

# **Chemokine Signalling in Malignant Cell Migration**

**Shirley Christine Mills**

**A Thesis presented for the Degree of Doctor of Philosophy from the School of  
Pharmacy at the University of East Anglia**

**May 2018**

© “This copy of the thesis has been supplied on condition that anyone who consults it is understood to recognise that its copyright rests with the author and that use of any information derived therefrom must be in accordance with current UK Copyright Law. In addition, any quotation or extract must include full attribution and may not be published without the author’s prior written consent”.

**Declaration:** This thesis is submitted to the University of East Anglia for the Degree of Doctor of Philosophy and has not been previously submitted at this or any other university for any assessment or degree. All this work is original and has been entirely carried out by the author alone. Shirley  
Christine Mills

## Abstract

Communication within and between cells is called signalling; elucidation of cell signalling in diseases, especially metastatic cancers, creates opportunities for developing therapeutic interventions. Signalling initiation occurs when a cell surface receptor binds a ligand; the signal then transmits via phosphorylation events through cytosolic signalling proteins to nuclear or effector proteins that orchestrate a cellular response. G-protein coupled receptors (GPCRs) are one type of receptor; a sub-family of GPCRs are chemokine receptors, their ligands, chemokines, can trigger directional migration. Homeostatic chemokine-triggered migration can be hijacked by cancer cells to facilitate metastasis. This study explored various poorly understood aspects of chemokine signalling that may support metastasis with the aim of identifying therapeutic targets.

Methodology employed THP-1, Jurkat and MCF7 cell-lines, the manipulation of signalling by antagonists, siRNA knockdown or plasmid modification, followed by calcium and chemotaxis assays, protein visualisation using immunofluorescence, flow cytometry and western blot.

Investigations found that in THP-1 cofilin phosphorylation temporally relates to CXCL12-stimulation and to chemotactic migration. In THP-1, but not Jurkat, JAK2 and STAT3 signalling support chemotaxis to CXCL12 and CCL2. Various NSAIDs, Aspirin and Paracetamol drug-specifically influenced chemokine-induced migration and cofilin activity. Rac1, FAK/Pyk2 and Pi3K were found important for chemotaxis to CXC- but not CC-chemokines and to modulate cofilin phosphorylation. Rac1 inhibitor NSC23766 was found to compete with CXCR4 ligands. Many signalling proteins involved in cancer, including GRKs, Src, Raf, MEK, ERK, Cdc42, ROCK,  $\beta$ -catenin and p38MAPK were shown to positively influence chemotactic migration, also Arrestin-2 to support chemotaxis to CXCL12, and Arrestin-3 chemotaxis to CCL3. Dynamin inhibitors and siRNA knockdown produced chemokine, cell type, and dynamin domain-specific responses, Dynamin's G-domain being important for CXCL12- and PH domain for CCL3-induced migration. PKC's role in malignancies was found contradictory and isoform specific; PKC $\epsilon$  and PKC $\delta$  supporting chemotaxis to CXCL12 but not CCL3, whereas PKC $\alpha$  and PKC $\zeta$  influenced migration to both CXCL12 and CCL3.

This thesis offers novel insights into the complexities of chemokine-induced migration. It examines many key signalling proteins implicated in cancer; reports that NSC23766 offers promise as a lead compound for developing CXCR4 biased antagonists; and offers possible mechanisms, through cofilin phosphorylation and effects on cell migration, for the mixed epidemiology reported for different NSAID's with respect to their influences on cancer incidence and progression, and suggests Ibuprofen may offer anti-metastatic efficacy.

## Table of Contents

<b>Abstract</b> .....	<b>iii</b>
<b>Acknowledgements</b> .....	<b>xiii</b>
<b>Published Papers</b> .....	<b>xiv</b>
<b>Chapter 1: Introduction</b> .....	<b>1</b>
1.1: Cells .....	1
1.2: Cell communication .....	3
1.3: Cancer and metastasis .....	3
1.3.1: Cell signalling in metastasis .....	4
1.4: G-Protein Coupled Receptors .....	4
1.5: Chemokines.....	5
1.6: Chemokine receptors.....	5
1.7: Inflammatory and homeostatic chemokines .....	6
1.8: Receptors CXCR4, CXCR7 (aka ACKR3) and their ligand CXCL12.....	7
1.9: ELR-positive and -negative CXC chemokines .....	7
1.10: Chemokines and T-lymphocytes (T-cells) .....	7
1.11: Chemokines and B-lymphocytes (B-cells).....	9
1.12: Tumour-associated macrophages, CCL2 and CCL3 .....	9
1.13: Tumorigenic signalling complexities, CXCL9, CXCL10, CXCL11 and CXCL12. ....	11
1.14: Oncogenic and epigenetic influences on chemokines.....	12
1.15: Chemokine receptor CXCR4 and metastasis.....	13
1.15.1: Structure of CXCR4 and its interactions with CXCL12.....	14
1.16: Introduction to Dynamin and Dynamin Like Proteins (DLPs) .....	16
1.16.1: Dynamin family proteins structure and domains .....	17
1.16.2: Dynamin polymerization.....	18
1.16.3: Membrane fission .....	19
1.16.4: Endocytosis plays a key role in regulation of intracellular signalling .....	19
1.16.5: Influences of cargo on endosome fate .....	20
1.16.6: Dynamin, $\beta$ -arrestins and the Rho GTPases.....	20
1.16.7: Dynamin's role in Clathrin-dependent endocytosis .....	20
1.16.8: Dynamin's role in clathrin-independent endocytosis.....	21
1.16.9: Dynamin and DLPs in disease.....	22
1.16.10: Dynamin in cancer development and progression .....	23
1.16.11: Drp-1, mitochondrial division and cancer.....	24



1.17: Protein Kinase C (PKC) .....	25
1.17.1: PKC structure, isoforms, location and function .....	25
1.17.2: PKC's phosphorylation of chemokine receptors.....	26
1.17.3: PKC activation .....	27
1.17.4: PKCs role in cancers .....	28
1.17.5: PKCs as oncoproteins and as tumour suppressors .....	29
1.18: JAK STAT Signalling.....	29
1.18.1: JAK2 in malignancies .....	30
1.19: Rho GTPases in cell migration.....	31
1.19.1: Controllers of Rho GTPases GDIs, GAPs and GEFs .....	32
1.20: Pi3K and FAK signalling in metastasis .....	33
1.21: Signalling linking cofilin to chemotactic metastasis.....	34
1.21.1: Cofilin phosphorylation and dynamics .....	34
1.21.2: Phospholipid phosphatidylinositol-(4,5)-bisphosphate influences on cofilin.....	36
1.22: Non-Steroidal-Anti-inflammatory Drugs (NSAIDs) and metastasis .....	37
1.22.1: Selective and non-selective NSAIDs.....	37
1.22.2: Paracetamol's complex mode of action .....	37
1.22.3: Leukocytes and PGE <sub>2</sub> .....	38
1.22.4: COX1 and COX2, inflammation and cancer.....	39
1.22.5: NSAIDs COX-independent antineoplastic effects .....	40
1.23: Research objectives .....	41
<b>Chapter 2: Materials and Methodology.....</b>	<b>43</b>
2.1: Reagents.....	43
2.1.1: Small Molecule Inhibitors .....	43
2.1.2: Peptides and Chemokines.....	45
2.1.3: Bacterial Plasmids .....	46
2.1.4: Antibodies .....	46
2.1.5: Small Interfering Ribonucleic Acids (siRNA).....	47
2.1.6: Imaging Stains and Activation Kits .....	48
2.2: Cell-lines.....	49
2.3: Cell culture .....	49
2.3.1: FCS Heat Inactivation .....	50
2.3.2: Propagating Cell Cultures.....	50
2.3.3: Cell Counting and Viability .....	50

2.3.4: Freezing and thawing cells .....	50
2.3.5: Harvesting Adherent Cells.....	50
2.3.6: Phorbol 12-myristate 13-acetate differentiation of THP-1 to macrophages.....	51
2.4: Chemotaxis .....	51
2.5: Wound-healing assays .....	51
2.6: Cytotoxicity Assays.....	52
2.6.1: CellTitre 96® Aqueous One Solution Cell Proliferation Assay .....	52
2.6.2: Manual Toxicity Assay .....	52
2.7: Fluorescent Phalloidin (Phalloidin) F-actin Stain .....	52
2.8: 4',6-diamidino-2-phenylindole (DAPI) stain.....	53
2.9: Receptor Immunofluorescence staining.....	53
2.10: Immunofluorescence staining of cellular proteins .....	54
2.11: Transfection of cells .....	54
2.11.1: siRNA Transfection.....	54
2.11.1.1: siRNA transfection using AMAXA Nucleofector.....	54
2.11.1.2: Chemical siRNA transfection.....	55
2.11.2: Plasmid transfection using AMAXA.....	55
2.11.3: Eugene or Lipofectamine plasmid transfection for adherent cells.....	55
2.12: Plasmid technology .....	56
2.12.1: DH5α Escherichia Coli transformation.....	56
2.12.2: Bacterial fermentation for plasmid DNA harvesting .....	56
2.12.3: Plasmid Purification (Qiagen Plasmid Midi Kit method).....	56
2.12.4: Confirming DNA on Agarose Gel .....	57
2.13: Peptide synthesis .....	57
2.14: SDS-PAGE and Western blot .....	58
2.14.1 Total protein extraction for Western Blot .....	58
2.14.2: Gel preparation for Western Blot .....	58
2.14.3: Protein transfer to membrane.....	59
2.14.4: Primary antibody labelling .....	59
2.14.5: Loading confirmation .....	59
2.15: Immunoprecipitation of CCR5 receptor.....	60
2.16: Analysis of intracellular calcium ion flux.....	60
2.17: Internalisation assay and flow cytometry analysis .....	61
2.18: Cyclic Adenosine Monophosphate (cAMP) Assay.....	61

2.19: Rac1 Activation Assay .....	62
2.20: Enzyme linked immunosorbance assay (ELISA) .....	63
2.21: Analysis of data .....	63
<b>Chapter 3: Exploring the intricacies of dynamin function in malignant cell migration .....</b>	<b>64</b>
3.1: Introduction .....	64
3.2: Results.....	65
3.2.1: The expression of CXCR4 and CCR5 in cell-lines .....	65
3.2.2: Exploring the role of dynamin in cell-lines.....	67
3.2.3: Immunofluorescence established dynamin's presence.....	68
3.2.4: Dynamin-2 siRNA knockdown inhibits wound-healing but not chemotaxis.....	68
3.2.5: Dynamin and Drp-1 inhibitors.....	71
3.2.6: Dynasore .....	72
3.2.7: Dyngo4a .....	76
3.2.8: MiTMAB and OcTMAB .....	77
3.2.8.1: MitMAB .....	78
3.2.8.2: OcTMAB .....	79
3.2.9: Rhododyn-C10™ .....	80
3.2.10: RTIL-13 .....	81
3.2.11: Pyrimidyn-7™ .....	83
3.2.12: Dynamin inhibitors can interrupt cytokinesis.....	84
3.3: Discussion .....	85
3.3.1: Dynasore may be inhibiting Drp-1 as well as dynamin.....	86
3.3.2: CCR5 and CXCR4 endocytosis kinetics .....	86
3.4: Conclusions .....	87
<b>Chapter 4: PKC and other key signalling proteins in cell migration towards CXCL12 and CCL3 in leukemic cells compared to breast cancer cells .....</b>	<b>90</b>
4.1: Introduction .....	90
4.2: Results.....	92
4.2.1: Rottlerin and PKCδ .....	92
4.2.2: Staurosporine, GF109203X and PKC isoform knockdown .....	94
4.2.3: PKD (PKCμ) activity is important for CCL3- but not CXCL12-induced chemotaxis in THP-1 cells, and for CXCL12-induced chemotaxis in Jurkat.....	100
4.2.4: PKD inhibition modulates cAMP levels .....	101
4.2.5: PKC inhibitors – effects on cellular calcium dynamics appear isoform specific .....	103

4.2.6: Src and Ras/Raf/MEK/ERK signalling appear important for CCL3 and CXCL12 induced migration in THP-1 and MCF7 and for CXCL12-induced migration in Jurkat .....	103
4.2.7: Src siRNA knockdown also inhibits cell migration .....	105
4.2.8: Signalling through the Ras/Raf/MEK/ERK pathway lacks chemokine or cell specificity .....	108
4.2.9: Inhibiting pairs of signalling proteins provides further evidence of signalling through Src and Ras/Raf/MEK/ERK pathways triggered by CXCL12 and CCL3.....	113
4.3: Discussion .....	116
4.3.1: Roles of PKC $\alpha$ in malignancies .....	117
4.3.2: PKC $\epsilon$ upregulation may support cell survival, invasion and motility .....	117
4.3.3: PKC signalling through GSK3, Slingshot and cofilin.....	119
4.4: Conclusions .....	121
<b>Chapter 5: CXCL12 and CCL3 chemokine-induced migration in leukaemic and breast cancer cells can involve cofilin phosphorylation, Pi3K and <math>\beta</math>-arrestins .....</b>	<b>123</b>
5.1: Introduction .....	123
5.2: Results.....	124
5.2.1: Cofilin modulates leading edge dynamics .....	124
5.2.2: Cofilin knockdown reduces migration to CCL3 and CXCL12 .....	125
5.2.3: Cofilin phosphorylation can be triggered by a range of chemokines .....	127
5.2.4: Chemotactic responses to chemokines are concentration dependent.....	127
5.2.5: Additive responses between chemokines may suggest dimerization .....	128
5.2.6: Pi3K inhibition and chemokine-induced migration .....	132
5.2.7: Pi3K siRNA knockdown also inhibits chemokine-induced migration in MCF7 and THP-1 .....	134
5.2.8: Cofilin phosphorylation is modified by Pi3K inhibition.....	136
5.2.9: G-protein coupled receptor kinases (GRKs).....	139
5.2.9.1: $\beta$ ARK.....	139
5.2.9.2: Ipyrimidine .....	141
5.2.10: $\beta$ -arrestins.....	143
5.2.10.1: Immunofluorescence demonstrates the presence of $\beta$ -arrestins in cell-lines ....	143
5.2.10.2: $\beta$ -arrestin transfection in CHO.CCR5 .....	144
5.2.10.3: $\beta$ -arrestin transfections in MCF7, THP-1 and Jurkat.....	145
5.2.11: Focal adhesion kinases play a role in chemokine chemotaxis.....	149
5.2.12: Rho Proteins.....	151
5.2.12.1: Rho activated coiled-coil kinase (ROCK) .....	152

5.2.13: Mitogen extracellular signal regulated kinase (MAPKK) (MEK) and Src .....	154
5.3: Discussion .....	156
5.3.1: Cofilin phosphorylation and chemokinesis .....	157
5.3.2: Additive or inhibitory effects can occur when chemotactic chemokines are used in tandem .....	158
5.3.3: Pi3K, Phosphatidylinositol 3,4,5 triphosphate (PIP3), Gβγ signalling and GEFs .....	158
5.3.4: Cofilin links to mitogenic signalling networks.....	160
5.3.5: GRKs and β-arrestin in chemokinesis.....	161
5.3.6: β-arrestin mediation of signalling leading to chemotaxis and chemokinesis.....	162
5.3.7: ROCK and MEK are key mediators of cofilin phosphorylation.....	163
5.3.8: FAK inhibition may support haematological malignancies .....	163
5.4: Conclusions .....	163
<b>Chapter 6: JAK2 and STAT3 play role in chemokine-induced chemotaxis and cofilin phosphorylation.....</b>	<b>166</b>
6.1: Introduction .....	166
6.2: Results.....	167
6.2.1: JAK2 and STAT3 inhibitors were examined for effects on cell metabolism and actin polymerisation .....	168
6.2.2: JAK2 and STAT3 role in chemotactic cell migration and chemokinesis. ....	169
6.2.3: The roles of JAK2 and STAT3 in calcium dynamics .....	172
6.2.4: cAMP and JAK STAT signalling.....	173
6.2.4.1: cAMP modulator Forskolin and PKA inhibitor H89HCL inhibit chemotaxis and chemokinesis.....	173
6.2.4.2: JAK2 and STAT3 inhibition did not statistically significantly increase cAMP levels .....	177
6.2.4.3: cAMP levels may modulate actin filaments.....	178
6.2.5: Forskolin increases cofilin phosphorylation.....	181
6.2.6: Cofilin phosphorylation in the presence of JAK2 and STAT3 VIII inhibition .....	182
6.2.6.1: CXCL12 induce cofilin phosphorylation and STAT3 phosphorylation.....	182
6.3: Discussion .....	184
6.3.1: JAK2, STAT3 and cofilin phosphorylation.....	185
6.3.2: cAMP involvement with JAK2 and STAT3 signalling .....	186
6.4: Conclusions .....	190
<b>Chapter 7: Direct and indirect effects of NSAIDs in chemotactic metastasis.....</b>	<b>192</b>
7.1: Introduction .....	192

7.2: Results.....	193
7.2.1: Aspirin and Naproxen .....	193
7.2.2: Ibuprofen .....	196
7.2.3: Celecoxib.....	199
7.2.4: Paracetamol .....	201
7.2.5: Paracetamol, Aspirin and NSAID's effects on cellular calcium dynamics .....	202
7.2.6: COX2-inhibition may modulate basal cAMP levels .....	205
7.2.7: NSAIDs and Paracetamol modulated cofilin phosphorylation.....	206
7.3: Discussion .....	208
7.3.1: Ibuprofen may have PGE <sub>2</sub> -independent effects on cell viability and migration.....	208
7.3.2: NSAIDS effects on calcium fluctuations .....	210
7.3.3: NSAIDs and basal cAMP levels .....	212
7.3.4: The Prostaglandin Cascade, cAMP and Cofilin.....	212
7.4: Conclusions .....	214
<b>Chapter 8: Rac1 mediates chemotaxis to CXCL12 but not CCL3, in leukaemic and breast cancer cell-lines, and Rac1 GEF inhibitor NSC23766 may have off-target effects on CXCR4/CXCR7 axis</b> .....	<b>216</b>
8.1: Introduction .....	216
8.2: Results.....	218
8.2.1: NSC23766 inhibits chemotaxis to CXCL12 but not CCL3.....	218
8.2.2: Rac1 inhibiting peptide W56 inhibits chemotaxis to CXCL12 but not CCL3 .....	220
8.2.3: NSC23766 and W56 inhibit CXCL12-induced but not CCL3-induced wound-healing in MCF7 .....	220
8.2.4: NSC23766, AMD3100 and ATI2341 inhibit CXCL12-induced Rac1 activation in MCF7	222
8.2.5: NSC23766 competes with CXCL12 for CXCR4 binding. ....	222
8.2.6: NSC23766 competes with CXCR4 antibody 12G5 and CXCL12.....	224
8.2.7: ATI2341, AMD3100 and NSC23766 are not chemotactic to Jurkat .....	224
8.2.8: CXCR4 inhibition in presence of NSC23766 .....	225
8.2.9: Flow cytometry demonstrated NSC23766 was displacing CXCR4 antibody 12G5 .....	226
8.2.10: Rac1 inhibitor ETH1864 does not modify 12G5 binding or CXCL12-triggered CXCR4 internalisation .....	228
8.2.11: Sucrose and sodium azide pre-treatment does not stop NSC23766 causing CXCR4 internalisation .....	228
8.2.12: NSC23766 may act as a biased antagonist with respect to cAMP signalling.....	229
8.2.13: cAMP levels may modulate PKC $\zeta$ signalling .....	230

8.2.14: Effects of NSC23766 on intracellular calcium .....	231
8.2.15: U73122 inhibits PLC signalling .....	234
8.2.16: Inhibiting Cdc42 reduced migration towards CCL3 and CXCL12 .....	236
8.2.17: W56 and NSC23766 both inhibit CXCL12- but not CCL3-induced cofilin phosphorylation .....	237
8.2.18: NSC23766 also inhibits chemotaxis of THP-1 to CXCL11 but not to CXCL9 or CCL2 ...	238
8.2.19: CXCL14 modulates CXCR4/CXCL12 signalling in Jurkat .....	238
8.3: Discussion .....	240
8.3.1: Rac1 inhibitor produces chemokine specific responses .....	240
8.3.2: Rac GEF inhibitor NSC23766 .....	241
8.3.3: NSC23766 competes with CXCL12 and 12G5 .....	242
8.3.4: CXCR7 receptor in cancer .....	243
8.3.5: NSC23766 can displace CXCR4 antibody 12G5 .....	243
8.3.6: Endocytosis inhibitors do not prevent NSC23766 triggered CXCR4 internalisation .....	244
8.3.7: cAMP levels are reduced by NSC23766 but not by AMD3100 .....	246
8.3.8: Biased signalling .....	247
8.3.9: cAMP levels may modulate PKC $\zeta$ signalling .....	247
8.3.9.1: PKC $\zeta$ knockdown inhibits CCL3 and CXCL12 MCF7 wound-healing and Jurkat chemotaxis to CXCL12 .....	248
8.3.9.2: Both PKC $\zeta$ over-expression and inactivation can support malignancies .....	248
8.3.10: Intracellular calcium, PLC and Rac1 .....	249
8.3.11: NSC23766 inhibits both early and late cofilin phosphorylation events in response to CXCL12 .....	250
8.3.12: Rac1 may be involved in CXCL11 but not CCL2 or CXCL9 chemotaxis .....	251
8.3.13: NSC23766 may potentiate CXCL14 inhibition of Jurkat chemotaxis to CXCL12 .....	252
8.4: Conclusions .....	253
<b>9: General Conclusions .....</b>	<b>255</b>
<b>10: Future Work .....</b>	<b>258</b>
<b>11: References .....</b>	<b>259</b>
<b>Appendix 1 - List of Tables .....</b>	<b>325</b>
Chapter 2 .....	325
Chapter 3 .....	325
<b>Appendix 2 - List of Figures .....</b>	<b>326</b>
Chapter 1 .....	326
Chapter 3 .....	326

Chapter 4.....	327
Chapter 5.....	329
Chapter 6.....	331
Chapter 7.....	332
Chapter 8.....	333
<b>Appendix 3 - List of Abbreviations .....</b>	<b>335</b>
Table A3 .....	335
<b>Appendix 4 - Small Molecule Inhibitor and Receptor Antagonist structures.....</b>	<b>342</b>
Table A4 .....	342
<b>Appendix 5 - Published Abstracts, Posters and Oral Presentations.....</b>	<b>347</b>
2014 .....	347
2015 .....	347
2016 .....	347
Oral Presentations .....	348
<b>Appendix 6 - Contributions to and Copies of Published Papers .....</b>	<b>348</b>



## Acknowledgements

Thank you to my supervisors Anja Mueller and Maria O'Connell who have given me the opportunity to plan and complete my thesis investigations with great freedom, follow my instincts and learn many different techniques. To my primary supervisor Anja for putting such a range of chemicals and tools at my disposal, I am grateful for your support.

My thanks also go to the following; to Leanne Stokes for training me in techniques including Flow Cytometry and for her kind support and scientific input. To Lesley Howell for training me in peptide synthesis and to Wafa Al-Jamal and Sara Pereira for use of their FACS machine; also to my lab colleague Jessica di Gesso for teaching me Western Blotting. Likewise thanks to Professor Mark Searcey, The School of Pharmacy and UEA for their support and their 'Do Different' scholarship.

I would also like to thank my viva examiners; Professor Robert Nibbs for his time providing constructive, thought-provoking comments and Zoë Waller for her helpful suggestions. Viva input from both examiners encouraged me to undertake improvements in the readability of this thesis.

Finally to the two people who stoically supported me all the way through this learning experience, my husband Ron and my daughter Emma; thank you for your love, patience and companionship.

## Published Papers

Jacques R O, Mills S C, Zerwes P, Fagade F O, Green J E, Downham S, Sexton D W, Mueller A. ***Dynamin function is important for chemokine receptor-induced cell migration.*** Cell Biochem Funct 2015 33(6):407-414

Mills S C, Goh P H, Kudatsih J, Ncube S, Gurung R, Maxwell W, Mueller A. ***Cell migration towards CXCL12 in leukaemic cells compared to breast cancer cells.*** Cell Signal 2016 28(4):316-324

Mills S C, Howell L, Beekman A, Stokes L, Mueller A. ***Rac1 plays a role in CXCL12 but not CCL3-induced chemotaxis and Rac1 GEF inhibitor NSC23766 has off target effects on CXCR4.*** Cell Signal 2018 42:88-96

## **Chapter 1: Introduction**

Most of us have heard of cancer, many will understand that early detection can offer cure, this is because survival rate is dramatically dashed by metastasis, the movement of a cancer cell from its primary site to a secondary niche which supports its growth and division. Cancers are diverse; they comprise normal cells with acquired genetic instability and abnormalities that render them refractory to normal controlling influences on their growth, lifespan and location [1, 2]. Metastasis can occur in response to 'come hither' signals from amongst others chemokines, small proteins secreted by immune and other cells [3]. The signalling networks driving metastasis are only partially understood, some component proteins and pathways have been identified but the full network and its spatiotemporal dynamics represents a major objective in oncology research. Cancer touches most people's lives at some point, either their own or someone dear to them; developing new therapies requires us to listen in and try to understand the conversations within and between our cells, contributing to our understanding of this signalling dialogue was the aim of my research.

This chapter aims to acquaint the reader with the basics and some of the intricacies of chemokines, chemokine receptors and immune cells; and introduce key signalling proteins relevant to the research work reported in later chapters.

### **1.1: Cells**

Eukaryotic cells are the basic structural and functional unit of the human body. Within each cell are many components each of which perform unique functions, figure 1. There are many different types of cells in humans together making up the different tissues; muscular, nervous, epithelial or connective. Some cells are dynamic and motile, cell movement often involves crawling over the extracellular matrix. This enables fibroblasts to move into wounds to support healing, and neutrophils and macrophages to respond to tissue invasion by pathogens. However with cancer cell movement facilitates metastasis [4].

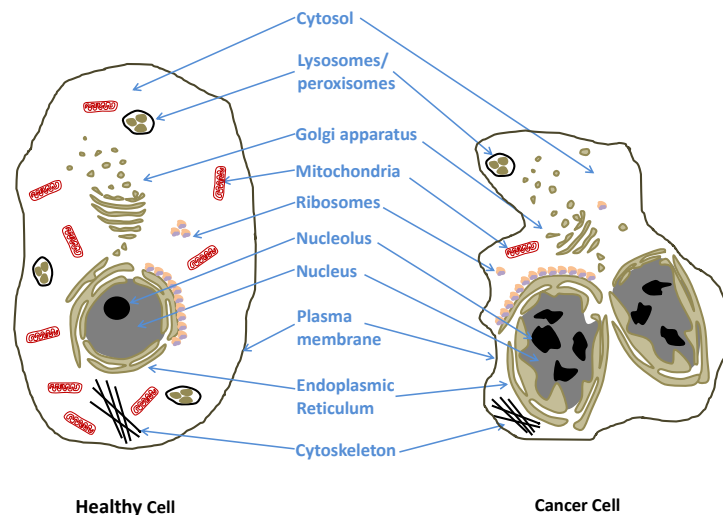


Figure 1.1: Cancer cells may contain many of the components of normal cells but often display reduced cytoplasm, an abnormal shape, plus multiple or enlarged dark staining nucleus with an irregular nuclear border, a nucleus containing clumpy chromatin and multiple nucleoli.

Cancer cells are normal cells that have acquired some or all of the following characteristics: Immortality so they are able to undergo repeated replication and resist apoptosis; DNA mutations and genome instability; an ability to induce angiogenesis, promote inflammation, avoid destruction by immune cells, and evade growth suppressors, also they may produce sustained proliferative signalling. Cancer cells also lose their ability to differentiate and have dysregulated cellular energetics [5]. For example a cell may become cancerous due to dysregulation of amino acid and glucose metabolism in response to abnormal growth factor signalling. Activation of a signalling pathway known as Pi3K/Akt may be key to this initial creation and support of a cancer cell because such signalling can trigger the reprogramming of mitochondrial metabolism [2]. Healthy cells compete for growth factors that govern their uptake of nutrients and maximise their ATP production via oxidative phosphorylation in mitochondria. However when growth factors are present in excess cells can increase their nutrient uptake and start using anabolic glycolysis, the energy production method commonly found in cancer cells. Nutrient supply appears key to cancer initiation [6]. Transcription factors are proteins that regulate the function of genes, oncogenes are genes that in some circumstances make a cell cancerous. Myc is an oncogene that can support this cancer initiation by promoting mitochondrial production of glutamine, a good carbon source and nitrogen donor, aiding macromolecule production and thus cell proliferation. Hence cancer can initiate from oncogene-directed metabolic reprogramming allowing anabolic growth, and cell proliferation [1].

### ***1.2: Cell communication***

Cells within any multicellular organism need to communicate with each other and respond to their environment. Cells talk to each other using small peptides or ions which, like words, can pass on an instruction or message and produce a physiological response. This talking is called cell signalling. Cell signalling can occur within cells (autocrine signalling), between neighbouring cells over short distances (paracrine signalling), or between cells or a collection of cells (a tissue) over longer distances (endocrine signalling). Intracellular communication between areas of the cell itself occurs via signalling pathways composed of membrane or cytosolic proteins. Passing the message (stimulus) between these proteins frequently involves protein phosphorylation which may activate or inactivate the next protein/s in the pathway. A cell's architecture is fundamental to its morphology and its mobility; signalling can modify a cell's morphology causing temporally and spatially transient changes in protein complexes within the many intracellular domains. The signalling cascade can initiate cellular responses e.g. activation of transcription factors, or cell movement [7, 8].

Immune cells employ a communication process facilitated by small protein signalling molecules that are secreted from one cell and detected by another cell or cells. Cells detect these signalling molecules, also called ligands, using receptors which are usually transmembrane proteins located within their plasma membrane. There are many different receptors, and each ligand will have affinity for and bind one or more receptors. Each receptor may bind one or more ligand. After binding the ligand/receptor pair can activate one or more intracellular signalling 'pathways' within the cell, usually producing an end response. Responses can include stimulating the cell to move up a chemical gradient which is termed cell migration [9, 10].

### ***1.3: Cancer and metastasis***

Cancer is where abnormal cells undergo uncontrolled division, often invading nearby normal tissues. Metastasis is the spread of these cells to a distant secondary site in the body. In cancer communication within and between cells goes wrong. Stem cells exist in a 'niche'; changes in their microenvironment or various transcription factors and signalling can activate them to make progenitor cells which then differentiate to generate tissues as required. When this goes wrong uncontrolled growth can initiate a benign tumour which may over time become cancerous. Cancer may also initiate through somatic mutation triggered by environmental stimulus, such as UV light or carcinogenic chemicals, or may arise from congenital insults, genetic defects, inflammation, ageing, and/or infection by virus or parasite [3, 11].

Cancer is not one disease; cancers are individual, complex and usually heterogeneous, so for example only some of the cells within a tumour will be capable of endless self-renewal i.e. malignant. Tumours are complex microenvironments composed of cohabiting malignant, healthy and immune cells. No two people's cancers are the same, as their oncogenic, genetic, epigenetic and immunological phenotypes will differ [11].

#### ***1.3.1: Cell signalling in metastasis***

Cell-cell communication in cancers encompasses many feedback loops that can activate or inhibit cell growth [3, 11]. The prevention of cancer progression, the migration of malignant cells from the localised primary tumour to secondary locations, requires a better understanding of cell signalling within malignant cells and between tumours and healthy tissues, as it is this communication that facilitates cell migration. Elucidating signalling pathways supporting metastasis is challenging, but considerable progress has been made, for example the dysregulation of calcium homeostasis has long been recognised as a casualty of cancer [12], with intracellular calcium dynamics modulating organelle functions, oncogenesis and ultimately cell death [13, 14]. Much is known about the role of cell energetics, glycolysis and mitochondrial respiration as mediators in cancer progression [2], and that mutations of receptors, key initiators of many signalling pathways, can also contribute to malignancy [15]. However to develop new therapies we need a better understanding of cell signalling. Immunotherapies, such as the checkpoint inhibitors, Programmed Death Protein-1 (PD-1) and Cytotoxic T Lymphocyte associated Antigen-4 (CTLA-4), are amongst the most innovative of the new treatments available for cancer. They are monoclonal antibodies that by binding inhibitory surface receptors on the cancer cells re-target cytotoxic T-cells to destroy cancer cells [16].

#### ***1.4: G-Protein Coupled Receptors***

The surfaces of most cells bristle with a multitude of different receptors which enable the cell to communicate with its environment. Contributing to this array is the family of G-Protein Coupled Receptors (GPCRs), of which there are over 800 distinctly different members [17]. GPCRs mediate responses to many different stimuli (agonists) which may arrive in the form of light, peptides, proteins, or sugars. Examples include hormones, neurotransmitters and immune system messaging proteins called cytokines. GPCRs are membrane proteins consisting of a peptide chain with a conserved basic tertiary structure that consists of seven hydrophobic transmembrane regions. When an agonist binds the GPCR, it undergoes a conformational change favouring its coupling with three intracellular heterotrimeric guanine nucleotide-binding proteins (G-proteins),  $G\alpha$ ,  $G\beta$  and  $G\gamma$ . Guanine exchange factors (GEFs) then promote GDP exchange for GTP on the  $G\alpha$

subunit; this allows G $\alpha$ -GTP and G $\beta\gamma$  to dissociate and interact with various effector proteins. The extracellular stimulus is translated into tightly regulated, highly specific, intracellular signalling cascades [18, 19]. GPCRs can be regulated by receptors becoming refractory to stimulus (desensitisation), receptor internalisation by endocytosis, and by longer term down-regulation of receptors. The desensitisation can be through the action of kinases; protein kinase A (PKA), protein kinase C (PKC), and G-protein receptor kinases (GRKs) which may trigger binding of  $\beta$ -arrestins, halt G-protein activation and trigger desensitisation of GPCR [20, 21].

### **1.5: Chemokines**

Cytokines are small secreted proteins that influence cell behaviour through modulation of cell signalling. Chemokines are a large subfamily of chemotactic cytokines [22]. Cell signalling allows cells to sense and respond to their environment and maintain homeostasis. Aberrant signalling between and within cells can initiate and perpetuate cancers [23]. Chemotactic chemokines can play a role in homeostasis. These small 8-12 kDa basic proteins regulate cell migration when they interact with and activate a specialist type of GPCR termed a Chemokine Receptor. Spatial and temporal expression of chemokines regulate the trafficking and locations of many cell types including leukocytes [24, 25].

There are four sub-families of chemokines classified by the arrangement of the initial two cysteines (C) with respect to non-cysteine residues (X) within each chemokine amino acid sequence. The largest two of these four families are the CXC chemokines, where one amino acid separates the first two cysteines at the N-terminal of the peptide chain, and the CC chemokines, where cysteines are adjacent. The other two families, known as XC and CXXXC, have very few members [26]. Although there is promiscuity in interactions between chemokines and their cognate GPCR, many restrict their ligand-binding to favoured partners [24, 25]. Leukocytes can express many different chemokine receptors. This differential expression allows the recruitment of specific cell types to specific tissues or locations providing a tailored appropriate immune response to the infective or inflammatory insult [26].

### **1.6: Chemokine receptors**

Chemokine receptors are subdivided into CC, CXC, XC and CXXXC with respect to their favoured ligands [25]. There are at least 18 G $\alpha_i$ -coupling chemokine receptors and 5 non-chemotactic Atypical Chemokine Receptors (ACKRs). ACKRs may undertake roles such as recycling or scavenging chemokines to maintain chemotactic gradients. Interestingly some chemokines have dual roles, as they can also act as classical receptor antagonists, antagonising ligand-receptor

interactions and responses. For example CXCL11 acts as a CCR5 antagonist and so hinders the binding of CCR5 ligand CCL3 [27, 28]. Some chemokine receptors are also the target of non-chemokine ligands e.g. macrophage migration inhibitory factor (MIF) is a cytokine that binds CXCR4 [29] as does extracellular ubiquitin [30] and nuclear protein HMGB1 [31].

On chemokine receptor activation the signal passes to GPCR-associated G-proteins, subunits  $\alpha$ ,  $\beta$  and  $\gamma$ . The GDP on the  $G\alpha$  subunit is phosphorylated to GTP,  $G\alpha$  dissociates from  $G\beta\gamma$  and, depending on stimulus, subunits trigger particular intracellular signalling proteins and pathways. There are at least four  $G\alpha$  subtypes  $G\alpha_s$ ,  $G\alpha_{i/o}$ ,  $G\alpha_{q/11}$ ,  $G\alpha_{12/13}$ . Chemokine chemotaxis purportedly mainly follows  $G_{\alpha i}$  or  $G_{\alpha 12/13}$  signalling and can involve Rho family GTPases, RhoA, Rac1 and Cdc42 [18, 32, 33]. Signalling cascades can be triggered through both  $G\alpha$  and  $G\beta\gamma$  and involve phospholipase C (PLC) isoforms. Diacylglycerol (DAG) and inositol 1,4,5-trisphosphate ( $IP_3$ ) produced in response to PLC signalling can trigger many converging or diverging signalling pathways within the cell; for example  $PLC\beta$  signalling via phosphoinositide 3-kinase (Pi3K) to phosphatase Slingshot (SSH), which can activate a small protein called cofilin which remodels the key cytoskeletal protein actin enabling leukocyte polarization and cell chemotaxis [34].

### 1.7: Inflammatory and homeostatic chemokines

Chemokines can also be classified into functional groups such as ‘inflammatory chemokines’, including CXCL9, CXCL10, CXCL11, which can act to produce increased inflammation. Inflammatory CC chemokines include CCL3 (MIP-1 $\alpha$ ) and CCL2 (MCP-1), figure 1.2. ‘Homeostatic chemokines’ is another classification. Many CC chemokines are coded on chromosome 17q12 and CXC chemokines on 4q13.3. However homeostatic chemokines are coded at other loci, for example CXCL12, on 10q11.21. [35]. CXCL12 is usually constitutively expressed in lymphoid tissues and can mediate homeostatic chemotaxis of lymphocytes and other cells. However CXCL12 can be upregulated and become inflammatory in disease including in cancers. Dysregulated chemokine or chemokine receptor expression can trigger or worsen prognosis in diseases including those involving inflammation or malignancy [3, 36].

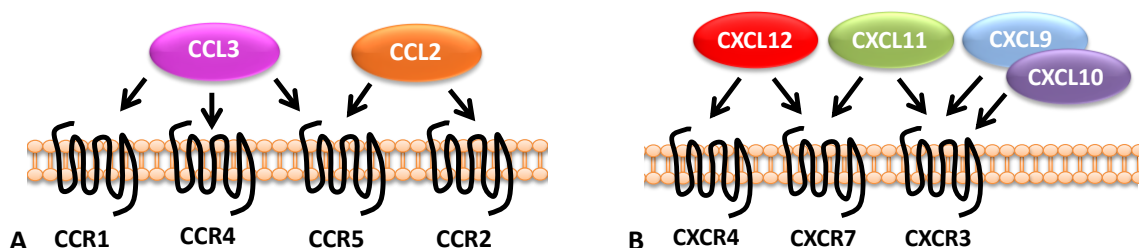


Figure 1.2: Examples of (A) CC and (B) CXC chemokine receptors and their ligands.



### **1.8: Receptors CXCR4, CXCR7 (aka ACKR3) and their ligand CXCL12**

CXCL12 is typical amongst homeostatic chemokines in binding only two chemokine receptors, each with non-redundant specific roles. CXCL12 binds CXCR4 and CXCR7, CXCL11 binds CXCR3 but also binds CXCR7 which is an ACKR. Atypical receptors are still seven transmembrane proteins but do not signal like classical chemokine receptors. They can lack the DRYLAIV motif in their second intracellular loop which aids coupling to G<sub>αi</sub> G-proteins [37, 38]. CXCR7 is well conserved across species [39]. It is known to dimerize with CXCR4 and may moderate the effects of CXCL12 binding CXCR4. CXCR7 may produce atypical signalling, not via G-proteins [40], and can act as a CXCL12 sink [41]. Interestingly although CXCR7 is not highly expressed in healthy tissues in an adult it is frequently present in malignant cells and through MAPK signalling can promote neo-angiogenesis [40]. CXCR4-CXCL12 signalling is key in keeping hematopoietic stem cells in the bone marrow [42]. Unfortunately this ability of CXCR4-CXCL12 signalling to support homing of stem cells can be hijacked by tumour cells, as CXCL12 can aid metastasis and the formation of secondary tumours [43].

### **1.9: ELR-positive and -negative CXC chemokines**

CXC chemokines can further be classified on the absence or presence of the glutamic acid-leucine-arginine (ELR) sequence occurring just prior to the CXC sequence. ELR-positive CXC chemokines mainly promote angiogenesis (examples include CXCL1, CXCL5 and CXCL8) whereas ELR-negative CXCs mainly inhibit angiogenesis [44]. CXCL9 (aka MIG), CXCL10 (aka IP-10) and CXCL11 (aka ITAC) are all ELR-negative and inhibit angiogenesis. They also attract anti-tumour T-lymphocytes and so may cause tumour regression [45-47]. CXCL9, CXCL10 and CXCL11 all bind CXCR3 which has three splice variants CXCR3-A, CXCR3-B and CXCR3-alt. CXCR3-A supports proliferation and chemotaxis, whereas CXCR3-B inhibits migration, proliferation and can trigger apoptosis [48, 49].

### **1.10: Chemokines and T-lymphocytes (T-cells)**

Chemotaxis is when a cell senses a chemokine and moves or 'taxes' towards it up the chemokine concentration gradient. In homeostasis this draws leukocytes towards damaged or infected cells releasing chemokines [50]. Chemokines can recruit effector T-cells including CD8<sup>+</sup> T-cells (cytotoxic T-cells) and T-helper CD4<sup>+</sup> cells type 1 and 2 (T<sub>H</sub>1 and T<sub>H</sub>2). Both types are T-helper cells supporting and regulating adaptive immune system function. T<sub>H</sub>1 and T<sub>H</sub>2 differ in the cytokines and type of immune responses they produce. Chemokines can also recruit Natural Killer (NK) cells which can engage with and cause apoptosis in malignant cells. T<sub>H</sub>1 and NK cells express CXCR3, the receptor for ligands CXCL9 and CXCL10; these chemokines draw T<sub>H</sub>1 and NK cells into the

tumour microenvironment, figure 1.3. The presence of  $T_H1$  and NK cells can improve patient prognosis and reduce metastasis [51, 52], and their presence in tumours improves outcomes as they increase  $CD8^+$  T-cell secretion of interferon- $\gamma$  and reduce metabolism of the chemotherapeutic agent cisplatin by tumour-associated fibroblasts [53].

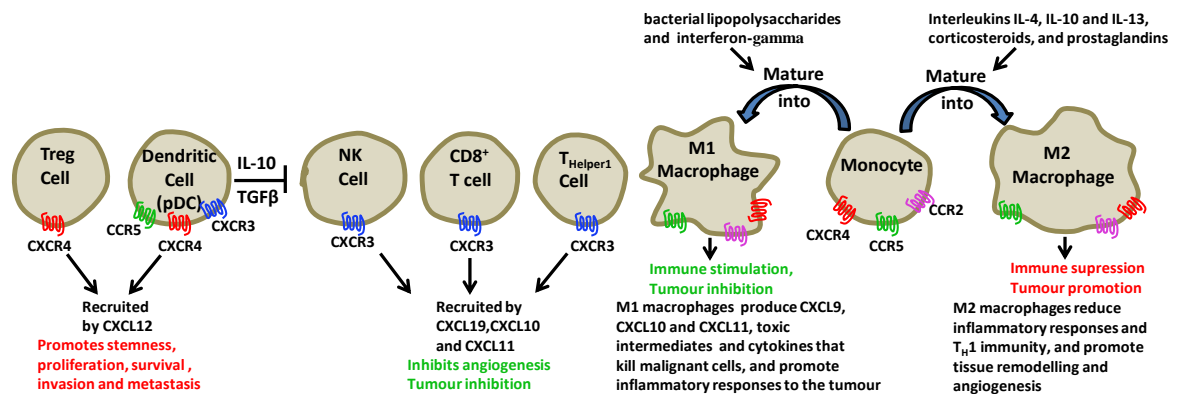


Figure 1.3: Immune cells can be recruited into the tumour microenvironment by chemokines; T-reg and Plasmacytoid Dendritic Cells (pDC) are recruited by CXCL12 and  $CD8^+$  T-cells, and T-helper cells and NK cells by CXCL9 and CXCL10. Monocytes differentiate into M1 and M2 macrophages. M1 macrophages stimulate the immune system, are microbicidal and cause tumour cytotoxicity, whereas M2 macrophages support tumour growth by promoting matrix remodelling and angiogenesis [43, 54-56].

Human T-helper-17 cell ( $T_H17$ ) function in human tumours is somewhat controversial [57] but they do express CXCR4 [58] which may aid their recruitment and retention in inflamed and malignant tissues where there are high levels of CXCL12.  $T_H17$  can recruit  $CD8^+$  T-cells, dendritic, and NK cells [59-62] into the tumour micro-environment; this is clinically helpful [63].

Tumour metastasis frequently occurs in the bone marrow, an immunosuppressive microenvironment that can aid malignant cell survival and growth. Regulatory T-cells (T-regs) aka suppressor T-cells maintain self-tolerance, preventing autoimmune disease, but also suppress immune responses to malignant cells [64]. T-regs can be recruited into the bone marrow and tumour microenvironments by CXCL12 as they express CXCR4. Increasing T-reg bone marrow load promotes an immune suppressive environment favouring implantation and growth of bone metastasis [65, 66].

NK cells express chemokine receptors including CXCR3, CCR2 and CCR5 [67]; CCR2 aids the movement of NK cells into tumours [68]. NK cells can activate  $CD8^+$  and other T-cells to attack and kill tumour cells. NK cells are part of the non-specific innate immune system. They have a single invariant antigen receptor which recognises a specific glycolipid antigen enabling them to activate

CD8<sup>+</sup> T-cells to target and kill MHC-positive tumour cells, whereas the NK cells themselves can kill MHC-negative tumour cells [55].

#### ***1.11: Chemokines and B-lymphocytes (B-cells)***

B-lymphocytes mature in the bone marrow and can develop into memory B-cells or plasma cells producing antibodies. Both form part of humoral immunity and the Adaptive Immune System. B-cells can act as Antigen Presenting Cells (APCs) and secrete cytokines [69], including some chemokines, and may also express CXCR4. Hence they may be recruited by CXCL12 into tumour microenvironments where they may improve prognosis [70, 71]. In lymphatic tissues associated with tumours B-cells may express chemokines which helpfully increase T-cell responses. B-cells can also serve as APCs in the tumour microenvironment and may positively or negatively influence anti-tumour immunity [72].

CXCL12 can recruit Plasmacytoid Dendritic Cells (pDC), which are part of the innate immune system. pDCs produce interferons and some chemokines including CXCL10 and CCL3 which attract immune cells to sites of infection or inflammation, and they also present antigens to CD4<sup>+</sup> T-helper cells. pDCs also express chemokine receptors including CXCR3, CXCR4, CCR2 and CCR5. pDCs need to express CCR2 and CCR5 to egress from the bone marrow whereas CXCR4 expression allows their retention in the bone marrow stroma where their development occurs, but also allows their attraction into CXCL12-producing tumour environments where they can impair T-cell destruction of malignant cells and so hinder prognosis [56, 73]. pDCs also produce pro-inflammatory cytokines and trigger immune tolerance favouring cancer progression [74].

#### ***1.12: Tumour-associated macrophages, CCL2 and CCL3***

Macrophages are large phagocytic leukocytes that develop from monocytes produced by stem cells in the bone marrow. Macrophages express CCR2 and so can respond to CCL2 and be attracted into tumours [75]. High numbers of Tumour Associated Macrophages (TAM) correlate with poor prognosis [76] as they can inhibit helpful T-cell activation [77], increase resistance to chemotherapy [78] and support metastasis [76]. This is because TAMs secrete CCL2, which can induce CCL3 secretion from metastasis-associated macrophages at metastatic sites; this can aid growth of secondary tumours [79]. However in some circumstances macrophages may aid survival. They can assist tumour-associated antigen T-cell 'cross-priming' by phagocytosing dead malignant cells then cross-presenting cancer antigens to cytotoxic T-cells, promoting the T-cells to attack live malignant cells [80]. Depending on the treatment employed macrophages may support or antagonise cancer therapy [81]. This is because TAMs can be influenced by their environment

to differentiate into an inflammatory (M1) or pro-tumour (M2) state. Bacterial lipopolysaccharides and interferon- $\gamma$  induce macrophage polarization into M1-subtypes that can kill cancer cells. However when entering tumours macrophages encounter cytokines such as interleukin-10 that can polarise them into M2-subtypes which can support tumour growth [54]. CCL2 is frequently produced by malignant tumours and the level of production correlates with macrophage infiltration. Excess CCL2 production can lead to TAM accumulation and tumour destruction, whereas modest accumulations can cause inflammation and tumour initiation. TAMs themselves may also produce CCL2 [82-84].

CCL2 and CCL3 can support tissue invasion as they stimulate the secretion of Matrix Metalloproteases (MMP), including MMP9, by monocytes. Matrix metalloproteases are molecular scissors, as they aid intracellular matrix penetration by migrating cells [85]. Circulating monocytes are precursors of macrophages [77]. CCL2 released from a tumour can recruit monocytes expressing CCR2 [86] from the blood. Treatment with the anti-CCL2 antibody, Carlumab, prevents this and reduces metastasis e.g. from breast to lung. However once Carlumab is withdrawn metastasis is accelerated. This could be due to a feedback mechanism accelerating tissue production of CCL2 [87], or that blocking CCL2 accumulates monocytes in the bone marrow which are released upon Carlumab withdrawal, allowing mass monocyte infiltration into metastatic tumours [88], which also increases local vascular endothelial growth factor (VEGF) and CXCL8 (interleukin-8) levels. CCL2 and CCL3 also support metastasis and angiogenesis, as the formation of new blood vessels allows tumours to grow [89]. However, even if TAM accumulation could be effectively prevented neutrophil accumulation may take its place, and have equally detrimental pro-tumour and pro-metastatic effects [85, 90]. Additionally CCL2 stimulates JAK2 and p38 mitogen-activated protein kinase (MAPK) signalling supporting metastasis [91]. CCL2 can also promote proliferation via activation of Rho GTPases [92], Epithelial Mesenchymal Transition (EMT) [93], and the survival and motility of cancer cells [92]. EMT is the process where epithelial cells lose their polarity, cell-cell adhesiveness, become migratory and invasive by gaining mesenchymal multipotent and stem-cell like properties. EMT is essential for embryogenesis but the process in later life facilitates metastasis of tumours [94].

CCL2 and CCL3 signalling can recruit macrophages into malignant tissues. These chemokines target CCR1, CCR2 and CCR5. Blocking this recruitment may inhibit accumulation of immunosuppressive leukocytes in the tumour microenvironment, stall metastasis and tumour neoangiogenesis [75, 79]; indeed, reducing macrophage load may increase anti-PD-L1 immunotherapy success [82]. However blocking chemokine production alone appears ineffective

[87], but may work synergistically with developing therapies such as cancer vaccines. For example CCL2 inhibition in mouse models potentiates cancer vaccines in lung cancer [95]. Recently clinical trials were conducted with a CCR2 antagonist CCX872-b [96], however treatment did not have a control so the benefits of adding CCX872-b to standard 5-fluorouracil, leucovorin, irinotecan, oxaliplatin regimens are not easily analysed. An anti-CCR2 monoclonal antibody Plozalizumab (MLN1202), which stops CCL2 binding CCR2, that reached phase-2 trials for bone metastasis has been withdrawn, although in trials for arthrosclerosis Plozalizumab did appear to reduce C-reactive protein levels, a marker for inflammation [97].

### ***1.13: Tumorigenic signalling complexities, CXCL9, CXCL10, CXCL11 and CXCL12.***

CXCL9, CXCL10 and CXCL11 chemotaxis and signalling through CXCR3 can be key in orchestrating anti-tumour immune responses such T<sub>H</sub>1 T-cell polarisation, the recruitment of cytotoxic T-cells, NK cells and IFN $\gamma$  production [98]. However these chemokines can also support metastasis and cell proliferation [99]. This converse situation illustrates the difficulty of designing effective immunotherapies. Immune cell chemotaxis is dependent on chemokine gradient and chemokine receptor expression but also on other modulators present *in vivo* for example CXCL9, CXCL10 and CXCL11 expression by monocytes and malignant cells is upregulated by cytokines such as TNF $\gamma$ , and Tumour necrosis factor alpha (TNF $\alpha$ ) [100, 101]. Additionally there are the CXCR3-A and CXCR3-B receptor subtypes whose responses differ [49] as well as factors such as CXCL9, CXCL10 and CXCL11 acting as antagonists to CXCR3 which itself stimulates T<sub>H</sub>2 polarization [102].

CXCL12 can work synergistically with VEGF to produce angiogenesis to support tumours [60]. CXCL12 supports malignant cell survival and proliferation [103], plus CXCL12-CXCR4 signalling promotes metastasis, invasion of cancer cells [104] and possibly radiation resistance [105]. When CXCL12 binds CXCR7, the receptor may act as a scavenger [106] but CXCL12-CXCR7 may also signal in malignant and associated endothelial cells via non-G-protein pathways e.g. CXCR7 is reportedly able to signal via ERK1/2 and p38 MAPK-kinase, G $_{\alpha i}$ -independently in Jurkat [107], and via JAK2/STAT3 upregulating  $\beta$ - and N-cadherin [108].  $\beta$ -catenin is involved in transcription, and along with N-cadherin, in cell-cell adhesion and migration.  $\beta$ -catenin expression and signalling can be upregulated in cancers and is reported to suppress chemokine expression and so the attraction and activation of effector T-cells.  $\beta$ -catenin signalling is tumorigenic, as it supports EMT and changes in cancer cells to a stem-cell-like phenotype [109].

Conversely CXCR7 signalling in astrocytes is reported to involve pertussis toxin sensitive G $_{\alpha i/o}$  G-proteins, and stimulate ERK1/2 and Akt via  $\beta$ -arrestin-2 triggered internalisation [110, 111].

CXCL12-CXCR7 signalling may support angiogenesis by increasing VEGF levels [112]. Inhibiting CXCR7 can inhibit T-cell chemotaxis [106]. CXCR7 expressed in malignant cells may increase survival, growth, adhesion and invasion of breast [113], prostate [114], and lung cancer cells [115] although CXCR7 expression may also aid lung repair after insult [116]. MCF7 breast cancer cells have been shown to express CXCR4, and at lower levels CXCR7. Knocking out CXCR7 with small interfering RNAs (siRNA) modestly reduced proliferation in MCF7, but no further inhibition of proliferation was observed if both CXCR4 and CXCR7 were depleted with siRNAs, suggesting proliferation in this cell-line involves CXCR4-CXCR7 dimerization. Interestingly MCF7 were found to strongly express both CXCL12 and CXCL11 [117]. The generally observed upregulation of CXCR7 in cancer cells compared to healthy cells may be a disease response aimed at repair.

#### ***1.14: Oncogenic and epigenetic influences on chemokines***

DNA methylation of genes can modulate the expression of chemokines such as CXCL9 and CXCL10 in malignant cells, and so influence the trafficking of cytotoxic and NK cells into cancerous tissues that may be critically important for the success of some immunotherapies such as PD-L1 inhibitors [118]. These are immune checkpoint inhibitors; they facilitate the immune system attacking the cancer cells but leaving healthy tissue alone. PD-1 is a checkpoint protein on T-cells; cancer cells can carry PD-L1, a protein which when it binds PD-1 stops the T-cells attacking and destroying them. Monoclonal antibodies that bind either PD-1 or PD-L1 block the interaction and the T-cells remain able to attack and destroy the cancer cells. Examples of PD-L1 monoclonal antibodies include Pembrolizumab and Nivolumab [119]. Drugs aiming to reprogram epigenetic signatures may restore chemokine expression and so also T-cell movement into tumours [118].

CXCR4 in malignant cells carrying a point mutation, making the receptor functionally active, showed increased signalling and chemotaxis to CXCL12, but conversely the mutation slowed tumour growth. Inhibition of this mutated CXCR4 with AMD3100, a small molecule CXCR4 antagonist, reversed this slowdown but only *in vitro* not *in vivo* [120]; chemokine gradients may have contributed to this outcome. Other genetic mutations can also increase CXCR4 expression, for example, in rhabdomyosarcoma fusion of PAX3 and FKHR genes occurs, which increases the cancer cells' invasiveness [121]. Hypoxia is a common feature in central zones of solid tumours, and it can stimulate CXCL12 [122] and CCL2 expression [123]. Transcription factors such as Hypoxia-Inducible Factor 1 (HIF1) mediate malignant cell responses to hypoxia [124]. HIF1 may bind the promoter region of CXCL12 gene-inducing translation of CXCL12 mRNA. Hypoxia can also stimulate both malignant cells and TAMs to express CXCR4 [125, 126] and inhibit expression of

CXCR7 [127]. Blocking CXCL12-CXCR4 signalling may be therapeutic in cancers as the signalling supports cell proliferation, invasiveness, angiogenesis and metastasis [128, 129].

### 1.15: Chemokine receptor CXCR4 and metastasis

CXCL12/CXCR4 aberrant signalling is heavily implicated in cancer, tumour angiogenesis and the survival and metastasis of malignant cells [130, 131]. The expression of CXCR4 is reportedly upregulated in many malignancies [132]. However CXCR4 can also be essential to maintain health. For example in B-cells CXCR4 expression facilitates immune responses to infection and autoimmune diseases [133]. Somatic homeostasis may also involve immune modulation by the sympathetic nervous system, for example adrenaline stimulation of  $\beta_2$ -adrenergic receptors may, through interaction with CCR7 and CXCR4 receptors, cause retention of lymphocytes in lymph nodes, resulting in reduced peripheral tissue concentrations of antigen-carrying T-cells in inflammatory diseases [134]. CXCR4 is therefore an attractive target for therapeutic manipulation. Blocking CXCR4/CXCL12 signalling with small molecule inhibitors has been shown to inhibit metastasis [135]. A simplification of the complex signalling through the CXCL12/CXCR4 axis in metastasis is illustrated in figure 1.4.

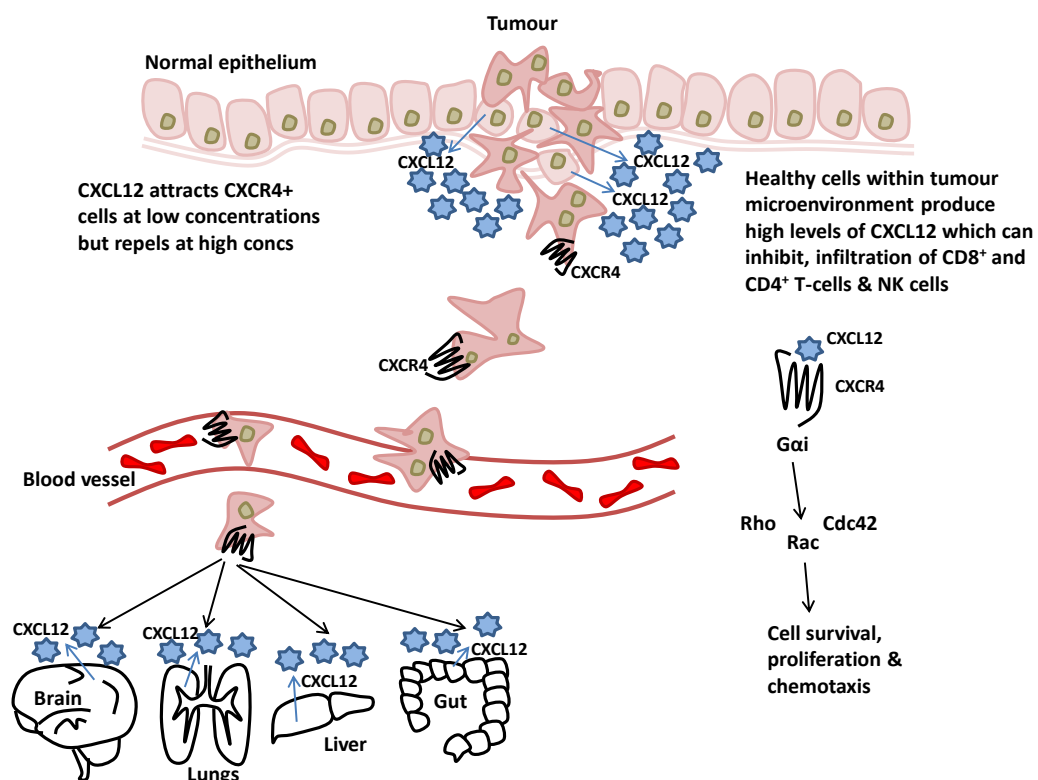


Figure 1.4: CXCR4/CXCL12 signalling supports tumour cell spread from primary to secondary locations [136-140].

### 1.15.1: Structure of CXCR4 and its interactions with CXCL12

The CXCR4/CXCL12 axis influences so many complex physiological activities that the simple interaction of CXCL12 with CXCR4 would offer insufficient specificity. It is known that the cell context, along with both CXCR4 oligmerization and CXCL12 oligmerization, adds levels of control [141, 142]. CXCR4 is a class A GPCR [143]. Dimerization of CXCR4 has been shown by investigations of crystal structures with small antagonists, fluorescence resonance energy transfer, bioluminescence and other techniques to be key in functional selectivity, and in the gain of function of mutated CXCR4 in cancers and WHIM syndrome where there are heterozygous mutations of CXCR4 [144]. Recent research and crystal structures suggests that CXCR4 may interact with CXCL12 in 1:1, 2:2 or 2:1 CXCR4: CXCL12 ratios [145, 146].

GPCRs have seven transmembrane helices which in CXCR4 are arranged in a goblet shape in such a way that two sub-pockets capable of accommodating ligands are available. These are known as the major pocket formed by helices 3, 4, 5, 6 and 7, and the minor pocket formed by helices 1, 2, 3 and 7 [147]. The G-protein binding site lies in the centre of the helices on the cytosolic side, figure 1.5.

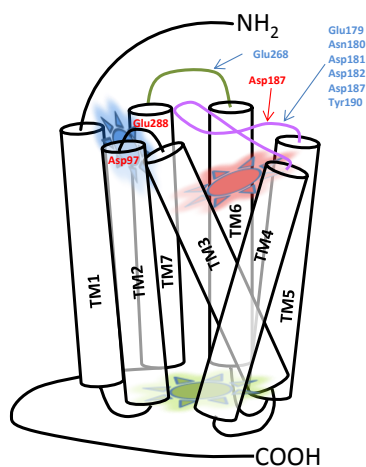


Figure 1.5: Basic goblet structure of the CXCR4 receptor. Major pocket - red star, minor pocket - blue star, G-protein binding site - green star, transmembrane domains (TM) - black, extracellular loop 2 (ECL2) - purple, ECL3 - green. Residues thought essential for CXCL12 binding - red, and for CXCL12 activation - blue [147-153].

Chemokine receptor activation may follow the chemokine binding to the N-terminal, major and minor pockets, triggering receptor conformation change and activation precipitating the binding of a G-protein to the intracellular site. Research on CXCR4 suggest the major and minor pockets are connected [147]. These pockets have been analysed using ligand structure activity and mutagenesis studies which allow their mapping. It has been found some CXCR4 ligands such as AMD3100 and AMD11070, figure 1.6, bind the major and minor pockets and their interface [147, 149].





Figure 1.6: Structures of CXCR4 inhibitors AMD3100 and AMD11070

Chemokine receptors, including CXCR4, differ from other class A GPCRs in the position of their helix bundle, extracellular, and ligand binding domains. Various standard sequences found in other GPCRs in specific locations, and the generic numbering system developed for GPCRs (which relies on conserved motifs and sequences e.g. DRY in transmembrane helix 3 (TM3)) does not translate completely to chemokine GPCRs [145, 154, 155].

CXCL12 itself may function differently when in monomeric or dimeric form. CXCL12 acts as a partial agonist incapable of inducing chemotaxis when dimeric, but still able to induce intracellular calcium flux [156-158]. Several residues are thought essential for CXCL12 binding, namely Asp97 in TM2, Asp187 in extracellular loop 2 (ECL2) and Glu288 in TM7. Others, such as Glu179 to Asp182, Asp187 and Tyr190 in ECL2, and Glu268 in ECL3 and Glu288 are thought important for CXCR4 signalling [150-153].

Research has employed NMR as well as site-directed mutagenesis studies. NMR studies show the first eight residues of CXCL12 N-terminus contain two amino acids that are essential for CXCR4 activation, namely Lys1 and Pro2 which may interact with CXCR4's Asp187 (ECL2) and Glu288 (TM7). Investigations so far have led to the theory that CXCL12 interacts with CXCR4 in a two-step process. Firstly the CXCL12 motif between amino acids 12 and 17, 'RFFESH' (Arg-Phe-Phe-Glu-Ser-His), binds CXCR4's N-terminus followed by CXCL12's N-terminus between amino acids 1 and 8. This locates into a transmembrane helix of CXCR4 triggering conformation change and activation [146, 150-153, 158-162]. Put together the extensive research completed supports the importance of the purported minor and major sub-pockets located in CXCR4's transmembrane cavities for CXCL12 binding. With the minor pocket formed by helices one, two, three, and seven [147], where ECL2's residues Glu179, Asp187, Tyr190 and Asp193, plus ECL3's Glu268 along with Trp94 and Asp97 (both in TM2) are key. The major pocket is surrounded by helices three, four, five, six and seven, with Asp171 (TM4), Tyr255 and Asp262 (both in TM6) being important. Also considered to contribute are Tyr116 (TM3) and Glu288 (TM7) which sit at the edge of the major and minor sub-pockets. The CXCL12 N-terminal Lys1 and Pro2 are thought to sit in CXCR4's minor sub-pocket in contact with Asp97 (TM2), Asp187 (ECL2) and Glu288 (TM7), three key activation residues, figure 1.7. What has also been explored is how one CXCL12 protomer could successfully bind a CXCR4 dimer. It is suggested that CXCL12's Lys1 and Pro2 could continue to occupy one CXCR4's minor

sub-pocket and still be in contact with activators Asp97 (TM2), Asp187 (ECL2) plus Glu288 (TM7) in a CXCR4 dimer. CXCL12 may remain longer in contact with a CXCR4 homodimer than a CXCR4 monomer, and also be in contact for longer when CXCL12: CXCR4 stoichiometry is 1:2 than would occur with 1:1 [147, 148].

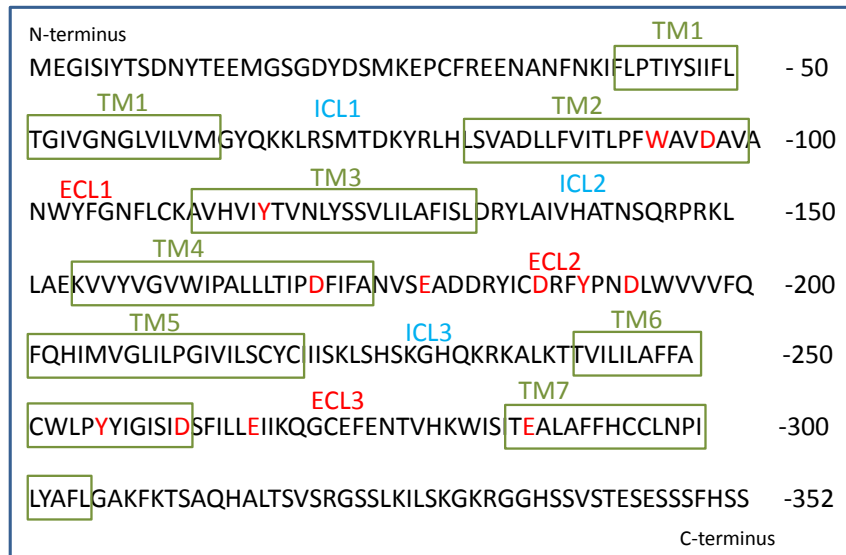


Figure 1.7: CXCR4 sequence with key binding residues for CXCL12 in red, TM = transmembrane region, ICL = intracellular loop, ECL = extracellular loop.

Having briefly explored the role of chemokines, chemokine receptors and the immune system in metastatic signalling, next key individual proteins will be introduced that are involved in transferring the message from an activated chemokine receptor onwards into a cell.

### 1.16: Introduction to Dynamin and Dynamin Like Proteins (DLPs)

For a receptor to internalise an endocytic vesicle needs to form from the cell membrane. This requires the recruitment of several cytosolic proteins including the GTPase dynamin. Dynamin is purported to aid the scission of vesicles from the membrane by forming helical oligomers around the necks of budding vesicles, before GTP hydrolysis creates conformational change in the dynamin polymer producing vesicle/membrane fission. However this is not dynamin's only role in cellular function [163, 164]. Dynamins are also involved in cytokinesis, organelle division, pathogen resistance and transport vesicle budding [165].

There are three dynamin mammalian genes producing at least twenty-five distinct splice forms of dynamin: eight variants of dynamin-1, mainly found in neurons; four variants of dynamin-2 which is ubiquitous; and thirteen variants of dynamin-3 mainly found in brain and testis [166],

suggesting varying specialist roles for dynamin throughout the body. Different isoforms can uniquely interact with specific proteins, for example dynamin-1 is found in presynaptic neuronal tissue and is involved with axon growth, whereas dynamin-3 is found in dendritic spines where it purportedly mediates remodelling [167, 168]. The main differences in dynamin-1, -2 and -3 are in the last 150 residues in the C-terminus proline-rich domain. Dynamin isoforms interact with various proteins and lipids with varying affinities and oligomerizability producing tissue-specific regulation [169].

Dynamin-1, -2, and -3 are members of the DLPs membrane remodelling GTPase family. Other DLP members include Dynamin-related protein-1 (Drp-1) and mitofusin (Mfn) both found in mitochondrial outer membranes. Drp-1 is involved in mitochondrial fission, whereas Mfn mediates mitochondrial fusion along with a DLP called Optic Atrophy-1 (OPA-1) found in mitochondrial inner membrane [170], figure 1.8.

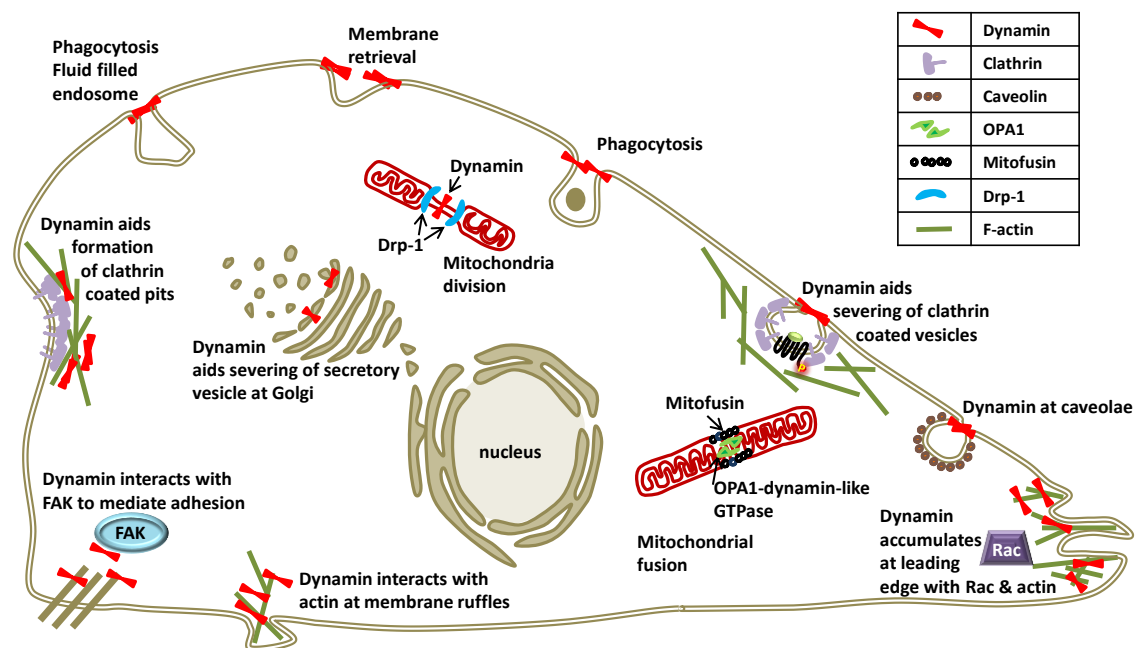


Figure 1.8: Dynamics of dynamin and dynamin-like proteins (DLPs) in a migrating cell [163, 170, 171].

### 1.16.1: Dynamin family proteins structure and domains

The dynamin monomers reside in the cytosol. Dynamin structural regions from the N-terminal consist of a G-domain, a stalk region, a Pleckstrin Homology (PH) domain, a GTPase Effector Domain (GED), and at the C-terminal a Proline-Rich Domain (PRD), figures 3.3 and 3.4. Phospholipids binding dynamin's PH domain can stimulate its activity, and dynamin's GTPase activity can be stimulated by oligomerization of the protein via interactions of GTPase domains,

the middle domains, and the GEDs. Stimulation also follows binding of SH3-domain proteins to dynamin's PRD [165]. Crystallographic studies show dynamin can form hairpin-like dimers, with the PH and GTPase domains sitting either side of a pocket, and juxtaposed BSE (stalks) interacting in a criss-cross arrangement. The PRDs do not appear in the crystal structure as they project out of the polymerized helix, figures 1.9 and 1.10.

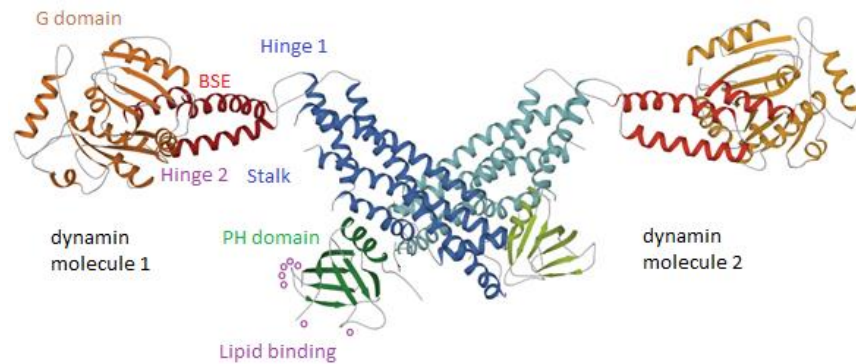


Figure 1.9: Regions of the crystal structure of a dynamin dimer [172, 173].

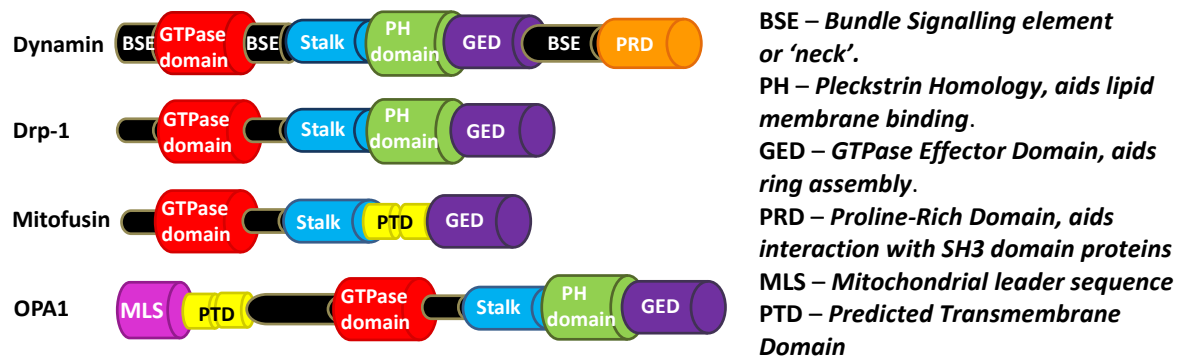


Figure 1.10: Structural elements of Dynamin and Dynamin-Like Proteins (DLPs) [163, 165].

### 1.16.2: Dynamin polymerization

Dynamin monomers form dimers, the basic unit, through interactions of the stalk regions, [174] then dimers themselves interact, forming oligomers. Different oligomeric rings of dynamin can link through the G-domains [175]. The PH domains, “the feet”, bind lipid membranes positioning the PRD region facing the cytosol, so ideally placed to interact with other proteins. The PH domain has affinity for acidic membrane phospholipids such as phosphatidylinositol-4,5-bisphosphate (PtdIns(4,5)P<sub>2</sub>) aka PIP<sub>2</sub> [176]. Curvature of the membrane itself may attract dynamin [177]. Antagonising the PH domain is known to impair clathrin-mediated endocytosis [178]. There are also hydrophobic (lipid binding) loops protruding from the PH domain, figure 3.2, which may promote curvature of the oligomer and membrane interactions [179]. The PRD domain strongly supports dynamin's interaction and co-ordination with SH3-motifs in other proteins, helps to draw dynamin to endocytic locations, and co-ordinate endocytosis [180].

### 1.16.3: Membrane fission

Dynamin's mode of membrane fission has been extensively investigated over many years [177, 181, 182] and there is consensus that dynamin can, in the presence of GTP, constrict or twist membranes facilitating fission. The oligomer must circle the membrane tube and connects with itself via the G-domains, as GTPase activity depends on G-domain dimerization. G-domain dimer GTP hydrolysis then produces a lever-like movement of dynamin's BSE domains which propagates along the dynamin subunits, thus narrowing the dynamin helix diameter constricting the membrane tube [183], figure 1.11.

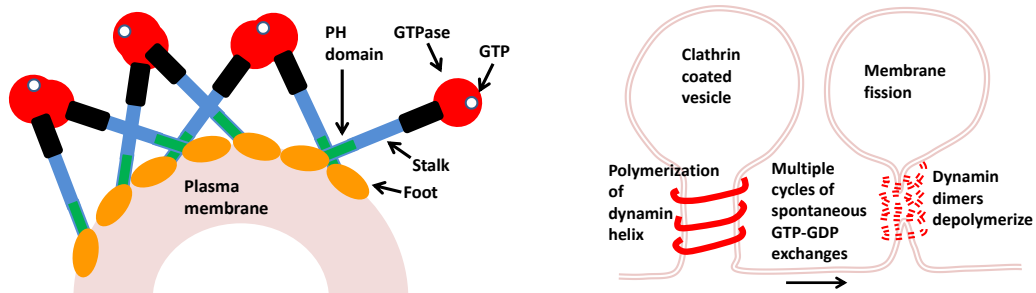


Figure 1.11: Mechanism of dynamin-mediated vesicle and membrane fission [163, 183].

Fission is thought not to occur solely due to shearing or tearing as tube radius decrease occurs too slowly [184]. Helix disassembly may trigger membrane destabilisation and fission [185], although this is still debated [184]. Other DLPs share some of dynamin's structural features and mode of action [186, 187]. Membrane severing can *in vitro* be achieved by dynamin alone, *in vivo* this may also involve other proteins and processes, such as actin polymerization or myosin providing membrane tension thus supporting membrane fission [188].

Dynamins catalyse scission but also may modulate clathrin-coated pit maturation. Over expressing dynamin-1 mutants, with GTPase domains inactivated, was found to accelerate clathrin-mediated endocytosis; how is not clear [189]. Dynamin-1 can alone curve membranes and catalyse fission. Dynamin-2 cannot shape membranes alone, it appears to need other curve-generating proteins to produce fission [190]. Dynamin-1 and dynamin-2 mRNA are equally present in non-neuronal tissues, however dynamin-1 may be phosphorylated and so inactivated by GSK3 $\beta$  which itself is constitutively active [191]. Inhibiting GSK3 $\beta$  can activate both dynamin-1 and clathrin-mediated endocytosis [192].

### 1.16.4: Endocytosis plays a key role in regulation of intracellular signalling

Endocytosis involves the inward budding of vesicles from the plasma membrane. Endocytosis allows the passage of components between cellular compartments but also mediates cellular signalling [193]. Vesicle cargo can include GPCRs with bound ligands. Endocytosis of the receptor can terminate signalling [194] or initiate signalling cascades from endosome complexes.

Endosomes can be classified as early, recycling or late endosomes. The pathway followed by endocytic vesicles and their intracellular fate can qualitatively and quantitatively control downstream signalling and hence cellular responses [193, 195]. This signalling can reciprocally also regulate both further receptor endocytosis, and the endocytic pathways followed by subsequent endocytic vesicles [196, 197]. This crosstalk can mediate cancer prognosis by modulating migratory, proliferative and survival signals supporting metastasis [198].

#### ***1.16.5: Influences of cargo on endosome fate***

Signalling from endosomes has been shown to influence post-uptake sorting decisions, between recycling to the membrane and degradation pathways [199]. Coated pits reportedly may themselves trigger signalling pathways e.g. through JAK2 and Akt [200], and even surviving flat clathrin lattices may act as signalling platforms [201], as do caveolar micro-domains which can support catabolic oxidative mitochondrial metabolism and cell signalling effects favouring malignancy [202]. Endosomes may contain signalling platforms that trigger Grb2-mSOS-Ras signalling [203] and determine signal strength and specificity [204]. For example endosomes containing APPL1 scaffolding protein can signal from Akt to GSK3 $\beta$ , whereas Akt signalling from the plasma membrane can follow the mTOR pathway [205].

#### ***1.16.6: Dynamin, $\beta$ -arrestins and the Rho GTPases***

When GPCRs signal through trimeric G-proteins the stimulated G-protein is inactivated by GPCR kinases,  $\beta$ -arrestin recruitment may follow [206].  $\beta$ -arrestins can also act as adaptors linking G-proteins to clathrin-coated pits and clathrin-mediated endocytosis. However, MAPK pathway signalling may continue from early endosomes via  $\beta$ -arrestins acting as scaffolds, or from GPCR/arrestin complexes [207, 208]. This secondary signalling may vary in specificity and strength from the original issuing from the GPCR/ligand at the plasma membrane [209], and be controlled by GPCR type. GPCRs may use PDZ-domain/s to interact with the actin cytoskeletal components and delay clathrin coated pit maturation and dynamin recruitment and/or receptor ubiquitination [197, 210]. This appears relevant for CXCR4 [211], and for CCR5 signalling as both receptors contain a C-terminus PDZ-binding sequence [212]. Endocytosis can be modulated by Ras and Rho GTPases. Rho GTPases support actin-dependent clathrin-independent endocytosis [209], but Rac and Rho activation may actin-independently inhibit clathrin-mediated endocytosis [213].

#### ***1.16.7: Dynamin's role in Clathrin-dependent endocytosis***

Clathrin-mediated endocytosis is one of several endocytic pathways [214]. It requires Adaptor Protein Complex-2 (AP2) to recruit clathrin proteins to the plasma membrane [215]. Supported by other endocytic assessor proteins a clathrin-coated pit develops around its cargo until it has formed a narrow neck connecting it to the plasma membrane. This neck triggers recruitment and

assembly of dynamin which triggers scission [216]. The endocytic vesicle may then fuse with others containing similar or different cargoes. These are early phosphatidylinositol-3-phosphate (PI3P) rich endosomes, which carry interacting scaffold proteins such as EEA1 or APPL1 that mediate endosome maturation and sort endosomes into three possible pathways [217]. Receptor cargoes can be (i) rapidly recycled back to the plasma membrane, (ii) slowly recycled to the membrane via perinuclear recycling endosomes or (iii) retained, ubiquitinated and degraded when endosomes fuse with lysosomes, this terminates signalling and down-regulates receptors [171].

Clathrin-dependent endocytosis is important in signalling from many receptors. It appears involved in the building of multi-protein clathrin-containing pits which enable surface receptors and their ligand to be internalised [218]. Dynamin may help modulate cell signalling by regulating receptor endocytosis, so clearance of receptors from the cell surface, and the formation of signal transduction complexes in endosomes [195, 219].

#### ***1.16.8: Dynamin's role in clathrin-independent endocytosis***

The endocytic protein endophilin-A recruits dynamin [220] and may play a subsidiary role in clathrin-mediated endocytosis, as may cofilin, a small protein controlling actin polymerization [188]. Endophilin-A also controls a clathrin-independent endocytic pathway, it carries an SH3-domain that strongly binds proline-rich motifs in some GPCRs, and is involved in some receptor-ligand stimulated endocytosis. Endophilin-A, but not clathrin, is found at the leading edge in some cells undergoing chemotaxis, whereas in non-migrating cells endophilin-A and clathrin-coated pits are equally present. Endophilin-A, F-actin and dynamin are all in plentiful supply at the leading edge of cells, and all participate in rapid  $\beta$ -arrestin-independent formation of clathrin-independent endophilin-A assemblies which facilitate receptor endocytosis, following GPCR stimulation [221]. Endophilin-A may interact with dynamin to produce the pulling-force needed for scission [222]. Such endophilin-A-rich endocytic vesicles then can be tracked from the membrane to perinuclear area. Growth factors can also facilitate this rapid endophilin-A-mediated endocytosis, or hinder it if absent. Fast endophilin-A-mediated endocytosis appears important in chemotaxis, and may also play a role in Raf, MEK, ERK (MAPK) and growth factor signalling, which produces chemotaxis. Although not affected by clathrin-knockdown or inhibition, endophilin-A-mediated endocytosis is hampered by dynamin knockdown or mutation (K44A dominant negative mutant), or dynamin inhibition using Dyngo4a, Dynasore, MitMAB and OctMAB. Endophilin-A-mediated budding and endocytosis is also inhibited by the inhibition of actin polymerization, Pi3K, Rho or Rac, whereas inhibiting Cdc42 increased endophilin-A-rich

vesicle formation. Overall endophilin-A-mediated endocytosis appears dependent on dynamin, actin, cholesterol, Rac, Rho, Pi3K and PAK1 [221].

Receptor-ligand binding may stimulate Pi3K to produce phosphatidylinositol(3,4,5)-triphosphate (aka  $\text{PtdIns}(3,4,5)\text{P}_3$  and  $\text{PIP}_3$ ) from  $\text{PtdIns}(4,5)\text{P}_2$  (aka  $\text{PIP}_2$ ).  $\text{PIP}_3$  is plentiful at a cell's leading edge. Once produced  $\text{PIP}_3$  is hydrolysed back to  $\text{PIP}_2$  by phosphatase PTEN [223]. PTEN inhibition increases leading edge endophilin-A levels, this is Pi3K-dependent. SHIP1 and SHIP2 hydrolyse  $\text{PIP}_3$  to  $\text{PtdIns}(3,4)\text{P}_2$  [224], this reduces leading edge endophilin-A levels. A  $\text{PtdIns}(3,4)\text{P}_2$ -binding protein lamellipodin binds endophilin-A at the leading edge, triggering fast endophilin-A-mediated endocytosis [225], figure 1.12.

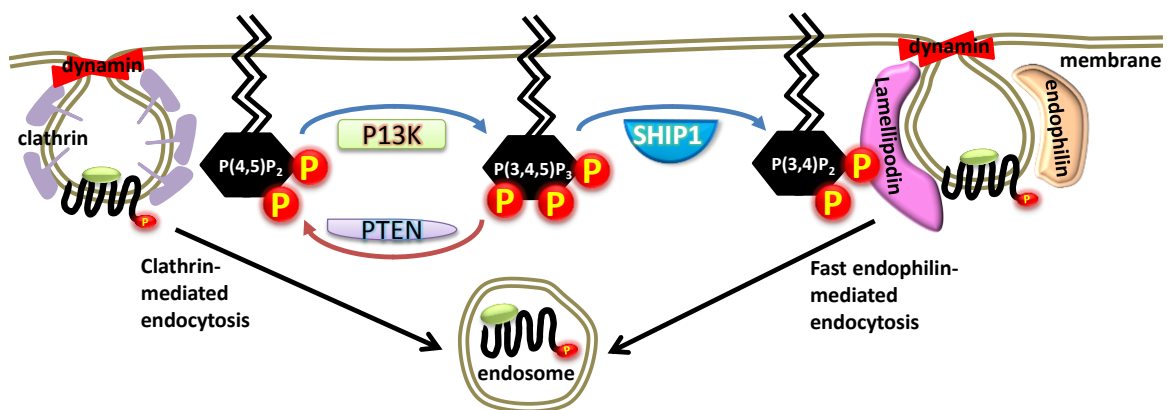


Figure 1.12: Dynamin contributes to both clathrin-dependent and endophilin-mediated endocytosis. Endophilin controls a leading edge fast-acting clathrin-independent pathway dependent on dynamin, Rac and actin that facilitated endocytosis of some GPCRs. SHIP1 dephosphorylates  $\text{P}(3,4,5)\text{P}_3$  forming  $\text{P}(3,4)\text{P}_2$ , SHIP2 recruits lamellipodin which summons endophilin [221, 223, 225].

#### 1.16.9: Dynamin and DLPs in disease

Aberrant dynamin and DLP's function has been linked to many diseases including cancer. Dynamin has been found to be upregulated in malignant cells, and to support increased cell migration *in vitro* and metastasis *in vivo* [226]. Dynamin interacts with microtubules and focal adhesion kinase to modulate cell migration [227], while also affecting lamellipodia formation [228]. Dynamin does this through interaction with a GTPase, Rac1's guanine exchange factor (GEF) Vav1. Vav1 along with other GEFs activates Rac1 [229]. Rac1 then regulates actin dynamics including the branching important in lamellipodia formation [230]. In T-cells dynamin-2 was shown to directly interact with Vav1 [231]. Vav1 is an oncogene expressed in many cancers [232, 233]. CXCL12 can activate JAK-Vav-Rac1 signalling in melanoma cells which then supports metastasis [234]. However in the



absence of active dynamin Vav1 interacts instead with Hsc70 chaperone protein which directs Vav1 to lysosomes for degradation [229].

Mutations in DLP Drp-1 has been found to drive mitosis in twenty-nine different cancer types and to modulate chemotherapy sensitivity of primary tumours. Relapse in ovarian cancers treated with platinum-based chemotherapy has been linked to Drp-1/mitochondrial-driven mitosis [235]. Inhibition of Drp-1 has been shown to reduce migration and invasion of thyroid cancer cells [236].

#### **1.16.10: Dynamin in cancer development and progression**

Cancer features unregulated cell proliferation, migration and endocytosis; signalling controls these factors and the survival of cancer cells. Endosomal signalling can enhance metastasis e.g. aberrant sorting decisions favouring endosome recycling over degradation for proliferative signalling cargoes [199].

Mutations and loss of proteins that ubiquitinate receptors in endosomes can change the fate of oncogenic receptors directed to lysosomes, causing them to be recycled back to the plasma membrane and prolong signalling. If this signalling supports cell proliferation and/or migration it can favour cancer and metastasis. Scaffolding proteins, cargo and dynamin can all influence the fate of the endosome [194, 198]. Mechanisms include upregulation of dynamin which can by increasing clathrin-coated pit initiation and maturation support aberrant clathrin mediated endocytosis [192].

Proliferative signalling can be produced by the Pi3K/PIP<sub>2</sub>/PIP<sub>3</sub>/Akt/mTOR pathway. PTEN tumour suppressor inhibits the PIP<sub>2</sub> to PIP<sub>3</sub> step, whereas Akt inhibits constitutively active GSK3 $\beta$  which when active suppresses dynamin-1. Overactive dynamin-1 enhances clathrin-coated pit initiation and clathrin-mediated endocytosis. Akt-GSK3 $\beta$  signalling is upregulated in endosomes with APPL1 scaffolds [192]. Activated dynamin-1 appears to support APPL1 endosome production and Akt signalling [196]. Akt inhibitors can be shown to dynamin-1-dependently inhibit clathrin-mediated endocytosis [192]. Dynamin-1 is controlled by phosphorylation so its activity and expression do not necessarily correlate. The calcium-dependent phosphatase calcineurin can dephosphorylate and so activate dynamin-1 [171]. Thus dynamin recruitment can regulate the initiation and maintenance of clathrin-coated pits, and increase endocytic activity which itself may correlate with metastatic potential.

#### **1.16.11: Drp-1, mitochondrial division and cancer**

Mitochondrial fusion is aided by the DLP Mfn isoforms Mfn1 and Mfn2 along with OPA1 [237], which create links between fusing mitochondria. Mfn2 also aids mitochondrial-Endoplasmic Reticulum (ER) linkage facilitating mitochondrial calcium uptake [238].

Mitochondria undergo division and fusion, governed by genes in the cell nucleus [239]. Disorders of mitochondrial dynamics can contribute to the pathology of cancer, since mitochondrial fission and fusion fine-tunes cell-cycle progression, majorly influencing ATP production, reactive oxygen species production, oxygen sensitivity and apoptosis [240]. Mitochondria associate with the ER facilitating localised peaks in calcium signalling [241], which can trigger apoptosis [242]. Calmodulin-dependent kinase links the phosphorylation of Drp-1 to calcium levels [243]. Defective mitochondria are disposed of by enclosing in autophagic vacuoles which then merge with lysosomes in a process called mitophagy [244]. Mitophagy is more efficient with smaller organelles created by mitochondria fission. Smaller mitochondria also more efficiently accelerate cell proliferation. Fission is facilitated by Drp-1 [245]. Drp-1 monomers co-operate, creating a ring-like structure which constricts and divides the mitochondrion [246].

In cancer there is excess proliferation along with apoptosis resistance. Respiration shifts from oxidative metabolism to aerobic glycolysis, this is called the 'Warburg Effect'. Mitochondrial pyruvate dehydrogenase kinase activation contributes to this by suppressing oxidative metabolism and inhibiting pyruvate dehydrogenase making the cell less susceptible to apoptosis [247, 248]. ATP production and mitochondrial division is needed before mitosis, these processes are co-ordinated as the cell cycles from stage G<sub>1</sub> to S. Drp-1 inhibition triggers mitochondrial hyperfusion into larger mitochondria, which facilitates increased ATP production [249]. DNA replication then occurs and cyclin E accumulates. Cyclin B1- cyclin-dependent kinase 1 (CDK1) initiates mitosis and activates Drp-1 via phosphorylation of its Ser<sup>616</sup>, this triggers mitochondria fission facilitating cell division [250]. Drp-1 is controlled by various kinases. Drp-1 activity, so mitochondrial replication, is increased by phosphorylation at Ser<sup>616</sup>, and decreased by phosphorylation of Drp-1 Ser<sup>637</sup> [251], figure 1.13.

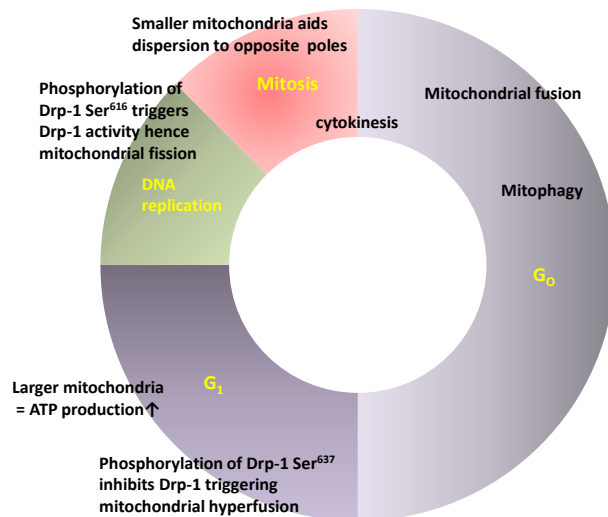


Figure 1.13: Drp-1 influences mitochondria fission/fusion dynamics during the cell cycle [249, 252].

Drp-1 inhibition can inhibit tumour growth, increasing spontaneous apoptosis and decreasing cell proliferation and metastasis [252, 253] and change cell morphology to a more rounded shape unsuited to migration [254].

Once initiated the signalling from a chemokine receptor is transmitted through various membrane and cytosolic proteins. A key protein often involved in this signal transduction is Protein Kinase C.

### 1.17: Protein Kinase C (PKC)

Homeostatic PKC signalling is exquisitely complex and in cancer this complexity increases. PKC responses can be modulated by chemokines. Differences in distribution of PKC isoforms in normal and malignant leukocytes have been reported [255, 256], hence PKC assays using cancer cell-lines may produce differing results to those in non-malignant cells.

Activating PKCs can protect against induced lung metastasis and reduce tumour growth (in mice) [257] and produce temporary remission from leukaemia in humans [258]. Hence in human cancers PKCs can act as tumour suppressors, however they can also act as oncogenes [259, 260]

#### 1.17.1: PKC structure, isoforms, location and function

PKC is transcribed from nine PKC genes producing twelve isoforms as some genes produce splice variants. All isoforms contain a C-terminal kinase and a variable N-terminal auto-inhibitory regulatory domain that determines both the PKC subfamily, and through interactions with its respective C-terminal kinase moiety, if the protein is active or not [261]. PKC isoforms are classified as conventional (isoforms  $\alpha$ ,  $\beta$ , and  $\gamma$ ), novel ( $\delta$ ,  $\epsilon$ ,  $\eta$ , and  $\theta$ ) and atypical ( $\zeta$  and  $\iota$ ), figure 1.14. PKC enzymes contain a catalytic C-terminal ATP binding domain, and a regulatory unit that keeps PKC inactive until triggered and controls its subcellular location.

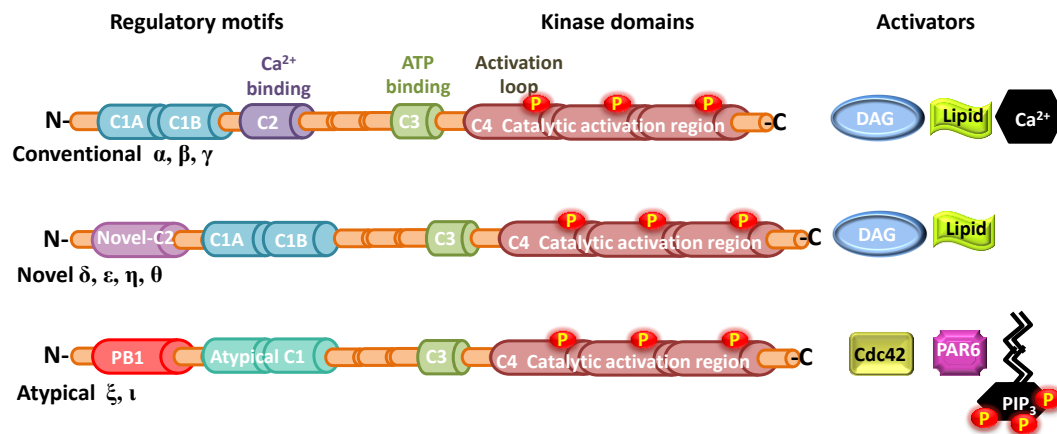


Figure 1.14: PKC isoenzymes, domains and activators [261, 262].

Diacylglycerol (DAG) can activate conventional and novel, but not atypical PKC isoforms. DAG is a lipid metabolism intermediate, its level in cells is modulated by PLC activation [263]. Conventional PKCs all have a C2 domain that calcium dependently binds phospholipids along with two cysteine-rich zinc finger regions C1a and C1b at the amino-terminus. Conventional PKCs remain in the cytosol until activated by the activation of DAG; they then translocate to the membrane to bind DAG [264].

Novel PKCs also have C1 and C2 domains but with the C2 nearest the N-terminus, and their C2 region lacks calcium binding regions so membrane translocation is not controlled by calcium or phospholipids but occurs just as efficiently as with conventional PKCs as their affinity for DAG is greater [265, 266].

Atypical PKC's activation is independent of DAG and calcium, their C1 domain is activated by  $\text{PIP}_3$  [267] or ceramide [268, 269]. Also they also have a PB1 motif at their N-terminal which reacts with other PB1 containing proteins and 3-phosphoinositide-dependent protein kinase 1 (PDK1) [270, 271]. Partition Defective Protein (PAR)-6 and  $\text{PKC}\zeta$  interact through their PB1 domains [272], PAR6 links  $\text{PKC}\zeta$  to Rho GTPases Rac1 and Cdc42 involved in Ras oncogenic transformation and cell polarity [273, 274].

### 1.17.2: PKC's phosphorylation of chemokine receptors

GPCR phosphorylation is a complex process involving many kinases. There is considerable redundancy with several kinases each able to phosphorylate several, usually C-terminal, sites. CXCL12/CXCR4 activation is no exception and purportedly involves multiple kinases including GPCR kinases (GRKs) and PKC isoforms [275-277]. CXCR4 C-terminal has three threonines and fifteen serines. Research has demonstrated phosphorylation of seven serines following CXCR4 stimulation by GRKs and PKC [278]. Other studies support phosphorylation by PKC of CXCR4

following CXCL12 binding [279]. Also CXCL12 induced CXCR4 C-tail phosphorylation can be inhibited by GRK, PKC $\alpha$  PKC $\delta$  or PKC $\zeta$  inhibition [280].

### **1.17.3: PKC activation**

PKC resides in the cytosol until activated by agonist interaction with receptor [262]. Activation triggers conformational changes allowing PKC to interact in specific cellular locations with defined substrates, which substrate is governed by PKC C1a domain [281]. With conventional PKC $\alpha$ , PIP2 hydrolysis leads to PKC activation, firstly by calcium binding PKC $\alpha$  C2 domain facilitating interactions with membrane phospholipids and PKC $\alpha$  activation by binding DAG embedded in membrane [282, 283].

The novel PKCs including PKC $\delta$  and PKC $\epsilon$  do not bind calcium but have a greater affinity for DAG than conventional PKC's so primarily move to and signal from Golgi membranes which are richer in DAG than cell membranes [261]. Atypical PKCs including PKC $\zeta$  have a lower catalytic activity than DAG-regulated novel or conventional PKCs; atypicals bind scaffold proteins e.g. PAR6 via PB1 Domains [284, 285]. Different scaffolds produce different PKC activity levels e.g. PAR6 activates, whereas PAR3 binds atypical PKC's active site preventing substrate access and activation [286].

Scaffolding proteins can modulate PKC location and signalling. PKC N-terminal regions contain regulatory regions that produce different isoform responses to different activators [287]. PKC isoforms can be activated by the same stimulus but then be directed to different cellular locations, for example Golgi, nuclear envelope, endoplasmic reticulum or specific cytoskeletal components inside mitochondria or the nucleus [288]. At these locations various scaffolding, adaptor or targeting proteins link the PKC with their substrates so can translate the extracellular signal to specific cellular microenvironments [289]. These PKC binding proteins include actin, importins, heat shock proteins (HSP), 14-3-3 proteins, receptors for activated C-kinase (RACKs), A-kinase-anchoring protein (AKAPs) and Annexins, figure 1.15.

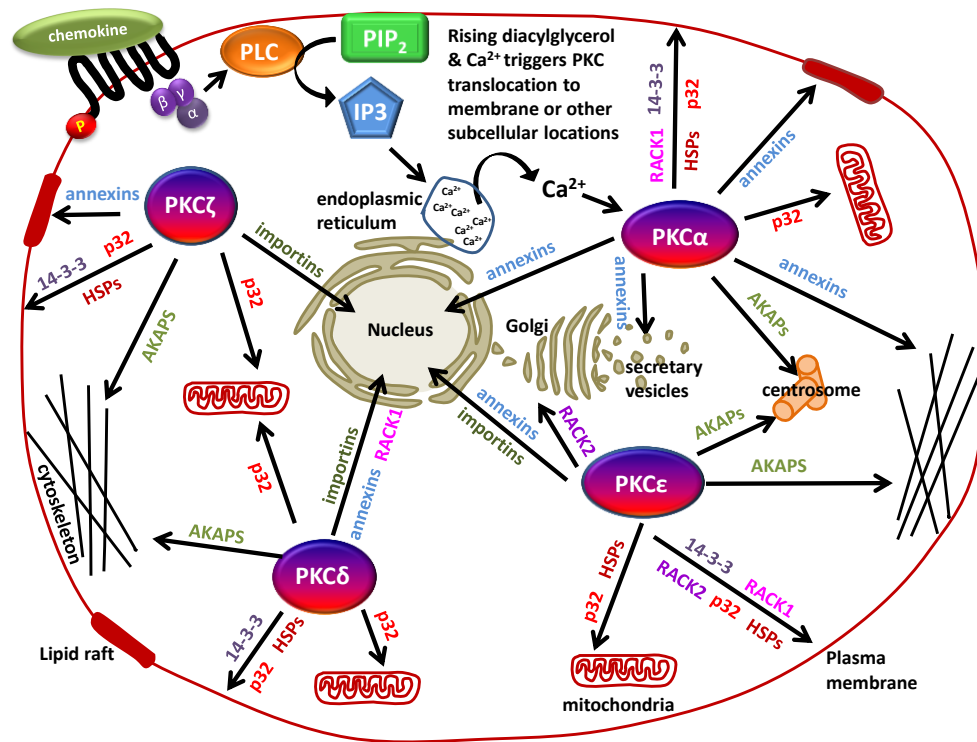


Figure 1.15: PKC isoenzymes interact with scaffolding proteins which can selectively modulate the PKCs location and signalling, for example an annexin or anchoring protein such as RACK1 can regulate recruitment of specific PKC isoenzyme to the membrane or other subcellular location where PKC may phosphorylate nearby substrates [287-289].

#### 1.17.4: PKCs role in cancers

Conventional and novel PKC inactivation is governed by metabolism and decay of DAG these PKCs then return to their auto-inhibited conformation and reside in the cytosol [290]. With atypical PKCs other PKC isoforms may be involved in their inactivation [291].

Abnormal PKC expression has been implicated in many pathophysiologies including cancers [292, 293]. However PKC is not a simple proto-oncogene, it actually supports homeostasis, but modifying PKC regulation may support malignancies [262]. This includes through Raf-1 signalling triggering Mitogen-Activation Protein Kinase (MAPK) promoted metastasis, and proliferation normally prevented by PKC regulation [294]. In cancers loss of function (LOF) or loss of normal signalling of PKC isoforms is common and gain of function (GOF) rare [261]. LOF mutations are generally heterozygous and can be dominant negative which then adversely influences global PKC signalling, i.e. one isoenzyme mutation may suppress other PKC isoenzyme signalling [259]. This may be due to common elements in PKC isoenzyme activation being sequestered by the mutated PKC e.g. PDPK1 [295]. It has been observed that PKCα has reduced function in pituitary tumours [296] and that PKCα inhibitors enzastaurin and aprinocarsen worsened outcomes when given with chemotherapy for lung cancers [297]. PKC signalling can suppress oncogenic mutated K-Ras signalling, and can inhibit oncogenic signalling by promoting internalisation of receptors such as

Epidermal Growth Factor Receptor (EGFR) and HER2 (Human-EFGR-2) which promote cell growth and survival [298-300]. Functional PKC can also keep growth factor receptor signalling in check, PKC may inhibit receptors, including GPCRs by phosphorylation of their cytoplasmic loops in a dynamin-dependent manner [301]. PKC $\alpha$  can also inhibit K-Ras, so may suppress malignant cell growth by suppressing oncogenes, as K-Ras is frequently mutated in cancers where there is LOF of PKC [259, 302].

The gene for PKC $\delta$  is deleted in many skin cancers, re-expression in a mouse model suppresses malignant cell growth [303]. However PKC $\delta$  is implicated in promoting pancreatic cancers [260] and in cell-lines PKC $\delta$  depletion can induce apoptosis and PKC $\delta$  upregulation protects from apoptosis [304], so depending on oncogene expression PKC $\delta$  can promote malignant growth, survival and ERK signalling downstream of PKC $\delta$  [305] or inhibit it. Results of PKC investigations in malignant cell-lines may therefore be cell-type specific.

#### ***1.17.5: PKCs as oncoproteins and as tumour suppressors***

Novel PKCs may act as oncoproteins e.g. PKC $\delta$  has roles in survival and apoptosis, opposing receptor-initiated apoptosis, and supporting apoptosis triggered by DNA damage [306, 307]. PKC $\delta$  increased expression may worsen outcome in HER2 positive breast cancer, but in endometrial cancers decreased PKC $\delta$  expression correlates with higher grade tumour, hence PKC $\delta$  can drive some cancers and inhibit others. Hormone sensitivity may govern if PKC GOF or LOF favours malignant cell survival [308, 309].

PKC $\epsilon$  expression can be elevated in prostate and breast cancers [310] and ablation of PKC $\epsilon$  may inhibit prostate cancer development and metastasis (in mice). Inhibiting PKC $\epsilon$  can cause G<sub>1</sub>/S cell cycle arrest. PKC $\epsilon$  can phosphorylate Signal Transducers and Activator of Transcription-3 (STAT3) Ser<sup>727</sup> triggering nuclear translocation; hence PKC $\epsilon$  can regulate transcription factors including, STAT3 activity in some cancers. STAT3 activation also links to COX-2 activation [311] so inflammation. STATs are transcription factors phosphorylated by receptor associated Janus Kinases (JAKs), which respond to specific cytokines, including chemokines, producing cell migration, proliferation and survival [312].

#### ***1.18: JAK STAT Signalling.***

The JAK family contains the ubiquitously distributed JAK1, JAK2 and Tyk2, plus JAK3 which is found mostly in hematopoietic cells. The STATs are intracellular transcription factors influencing cell immunity, differentiation, proliferation and apoptosis. The STAT family consists of STAT1-STAT4, STAT5 (A & B) and STAT6. STAT3 is often activated in tumours and has been implicated in in

cancer progression. STAT3 appears important in immune responses to malignancy and in resistance to chemotherapy. GPCR's activation of STAT3 via JAK2 is associated with cancer [312-316]. STAT3 appears to hold a key role in cancer initiation, progression and prognosis, and is often elevated in blood and breast malignancies [317, 318].

Tyrosine phosphorylation by JAKs is purportedly required for most cytokine responses. JAKs' association with cytokine receptors is enhanced by cytokine ligand binding, and JAK responses include tyrosine phosphorylation of their associated receptor, this opens docking sites for both STATs and PLC; activated PLC signalling can then trigger calcium release from intracellular reservoirs [319-321]. JAKs' phosphorylation of receptor tyrosines facilitates STAT phosphorylation, dimerization, transfer to nucleus and initiation of transcription [312].

G<sub>αi</sub> can be inactivated by pertussis toxin (PTX). PTX is an A-B toxin, the A subunit ribosylates and uncouples α subunits of G<sub>αi</sub> from the receptor, the B protomer reportedly can bind cell surface proteins including Toll-like receptor 4 and activate intracellular signalling cascades [322] hence PTX can be used to investigate the involvement of G<sub>αi</sub> in CXCR4/CXCL12 signalling. Vila-Coro *et al.* (1999) published evidence that CXCR4/CXCL12 signalling involved G<sub>αi</sub>, JAK phosphorylation, JAK phosphorylation of CXCR4 dimers, STAT association with CXCR4 and subsequent dimerization via SH2-phosphotyrosyl interactions then movement to the nucleus [323].

#### **1.18.1: JAK2 in malignancies**

JAK2 gene mutations are common in myeloproliferative neoplasms. STAT signalling downstream of JAK kinases is reportedly enhanced in malignant cells [324]. JAK2 mutations have been shown to increase chemotactic responses of CXCR4 to CXCL12 and also both retention and maintenance of haematopoietic stem cells in bone marrow, plus their movement to extramedullary sites producing myelofibrosis. Normally haematopoietic stem cells and haematopoietic stem progenitor cells divide and differentiate in the bone marrow but in myeloproliferative neoplasms extramedullary haematopoiesis occurs for example in the spleen [325]. CXCR4 functions to retain haematopoietic stem cells in the bone medullary this can be antagonised by CXCR4 inhibitors including AMD3100 (Plerixafor) [326]. In myeloproliferative neoplasms CXCR4 sensitivity may be increased even in CXCR4 downregulation [327]. JAK2 mutations or cytokines may trigger oncogenic activation synergistically with CXCR4/CXCL12 signalling facilitating Pi3K signalling and chemotaxis [328]. A JAK1/2 inhibitor ruxolitinib is currently licenced for treating myeloproliferative neoplasm polycythemia vera [329].

PKC and JAK2 signalling may influence metastasis, but the process of cell migration is co-ordinated by Rho GTPases regulating cell polarity, adhesion, actin polymerization and cytoskeletal dynamics.



### 1.19: Rho GTPases in cell migration

Rho GTPases are members of the Ras family of proteins and are molecular switches, they are 'off' when GDP-bound and 'on' when in GTP-bound conformation but are also modulated by post-translational modifications and influenced by other proteins when in complexes [330]. Active Rho GTPases interact with effectors downstream to initiate various signalling pathways [331]. Location is key for Rho GTPases. Although Rho GTPases have sequence and structural homology each can control specific cellular responses within tightly controlled spatial-temporal activation and signalling [332].

There are over twenty Rho GTPase family members, each with several isoforms, three Rho GTPases involved with the actin cytoskeleton are RhoA, Rac1 and Cdc42. RhoA is involved with contraction at the cell's rear related to actomyosin, Cdc42 with filopodia formation at the leading edge, and Rac1 with lamellipodia and membrane ruffles [331, 333]. Rac1 regulates lamellipodia formation and so is key to cell motility; it is most active at a cell's leading edge [334].

Rho GTPases can undergo lipid modification of their C-terminal. Usually this is prenylation, the addition of farnesyl or geranylgeranyl unit to a C-terminal cysteine commonly the Cys in terminal CAAX motif. This may be followed by S-palmitoylation at a nearby cysteine. The effect of prenylation is to allow the GTPase to insert and anchor in a cell or organelle membrane. For example Rac1 palmitoylation increases the GTPase stability and activity, and may determine the subcellular location of the protein. Rac1 is prenylated at Cys<sup>189</sup>, then palmitoylated at Cys<sup>178</sup> [335], figure 1.16.

MQAI--KCVVVG DGAVGKTCLISYTTNAFPGEYIPTVFDNYSANVM	VDG	- 48
Switch I		
KPVNLGLWDTAGQEDYDRLRPLSYPQTDVFLICFSLVSPASFENVRAKWY		- 98
Switch II		
PEVRHHCPNTPILVGTKLDLRDDKDTIEKLKEKKLTPTYPQGLAMAKE		- 148
IGAVKYLECSALTQRGLKTVFDEAIRAVLCPPPVKKR -- KRKC	LLLC	C-terminus - 192

Figure 1.16: Human Rac1 sequence, showing Switch I and Switch II regions, C-terminus cysteines Cys<sup>178</sup> and Cys<sup>189</sup> (underlined), and W56 Rac1 active peptide (used in chapter 8) residues in red.

### **1.19.1: Controllers of Rho GTPases GDIs, GAPs and GEFs**

Cellular activity and levels of Rho GTPases are also controlled by epigenetic and microRNA regulation, phosphorylation, and in the case of Rac1, addition of ubiquitin-like proteins (sumoylation) which help to keep Rac1 in an active state, or subject to ubiquitination and degradation in proteasomes [330]. Rho GTPases can be activated by GPCRs including chemokine receptors [336].

There are three controllers of Rho GTPases. (i) Firstly Rho-specific guanine nucleotide dissociation inhibitors (Rho GDIs), these can bind GDP-bound Rho GTPases and can sequester them in the cytosol by masking the COOH prenylation [337]. There are at least three known Rho GDI mammalian isoforms each containing two key motifs, the N-terminal domain which binds Rho GTPases' Switch I and Switch II regions, see figure 1.16, and the C-terminus domain which through interactions with Rho GTPases including the Switch II region facilitate the release of Rho GTPases from lipid membranes [338-340]. (ii) Secondly there are GTPase-Activating Proteins (Rho GAPs) which by augmenting the speeding up of the intrinsic GTPase-hydrolysis turn the GTPase 'off'. Several Rho GAPs have been identified, many exhibiting Rho GTPase specificity, including ARHGAP15 and FilGAP which act on Rac1 [341, 342]. (iii) Finally there are guanine nucleotide exchange factors (Rho GEFs) which promote activation of the GTPase and so exchange of GDP for GTP [338].

There are seventy or more Rho GEFs classified into two families, DOCK and DBL, depending on structure; they interact with GTPase Switch regions as do GAPs and GDIs [330, 343]. Rho GEFs are usually regulated by phosphorylation, which may activate or inhibit depending on GEF. Phosphorylation produces 14-3-3 protein docking sites. 14-3-3 proteins usually inhibit GEF activity. 14-3-3 $\zeta$  binds GEF T-lymphoma invasion and metastasis-inducing protein-1 (Tiam1) recruiting Tiam1 to adhesion complexes where it activates Rac1 supporting cell migration and chemotaxis [344]. Tiam1 is a pro-invasion factor of T-lymphocytes. It activates Rac1 but also influences polarity in migrating cells, by binding PAR3 in the PAR polarity complex, which includes PAR3, PAR6 and atypical PKC. Tiam1 promotes the PAR complex which regulates cell front-rear polarization and the formation of cell-cell junctions [345]. Inhibition of TIAM1 can support migration indirectly by promoting cell-cell junction disassembly. Also inhibition of PKC can inhibit chemotaxis. Tiam1 therefore exhibits some control over chemotaxis via the PAR complex. Research suggests different cell-lines appear to have different GEFs activating Rac1. In lymphocytes Rac activation can be triggered via Rac-specific GEF DOCK2 only found in

hematopoietic cells. In HER2 positive breast cancers Rac1 was found activated through Akt signalling stimulating Tiam1 and via PKC signalling inhibiting a Rac1 guanine nucleotide dissociation inhibitor, RhoGDI2 [346-350].

Additionally GTPase Rac1 can be regulated by phosphorylation, including by focal adhesion kinase (FAK) or SRC on Tyr<sup>64</sup>, and by AKT on Ser<sup>71</sup>, both raise levels of GDP-bound Rac1. Tyr<sup>64</sup> and Ser<sup>71</sup> lie in the Rac1's Switch II region, figure 1.16; phosphorylation of these residues appears to hinder GTP binding [351, 352]. ERK can trigger Rac1 phosphorylation at Thr<sup>108</sup> causing Rac1 translocation into nucleus where it is unavailable to GEFs, and can interact with NFκB and β-catenin and may support Wnt signalling plus RhoA-governed malignant cell invasion [353-356].

### ***1.20: Pi3K and FAK signalling in metastasis***

Sequences of events following a cell surface receptor sensing a chemokine gradient can include phosphoinositide-3-kinase (Pi3K) signalling which triggers the formation of PIP<sub>3</sub> at the cell's leading edge and actin cytoskeleton reorganisation resulting in lamellipodia formation [357]. This involves a dense intracellular matrix of actin filaments forming within the lamellipodium which can move the cell membrane forward, but also supports the formation of adhesion complexes that link to and grip the extracellular matrix (ECM) meshwork giving the cell traction to flow forward [358]. Adhesion complexes are dynamic structures composed of scaffolding proteins such as integrins that bind to ECM fibronectin and to actin via proteins such as paxillin and talin [359]. These adhesion complexes grip the ECM as the cell flows past their location, then are disassembled when located near the uropod, by microtubules transporting calpains and FAK to the complex [227, 360]. FAK phosphorylation of paxillin, and calpain's severing of talin, effectively then disunite the ECM link. Adhesion complex proteins and FAK may then undergo ubiquitination or be recycled back to the leading edge [361, 362]. Membrane phospholipids to expand the lamellipodium leading edge in response to chemotactic chemokines can be supplied by polarized microtubule exocytosis and facilitated by autophagy. Autophagy includes facilitated degradation of focal adhesion proteins and actin remodelling proteins. Chemokine receptors such as CXCR4 have been implicated in the control of autophagic flux facilitating metastasis [363].

Thus metastasis involves cell polarisation and leading edge formation involving Rho family members Cdc42, Rac and Rho interacting with Pi3K signalling and FAK phosphorylation, however another key protein involved with actin filament dynamics is cofilin.

### ***1.21: Signalling linking cofilin to chemotactic metastasis***

Actin filament remodelling is essential for cells to physically migrate. Actin filaments mainly grow from 'barbed' ends. Such actin dynamics can be modulated by cofilin, a small 19 kDa protein which forms co-filaments with actin, initiating actin severing and depolymerisation and so providing a source of actin initiation barbed ends along with monomers which can be recycled to growing actin filaments at a cell's leading edge which then push the cell membrane forward, facilitating chemotaxis. This is an ATP-dependent process; cofilin has high affinity for ADP-actin and low affinity for ATP-actin and so functions to break-up old filaments [364, 365].

Studies show cofilin expression is upregulated in many solid tumours, in adherent cell-lines including A549 and HeLa, and in malignant leukocytes and suspension cell-lines including Jurkat and HL60. Cofilin has also been shown to aid EMT and metastasis. Chemotaxis has been shown to positively correlate with cofilin expression [366-372].

#### ***1.21.1: Cofilin phosphorylation and dynamics***

Active cofilin binds actin filaments, disassembling them from the minus end by modifying the actin twist causing filament strain followed by filament fragmentation. Cofilin is activated by dephosphorylation on Ser<sup>3</sup>, which lies in its actin-binding site [373, 374], by phosphatases including PP1/PP2, Calcineurin and Slingshot, activation can be modulated by signalling including through Pi3K [375, 376]. Cofilin is inactivated by LIM kinase (LIMK) phosphorylation, which is mediated by Rho GTPases [377]. However cofilin's cellular activities are multi-layered and complex; for example, cofilin may have feedback effects on stimulated receptors by interacting with phospholipase D1, as phosphorylated cofilin can stimulate phospholipase D1 activity triggering cellular responses such as calcium mobilisation and apoptosis, membrane hydrolysis, and actin stress fibre formation [378]. Cofilin phosphorylation is also influenced by pH, ROS and membrane lipids. Only un-phosphorylated cofilin can sever actin [377, 379].

Three isoforms of Slingshot occur in humans, SSH1L, SSH2L and SSH3L. The activities of slingshot phosphatases are influenced by regulatory proteins including 14-3-3. 14-3-3 proteins bind phosphorylated Slingshot sequestering the phosphatase in the cytoplasm away from F-actin in the lamellipodia and cell protrusions [380]. Protein Kinase D (PKD) can phosphorylate serines in the carboxy-terminus of Slingshot, and this induces 14-3-3 scaffold proteins to bind and sequester Slingshot in the cytoplasm, reducing active Slingshot levels in lamellipodia. Reducing phosphatase activity on cofilin can increase local levels of phosphocofilin occur in lamellipodia. Slingshot also dephosphorylates and inactivates LIMK1. 14-3-3 bound Slingshot may then dephosphorylate LIMK1 in the cytosol, leaving active cofilin in the actin-rich lamellipodia in migrating cells [381-

383]. In metabolic stress, which can be triggered by high cholesterol or blood glucose, 14-3-3 $\zeta$  undergoes S-glutathionylation and degradation by caspases. This frees Slingshot to activate cofilin, stimulating actin turnover plus remodelling, and has been found to increase THP-1 sensitivity towards CCL2 [384].

There are two LIMK subtypes, LIMK1 and LIMK2; they are serine-threonine specific and both contain many cysteine residues and two zinc fingers. LIMKs can be regulated by Rho GTPases [385]. LIMKs are involved in a wide range of cellular processes including mediating the actin cytoskeletal structure via phosphorylation of cofilin [386]. LIMK can be activated by several routes including: phosphorylation of a threonine in LIMK's catalytic domain [385, 387, 388]; phosphorylation of Ser<sup>323</sup>; and inactivated by caspase-3 proteolysis of LIMK Asp-240 [389, 390], figure 1.17.

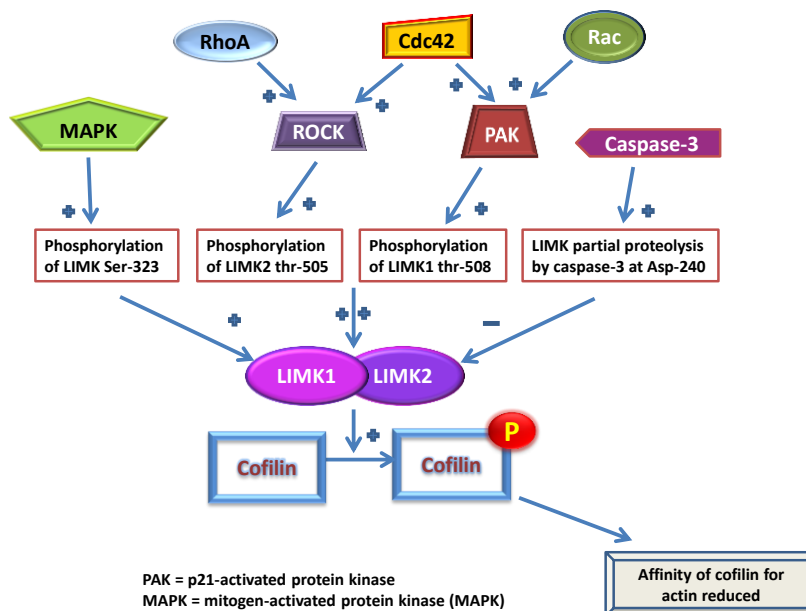


Figure 1.17: Some of the many signalling pathways modulating LIMK activation [385, 387-390].

Both LIMK and cofilin have been shown to moderate other signalling pathways; and dephosphorylated cofilin to localise to mitochondria [391]. If dephosphorylated cofilin translocates to mitochondria it raises membrane permeability allowing cytochrome C release, caspase 9 Apat-1 cleavage and activation, then caspase-3 activation and cell apoptosis [391]. Overall the literature suggests the many influences on cofilin activation may interact and are often cell type specific.

Cofilin phosphorylation state is not a direct measure of cofilin activity, although total phosphorylation has been shown to increase following ligand stimulation of cells [392]. This is explained as the active cofilin (un-phosphorylated) and phosphocofilin may be in different cellular 'locations' such as the cytosol, the F-actin location between cytosol and membrane, and at the membrane. Cofilin does not evenly spread throughout the cell, it clusters. Where clusters are

juxtaposed to older actin filaments un-phosphorylated cofilin can sever actin, forming new barbed ends and monomers which trigger actin polymerization, that is key to cell migration and metastasis [373, 379, 393]. Also cofilin's protein sequence contains nuclear location signals which allow cofilin to carry depolymerized actin into the nucleus [394]. In the nucleus cofilin may form actin rod-like structures [395], and be phosphorylated by LIMK1 [396]; the transported actin may remodel chromatin [397] and bind RNA polymerase modulating gene transcription [398]. Hence cofilin may indirectly influence gene expression.

### 1.21.2: Phospholipid phosphatidylinositol-(4,5)-bisphosphate influences on cofilin

Cofilin activity can be assisted by actin-interacting protein (Aip1) and adenyl cyclase-associated protein (CAP). Aip1 and cofilin form a complex that can stop severed actin reannealing by capping barbed ends. An Aip1:cofilin:CAP complex then frees cofilin from ADP-actin to continue severing [399]. PIP<sub>2</sub> in the cell membrane can also sequester the Ser<sup>3</sup> site of cofilin, rendering notionally 'active' un-phosphorylated cofilin inactive. The cofilin-PIP<sub>2</sub> complex is transient and dynamic, with membrane PIP<sub>2</sub> rapidly binding then releasing active cofilin. PLC $\gamma$  activation causes a decrease in levels of PIP<sub>2</sub>, and so reduces the amount available that can bind cofilin i.e. decreases binding but not the release of cofilin; hence this can effectively increase the actual levels of active cofilin near the membrane juxtaposed to plentiful F-actin [379, 400, 401]. CXCL12/CXCR4 signalling through Pi3K, Rho and Rho-associated protein kinase (ROCK) pathways can activate LIMK and PLC $\gamma$ . Whereas LIMK causes generalised cofilin phosphorylation throughout the cytosol, PLC $\gamma$  acts locally near the membrane increasing levels of active cofilin, as explained above, near the receptors receiving CXCL12 stimulus, supporting directional lamellipodium formation towards the chemokine stimulus [379, 402-405]. Additionally, a pH rise may cause a decrease in PIP<sub>2</sub>/cofilin affinity and increases PLC $\gamma$  activation of cofilin [406], figure 1.18.

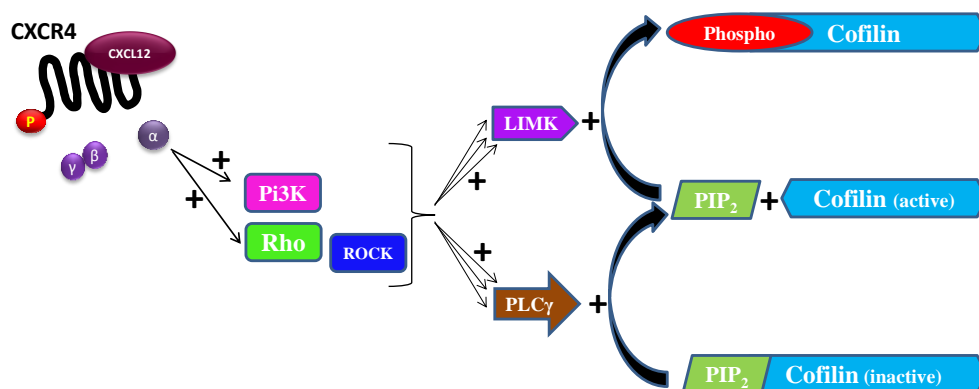


Figure 1.18: Signalling resulting in phospholipid PIP<sub>2</sub> sequestering cofilin [379, 402-406].

Cofilin activity upregulation in cancer cells can be a major driver of metastasis and hamper DNA repair [407, 408]. Prostaglandin E<sub>2</sub> (PGE<sub>2</sub>) can stimulate PTEN to dephosphorylate so activate cofilin [409]. Hence blocking PGE<sub>2</sub> production using Non-Steroidal Anti-inflammatory Drugs (NSAIDs) may, via inhibition of cofilin, inhibit cell migration.

### ***1.22: Non-Steroidal-Anti-inflammatory Drugs (NSAIDs) and metastasis***

The connection between inflammation and cancer is well established; inflammation is purportedly highly tumorigenic and links to chemokine chemotaxis [410, 411]. NSAIDs are reported to have useful prophylactic effects for some solid tumours, although effects on haematopoietic malignancies risk are less clear [412]; also they may affect metastatic spread [413].

#### ***1.22.1: Selective and non-selective NSAIDs***

Commonly prescribed NSAIDs include ibuprofen, naproxen, aspirin and celecoxib. Ibuprofen, aspirin and naproxen are non-selective inhibitors of prostaglandin-endoperoxide synthase 1 and 2 more commonly known as cyclooxygenase 1 (COX1) and 2 (COX2), whereas celecoxib is a selective COX2 inhibitor [414]. All NSAIDs inhibit COX1 or COX2 or both, these enzymes catalyse the conversion of Arachidonic Acid (AA) to Prostaglandin H<sub>2</sub> (PGH<sub>2</sub>). The fatty acid AA is produced by hydrolysis of the fatty acid/glycerol bond in membrane phospholipids by one of the many phospholipase A<sub>2</sub> isoenzymes [415]. COX enzymes have cyclooxygenase and peroxidase actions; they catalyse the cyclization of AA to unstable 15-hydroxyperoxide then their peroxidase action produces PGH<sub>2</sub>. PGH<sub>2</sub> is also unstable and so is converted by isomerases to prostaglandins (PGD<sub>2</sub>, PGE<sub>2</sub> or PGF<sub>2</sub>), prostacyclin (PGI<sub>2</sub>) or thromboxanes (TXA<sub>2</sub>, TXB<sub>2</sub>) depending on tissue isomerase/s present. Many of these derivatives have inflammatory, pyretic or nociceptive effects [416]. PGE<sub>2</sub> is also produced by cancer cells as COX2 expression is induced by inflammatory and mitogenic stimuli, such as cytokines and growth factors. PGE<sub>2</sub> supports inflammatory T-cell Th<sub>17</sub> activity, and recruits monocytes and neutrophils. Also COX2 derived PGE<sub>2</sub> can promote angiogenesis [417].

#### ***1.22.2: Paracetamol's complex mode of action***

Paracetamol is widely used in pain management, it also inhibits COX enzymes but its mode of action is complex; it appears to act locally [418]; peripherally [419] including through cannabinoid receptors; centrally in the spine [420] including via serotonin 5-HT<sub>3</sub> receptors coupling to Gs and cAMP production; and in the brain via transient receptor potential vanilloid subtype 1 (TRPV1) non-selective Ca<sup>2+</sup> channels [421]. Paracetamol weakly inhibits prostaglandin synthesis with more COX2 than COX1 activity, it has weaker analgesic effects than NSAIDs and few anti-inflammatory effects [422]. Paracetamol appears to inhibit the peroxidase function of COX enzymes only when low, not high, levels of AA are available, and hence fails to effectively suppress inflammation.

Paracetamol also non-selectively inhibits other peroxidases. In monocytes paracetamol can reduce COX2 activity by 80% [423]. Centrally paracetamol has an anti-nociceptive effect on 5-HT<sub>3</sub> serotonin receptors; this can be blocked with 5-HT<sub>3</sub> antagonists [424, 425]. PGE<sub>2</sub> modulates nociceptive signals via the serotonergic anti-nociceptive system [426] so paracetamol's analgesic effect may be directly on 5-HT<sub>3</sub> receptors or via cyclooxygenases, figure 1.19.

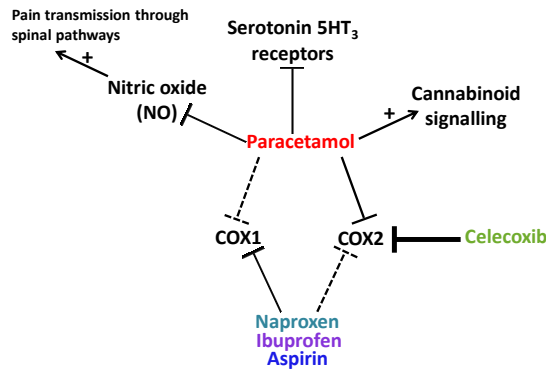


Figure 1.19: Modes of action of paracetamol, ibuprofen, naproxen and celecoxib [423, 424, 427, 428].

Paracetamol can be de-acetylated to p-aminophenol which interacts with AA to form N-arachidonoyl phenylamine aka N-arachidonoyl aminophenol, which, by inhibiting the degradation and uptake of anandamide, can (i) indirectly increase activity of cannabinoid receptors [428] inhibiting endogenous cannabinoid reuptake, (ii) activate TRPV1 channels, agonists of which can inactivate nociceptive nerve fibres, cause vasodilation and modulate thermoregulation reducing temperature [427, 429, 430], (iii) inhibit cyclooxygenases and (iv) inhibit selective transport and internalisation of anandamide by neurones [431]. Anandamide concentration appears key to paracetamol's efficacy [432, 433]. Endogenous cannabinoids have an anti-nociceptive action on spinal cord and brain pain pathways [427]. If cannabinoid receptors are inhibited paracetamol's analgesic and antipyretic effect is blocked [434]. Paracetamol may also inhibit formation of the neurotransmitter nitrous oxide (NO). Substance P and NMDA receptors activate NO synthesis, NO acts on the nociceptive pathways in the spinal cord leading to the brain [435, 436].

### 1.22.3: Leukocytes and PGE<sub>2</sub>

Prostaglandins such as PGE<sub>2</sub> are inflammatory mediators; macrophage response to cytokines includes the secretion of PGE<sub>2</sub> which through autocrine signalling regulates their activity. PGE<sub>2</sub> can be produced by many tissues, and its production can be increased in cancer [437]. Raised PGE<sub>2</sub> levels can be immunosuppressive [438], additionally PGE<sub>2</sub> has been shown to increase cell proliferation, migration and angiogenesis [439]. COX1 contributes to homeostasis, and is constitutively expressed in most cell types whereas COX2 can be induced in macrophages by mediators of inflammation. PKCα regulates macrophage PGE<sub>2</sub> responses to bacterial lipopolysaccharides and interferon-gamma via modulation of COX2 expression [440].



PGE<sub>2</sub> suppresses leukocyte activation and binds G-protein coupled E-prostanoid receptors 1 to 4 (EP1-EP4). EP1 receptors increase G<sub>q</sub> G-protein and Ca<sup>2+</sup> responses; EP2 and EP4 receptors through G<sub>s</sub> G-proteins increase Adenylyl Cyclase and cAMP levels; and EP3 receptors through G<sub>i</sub> G-proteins reduce cAMP levels [441]. COX2 is the target of transcription factor Activator Protein-1 (AP-1). AP-1 consists of cFos and cJun subunits expressed in response to stimuli including cytokines [442]. COX2 is one of the rate limiting enzymes in PGE<sub>2</sub> production; excess PGE<sub>2</sub> inhibits macrophage and NK cell tumouricidal activity [443].

#### **1.22.4: COX1 and COX2, inflammation and cancer**

COX1 is constitutively active whereas COX2 isoform expression is inducible, for example, by mitogens or cytokines as COX2 is involved in inflammation [444]. NSAIDs may be therapeutic in malignant cells exhibiting certain mutations such as in Pi3K signalling [445]. Non-selective NSAIDs inhibit both COX1 and COX2 and may inhibit proliferation and accelerate apoptosis [446]. High levels of COX2 which is overexpressed in some cancers correlates with angiogenesis and mutagenesis [447]. Although epidemiological evidence shows aspirin and some NSAIDs can protect against tumour development or progression in the gut, dose and duration appear critical [448, 449], and the mechanisms need further elucidation. COX1 and COX2 are coded on separate genes [450].

Prostaglandins are involved in cellular differentiation; PGE<sub>2</sub> production by COX2 appears important for colorectal cancer initiation and progression via stimulation of malignant cell proliferation, survival, invasiveness and tumour angiogenesis [451, 452]. NSAIDs may hamper colorectal carcinogenesis by stimulating apoptosis or programmed cell death, as PGE<sub>2</sub> stimulates Pi3K/Akt pathways that protect colon cancer from apoptosis [453]. The Akt substrate GSK3 $\beta$  inactivates cJun and cMyc oncogenic transcription factors and negatively regulates Wnt signalling and  $\beta$ -catenin proto-oncoprotein and so suppresses tumour initiation [454]. Regular NSAIDs or aspirin may halve bowel cancer risk [455], and reduce polyp formation in familial adenomatous polyposis [456].

Chemotherapy with cisplatin and radiation treatments may leave patients more vulnerable to the metastatic spread of tumour cells, spared by these therapies, as responses can include production of chemotactic cytokines, and tumour cell growth in damaged tissues. This vulnerability may be ameliorated by ibuprofen treatment [457], possibly due to ibuprofen's ability to inhibit PGE<sub>2</sub> production, and modulate calcium dynamics in remaining malignant cells [458].

NSAIDs may have a COX-independent mechanism of opposing various malignancies. Non-selective NSAIDs irreversibly acetylate COX1 and competitively inhibit COX2 [459], but different NSAIDs may act at different concentrations in different tissues e.g. Aspirin at low dose relatively selectively inhibits COX1 in platelets but above 500  $\mu$ M only inhibits COX2 [460, 461]. Inhibition of COX1 purportedly can cause gut ulceration, but COX2 expressed in the presence of damage may support mucosal integrity [462]. There is a link between inflammation and cancer, and pro-inflammatory IL-1 $\beta$  and TNF $\alpha$  are potent inducers of COX2. Chronic inflammation can trigger malignant transformation. PGE<sub>2</sub> levels are reported to positively correlate with metastatic potential of breast cancers [463]. Smoking can induce COX2 expression and PGE<sub>2</sub> release in metastatic breast cancer via phospholipid A2-dependent pathways that support cell proliferation and migration [415]. PGE<sub>2</sub> may be able to inhibit apoptosis, reduce cellular adhesion, increase motility, promote immunosuppression and angiogenesis [464, 465]. PGE<sub>2</sub> may promote anti-apoptotic effects via Pi3K-Akt & PPAR $\delta$  signalling [466]; support VEGF expression which itself stimulates cell proliferation [467]; and induce cell proliferation by Raf/MEK/ERK and Pi3K/Akt signalling [468] that itself supports motility and invasion and through ERK2/JNK1 signalling angiogenesis [469].

COX2-produced PGE<sub>2</sub> is the principle prostaglandin produced in solid tumours [470, 471]. In mice if EP1, EP2 and EP4 are deleted or blocked by antagonists the animals resist carcinogen-mediated cancers [472-474]. EP1, EP2 and EP4 over-expression occurs in breast cancers [475]. COX2/PGE<sub>2</sub> may contribute to breast cancer growth via EP1-PKC or PKA signalling upregulating aromatase, an enzyme which catalyses oestrogen biosynthesis in adipose tissues; if adjacent to tumours this can support malignancy [476, 477].

#### ***1.22.5: NSAIDs COX-independent antineoplastic effects***

Individual NSAIDs may have COX-independent prostaglandin-independent antineoplastic effects, e.g. celecoxib can induce expression of cyclins A, B and D causing cell cycle arrest in G1 phase [478], this may occur due to inhibition of PKB/Akt or PDK-1 [479]. Celecoxib can also activate apoptosis by the intrinsic pathway, i.e. cytochrome C release by mitochondria activating caspases-3, 8, and 9 [480, 481].

NSAIDs have also shown anti-tumour effects on COX2-null cell lines as NSAIDs independently of COX2 inhibition can stimulate the transcription and translation of 15-hydroxyprostaglandin dehydrogenase (15-PGDH) which degrades inflammatory prostaglandins so physiologically antagonises COX2. 15-PGDH may inhibit colon malignancy [482]. NSAIDs may raise levels of 15-PGDH by (i) down-regulation of matrix metalloproteinase-9 (MMP-9) which can degrade 15-PGDH

and (ii) by upregulating Tissue inhibitor of metalloproteinase-1 (TIMP-1) an inhibitor of MMP-9 [483]. Ibuprofen is reported to upregulate metalloprotease-13 (MMP-13) and Paracetamol to suppress it [484]. Ibuprofen may also down regulate MMP-2, MMP-9 [485], as well as TNF $\alpha$  stimulated IL-6 and IL-8 [486]. Finally NSAIDs' purported anti-cancer effects include inhibition of calcium ATPases preventing cytosolic calcium re-uptake and so elevating intracellular calcium concentrations [487].

### **1.23: Research objectives**

Malignant cell migration facilitates metastasis, frequently the final fatal stage in cancer progression. Interest is growing in modulation of chemokine signalling as a therapeutic tool in cancer. For example, a CXCR4 peptide antagonist (LY2510924) has been used in clinical trials as adjunct therapy, with a variety of established chemotherapeutic agents, but as yet there have been no positive outcomes reported. Sadly LY2510924 reduced overall survival (OS) time in metastatic renal cell carcinoma from 12 to 8 months when added to Sunitinib [488]; and reduced OS time from 11 to 9 months in small cell lung cancer when added to carboplatin and etoposide therapy [489]. These results confirm further elucidation and understanding of chemokine signalling is urgently required.

**Hypothesis:** Many chemokines, including CCL3 and CXCL12 along with their cognate receptors, are instrumental in supporting metastasis.

**Aim:** Elucidate the importance of key intracellular signalling proteins in CCL3- and CXCL12-triggered cancer cell migration.

**Objective:** To use small molecule antagonism, siRNA knockdown or plasmid modification of chemokine receptors and important intracellular signalling proteins to further elucidate these proteins role in chemokine-induced cell migration *in vitro*, as this may relate to metastasis *in vivo*. The focus was on CXCL12-, CCL3- and CCL2-induced chemotaxis in THP-1 monocyte, and Jurkat T-cell suspension cell-lines also CXCL12- and CCL3-stimulated random motility (chemokinesis) in MCF7 a breast-cancer adherent cell-line.

**Limitations:** The investigations in this thesis solely used cancer cell-lines to understand the fundamentals of these specific chemokine signalling pathways, the identities of the cell-lines were presumed to be as supplied from ATCC. Cell-lines offer easy access and excellent reproducibility as a first step before expanding into patient samples or animal models both of which also have

their limitations. Malignant cells are unique to each and every patient so tissue samples must be drawn from many different patients to get a clear picture of inhibitor effects. Animal models, usually mice, are also very useful, more homogeneous; however the important differences in the chemokine systems of mice and men are a limiting factor. Cell-lines can establish the importance of a signalling protein in chemotactic signalling laying the groundwork for further investigations in animal models and patient samples which precede clinical trials in people. For example this was the route that has led to the now extensive clinical use of tyrosine kinase inhibitors in the treatment of many cancers [490].

## Chapter 2: Materials and Methodology

### 2.1: Reagents

#### 2.1.1: Small Molecule Inhibitors

Table 2.1: Small Molecule Inhibitors (solvent DMSO unless otherwise stated)

Small molecule Inhibitor	Supplier	Experimental conc.
<b>Dynamin Inhibitors</b>		
MitMAB	Ascent Scientific	10 $\mu$ M
OctMAB	Ascent Scientific	5 $\mu$ M
Dynasore	Abcam	40, 60, 80 $\mu$ M
Dyngo 4a	Abcam	80 $\mu$ M
RTIL-13 <sup>TM</sup>	Abcam	2.5, 5, 10 $\mu$ M
RhodadynC10 <sup>TM</sup>	Abcam	20 $\mu$ M
Pyrimidyn-7 <sup>TM</sup>	Abcam	10 $\mu$ M
<b>PKC Inhibitors</b>		
Rottlerin (solvent ethanol)	Tocris	2-4 $\mu$ M
Staurosporine	Tocris	10 nM
GF109203X (solvent ethanol)	Tocris	5 $\mu$ M
<b>PKD Inhibitor</b>		
CID755673	Tocris	5 $\mu$ M
<b>Raf-1 Inhibitor</b>		
L779450	Abcam	0.5, 1, 5 $\mu$ M
<b>cAMP Activator</b>		
Forskolin	Abcam	20, 50 $\mu$ M
<b>ERK/MEK inhibitors</b>		
SL327	Abcam	1 $\mu$ M
PD98059	Abcam	10, 25 $\mu$ M
<b>Rac Inhibitors</b>		
NSC23766 (solvent water)	Abcam	12.5, 25, 50, 100 $\mu$ M
EHT1864	Cambridge Biosciences	10 $\mu$ M
<b>FAK/Pyk2 Inhibitors</b>		
PF-562271	Abcam	10 -25 $\mu$ M
FAK Inhibitor PF-228	Sigma-Aldrich	10 $\mu$ M

Table 2.1 continued: Small Molecule Inhibitors (solvent DMSO unless otherwise stated)

Small molecule Inhibitor	Supplier	Experimental conc.
<b>Kinase Inhibitors</b>		
SB203580	Abcam	10 $\mu$ M
$\beta$ -ARK-1	Calbiochem	1 – 2 $\mu$ M
Bosutinib	Selleck Biochem	0.5, 1, 2.5, 5, 10 $\mu$ M
H89 HCL	Abcam	0.5, 1 $\mu$ M
Y27632	Tocris	1, 5, 10 $\mu$ M
<b>Pi3K Inhibitors</b>		
AS605240	Tocris	1, 5 $\mu$ M
LY294002	Tocris	10 $\mu$ M
<b>GRK Inhibitor</b>		
lpyrimidine (4-Amino-5-ethoxymethyl-2-methylpyrimidine)	Abcam	1, 5 $\mu$ M
<b>JAK2 II Inhibitor</b>		
Hexabromocyclohexane (HBC)	Calbiochem	10 $\mu$ M
<b>STAT3 III Inhibitor</b>		
WP1066	Calbiochem	2 $\mu$ M
<b>STAT3 VIII Inhibitor</b>		
5,15-Diphenylporphyrin (5,15-DPP)	Calbiochem	10 $\mu$ M
<b><math>\beta</math>-catenin Inhibitor</b>		
FH535	Abcam	1, 5 $\mu$ M
<b>Cdc 42 Inhibitors</b>		
ZCL278	Abcam.	10, 20 $\mu$ M
<b>Phospholipase C Inhibitors</b>		
U73122	Tocris	10 $\mu$ M
<b>NSAIDs</b>		
Celecoxib	Sigma-Aldrich	50 $\mu$ M
Ibuprofen	Aspar Pharmaceuticals	290 $\mu$ M
Naproxen (solvent water)	Aspar Pharmaceuticals	217 $\mu$ M
Aspirin (solvent water)	Aspar Pharmaceuticals	555 $\mu$ M
Paracetamol	Aspar Pharmaceuticals	130 $\mu$ M

Table 2.2: Small Molecule Inhibitors and Receptor Antagonists (solvent DMSO unless otherwise stated)

Small molecule inhibitor	Supplier	Experimental conc.
<b>CXCR4 antagonist</b> ATI2341 (solvent water)	Tocris	10 $\mu$ M
<b>CCR1/CCR3 antagonist</b> J113863	Tocris	1 nM, 20 nM
<b>CCR5 antagonist</b> Maraviroc	Tocris	50 nM
<b>G<math>\beta</math>y Inhibitor</b> Gallein	Tocris	10 $\mu$ M
<b>Cytoskeletal Inhibitors</b> Nocodazole	Sigma-Aldrich	7.5 $\mu$ M

### 2.1.2: Peptides and Chemokines

Table 2.3: Peptide Inhibitors (solvent water)

Peptide	Sequence	Experimental Conc.
Rac-1 active peptide (W56)	VDGKPVNLGLWDTAG	280 – 560 $\mu$ M
Rac-1 control peptide (F56)	VDGKPVNLGLFDTAG	280 – 560 $\mu$ M

Table 2.4: Chemokines (solvent water)

Chemokines (Human)	Supplier	Experimental Conc.
CXCL9	PeptoTech London, UK	1 – 5 nM
CXCL11	PeptoTech London, UK	1 – 5 nM
CXCL12	PeptoTech London, UK	0.1 – 10 nM
CXCL14	PeptoTech London, UK	1 – 600 nM
CCL2	PeptoTech London, UK	1 – 5 nM
CCL3 (2-70) (D26A) [491]	British Biotech Oxford UK*	1 – 10 nM

\*Generously donated by Lloyd Czaplewski of British Biotech (Oxford, UK). CCL3 (2–70) (D26A) a form of CCL3 which has reduced aggregation propensity but similar affinity for CCR5 as well as ability to stimulate both calcium mobilisation and chemotaxis as endogenous CCL3, although CCL3 (2–70) (D26A) has a reduced gene sequence [492].

### 2.1.3: Bacterial Plasmids

Table 2.5: Bacterial Plasmids

Plasmid	Source / Addgene plasmid reference
$\beta$ -arrestin 1 aka Arrestin-2	pcDNA3 arr2 (arrestin-2) a gift from Eamond Kelly [493]
$\beta$ -arrestin 2 aka Arrestin-3	pcDNA3 arr3 (arrestin-3) a gift from Eamond Kelly [493]
eGFP control	pEGFP.C2 (Clontech, France) plasmid DNA coding green fluorescent protein at the C-terminus
Arrestin-2 mutant	PcDNA3-arr2 mutant – arrestin-2 component is mutated by substitution of a valine for an aspartic acid at the start of the arrestin sequence i.e. $\beta$ -arrestin-1-V53D [494]
dsRed-Mito	Mitochondrial targeting sequence fused to 5' of DsRed vector has CMV promoter, pUC, fl and SV40 origins of replication. Kanamycin / G418 resistance (Clontech, France)

Plasmids above were produced by cloning arrestin DNA into pEGFP-N1 plasmids (Clontech, France) using a Hind III/Apa I digest. pEGFP.C2 plasmids (Clontech, France) were used as transfection controls.

### 2.1.4: Antibodies

Table 2.6: Primary Antibodies

Primary Antibody	Species	Supplier	Dilution*
Cofilin #3312 mAb (Immunofluorescence)	Rabbit	Cell Signaling Tech.	1 in 1000
Cofilin (D3F9)XP™ mAb (Western Blots)	Rabbit	Cell Signaling Tech.	1 in 5000
Phospho-cofilin (Ser3) (77G2) #3313 mAb	Rabbit	Cell Signaling Tech.	1 in 1000
Dynamin-2 Ab65556 mAb	Rabbit	Abcam	1 in 1000
$\beta$ -actin (C4) sc47778 mAb	Mouse	Santa Cruz Biotech	1 in 5000
$\beta$ -Arrestin-1/2 Antibody (A-1): sc-74591 mAb	Mouse	Santa Cruz Biotech	1 in 1000
Src: 3389 #327537 mAb	Mouse	R & D Systems Biot.	1 in 1000
PKC alpha (H-7): sc-8393	Mouse	Santa Cruz Biotech	1 in 5000
PKC zeta (H-1):sc-17781	Mouse	Santa Cruz Biotech	1 in 10,000
PI3 Kinase p85 $\alpha$ (6G10) #13666 mAb	Mouse	R & D Systems Biot.	1 in 1000
CXCR4 12G5	Mouse	Santa Cruz Biotech	1 in 5000
CCR5 HEK/1/85a/7a cell growth supernatant	Rat	**	undiluted
p-STAT3 (B-7): sc-8059	Mouse	Santa Cruz Biotech	1 in 1000

(\*working dilution in 5% bovine serum albumin (BSA) in Tris Buffered Saline + Tween (TSBT)

\*\*Gift from J.A. McKeating, Reading.



Table 2.7: Secondary Antibodies

Secondary Reagent	Species	Supplier	Dilution*
Horseradish peroxidase	Mouse	Sigma Aldrich	1 in 20,000
Horseradish peroxidase	Rabbit	Sigma Aldrich	1 in 20,000
Horseradish peroxidase	Rat	Sigma Aldrich	1 in 10,000
Fluorescein isothiocyanate (FITC)	Mouse	Sigma Aldrich	1 in 500 - 1000
Fluorescein isothiocyanate (FITC)	Rabbit	Santa Cruz Biotechnology	1 in 500 - 1000
Fluorescein isothiocyanate (FITC)	Rat	Santa Cruz Biotechnology	1 in 500 - 1000
(*working dilution in 5% BSA in TSBT)			

### 2.1.5: Small Interfering Ribonucleic Acids (siRNA)

Table 2.8: siRNAs (All used at 50 nM in RNAase-free water)

siRNA	Supplier / Reference	Target sequence 5'-3'
<b>QIAGEN</b>		
PKC $\alpha$	Hs_PRKCA_5	AACCATCCGCTCCACACTAAA
PKC $\delta$	Hs_PRKCD_11	CAGCAGCAAGTGCAACATCAA
PKC $\epsilon$	Hs_PRKCE_6	CACGGAAACACCCGTACCTTA
PKC $\zeta$	Hs_PRKCZ_6	GACCAAATTTACGCCATGAAA
Scr-Xerogon Allstars Neg Modf.s: 3'Rh	Cat1027291,B/Noas173445 (Nonsense sequences)	Rhodamine (20 nmol) S177811
<b>On-TARGETplus Human - Individual</b>		
Pi3K J-003020-16-0005	PIK3R1(5296)	GACGAGAGACCAAUACUUG
SRC	SRC (6714)	GGGAGAACCUCUAGGCACA

Table 2.9: SMARTpool siRNAs (All used at 50 nM in RNAase-free water)

On-TARGETplus Human - SMARTpool	Dharmacon	Target sequences
Dynamin-2	DMN2(1785)-05	<b>Dynamin-2 Pool sequences</b> GGCCCUACGUAGCAAACUA
	DMN2(1785)-06	GAGAUCAAGGUGGACACUCU
	DMN2(1785)-07	CCGAAUCAAU CGCAUCUUC
	DMN2(1785)-08	GAGCGAAUCGUCACCACUU
Cofilin-1	CFL1(1072)-05	<b>Cofilin-1 Pool sequences</b> CCUCUAUGAUGCAACCUAU
	CFL1(1072)-06	CAUGGAAGCAGGACCAGUA
	CFL1(1072)-07	UAAAUGGAAUGUUGUGGAG
	CFL1(1072)-08	ACUCUGUGCUUGUCUGUUU

#### 2.1.6: Imaging Stains and Activation Kits

Table 2.10: Imaging Stains

Cell stains	Synonym	Supplier	Experimental conc.
Alexa Fluor™ 488 Phalloidin	Phalloidin	Sigma Aldrich	1:200
4',6-Diamidino-2-phenylindole dihydrochloride	DAPI	Sigma Aldrich	1:5000

Table 2.11: Activation Kits

Kit	Reference	Supplier
CatchPoint cyclic-AMP Fluorescent Assay Kit	#R8089	Molecular Devices
Rac1 Activation Assay Biochem Kit™	#BK035-S	Cytoskeleton, Inc
PhosphoSTAT3 (Tyr705) InstantOne ELISA™	#85-86102-11	eBioscience

## 2.2: Cell-lines

Table 2.12: Cell-lines

Cell-line	Source	Supplier
<b>THP-1</b>	Homo sapiens blood monocyte cell line originating from the peripheral blood of a one year old male donor suffering acute monocytic leukaemia	ATCC*
<b>Jurkat</b>	Homo sapiens blood T-lymphocyte cell line originating from the peripheral blood of a male donor suffering acute T-cell leukaemia	ATCC*
<b>MCF7</b>	Homo sapiens epithelial breast cell line originating from the pleural effusions of a 69 yr old female suffering metastatic breast adenocarcinoma (Michigan Cancer Foundation-7)	ATCC*
<b>PC3</b>	Homo sapiens prostate cell line originating from metastatic growth in bone producing grade IV adenocarcinoma in 62 yr old male	ATCC*
<b>CHO.CCR5</b>	Chinese Hamster Ovary cell line transfected with pcDNA3 encoding chemokine receptor CCR5 and resistance gene to antibiotic G418 maintained by culturing cells in presence of 200µg/mL G418	J. McKeating Reading[495]

\*original source American Type Culture Collection (ATCC) - cell line identities were presumed to be as supplied.

## 2.3: Cell culture

Table 2.13: Cell Culture Mediums

Medium	Contents
RPMI Complete	500 mL Roswell Park Memorial Institute 1640 medium + 50 mL Heat inactivated FCS + 5 mL L-glutamine 200 mM + 5 mL MEM Non-essential Amino Acid Solution (100 X)
DMEM Complete	500 mL Dulbecco's Modified Eagle's Medium-high glucose + 50 mL Heat inactivated FCS + 5mL L-glutamine 200 mM + 5 mL MEM Non-essential Amino Acid Solution (100 X)

### **2.3.1: FCS Heat Inactivation**

FCS was thawed, warmed to 55°C in a water bath, maintained at 55°C ± 2°C for 30 ± 2 minutes then cooled, then aseptically aliquoted and frozen for future use.

### **2.3.2: Propagating Cell Cultures**

Adherent cells were cultured in DMEM complete and split at 80% confluency. Suspension cells were maintained in RPMI complete at approximately  $80 \times 10^4$  cells/mL

### **2.3.3: Cell Counting and Viability**

0.1 mL of 0.4% Trypan Blue in PBS was added to 0.1 mL of cell suspension, incubated for 15 minutes, and the mixture used to load Neubauer haemocytometer. Blue cells were non-viable. Cells were counted using light microscopy, at X400. Viability was calculated as % viable =  $[1 - (\text{blue cells} / \text{total cells})] \times 100$ . Cells were only used if viability was above 95%.

### **2.3.4: Freezing and thawing cells**

Freezing:  $5 \times 10^6$  cells in logarithmic growth phase were aseptically centrifuged (900 rpm/5 minutes), the supernatant was discarded, then cell pellet re-suspended in 1 mL freezing mixture (sterile FCS+10% sterile DMSO), transferred to 2 cryogenic tubes (Fisher), wrapped in several layers of tissue to slow freezing rate and immediately placed at -70°C for ≥ 24 hours, once fully frozen tubes were transferred to liquid nitrogen storage (-195°C).

Thawing: A cryogenic tube was warmed rapidly to 37°C, once contents were freely moving they were aseptically tipped into 5 mL simple medium (37°C), shaken gently, centrifuged (900 rpm, 5 minutes), the supernatant discarded, and pellet re-suspended in 5 mL warmed complete medium maintain at 37°C 5 % CO<sub>2</sub>.

### **2.3.5: Harvesting Adherent Cells**

Concentrated EDTA solution (0.5 M) was prepared by weighing 37.224 g EDTA, adding to 100mL of Millipore filtered distilled water, then placing on a magnetic stirrer in plastic beaker, 6-10 pellets of sodium hydroxide added, and stirred until all solids were in solution. The pH was adjusted if necessary with HCl 5 M to give pH 7-8, solution was transferred to a 200 mL glass bottle and autoclaved, 121°C, 15 minutes. 2mL of this sterile 0.5 M EDTA was then added aseptically to 200 mL of sterile PBS to prepare working ~5 mM EDTA. Adherent cells were detached by pouring off medium, adding 4 mL of 5 mM EDTA/PBS, incubating (37°C, 5% CO<sub>2</sub>, 10 minutes), the flask tapped until cells detached, cells were then centrifuged and washed with PBS (37°C) to remove EDTA.

Harvesting using Trypsin/0.05% EDTA (Gibco-invitrogen): Medium was tipped out from 75 cm<sup>2</sup> flasks, and attached cells rinsed with PBS, before adding 2.5 mL Trypsin/0.05% EDTA solution,

flasks were then left for 10 seconds, before 1.5 mL of Trypsin/0.05% EDTA was removed leaving 1 mL on cells, flasks were then briefly incubated (2 minutes, 37°C, 5% CO<sub>2</sub>), and flask tapped until cells detached. Cells were used without further rinsing as the new medium dilutes remaining trypsin/EDTA enough so it does not impede attachment or growth.

#### **2.3.6: Phorbol 12-myristate 13-acetate differentiation of THP-1 to macrophages**

THP-1 were centrifuged, re-suspended at  $20 \times 10^4$  cells/mL in fresh RPMI complete, and 25-50 ng/mL Phorbol 12-myristate 13-acetate (PMA, TPA) added, e.g. 1.5 µL per 30 - 60 mL cell suspension. For cell staining 5 mL of cell suspension was added to each well of 6 well plate containing glass coverslips previously sterilised in ethanol 70%, plates were left 72 hours for cells to adhere and grow on coverslips.

#### **2.4: Chemotaxis**

The wells in a Neuro Probe ChemoTx® System micro-chemotaxis plate (ChemoTx# 101-5 with 5 µm pores) were blocked with 30 µL blocking buffer (1% BSA in RPMI without additives) for at least 30 minutes at room temperature. Chemokine solutions were prepared at working concentration/s, 1 nM unless otherwise stated, in working buffer (0.1% BSA in RPMI without additives). Jurkat or THP-1 cells were spun at 900 rpm and re-suspended in working buffer to give  $25 \times 10^4$  cells per well. Inhibitors at the required concentrations were added and cells incubated (37°C 30 minutes). Blocking buffer was removed from the plate and replaced with 31 µL of the relevant chemokine solution or working buffer for the control. The membrane was attached and 20 µL of cell suspension was added to the top surface. The plate was placed in a humidified chamber which was then incubated for 4 hours at 37°C, 5% CO<sub>2</sub>. Next the remaining cell solution on membrane was carefully removed, the membrane detached, and the cells that had migrated through the pores into in each well counted using a haemocytometer. Each data point was performed in duplicate, and the whole experiment repeated on three or more occasions.

#### **2.5: Wound-healing assays**

MCF7 cells were removed from flasks using EDTA 0.5 mM/PBS, centrifuged, (transfected if required), seeded onto 12 well plates, incubated (37°C, 5% CO<sub>2</sub>) for 24 hours. A scratch was introduced to the monolayer with 200 µL pipette tips (time point 0), medium and loose cells removed, monolayer washed once in DMEM, then 500 µL DMEM without additives was added along with inhibitors or vehicle control and plates incubated (37°C, 5% CO<sub>2</sub> 30 minutes). Chemokines (at 10 nM unless otherwise stated) were added to the cells and pictures were taken (time point 0). Plates were incubated (37°C, 5% CO<sub>2</sub> 24 hours) then imaging repeated (time point

24 hours), using an inverted Leica microscope 10 times magnification. Images were analysed and the width of the wound was measured for control and with inhibitor treatment (with and without chemokine) at 0 hours and 24 hours. Ratios were calculated (width of the wound after 24 hours divided by the width of the wound at 0 hours) and the effects of inhibitor and chemokine analysed. The nearer the result is to 1 the more effective the inhibitor in preventing migration.

## **2.6: Cytotoxicity Assays**

### **2.6.1: CellTiter 96® Aqueous One Solution Cell Proliferation Assay**

3-(4,5-dimethylthiazol-2-yl)-5-(3-carboxymethoxyphenyl)-2-(4-sulfophenyl)-2H-tetrazolium (MTS) assays were performed using Promega's CellTiter 96® Aqueous Non-Radioactive Cell Proliferation Assay and 96 well plates. Suspension cells were spun down, and re-suspended in RPMI complete at  $1 \times 10^6$  cells/mL, 100  $\mu$ L of cell solution was placed in each well. (For adherent cells these were seeded into the plate and incubated (37°C, 5% CO<sub>2</sub>) in complete medium overnight to form a monolayer, medium was then pipetted out and 100  $\mu$ L of complete medium per well added). Then for both adherent and suspension cells inhibitors were added at the required concentrations. Each condition/inhibitor was duplicated. Plates were incubated for 4 hours at 37°C before 20  $\mu$ L of the MTS solution was added per well and the plate incubated for 2-5 hours at 37°C. The MTS is reduced by live cells to a red/brown soluble formazan that absorbs at 490 nm. Once sufficiently coloured the plate was read in a BMG Labtech Fluostar OPTIMA fluorometer at 490 nm.

### **2.6.2: Manual Toxicity Assay**

Inhibitors that are chromophores that absorb light at 490 nm can give erroneous results with any absorbance tests. The inhibitor  $\beta$ -ARK-1 was a good example. At 190  $\mu$ M  $\beta$ -ARK-1 no toxicity is detected by MTS assays, yet  $\beta$ -ARK-1 IC<sub>50</sub>, depending on cell type, was nearer 10  $\mu$ M. Manual toxicity assay were undertaken as above (2.6.1) except MTS was not used instead cells are counted manually after required incubation time with inhibitors. 20  $\mu$ L of cell suspension was added to 20  $\mu$ L of Trypan blue 0.4% filtered solution, mixed, incubated (37°C, 5% CO<sub>2</sub>, 15 minutes), then loaded into a haemocytometer and any live cells counted manually. Dead cells stained completely blue, live cells stayed clear.

## **2.7: Fluorescent Phallotoxin (Phalloidin) F-actin Stain**

Twelve well plates were prepared aseptically, each well with one glass cover slip dipped in 70% ethanol. Adherent cells were detached using 0.5mM EDTA/PBS, and sparsely seeded into wells, 500  $\mu$ L complete medium was added to each well and plate incubated overnight to allow cell

attachment and growth on glass coverslips. Complete medium was then removed aseptically and 500µL of medium without additives placed in each well. Inhibitors were added in duplicates and plate incubated (37°C, 5% CO<sub>2</sub>, 30 minutes). Chemokines were then added to one of each duplicate and plate incubated for a further hour. Solutions were then removed, coverslips gently washed with cold PBS, and 100 µL 4% paraformaldehyde added, and plate left at room temperature for 10-15 minutes. Paraformaldehyde was then removed, coverslips gently washed with cold PBS and 100 µL of 0.1% Triton X-100 added for 3-5 minutes. Triton X-100 was then removed, coverslips washed with cold PBS, and 50µL per well of Phalloidin Daylight™488 Conjugated (1 µL per 100 µL cold PBS) added. Plate was covered to exclude light and kept at room temperature for 20 minutes. Phalloidin solution was pipetted off, coverslips were washed once with cold PBS, then if required DAPI staining was undertaken next (see methodology below). Finally coverslips were lifted from wells and mounted face down on a labelled glass slide/s using a spot of DPX mounting medium or PBS/glycerol 50/50 mix and nail varnish to seal edges of coverslip onto glass slide.

#### ***2.8: 4',6-diamidino-2-phenylindole (DAPI) stain***

This can be used after actin or receptor staining, where cells were fixed with paraformaldehyde and permeabilised with 0.1% Triton X-100. 1 µL of DAPI was diluted in 1 mL PBS (300 nM) and 50 µL placed on coverslip in well, plate incubated at room temperature for 5 minutes in dark, DAPI solution removed and wells rinsed three times cold PBS, coverslips were mounted on glass slides as above.

#### ***2.9: Receptor Immunofluorescence staining***

For suspension cells, cells were centrifuged, washed 1 x cold PBS, re-suspended at  $5 \times 10^6$  cells/mL in cold 0.5% BSA in PBS, and primary antibody (1:1000) in 0.5% BSA in PBS added or control (0.5% BSA in PBS). Cells were incubated (4°C, 1 hour) washed twice in cold 0.5% BSA in PBS, before re-suspended in fluorescein isothiocyanate (FITC) labelled immunoglobulin secondary antibodies (1:100 in 0.5% BSA in PBS) for 1 h at 4°C. Cells were then washed twice (0.5% BSA in PBS) and a droplet placed onto a labelled glass slide and a coverslip added before imaging using an inverted Leica DMII fluorescence microscope magnification 500X – 1000X UV excitation 435 nM emission 480 nM. For adherent cells, cells were seeded, as in Phalloidin actin stain above, onto glass coverslips in 12 well plates, incubated overnight (37°C, 5%CO<sub>2</sub>) on coverslips, washed with 0.5% BSA/PBS, then stains and washes were added to wells as described above, and coverslips mounted as in Phalloidin actin stain.

## **2.10: Immunofluorescence staining of cellular proteins**

Twelve well plates were prepared aseptically, each well with one glass cover slip dipped in 70% ethanol. Adherent cells were detached using 0.5 mM EDTA/PBS, and sparsely seeded into wells, 500  $\mu$ L complete medium was added to each well and plate incubated overnight to allow cell attachment and growth on glass coverslips. Solutions were then removed, coverslips gently washed with cold PBS, and 100  $\mu$ L 4% paraformaldehyde added, and plate left at room temperature for 10-15 minutes. Paraformaldehyde was then removed, coverslips gently washed with cold PBS and 100  $\mu$ L of 0.1% Triton X-100 added for 3-5 minutes. Triton X-100 was removed, coverslips washed 3x with cold PBS. Cells were incubated in 1% BSA in PBS + 1% Tween 20 (PBST) for 30 minutes (blocks non-specific binding). Then incubated in desired antibody (1:1000) in 1% PBST in humidified chamber 1 hour RT, before antibody was removed, washed 3x with cold PBS for 5 minutes, secondary antibody (1:1000) in 1% BSA in PBST added, and plate kept 1 hour RT (in dark). Secondary antibody was then pipetted off, coverslips washed with cold PBS (3x 5 minutes), then mounted with drop of DPX, and stored at 4°C in dark, imaged using an inverted Leica DMII fluorescence microscope magnification 500X – 1000X UV excitation 435 nM emission 480 nM.

## **2.11: Transfection of cells**

### **2.11.1: siRNA Transfection**

#### **2.11.1.1: siRNA transfection using AMAXA Nucleofector**

siRNA was prepared by adding 200  $\mu$ L of RNase free siRNA suspension buffer (Qiagen Sciences) to 5 nmol of siRNA to produce 25  $\mu$ M (approximate) stock, tube was centrifuged briefly and placed on the orbital shaker (30 minutes, RT). 2  $\mu$ L of 25  $\mu$ M siRNA stock was added to 198  $\mu$ L RNase free suspension buffer to produce approximate 250 nM stock. Solution concentration was confirmed using Nanodrop readings on the RNA/DNA tab. The average of three RNA readings was used and concentration calculated using formula  $13.4 \text{ ng}/\mu\text{L} = 1 \mu\text{M}$  - formula uses average siRNA mol. wt. = 13,400 g/mol (Dharmacon, UK).

Adherent cells were removed from flasks using 0.5mM EDTA/PBS or suspension cells were harvested. Cells were then counted, centrifuged and re-suspended in electroporation buffer (EPB) containing Hepes 20 mM 4.766 g, NaCl 137 mM 8.0063 g, KCl 5 mM 372.8 mg, Dextrose (D-glucose) 6 mM 1.081 g, Na<sub>2</sub>HPO<sub>4</sub> 0.7 mM 99.372 mg, H<sub>2</sub>O to 1000 mL. The pH was adjusted to 7.5 using KOH to raise pH or HCl to lower pH, before filter sterilising through a 0.22  $\mu$ m Millipore filter.  $3 \times 10^6$  cells were used per 200  $\mu$ L per cuvette (Gene Pulser Cuvette 0.4 cm electrode gap). siRNA was added to cuvette to produce final concentration of 50 nM. Cuvette was treated in



Lonza Amaxa Nucleofector II according to manufacturer's instructions on programme U001, then contents immediately aseptically transferred to pre-warmed complete medium. Suspension cells were grown for 24 hours before chemotaxis or preparation of proteins for western blotting. Adherent cells were seeded directly after AMAXA treatment into 12 well plates prepared for scratch assay. Controls were nonsense siRNA (Scr) also at 50 nM and AMAXA only treatment of cells in absence of siRNA.

#### ***2.11.1.2: Chemical siRNA transfection***

Adherent cells were also transfected with siRNAs using Lipofectamine RNAi (ThermoFisher Scientific) according to manufacturer's instruction. Controls were nonsense siRNA (Scr) also at 50 nM, and transfection agent only treatment in absence of siRNA.

#### ***2.11.2: Plasmid transfection using AMAXA***

Cells were counted, centrifuged and re-suspended at (per cuvette)  $3 \times 10^6$  cells in 200  $\mu$ L electroporation buffer, plus 12.5  $\mu$ L tRNA and 2  $\mu$ g plasmid DNA, with only tRNA as one control. Other controls were 2  $\mu$ g mutant arrestin plasmid or eGFP plasmid. Each cuvette was then placed in turn into the AMAXA and treated on programme U001. Next 250  $\mu$ L warm RPMI was immediately added to each cuvette, then entire contents transferred to 5 mL warmed complete medium. Plates or flasks were incubated for 24 hours (37°C, 5% CO<sub>2</sub>) before use in experiments. Adherent cells were transfected in the same way after detaching from plastic using 0.5 mM EDTA/PBS or were transfected following Lipofectamine DNA (ThermoFisher Scientific) following manufacturer's instructions.

#### ***2.11.3: Fugene or Lipofectamine plasmid transfection for adherent cells***

Previously seeded cells growing on cover slips in a 12 well plate were used, or cells directly seeded onto the plate (for scratch assays). Old medium was removed, replaced with 500  $\mu$ L of medium without supplements, and plate replaced into an incubator to allow 5% CO<sub>2</sub> to acidify medium pH (important for transfection success). Next one Eppendorf with 100  $\mu$ L simple medium for each transfection, plus one as a Fugene or Lipofectamine control was prepared. Then either 3  $\mu$ L of Fugene or 5  $\mu$ L of Lipofectamine was added rapidly, and the Eppendorfs left standing under laminar flow (RT) for 10 minutes, before 1  $\mu$ g of plasmid DNA per Eppendorf was added and again left for 5 minutes under laminar flow (RT). Then the contents of each Eppendorf were added to one well of a 12 well plate along with 200  $\mu$ L simple medium. Plate was incubated (37°C, 5% CO<sub>2</sub>, 4-8 hours) then 500  $\mu$ L of complete medium added to each well. A check for fluorescence (UV excitation 435 nM emission 480 nM) was carried out at 24 hours.

## **2.12: Plasmid technology**

### **2.12.1: DH5α *Escherichia Coli* transformation**

2 ng of relevant plasmid was added to 50 µL of freshly thawed DH5α *E. coli* on ice, tube flicked gently 4-5 times to mix, incubated (4°C, 30 minutes), heat shocked (42°C, 30 seconds), placed on ice (4°C, 2 minutes), tube incubated (37°C, 40 minutes), tube flicked gently every 5 minutes. Agar petri plates were prepared using agar containing the relevant antibiotic (10 µg/mL kanamycin for arrestin plasmids), plates were inoculated using sterilised spreader, incubated overnight (37°C), colony collected and transferred to bacterial fermentation (2.12.2).

### **2.12.2: Bacterial fermentation for plasmid DNA harvesting**

One litre of Luria Broth (LB), was prepared and sterilised (by autoclaving), 10mg/mL of antibiotic relevant to resistant gene in plasmid (Kanamycin used for arrestin plasmids) added aseptically once broth cool.

100 mL conical flask/s were sterilised, using foil to cover tops, then to each 20 mL LB/ kanamycin broth added, plus 20 µL DH5α *E. coli* carrying plasmid to each flask, flasks were placed on shaker to oxygenate at 37 °C for 12-24 hours until contents became cloudy, (aliquots of this cloudy culture were frozen for later use). 10 mL of the first culture was then transferred to sterile LB broth + Kanamycin 10 µg/mL (150 mL) in a 250 mL sterile foil covered conical flask, then shaken overnight at 37 °C. Content of flask were then centrifuged to pellet bacteria in 50 mL tube/s (4000 rpm 5 minutes), supernatant discarded and pellet then processed or stored at -20°C, for later purification (2.12.3).

### **2.12.3: Plasmid Purification (Qiagen Plasmid Midi Kit method)**

Qiagen Midi Kit protocol was followed using buffers provided briefly: 4 mL Buffer P1 was added to each 50 mL tube to lyse bacteria, pipetted up and down to create a suspension then the lysis mix transferred into the next 50 mL tube containing a bacteria pellet, process was repeated for up to four pellets. 4 mL of Buffer P2 (contains NaOH and SDS) to 4 mL of re-suspended cells in P1 was gently added. Tube lid put on and tube inverted two or three times, before waiting 3 minutes. Then 4 mL buffer P3 (contains Acetic Acid) which neutralises and precipitates proteins was added and tube shaken vigorously 2-3 times, then centrifuged (4000 rpm 5 minutes). A Qiagen Plasmid Midi Kit column was suspended over a new 50mL centrifuge tube, and equilibrated by adding 5 mL of QBT Buffer. Once QBT had run through the column centrifuged tube was carefully lifted from centrifuge, it contained a white pellet of protein below and above a clear solution. Tube was poured carefully into equilibrated column so that the clear solution went into the columns the white pellet and surface should stay in centrifuge tube. Clear solution was allowed to run through

column and the eluate discarded, as plasmid DNA had bound solid phase in column. Once all supernatant from bacteria proteins had run through column was filled with QC wash buffer, and again eluate discarded. Column was then suspended over a new 50 mL tube, and 5 mL QF elution buffer added to elute DNA off column, eluate was collected then column discarded.

3.5 mL isopropanol was added to 5 mL eluted DNA solution in centrifuge tube (5 mL x 0.7 = 3.5 mL) tube capped and tipped 3 or 4 times, then centrifuged (4°C, 4000 rpm, 1 hour). Supernatant was then poured off, 1 mL 70% ethanol added to pellet without mixing, and tube centrifuged (4°C, 4000 rpm 15 minutes), before ethanol was tipped off and tube inverted onto tissue to drain (RT, 1 hour). DNA pellet was then re-suspend in sterile distilled H<sub>2</sub>O (200-500 µL), nano-dropped for DNA concentration and then diluted if necessary in water down to 1 µg/µL, before freezing (-20°C). Alternatively pellet was re-suspend in TrisEDTA buffer and solution stored at 4°C.

#### ***2.12.4: Confirming DNA on Agarose Gel***

The DNA digest mixture was set up as follows: 2 µL of plasmid DNA, 1 µL of 10x HIND3 buffer, 1 µL enzyme HIND3 restriction enzyme (in glycerol), 6 µL water, mixture was incubated (1 hour, 37°C). Agarose Gel was prepared and run as follows: 50 x TAE buffer was mixed containing: Tris Base 24.218g, Sodium acetate 2.05g (water free), EDTA 1.86 g, Acetic acid 5 mL, Water to 100 mL. The agarose gel was made by heating 0.1 g Agarose with TAE to 100 mL, solution was cooled, 2 µL non-toxic DNA dye added, before gel was poured into mould to set. Loading buffer was added to each sample, then sample/s, and a DNA ladder to check plasmid size, loaded into gel wells.

#### ***2.13: Peptide synthesis***

Two 15 mer peptides were synthesized on a Multisynthtech Syro I automated peptide synthesiser using standard N $\alpha$ -Fmoc-based solid-phase peptide synthesis, an active peptide called W56 with the sequence VDGKPVNLGLWDTAG and an inactive peptide called F56 with the sequence VDGKPVNLGLFDTAG. The synthesis was carried out on a NOVA PEG Rink amide polystyrene resin (substitution: 0.49 mmol/g) employing methodology similar to that described by Malkinson [496], varying only in that Fmoc de-protection was carried out with 40% piperidine (1 x 10 minutes) and 20% piperidine (2 x 5 minutes). Next the peptides were cleaved from the resin by shaking the resin beads in 5 mL trifluoroacetic acid (TFA), water and triisopropylsilane (TIPS) mixture i.e. TFA/H<sub>2</sub>O/TIPS (95:2.5:2.5% v/v) solution for 3 hours. The beads were then filtered from the solution and washed with neat TFA then combined with TFA/H<sub>2</sub>O/TIPS (95:2.5:2.5% v/v) which was then evaporated under vacuum. The crude peptide was then precipitated with cold diethyl ether before being filtered. The peptides were purified using reverse phase chromatography on a

Biotage Isolera Four (SNAP Cartridge KP-C18-HS 12 g) using two phases. Mobile phase A: 5% methanol in H<sub>2</sub>O + 0.05% TFA. Mobile phase B: 5% H<sub>2</sub>O in methanol + 0.05% TFA. The gradient employed was 0→100%B over one hour. Next the fractions containing the peptides were evaporated under vacuum, and the peptides dissolved in purified water before being freeze dried. Peptide purity was examined using analytical HPLC (column ZORBAX Eclipse XBD-C18) Mobile phase A: H<sub>2</sub>O + 0.05% TFA. Mobile phase B: methanol + 0.05% TFA. Gradient 5→95%B over 20 minutes; the peptides were found to be ≥ 90% pure. Finally the mass of the peptides was examined using MALDI mass spectrometry, the active W56 peptide gave readings of (M+Na, 1562) and (M+K, 1578), and the control F56 peptide readings of (M+Na, 1523) and (M+K, 1539).

#### **2.14: SDS-PAGE and Western blot**

##### **2.14.1 Total protein extraction for Western Blot**

Unless otherwise stated cells were exposed to treatment with inhibitors or controls (30 minutes, at 37°C, 5% CO<sub>2</sub>) then to chemokines at 5 nM or H<sub>2</sub>O control (15 minutes at 37°C, 5% CO<sub>2</sub>), before cells were harvested, washed (ice-cold PBS), re-suspended in minimum volume of ice-cold PBS, before an equal volume of Mammalian Protein Extraction Buffer (GE Healthcare), with 5 mM Dithiothreitol (DTT) was added. Solutions were then rapidly mixed (using Gilson), and Eppendorfs kept on ice for 40 minutes, vibrated every 5 minutes to mix, then centrifuged (10 minutes, 13,000 rpm, 4°C), then the clear supernatant was pipetted into fresh Eppendorfs, which were kept on ice. Supernatant protein concentrations was analysed at 280 nm absorbance (Nanodrop Spectrometer ThermoFisher Scientific). The average of 3 readings were recorded as protein content, proteins were used immediately or flash frozen and store at -20°C. The volumes of protein extracts required to give equal protein content (µg) in all lanes were calculated, mixed 50:50 with 2xSB buffer + 5 mM DTT, boiled 5 minutes, spun briefly to return condensation to solution, and loaded onto a 10% Acrylamide gel.

##### **2.14.2: Gel preparation for Western Blot**

Using BioRAD system, glass plates were cleaned with 70% ethanol, fixed into holder, and 10% gels prepared (ideal separation for ~30-90 kDa proteins), then upper gel added with 10 well combs.

Bottom gel (10%) contained: 6 mL H<sub>2</sub>O, 3.7 ml Bottom gel stock (hydroxymethyl aminomethane aka Tris 90.75g, 20% SDS 10ml, pH to 8.8 water to 500ml), 5ml Bis-acrylamide (30% acrylamide), 130 µL 10% ammonium persulfate (APS), 13 µL TEMED. Solution was mixed, rapidly pipetted between prepared plates, and immediately overlaid with water and left until set.

Upper gel contained: 600  $\mu$ L Upper gel stock (Tris 12.11g, SDS 20% 4mL, pH to 6.8 water to 200 mL), 4.25 mL  $H_2O$ , 1 mL Bis-acrylamide, 75  $\mu$ L APS 10%, 7.5  $\mu$ L TEMED, Solution was mixed, pipetted into gap above bottom gel, comb inserted immediately, then left to set.

BioRAD electrode chamber was set up with gel plates and running buffer (Laemmli buffer) containing: Tris 17.5g, Glycine 72g, 5g sodium dodecyl sulfate (SDS),  $H_2O$  to 5 Litres. Combs were removed, 5  $\mu$ L of pre-stained protein ladder (Thermo Scientific #26612), 20-120 kDa, loaded in well 1, and then prepared protein samples in wells 2-10 as needed. BioRAD was operated at 25 amps until proteins had advanced close to base of gels.

#### ***2.14.3: Protein transfer to membrane***

Using PVC gloves Whatman Protran pore 0.45  $\mu$ m nitrocellulose membrane was cut to size, labelled, soaked (30 minutes  $H_2O$ ), gel was extracted from glass plates and sandwiched with membrane between ten blotting paper layers, laid on semidry blotter and soaked with transfer/blotting buffer containing: 14.4 g Glycine, 3 g Tris, 200 ml Methanol, 2.5 mL 20% SDS, water to 1 L. BioRAD semi-dry blotter was assembled and run at 10 volts for 2 hours. Membranes were then extracted, washed TBST, and blocked in 5% BSA/TBST, or 5% dried skimmed milk/TBST for one hour RT in 50 mL centrifuge tubes. TBST contained: 2.4 g Tris Base, 8.8 g NaCl, 1 mL Tween 20,  $H_2O$  to 1000 mL (pH 7.6).

#### ***2.14.4: Primary antibody labelling***

Blocking solution was poured off, 5mL primary antibody diluted (usually 1:1000) in 5% BSA/TBST added, and tube was rolled at RT for 2 hours or 4°C for 12 hours. Then the primary antibody solution was removed the membrane washed with TBST (3 x 5 minutes), drained, rolled with 5 mL species specific horseradish peroxidase diluted in 5% BSA/TBST, or 5% dried skimmed milk/TBST (usually 1:20,000, 1 hour). Horseradish peroxidase solution was then drained off, membrane washed TBST (3 x 5 minutes), membrane blotted then covered with Pierce® ECL Western Blotting Substrate mix, (RT, 3 minutes) blotted, placed between two pieces of clear acetate and imaged in camera (G-BOX SynGene Imager using Gene Snap Software).

#### ***2.14.5: Loading confirmation***

Membranes were stripped by either rolling with Millipore Stripping Solution (Millipore, Temecula California) for 20 minutes, followed by 3 washes (TBST) then re-blocked 5% BSA/TBST or 5% Milk/TBST (1 hour) or using Stripping buffer (7.5 g Glycine, 0.5 g SDS, 5 mL Tween 20, water to 500 mL pH to 2.2 with concentrated HCl). Membrane was placed in stripping tray, covered with stripping buffer, shaken (10 minutes), step repeated with fresh stripping solution, membrane washed twice with PBS by shaking in tray (2 x 10 minutes), washed twice with TBST (2 x 5

minutes), membrane placed in tube and blocked with 5% BSA/TBST or 5% Milk/TBST for 1 hour then treated with loading control e.g. Beta-actin.

### ***2.15: Immunoprecipitation of CCR5 receptor***

1 x 10<sup>7</sup> THP-1 cells were centrifuged, washed 2 x cold PBS, and 1 mL of lysis buffer (150 mM NaCl, 20 mM Tris, 20 mM EDTA, with 0.5 mL polyoxyethylene 10 oleoyl ether (Brij 97), plus 1 protease inhibitor tablet per 50 mL) added. Cells were pipetted up and down to lyse, left suspended in lysis buffer (40-60 minutes 4°C) with gently mixing. Centrifuged 17,000g in Eppendorfs (4°C, 25 minutes) to produce a white pellet of nuclear proteins, pellet was discarded and the supernatant put into two Eppendorfs (labelled CCR5 and control). 500 µL (5 µg) Rat HEK/1/85a/7a CCR5 antibody was added to 500 µL supernatant for active, and 5 µg control (Rat IgG isotype) protein to control. Eppendorfs were left on ice (4°C, 1 hour). Next G-sepharose was prepared (using G-sepharose for rat antibodies as A-sepharose will not bind rat). G-sepharose was centrifuged (13,000 rpm, 2 minutes), supernatant pipetted off. G-sepharose pellet washed in cold PBS twice. 200 µL G-sepharose diluted with 200 µL cold PBS making a slurry. 25 µL G-sepharose slurry was added to 25 µL supernatant for active and for control mixtures, then Eppendorfs put on turning device overnight for 14 hours (4°C), or left in fridge overnight and turned for 1 hour (RT) in morning. Eppendorfs were wrapped in Parafilm to stop evaporation. Eppendorfs were centrifuged (13,000 rpm 2 minutes). Pellet washed 4 X with 1 mL ice cold lysis buffer (without pipetting up and down, mix re-suspended itself (care with pellet, just to take off most of supernatant). After last wash tube was centrifuged (13,000 rpm, 3 minutes), supernatant discarded with care. Pellet was re-suspended in 20 µL sample buffer, boiled for 5 minutes, centrifuged, and supernatant loaded onto Western gel as above. Gel was transferred to nitrocellulose membrane as above. Membrane was blocked with 5% Milk/PBS for 1 hour, rolled with 1 mL HEK/1/85a/7a CCR5 antibody in 25 mL 5% milk/PBS for 1 hour, washed (3 x 5 minutes) cold PBS. Rolled with Rat Horseradish Peroxidase 5 µL in 25 mL 5% milk/PBS for 1 hour washed (3 x 5 minutes) cold PBS, then visualised using Pierce® ECL solution following manufacturer's instructions.

### ***2.16: Analysis of intracellular calcium ion flux***

Cells were harvested, centrifuged, washed in calcium flux buffer (NaCl 137 mM, KCl 5 mM, MgCl<sub>2</sub> 2 mM, CaCl<sub>2</sub> 1.5 mM, HEPES 10 mM, D-Glucose 25 mM pH to 7.4) and re-suspended in calcium flux buffer. Fura2 (2 µM) was mixed with cells and cell solution aliquoted into 200 µL portions in Eppendorfs, inhibitors or controls were added, Eppendorfs were incubated (30 minutes, 37°C,

5%CO<sub>2</sub>). Then using calcium flux buffer, cells were washed twice before being re-suspended at 2x10<sup>6</sup> cells/mL. 100 µL aliquots from each 200 µL sample were pipetted into two wells in a black 96 well plate producing duplicates. Fluorescence was measured in response to a 20 µL injection of a 100 nM chemokine solution giving a final concentration of approximately 16.7 nM (unless otherwise stated), added either 15 or 30 seconds after incubation. Calcium mobilisation was measured by a BMG Labtech Fluostar OPTIMA fluorimeter, or calcium mobilisation and Area Under Curve (AUC) of mobilisation trace by a Flexstation III ROM V3.0.22 (Molecular Devices Ltd, Wokingham, UK) using SoftMax Pro, Excel and GraphPad Prism. Fura2-AM binds free intracellular calcium; it absorbs and is excited by wavelengths 340 nm and 380 nm and emits at 510 nm, and the 340/380 ratio allows the measurement of intracellular calcium concentrations. Using ratios eliminates any effects of uneven dye loading or leakage, and photo-bleaching. Results are displayed as either as a 340/380 ratio trace or as bar charts (n≥3) showing changes in fluorescence ratio i.e. peak fluorescence with chemokine minus basal fluorescence before chemokine addition, mean ± SEM, or as Area Under Curve (AUC), mean ± SEM.

### ***2.17: Internalisation assay and flow cytometry analysis***

Cells were harvested, allowing 50 x 10<sup>4</sup> cells per sample, cells were suspended at 5 x 10<sup>5</sup> cells/mL in 0.1% BSA/RPMI with inhibitors or vehicle control at either 37°C or 4°C for 30 minutes, then were treated with CXCL12 (15 nM) or control (H<sub>2</sub>O) at either 37°C or 4°C for 15 minutes. Cells were then washed with ice-cold 0.5% BSA/PBS, and re-suspended in 0.5% BSA/PBS containing anti hCXCR4 clone 12G5 antibody from R&D Systems (1:2000) or control (0.5% BSA/PBS) for 1 hour at 4°C. (NB. An alternative and better control would have been isotype control antibody.) Cells were then washed 3 times with ice-cold 0.5% BSA/PBS, then re-suspended in 0.5% BSA/PBS containing 1:500 mouse fluorescein isothiocyanate (FITC)-conjugated anti-mouse IgG antibody for 1 hour at 4°C. Stained cells were centrifuged, washed, and re-suspended in 300 µL 0.5% BSA/PBS, gated to exclude dead cells using FSC versus SSC and quantified using a FACS Calibur, and data analysed using CellQuest software version 3.1 (Becton Dickinson, San Jose, CA).

### ***2.18: Cyclic Adenosine Monophosphate (cAMP) Assay***

Cyclic Adenosine Monophosphate (cAMP) assays were performed following Molecular Devices kit instructions and using CatchPoint buffers and protocols for cAMP analysis. Cells were harvested, allowing 8 x 10<sup>4</sup> cells per well, cells were re-suspended at 2 x 10<sup>6</sup> cells/mL in 0.1% BSA/RPMI, aliquoted into Eppendorfs and treated with inhibitor or vehicle control for 15 minutes (37°C, 5%, CO<sub>2</sub>). Cells were centrifuged, washed once in Krebs-Ringer bicarbonate buffer KRBG (D-Glucose

1.8 g,  $\text{MgCl}_2 \cdot 6\text{H}_2\text{O}$  0.1 g, KCl 0.34 g NaCl 7.0 g,  $\text{Na}_2\text{HPO}_4$  0.1 g,  $\text{NaH}_2\text{PO}_4 \cdot 2\text{H}_2\text{O}$  0.234 g,  $\text{H}_2\text{O}$  to 1 Litre, pH to 7.4), sterilised with 0.22  $\mu\text{m}$  Millipore filter, pelleted and then re-suspended in stimulation buffer (0.75 mM 3-Isobutyl-1-methylxanthine (IBMX) in KRBG) at  $2 \times 10^6$  cells/mL and incubated for 10 minutes RT. Cells were pipetted gently to re-suspend and 40  $\mu\text{L}$  added to desired wells of a 96 well round-bottomed plate. 2 mL of 60  $\mu\text{M}$  Forskolin in PBS was prepared, and 20  $\mu\text{L}$  (or 20  $\mu\text{L}$  PBS for control) pipetted onto cells in wells, plate was gently agitated to mix and incubated (37°C, 5%  $\text{CO}_2$ , 15 minutes). Chemokines to produce 10 nM (6  $\mu\text{L}$  of 100 nM CXCL12, 6  $\mu\text{L}$  of 1  $\mu\text{M}$  CCL3 or 6  $\mu\text{L}$   $\text{H}_2\text{O}$  for controls), were then added for set periods (20 minutes, 10 minutes, 5 minutes and 1 minute), wells were gently agitated. Next 20  $\mu\text{L}$  lysis buffer was added to all wells and plates incubated for 10 minutes on a shaker to lyse cells. Samples were then transferred to a CatchPoint cAMP 96 well assay plate, and the cAMP protocol was followed exactly using CatchPoint buffers to produce both a standard curve, and analyse the samples. Results were read at excitation 530 nm, emission 585 nm, cut off 570 nm, gain 20%, using Flexstation III ROM v3.0.22.

### **2.19: Rac1 Activation Assay**

Cells were serum starved for 24 hours, treated at 37°C with inhibitors for 30 minutes then with 10 nM CXCL12 for 15 minutes. Cells were then washed with ice cold PBS, then lysed on ice using Cytoskeleton Rac1 Activation Assay Biochem Kit supplied Cell Lysis Buffer (50 mM Tris pH 7.5, 10 mM  $\text{MgCl}_2$ , 0.5 M NaCl, 2% Igepal) plus 1x protease inhibitor cocktail (100x contains 62  $\mu\text{g}/\text{mL}$  Leupeptin, 62  $\mu\text{g}/\text{mL}$  Pepstatin A 14 mg/mL Benzamidine, 12 mg/mL tosyl arginine methyl ester). Cells were harvested with a cell scraper and cells transferred to ice cold pre-labelled Eppendorfs, centrifuged (13,000 rpm 1 min), then the clarified lysate was collected, transferred to ice cold labelled tubes and flash frozen using dry ice and ethanol mix. 20  $\mu\text{L}$  was retained of each sample for protein quantification using Nanodrop analysis. 800  $\mu\text{g}$  protein in 800  $\mu\text{L}$  lysis buffer per sample was used in Rac1 Activation pull down assay along with 10  $\mu\text{g}$  of PAD-PBD beads following Cytoskeleton protocol. Briefly protein samples were rolled with beads (4°C, 60 minutes), centrifuged (3000 g, 4°C, 1 minute), 90% supernatant removed. Beads washed with 500  $\mu\text{L}$  wash buffer for 30 seconds, centrifuged (3000g, 4°C, 3 minutes), supernatant removed without disturbing beads, 15  $\mu\text{L}$  of 2X Laemmli sample buffer (125 mM Tris pH 6.8, 20% glycerol, 4% SDS, 0.005% bromophenol blue, 5 %  $\beta$ -mercaptoethanol) added. Samples were boiled 2 minutes, then beads and samples were loaded together into gel lanes (beads stayed in well and only the proteins moved down gel). His-Rac1 control protein was run with samples. On a second gel 10  $\mu\text{g}$  of protein per sample was run for analysing total Rac. The samples were separated on 10% gels



and electrophoretically transferred to a nitro-cellulose membrane as described in detail above. The membranes were blocked with 5% non-fat powdered milk in TBST (30 minutes, RT), then incubated at 4°C overnight with 1:500 anti-Rac1 antibody (ARC03) in TBST, (no blocker) then rinsed (50 mL TBST, 1 minute) and then incubated with 1:10,000 goat anti-mouse HRP conjugate in TBST (1 hour, RT) (with no blocking agent), then membrane washed with TBST (5x10 minutes). The blots were developed using Pierce® ECL western blotting substrate (ThermoFisher Scientific) as per manufacturer's instructions.

### ***2.20: Enzyme linked immunosorbance assay (ELISA)***

Using InstantOne™ STAT3 phosphotyrosine 705 ELISA eBiosciences, UK according to protocol THP-1 cells were harvested, centrifuged and re-suspended at  $1 \times 10^6$  cells/200  $\mu$ L in simple DMEM per Eppendorf, treated with inhibitor or control (1% DMSO), incubated (37°C, 5% CO<sub>2</sub>, 30 minutes), then CXCL12 was added to the relevant samples to produce a final concentration of 5 nM and incubated (37°C, 5% CO<sub>2</sub>, 0, 1, 5 or 10 minutes). Cells were washed once with cold PBS, centrifuged and supernatant removed from pellet. 50  $\mu$ L of supplied 1X lysis buffer was added per pellet, mixed and shaken (RT, 10 minutes, 140 rpm). Then 50  $\mu$ L of lysate was added to each well of ELISA plate with 50  $\mu$ L of kit antibody cocktail. Plate was shaken (RT, 60 minutes 140 rpm). Samples were then washed with kit buffer (3 x 200  $\mu$ L) and 100  $\mu$ L pre-equilibrated detection reagent added to all wells and plate incubated (RT, 30 minutes, covered). 100  $\mu$ L of the supplied stop reagent was added to all wells and the plate was read at 450 nM using BMG Fluostar OPTIMA fluorimeter.

### ***2.21: Analysis of data***

Chemotaxis, Calcium and MTS data were analysed using one-way ANOVA followed by Bonferroni post hoc tests, or when only two samples were being compared by Students t-Test. Throughout a p value greater or equal to 0.05 was considered significant and represented on graphs and figures as one star (i.e. \* =  $p \leq 0.05$ ), two stars was considered very significant (\*\* =  $p \leq 0.01$ ), and three stars highly significant (\*\*\*) =  $p \leq 0.001$ ). Data represent the mean  $\pm$  standard error of mean, of at least three independent experiments. GraphPad Prism 4 (GraphPad Software Inc Ca, USA) was used for all statistical tests.

## **Chapter 3: Exploring the intricacies of dynamin function in malignant cell migration**

### **3.1: Introduction**

For a receptor to internalise an endocytic vesicle needs to form from the cell membrane. This requires the recruitment of several cytosolic proteins including the ~98 kDa GTPase dynamin. Dynamin is purported to aid the scission of vesicles from the membrane by forming helical oligomers around the necks of budding vesicles, before GTP hydrolysis creates conformational change in the dynamin polymer producing vesicle/membrane fission. However this is not dynamin's only role in cellular function [163, 164], dynamins are also involved in cytokinesis, organelle division, pathogen resistance and transport vesicle budding [165]. Dynamin other important cellular functions including roles in signalling and the endocytosis of receptors [164, 497].

There are many dynamin splice variants and 3 key isoforms, Dynamin-1, -2 and -3. Dynamin-2 is ubiquitous [166-168]. The closely related Dynamin-like proteins (DLP) include Dynamin-related-protein one (Drp-1), mitofusin (Mfn), and Optic Atrophy protein 1 (OPA1) involved in the mitochondrial fission and fusion essential for cell division [170, 498]. The dynamin protein contains five regions including a Pleckstrin homology (PH) and GTPase domains. Dynamin monomers form dimers which can then oligomerise to produce constricting rings round endosomal vesicles containing receptors which cause vesicle scission [165, 497]. Dynamin-1, -2 and -3 have differing abilities to curve membranes to produce endosome fission [177-179]. The pathways and fates of endocytic vesicles can qualitatively and quantitatively control downstream signalling and cellular responses that mediate cancer prognosis and metastasis. Endosome cargo such as specific GPCRs can influence sorting decisions between recycling to cell surface and ubiquitination and degradation [193-195]. Endosomes can also contain signalling platforms such as GPCR/ $\beta$ -arrestin complexes that can trigger signalling favouring malignancy [196, 198, 199]. Endocytosis can be clathrin-dependent or independent; dynamin plays a role in both [189]. Dynamin may rate-limit the former and, along with EndophilinA and F-actin, facilitate vesicle scission in the later, along with signalling through Pi3K, Rho and Rac [221-224]. Aberrant function of dynamin and DLPs such as Drp-1 are implicated in metastasis [226]. Dynamin-2 interactions with oncogenes expressed in many cancers can activate CXCL12 signalling through Akt, JAK and Rac1 favourable to metastasis [229-234]. Drp-1 drives mitosis in many cancers. Drp-1, OPA-1 and Mfn modulate mitochondrial fission and fusion in cell division. Drp-1 inhibition can increase malignant cell apoptosis and decrease cell proliferation [235, 236]. Thus dynamin plays

importance roles both in homeostasis and malignancies. What is less well understood is dynamins role in metastasis supported by chemokines. This work explored the role of dynamin in malignant cell migration through chemotaxis assays in THP-1 monocytes and Jurkat T-cells, along with wound-healing assays of chemokinesis in MCF7 breast cancer cells.

**Hypothesis:** Dynamin supports chemotactic migration of cancer cells; therefore inhibition of dynamin may prevent metastasis.

**Aim:** To expose the role of dynamin in CCL3 and CXCL12-chemotactic migration in cancer cell-lines THP-1 and Jurkat along with dynamins role in CCL3 and CXCL12 supported wound-healing in MCF7.

**Objectives:**

- (i) Establish the presence of CCR5 and CXCR4 in cell-lines.
- (ii) Establish that dynamin is expressed in THP-1, Jurkat and MCF7.
- (iii) Explore the effects of siRNA knockdown of dynamin in THP-1, Jurkat and MCF7.
- (iv) Observe the effects of a range of small molecule inhibitors of dynamin on chemotaxis in Jurkat and THP-1 looking for any chemokine and/or dynamin domain-specific effects.

### **3.2: Results**

Please note controls are common between graphs where experiments were conducted simultaneously; results for each inhibitor have been displayed separately for ease of description of results, this applies to: figures 3.8 and 3.15; 3.16 and 3.19; 3.23 and 3.24.

#### **3.2.1: The expression of CXCR4 and CCR5 in cell-lines**

First the expression of CXCR4 in THP1, Jurkat and MCF7 was examined by flow cytometry, levels appeared highest in Jurkat, figure 3.1.

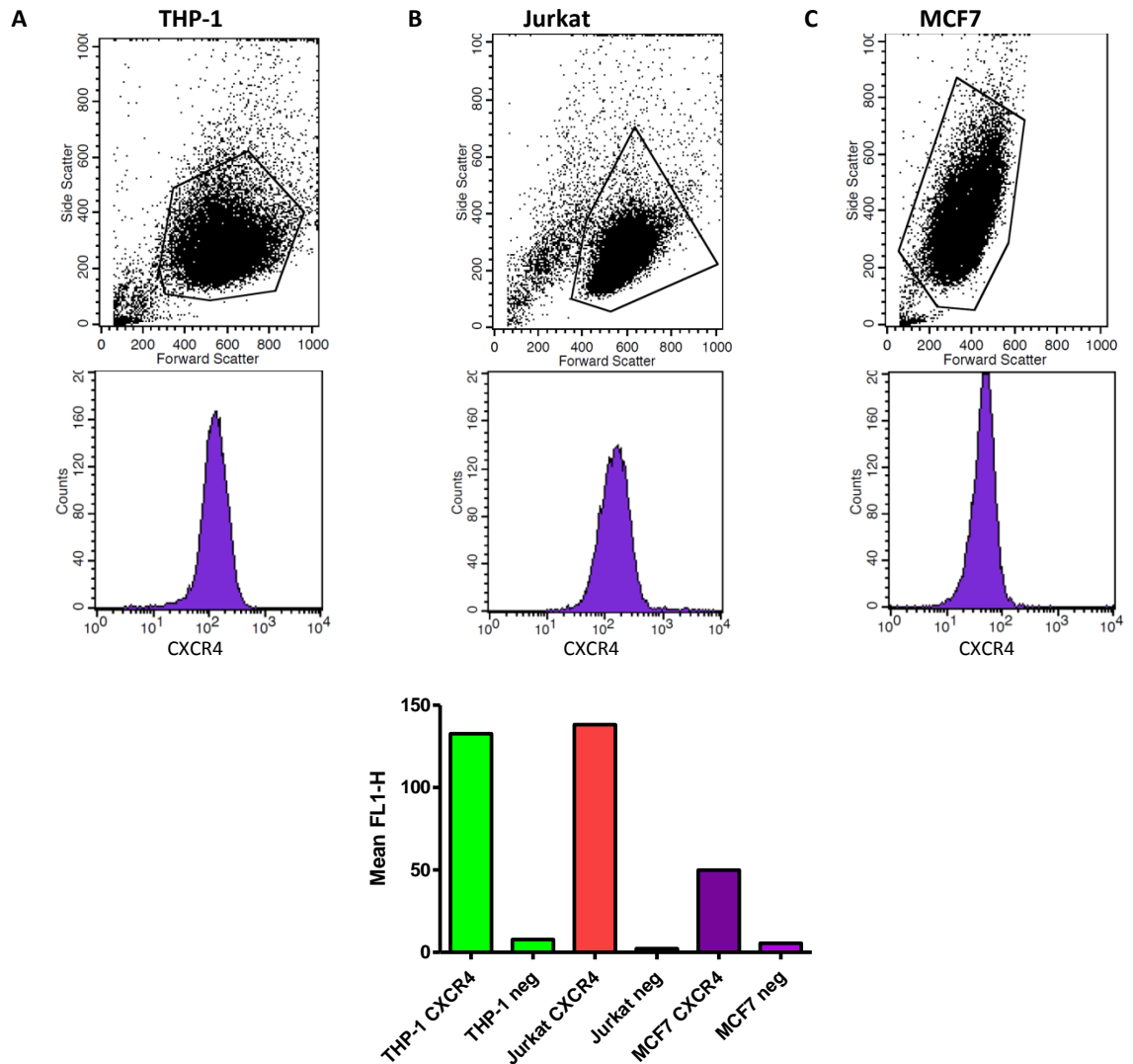


Figure 3.1: CXCR4 expression in (A) THP-1, (B) Jurkat and (C) MCF7. Flow cytometry analysis of 20,000 events following incubation with 12G5 (10  $\mu$ g/mL, 60 mins, 4°C) then FITC (1 in 500, 60 mins, 4°C), n=1.

CXCR4 and CCR5 receptors were then visualised on MCF7 and THP-1 cells by immunofluorescence, figure 3.2.

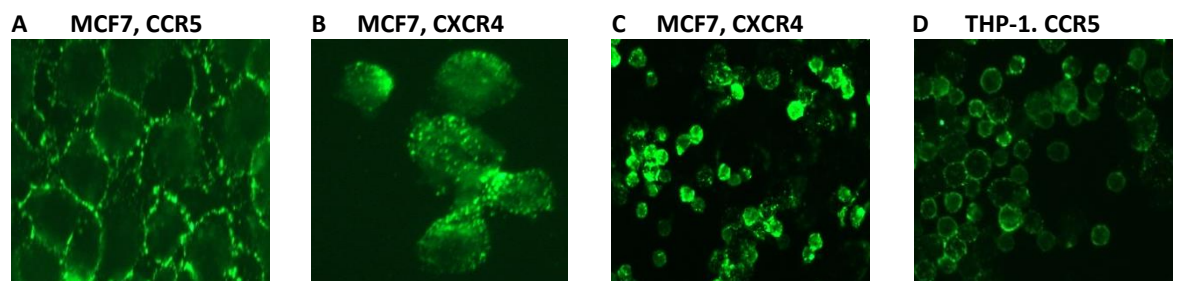


Figure 3.2: Anti-CCR5 (HEK/1/85a/7a) antibody (1hr, 4°C) followed by FITC (1 hr, 4°C) confirm expression of CCR5 on (A) MCF7 and (D) THP-1. Anti-CXCR4 (12G5) (1hr, 4°C) followed by FITC (1hr, 4°C) confirms expression of CXCR4 on (B) MCF7 and (C) THP-1. Imaged UV inverted microscopy (Leica DMII Fluorescence microscope 500x Ex 490 nm, Em 520 nm).

The presence of CCR5 in THP-1 was demonstrated using Immunoprecipitation as expression is relatively low, and in CHO.CCR5 by immunofluorescence and Western blot, figure 3.3.

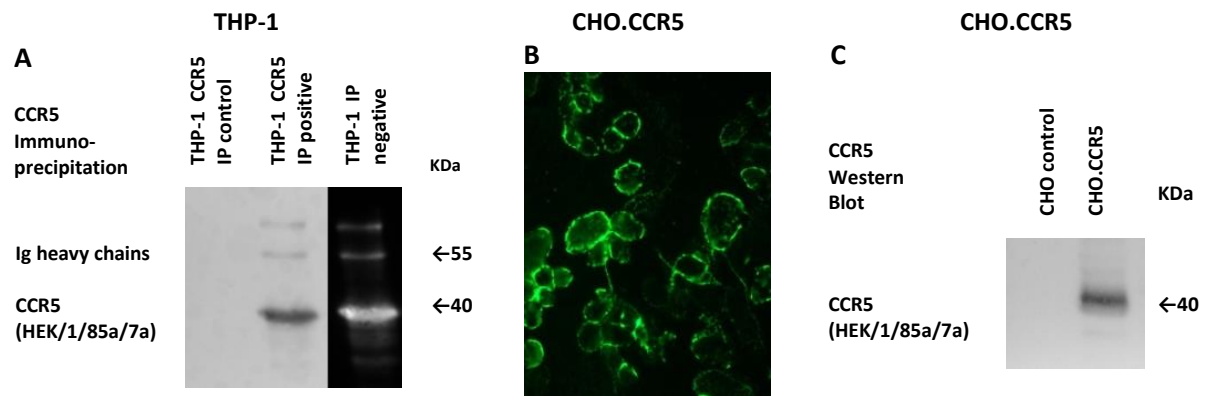


Figure 3.3: Anti-CCR5 (HEK/1/85a/7a) antibody reveals presence of CCR5 in (A) THP-1 using IP (C) CHO.CCR5 using western blot. (B) CHO.CCR5 using immunofluorescence, HEK/1/85a/7a (1hr, 4°C) followed by FITC (1hr, 4°C) Imaged UV inverted microscopy (Leica DMII Fluorescence microscope 500x Ex 490 nm, Em 520 nm).

CCL3 may illicit responses through binding CCR1 or CCR5. Inhibition of CCR1 using J113863, or CCR5 using Maraviroc both significantly inhibit chemotaxis of THP-1 to CCL3, suggesting both receptors were expressed by THP-1, and relevant to CCL3-induced chemotaxis, figure 3.4.

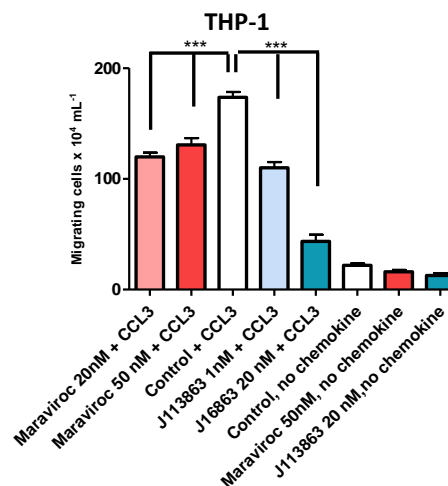


Figure 3.4: Chemotaxis of THP-1 to 1 nM CCL3 following pre-treatment with CCR1 inhibitor J113863 or CCR5 inhibitor Maraviroc or control (DMSO). Means  $\pm$  SEM, one-way ANOVA, post-hoc Bonferroni,  $n \geq 3$  independent experiments, \*\*\*= $p < 0.001$

### 3.2.2: Exploring the role of dynamin in cell-lines

Next the presence and location of dynamin in cell-lines was established using immunofluorescence. The effects of dynamin siRNA knockdown, and various small molecule inhibitors of dynamin, such as Dynasore (a small molecule inhibitor of both dynamin, and at lower concentrations, Drp-1 [499]) were explored, using CCL3 and CXCL12-induced chemotaxis in THP-1, CXCL12 chemotaxis in Jurkat, and wound-healing in MCF7.

### 3.2.3: Immunofluorescence established dynamin's presence

Although dynamin plays roles at the membrane and in the cytoplasm, figure 1.4, dynamin-2 appeared more concentrated in nucleus than membranes of THP-1 and MCF7, figure 3.5, possibly because both are cancer cell-lines.

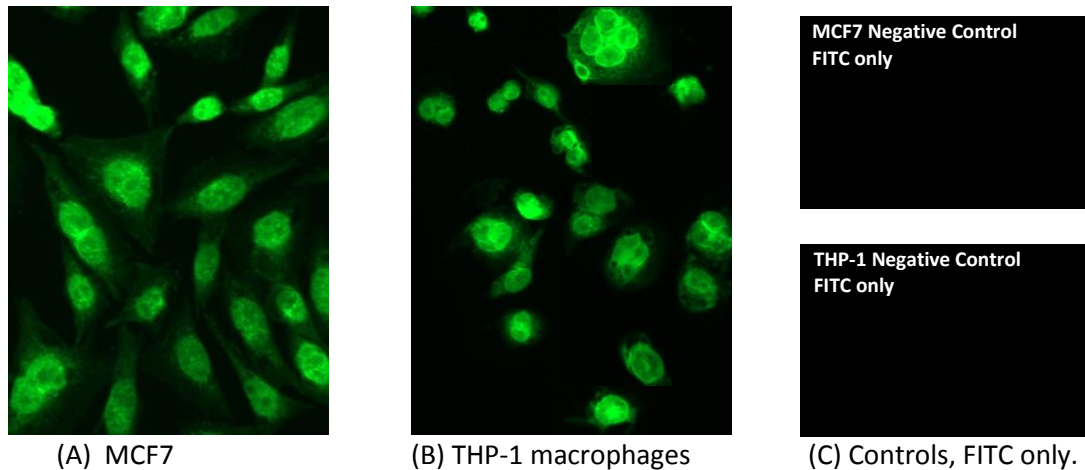


Figure 3.5: Dynamin-2 immunofluorescent staining. (A) THP-1, pre-treatment 25 nM PMA or (B) MCF7, grown on glass for 24 hours, fixed (4% paraformaldehyde), incubated with anti-dynamin-2 then probed with FITC. Imaged UV inverted microscopy (Leica DMII Fluorescence microscope 500x Ex 490 nm, Em 520 nm).

Immunofluorescent staining on adherent MCF7 and THP-1 after differentiation to macrophages demonstrated that Dynamin-2 was present in both, figure 3.5. Jurkat, a suspension cell-line were not successfully differentiated, however dynamins presence in Jurkat was clearly demonstrated by Western Blot, figure 3.6 below.

### 3.2.4: Dynamin-2 siRNA knockdown inhibits wound-healing but not chemotaxis

Dynamin-2 knockdown with siRNA in THP-1 and Jurkat cells had no significant inhibitory effect on chemotaxis to CCL3 and CXCL12 respectively, figure 3.6.

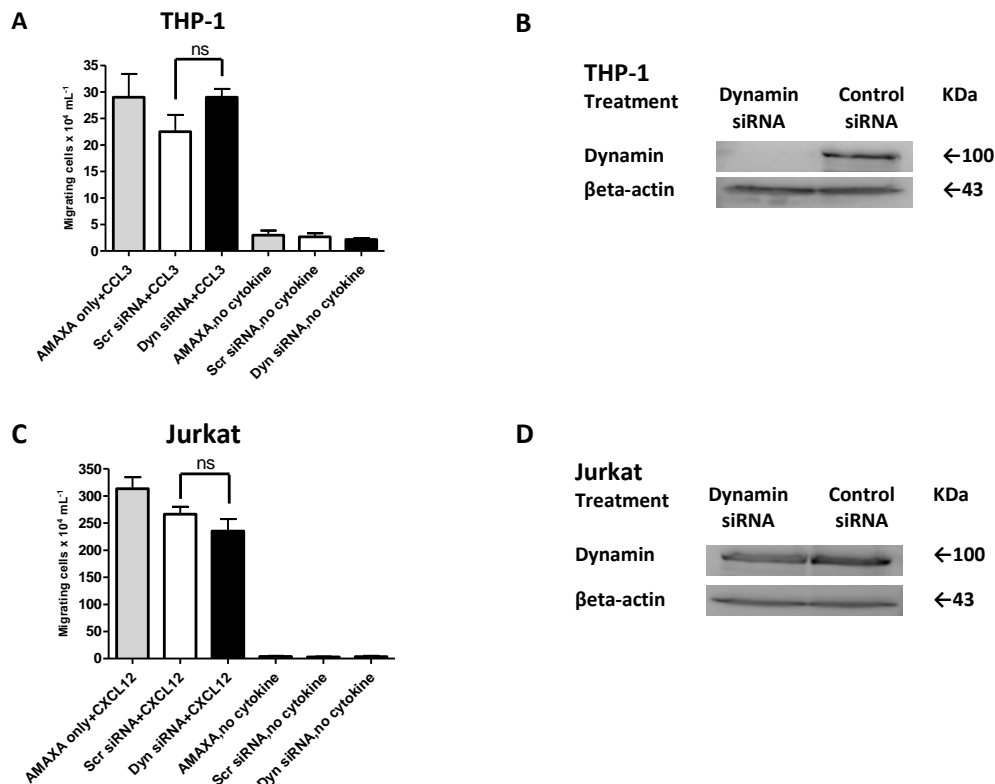


Figure 3.6: Dynamin-2 siRNA knockdown. Cells transfected with 50 nM Human Dynamin-2 or 50 nM nonsense siRNA (Scr) control, chemotaxis assays and Western Blots undertaken 24 hours after transfection. (A) THP-1 chemotaxis to 1 nM CCL3 (B) Western Blot of THP-1, loading confirmed with  $\beta$ -actin (C) Jurkat chemotaxis to 1 nM CXCL12 (D) Western Blot of Jurkat, loading confirmed with  $\beta$ -actin. Means  $\pm$  SEM, one-way ANOVA, post-hoc Bonferroni,  $n \geq 3$  independent experiments, ns= $p > 0.05$ .

Dynamin-2 siRNA almost complete knockdown did not significantly affect chemotaxis of THP-1 to CCL3 or Jurkat chemotaxis to CXCL12. Knockdown was very effective in THP-1 but less so in Jurkat where dynamin knockdown may have been partial in all cells or complete in a proportion of Jurkat hence a more effective knockdown in Jurkat may have produced a very different result.

However effective Dynamin-2 knockdown did significantly inhibited wound-healing in MCF7 cells, possibly indicating a differential use of Dynamin-2 in adherent and suspension cell-lines, figure 3.7.

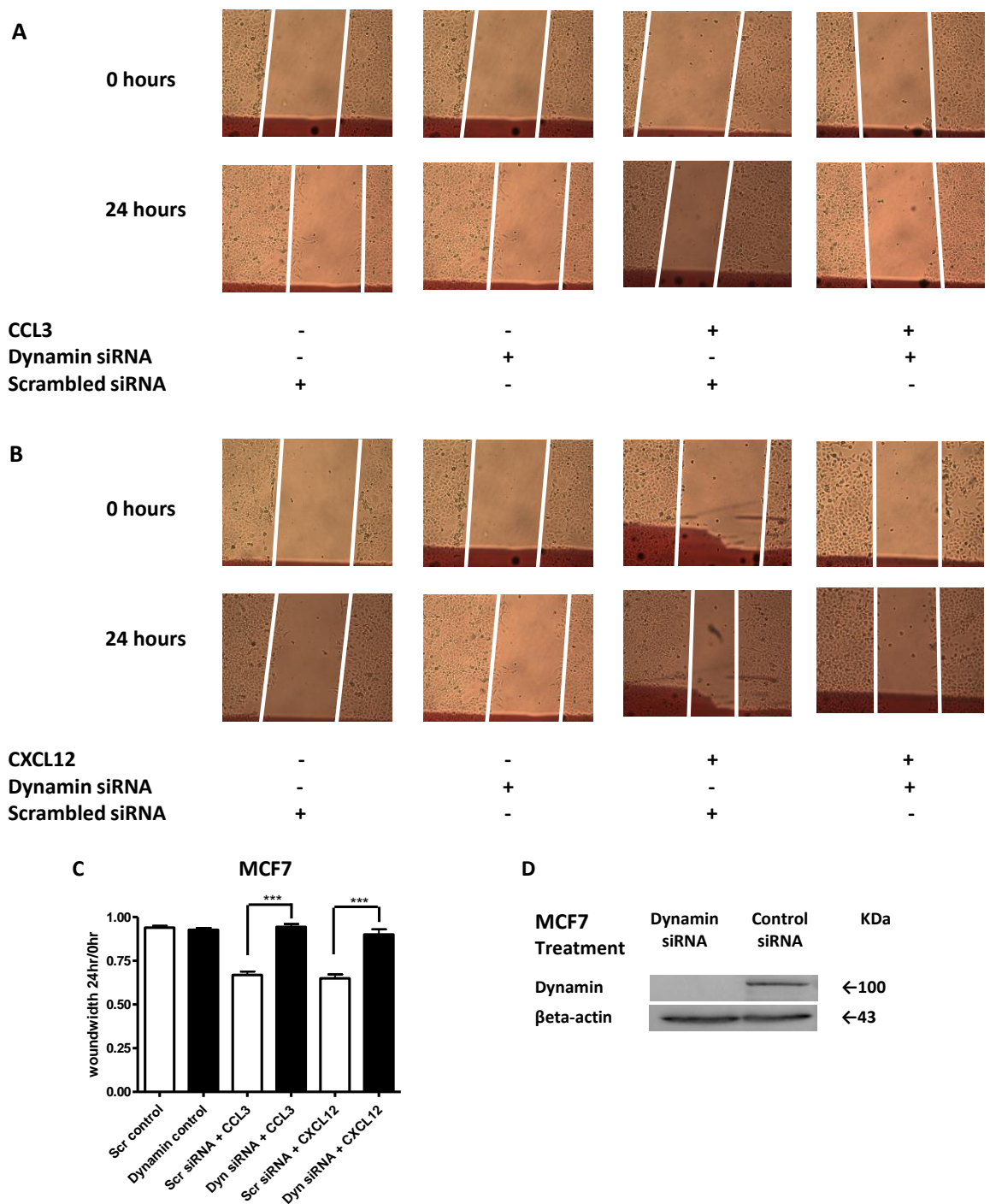


Figure 3.7: MCF7 wound-healing assays following transfection with 50 nM Dynamin-2 siRNA or nonsense siRNA (Scr) control. Analysis 24 hours after (A and C) 10 nM CCL3, or (B and C) 10 nM CXCL12. (D) Western blot dynamin-2 expression 24 hours after siRNA knockdown,  $\beta$ -actin loading control. Means  $\pm$  SEM, one-way ANOVA, post-hoc Bonferroni,  $n \geq 3$  independent experiments, \*\*\*= $p < 0.001$ .

In both MCF7 and THP-1 Western Blots indicated Dynamin-2 siRNA knockdown was complete. CCL3 chemotaxis in THP-1 was not significantly inhibited however in MCF7 CCL3 (and CXCL12) wound-healing was dramatically reduced. The assays differ in that cell movement in wound-healing is non-directional whereas in chemotaxis it is; suggesting either that there may be a differential use of dynamin-2 in these cell lines or that dynamin-2 is important for other factors



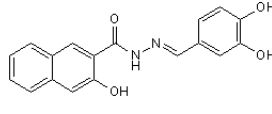
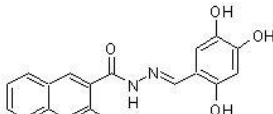
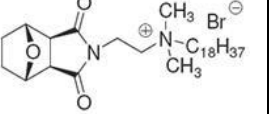
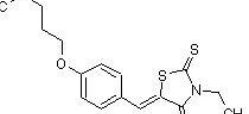
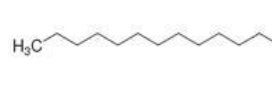
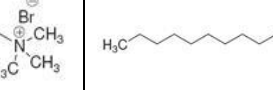
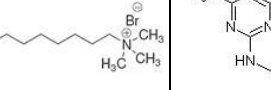
involved in wound-healing. Such factors may involve haptokinetic (random) migration, or haptotaxis migration along a substrate [500], *In vivo* substrate may be the extracellular matrix, to which chemokine gradient may be bound. *In vitro* the plastic substrate of a wound-healing assay may absorb chemokine, but gradients are absent, hence chemotaxis which involves a cell extending a leading edge towards and then moving up a diffusing chemokine gradient does not occur, but chemokinesis random migration prompted by a chemokine can.

To further analyse the effects of dynamin in chemotaxis a range of small molecule inhibitors were employed in THP-1 and Jurkat chemotaxis assays. Inhibitors were chosen with structural similarities such as MitMAB with OcTMAB, and Dynasore with Dyngo4a, along with inhibitors with unique structures, such as RTIL-13, table 3.1. This range of inhibitors will block either dynamin recruitment at the plasma membrane (MitMAB, OcTMAB or RTIL-13) or inhibit dynamins functions once at the membrane (Dynasore, Dyngo4a) [501]. With these tools it was hoped to fully probe the functions of dynamin in chemotaxis to CCL3 and CXCL12.

### **3.2.5: Dynamin and Drp-1 inhibitors**

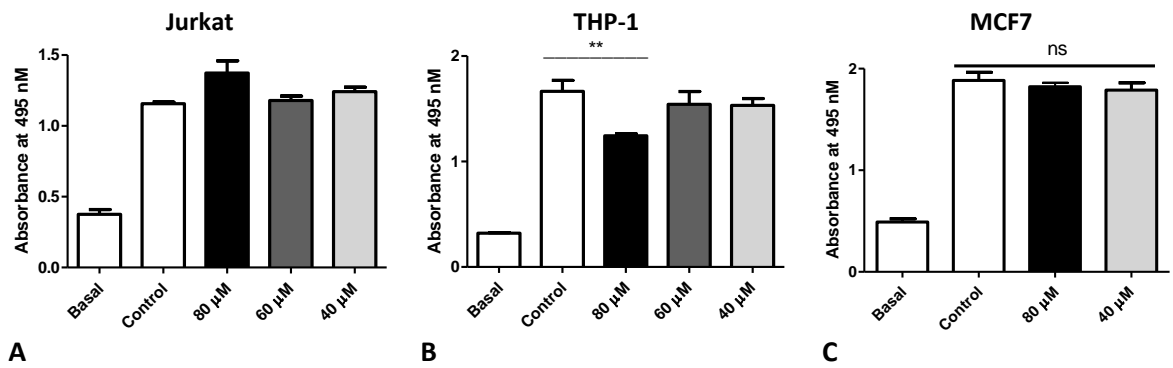
Dynamin inhibitors are anti-mitotic and so potential anti-cancer drugs. The dynamin inhibitors used here include (i) the first dynamin inhibitor synthesised, Dynasore, a cell-permeable reversible non-competitive inhibitor of the dynamin GTPase and at lower concentrations Drp-1 [499]. (ii) A Dynasore analogue with purportedly greater specificity and potency and less cytotoxicity, Dyngo4a [502]. (iii) The long-chain ammonium salt inhibitors MitMAB and OcTMAB which target the PH domain of dynamin [503]. (iv) Room Temperature Ionic Liquid 13 (RTIL-13) which targets both dynamins PH and GTPase domains. (v) RhodadynC10 a Rhodanine N-ethyl analogue with a potency at least as good as other in-cell dynamin inhibitors [504], which targets dynamin's GTPase domain and Transferin-A, and (vi) Pyrimidyn7, one of the most potent dynamin inhibitors available which inhibits dynamin-1 interactions with both GTP and phospholipid [505, 506]. Table 3.1 illustrates the site/s of action of dynamin inhibitors used in this investigation.

Table 3.1: Small molecule inhibitors of dynamin, their structures, target region/s and reported IC<sub>50</sub>'s [499, 502-506].

Dynamin region	BSE	G-domain	BSE	Stalk	PH	Stalk	BSE	PRD
Inhibitor Targeting region		<b>Dynasore</b> IC <sub>50</sub> = 15 μM			<b>MitMAB</b> IC <sub>50</sub> = 3.15 μM			
		<b>Dyngo 4a</b> IC <sub>50</sub> = 2.6 μM			<b>OctMAB</b> IC <sub>50</sub> = 4.4 μM			
		<b>RhodadynC10</b> IC <sub>50</sub> = 30.3 μM			<b>RTIL-13</b> IC <sub>50</sub> = 2.3 - 9.3 μM			
		<b>Pyrimidyn-7<sup>TM</sup></b> IC <sub>50</sub> = 1.8 μM			<b>Pyrimidyn-7<sup>TM</sup></b> IC <sub>50</sub> = 1.8 μM			
								
Dynasore		Dyngo 4a		RTIL-13 <sup>TM</sup>		RhodadynC10 <sup>TM</sup>		
								
MitMAB		OctMAB		Pyrimidyn-7 <sup>TM</sup>				

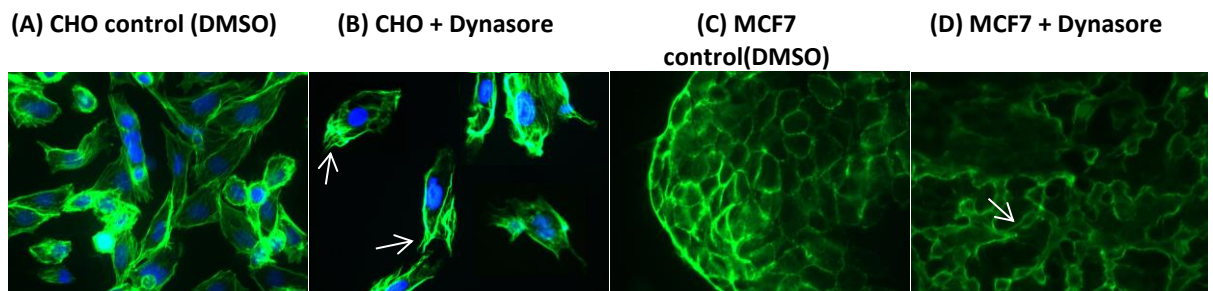
### 3.2.6: Dynasore

The non-competitive inhibitor Dynasore dose-dependently blocks the GTPase activity in dynamin-1 and dynamin-2 at the membrane and Drp-1 [507]. Actin filament remodelling enables cell motility and metastatic invasion of tissues. Dynasore inhibits actin dynamic remodelling and malignant cell invasion [508]. Dynasore has reported relatively low potency and specificity, compared to Dyngo4a, [501] hence Dynasore has been used at 100 µM in cell assays by others [509] however MTS assays illustrated at 80 µM Dynasore caused cytotoxicity in THP-1 cells but not in Jurkat. At 60 µM or below this toxicity was lost, figure 3.8.



**Figure 3.8:** Cytotoxicity assays for Dynasore. MTS assays were over 7 hours in (A) Jurkat and (B) THP-1 and over 24 hours in (C) MCF7 cells. Basal absorbance occurs in presence of medium after MTS treatment in the absence of cells. Means  $\pm$  SEM, one-way ANOVA, post-hoc Bonferroni,  $n \geq 3$  independent experiments,  $**=p < 0.01$ ,  $ns=p > 0.05$ .

Dynasore contains a chromophore explaining the increased absorbance seen at 80  $\mu$ M in Jurkat, figure 3.8A, this is likely to have also have affected MTS results in THP-1 and MCF7, possibly disguising Dynasore toxicity at lower concentrations. Dynasore was also found to cause cytoskeletal damage, adherent cells were seen to develop membrane ruffles, neural-like projections and have a tendency to detach from surfaces, leading to less cell density on the slides, figure 3.9B (control and treated slides were seeded at the same density). This is expected as dynamin mechanistically interacts with myosin and actin. Others have observed these effects with Dynasore at 80  $\mu$ M [510], figure 3.9.



**Figure 3.9:** Filament actin stain following Dynasore. Alexa-488 Phalloidin (green) and DAPI nuclear stains (blue) of CHO.CCR5 and MCF7 following pre-treatment with 80  $\mu$ M Dynasore (1 hr). Imaged UV inverted microscopy (Leica DMII Fluorescence microscope 500x Ex 490 nm, Em 520 nm).

The effect of Dynasore on CXCL12 and CCL3-induced chemotaxis in Jurkat and THP-1 cells was explored using different inhibitor concentrations. At 80  $\mu$ M, figure 3.10, probably due to toxicity cytotoxicity suggested by the MTS assays, figure 3.8B, Dynasore produced significant inhibition of chemotaxis in THP-1 ( $p < 0.001$ ), as well as non-significantly reducing basal migration, figure 3.10C. Hence using Dynasore at 80  $\mu$ M in THP-1 does not inform on dynamin function in THP-1 chemotaxis.

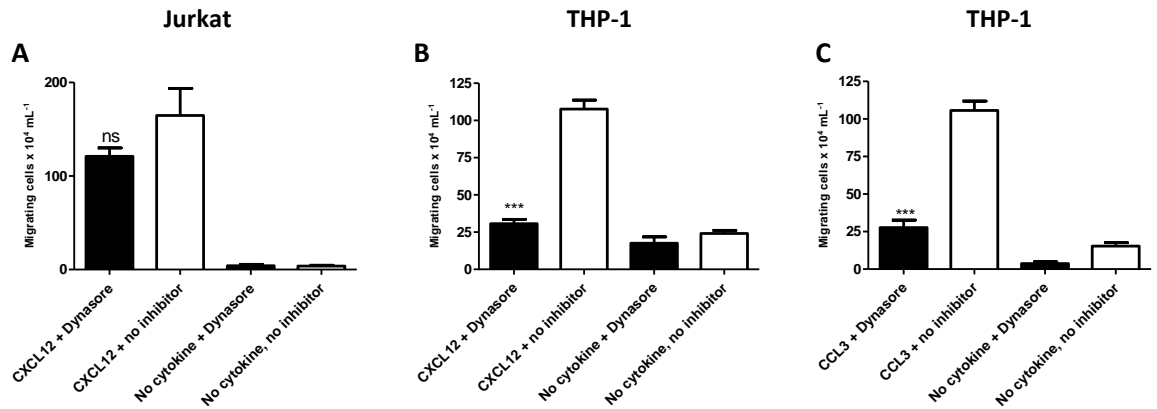


Figure 3.10: Chemotaxis assays following pre-treatment with 80  $\mu$ M Dynasore or control (DMSO). (A) Chemotaxis of Jurkat to 1 nM CXCL12. (B) THP-1 chemotaxis to 1 nM CXCL12. (C) THP-1 chemotaxis to 1 nM CCL3. Means  $\pm$  SEM, one-way ANOVA, post-hoc Bonferroni,  $n \geq 3$  independent experiments, \*\*\*= $p < 0.001$ , ns= $p > 0.05$ .

Due to indicated toxicity chemotaxis assays were repeated with Dynasore at concentrations of 60  $\mu$ M, results mirrored those at 80  $\mu$ M, figure 3.11A, Jurkat inhibition was absent but in THP-1 inhibition was still highly significant, figure 3.11B and 3.11C.

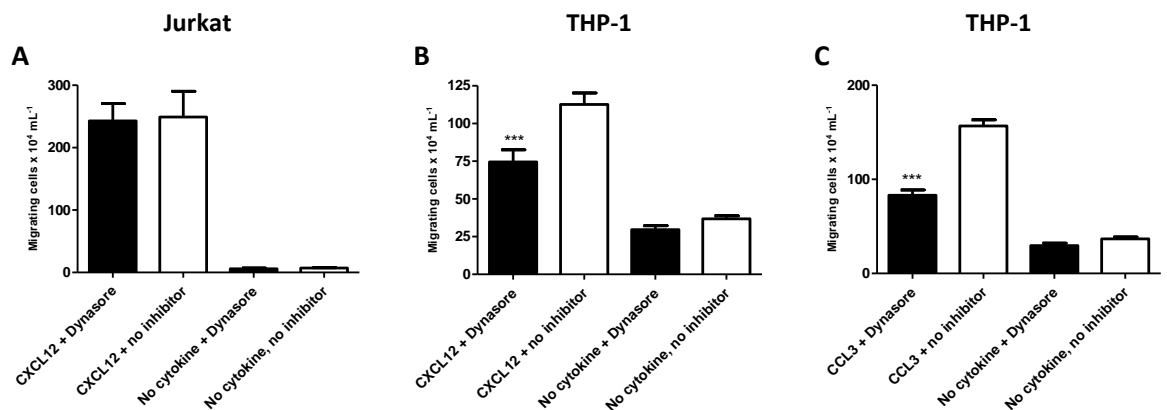


Figure 3.11: Chemotaxis assays following pre-treatment with 60  $\mu$ M Dynasore or control (DMSO). (A) Chemotaxis of Jurkat to 1 nM CXCL12. (B) THP-1 chemotaxis to 1 nM CXCL12. (C) THP-1 chemotaxis to 1 nM CCL3. Means  $\pm$  SEM, one-way ANOVA, post-hoc Bonferroni,  $n \geq 3$  independent experiments, \*\*\*= $p < 0.001$ .

Surprisingly at 40  $\mu$ M Dynasore had no effect on CXCL12-chemotaxis in Jurkat or THP-1, but still caused highly significant inhibition to CCL3-induced chemotaxis in THP-1, figure 3.12.

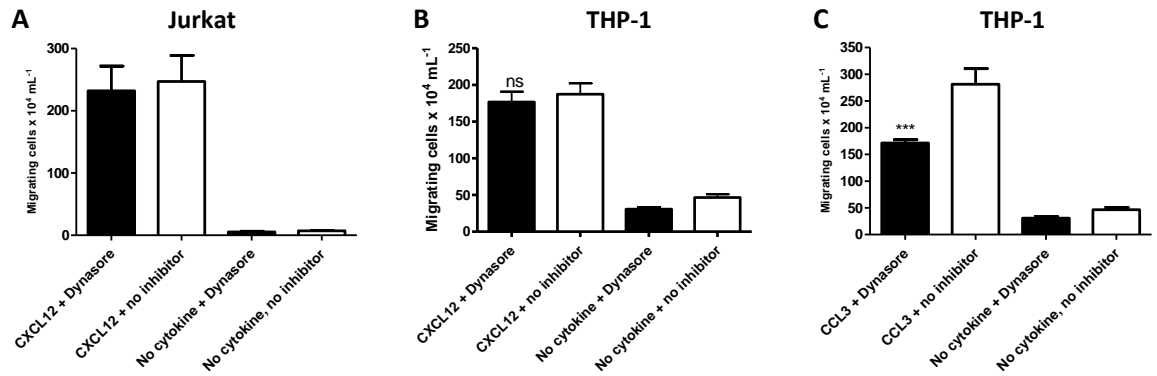


Figure 3.12: Chemotaxis assays following pre-treatment with 40  $\mu\text{M}$  Dynasore or control (DMSO). (A) Chemotaxis of Jurkat to 1 nM CXCL12. (B) THP-1 chemotaxis to 1 nM CXCL12. (C) THP-1 chemotaxis to 1 nM CCL3. Means  $\pm$  SEM, one-way ANOVA, post-hoc Bonferroni,  $n \geq 3$  independent experiments, \*\*\*= $p < 0.001$ , ns= $p > 0.05$ .

Dynasore is also reported to dynamin-independently disrupt lipid rafts and membrane cholesterol homeostasis [511]. Dynasore application at 80  $\mu\text{M}$  has been shown to inhibit dynamin-dependent endocytic pathways rapidly stopping coated vesicle formation causing the accumulation of partly formed pits and arresting the pinching off of vesicles [512], suggesting dynamin is essential in coated vesicle formation and endocytic vesicle scission. However, Dynasore and another dynamin, G-domain inhibitor Dyngo-4a, have been shown to produce off-target effects. In cells where dynamin isoforms 1, 2, and 3 were knocked out, Dynasore at 80  $\mu\text{M}$  and Dyngo-4a at 30  $\mu\text{M}$  both still inhibited membrane ruffles, cell attachment and spreading, as well as inhibiting F-actin and lamellipodia formation [513]. Dynasore at 75  $\mu\text{M}$  is also reported to increase calcium levels at the membrane [514]. The effects of Dynasore on CCL3 and CXCL12-induced calcium release were explored; the results did not mimic those from the chemotaxis, figure 3.13.

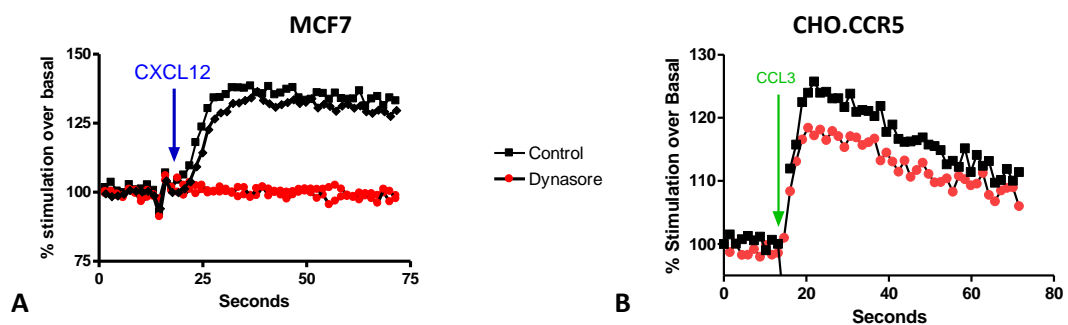


Figure 3.13: Intracellular calcium responses to 80  $\mu\text{M}$  Dynasore. (A) Representative traces following stimulation of MCF7 with 10 nM CXCL12 following pre-treatment with Dynasore or DMSO control. (B) Representative trace following stimulation of CHO.CCR5 with 10 nM CCL3 following pre-treatment with Dynasore or DMSO control,  $n=1$ .

Dynasore at 80  $\mu\text{M}$  eliminated release of intracellular calcium in response to CXCL12 in MCF7, and reduced calcium release in response to CCL3 in CHO.CCR5, figure 3.13, again indicating cell-specific responses to dynamin inhibition or Dynasore toxicity.

### 3.2.7: Dyngo4a

Dyngo4a is a Dynasore analogue, table 3.1, with reportedly 40-fold improved potency over Dynasore and more specificity as explained above [501]. It has reported  $\text{IC}_{50}$  values of 380 nM and 2.6  $\mu\text{M}$  at dynamin-1 and -2 respectively compared to Dynasore  $\text{IC}_{50}$  of 15  $\mu\text{M}$ . Both Dyngo4a and Dynasore target the GTPase activity of dynamin-1 and dynamin-2 [515]. Membrane-permeable Dyngo4a, like Dynasore, inhibits dynamin by binding to an allosteric site within the GTPase domain of both dynamin-1 and -2 [516], and both inhibitors block dynamin function after membrane recruitment [501]. However here Dyngo4a was only found to inhibit chemotaxis to CXCL12 and CCL3 at concentrations of 80  $\mu\text{M}$ , figure 3.14, but not to have any significant effects on chemotaxis at lower concentrations (data not shown). Suggesting Dyngo4a's reported increased potency over Dynasore is not applicable to chemotaxis of THP-1 or Jurkat. MTS assays showed that Dyngo4a's observed effects were not due to toxicity, figure 3.15.

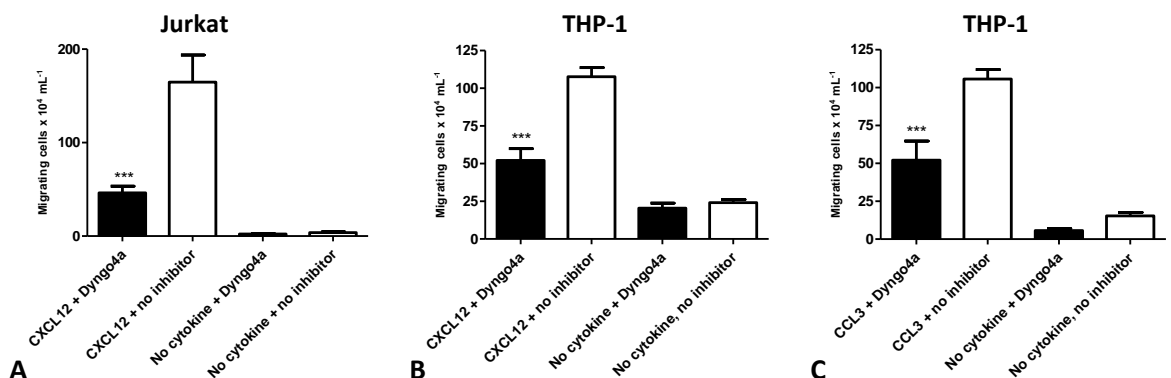


Figure 3.14: Chemotaxis assays following pre-treatment with 80  $\mu\text{M}$  Dyngo4a or control (DMSO). (A) Chemotaxis of Jurkat to 1 nM CXCL12. (B) THP-1 chemotaxis to 1 nM CXCL12. (C) THP-1 chemotaxis to 1 nM CCL3. Means  $\pm$  SEM, one-way ANOVA, post-hoc Bonferroni,  $n \geq 3$  independent experiments, \*\*\*= $p < 0.001$ .

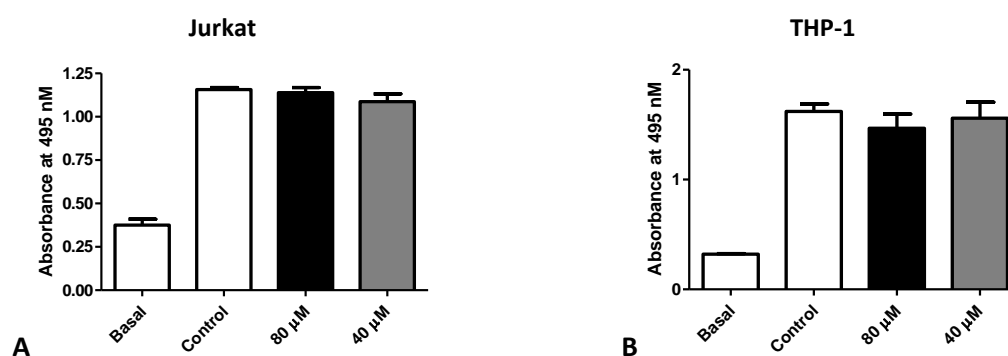


Figure 3.15: Cytotoxicity assays for Dyngo4a. MTS assays were over 7 hours in (A) Jurkat and (B) THP-1. Basal absorbance occurs in presence of medium after MTS treatment in the absence of cells. Means  $\pm$  SEM,  $n \geq 3$  independent experiments, one-way ANOVA with post-hoc Bonferroni revealed no significant differences.

The results of the chemotaxis and cytotoxicity assays for Dyngo4a indicate its reported 40-fold increased potency over Dynasore with respect to dynamin either does not apply in THP-1 or Jurkat or that Dyngo4a does indeed target dynamin more effectively than Dynasore, blocking both endocytosis and clathrin-mediated endocytosis [501], with less off target toxicity than Dynasore. Suggesting the above Dynasore results could be due more to off target toxicity than dynamin inhibition, as the chemokine specific response produced by 40  $\mu$ M Dynasore was not repeated by Dyngo4a.

### 3.2.8: MiTMAB and OcTMAB

Next the effects of MiTMAB and OcTMAB, inhibitors of dynamins PH domain were explored. MiTMAB and OcTMAB are water-soluble, cell-permeable and block cytokinesis without any other effects on mitosis and also induce apoptosis in cancer cells [517]. Their toxicity in cancer cells is higher than in healthy cells. Classical anti-mitotics such as taxanes and vinca alkaloids target microtubules, but tubulin is important for function of healthy and non-dividing cells [518]. Other anti-mitotics target kinases and kinesin spindle proteins expressed in dividing cells, and so also target the mitotic spindle early in cell division [519]. Targeting dynamin does not target the mitotic spindle; blocking dynamin prevents the necessary dynamin activation of phosphatase calcineurin to produce cytokinesis. Hence MiTMAB and OcTMAB block the abscission phase of cytokinesis producing polyploidy without affecting any other stage of mitosis and they are selective for cancer cells [520, 521]. Apoptotic death may not follow cytokinesis failure, senescence and reversible mitotic arrest may occur [522]. In cancer cells responses to MiTMAB and OcTMAB negatively correlate with levels of Bcl-2 and Mcl-1, another Bcl-2 protein family member. MiTMAB/OcTMAB-induced apoptosis is caspase-dependent. If cell-lines express Bcl-2, an anti-apoptotic protein, they are resistant to MiTMAB and OcTMAB [517].

MitMAB and OctMAB inhibit the recruitment of dynamin to membranes [523]. MitMAB inhibits dynamin-1 and -2 with an  $IC_{50}$  of 3.1  $\mu$ M and 8.4  $\mu$ M respectively competing with the lipid-binding pleckstrin homology but not the GTPase.  $IC_{50}$  for inhibiting dynamin-1 and -2 receptor-mediated endocytosis is 19.9  $\mu$ M and 2.2  $\mu$ M respectively [503, 520].

### 3.2.8.1: MitMAB

MitMAB targets the dynamin-phospholipid interactions, may interact with phospholipase-C $\delta$  PH domain, and has been shown to block calcium influx [524], hence may inhibit endocytosis through an effect on calcium channels [525]. Cytosolic calcium changes support a shift from early to late endocytosis [526, 527]. MitMAB has also been shown to inhibit nicotinic acetylcholine receptors [523]. In cancer cells MitMAB can block dynamin-2, as it inhibits cytokinesis and cell proliferation but not any other cell-cycle stage [520]. MTS assays indicated cytotoxicity at 10  $\mu$ M in THP-1 and Jurkat, figure 3.16. MitMAB at 10  $\mu$ M had no effect on calcium release (data not shown).

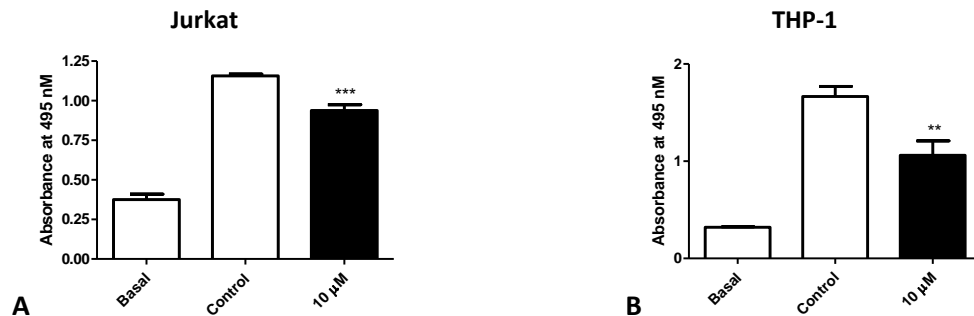


Figure 3.16: Cytotoxicity assays for 10  $\mu$ M MitMAB. MTS assays over 7 hours in (A) Jurkat and (B) THP-1. Basal absorbance occurs in presence of medium after MTS treatment in the absence of cells. Means  $\pm$  SEM, one-way ANOVA, post-hoc Bonferroni,  $n \geq 3$  independent experiments, \*\*= $p < 0.01$ , \*\*\*= $p < 0.001$ .

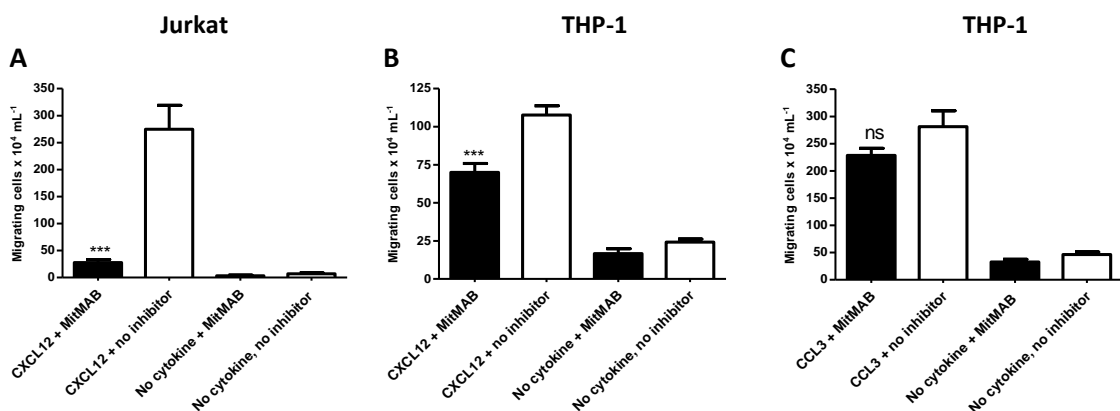


Figure 3.17: Chemotaxis assays following pre-treatment with 10  $\mu$ M MitMAB or control (DMSO). (A) Chemotaxis of Jurkat to 1 nM CXCL12. (B) THP-1 chemotaxis to 1 nM CXCL12. (C) THP-1 chemotaxis to 1 nM CCL3. Means  $\pm$  SEM, one-way ANOVA, post-hoc Bonferroni,  $n \geq 3$ , \*\*\*= $p < 0.001$ , ns= $p > 0.05$ .



MitMAB at 10  $\mu\text{M}$  very significantly inhibited chemotaxis to CXCL12 in both Jurkat and THP-1 but not CCL3-induced chemotaxis in THP-1, figure 3.19. Therefore further investigations probed differences in effects between CCL3 and CXCL12 chemotaxis in THP-1 as such differences in response were not found in the literature.

Dynasore and MitMAB have been shown to produce temporally distinct effects. Dynasore but not MitMAB block dynamin-1 GTPase activity, and so may block the early stages of endocytosis when receptor stimulus is still present, whereas MitMAB, a competitive inhibitor, may block dynamin binding to phospholipid membranes later in the endocytosis process [523]. Suggesting the endocytosis kinetic differences in CXCR4/CXCL12 and CCL3/CCR5 could explain results, see discussion.

### 3.2.8.2: OcTMAB

OcTMAB, like MiTMAB, is an inhibitor of dynamin-1 and -2,  $\text{IC}_{50}$  is approximately 1.9  $\mu\text{M}$ , and 4.4  $\mu\text{M}$  respectively, about half that of MiTMAB. OcTMAB  $\text{IC}_{50}$  for inhibiting receptor-mediated endocytosis is approximately 6.7  $\mu\text{M}$  OcTMAB also competes for phospholipids for the lipid binding pleckstrin homology of dynamins  $\text{IC}_{50} \sim 16 \mu\text{M}$  all values depend on cell type [501]. OcTMAB modestly inhibited chemotaxis to CXCL12 in Jurkat and THP-1, but not to CCL3 in THP-1, figure 3.18. OcTMAB at 5  $\mu\text{M}$  had no effect on calcium release (data not shown) and displayed no toxicity in MTS assays, figure 3.19.

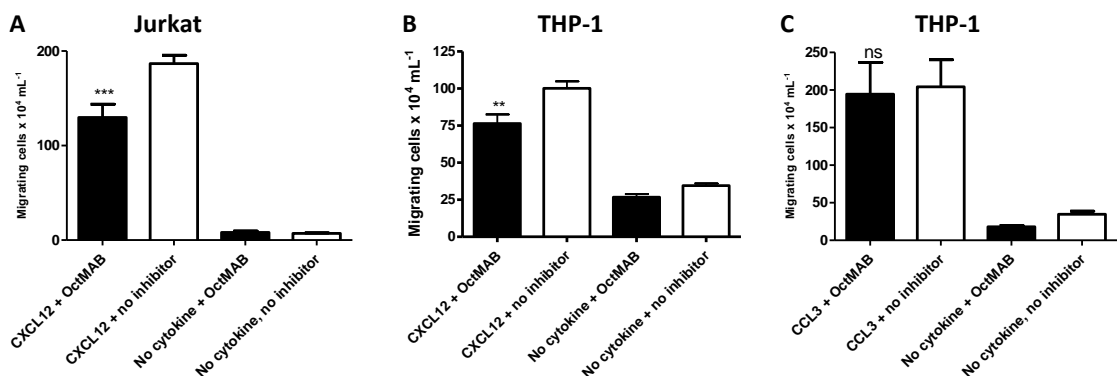


Figure 3.18: Chemotaxis assays following pre-treatment with 5  $\mu\text{M}$  OcTMAB or control (DMSO). (A) Chemotaxis of Jurkat to 1 nM CXCL12. (B) THP-1 chemotaxis to 1 nM CXCL12. (C) THP-1 chemotaxis to 1 nM CCL3. Means  $\pm$  SEM, one-way ANOVA, post-hoc Bonferroni,  $n \geq 3$  independent experiments, \*\*\*=  $p < 0.001$ , \*\*=  $p < 0.01$ , ns =  $p > 0.05$ .

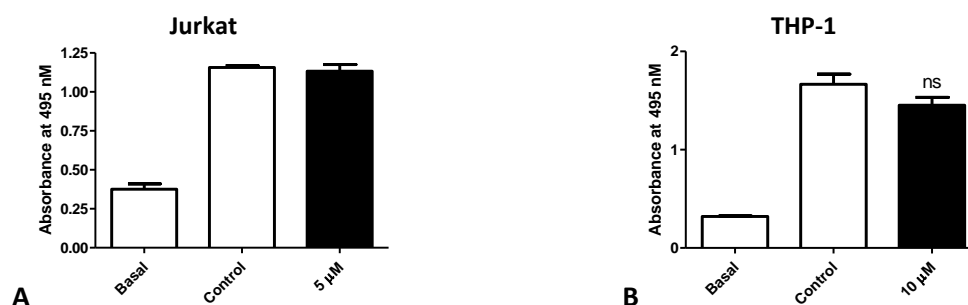


Figure 3.19: Cytotoxicity assays for OctMAB. MTS assays over 7 hours in (A) Jurkat and (B) THP-1. Basal absorbance occurs in presence of medium after MTS treatment in the absence of cells. Means  $\pm$  SEM, one-way ANOVA, post-hoc Bonferroni,  $n \geq 3$  independent experiments, ns= $p > 0.05$ .

Thus MiTMAB and OcTMAB, both reported as inhibitors of dynamins PH domain, at the concentrations employed selectively inhibited CXCL12 but not CCL3 chemotaxis. Next the effects of Rhodadyn-C<sup>10</sup>, purportedly an inhibitor of Dynamins GTPase domain [504] were explored.

### 3.2.9: Rhodadyn-C10<sup>TM</sup>

Rhodadyn-C10 is the N-ethyl analogue of a rhodanine scaffold. It is cell-permeable and inhibits dynamin-1 and -2 GTPase activity  $IC_{50}$  values are reported as 6.4  $\mu$ M and 30.3  $\mu$ M at dynamin-1 and dynamin-2 respectively. Rhodadyn-C10 also blocks clathrin-mediated endocytosis of transferrin and receptor-mediated endocytosis with an  $IC_{50}$  of 7.0  $\mu$ M [504]. Rhodadyn-C10 at 20  $\mu$ M did significantly inhibit CXCL12 chemotaxis of Jurkat, and to a much lesser extent CCL3 chemotaxis in THP-1 but MTS assays indicated significant toxicity over seven hours in both cell lines, figure 3.20. At concentrations of 20  $\mu$ M Rhodadyn-C10 had no effect on calcium release and at concentrations below 20  $\mu$ M Rhodadyn-C10 had no effect on chemotaxis.

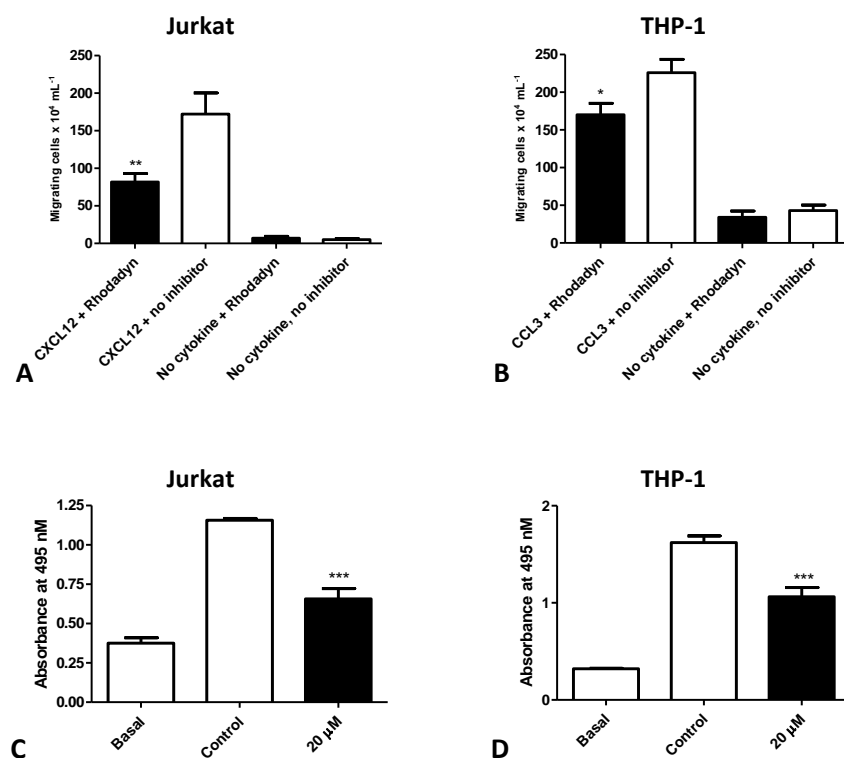


Figure 3.20: Chemotaxis assays following pre-treatment with 20  $\mu$ M Rhodadyn-C10 or control (DMSO). (A) Chemotaxis of Jurkat to 1 nM CXCL12. (B) THP-1 chemotaxis to 1 nM CCL3. (C) Cytotoxicity (MTS) assay for Rhodadyn-C10 over 7 hours in Jurkat and (D) THP-1. Basal absorbance occurs in presence of medium after MTS treatment in the absence of cells. Means  $\pm$  SEM, one-way ANOVA, post-hoc Bonferroni,  $n \geq 3$  independent experiments, \*\*\*= $p < 0.001$ , \*\*= $p < 0.01$ , \*= $p < 0.05$ .

Results with Rhodadyn-C10 did not support the theory that the G-domain is more applicable to CCL3- than CXCL12-chemotaxis, however its cytotoxicity limited its usefulness. Next the effects of two dynamin inhibitors credited with inhibiting both dynamins G- and PH- domains, RTIL-13 and Pyrimidyn-7<sup>TM</sup> were examined.

### 3.2.10: RTIL-13

Room Temperature Ionic Liquids (RTILs) are salts with high melting points ( $>150^{\circ}\text{C}$ ) used as replacements for volatile organic solvents in chemical synthesis as they produce faster, cleaner reactions, however predicting any individual RTIL's properties is difficult. RTIL-13 (4-(N,N-dimethyl-N-octadecyl-N-ethyl)-4-aza-10-oxatricyclo[5.2.1]decane-3,5-dione bromide) was developed as a tool to solubilise the PH domain of dynamin for protein experiments, and was found to inhibit dynamin GTPase with an  $\text{IC}_{50}$  of 2.3  $\mu\text{M}$ . Hence RTIL-13 targets both dynamin's lipid binding PH domain and its GTPase domain [528]. Abcam claim RTIL-13 also inhibits receptor-mediated endocytosis ( $\text{IC}_{50}$  9.3  $\mu\text{M}$ ) and synaptic vesicle endocytosis ( $\text{IC}_{50}$  7.1  $\mu\text{M}$ ). RTIL-13 at concentrations between 5 and 20  $\mu\text{M}$  inhibited chemotaxis of Jurkat and THP-1. Levels of

inhibition steadily increased from significant ( $p<0.05$ ) at 5  $\mu\text{M}$  (data not shown) to very highly significant ( $p<0.001$ ) at 20  $\mu\text{M}$ , figure 3.21A and B, and was not cell type or chemokine specific. However even at 20  $\mu\text{M}$  RTIL-13 did not have any impact on calcium release, figure 3.21C.

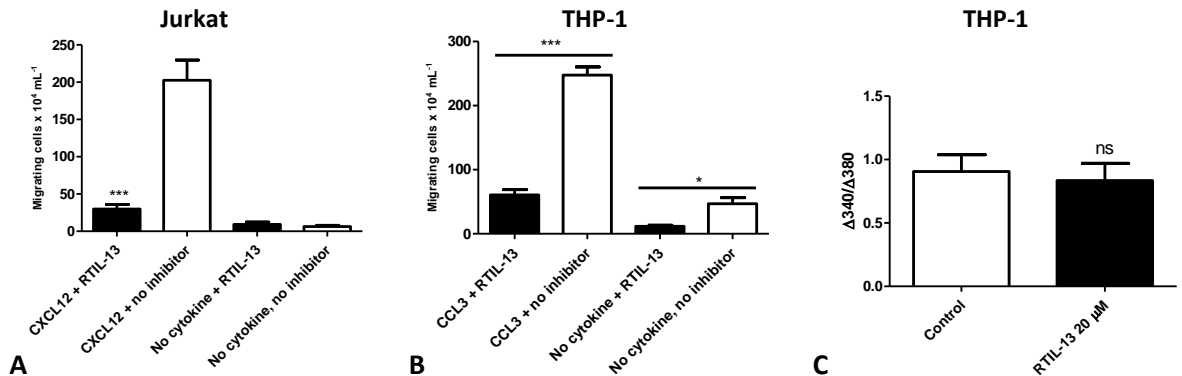


Figure 3.21: Chemotaxis assays following pre-treatment with 20  $\mu\text{M}$  RTIL-13 or control (DMSO). (A) Chemotaxis of Jurkat to 1 nM CXCL12. (B) THP-1 chemotaxis to 1 nM CCL3. (C) Fura2  $\text{Ca}^{2+}$  assay in THP-1 following 20  $\mu\text{M}$  RTIL-13 or control (DMSO). Data expressed as fluorescence ratio change ( $\Delta 340/\Delta 380 \text{ nm}$ ), i.e. peak fluorescence following 10 nM CCL3 addition minus basal fluorescence (prior to chemokine). (A) & (B) one-way ANOVA (C) t-test, Means  $\pm$  SEM,  $n \geq 3$  independent experiments, \*\*\*= $p<0.001$ , \*= $p<0.05$ , ns= $p>0.05$ .

In THP-1 chemotaxis to CCL3 RTIL-13 at 20  $\mu\text{M}$  significantly ( $p<0.05$ ) inhibited basal migration in the absence of chemokine, figure 3.21B, as this could be caused by cytotoxicity MTS assays using a range of RTIL-13 concentrations were undertaken in both THP-1 and Jurkat, figure 3.23.

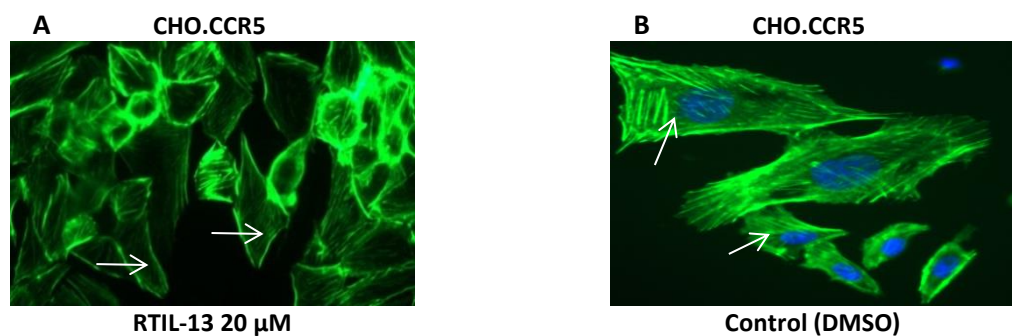


Figure 3.22: Actin filament staining following RTIL-13. Alexa-488 Phalloidin (green) and DAPI nuclear stains (blue) of CHO.CCR5 following pre-treatment with (A) 20  $\mu\text{M}$  RTIL-13 or (B) Control (1 hr). Imaged UV inverted microscopy (Leica DMII Fluorescence microscope 500x Ex 490 nm, Em 520 nm).

RTIL-13 at 20  $\mu\text{M}$  slightly lessened Phalloidin staining but did not distort or eliminate actin filaments, figure 3.22.

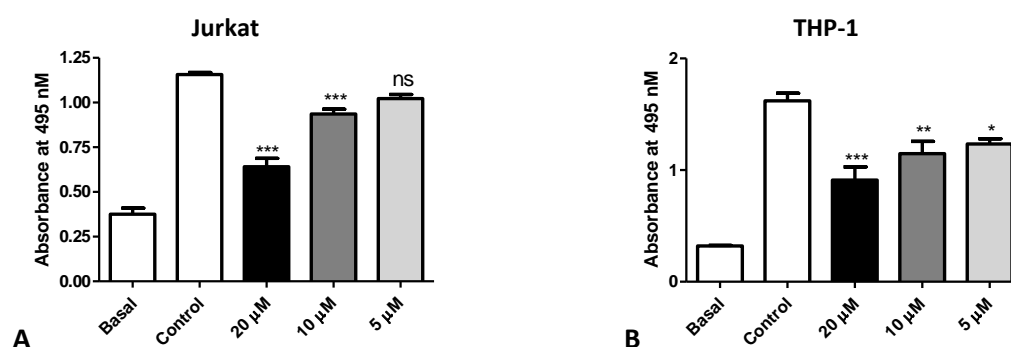


Figure 3.23: Cytotoxicity assays for RTIL-13. MTS assays were over 7 hours in (A) Jurkat and (B) THP-1. Basal absorbance occurs in presence of medium after MTS treatment in the absence of cells. Means  $\pm$  SEM, one-way ANOVA, post-hoc Bonferroni,  $n \geq 3$  independent experiments, \*\*\*= $p < 0.001$ , \*\*= $p < 0.01$ , \*= $p < 0.05$ , ns= $p > 0.05$ .

MTS assays indicated RTIL-13 caused significant cytotoxicity at 10  $\mu$ M and above in Jurkat and at 5  $\mu$ M and above in THP-1.

Thus although 20  $\mu$ M RTIL-13 significantly reduced cell migration figure 3.21A and B, cytotoxicity assays, figure 3.23, and the significant inhibition of basal migration, figure 3.21B, indicated this may have been due to toxicity. Also Phalloidin stains in CHO.CCR5 following treatment with 20  $\mu$ M RTIL-13 illustrated that loss of actin filaments may have also contributed to reduced cell migration. Hence it is hard to isolate and effectively evaluate RTIL-13's effects on dynamin using chemotaxis assays.

### 3.2.11: Pyrimidyn-7<sup>TM</sup>

Pyrimidyn-7 inhibits the binding of dynamin to phospholipid, by binding membrane phosphatidylserine. Phosphatidylserine binds the PH domain of dynamin and aids its GTPase activity by enhancing co-operative helix oligomerization [175, 176, 529]. Pyrimidyn-7 shares structural similarities with ammonium salt inhibitors of dynamin, such as MiTMAB and some RTILs, and so has amphiphilic properties that inhibit dynamin-binding phospholipids. Also Pyrimidyn-7 is a nucleotide analogue and so mimics GTP and targets the GTPase domain of dynamin competing with GTP for binding. Pyrimidyn-7 targets dynamin-1 ( $IC_{50}$ , 1.1  $\mu$ M) and dynamin-2 ( $IC_{50}$ , 1.8  $\mu$ M) with nearly equal potency, competitively inhibiting both basal and phosphatidylserine-stimulated activity [506].

Pyrimidyn-7 has been shown to reversibly inhibit vesicle endocytosis and clathrin-mediated endocytosis possibly because dynamin inhibition can inhibit endocytosis. Pyrimidyn-7 at 30-40  $\mu$ M can reversibly block clathrin-mediated endocytosis in cell lines. This is reversible after washout, and endocytosis activity is restored within an hour. At 30  $\mu$ M Pyrimidyn-7 is reported to abolish dynamin-PH binding and dynamin localisation to the membrane, and hence blocks clathrin-mediated endocytosis. At low concentrations (10  $\mu$ M) pyrimidyn-7 inhibits cell proliferation,

increasing DNA fragmentation and causing apoptosis in cancer cells. At concentrations of 1.3 to 3.2  $\mu\text{M}$  pyrimidin-7 inhibited growth of many different cancer cell-lines, suggesting potential therapeutic anticancer effects [506]. MTS assays confirmed Pyrimidin-7 at 10  $\mu\text{M}$  inhibited metabolism in both THP-1 and Jurkat cells, figure 3.24.

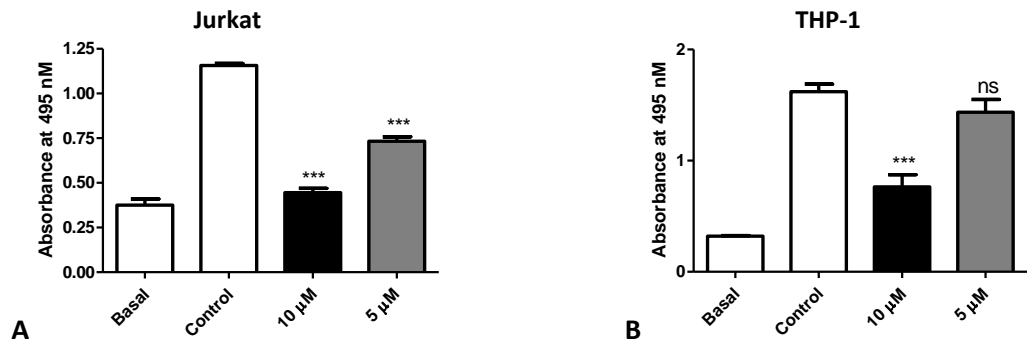


Figure 3.24: Cytotoxicity assays for Pyrimidin-7<sup>TM</sup>. MTS assays were over 7 hours in (A) Jurkat and (B) THP-1. Basal absorbance occurs in presence of medium after MTS treatment in the absence of cells. Means  $\pm$  SEM, one-way ANOVA, post-hoc Bonferroni,  $n \geq 3$  independent experiments, \*\*\*= $p < 0.001$ , ns= $p > 0.05$ .

Cytotoxicity assays of Pyrimidin-7<sup>TM</sup> indicated inhibition of cell metabolism in Jurkat at 5  $\mu\text{M}$  and above, and in THP-1 at 10  $\mu\text{M}$ , figure 3.24. At 10  $\mu\text{M}$  Pyrimidine-7 was found to inhibit CXCL12- but not CCL3-induced chemotaxis in THP-1 and CXCL12-induced chemotaxis in Jurkat, figure 3.25, again suggesting that unlike with CXCR4/CXCL12 chemotaxis, for CCR5/CCL3-induced signalling dynamin-involved receptor endocytosis may not be essential.

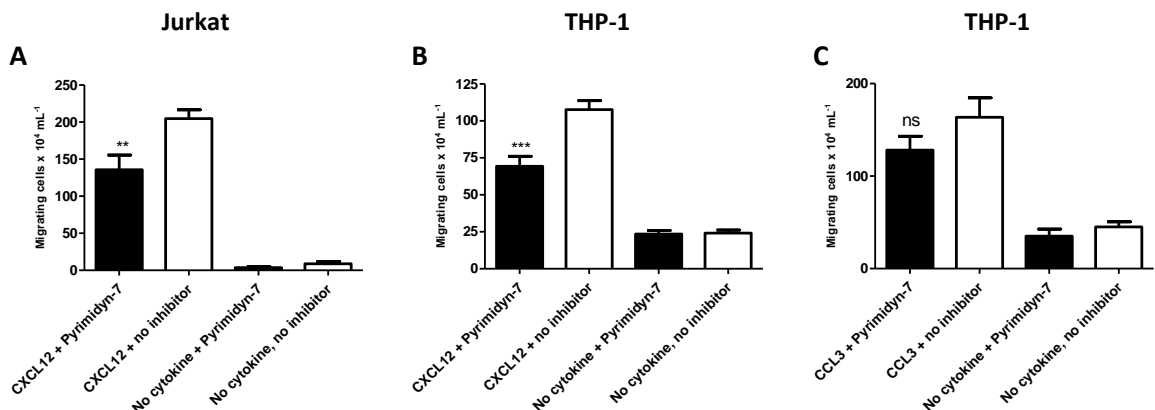


Figure 3.25: Chemotaxis assays following pre-treatment with 10  $\mu\text{M}$  Pyrimidin-7 or control (DMSO). (A) Chemotaxis of Jurkat to 1 nM CXCL12. (B) THP-1 chemotaxis to 1 nM CXCL12. (C) THP-1 chemotaxis to 1 nM CCL3. Means  $\pm$  SEM, one-way ANOVA, post-hoc Bonferroni,  $n \geq 3$  independent experiments, \*\*\*= $p < 0.001$ , \*\*= $p < 0.01$ , ns= $p > 0.05$ .

### 3.2.12: Dynamin inhibitors can interrupt cytokinesis

Treatment with MitMab and OctMAB appears to interrupt cell cycle progression, increasing the proportion of cells in late G2 to M stage with effectively 4N content of DNA. This may be due to

interruption of the cell cycle progression or due to failure of cytokinesis [520]. Inhibition of dynamin-2's role in cytokinesis, where it may stabilise the actin filaments in the contractile ring, [530] is one explanation. Here THP-1 cells differentiated to macrophages were transfected with eGFP plasmids then treated with Dynasore 40  $\mu$ M; many of these cells showed defective cytokinesis, figure 3.26. Similar effects were seen with THP-1 treated RTIL-13 20  $\mu$ M or Dynasore 40  $\mu$ M then stained with CCR5 antibody, figure 3.27. Cytokinesis requires membrane ingression then abscission. Actin and myosin both form filaments in line with the mitotic spindle; dynamin stabilises the actin filaments and hence plays a role in abscission [531].

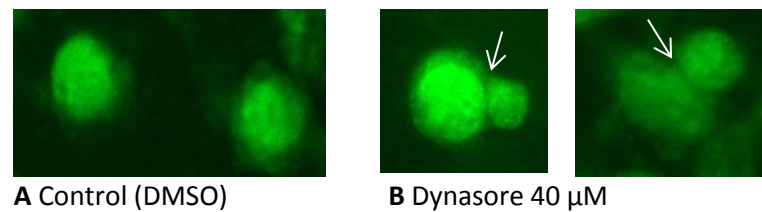


Figure 3.26: THP-1 transfected with eGFP (pEGFP.C2) plasmids. Cell treatment 40  $\mu$ M Dynasore or control (DMSO) for 12 hours, fixed (4% paraformaldehyde). Imaged UV inverted microscopy (Leica DMII Fluorescence microscope 500x Ex 490 nm, Em 520 nm).

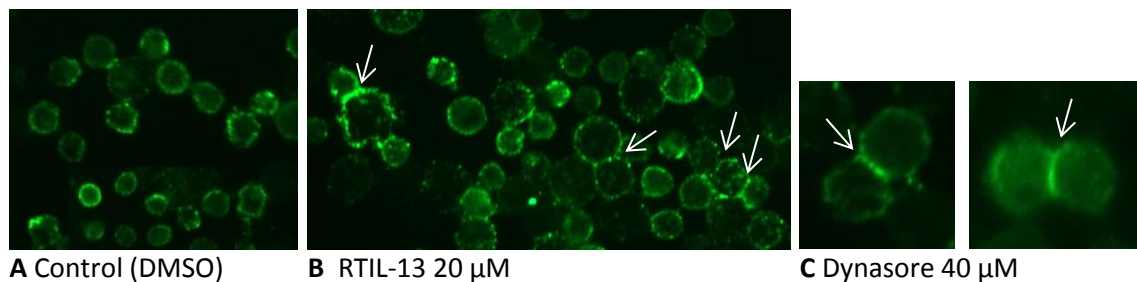


Figure 3.27: CCR5 receptor immunofluorescent staining following Dynamin inhibitors. (A) THP-1, pre-treatment 25 nM PMA grown on glass for 24 hours, treated 20  $\mu$ M RTIL-13 or 40  $\mu$ M Dynasore or DMSO (6 hrs), fixed (4% paraformaldehyde), incubated with CCR5 antibody (HEK/1/85a/7a) (1 hr) then probed with rat FITC. Imaged UV inverted microscopy (Leica DMII Fluorescence microscope 500x Ex 490 nm, Em 520 nm).

### 3.3: Discussion

The above results may suggest that in CCL3 but not CXCL12-induced chemotaxis in THP-1 the dynamin G-domain has important for chemotaxis. The results in the Jurkat provide some support for this conclusion although it cannot be confirmed as Jurkat do not migrate to CCL3. This suggests that receptors CCR5 and/or CCR1, the likely targets of CCL3 [532], but not CXCR4, the

likely target of CXCL12, require an active dynamin G-domain for endocytosis. Others have found dynamin important in CC (CCR2) chemokine-induced endocytosis [533].

### **3.3.1: Dynasore may be inhibiting Drp-1 as well as dynamin**

Dynasore at low concentrations (1-10  $\mu\text{M}$ ) inhibits mitochondrial Drp-1 as well as dynamin-1 and -2, hence at 40  $\mu\text{M}$  it will produce significant inhibition of Drp-1. It is possible CCL3-induced chemotaxis in THP-1 is more sensitive to inhibition of Drp-1 than Jurkat chemotaxis to CXCL12. Increased Drp-1 expression confers resistance to chemotherapy, e.g. in T-cell lymphoblastic leukaemia [534], Drp-1 can also increase disease virulence [252] by producing mitochondrial fragmentation which itself can accelerate mitosis and prevent homeostatic intra-mitochondrial calcium fluxes which can mediate apoptosis [242]. By inhibiting Drp-1 for example with 1, 3 and 10  $\mu\text{M}$  Dynasore [535] proliferation can be inhibited and apoptosis supported. Whereas Dynasore at 80  $\mu\text{M}$  has been shown to prevent receptor endocytosis [252, 536].

Drp-1 upregulation is found in many cancers [240] and Drp-1 mutations can support hypoxia-induced migration *in vitro* in malignant glioblastoma cells [537]. MAPK/ERK pathway signalling leads to phosphorylation of Drp-1 on Ser<sup>616</sup> [538] which can be suppressed by ERK inhibition. MAPK/ERK signalling is reportedly very active in Jurkat, and MAPK/ERK signalling also supports the phosphorylation of Drp-1 Ser<sup>616</sup>, and so activation of Drp-1 which modifies mitochondrial metabolism [534].

### **3.3.2: CCR5 and CXCR4 endocytosis kinetics**

There are important differences in the endocytosis kinetics and routes of the CCR5 and CXCR4 receptors which offers an alternative explanation of the different responses of CXCL12- and CCL3-induced chemotaxis to some dynamin inhibitors such as Dynasore. CXCL12-bound CXCR4 receptors start to internalise within two minutes and bound receptor internalisation is complete within 20 minutes. A likely target of CCL3 are CCR5 receptors; these have an extended conformation fatty acid saturated C-tail facilitating insertion into membrane lipid rafts, which slows internalisation by about 10-fold compared to CXCR4 in T-cells. CCR5 internalises very slowly, it can take up to 40 minutes to get underway and two hours to complete. The longer transit time of the CCR5 may allow ligand release, receptor re-sensitisation, re-stimulation and further signalling. Also CXCR4-internalisation can be clathrin-dependent, and CCR5-clathrin-independent, as CCR5 may internalise via caveolae or glycolipid rafts [539]. These factors could explain the discordant effects of dynamin inhibition on CCL3 and CXCL12-induced chemotaxis, if the CCR5 longer residency time on the membrane makes the receptor more sensitive to dynamin inhibitors such as Dynasore, figure 3.28



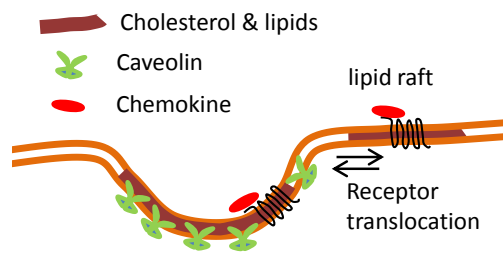


Figure 3.28A: Caveolae invaginations can recruit signalling receptors which may translocate between lipid rafts within and without caveolae while continuing to signal; they may or may not undergo endocytosis [540]. CCR5 may signal via this mechanism [539]

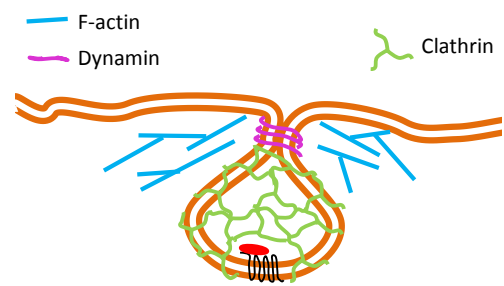


Figure 3.28B: Clathrin-mediated endocytosis is initiated when the ligand binds the receptor, clathrin is recruited for coating pit, F-actin and dynamin promote membrane curvature and dynamin neck scission endocytosis follows [541]. CXCR4 may be internalised by this method [539]

Dynamin along with many other players such as Bin-Amphiphysin-RVS (BAR) proteins are key in both clathrin-coated pit formation and in vesicle neck strain and scission [542]. However there are many endocytic accessory proteins (EAPs) involved in clathrin and/or caveolin-mediated endocytosis. These can vary with cell type [543] and may be modified in cells with mutated DNA such as cancer cell-lines. EAPs include Adaptor proteins with basic motifs that bind negative PIP<sub>2</sub> or phosphatidylserine [544] and so trigger clathrin-coated pit initiation. Knockdown of one of these Adaptor Protein Complexes, AP2, inhibits clathrin-coated pit formation and to some extent receptor-internalisation [545]. This appears to be because stoichiometrically two AP2 complexes associate with PIP<sub>2</sub> and a clathrin triskelion to initiate clathrin-coated pit formation [546]. Therefore if any of the dynamin small molecule inhibitors used in this investigation have off-target effects on adaptor proteins that play a role in one but not both cell-lines employed this could also explain discordant effects of the inhibitor on one but not both Jurkat and THP-1 chemotaxis.

### 3.4: Conclusions

Western Blot confirmed dynamin-2 was present in Jurkat, THP-1 and MCF7, Immunofluorescence confirmed in THP-1 and MCF7 the highest dynamin-2 concentrations were in the nucleus. Knockdown of Dynamin-2 very significantly inhibited wound-healing supported by CCL3 or CXCL12 in MCF7, suggesting an important role for dynamin in chemokinesis. However even complete dynamin-2 knockdown had no significant effect on CCL3 chemotaxis in THP-1. Dynamin siRNA investigations in Jurkat were somewhat inconclusive due to incomplete knockdown.

Dynamin was concluded to be important in cell division as inhibition, with RTIL-13 or Dynasore, interrupted cytokinesis producing conjoined cells.

Drawing conclusions from the results with Rhodadyn-C10, RTIL-13 and Pyrimidyn-7 are hampered by these inhibitors toxicity at concentrations needed to inhibit chemotaxis. Pyrimidyn-7 inhibits both the GTPase and PH domains of dynamin [506]. At 10  $\mu$ M Pyrimidyn-7 inhibited CXCL12 but not CCL3 chemotaxis, although it also inhibited cell metabolism in both THP-1 and Jurkat. Pyrimidyn-7's differing effects on CXCL12 and CCL3 chemotaxis may be due to CXCR4/CXCL12 but not CCR5/CCL3-induced signalling requiring rapid receptor endocytosis to produce signalling leading to chemotaxis.

Dynasore targets dynamins GTPase domain [512], at 40  $\mu$ M it selectively inhibited CCL3 but not CXCL12 chemotaxis. As discussed this may be due to differing endocytosis kinetics and/or mechanisms of CXCR4 and CCR5, or due to the G-domain being important for CXCL12 but not CCL3 chemotaxis. However as Dynasore at much lower concentrations inhibits Drp-1 [499] therefore the effects of Dynasore at 40  $\mu$ M on CCL3 assays could be partly due to inhibiting Drp-1 modulated motility. This conclusion is supported by dynamin-2 siRNA knockdown not significantly inhibiting chemotaxis in THP-1. Dyngo4a, which also purportedly inhibits dynamin GTPase domain, inhibited equally both CCL3 and CXCL12 chemotaxis so also did not confirm differential results from Dynasore. These contrasting effects of Dynasore and Dyngo4a were seen at inhibitor concentrations that did not cause toxicity. MiTMAB was seen to inhibit CXCL12 chemotaxis in THP-1 and Jurkat but not CCL3 chemotaxis in THP-1, suggesting the PH domain may be more important for CXCL12 than CCL3 chemotaxis.

Overall results demonstrate that dynamin is clearly present in these cell-lines and plays an important role in both CCL3 and CXCL12 chemokinesis in MCF7. Results in THP-1 and Jurkat suggest differential use of dynamin domains in CCL3 and CXCL12 stimulated chemotaxis. With the PH domain being more important for CXCL12-chemotaxis and the GTPase domain for CCL3-chemotaxis, figure 3.29. However factors such as the role of Drp-1 and the very different endocytosis kinetics between CCR5 in and CXCR4 receptors may have influenced these results.

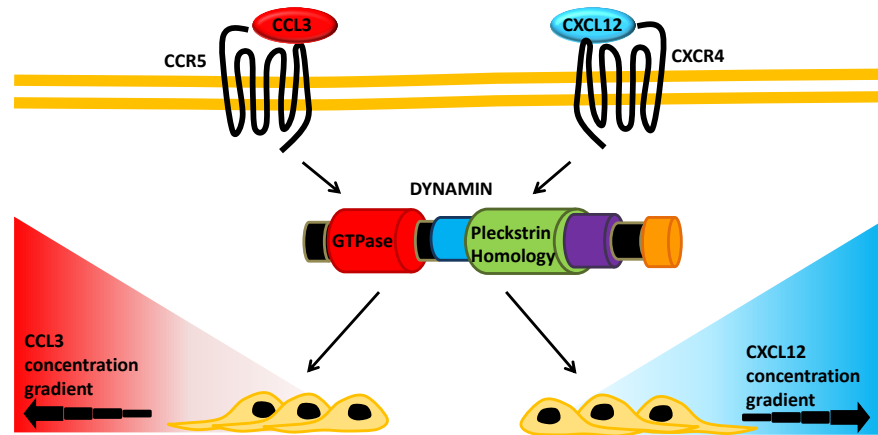


Figure 3.29: Different dynamin domains are involved in CCL3- compared to CXCL12-chemotaxis. In some cell types dynamin can support chemotaxis to both CCL3 and CXCL12, however dynamins PH domain may be more important for chemotaxis to CXCL12 and dynamins GTPase domain for chemotaxis to CCL3 [547].

Dynamins diverse roles are only part of the chemokine signalling story leading to chemokinesis and chemotaxis supporting spread of cancer cells to secondary sites. Other key players in metastasis include PKC, Src, ROCK and the Raf/MEK/ERK signalling cascade; investigations into these proteins are reported in chapter 4.

## **Chapter 4: PKC and other key signalling proteins in cell migration towards CXCL12 and CCL3 in leukemic cells compared to breast cancer cells**

### ***4.1: Introduction***

Key signalling in metastasis includes through the Ras/Raf/MEK/ERK pathway, Src and PKC. PKC is an important chemokine signalling transducer in health and disease [548, 549]. There are many PKC isoforms, activation of which can trigger their cellular translocation. PKC activation and structure is isoform dependent [261]. Abnormal PKC expression is observed in many pathologies, in malignancies PKC plays a complex role, isoforms may act as oncoproteins or tumour suppressors [306, 307]. PKC isoforms are involved with other kinases in GPCR phosphorylation [275, 277]. Including of CXCR4 following CXCL12 binding [279], as this can be prevented by PKC $\alpha$  inhibition [280]. PKC also modulates signalling through GSK3 a key protein in many signalling pathways including those involving Pi3K, Akt, PKA and Wnt [550-552].

Src plays a key role in cell proliferation and metastasis [553]. Src levels can modulate cell adhesion and cell migration interacting with many cellular proteins [554]. Deregulation of Src is key to survival of many malignant cells [555]. Proliferative and pro-migratory signalling also occurs via the Ras/Raf/MEK/ERK pathway [556, 557]. Raf kinases activating MEK1 and MEK2 which subsequently activate ERK1 and ERK2 although there is also purportedly cross-talk between all these signalling proteins, figure 4.1 [558, 559].

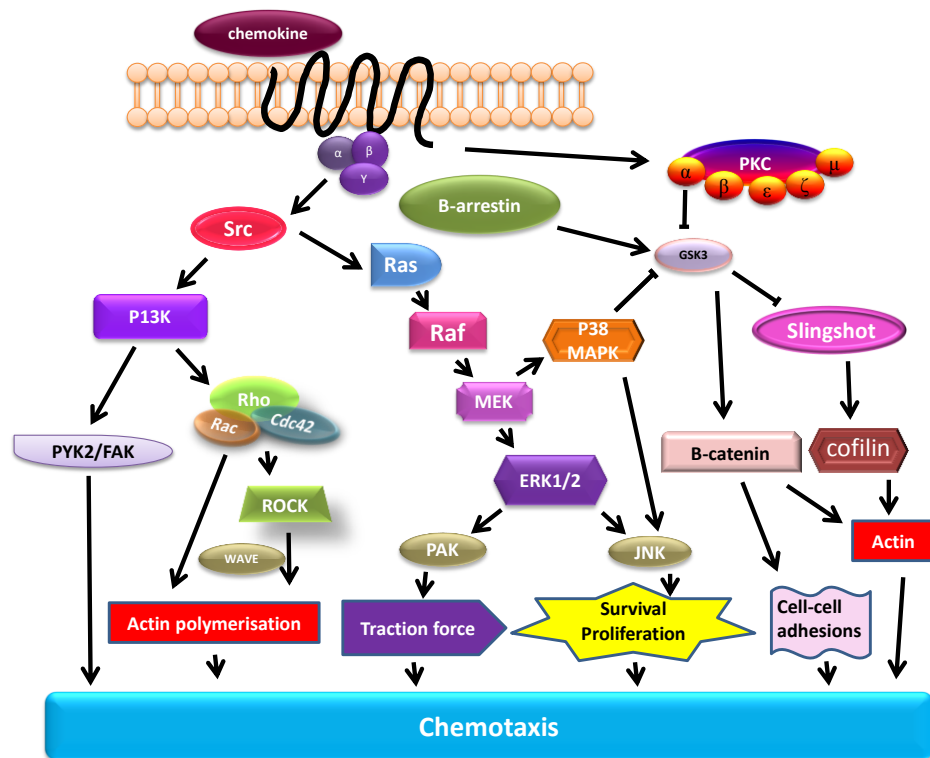


Figure 4.1: PKC and other key signalling proteins involved in chemotaxis and metastasis.

**Hypothesis:** Signalling through PKC, Src, ROCK and the Ras/Raf/MEK/ERK pathway can initiate metastasis, therefore inhibition of these proteins may prevent migration supported by chemokines CCL3 and CXCL12.

**Aim:** To explore the role of PKC isoforms, Src, ROCK, Raf, MEK and ERK in CCL3 and CXCL12-chemotactic migration in cancer cell-lines THP-1 and Jurkat along with PKCs role in CCL3 and CXCL12 supported wound-healing in MCF7.

**Objectives:**

- (i) Using small molecule inhibitors siRNA knockdown explore the role of PKC isoforms in CXCL12 and CCL3 chemotactic migration of THP-1 and Jurkat along with CXCL12 and CCL3-supported wound-healing in MCF7.
- (ii) Explore the effects of PKC small molecule inhibitors on cAMP production in THP-1 and Jurkat
- (iii) Investigate the effects of PKC inhibition on calcium dynamics in THP-1 and Jurkat.
- (iv) Use small molecule inhibition of  $\beta$ -catenin to look for effects on chemotaxis to CCL3 and CXCL12 in THP-1 and Jurkat.

(v) Apply small molecule inhibition and siRNA knockdown to explore the role of Src in CXCL12 and CCL3 chemotactic migration of THP-1 and Jurkat along with CXCL12 and CCL3-supported wound-healing in MCF7.

(vi) Use small molecule inhibitors of Raf, MEK, ERK or ROCK to see if these proteins supported chemotaxis of THP-1 or Jurkat to CCL3 or CXCL12.

## **4.2: Results**

Please note controls are common between graphs where experiments were conducted simultaneously; results for each inhibitor or siRNA have been displayed separately for ease of description of results, this applies to: figures 4.2A and 4.4A; 4.2B, 4.7A and 4.7B; 4.3A, 4.4B, 4.6E, 4.12A, 4.17B, and 4.23B; 4.3B, 4.4C, 4.6F, 4.11A, 4.24C and 4.29C; 4.18 and 5.15; 4.8A and 4.8B; 4.6D and 4.12B; 4.30A, 4.31A, 4.33B, 4.34B.

There are several key proteins implicated in metastasis and in chemokine signalling. These include PKC, Src, MEK, ERK, and Pi3K. Here the effect of pharmacological blockage of these signalling proteins on CXCL12- and CCL3- supported cell migration was explored using three different cell-lines, THP-1, Jurkat and MCF7.

Firstly the role of PKC in CXCL12-induced signalling was explored in three cell lines Jurkat, THP-1, and MCF7. Tools employed were small molecule inhibitors, Rottlerin, Staurosporine, CID755673, GF109203X (for structures see appendix 4), along with PKC siRNA knockdown of PKC $\alpha$ ,  $\delta$ , and  $\epsilon$ . Responses to PKC manipulation were analysed by chemotaxis-, cAMP- and calcium-assays.

### **4.2.1: Rottlerin and PKC $\delta$**

Rottlerin has been used in many studies as a selective PKC $\delta$  inhibitor, but it is not specific, it uncouples mitochondria so reduces ATP levels which may hinder PKC $\delta$  tyrosine phosphorylation. Rottlerin also is reported to block other kinases and inhibit sodium-dependent glutamate transport and accelerate the transporter degradation, it may also activate calcium and potassium channels hence Rottlerin can produce effects on cells where PKC $\delta$  is deleted [560, 561].

The effects of Rottlerin and siRNA PKC $\delta$  inhibition on CXCL12-induced chemotaxis in Jurkat was explored, along with siRNA PKC $\delta$  inhibition of CXCL12-induced MCF7 wound-healing. siRNA controls were transfected with nonsense siRNA (Scr), figure 4.2.

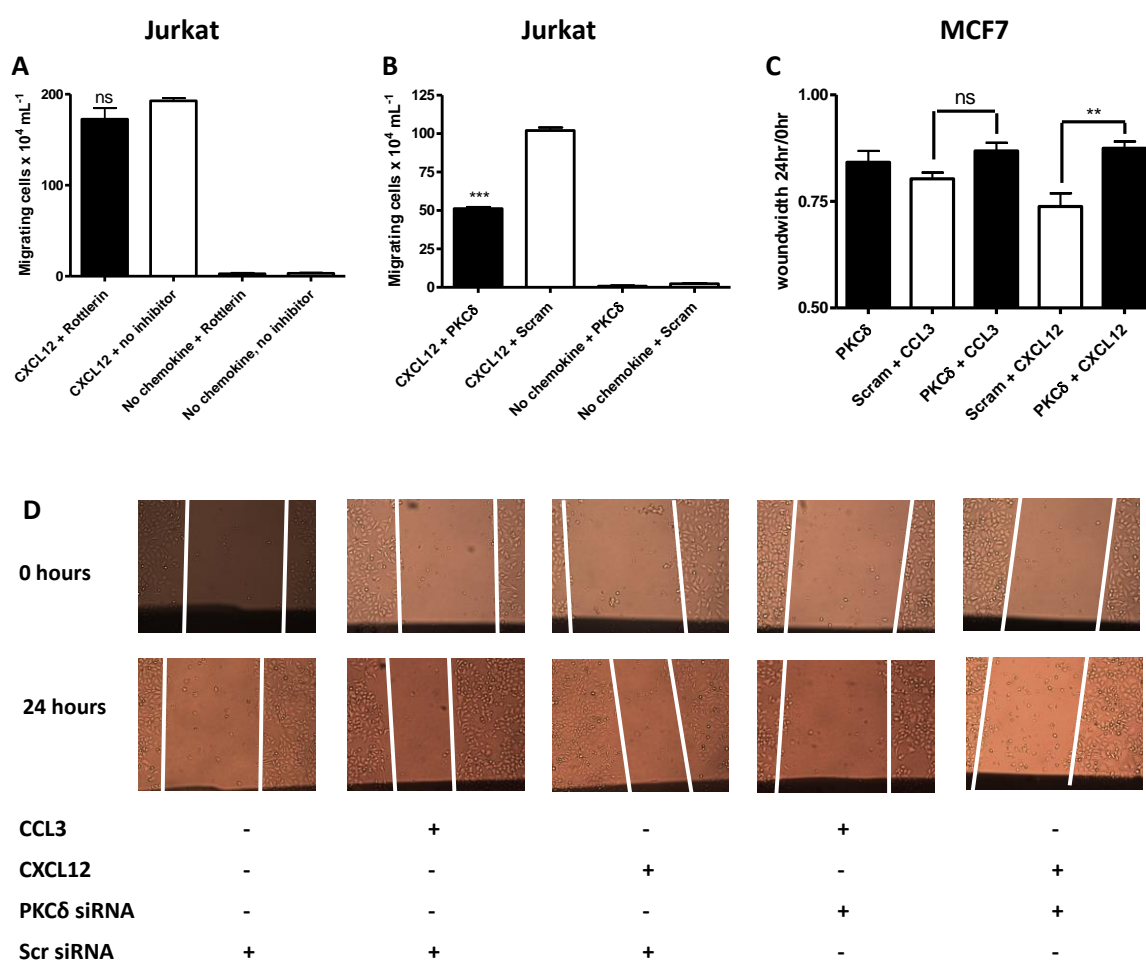


Figure 4.2: Chemotaxis of Jurkat to 1 nM CXCL12 following pre-treatment with (A) Rottlerin 2  $\mu$ M or control (Ethanol) or (B) following transfection with 50 nM PKC $\delta$  siRNA or nonsense siRNA (Scram) control. (C & D) MCF7 wound-healing assays supported by 10 nM CCL3 or 10 nM CXCL12 following transfection with 50 nM PKC $\delta$  siRNA or nonsense siRNA control. Means  $\pm$  SEM, one-way ANOVA, post-hoc Bonferroni,  $n \geq 3$  independent experiments, ns= $p > 0.05$ , \*\*= $p < 0.01$ , \*\*\*= $p < 0.001$ .

Chemotaxis of Jurkat to CXCL12 was not inhibited by Rottlerin 2  $\mu$ M but was very significantly inhibited ( $p < 0.001$ ) by siRNA knockdown of PKC $\delta$ . MCF7 wound-healing confirmed that siRNA PKC $\delta$  knockdown has no significant effect on CCL3-induced wound-healing but significantly ( $p < 0.01$ ) inhibits CXCL12-induced wound-healing, figure 4.2A-D. Unfortunately no antibody was available to confirm the extent of PKC $\delta$  knockdown.

Others have shown a relationship between PKC $\delta$  and cAMP [562] so the effect of Rottlerin on CXCL12 modulation of cAMP production and also calcium release in Jurkat was explored, figure 4.3.

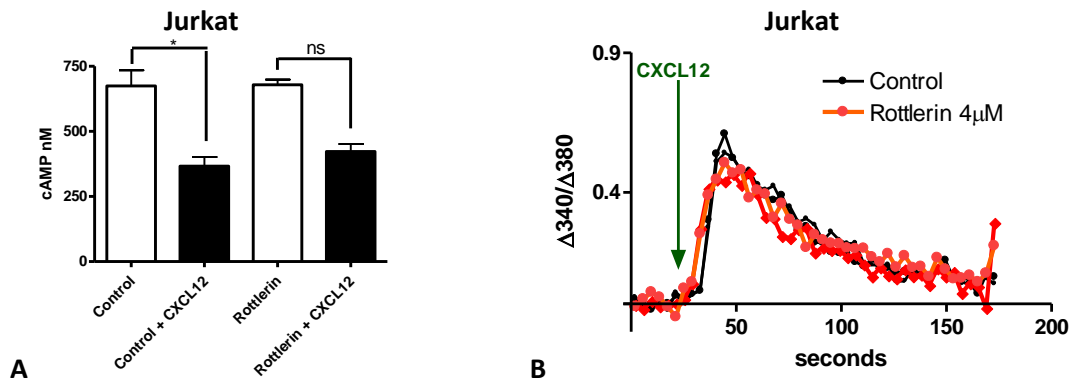


Figure 4.3: Effects of Rottlerin 4  $\mu$ M on cAMP and calcium responses to CXCL12 10 nM. (A) cAMP production in Jurkat following Rottlerin or control measured before or after 20 minutes CXCL12 stimulation. Means  $\pm$  SEM, one-way ANOVA, post-hoc Bonferroni,  $n \geq 3$  independent experiments,  $*=p < 0.05$ . (B) Fura2  $\text{Ca}^{2+}$  assay in Jurkat following Rottlerin or control (Ethanol). Data expressed as fluorescence ratio change ( $\Delta 340/\Delta 380$  nm) i.e. peak fluorescence following CXCL12 addition minus basal fluorescence (prior to chemokine),  $n=1$ .

Jurkat pre-treatment with Rottlerin 4  $\mu$ M blunted cAMP production but had no significant effect calcium responses in response to CXCL12 stimulation.

Rottlerin at 2  $\mu$ M was found to have no significant inhibitory effects on chemotaxis, or at 4  $\mu$ M on calcium responses, although it blunted cellular cAMP reduction following CXCL12 stimulation. However PKC $\delta$  siRNA knock-down did inhibit Jurkat chemotaxis, suggesting that if there are any Jurkat responses to Rottlerin they are complex. It is possible Rottlerin's off target effects masked any inhibitory effects. Rottlerin was found to reduce the establishment of cell-cell contacts due to E-cadherin and  $\beta$ -catenin internalization [563], and may therefore reduce the cell clumping often observed in Jurkat. Additionally ethanol, the inhibitors solvent, could dehydrate cells, and either effect, less clumping or cell shrinkage, could aid passage through the pores of the Transwell® chemotaxis assay plates and skew results. Additionally Rottlerin at 4  $\mu$ M is reported to cause apoptosis body formation, this may be via death receptor 5 up-regulation [564]. Apoptosis-body formation causes the cells to shrink as contents are lost, this could also explain reported increases in chemotaxis assays through the 5  $\mu$ m pores [565]. MCF7 scratch assays indicated PKC $\delta$  is more relevant to CXCL12 rather than CCL3-induced wound-healing, figure 4.2C.

#### 4.2.2: Staurosporine, GF109203X and PKC isoform knockdown

Staurosporine is a natural product, an alkaloid isolated from *Streptomyces staurosporeus*, that has anti-proliferative actions on many cancer cell-lines as it arrests the cell cycle at G2/M. Staurosporine is also a non-selective inhibitor of PKC with  $\text{IC}_{50} \sim 3$  nM, and for cAMP-dependent protein kinase  $\sim 8$  nM. Jurkat caspase-3 induced-apoptosis, and the release of microparticles (apoptotic bodies), is reported within 2 hours of treatment with staurosporine [566, 567]. Staurosporine 10 nM treatment of Jurkat caused little inhibition of chemotaxis, no



effects on calcium production, but did blunt cAMP reduction in Jurkat but not THP-1, all response to CXCL12, figure 4.4, also in wound-healing assays caused apoptosis of MCF7 over 24 hours of incubation (data not shown).

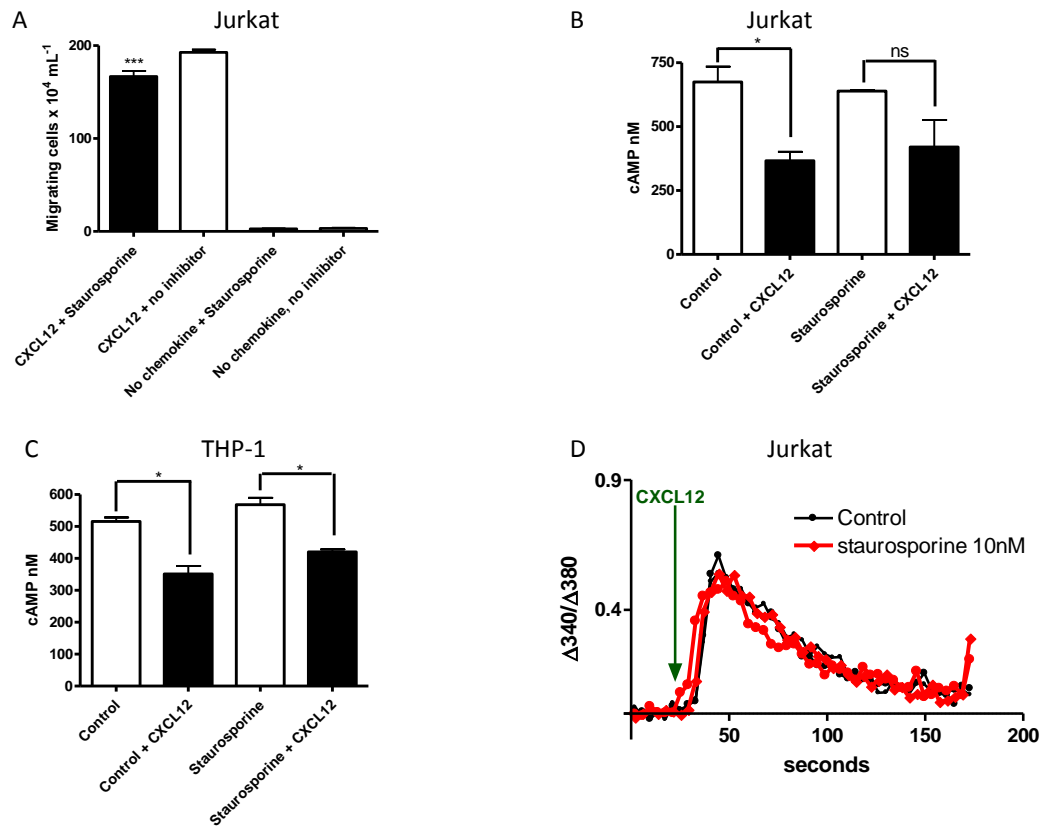


Figure 4.4: Effects of Staurosporine 10 nM on chemotaxis, cAMP and calcium responses to CXCL12 in Jurkat. (A) Chemotaxis to 1 nM CXCL12. (B and C) cAMP production following Staurosporine or control measured before or after 20 minutes CXCL12 10 nM stimulation. Means  $\pm$  SEM, one-way ANOVA, post-hoc Bonferroni,  $n \geq 3$  independent experiments, \*\*\* =  $p < 0.001$ , \* =  $p < 0.05$ . (D) Fura2  $\text{Ca}^{2+}$  assay following Staurosporine or control. Data expressed as fluorescence ratio change ( $\Delta 340/\Delta 380$  nm) i.e. peak fluorescence following CXCL12 addition minus basal fluorescence (prior to chemokine).  $n=1$ .

GF109203X is a pan PKC inhibitor, reported to inhibit PKCs with an  $\text{IC}_{50}$  values of  $\sim 0.008 \mu\text{M}$  ( $\text{PKC}\alpha$ ),  $0.21 \mu\text{M}$  ( $\text{PKC}\delta$ ),  $0.132 \mu\text{M}$  ( $\text{PKC}\epsilon$ ) and  $5.8 \mu\text{M}$  ( $\text{PKC}\zeta$ ) respectively, it caused significant toxicity in MCF7 and THP-1, figure 4.5

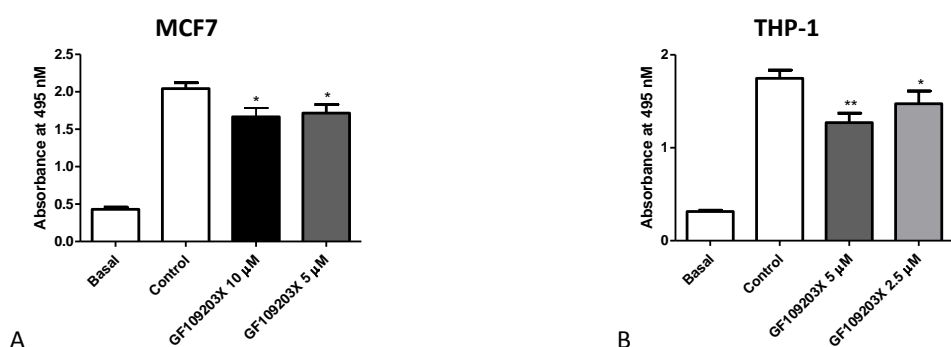


Figure 4.5: Cytotoxicity assays for GF109203X. MTS assays were over 24 hours in (A) MCF7 and over 7 hours in (B) THP-1. Basal absorbance occurs in presence of medium after MTS treatment in the absence of cells. Means  $\pm$  SEM, one-way ANOVA, post-hoc Bonferroni,  $n \geq 3$  independent experiments, \*\*= $p < 0.01$ , \*= $p < 0.05$ .

GF109203X inhibited metabolism at 5 and 10  $\mu$ M in MCF7 over 24 hours and at 2.5 and 5  $\mu$ M in THP-1 over 7 hours. The effects of GF109203X at 5  $\mu$ M which should inhibit all PKC isoenzymes was explored in Jurkat and THP-1 cells using chemotaxis, cAMP and calcium assays, figure 4.6, the small effects observed on chemotaxis and cAMP assays in THP-1 may be explained by toxicity rather than any direct effects on PKC's within cells.

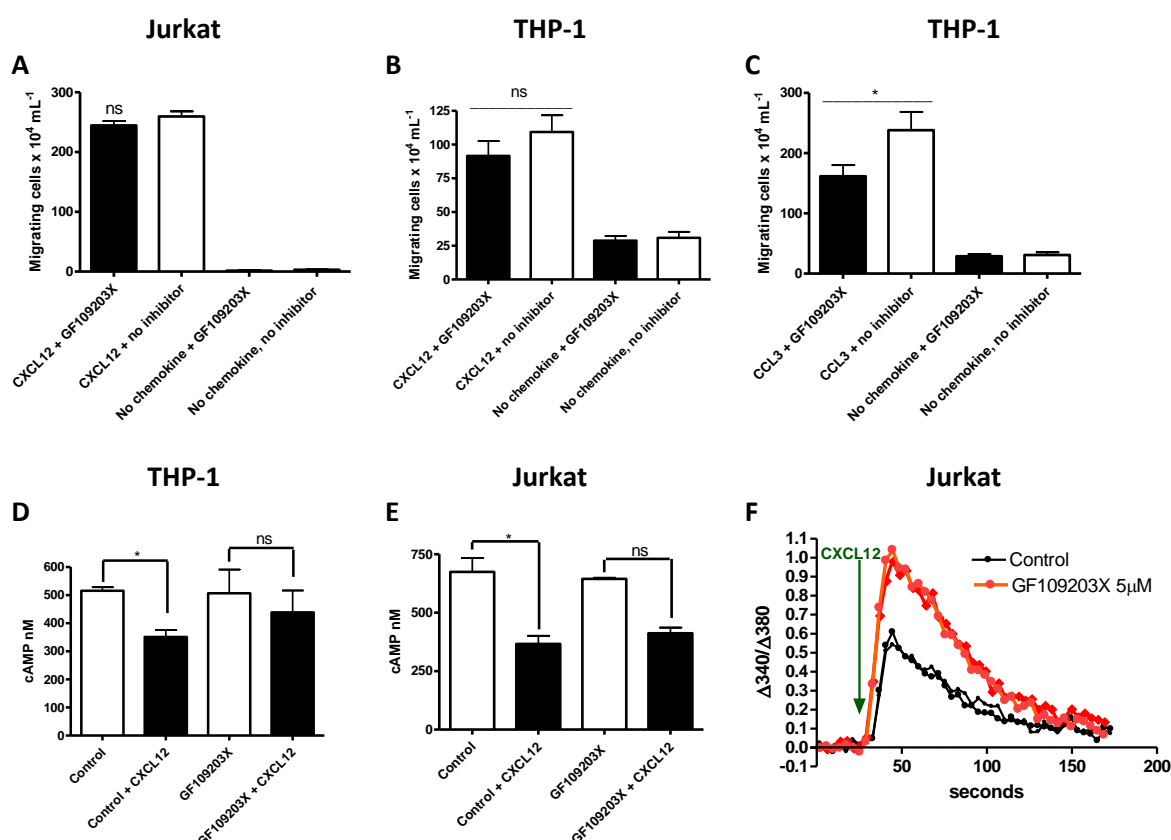


Figure 4.6: Chemotaxis, cAMP and calcium assays following pre-treatment with GF109203X at 5  $\mu$ M or control (DMSO). (A) Chemotaxis of Jurkat to 1 nM CXCL12. (B) THP-1 chemotaxis to 1 nM CXCL12. (C) THP-1 chemotaxis to 1 nM CCL3. (D) cAMP production in THP-1 and (E) Jurkat both measured before or after 20 minutes CXCL12 10 nM stimulation measured before or after 20 minutes CXCL12 10 nM stimulation. Means  $\pm$  SEM, one-way ANOVA, post-hoc Bonferroni,  $n \geq 3$  independent experiments. (F) Fura2 Ca<sup>2+</sup> assay in Jurkat,  $n=1$ , data expressed as fluorescence ratio change ( $\Delta 340/\Delta 380$  nm) i.e. peak fluorescence following 10 nM CXCL12 addition minus basal fluorescence (prior to chemokine), \*= $p < 0.05$ , ns= $p > 0.05$ .

GF109203X at 5  $\mu$ M did not prevent Jurkat or THP-1 chemotaxis to CXCL12, but slightly inhibited chemotaxis of THP-1 to CCL3. Also GF109203X significantly modify cAMP in response to 20 minutes CXCL12 10 nM in THP-1 and Jurkat. An increase in calcium responses to CXCL12 10 nM in Jurkat was also observed.

The only dramatic effect of GF109203X appeared to be on calcium responses. GF109203X at 5  $\mu$ M can be shown to strongly inhibit CXCL12-induced wound-healing in MCF7 cells [565] however this could be due to its cytotoxicity. Although at 5  $\mu$ M GF109203X would be expected to inhibit PKC $\alpha$ ,  $\epsilon$  and  $\zeta$ . PKC LOF mutations may remove the breaks on GPCR signalling possibly suggesting in certain circumstances PKC inhibitors could increase chemotactic responses. PKC $\alpha$  but not PKC $\epsilon$

was observed to suppresses signalling via Pi3K, PKC $\alpha$  may inhibit the catalytic subunit of Pi3K [568], and inactivate proto-oncogene Akt, this may be prevented by GF109302X [569]. This provides a possible mechanism for GF109302X to increase calcium responses, as observed above; however the very strong orange colouring of GF109302X may also impact on fluorescent assay accuracy. Therefore next the effects of PKC $\alpha$ , and PKC $\epsilon$  siRNA knockdown on MCF7 scratch assays and Jurkat chemotaxis were explored, figures 4.7 and 4.8.

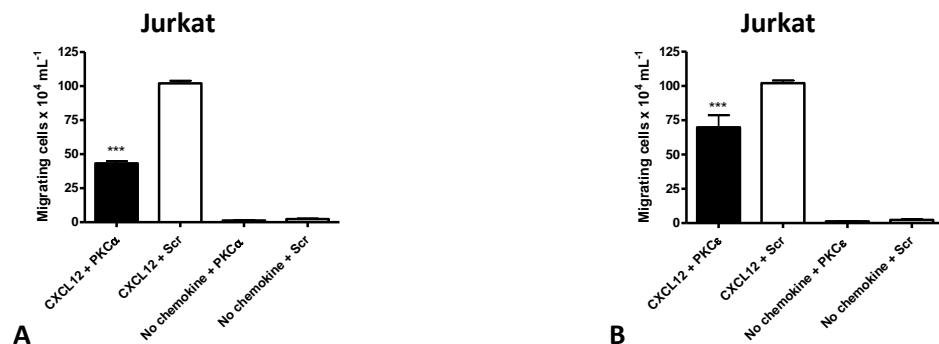


Figure 4.7: PKC $\alpha$  and PKC $\epsilon$  siRNA knockdown in Jurkat. Cells transfected with 50 nM Human PKC $\alpha$ , PKC $\epsilon$  or nonsense siRNA (Scr) control. Chemotaxis assays undertaken 24 hours after transfection to CXCL12 1nM, (A) after PKC $\alpha$  knockdown, (B) after PKC $\epsilon$  knockdown. Means  $\pm$  SEM, one-way ANOVA, post-hoc Bonferroni,  $n \geq 3$  independent experiments, \*\*\*= $p < 0.001$ .

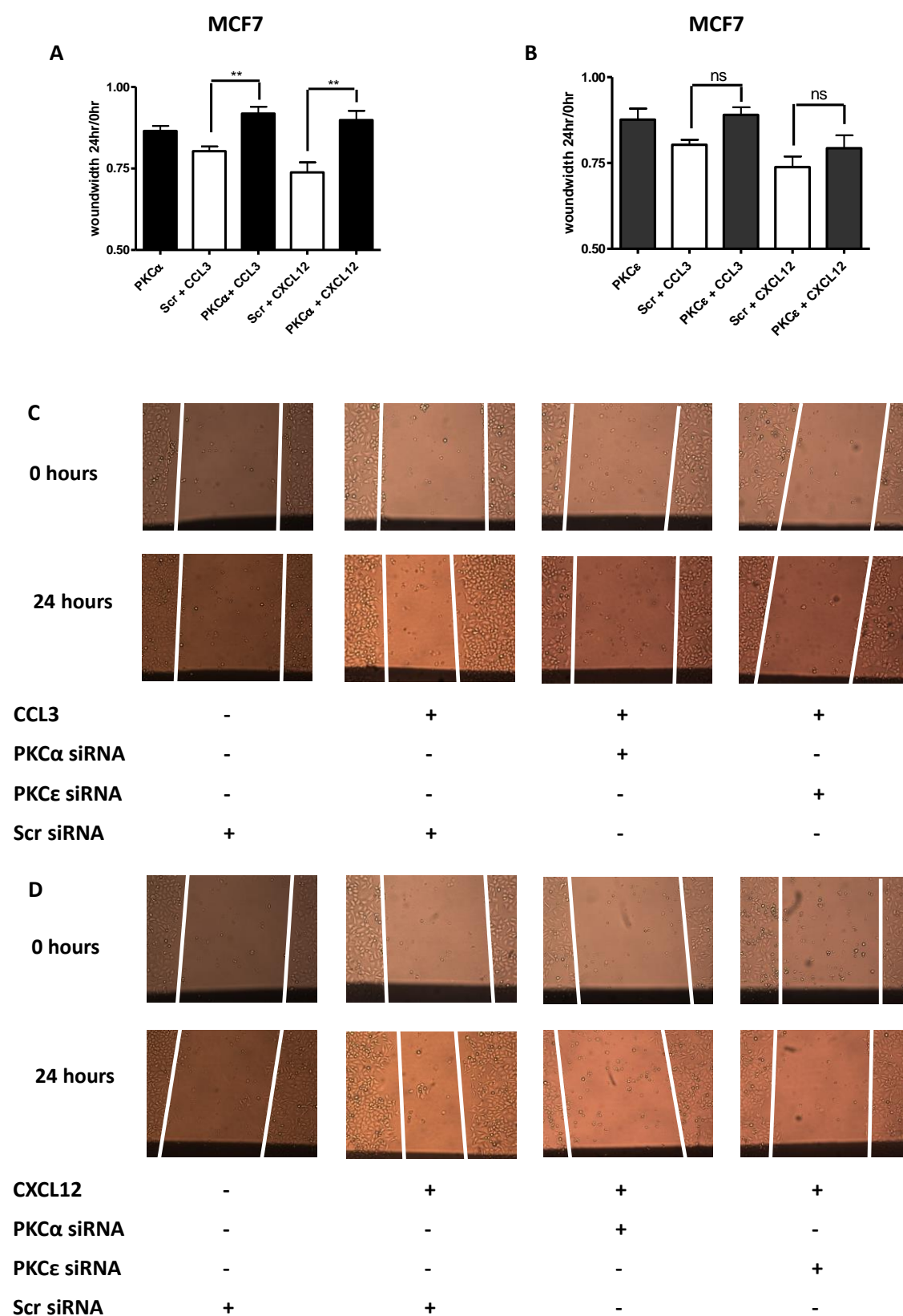


Figure 4.8: PKC $\alpha$  and PKC $\epsilon$  siRNA knockdown in MCF7. Wound-healing assays 24 hours after transfection supported by (A & C) CCL3 10 nM, or (B & D) CXCL12 10 nM, following transfection with 50 nM human PKC $\alpha$ , PKC $\epsilon$  or 50 nM nonsense siRNA (Scr) control. Means  $\pm$  SEM, one-way ANOVA, post-hoc Bonferroni,  $n \geq 3$  independent experiments, \*\*= $p < 0.01$ , ns= $p > 0.05$ .

The success of the PKC $\alpha$  siRNA knock-down was confirmed by western blotting. Knockdown was more complete in MCF7 than Jurkat, figure 4.9, overall suggesting that Jurkat chemotaxis to CXCL12 is highly sensitive to PKC $\alpha$  knockdown.

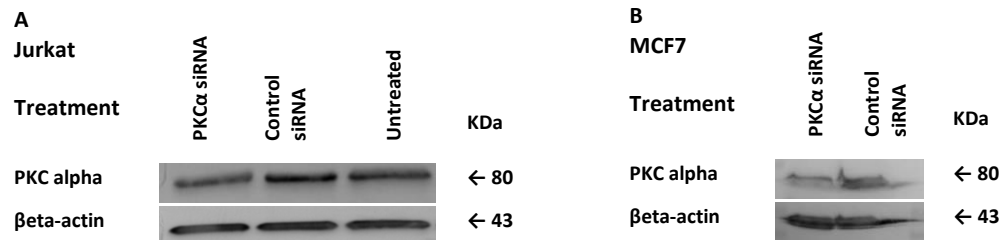


Figure 4.9: siRNA PKC $\alpha$  knockdown was confirmed by Western Blot 24 hours post-transfection, for (A) Jurkat and (B) MCF7, loading confirmed with  $\beta$ -actin.

The chemotaxis assays suggested that in Jurkat CXCL12-induced chemotaxis may be more sensitive to PKC $\alpha$  and PKC $\delta$  inhibition than PKC $\epsilon$ , further experiments are required to confirm this, but one influence on results may be the low expression of novel and atypical PKCs in Jurkat [570]. MCF7 CXCL12- and CCL3-induced wound-healing was inhibited by PKC $\alpha$  but not by PKC $\epsilon$ , whereas PKC $\delta$  knockdown specifically inhibited CXCL12 but not CCL3 migration, figure 4.2 above. PKC $\zeta$  knockdown was also explored in Jurkat and MCF7, see chapter 8 section 8.2.13.

#### **4.2.3: PKD (PKC $\mu$ ) activity is important for CCL3- but not CXCL12-induced chemotaxis in THP-1 cells, and for CXCL12-induced chemotaxis in Jurkat**

Protein Kinase D (aka PKC $\mu$ ) is a calmodulin-dependent kinase so also a target of DAG. There are 3 PKD isoforms PKD1, PKD2 and PKD3. PKD is controlled by PKC-dependent mechanisms. PKC isoforms activate PKD by serine phosphorylation of PKD's activation loop. The PKD pathway is involved through NF $\kappa$ B in cell survival and proliferation, and transport of proteins from Golgi to plasma membrane and cell migration [571, 572]. Transmembrane glycoprotein E-cadherin, critical for cell-cell adhesions, can be phosphorylated by PKD1 when they co-localise. In cancer such phosphorylation reduces cellular motility. E-cadherin's cytoplasmic tail is anchored to actin via catenins, including  $\beta$ -catenin [573]. When a cell migrates a lamellipodium pushes out at the leading edge, attaches to substrate, and pulls the cell forward, if anchorage is not achieved the lamellipodium flows back into the cell forming a membrane ruffle, any particles adhering to the top or bottom surfaces also move back, this is retrograde flow. Inhibiting PKD inhibits retrograde membrane transport and actin-dependent membrane ruffles hence cytoskeleton dynamics. PKD is reported to be involved in directional lamellipodia formation. In the absence of PKD Rac1 can restore lamellipodia formation but there is still loss of directional migration [574].

The effects of the PKD inhibitor CID755673 and  $\beta$ -catenin inhibitor FH535 were explored in Jurkat and THP-1. In MCF7 wound-healing assays 5  $\mu$ M CID755673 over 24 hours caused cell death (data

not shown) reflecting the significant inhibition of metabolism shown in MTS assay over 24 hour, figure 4.15A. CID755673 did not significantly inhibit metabolism in THP-1, figure 4.15B, but very significantly inhibited Jurkat chemotaxis and calcium flux and produced chemokine specific responses on THP-1 migration, figures 4.10 and 4.11.

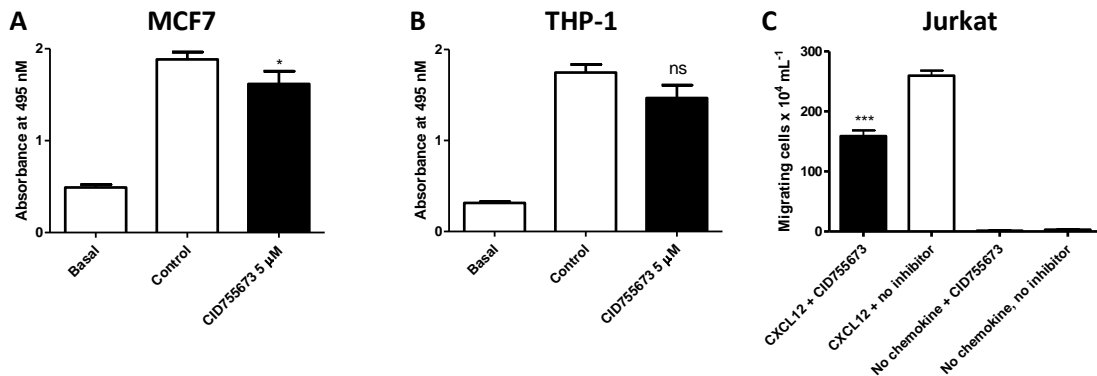


Figure 4.10: Cytotoxicity assays for CID755673. MTS assays were over 24 hours in (A) MCF7 and over 7 hours in (B) THP-1. Basal absorbance occurs in presence of medium after MTS treatment in the absence of cells. (C) Chemotaxis of Jurkat to 1 nM CXCL12. Means  $\pm$  SEM, one-way ANOVA, post-hoc Bonferroni,  $n \geq 3$  independent experiments,  $*$ = $p < 0.05$ ,  $***$ = $p < 0.001$ ,  $ns$ = $p > 0.05$ .

CID755673 at 5  $\mu$ M caused significant inhibition of CXCL12-induced calcium flux in Jurkat but only inhibited CCL3-induced, not CXCL12-induced, chemotaxis in THP-1, figure 4.11.

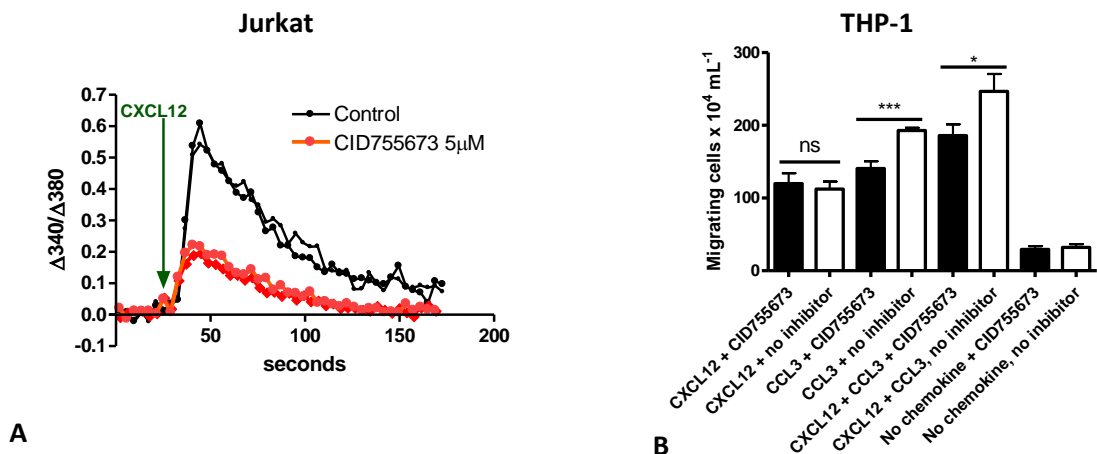


Figure 4.11: Calcium and chemotaxis responses to CID755673 5  $\mu$ M. (A) Fura2  $Ca^{2+}$  assay in Jurkat. Data expressed as fluorescence ratio change ( $\Delta 340/\Delta 380$  nm) i.e. peak fluorescence following 10 nM CXCL12 addition minus basal fluorescence (prior to chemokine). Means  $\pm$  SEM, Student t-test,  $n \geq 3$  independent experiments,  $***$ = $p < 0.001$ ,  $*$ = $p < 0.05$ ,  $ns$ = $p > 0.05$ .

#### 4.2.4: PKD inhibition modulates cAMP levels

PKD inhibition modulated cAMP levels in both THP-1 and Jurkat producing cell type specific effects, figure 4.12.

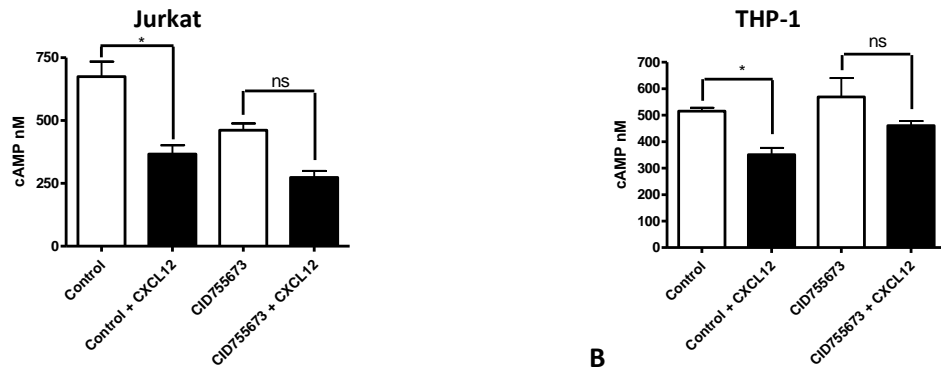


Figure 4.12: cAMP production in (A) Jurkat and (B) THP-1 following 5  $\mu$ M CID755673 or control measured before or after 20 minutes CXCL12 10 nM stimulation. Means  $\pm$  SEM, one-way ANOVA  $n \geq 3$  independent experiments  $*=p < 0.05$ .

CID755673 at 5  $\mu$ M blunted cAMP responses to CXCL12, non-significantly decreased basal and post CXCL12 levels in Jurkat and non-significantly increasing them in THP-1. Possibly supporting the conclusions from the chemotaxis assays that PKD inhibition may produce modest cell-type and chemokine specific effects.

In contrast  $\beta$ -catenin inhibition reduced Jurkat and THP-1 chemotaxis to CXCL12 as well as THP-1 chemotaxis towards CCL3. MTS assays indicated this was not due to inhibitor toxicity, figure 4.13.

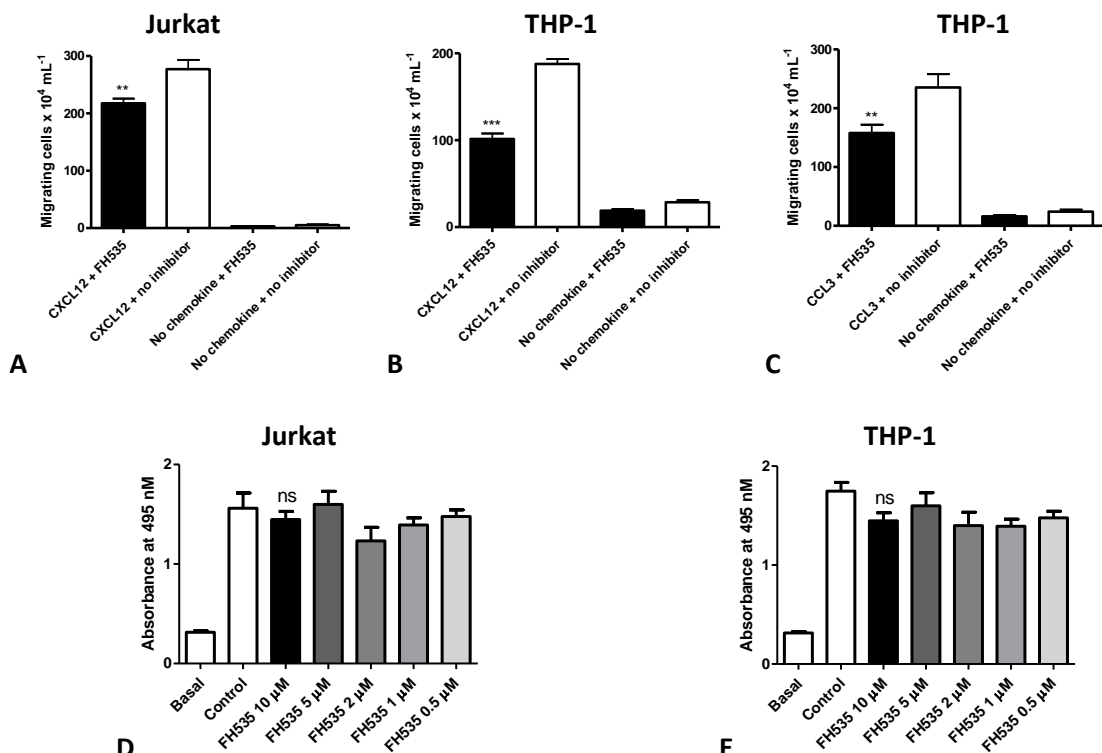


Figure 4.13: Chemotaxis following pre-treatment with FH535 1  $\mu$ M or control (DMSO). (A) Chemotaxis of Jurkat to 1 nM CXCL12. (B) THP-1 chemotaxis to 1 nM CXCL12. (C) THP-1 chemotaxis to 1 nM CCL3. (D & E) Cytotoxicity assays for FH535. MTS assays were over 7 hours in (D) Jurkat and (E) THP-1. Basal absorbance occurs in presence of medium after MTS treatment in the absence of cells. Means  $\pm$  SEM, one-way ANOVA, post-hoc Bonferroni,  $n \geq 3$  independent experiments,  $***=p < 0.001$ ,  $**=p < 0.01$ ,  $ns=p > 0.05$ .



#### 4.2.5: PKC inhibitors – effects on cellular calcium dynamics appear isoform specific

As displayed above Staurosporine and Rottlerin did not change calcium release compared to control, GF109203X increased both peak fluorescence and total calcium release whereas PKD inhibitor CID755673 highly significantly reduced both calcium release and chemokine induced peak fluorescence, these results, shown separately above, are summarised in figure 4.14.

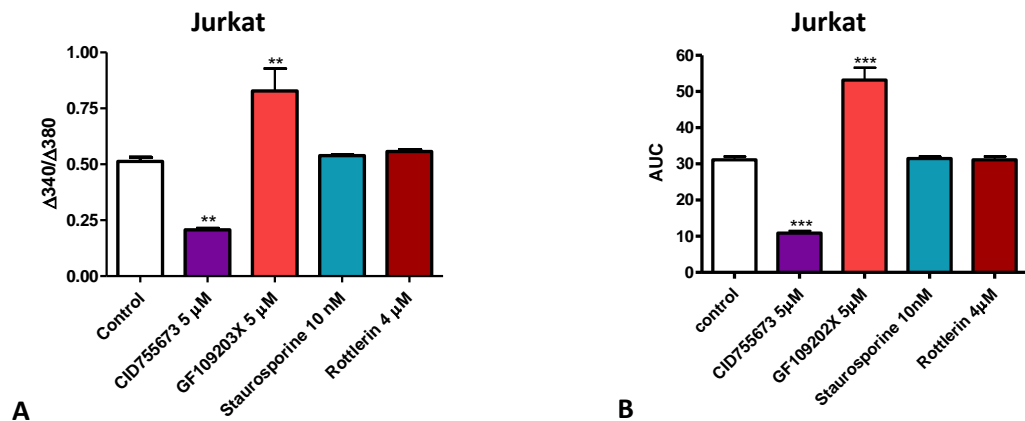


Figure 4.14: Fura2  $\text{Ca}^{2+}$  assay in Jurkat following treatment with PKC inhibitor or control. Data expressed as (A) fluorescence ratio change ( $\Delta 340/\Delta 380$  nm) i.e. peak fluorescence following 10 nM CXCL12 additions minus basal fluorescence (prior to chemokine); (B) Area under curve (AUC). Means  $\pm$  SEM, one-way ANOVA, post-hoc Bonferroni,  $n \geq 3$  independent experiments, \*\*\*= $p < 0.001$ , \*\*= $p < 0.01$ .

Overall results suggest PKD is important in Jurkat for calcium, cAMP and chemotactic responses to CXCL12. Inhibiting PKC $\mu$  (PKD) in Jurkat reduces calcium responses, but inhibiting PKC with Rottlerin and Staurosporine have no significant effect the effects. GF109203X inhibits PKC $\alpha$ ,  $\epsilon$  and  $\zeta$ ; may increase calcium flux or its effects may be due to fluorescent assay interference as the inhibitor has a strong fluorescent orange colouring. Overall results suggest PKC signalling in MCF7, THP-1 and Jurkat is isoform, chemokine and cell-type specific.

#### 4.2.6: Src and Ras/Raf/MEK/ERK signalling appear important for CCL3 and CXCL12 induced migration in THP-1 and MCF7 and for CXCL12-induced migration in Jurkat

c-Src protein tyrosine kinases (Src) are a family of non-receptor tyrosine kinases which have roles in cell signalling, adhesion, proliferation and migration. Src functions in agonist-induced receptor desensitization [553]. Both raised and lowered Src activity can alter cell migration. Over expression of Src can modulated cell dynamics and adhesion to other tissues. Src supports migration by aiding both cell adhesion to integrins and also disruption of cell-cell focal contacts, so has the potential to help leukocytes move through the extracellular matrix. Cofilin is involved in cellular dynamics and Focal Adhesion Kinase (FAK) in cell adhesion. Upregulation of Src does not alter the levels of FAK but increases its phosphorylation state, whereas Src upregulation decreases phosphorylation of cofilin, increasing F-actin dynamics, triggering cellular activity such as filopodia

formation. Filopodia are thin projections that can extend out from a migrating cell's leading edge, they are produced by actin bundles in the cytoplasm [554]. Inhibition of Src with 4-[(2,4-Dichloro-5-methoxyphenyl)amino]-6-methoxy-7-[3-(4-methyl-1 piperazinyl) propoxy]-quinolinecarbo nitrile (bosutinib) a Src tyrosine kinases inhibitor significantly inhibited chemotaxis to CXCL12 and CCL3 by THP-1 and to CXCL12 by Jurkat. Bosutinib did not inhibit cell metabolism at concentrations used, figures 4.15 and 4.16. Bosutinib also inhibits wound-healing in MCF7 [565].

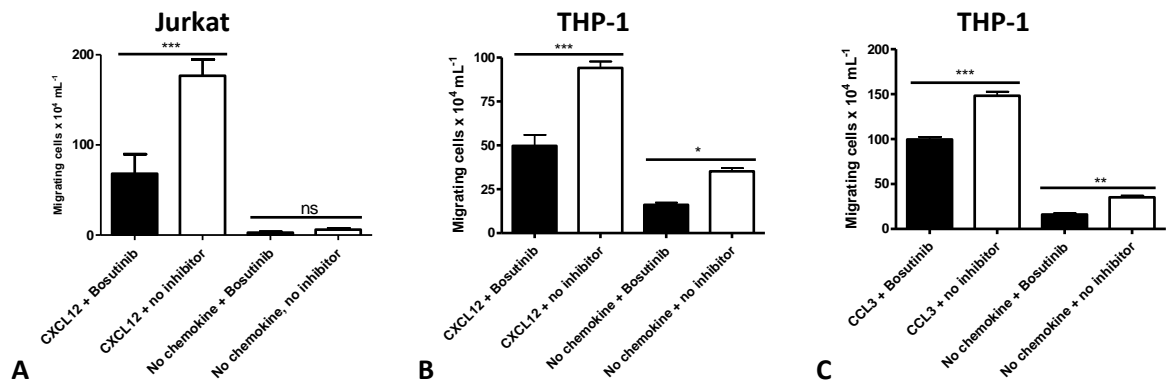


Figure 4.15: (A) Chemotaxis of Jurkat to CXCL12 1nM following pre-treatment with 1.25  $\mu\text{M}$  Bosutinib or control (DMSO). (B) Chemotaxis of THP-1 following pre-treatment with 0.5  $\mu\text{M}$  Bosutinib to CXCL12 1 nM or (C) CCL3 1 nM. Means  $\pm$  SEM, one-way ANOVA, post-hoc Bonferroni,  $n \geq 3$  independent experiments, \*\*\*= $p < 0.001$ , \*\*= $p < 0.01$ , \*= $p < 0.05$ .

MTS assays over 7 hours in Jurkat and THP-1 indicated in these cell lines that concentrations of Bosutinib at 5  $\mu\text{M}$  and above were toxic, however no toxicity was observed even at 10  $\mu\text{M}$  in MCF7 over 24 hours, figure 4.16.

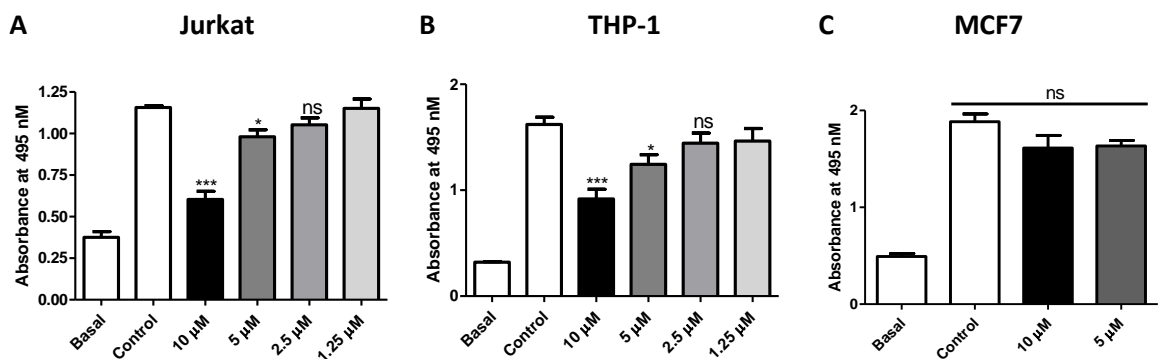


Figure 4.16: Cytotoxicity assays for Bosutinib. MTS assays were over 7 hours in (A) Jurkat and (B) THP-1 and over 24 hours in (C) MCF7 cells. Basal absorbance occurs in presence of medium after MTS treatment in the absence of cells. Means  $\pm$  SEM, one-way ANOVA, post-hoc Bonferroni,  $n \geq 3$  independent experiments, \*\*\*= $p < 0.001$ , \*= $p < 0.05$ , ns= $p > 0.05$ .

Bosutinib had no effect on calcium assays in THP-1, figure 4.17A but in cAMP assays in Jurkat at 5  $\mu$ M Bosutinib reduce basal levels of cAMP but had no significant effect on levels following 20 minutes of CXCL12 stimulation, figure 4.17B. Actin fibre visualisation following treatment of CHO.CCR5 cells with 5  $\mu$ M Bosutinib indicated inhibition of migration see in above assays may be due to disruption of F-actin formation, figure 4.17C. Bosutinib is reported to damage cell morphology [575] in cell-lines.

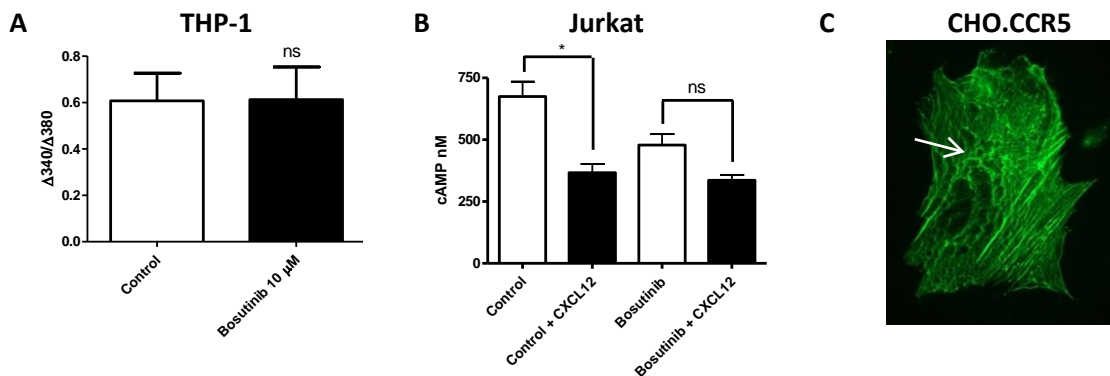


Figure 4.17: Calcium and cAMP assays with Bosutinib. (A) Fura2  $\text{Ca}^{2+}$  assay in THP-1 following 10  $\mu$ M Bosutinib or control (DMSO). Data expressed as fluorescence ratio change ( $\Delta 340/\Delta 380$  nm) i.e. peak fluorescence following 10 nM CCL3 addition minus basal fluorescence (prior to chemokine). Means  $\pm$  SEM, Student t-test. (B) cAMP production in Jurkat following 5  $\mu$ M Bosutinib measured before or after 20 minutes CXCL12 stimulation. Means  $\pm$  SEM, one-way ANOVA, post-hoc Bonferroni,  $n \geq 3$  independent experiments, ns= $p > 0.05$ , \*= $p < 0.05$ . (C) Alexa-488 Phalloidin actin-stain of CHO.CCR5 following pre-treatment with 5  $\mu$ M Bosutinib (1 hr). Imaged UV inverted microscopy (Leica DMII Fluorescence microscope 500x Ex 490 nm, Em 520 nm).

It can be seen that Bosutinib even at low concentrations significantly inhibits basal migration in THP-1, figure 4.15B & C, and appears to modify filament actin formations in CHO.CCR5. Bosutinib did not significantly modify calcium signalling but reduced cAMP levels, figure 4.17. However in addition to inhibiting Src Bosutinib also inhibits Src-family kinases Lyn and HCK, and is also reported to reduce signalling via Pi3K/Akt/mTOR, JAK/STAT3 and MAPK/ERK pathways [575]. The above results show Bosutinib can inhibit cell migration in presence and absence of chemokines CCL3 and CXCL12, but to explore if this was due to Src inhibition alone siRNA knockdown was undertaken.

#### 4.2.7: Src siRNA knockdown also inhibits cell migration

Src knockdown, using Src siRNA at 50 nM confirmed the importance of Src signalling in MCF7 and THP-1 migration to CCL3 and CXCL12 and Jurkat chemotaxis to CXCL12, figures 4.18 and 4.19.

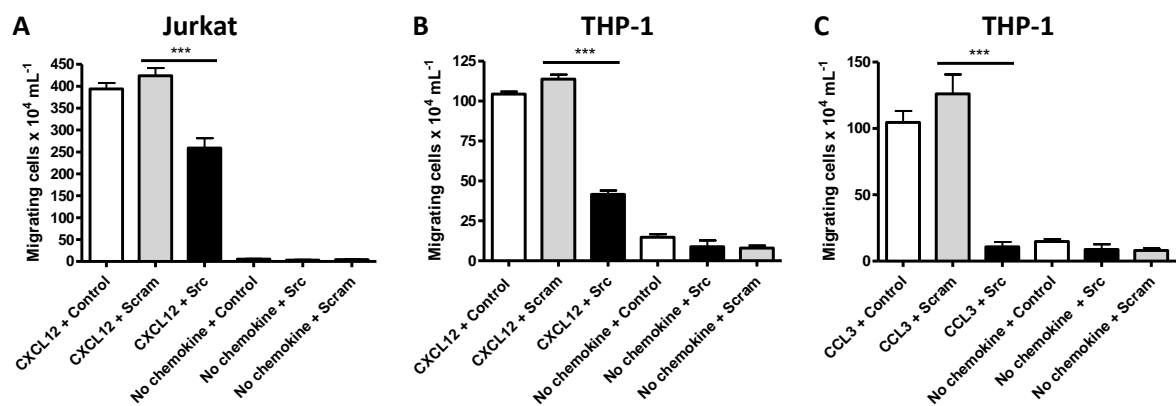


Figure 4.18: Src siRNA knockdown. Cells transfected with 50 nM Human Src or 50 nM nonsense siRNA (Scr) control, chemotaxis assays undertaken 24 hours after transfection. (A) Jurkat chemotaxis to 1 nM CXCL12 (B) THP-1 chemotaxis to 1 nM CXCL12 (C) THP-1 chemotaxis to 1 nM CCL3 (D). Means  $\pm$  SEM, one-way ANOVA, post-hoc Bonferroni,  $n \geq 3$  independent experiments, \*\*\*= $p < 0.001$ .

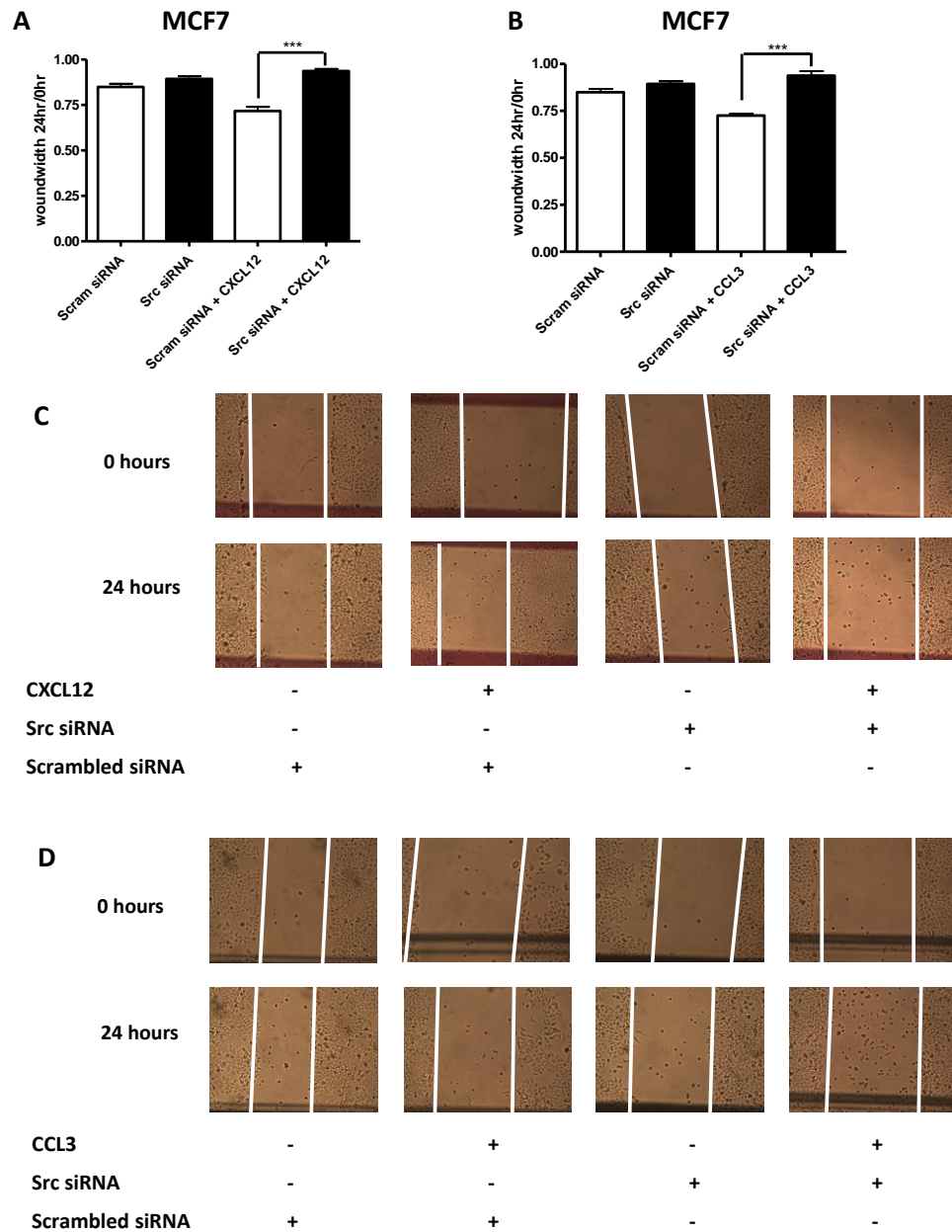


Figure 4.19: Src siRNA knockdown in MCF7. Wound-healing assays undertaken 24 hours after transfected with 50 nM Human Src or 50 nM nonsense siRNA (Scr) control. (A and C) Wound-healing supported by 10 nM CXCL12, or (B and D) 10 nM CCL3. Means  $\pm$  SEM, one-way ANOVA, post-hoc Bonferroni,  $n \geq 3$  independent experiments, \*\*\*= $p < 0.001$ .

siRNA knockdown of Src was confirmed by western blot, figure 4.20.

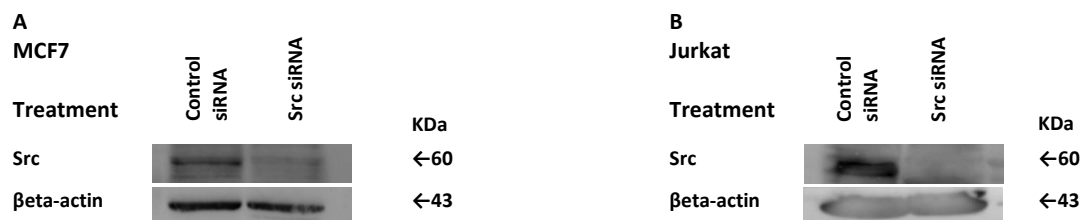


Figure 4.20: Anti-Src Western Blot following transfection with 50 nM Human Src or 50 nM nonsense siRNA (Scr) control (A) MCF7 and (B) Jurkat. Loading confirmed with  $\beta$ -actin.

siRNA knockdown of Src inhibited MCF7 wound-healing supported by CXCL12 or CCL3 and chemotaxis of THP-1 to both CCL3 and CXCL12 and Jurkat to CXCL12, figures 4.18-4.20. The above data confirms other studies that suggest Src signalling is critically important in chemokine-induced migration in both leukemic and breast cancer malignancies. For example Src deregulation is important in the cell proliferation, adhesion, invasion, migration and survival of breast malignancies; and in oncogenic resistance by protecting cells from chemotherapy-induced apoptosis [555]. CXCR4 expression correlates with breast cancer aggressiveness and poor prognosis [576]. Also CXCL12 signalling through CXCR4 links to the BCR/ABL fusion oncoprotein which causes and maintains chronic myelogenous leukaemia (CML). BCR/ABL phosphorylates so activates and dysregulates normal bone marrow progenitor and stem cells causing immature dysfunctional cells to populated the blood and spleen, the phenotype of CML. CXCL12/CXCR4 signalling via Src facilitates BCR/ABL oncoprotein to control CXCL12 signalling through both Pi3K and Ras/MAPK pathways [577, 578].

#### ***4.2.8: Signalling through the Ras/Raf/MEK/ERK pathway lacks chemokine or cell specificity***

The effects of p38 MAPK inhibition and ERK inhibition on CCL3 and CXCL12-induced chemotaxis in leukemic cells was explored using the following small molecule inhibitors, SB203580, which inhibits p38-MAPK stimulation of MAPK APK2 and total SAPK/JNK activity. L779450 which inhibits Raf kinase, and PD98059 which inhibits ERK1/2 and SL327 which inhibits MEK1/2. MAPK/ERK signalling involves the activation by GRKs of small G-protein Ras followed by a Raf, MEK and ERK protein kinases phosphorylation cascade. Malignancies involve uncontrolled growth; this is often due to aberrant MAPK/ERK signalling.

There are three homologues of Raf; B-Raf, A-Raf and Raf 1 also known as C-Raf. In humans, all are kinase components of the Ras/Raf/MEK/ERK signalling pathway. Raf kinases activate MEK1 and MEK2 also known as type 1 and 2 MAP kinase kinases and Mitogen Extracellular signal regulated kinase (MAPKK). MEK threonine and tyrosine kinases subsequently phosphorylate ERK1 and ERK2 thus signals are transferred from cell membrane to cellular effectors regulating cell motility, proliferation and apoptosis [556, 557, 579]. Of the three Raf proteins B-Raf may be the most potent due to its high affinity for MEK1 [580], however there may be cross-talk between Raf homologues [558] and feedback from ERK1 and ERK2 may inhibit Raf-1 phosphorylation so activation [556] while downregulating MEK2 and upregulating MEK1 [559], figure 4.21.

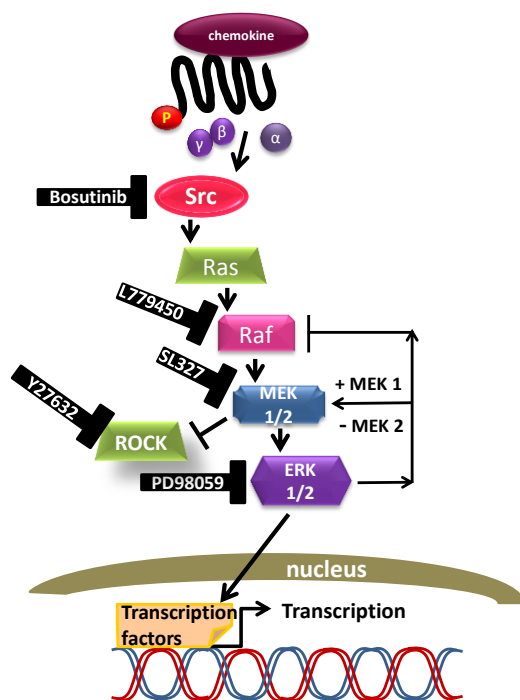


Figure 4.21: Inhibitors and feedback affecting the mitogenic Ras/Raf/MEK/ERK and ROCK signalling pathways [556-558, 579, 580].

Others have used the Raf-1 inhibitor 2-Chloro-5-[2-phenyl-4-(4-pyridinyl)-1H-imidazol-5-yl]phenol (L779450) (for structure see appendix 4), at 10  $\mu$ M for 24 hours to explore the relationship between Raf-1 inhibition and apoptosis regulation, L779450 was found to have a pro-apoptosis affect, and this was attributed to its ability to inhibit Raf-1 [579]. MTS assay here found L779450 at the concentrations used here had no effect on cell metabolism over seven hours but caused significant toxicity over twenty-four hours, figure 4.23, hence L779450, which inhibits Raf-1 by competing for ATP at the protein kinase catalytic site, was only used to explore the effect of Raf-1 inhibition on chemotaxis in Jurkat cells to CXCL12 and THP-1 cells to CXCL12 and CCL3. Inhibition of Raf 1 with 1  $\mu$ M L779450 significantly reduced CXCL12- and CCL3-induced chemotaxis in THP-1 and CXCL12-induced chemotaxis in Jurkat, figures 4.22.

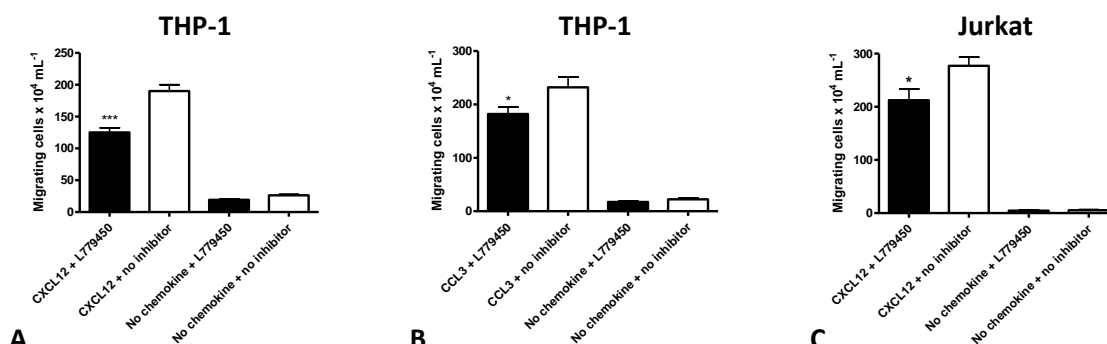


Figure 4.22: Chemotaxis assays following pre-treatment with L779450 or control. (A) Chemotaxis of THP-1 to 1 nM CXCL12, (B) THP-1 chemotaxis to 1 nM CCL3. (C) Jurkat chemotaxis to 1 nM CXCL12. Means  $\pm$  SEM, one-way ANOVA, post-hoc Bonferroni,  $n \geq 3$  independent experiments, \*\*\*= $p < 0.001$ , \*= $p < 0.05$ .

Cytotoxicity assay of in THP-1 showed at 1  $\mu$ M L779450 did not inhibit THP-1 metabolism but in MCF7 over 24 hours caused highly significant inhibition of metabolism. Also 5  $\mu$ M L779450 in Jurkat had no effect on basal cAMP levels or 20 minutes response to CXCL12, figure 4.23.

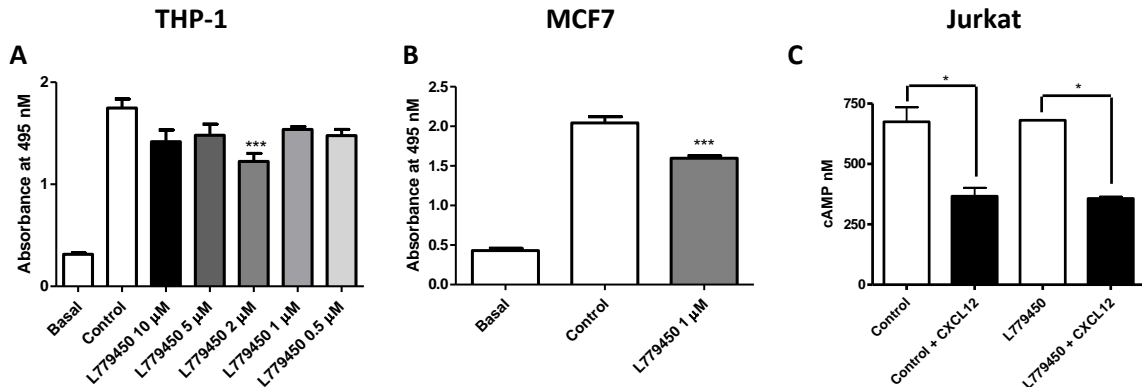


Figure 4.23: Cytotoxicity assays for L779450. MTS assays were over 7 hours in (A) THP-1 and over 24 hours in (B) MCF7 cells. Basal absorbance occurs in presence of medium after MTS treatment in the absence of cells. (C) cAMP production in Jurkat following 5  $\mu$ M L779450 or control measured before or after 20 minutes 10 nM CXCL12 stimulation. Means  $\pm$  SEM, one-way ANOVA, post-hoc Bonferroni,  $n \geq 3$  independent experiments, \*\*\*= $p < 0.001$ , \*= $p < 0.05$ .

L779450 also modestly inhibited calcium responses of Jurkat to CXCL12 and THP-1 to CCL3, figure 4.24.

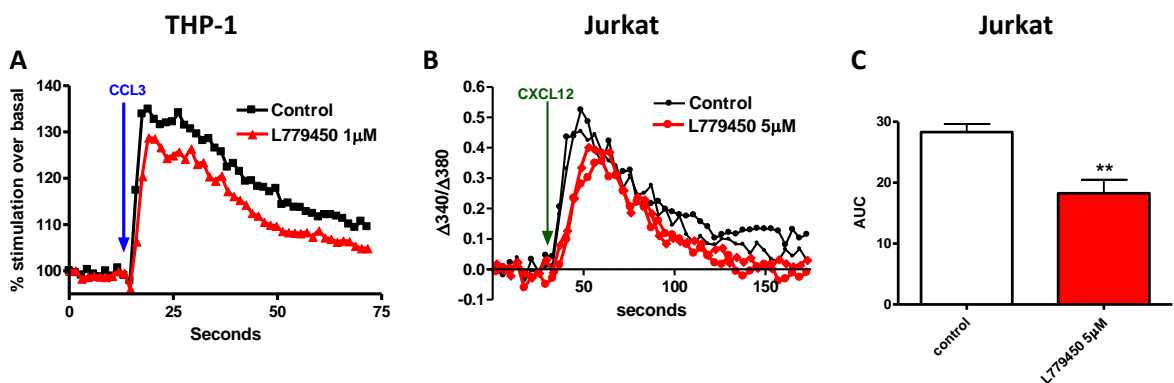


Figure 4.24: Fura2  $Ca^{2+}$  assays following L779450 or control (DMSO). In (A) THP-1 trace, (% stimulation over basal)  $n=1$  (B) Jurkat, Data expressed as fluorescence ratio change ( $\Delta 340/\Delta 380$ ) nm i.e. peak fluorescence following 10 nM CCL3 or 10 nM CXCL12 addition minus basal fluorescence (prior to chemokine),  $n=1$ . (C) Jurkat 10 nM CXCL12, Area under curve (AUC), Means  $\pm$  SEM, Student t-test,  $n \geq 3$  independent experiments, \*\*= $p < 0.01$ .

CXCL12 can induce chemotaxis but can also in some circumstances induce proliferation, for example in leukemic cells in stromal cultures. Such proliferation can be prevented by CXCR4 antagonists such as AMD3100 [581]. CXCL12 appears not to have proliferative effects on normal leukocytes in stromal cultures [582]. This suggests CXCL12 is working in synergy with other factors



present in malignancies, possibly other cytokines such as IL-3 and IL-7 present in the stromal support. Pre-treatment of leukemic cells with ERK1/ERK2 inhibitor PD98059 or p38 MAPK inhibitor SB203580 was found to inhibit proliferation triggered by CXCL12 in the presence of stromal tissue [583]. Here the effects of PD98059 and SB203580, (for structures see appendix 4), on CXCL12 and CCL3-induced chemotaxis in Jurkat and THP-1 were explored after MTS assays established concentrations that did not inhibit metabolism, figures 4.25-4.28.



Figure 4.25: Cytotoxicity assays for 10 µM SB203580. MTS assays were over 7 hours in (A) THP-1 and (B) Jurkat. Basal absorbance occurs in presence of medium after MTS treatment in the absence of cells. Means  $\pm$  SEM, one-way ANOVA, post-hoc Bonferroni,  $n \geq 3$  independent experiments, ns= $p > 0.05$ .

At 5 µM SB203580 had little impact on chemotaxis (data not shown) but at 10 µM inhibited CXCL12-induced chemotaxis in both Jurkat and THP-1 and THP-1 to CCL3, figure 4.26.

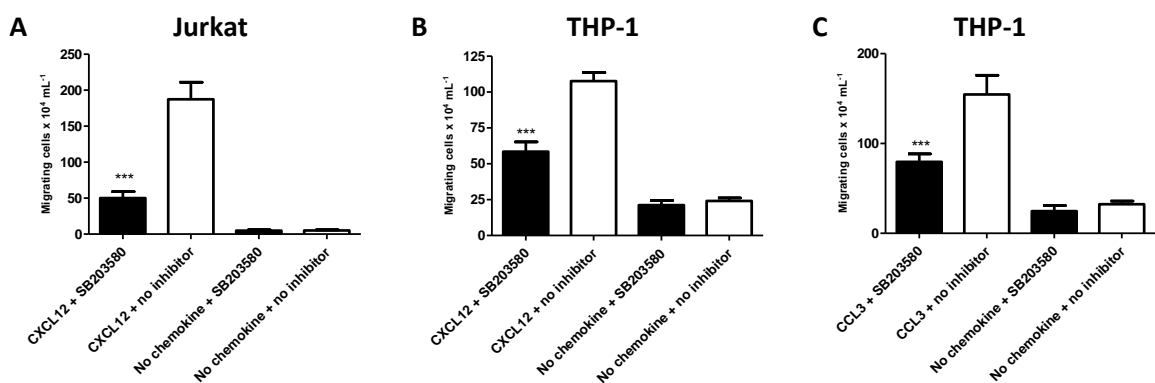


Figure 4.26: Chemotaxis assays following pre-treatment with 10 µM SB203580 or control (DMSO). (A) Chemotaxis of Jurkat to 1 nM CXCL12. (B) THP-1 chemotaxis to 1 nM CXCL12. (C) THP-1 chemotaxis to 1 nM CCL3. Means  $\pm$  SEM, one-way ANOVA, post-hoc Bonferroni,  $n \geq 3$  independent experiments, \*\*\*= $p < 0.001$ .

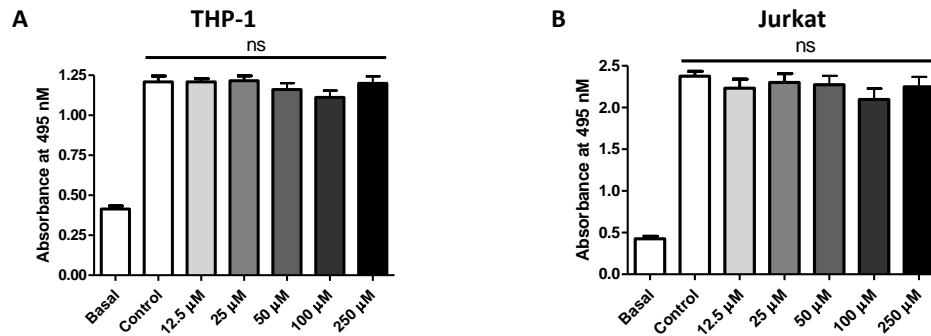


Figure 4.27: Cytotoxicity assays for PD98059. MTS assays were over 7 hours in (A) THP-1 and (B) Jurkat. Basal absorbance occurs in presence of medium after MTS treatment in the absence of cells. Means  $\pm$  SEM, one-way ANOVA, post-hoc Bonferroni,  $n \geq 3$  independent experiments, ns= $p > 0.05$ .

PD98059 at 25  $\mu$ M significantly inhibited both Jurkat chemotaxis to CXCL12 and THP-1 chemotaxis to CCL3. At 25  $\mu$ M PD98059 blunted cAMP responses to CXCL12 in Jurkat, possibly by reducing basal levels, figure 4.28.

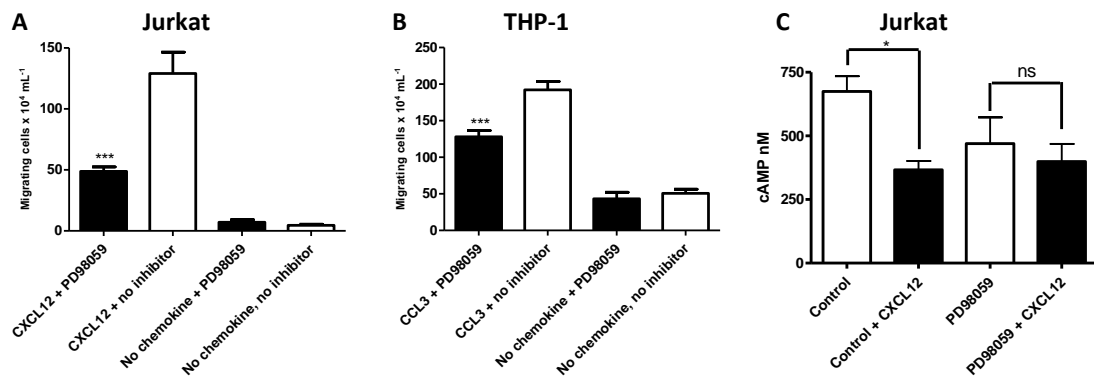


Figure 4.28: Chemotaxis assays following pre-treatment with 25  $\mu$ M PD98059 or control (DMSO). (A) Chemotaxis of Jurkat to 1 nM CXCL12. (B) THP-1 chemotaxis to 1 nM CCL3. (C) cAMP production in Jurkat following 25  $\mu$ M PD98059 or control measured before or after 20 minutes 10 nM CXCL12 stimulation. Means  $\pm$  SEM, one-way ANOVA, post-hoc Bonferroni,  $n \geq 3$  independent experiments, \*\*\*= $p < 0.001$ , \*= $p < 0.05$ .

PD98059 at 25 $\mu$ M was found to have no effect on calcium signalling in response to CXCL12 or CCL3, figure 4.29.

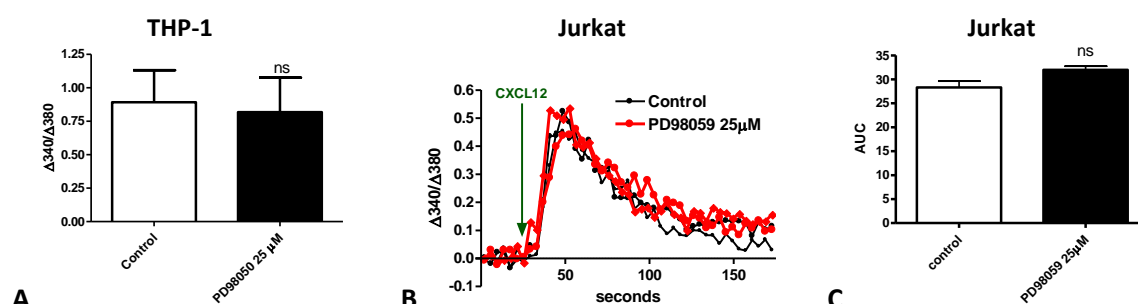


Figure 4.29: Fura2  $\text{Ca}^{2+}$  assay following 25  $\mu\text{M}$  PD98059 or control (DMSO). (A) THP-1 responses to 10 nM CCL3 (B & C) Jurkat responses to 10 nM CXCL12. (A & B) Data expressed as fluorescence ratio change ( $\Delta 340/\Delta 380$  nm) i.e. peak fluorescence following 10 nM CCL3 or 10 nM CXCL12 addition minus basal fluorescence (prior to chemokine) (C) Area under curve. Means  $\pm$  SEM, Student t-test,  $n \geq 3$  independent experiments, (B, trace  $n=1$ ),  $ns=p>0.05$ .

Results show targeting signalling through ERK1/ERK2 with PD98059 or p38 MAPK with SB203580 can specifically inhibit chemotaxis in Jurkat and THP-1 to these chemokines, and that the reduction in chemotaxis is not due to toxic effects of the inhibitors on cell metabolism.

#### ***4.2.9: Inhibiting pairs of signalling proteins provides further evidence of signalling through Src and Ras/Raf/MEK/ERK pathways triggered by CXCL12 and CCL3.***

The Ras/Raf/MEK/ERK pathway is often dysregulated in malignancies. This can be due to BRAF or NRAS mutations [584]. BRAF and NRAS can be targeted therapeutically but often resistance develops [585, 586]. A situation where targeting downstream Raf, MEK or ERK signalling may be helpful. However MEK inhibition may induce unhelpful Pi3K signalling [587]. Metastatic cells can invade or escape tissues by stimulating matrix metalloproteases (MMP's) digestion of the extracellular matrix (ECM), this can be activated by MEK/ERK signalling. To migrate cancer cells attach to the extracellular matrix and then need to change shape, which requires Rho/ROCK-mediated actin dynamics [588]. Cell movement requires integrin-mediated ECM adhesion which is itself regulated by SRC kinases, and can be inhibited by Src inhibitors [589]. Src kinases are implicated in both cell invasion and cell migration, and aberrant Src signalling is implicated in many cancers [590]. Inhibition of pairs of proteins involved in Src/Ras/Raf/MEK/ERK CXCL12 and CCL3 signalling was explored to look for synergistic inhibition of chemotaxis that may be applicable to preventing metastatic spread, figures 4.30-4.34.

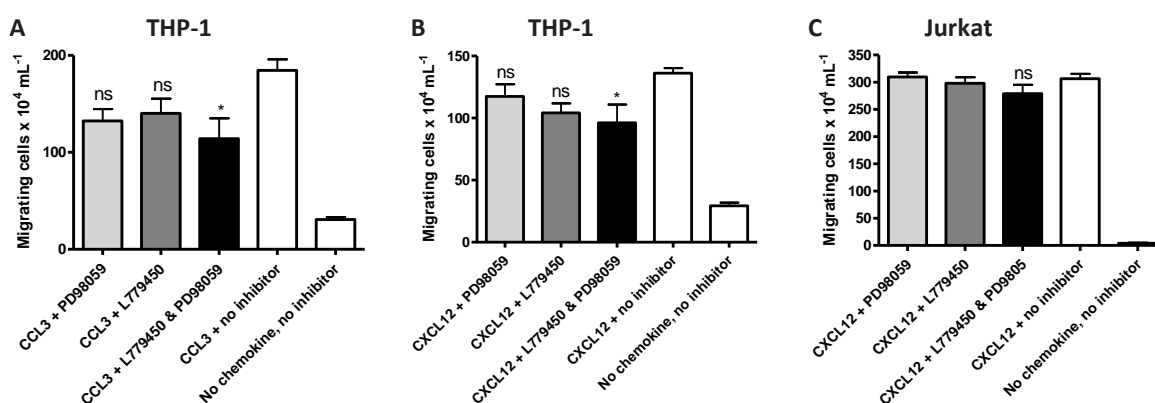


Figure 4.30: Chemotaxis assays following pre-treatment with 0.5  $\mu\text{M}$  L779450 and/or 12.5  $\mu\text{M}$  PD98059 or control (DMSO). (A) Chemotaxis of THP-1 to 1 nM CCL3. (B) THP-1 chemotaxis to 1 nM CXCL12. (C) Jurkat chemotaxis to 1 nM CXCL12. Means  $\pm$  SEM, one-way ANOVA, post-hoc Bonferroni,  $n \geq 3$  independent experiments,  $*$ = $p < 0.05$ , ns= $p > 0.05$ .

Combined low dose Raf (0.5  $\mu\text{M}$  L779450) and ERK (12.5  $\mu\text{M}$  PD98059) inhibition produces slightly greater inhibition of chemotaxis than L779450 or PD98059 at the same concentrations alone in THP-1 to CCL3 or CXCL12 but not in Jurkat to CXCL12, figure 4.30. For chemical structures of inhibitors used in this section please see appendix 4.

Similarly in THP-1 combined low dose Raf (0.5  $\mu\text{M}$  L779450) and MEK (0.5  $\mu\text{M}$  SL327) inhibition produced only slightly greater inhibition ( $p < 0.05$ ) than Raf or MEK inhibition alone in CCL3 and a slightly increased response ( $p < 0.01$ ) in CXCL12-induced chemotaxis, figure 4.31.

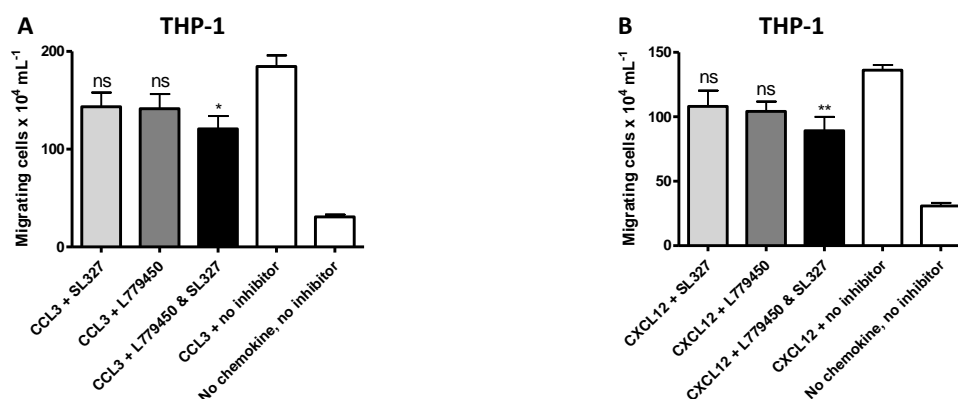


Figure 4.31: Chemotaxis assays following pre-treatment with 0.5  $\mu\text{M}$  L779450 and/or 0.5  $\mu\text{M}$  SL327 or control (DMSO). (A) Chemotaxis of THP-1 to 1 nM CCL3. (B) THP-1 chemotaxis to 1 nM CXCL12. Means  $\pm$  SEM, one-way ANOVA, post-hoc Bonferroni,  $n \geq 3$  independent experiments,  $**$ = $p < 0.01$ ,  $*$ = $p < 0.05$ , ns= $p > 0.05$ .

Raf and ROCK simultaneous inhibition produced more chemokine and cell-type specific responses. Combined Raf (0.5  $\mu\text{M}$  L779450) and ROCK (0.5  $\mu\text{M}$  Y27632) inhibition produced very significantly ( $p < 0.001$ ) increased inhibition of chemotaxis compared to Raf or ROCK inhibition alone in CXCL12-

induced chemotaxis in THP-1 but less inhibition ( $p<0.01$ ) in CCL3-induced chemotaxis in THP-1 or CXCL12-induced chemotaxis in Jurkat ( $p<0.05$ ), figure 4.32.

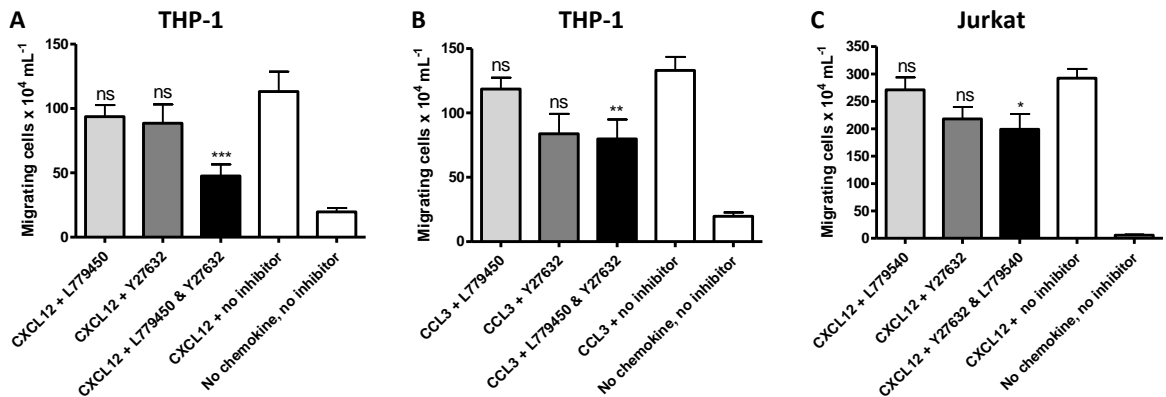


Figure 4.32: Chemotaxis assays following pre-treatment with 0.5  $\mu$ M L779450 and/or 0.5  $\mu$ M Y27632 or control (DMSO). (A) Chemotaxis of THP-1 to 1 nM CXCL12. (B) THP-1 chemotaxis to 1 nM CCL3. (C) Jurkat chemotaxis to 1 nM CXCL12. Means  $\pm$  SEM, one-way ANOVA, post-hoc Bonferroni,  $n\geq 3$  independent experiments,  $*$ = $p<0.05$ ,  $**$ = $p<0.01$ ,  $***$ = $p<0.001$ , ns= $p>0.05$ .

Raf inhibition with 0.5  $\mu$ M L779450 and Pi3K inhibition with 5  $\mu$ M LY294002 was found to be additive compared to Pi3K inhibition alone in CXCL12 but not CCL3-induced chemotaxis in THP-1, Pi3K itself producing a chemokine specific effect, i.e. no significant inhibition of CCL3-induced chemotaxis, figure 4.33.

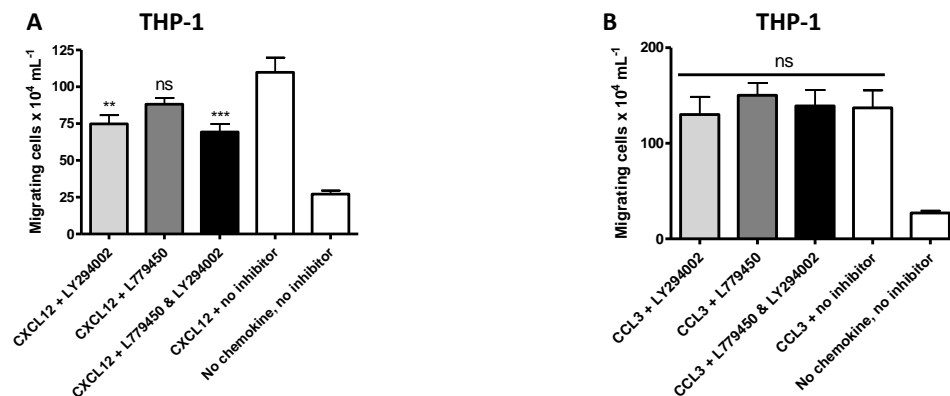


Figure 4.33: Chemotaxis assays following pre-treatment with 0.5  $\mu$ M L779450 and/or 5  $\mu$ M LY294002 or control (DMSO). (A) Chemotaxis of THP-1 to 1 nM CXCL12. (B) THP-1 chemotaxis to 1 nM CCL3. Means  $\pm$  SEM, one-way ANOVA, post-hoc Bonferroni,  $n\geq 3$  independent experiments,  $***$ = $p<0.001$ ,  $**$ = $p<0.01$ , ns= $p>0.05$ .

Similarly 0.5  $\mu$ M L779450 and Pi3K inhibition with 0.5  $\mu$ M AS605240 in THP-1 produced similar additive and chemokine specific effects as L779450 with LY294002, no greater inhibition than Pi3K inhibition alone in CXCL12-induced chemotaxis and no significant inhibition of CCL3-induced chemotaxis, figure 4.34.

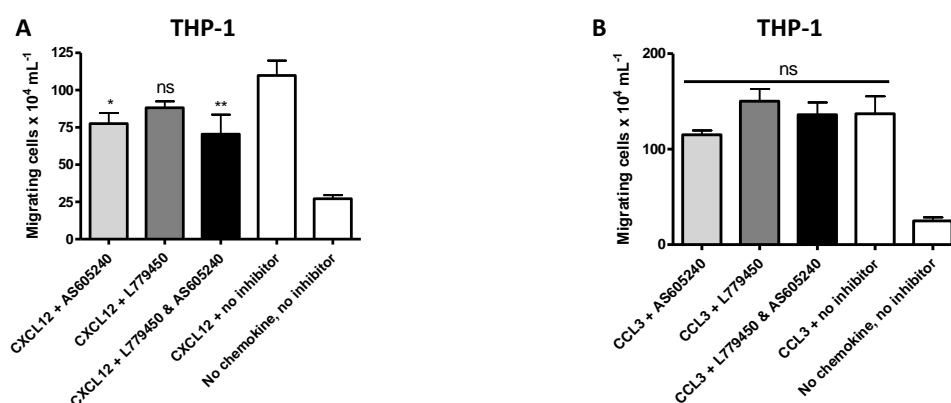


Figure 4.34: Chemotaxis assays following pre-treatment with 0.5  $\mu\text{M}$  L779450 and/or 0.5  $\mu\text{M}$  AS605240 or control (DMSO). (A) Chemotaxis of THP-1 to 1 nM CXCL12. (B) THP-1 chemotaxis to 1 nM CCL3. Means  $\pm$  SEM, one-way ANOVA, post-hoc Bonferroni,  $n \geq 3$  independent experiments, \*\*= $p < 0.01$ , \*= $p < 0.05$ , ns= $p > 0.05$ .

Whereas Src inhibition and Raf inhibition produced no greater effect than Src inhibition alone, figure 4.35.

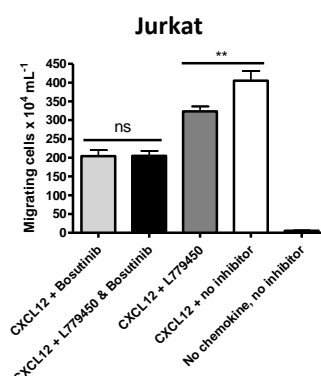


Figure 4.35: Chemotaxis assays following pre-treatment with 0.5  $\mu\text{M}$  Bosutinib and/or 0.5  $\mu\text{M}$  L779450 or control (DMSO). Chemotaxis of THP-1 to 1 nM CXCL12. Means  $\pm$  SEM, one-way ANOVA, post-hoc Bonferroni,  $n \geq 3$  independent experiments, \*\*= $p < 0.01$ , ns= $p > 0.05$ .

### 4.3: Discussion

Here Rottlerin at 2-4  $\mu\text{M}$  failed to inhibit cell migration, calcium flux, or cAMP reduction in response to CXCL12 in Jurkat cells, figures 4.2-4.3. At the higher concentration ethanoic solutions of Rottlerin may increase migration in Jurkat towards CXCL12 [565], this may be as Rottlerin has been shown to induce malignancy in human and rat fibroblasts and can block apoptosis in cells suffering DNA damage [591]. Rottlerin therefore may inhibit cell death in malignant cell-lines such as Jurkat. The Rottlerin used in these experiments was active as was shown to inhibit MCF7 wound-healing (published experiments undertaken by Dr Anja Mueller [565]). Here very different effects were found with siRNA knockdown of PKC $\delta$  compared to Rottlerin treatment, chemotaxis was significantly reduced by PKC $\delta$ , figure 4.2. This was somewhat surprising as PKC $\delta$  can act as a tumour suppressor as over expression can stall the cell cycle at G2/M, and its inhibition is reported to support malignancies [592]. PKC $\delta$  and PKC $\epsilon$  can have opposite effects. PKC $\delta$  can be

pro-apoptotic and inhibit cell proliferation, and can reduce mitochondrial activity inducing apoptosis, whereas in ischaemia PKC $\epsilon$  can prevent mitochondrial damage and cell death [593]. Similarly PKC $\epsilon$  supports NIH3T3 fibroblast cell-line proliferation whereas PKC $\delta$  may support myeloid and epithelial cell differentiation [594, 595]. PKC $\delta$  may be activated by Caspase-mediated proteolytic mechanisms aiding apoptosis in UV or carcinogen damaged keratinocytes preventing skin cancers [596]. Also PKC $\delta$  inhibition can support neoplastic transformation. Ras activating mutations, acting via Transforming Growth Factor alpha (TGF $\alpha$ ) can have opposing effects reducing PKC $\delta$  activation via phosphorylation and expression but not inhibiting PKC $\alpha$ , PKC $\epsilon$  or PKC $\zeta$  [597].

#### ***4.3.1: Roles of PKC $\alpha$ in malignancies***

PKC $\alpha$  is ubiquitously expressed, it promotes cell growth, migration and inhibits apoptosis [598], but PKC $\alpha$  can support both pro- and anti-tumorigenic signalling. PKC effects can show cell-type specificity, but also produce opposite effects in similar cells. For example PKC $\alpha$  upregulated ERK1/2 signalling supporting PAR2-induced cell proliferation, migration and survival in a metastatic colon cell-line [599]. Conversely PKC $\alpha$  can phosphorylate  $\beta$ -catenin marking it for proteasome degradation, reducing Wnt/ $\beta$ -catenin signalling and the cyclin D1 and c-Myc expression which supports proliferation of colon cancers [600]. Also inhibition of PKC $\alpha$  has been shown to inhibit the mesenchymal-amoeboid transition of cells including MDA-MB-231 breast cancer cells, reducing amoeboid invasiveness, hence PKC $\alpha$  may support breast cancer metastasis [601]. This may explain why here knockdown of PKC $\alpha$  reduced CCL3- and CXCL12-induced wound-healing in MCF7 breast cancer cell-line, figure 4.8.

PKC expression levels in cancers can vary as every cancer is genetically different, but also as PKC-regulated signalling pathways can be modulated by the oncogenes expressed in any particular cancer or cell-line [602]. For example PKC $\alpha$  deletion increased lung mutations where K-Ras was activated [603] and PKC $\alpha$  inhibitor GÖ6976 decreased migration of colon cancer cells SW480 [604] whereas in MDA-MD-231 breast cancer cells PKC $\alpha$  activation inhibited cell motility [605]. This may be why assays comparing small molecule inhibitors with siRNA knockdown, and result in different cell-lines can lead to opposite conclusions. Also small molecule inhibitors are rarely specific for example GÖ6976 is marketed as a specific PKC $\alpha$  inhibitor but also hits PKC $\beta$  [606] JAK2, FLT3 [607], and PKC $\mu$  (PKD) [608].

#### ***4.3.2: PKC $\epsilon$ upregulation may support cell survival, invasion and motility***

PKC $\epsilon$  upregulation is seen in some cancers [609], it has been found to increase the rate of cell replication in some cell-lines [610], and the malignant transformation potential of other

carcinogens albeit in mice [611]. PKC $\epsilon$  over expression also inhibits apoptosis in leukaemic [612] and breast cancer cells [613]. PKC $\epsilon$  inhibits programmed cell death triggered both through the extrinsic pathway, through ligand activation of receptors [614], and the intrinsic pathway involving mitochondrial release of apoptotic factors in cellular stress. These direct Activating Transcription Factor 2 (ATF2) to mitochondria increasing membrane permeability and cytochrome C release which activates caspases triggering apoptosis [615]. PKC $\epsilon$  can phosphorylate ATF2 causing its translocation to the nucleus, therefore overexpression of PKC $\epsilon$  can inhibit mitochondrial triggered apoptosis. This has been observed in MCF7 [613]. TNF can produce extrinsic triggered apoptosis, overexpression of PKC $\epsilon$  inhibits this process [616]. Inhibiting PKC $\epsilon$  inhibits apoptotic effects of TNF in lymphomas cells [617]. So PKC $\epsilon$  can promote cell proliferation and inhibit apoptosis [262]. Certainly here siRNA knockdown of PKC $\epsilon$  appeared to have less effect than knockdown of PKC $\alpha$ , figures 4.7-4.8 however the extent of PKC $\epsilon$  knockdown was not established.

PKB (Akt) regulates cell survival, proliferation [618] and metastasis. In MDA-MB-231 breast cancer cells which overexpress PKC $\epsilon$  silencing PKC $\epsilon$  decreased proliferation, invasion and motility and metastasis (in mice) [619] similar results were seen in HNSCC cells where PKC $\epsilon$  supported RhoA and RhoC signalling [620]. Here PKC $\epsilon$  knockdown appeared have greater effects in Jurkat than MCF7, figures 4.7-4.8, but again the extent of knockdown was not analysed as no PKC $\epsilon$  antibody was available in the laboratory.

Non-selective PKC inhibitor staurosporine had no effect on Jurkat CXCL12-stimulated chemotaxis, cAMP or calcium assays, figures 4.4 and 4.14. Staurosporine's effects on Jurkat have been studied by others. CXCR4 undergoes slow CXCL12-independent internalisation and recycling. PKC can trigger endocytosis signalling, but CXCR4 trafficking can vary by cell type [279]. Pre-treatment of Jurkat with 10 nM Staurosporine was shown to restore CXCR4 expression reduced by phorbol ester (PMA) treatment, leading researchers to conclude that CXCR4 internalisation in Jurkat is via PKC [570]. CXCR4 internalisation has previously been shown to be mediated by PKC, however CXCL12 and phorbol ester may induced CXCR4 internalisation involving differing pathways, whereas phorbol esters require PKC, PKC usage via CXCL12 induced CXCR4 internalisation was not inhibited by Staurosporine [279, 621]. Therefore the slight inhibition of chemotaxis observed here, figure 4.4, may be due more to Staurosporine off target effects than PKC inhibition.

Pan PKC inhibitor GF109203X in Jurkat had no effect on CXCL12-induced cAMP production or chemotaxis but dramatically increased calcium flux whereas in THP-1 GF109203X reduced CCL3- but not CXCL12-induced chemotaxis, figures 4.5-4.6 and 4.14.





cell-lines. The cAMP responses suggest cross-talk, possibly through GSK3, figure 4.36, and/or other intermediaries may influence chemotaxis. Similarly p38 MAPK inhibitor SB203580 strongly inhibits chemotaxis of Jurkat to CXCL12 and THP-1 to CCL3, figure 4.25-4.26.

Combining Raf and Pi3K inhibition produced additive effects on CXCL12 but not CCL3-induced chemotaxis, figures 4.33-4.34, suggesting biased signalling, Pi3K being more important for CXCL12 but not CCL3-triggered chemotaxis, this is covered further in chapter 5, section 5.2.6 of this thesis.

Combining Src with Raf inhibition, using Bosutinib with L779450, produced no greater inhibition than Src alone, suggesting Src operates near the receptor, high in the signalling pathway, figure 4.35. Whereas Raf with MEK (SL327), Raf with ERK 1/2 (PD98059), and Raf with ROCK (Y27632) inhibition all produced additive inhibitory effects on effect chemotaxis to CXCL12 and CCL3, figures 4.30-4.32. Again this indicated the importance of Raf/MEK/ERK signalling for chemotaxis in these cell-lines, but also suggesting cross-talk with ROCK, occurs from the Raf/Ras/MEK/ERK cascade.

Inhibition of ROCK in adherent cells can inhibit detachment apoptosis which is linked to Rho/ROCK pathway phosphorylation (activation) of cytoskeletal components and actin-myosin contraction which disrupts the E-cadherin mediated cell-cell adhesion balance with actin-myosin contraction [623]. By suppressing ROCK PPAR $\gamma$  is upregulated and PPAR $\gamma$  inhibits GSK3B which allows more  $\beta$ -catenin to move to membrane supporting E-cadherin cell-cell adhesion. Selective PPAR $\gamma$  agonists such as pioglitazone are reported to add to the effects of ROCK inhibitor Y27632 [624].

E-cadherin by recruiting  $\beta$ -catenin inhibits  $\beta$ -catenin nuclear translocation where it will aid the transcription of genes such as c-myc and cyclin D1 facilitating cell proliferation [624, 625], figure 4.37.  $\beta$ -catenin inhibition with FH535, figure 4.13, was found to significantly reduce CXCL12-induced chemotaxis in Jurkat and CXCL12 and CCL3-induced chemotaxis in THP-1.

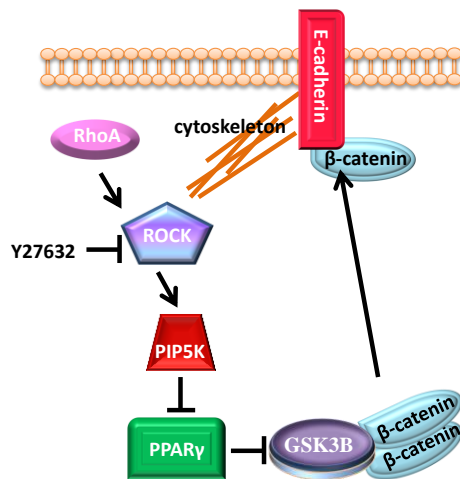


Figure 4.37: Effects of ROCK inhibition on  $\beta$ -catenin signalling [552, 623, 625].

GSK3 inhibition reportedly does not stop CXCL12 phosphorylation of serines in CXCR4 C-terminal [280] however GSK3 can inactivate Slingshot (SSH) [34]. Slingshot dephosphorylates (activates) cofilin, a key protein in cell migration, figure 4.38, discussed further here in chapters 5-8.

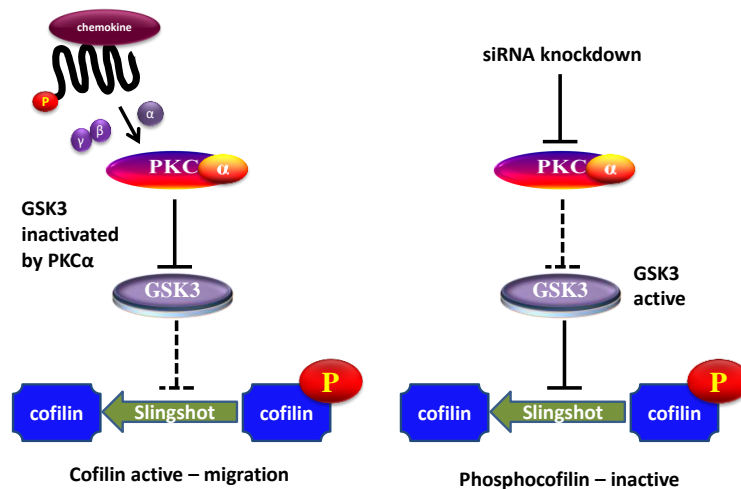


Figure 4.38: PKC signalling through GSK3, Slingshot and cofilin [34, 280].

#### 4.4: Conclusions

The above data suggest Src and PKC are key signalling proteins in CXCL12- and CCL3-induced migration of both the leukaemic and breast cancer cell-lines employed here. Src knockdown with siRNA and small molecule inhibitor Bosutinib produced similar responses. PKC isoenzyme specific responses were apparent with PKC $\alpha$ , PKC $\delta$  and PKC $\mu$  (PKD) being key for CXCL12 signalling, off target effects were possible issues with some small molecule inhibitors of PKC. Overall PKC involvement in CCL3 and CXCL12-induced migration was found to be isoform and cell type specific. Signalling through  $\beta$ -catenin, Src and the Raf/MEK/ERK pathway was not found to be chemokine specific, all of the pathway proteins were important for CCL3- and CXCL12-induced chemotaxis in THP-1 and Jurkat. This conclusion was supported by the additive effects found between inhibition of Raf plus ERK, Raf plus MEK, and Raf plus ROCK. Inhibition of Raf plus Pi3K

produced inhibition of CXCL12- but not CCL3-induced chemotaxis, suggesting CXCL12/CCL3 biased signalling through Pi3K and supporting the use of combination therapies to inhibit more than one mitogenic signalling pathway in metastatic cancers.

The data presented provides evidence for chemokine and cell-type favoured signalling pathways but also obvious cross talk, as where one signalling pathway or component is inhibited other signalling routes appear to ensure chemotactic attraction continues albeit to a reduced extent. Thus signalling pathways originating from any specific receptor, such as CXCR4 or CCR5, cannot be generalised between chemokines or between cell types; this may frustrate pharmacologists but may provide oncologists opportunities to develop targeted therapeutic molecules.

There are many other proteins purportedly involved in cell migration leading to metastasis, important ones include  $\beta$ -arrestins along with cofilin, a cytoskeleton-associated protein that controls actin dynamics.  $\beta$ -arrestins can dephosphorylate and so activate cofilin and spatially regulate cofilin activity [626] therefore in chapter 5 the CXCL12 and CCL3 signalling involving these proteins was explored.

## Chapter 5: CXCL12 and CCL3 chemokine-induced migration in leukaemic and breast cancer cells can involve cofilin phosphorylation, Pi3K and $\beta$ -arrestins

### 5.1: Introduction

Cell dynamics leading to metastasis involves a myriad of signalling and mechanical proteins and the hijacking of homeostatic chemotactic cell migration. Chemotaxis requires a directional leading edge; a small protein called cofilin is key to this process. Cofilin forms **co-filaments** with actin facilitating both EMT and metastasis [627]. Cofilin has three isomers cofilin-1 (non-muscle), cofilin-2 (muscle) and destrin (aka ADF) [628, 629]. Throughout this thesis reference to cofilin refers to cofilin-1. Cofilin expression is upregulated in many cell lines and cofilin activity is controlled by phosphorylation and ATP. De-phosphorylation by phosphatases such as PP2 and Slingshot, itself directed by proteins such as Pi3K, activates cofilin [375, 376]. This allows cofilin to bind actin, causing filament fragmentation and so producing a source of actin filament-initiation barbed ends and actin monomers to build new filaments [373]. Cofilin is inactivated by LIMK phosphorylation mediated by Rho GTPases Rac, Rho and Cdc42 [630, 631]. Metastasis and malignant cell invasion of healthy tissue have been associated with reduced LIM kinase (LIMK) expression and associated lower levels of phosphorylated cofilin [632]. Cell location of phosphorylated cofilin is influenced by 14-3-3 regulatory proteins sequestering Slingshot and also cell membrane PIP<sub>2</sub> sequestering cofilin. PIP<sub>2</sub> itself can be modulated by PLC $\gamma$  [381, 384], figure 5.1.

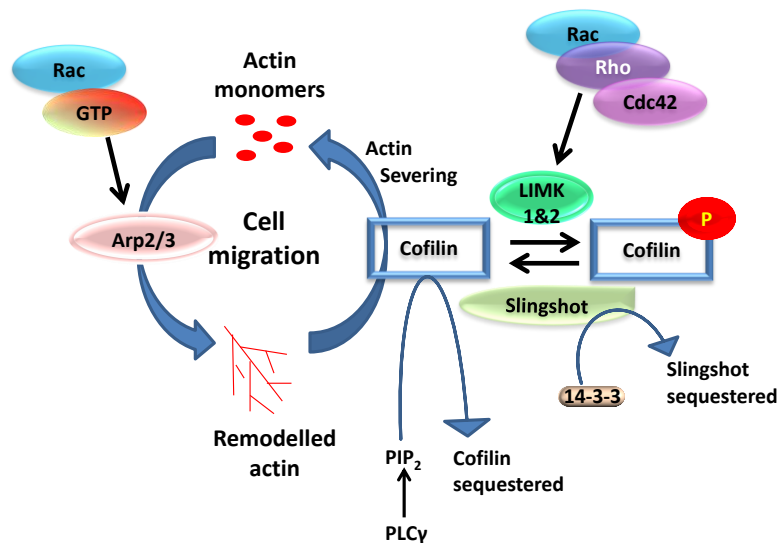


Figure 5.1: Summary of actin remodelling and the involvement of cofilin [375, 376, 386, 630].

**Hypothesis:** Cofilin supports chemokinesis in cancer cells, and is mediated by key signalling pathways involved in metastasis.

**Aim:** To explore the role of  $\beta$ -arrestin and cofilin in CCL3 and CXCL12 chemokinesis; observe the effects, on chemotaxis and cofilin phosphorylation, of inhibition of signalling transducers  $G\beta\gamma$  and GRKs, and key signalling proteins in metastasis Raf, MEK, Pi3K, ROCK and Src.

**Objectives:**

- (i) Establish that cofilin is expressed in cell-lines
- (ii) Explore the effects of siRNA knockdown of cofilin
- (iii) To investigate the effect of chemokines alone and in combinations on chemotactic migration and cofilin phosphorylation
- (iv) Explore the effects on chemotaxis and cofilin phosphorylation of Pi3K inhibition and Pi3K siRNA knockdown, and also of  $G\beta\gamma$ , GRK, FAK, ROCK, and MEK small molecule inhibition.
- (v) Explore the effects of over-expression of  $\beta$ -arrestins on chemokinesis in MCF7, and chemotactic migration in THP-1 and Jurkat.

## **5.2: Results**

Please note controls are common between graphs where experiments were conducted simultaneously; results for each inhibitor or siRNA have been displayed separately for ease of description of results, this applies to: figures 5.15 and 4.18; 5.21D and 5.27.

### **5.2.1: Cofilin modulates leading edge dynamics**

Cofilin is highly expressed in human T-cells; it regulates their movement especially through 3D environments [633]. Therefore Jurkat were first explored as a tool for examining cofilin phosphorylation in response to CXCL12 stimulus. However westerns extracting cytoplasmic but not nuclear cofilin, showed consistent high expression of both phosphorylated cofilin and cofilin, in the presence or absence of CXCL12, figure 5.2. Hence Jurkat did not offer a sensitive readout tool.

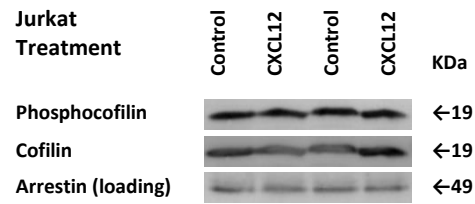


Figure 5.2: Western Blot with total-cofilin and phosphocofilin (Ser3) antibodies reveals cofilin phosphorylation levels in Jurkat in presence and absence of CXCL12 (5 nM, 15 mins before lysis). Arrestin-2 loading control.

### 5.2.2: Cofilin knockdown reduces migration to CCL3 and CXCL12

Cofilin expression in THP-1 and MCF7 was then explored with western blot or immunofluorescence assays. MCF7 were also modified using cofilin siRNA, with knockdown confirmed using western blot, and the effect of this on wound-healing triggered by CCL3 and CXCL12 explored, figure 5.3.

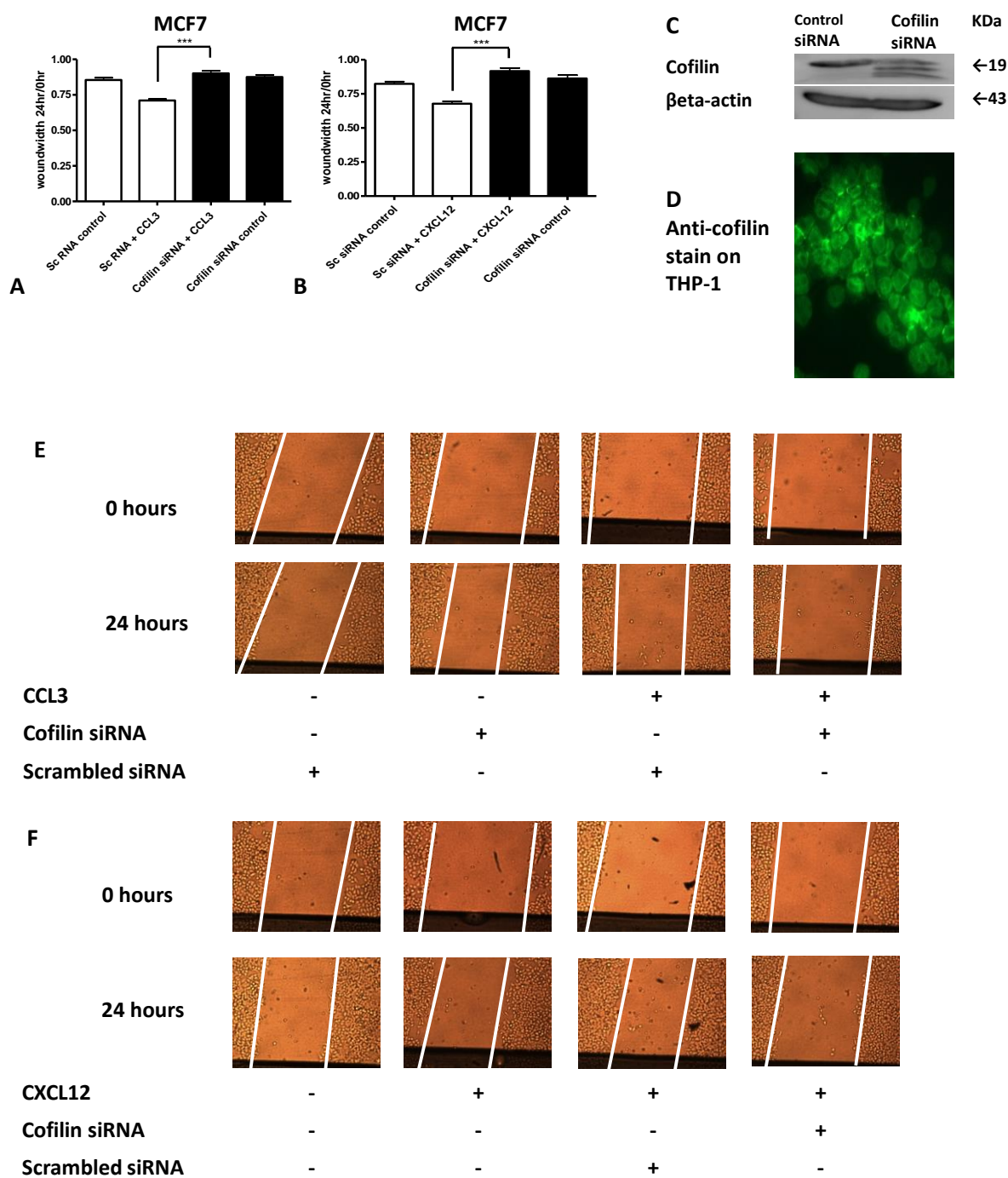


Figure 5.3: Cofilin siRNA knockdown reduced CXCL12 and CCL3 chemokinesis. MCF7 wound-healing assays 24 hours after transfection with 50 nM Cofilin siRNA or nonsense siRNA (Scr) control. Analysis 24 hours after (A and E) 10 nM CCL3, (B and F) 10 nM CXCL12. Means  $\pm$  SEM, one-way ANOVA, post-hoc Bonferroni,  $n \geq 3$  independent experiments, \*\*\*= $p < 0.001$ . (C) Western Blot MCF7 total-cofilin expression 24 hours after siRNA knockdown,  $\beta$ -actin loading control. (D) Immunofluorescent shows THP-1 cofilin expression. THP-1 incubated with anti-cofilin then probed with FITC. Imaged UV inverted microscopy (Leica DMII Fluorescence microscope 500x Ex 490 nm, Em 520 nm).

Complete cofilin knockdown in MCF7 was found to be lethal, whereas partial knockdown producing low expression of cofilin (19 kDa) and cofilin breakdown products with lower molecular



weights, figure 5.3C, very significantly ( $p < 0.001$ ) inhibited wound-healing in MCF7. Complete cofilin knockdown in THP-1 and Jurkat also proved lethal to cells.

### 5.2.3: Cofilin phosphorylation can be triggered by a range of chemokines

Westerns revealed cofilin phosphorylation state could be manipulated by several CC and CXC chemokines in THP-1 to a much greater extent than by CXCL12 in Jurkat, figure 5.4.

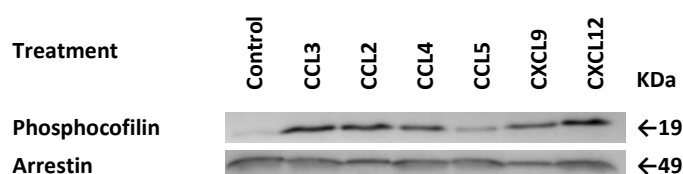


Figure 5.4: Western Blot with phosphocofilin (Ser3) antibody reveals cofilin phosphorylation levels in THP-1 in presence and absence of various chemokines (5 nM, 15 mins before lysis), Arrestin-2 loading control.

In THP-1 various chemokines were found to dramatically alter the phosphorylation state of cofilin, figure 5.4. Results showed that cofilin is present in the phosphorylated and un-phosphorylated forms in unstimulated THP-1 cells at variable levels, so the phosphorylation state of the control, which must be prepared at the same time, was considered alongside results. Basal phosphorylation state may be partly due to the phosphatase activity of Slingshot whose concentration has been shown to vary between different subcellular compartments, and observed to change during the cell division cycle in cultured cells; levels increasing as mitosis proceeds, with maximum levels during telophase and cytokinesis when Slingshot is required to dephosphorylate and reactivate cofilin [634-636].

### 5.2.4: Chemotactic responses to chemokines are concentration dependent

Many chemokines can be shown to induce chemotaxis in THP-1 cells, figure 5.5A, although Jurkat only significantly respond to CXCL12. A Gaussian distribution response to CXCL12 chemokine dose was observed for both cell types; this is also the case for THP-1 chemotaxis to CCL3, figures 5.5 and 5.6.

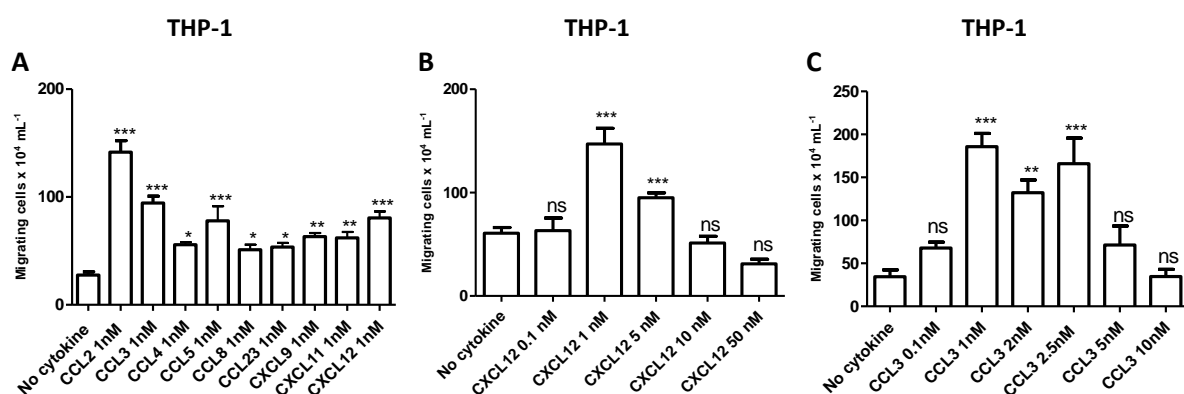


Figure 5.5: (A) THP-1 chemotactic response to various chemokines. (B) THP-1 Chemotactic dose-responses to CXCL12 and (C) to CCL3. Means  $\pm$  SEM, one-way ANOVA comparing to no chemokine, post-hoc Bonferroni,  $n \geq 3$  independent experiments, \*\*\*= $p < 0.001$ , \*\*= $p < 0.01$ , \*= $p < 0.05$ , ns= $p > 0.05$ .

Results in THP-1 suggested that if a chemokine produced cofilin phosphorylation it may also be chemotactic.

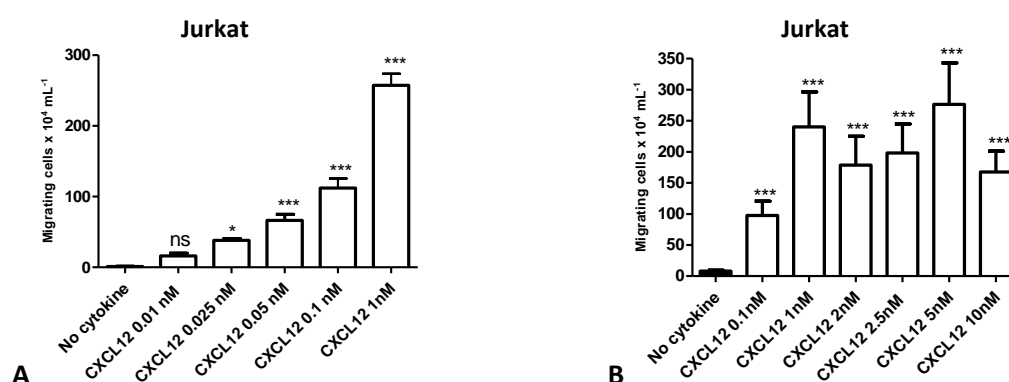


Figure 5.6: Jurkat chemotactic dose-responses to CXCL12 (A) low dose and (B) higher dose. Means  $\pm$  SEM, one-way ANOVA comparing to no chemokine, post-hoc Bonferroni,  $n \geq 3$  independent experiments, \*\*\*= $p < 0.001$ , \*\*= $p < 0.01$ , \*= $p < 0.05$ , ns= $p > 0.05$ .

### 5.2.5: Additive responses between chemokines may suggest dimerization

Chemotaxis responses in THP-1 were additive if both CCL3 and CXCL12 were used in tandem. Such co-operation appeared not always to be the case between CC- and CXC- chemokines; for example in THP-1 with CCL2 and CXCL11, or CCL2 and CXCL9, there was no significant additive effect. CXCL11 produced chemotaxis in THP-1 but little response in Jurkat, however in THP-1 and Jurkat CXCL11 significantly reduced chemotaxis to CXCL12. CXCL11 purportedly can bind CXCR7 and CXCR3, therefore these results may suggest that stimulation of CXCR7 by CXCL12 contributes to CXCR4-induced chemotaxis, figure 5.7. Other concentration combinations of these chemokines may produce different responses.

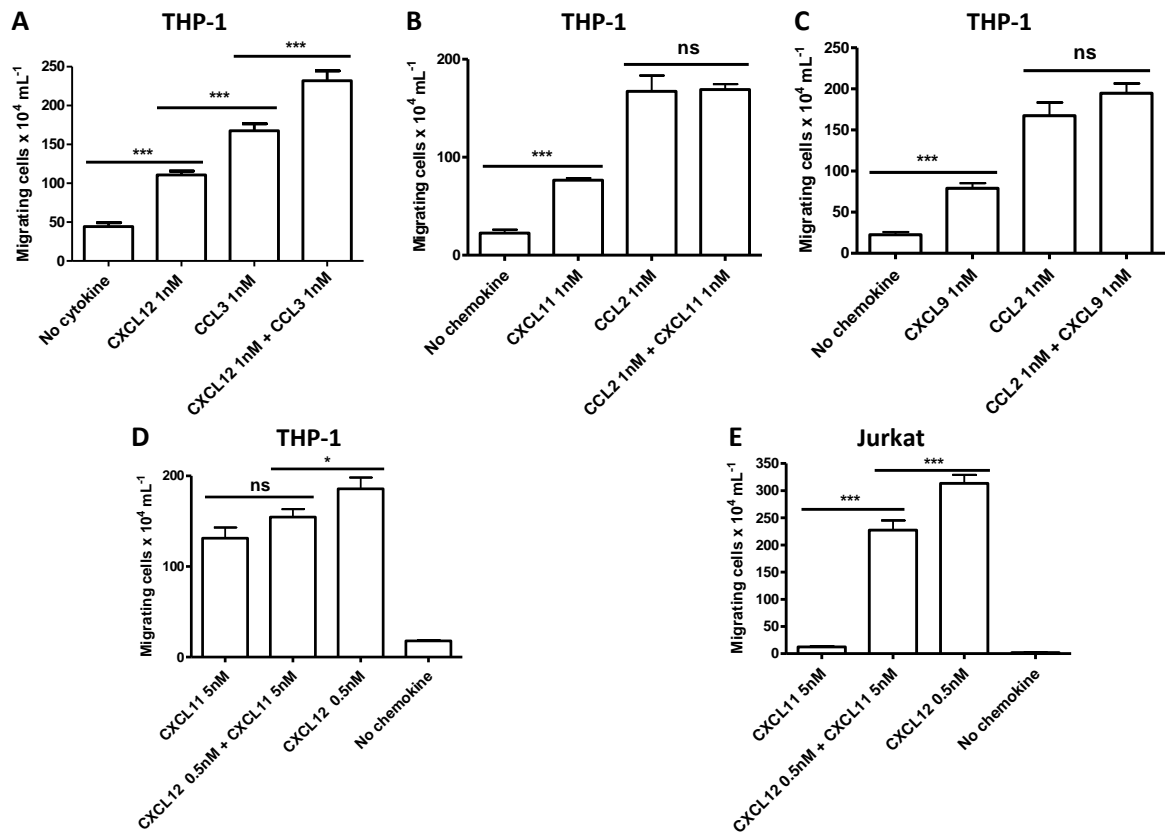


Figure 5.7: (A) THP-1 chemotaxis to CCL3 and/or CXCL12 (B) THP-1 chemotaxis to CCL2 and/or CXCL11. (C) THP-1 chemotaxis to CCL2 and/or CXCL9 (D) THP-1 chemotaxis to CXCL11 and/or CXCL12 (E) Jurkat chemotaxis to CXCL11 and/or CXCL12 Means  $\pm$  SEM, one-way ANOVA, post-hoc Bonferroni,  $n \geq 3$  independent experiments, \*\*\*= $p < 0.001$ , \*\*= $p < 0.01$ , \*= $p < 0.05$ , ns= $p > 0.05$ .

The antibody 12G5 binds CXCR4 inhibiting chemotaxis to CXCL12 in both Jurkat and THP-1. Pre-treatment with 12G5 antibody also inhibited chemotaxis to CXCL11 and CCL3 in THP-1 possibly indicating that CXCR4 supports chemotaxis to both these chemokines in this cell type. In Jurkat pre-treatment with 12G5 reversed some of the negative effects of adding CXCL11 to CXCL12 as a chemoattractant, suggesting the Jurkat expressed CXCR4 and CXCR7, but not CXCR3. In Jurkat and THP-1 pre-treatment with CXCL11 reduced chemotaxis to CXCL12 and combined CXCL12 and CXCL11, pointing to these cells expressing CXCR4, CXCR3 and/or CXCR7, figure 5.8.

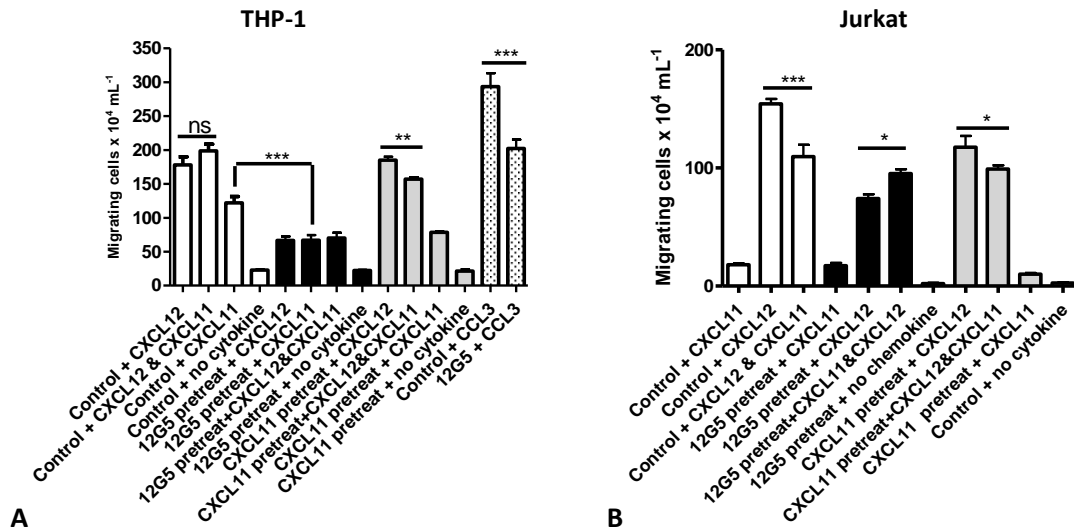


Figure 5.8: (A) THP-1 Chemotaxis to CCL3 1 nM, CXCL11 5nM and CXCL12 0.5 nM after CXCL11 25nM or 12G5 12.5ng/ $\mu\text{L}$  pre-treatment (37°C, 30 mins). (B) Jurkat chemotaxis to CXCL11 5 nM or CXCL12 0.5 nM after CXCL11 25 nM or 12G5 12.5 ng/ $\mu\text{L}$  pre-treatment (37°C, 30 mins). Means  $\pm$  SEM, one-way ANOVA, post-hoc Bonferroni,  $n \geq 3$  independent experiments, \*\*\*= $p < 0.001$ , \*\*= $p < 0.01$ , \*= $p < 0.05$ , ns= $p > 0.05$ .

These results suggest co-operation or dimerization of chemokine receptors or indeed chemokines may contribute to chemotaxis in both THP-1 and Jurkat. Co-operative effects of chemokines on calcium flux were also investigated in MCF7 and THP-1 cells. Both cell types respond well to CCL3 and CXCL12, MCF7 have been shown to highly express CXCR4 and CXCR7 but not CXCR3 [637]. CXCR7 and CXCR3 respond to CXCL11.

CXCL11 pre-treatment of MCF7 cells before calcium flux induced by CXCL12 indicated pre-stimulation of CXCR7 inhibited calcium oscillations, figure 5.9. Overall these results suggest that CXCL11 supports dimerization or co-internalisation of CXCR7 and CXCR4 receptors in MCF7, THP-1 and Jurkat.

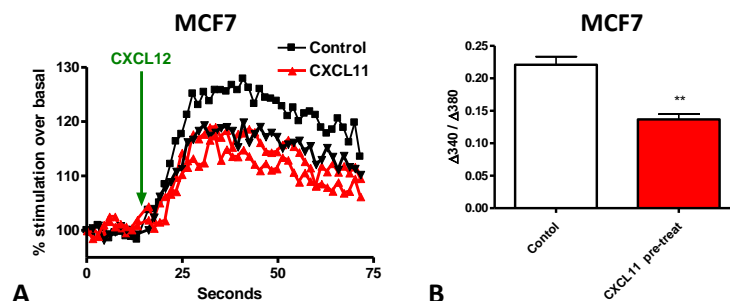


Figure 5.9: Fura2  $\text{Ca}^{2+}$  assay in MCF7 following pre-treatment with CXCL11 10 nM or control ( $\text{H}_2\text{O}$ ). Data expressed as fluorescence ratio change ( $\Delta 340 / \Delta 380 \text{ nm}$ ) i.e. peak fluorescence following 10 nM CCL3 addition minus basal fluorescence (prior to chemokine). (A) trace  $n=1$ , (B) Means  $\pm$  SEM, Student t-test,  $n \geq 3$  independent experiments, \*\* =  $p < 0.01$ .

CXCL12 but not CCL3 signalling is purportedly triggered through Gβγ subunits [638] to Pi3K this signalling can aid malignant cell invasiveness and metastasis. The small molecule inhibitor Gallein can prevent βγ subunit interactions with Pi3K [639]. Here Gallein was shown to specifically inhibit CXCL12 but not CCL3 chemotaxis in THP-1, however in the presence of both chemokines Gallein's inhibitory effects on chemotaxis increased, this was not due to cytotoxicity, figure 5.10.

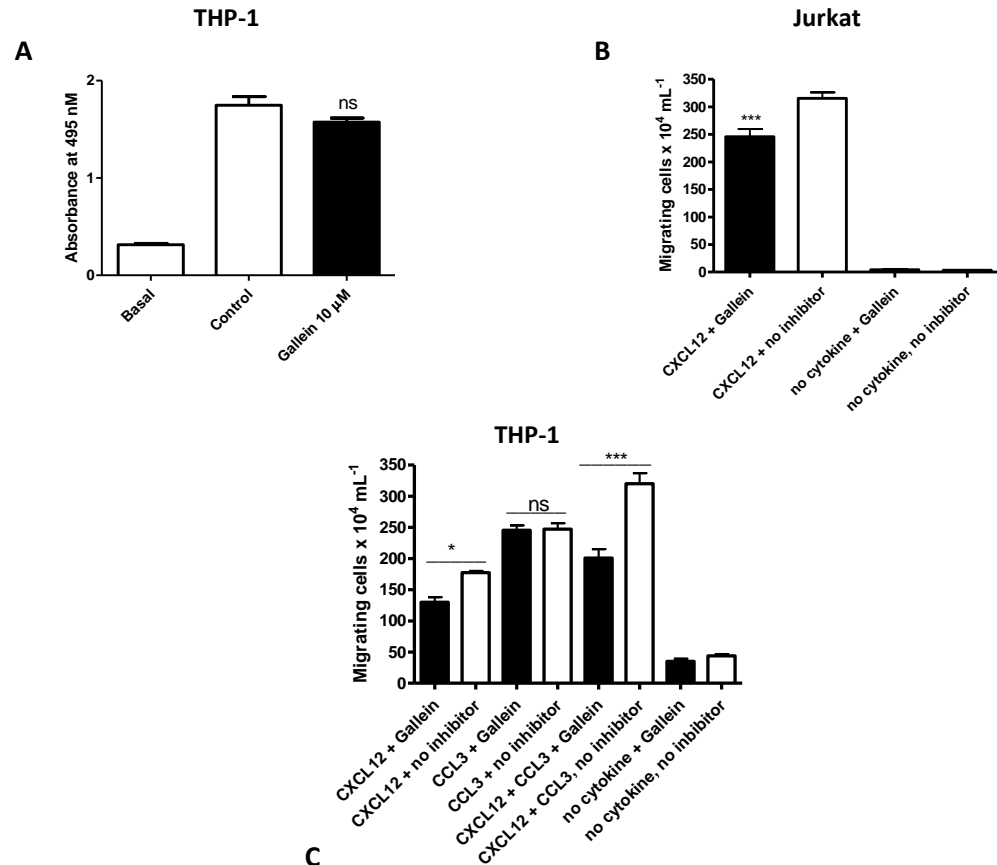


Figure 5.10: The effects of Gallein 10 μM. (A) Cytotoxicity assays over 7 hours in THP-1. (B) Chemotaxis of Jurkat to 1 nM CXCL12. (C) THP-1 chemotaxis to 1 nM CXCL12, 1 nM CCL3 or both. Means ± SEM, one-way ANOVA, post-hoc Bonferroni, n≥3 independent experiments, \*\*\*=p<0.001, \*\*=p<0.01, \*=p<0.05, ns=p>0.05.

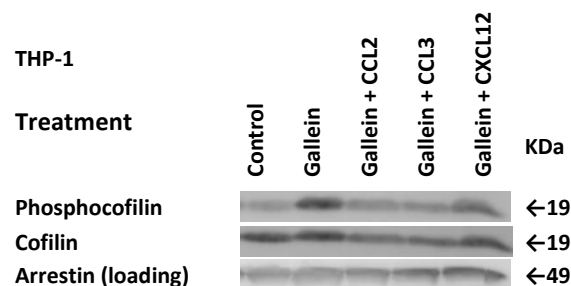


Figure 5.11: Western Blot with total-cofilin and phosphocofilin (Ser3) antibodies reveals cofilin phosphorylation levels in THP-1 following pre-treatment with Gallein 10 μM (37°C, 30 mins) in presence and absence of CCL2, CCL3 or CXCL12 (5 nM, 15 mins before lysis). Arrestin-2 loading control.

Gallein caused phosphorylation of cofilin before stimulation with chemokines but reduced cofilin phosphorylation seen previously in the presence of CCL2 and CCL3, figure 5.4, possibly suggesting  $\beta\gamma$  is involved in CCL2, CCL3 and CXCL12 signalling. Hence next the effect of Pi3K inhibition on cofilin phosphorylation and cell migration was examined.

There are many Pi3K subtypes [640] including dimer 1A which can act as a lipid and protein kinase, it contains catalytic subunit p110 and regulatory subunit p85. Binding of p110 to Ras causes Pi3K activation producing second messenger  $PIP_3$  at the membrane.  $PIP_3$  binds Akt and the kinase PDK1 which itself binds and activates Akt and Rac. Akt can then activate and inhibit various downstream proteins including Caspase-9 and NF $\kappa$ B regulating for example apoptosis, proliferation, and migration [641]. Rac activity may be essential for lamellipodia formation [642]. By influencing Slingshot and thus cofilin phosphorylation Pi3K may mediate actin filament formation and membrane protrusion [643].

#### ***5.2.6: Pi3K inhibition and chemokine-induced migration***

Previous studies have indicated that inhibiting Pi3K signalling may block cofilin dephosphorylation [644, 645]. Chemotaxis investigations using inhibitors LY294002 which reversibly inhibits Pi3K $\alpha$ , Pi3K $\delta$  and Pi3K $\beta$  with  $IC_{50}$ 's of 0.5  $\mu$ M, 0.57  $\mu$ M and 0.97  $\mu$ M, respectively, along with AS605240 a potent and selective inhibitor of Pi3K $\gamma$  with an  $IC_{50}$  of 8 nM and a 30-fold selectivity over Pi3K $\delta$  and Pi3K $\beta$  and 7.5-fold selectivity over Pi3K $\alpha$  indicate that the Pi3K pathway may be involved in migration towards CXCL12 in Jurkat and THP-1, and that Pi3K may have little or no involvement in CCL3-induced chemotaxis in THP-1, figures 5.12 and 5.13. The inhibitors did not inhibit cell metabolism, figure 5.14.

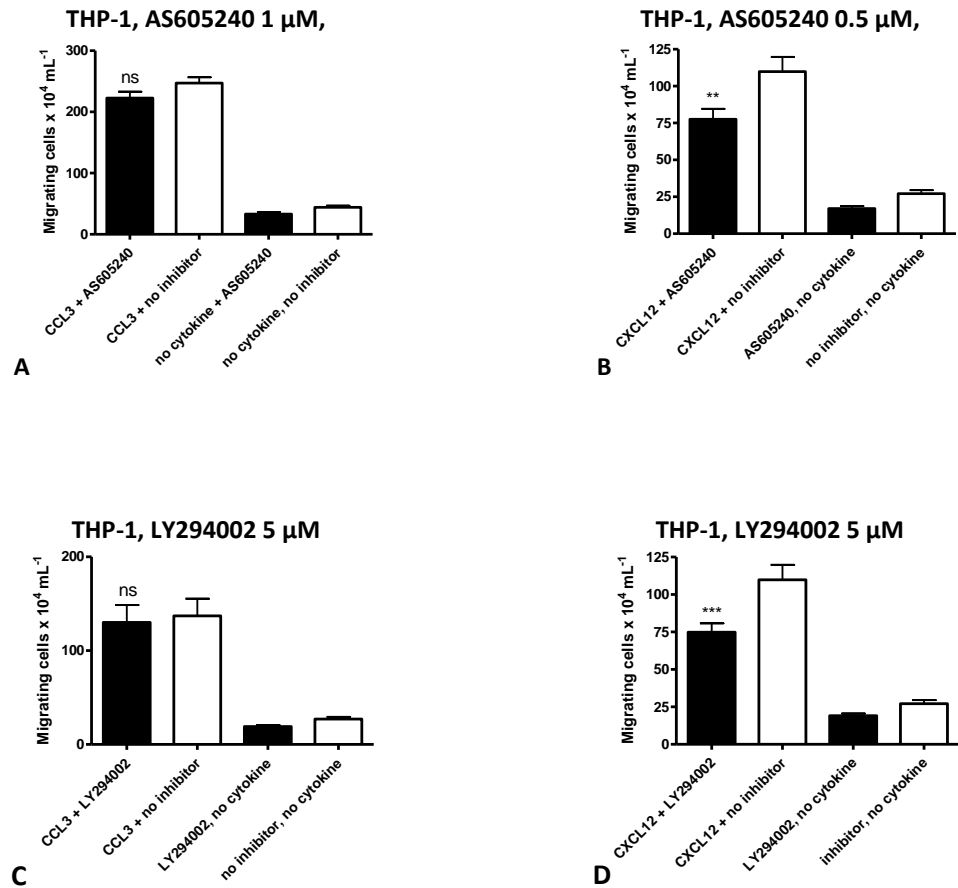


Figure 5.12: Chemotaxis assays of THP-1 following pre-treatment with LY294002 or AS605240 or control (DMSO) (A) to 1 nM CCL3 (B) to 1 nM CXCL12 (C) to 1 nM CCL3 (D) to 1 nM CXCL12. Means  $\pm$  SEM, one-way ANOVA, post-hoc Bonferroni,  $n \geq 3$  independent experiments, \*\*\*= $p < 0.001$ , \*\*= $p < 0.01$ , \*= $p < 0.05$ , ns= $p > 0.05$ . Note: 5.12B data also displayed in figure 4.34; 5.12C & D data also in figure 4.33.

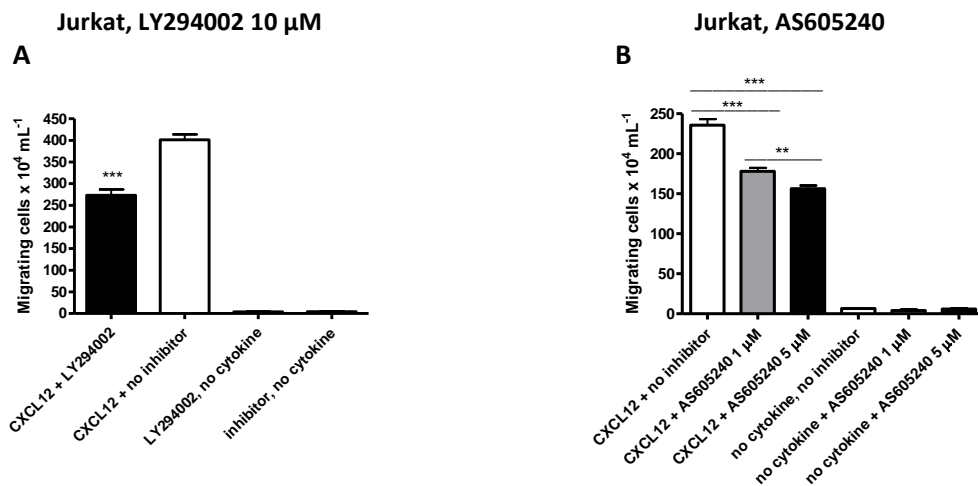


Figure 5.13: Chemotaxis assays of Jurkat to CXCL12 1 nM following pre-treatment with (A) 10  $\mu$ M LY294002 or (B) 1 or 5  $\mu$ M AS605240 or control (DMSO). Means  $\pm$  SEM, one-way ANOVA, post-hoc Bonferroni,  $n \geq 3$  independent experiments, \*\*\*= $p < 0.001$ , \*\*= $p < 0.01$ , \*= $p < 0.05$ , ns= $p > 0.05$ .

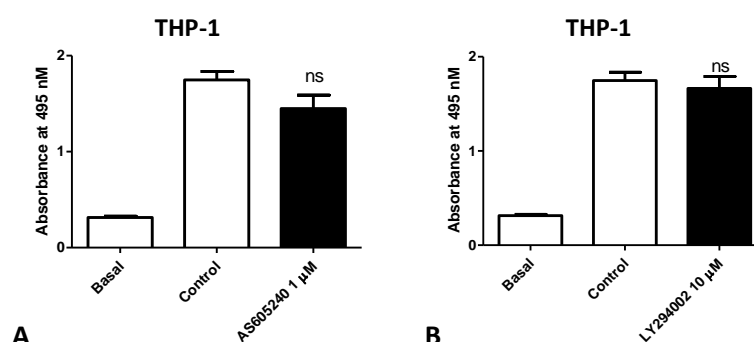


Figure 5.14: Cytotoxicity assays over 7 hours in THP-1 for (A) AS605240 1  $\mu$ M and (B) LY294002 10  $\mu$ M. Basal absorbance occurs in presence of medium after MTS treatment in the absence of cells. Means  $\pm$  SEM, one-way ANOVA, post-hoc Bonferroni,  $n \geq 3$  independent experiments, ns= $p > 0.05$ .

### 5.2.7: Pi3K siRNA knockdown also inhibits chemokine-induced migration in MCF7 and THP-1

These effects of Pi3K inhibition with small molecule inhibitors AS605240 and LY294002 on cell migration were confirmed using siRNA knockdown of Pi3K in THP-1, Jurkat and MCF7 cells, figures 5.15 and 5.15.

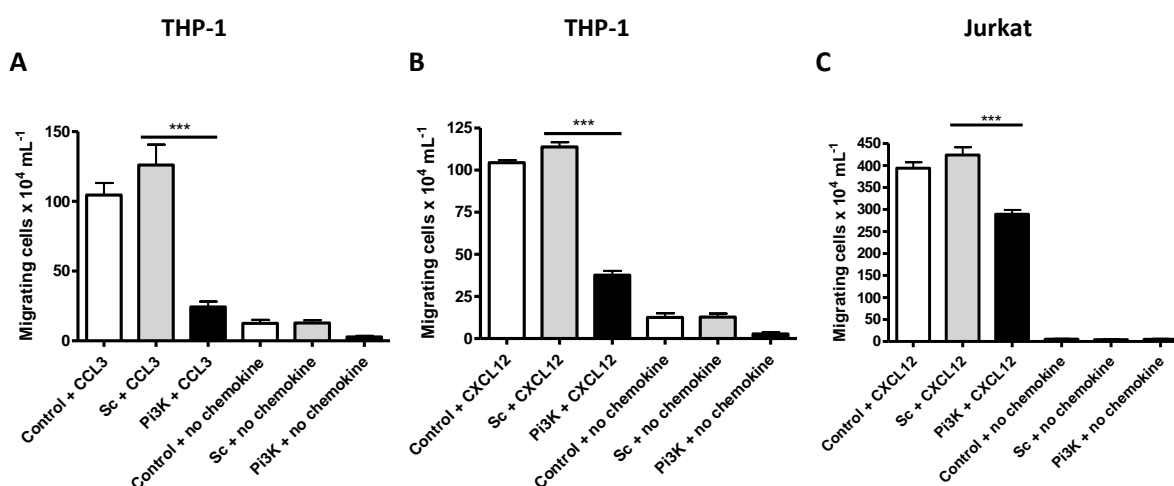


Figure 5.15: Pi3K siRNA knockdown. Cells transfected with 50 nM Human Pi3K or 50 nM nonsense siRNA (Sc) control, chemotaxis assays undertaken 24 hours after transfection. (A) THP-1 chemotaxis to 1 nM CCL3 (B) THP-1 chemotaxis to 1 nM CXCL12 (C) Jurkat chemotaxis to 1 nM CXCL12. Means  $\pm$  SEM, one-way ANOVA, post-hoc Bonferroni,  $n \geq 3$ , \*\*\*= $p < 0.001$ .



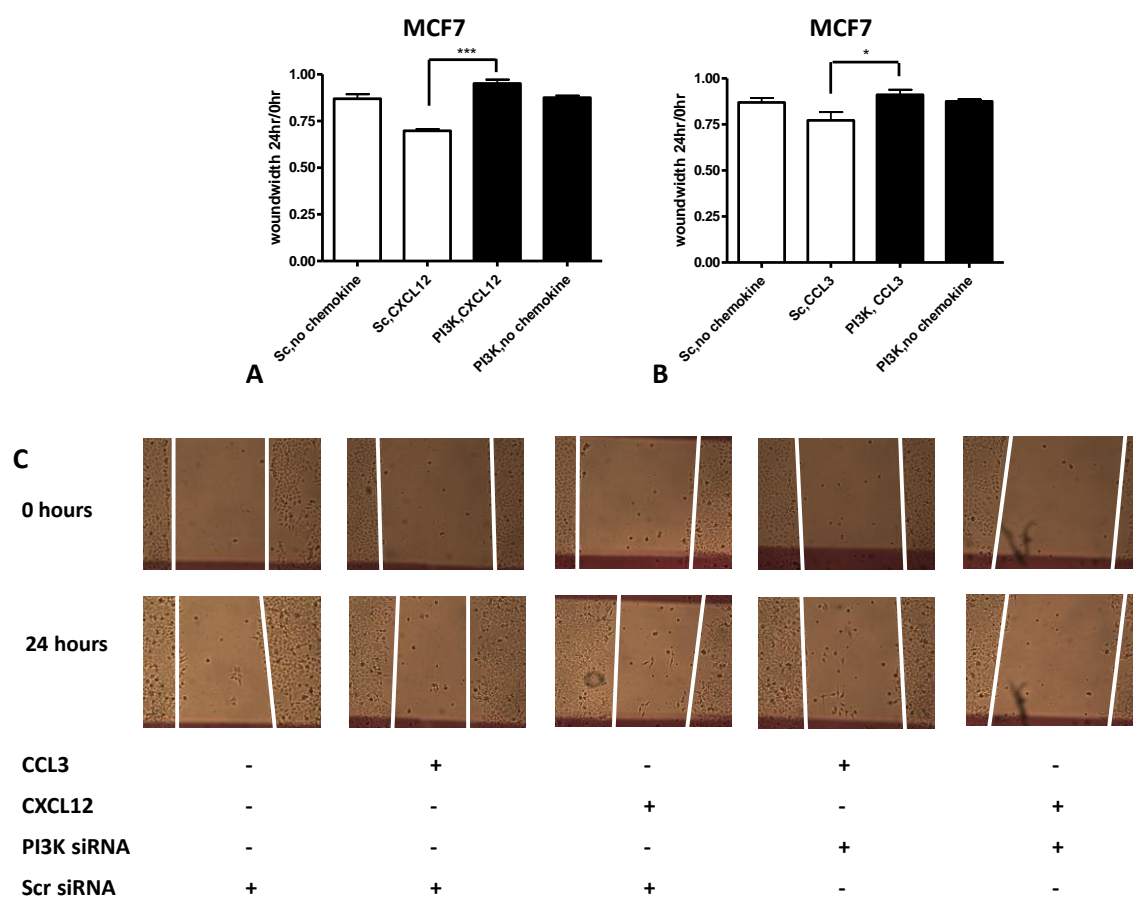


Figure 5.16: MCF7 Pi3K siRNA knockdown. Wound-healing assays following transfection with 50 nM Pi3K siRNA or nonsense siRNA (Scr) control. Analysis 24 hours after (A and C) 10 nM CXCL12, or (B and C) 10 nM CCL3. Means  $\pm$  SEM, one-way ANOVA, post-hoc Bonferroni,  $n \geq 3$ ,  $*=p < 0.05$ ,  $***=p < 0.001$ .

Pi3K knockdown highly significantly inhibited chemotaxis assays in THP-1 and Jurkat, figure 5.15, along with wound-healing in MCF7 induced by CXCL12, and to a lesser extent CCL3, figure 5.16. siRNA knockdown was confirmed with western blots figure 5.17, Pi3K knockdown was less effective in Jurkat than THP-1 or MCF7, possibly explaining the greater effect of Pi3K knockdown on chemotaxis in THP-1 than Jurkat, figure 5.15.

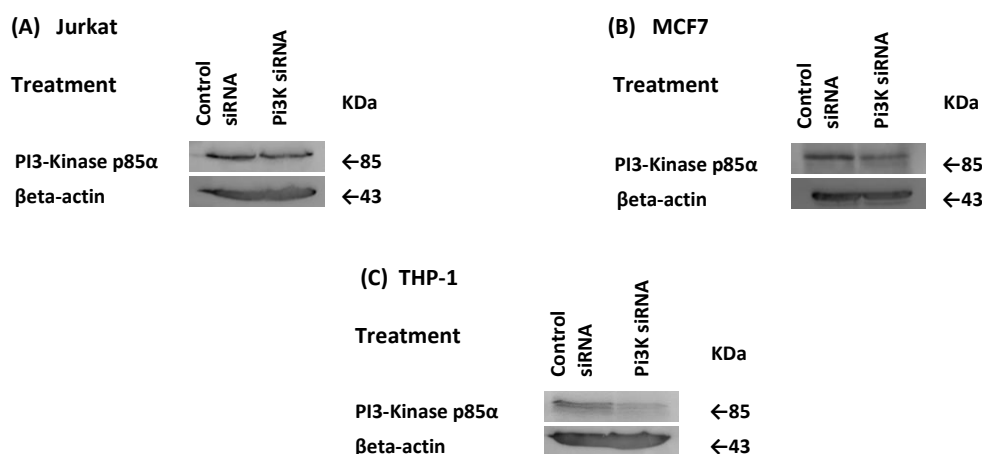


Figure 5.17: Pi3K siRNA knockdown. Cells transfected with 50 nM Human Pi3K or nonsense siRNA control. Western Blot 24 hours post-transfection using anti-Pi3K(p85α) antibody, loading confirmed with β-actin in (A) Jurkat, (B) MCF7 and (C) THP-1.

As above results indicate cofilin's phosphorylation state correlates with a cell's ability to migrate towards a chemokine, and chemotaxis to CCL3 and CXCL12 involves Pi3K. Possibly due to Pi3K signalling influencing phosphatase slingshot's modification of cofilin's phosphorylation state [645]. The ability of Pi3K inhibition to directly modulate cofilin phosphorylation was investigated.

### 5.2.8: Cofilin phosphorylation is modified by Pi3K inhibition

Cofilin phosphorylation was explored in THP-1 in the presence and absence of Pi3K inhibitors LY294002 (LY) 20 μM and AS605240 (AS) 5 μM. Cells were treated with inhibitors followed by CXCL12 or CCL3 at different concentrations, figure 5.18.

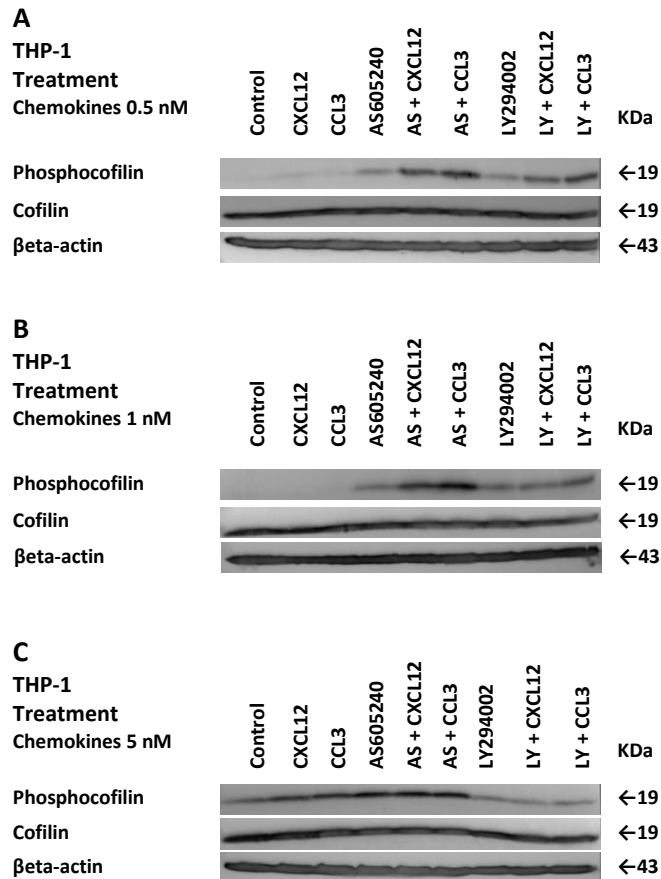


Figure 5.18: Western Blot with total-cofilin and phosphocofilin (Ser3) antibodies reveals cofilin phosphorylation levels in THP-1 following pre-treatment with AS605240 (AS) 5  $\mu$ M or LY294002 (LY) 20  $\mu$ M (37°C, 30 mins) in presence and absence of CXCL12, or CCL3 (0.5, 1 or 5 nM, 15 mins before lysis).  $\beta$ -actin loading control.

In THP-1 at higher levels of chemokines (5 nM) AS605240 continued to increase phosphorylation responses in presence and absence of chemokine whereas LY294002 decreased them. However in Jurkat the cofilin phosphorylation showed little response to Pi3K inhibition or CXCL12 stimulation, figure 5.19, this may be due to differences between untransformed T-lymphocytes and Jurkat (a T-cell lymphoma cell line) with respect to Ras signalling. In Jurkat Ras fails to activate Pi3K [646] whereas in untransformed T-lymphocytes it can [647].

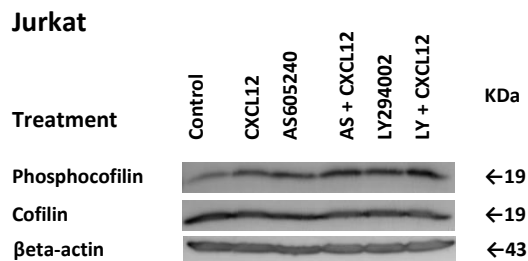


Figure 5.19: Western Blot with total-cofilin and phosphocofilin (Ser3) antibodies reveals cofilin phosphorylation levels in Jurkat following pre-treatment with AS605240 (AS) 5  $\mu$ M or LY294002 (LY) 20  $\mu$ M (37°C, 30 mins) in presence and absence of CXCL12 (5 nM, 15 mins before lysis).  $\beta$ -actin loading control.

As explained cofilin is able to modify the assembly and reorganisation of actin filaments, so the effects of the Pi3K inhibitors on actin fibres in CHO.CCR5 cells were examined using Phalloidin, figure 5.20.

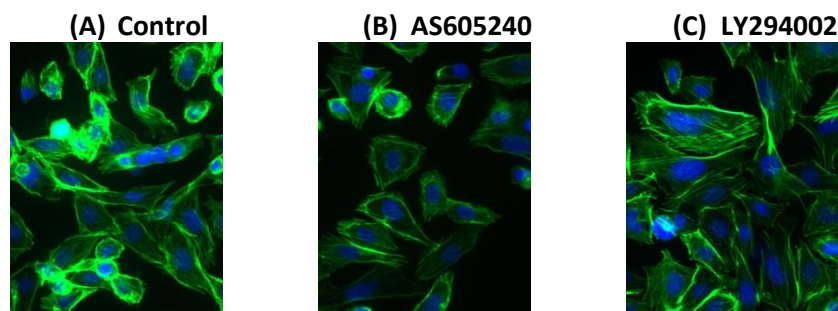


Figure 5.20: Filament actin stains following Pi3K inhibition. Alexa-488 Phalloidin (green) and DAPI nuclear stains (blue) of CHO.CCR5 following pre-treatment with (A) DMSO control (B) 5  $\mu$ M AS605240 or (C) 10  $\mu$ M LY294002 (1 hr, 37°C). Imaged UV inverted microscopy (Leica DMII Fluorescence microscope 500x Ex 490 nm, Em 520 nm).

AS605240 or LY294002 show no adverse effects on actin filament structure, therefore these inhibitors effects on chemotaxis are unlikely to be due to destruction of the cell's actin cytoskeleton.

Modification of GRK, Src, ROCK, Raf and MEK signalling, using small molecule inhibitors, also influences chemotaxis of THP-1 and Jurkat to CCL3 and/or CXCL12, so the influence of these inhibitors on cofilin phosphorylation was examined. GRK activity is linked to the actions of  $\beta$ -arrestin, hence the effects of transfection of cells, with plasmids to increase or decrease  $\beta$ -arrestin levels, on cell migration were also explored.

### 5.2.9: G-protein coupled receptor kinases (GRKs)

GRKs are a family of protein kinases that can support malignancies; they modulate survival, proliferation and invasion of cancers [648]. Activated chemokine receptors couple to G-proteins, enabling the exchange of GDP for GTP on the  $G\alpha$  subunit, which causes the  $G\alpha$  and the  $G\beta/\gamma$  dimers to dissociate and interact with downstream effectors such as adenylyl cyclase. This activation of the chemokine receptor causes the translocation of GRKs from the cytosol to the plasma membrane, and GRKs then phosphorylates serine/threonine residues on the receptor. This phosphorylation recruits  $\beta$ -arrestins (a non-visual arrestin) to the receptor.  $\beta$ -arrestins cause receptor desensitisation, that is uncoupling the chemokine receptor from the  $G\alpha$  and  $G\beta/\gamma$  G-proteins [649]. However,  $\beta$ -arrestins can also act as scaffolding proteins and mediate signalling and receptor internalisation [650], hence GRKs influence the balance of  $\beta$ -arrestin and G-protein signalling [651].

#### 5.2.9.1: $\beta$ ARK

The original GRK identified was the enzyme which phosphorylates rhodopsin, now called GRK1. Next,  $\beta$ -adrenergic receptor kinase ( $\beta$ ARK), an enzyme that could phosphorylate and desensitizes an agonist bound GPCR was discovered,  $\beta$ ARK is now called GRK2 [649]. There are at least six GRK isoforms, and some isoforms are involved in malignant cell migration and apoptosis [652]. Here the effects of a specific  $\beta$ ARK inhibitor, Methyl 5-[2-(5-nitro-2-furyl)vinyl]-2-furoate ( $\beta$ -ARK-1) were explored, figure 5.21.

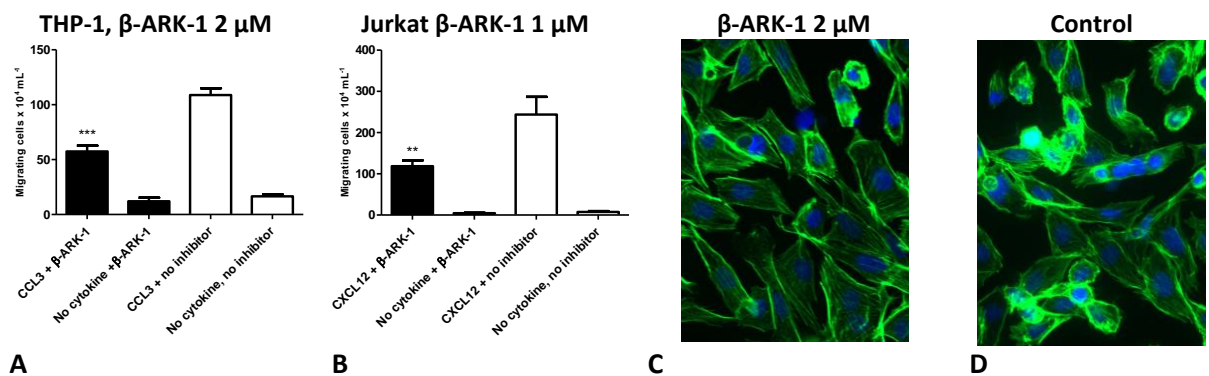


Figure 5.21: Chemotaxis assays following pre-treatment with  $\beta$ -ARK-1 or control (DMSO). (A) Chemotaxis of THP-1 to 1 nM CCL3. (B) Jurkat chemotaxis to 1 nM CXCL12. Means  $\pm$  SEM, one-way ANOVA, post-hoc Bonferroni,  $n \geq 3$  independent experiments, \*\*\*= $p < 0.001$ , \*\*= $p < 0.01$ . (C and D) Filament actin stains. Alexa-488 Phalloidin (green) and DAPI nuclear stains (blue) of CHO.CCR5 following pre-treatment with 2  $\mu$ M  $\beta$ -ARK-1 (1 hr, 37°C). Imaged UV inverted microscopy (Leica DMII Fluorescence microscope 500x Ex 490 nm, Em 520 nm).

$\beta$ -ARK-1 highly significantly inhibited chemotaxis of THP-1 to CCL3 and Jurkat to CXCL12 and had little effect on actin polymerization in CHO.CCR5, figure 5.21. The  $IC_{50}$  of  $\beta$ -ARK-1 is reported as 126  $\mu$ M [653], however this figure was derived from a  $\beta$ ARK activation assay not a MTS or MTT toxicity assay. MTS assay results were deceptive with this highly coloured chromophore compound as they indicated inhibition of metabolism at low concentrations ( $\sim 6 \mu$ M) but not at high concentrations (190  $\mu$ M), figure 5.22A. Therefore manual toxicity assays were undertaken, over 24 and 48 hours showed above  $\sim 3 \mu$ M produced inhibition of proliferation and at higher concentrations  $\beta$ -ARK-1 produced cell death in Jurkat whereas in THP-1 cells toxicity was relatively consistent across all  $\beta$ -ARK-1 concentrations, figure 5.22B-E

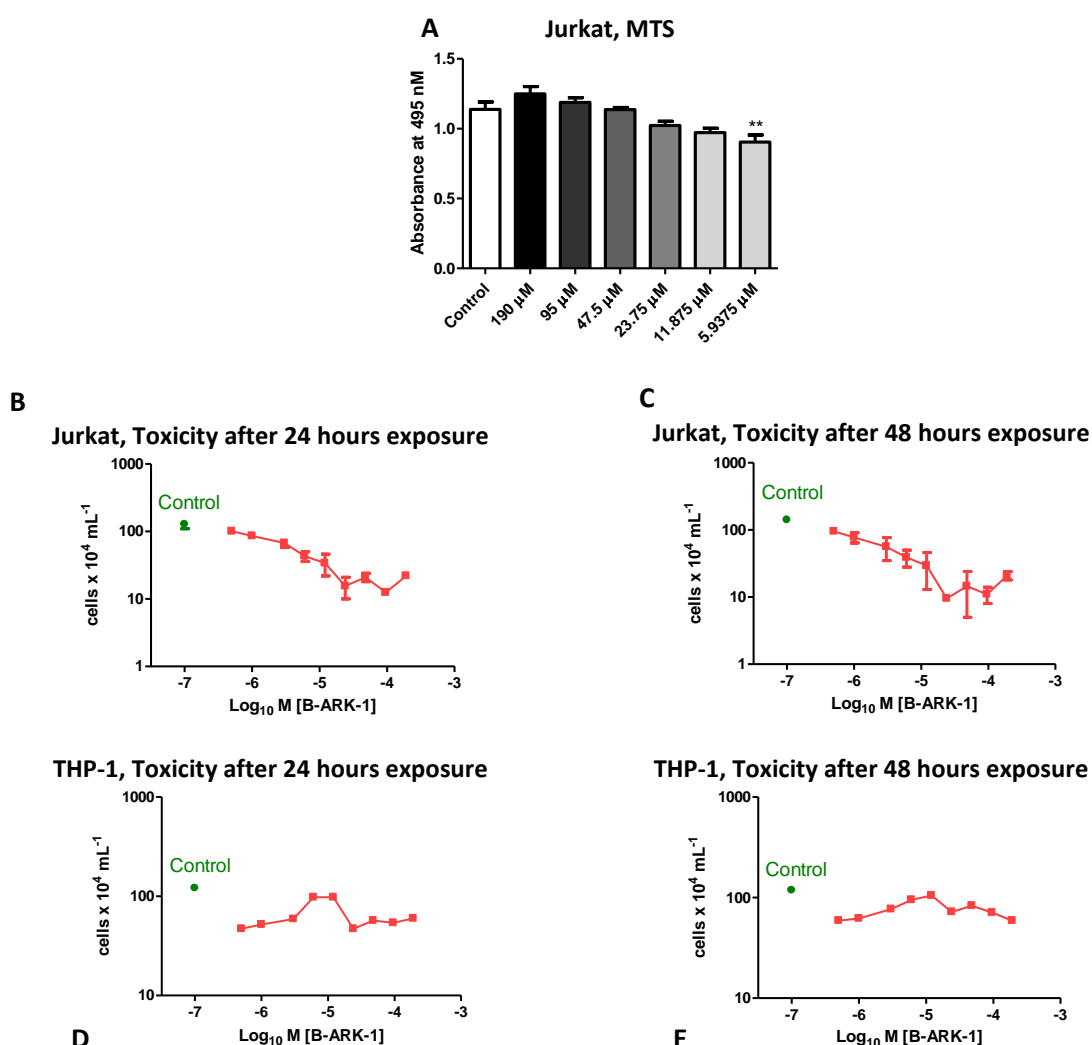


Figure 5.22: Cytotoxicity assays for  $\beta$ -ARK-1. (A) MTS assays were over 24 hours in Jurkat Basal absorbance occurs in presence of medium after MTS treatment in the absence of cells. Means  $\pm$  SEM, one-way ANOVA, post-hoc Bonferroni,  $n \geq 3$  independent experiments,  $**=p < 0.01$ . (B-E) Manual cytotoxicity assays, trypan blue staining allowed live cell counts after 24 or 48 hours of  $\beta$ -ARK-1 exposure (B and C  $n=2$ , D and E  $n=1$ ).

Chemotaxis and toxicity assays indicate Jurkat are more sensitive to  $\beta$ -ARK-1 inhibition of GRK2 than THP-1. This may relate to Pi3K being constitutively active in Jurkat [654] and important for Jurkat chemotaxis [565], as Pi3K signalling can trigger nuclear location of Mdm2, which then impedes Mdm2 E3-ubiquitin ligase-mediated GRK2 degradation [655].

#### 5.2.9.2: *l*pyrimidine

*l*pyrimidine (4-Amino-5-ethoxymethyl-2-methylpyrimidine) is a relatively new small molecule inhibitor stated to target GRKs, but which GRK/s are not specified, and to-date there have been no publications detailing use of this inhibitor. Exploration of *l*pyrimidine's effects showed it to significantly inhibit chemotaxis in THP-1 and Jurkat, figure 5.23.

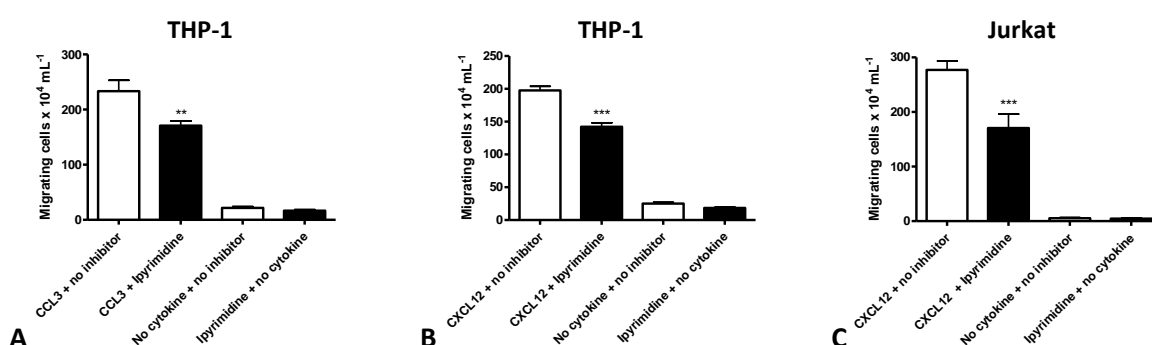


Figure 5.23: Chemotaxis assays following pre-treatment with 5 $\mu$ M *l*pyrimidine or control (DMSO). (A) Chemotaxis of THP-1 to 1 nM CCL3. (B) THP-1 chemotaxis to 1 nM CXCL12. (C) Jurkat chemotaxis to 1 nM CXCL12. Means  $\pm$  SEM, one-way ANOVA, post-hoc Bonferroni,  $n \geq 3$  independent experiments, \*\*\*= $p < 0.001$ , \*\*= $p < 0.01$ .

MTS assays using concentration up to 10  $\mu$ M *l*pyrimidine showed no evidence of significant cell toxicity in THP-1 over 7 hours, but over 24 hours in MCF7 cells very significant inhibition of cell metabolism was observed even at 5  $\mu$ M, figure 5.24. The possibility that *l*pyrimidine has off-target effects still needs exploring as another pyrimidine structure, 4-amine-5-(4-chlorophenyl)-7-(*t*-butyl)pyrazolo[3,4-*d*]pyrimidine, reportedly inhibits Src kinase activity [553], and both structures may be able to bind similar protein sites, as both contain a central pyrimidine, with an electronegative group on one side and aliphatic group on other, figure 5.25. Although as Src purportedly phosphorylates and activates GRK [553] the end result may be the same.

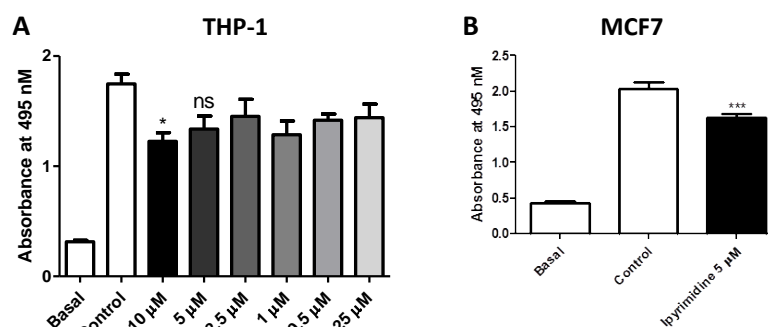


Figure 5.24: Cytotoxicity assays for Ipyrimidine. MTS assays were over 7 hours in (A) THP-1 and over 24 hours in (B) MCF7 cells. Basal absorbance occurs in presence of medium after MTS treatment in the absence of cells. Means  $\pm$  SEM, one-way ANOVA, post-hoc Bonferroni,  $n \geq 3$  independent experiments, \*\*\*= $p < 0.001$ , \*= $p < 0.05$ , ns= $p > 0.05$ .

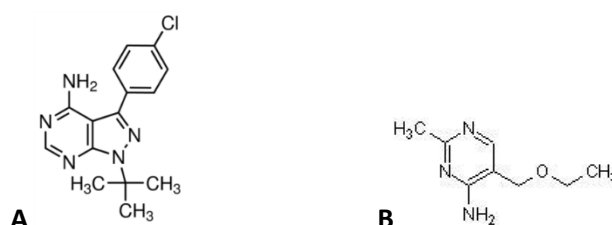


Figure 5.25: The structures of (A) 4-Amino-5-(4-chlorophenyl)-7-(t-butyl)pyrazolo[3,4-d]pyrimidine and (B) 4-Amino-5-ethoxymethyl-2-methylpyrimidine (Ipyrimidine).

Western blots revealed that in THP-1 Ipyrimidine increased basal cofilin phosphorylation, and modestly reduced CXCL12-induced, but had little effect on CCL3-induced cofilin phosphorylation, figure 5.26.

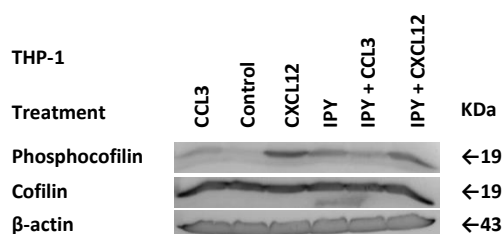


Figure 5.26: Western Blot with total-cofilin and phosphocofilin (Ser3) antibodies reveals cofilin phosphorylation levels in THP-1 following pre-treatment with 10  $\mu$ M Ipyrimidine (IPY) (37°C, 30 mins) in presence and absence of CXCL12 or CCL3 (5 nM, 15 mins before lysis).  $\beta$ -actin loading control.

Ipyrimidine inhibition of GRKs may partly block the chemokine stimulation triggering cofilin phosphorylation. Phalloidin actin stains in CHO.CCR5 cells indicated Ipyrimidine treatment at 10  $\mu$ M may reduce actin filament polymerisation, figure 5.27, possibly through modification of cofilin phosphorylation which would also explain the inhibition of chemotaxis, figure 5.23.



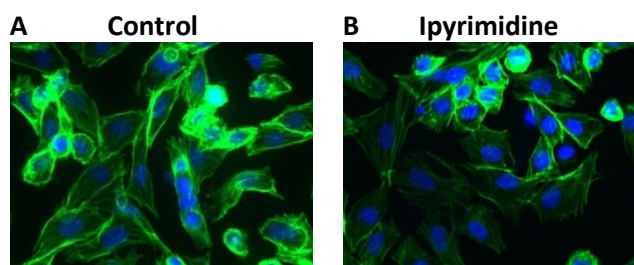


Figure 5.27: Filament actin stain. Alexa-488 Phalloidin (green) and DAPI nuclear stains (blue) of CHO.CCR5 following pre-treatment with (A) DMSO (B) 10  $\mu$ M Ipyrimidine (1 hr, 37°C). Imaged UV inverted microscopy (Leica DMII Fluorescence microscope 500x Ex 490 nm, Em 520 nm).

#### 5.2.10: $\beta$ -arrestins

Downstream of CXCR4  $\beta$ -arrestin mediates receptor trafficking and GRK signalling.  $\beta$ -arrestin may also play a role in CXCR7 activation of ERK 1/2 resulting in increasing cancer cell adhesion and proliferation [113, 656, 657]. GPCR overstimulation may cause cytotoxicity;  $\beta$ -arrestin can act to desensitize receptors preventing G-protein-receptor association over the short term, and over a longer term receptors can be internalised and degraded [658].

$\beta$ -arrestins may sequester RhoGEFs and RhoA in the cytosol producing compartment-specific regulation inhibiting spatial and temporal activities critical for cell migration [659]. B-arrestin-1 aka Arrestin-2, and  $\beta$ -arrestin-2 aka Arrestin-3, are implicated in cancer and cell migration. Both arrestins are expressed in haematopoietic cells, and may modulate the Wnt/ $\beta$ -catenin signalling pathway in stem cell maintenance of leukaemia [660]. Arrestin-2 in conjunction with  $G\alpha_{q/11}$  influences RhoA-triggered stress-fibre formation and so actin remodelling [661], and also some cancer derived cell-lines show raised Arrestin-2 expression [662]. Arrestin-2 may regulate Rho GTPases through RhoGAPs [663] and RhoGEFs [664]. Active Rac reportedly increases cofilin phosphorylation, and depletion of Arrestin-2 is reported to cause reduced directional migration and cofilin phosphorylation in transfected HEK cells [665]. In leukocytes  $\beta$ -arrestins scaffold cofilin with phosphatases at membrane protrusions controlling location of actin filament severing [626].

##### 5.2.10.1: Immunofluorescence demonstrates the presence of $\beta$ -arrestins in cell-lines

The presence of arrestins in cell-lines was demonstrated using immunofluorescent staining and UV microscopy, figure 5.28. Jurkat and undifferentiated THP-1 also express Arrestin-2, figures 5.2 and 5.11.

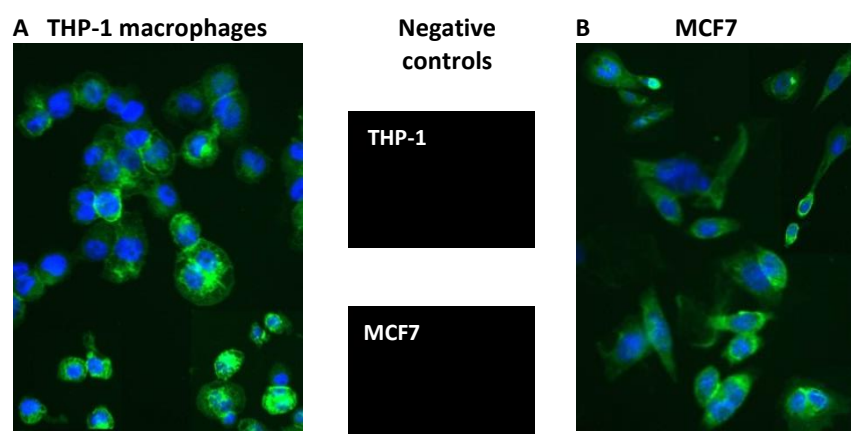


Figure 5.28: Arrestin immunofluorescent staining. (A) THP-1, pre-treatment 25 nM PMA or (B) MCF7, grown on glass for 24 hours, fixed (4% paraformaldehyde), incubated with anti-arrestin-2 then probed with FITC. Imaged UV inverted microscopy (Leica DMII Fluorescence microscope 500x Ex 490 nm, Em 520 nm).

#### 5.2.10.2: $\beta$ -arrestin transfection in CHO.CCR5

The immunofluorescent staining showed the cell-lines expressed arrestin-2. Plasmids, carrying GFP-tagged Arrestin-2, Arrestin-3 or mutant Arrestin-2, were transfected into cells. These caused over- or in the case of the mutant dominant negative expression of arrestin, and so allowed the influence chemokines on the arrestin subtypes to be visualised and explored. The mutant arrestin-2 ( $\beta$ -arrestin-1-V53D) has a valine substituted for an aspartic acid. It is understood to interact normally with GPCR but then fail to facilitate sequestration to endocytic pathways so the mutant inhibits normal  $\beta$ -arrestin binding, uncoupling the receptor, and mediating receptor desensitisation, sequestration and subsequent recycling and re-sensitisation [494]. The effect of CCL3 on arrestin-transfected CHO.CCR5 was explored first, figure 5.29.

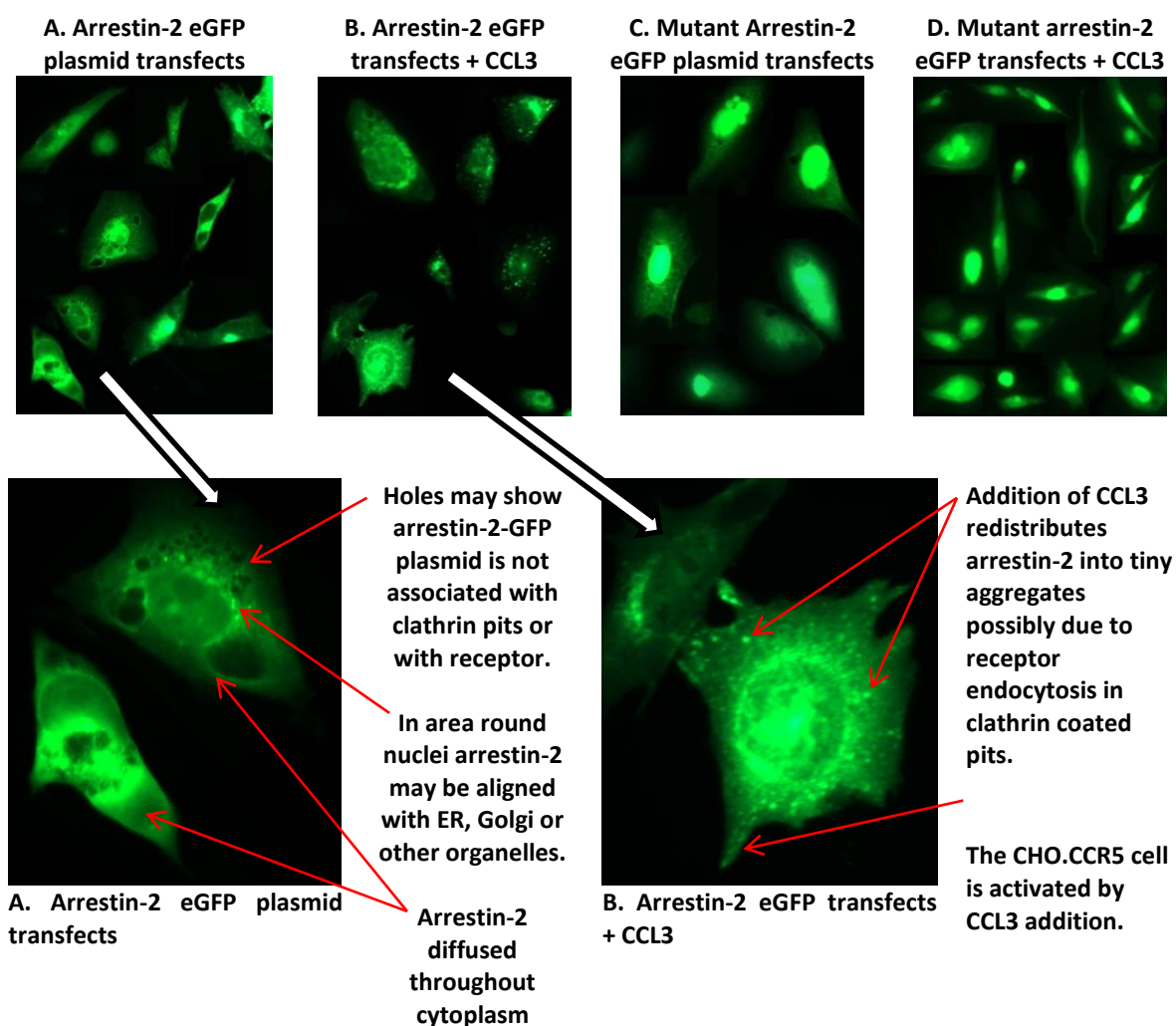


Figure 5.29: CHO.CCR5 were transfected with (A and B) Arrestin-2 eGFP or (C and D) mutant Arrestin-2 eGFP plasmids, grown on glass coverslips (24 hrs, 37°C, 5% CO<sub>2</sub>), (B and D) treated with CCL3 (10 nM, 15 mins, 37°C), fixed (4% paraformaldehyde) then imaged UV inverted microscopy (Leica DMII Fluorescence microscope 500x Ex 490 nm, Em 520 nm).

Arrestin-2 eGFP plasmids clearly respond to CCL3 whereas mutant Arrestin-2 eGFP plasmids accumulate in the CHO's nucleus, and transfects' appearance is not altered in response to CCL3 treatment.

#### 5.2.10.3: $\beta$ -arrestin transfections in MCF7, THP-1 and Jurkat

Similar responses, redistribution into aggregates are seen in MCF7 cells transfected with the Arrestin-2 eGFP plasmids then treated with CXCL12 or CCL3 (arrowed), figure 5.30, whereas after transfection with Arrestin-3 eGFP plasmids dense areas were apparent both before and after chemokine addition (arrowed), figure 5.31.

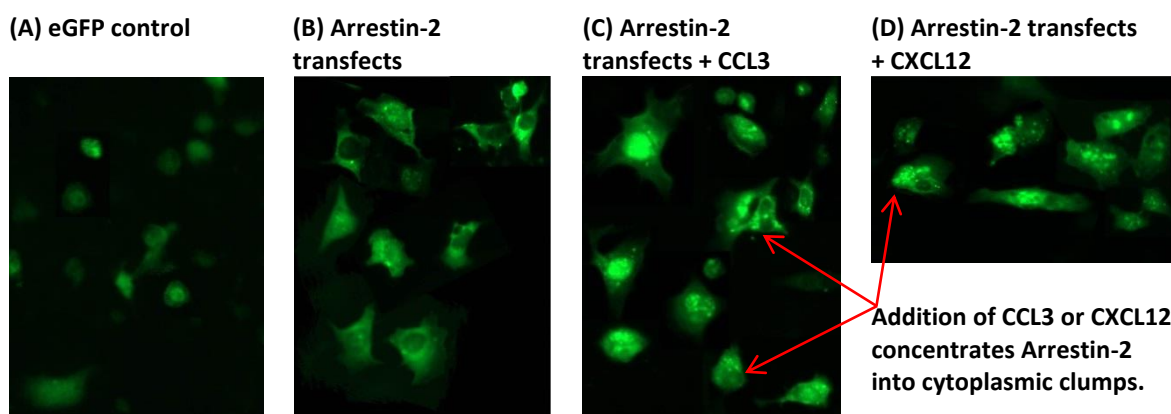


Figure 5.30: MCF7 were transfected with (A) eGFP control plasmids or (B, C and D) Arrestin-2 eGFP plasmids, grown on glass coverslips (24 hrs, 37°C, 5% CO<sub>2</sub>), (C and D) treated with CCL3 or CXCL12 (10 nM, 15 mins, 37°C), fixed (4% paraformaldehyde), then imaged UV inverted microscopy (Leica DMII Fluorescence microscope 500x Ex 490 nm, Em 520 nm).

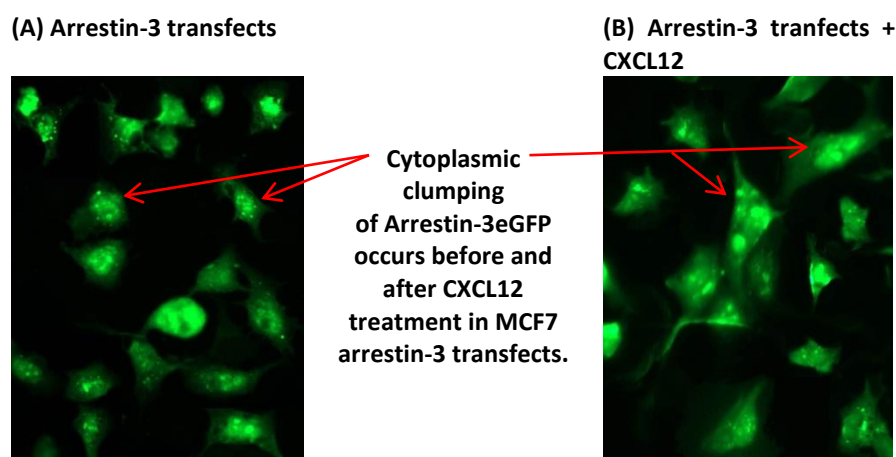


Figure 5.31: MCF7 were transfected with (A and B) Arrestin-3 eGFP plasmids grown on glass coverslips (24 hrs, 37°C, 5% CO<sub>2</sub>), (B) treated with CXCL12 (10 nM, 15 mins, 37°C), fixed (4% paraformaldehyde) then imaged UV inverted microscopy (Leica DMII Fluorescence microscope 500x Ex 490 nm, Em 520 nm).

In Jurkat which express CXCR4, chemotaxis of cells transfected with mutant or active Arrestin-2 eGFP plasmids suggests overexpression of Arrestin-2 may very modestly positively modify migration towards CXCL12 compared to eGFP control plasmids, figure 5.33A. In THP-1 transfections with Arrestin-3 plasmids produced an increased migration towards both CCL3 and CXCL12, whereas Arrestin-2 plasmids only increased migration towards CXCL12, however both are compared to mutant Arrestin-2 plasmid transfection which may reduce migration, figures 5.33B and C. In MCF7 cells transfection with Arrestin-2 again modestly significantly increases chemokinesis in the presence of CCL3. Whereas Arrestin-3 and mutant Arrestin-2 plasmid

transfection did not increase wound-healing in response to CCL3 or CXCL12. What is not known is if eGFP plasmids used as control aid or impede wound-healing, figure 5.34. Overall response to overexpression of  $\beta$ -arrestins by plasmid transfection demonstrated both cell type and chemokine specific responses. Before chemotaxis experiments transfection efficiency was checked in Jurkat and THP-1 cells using UV imaging, figure 5.32.

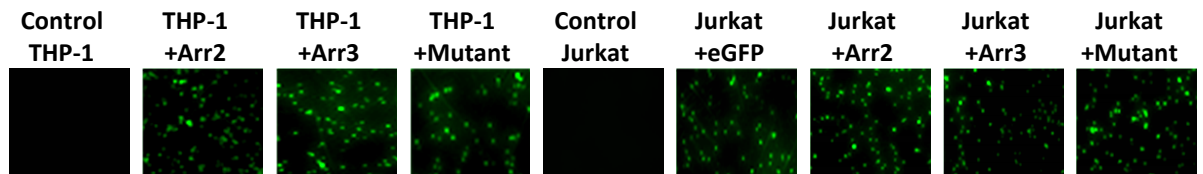


Figure 5.32: Transfection efficiency was established using UV inverted microscopy (Leica DMII Fluorescence microscope 500x Ex 490 nm, Em 520 nm).

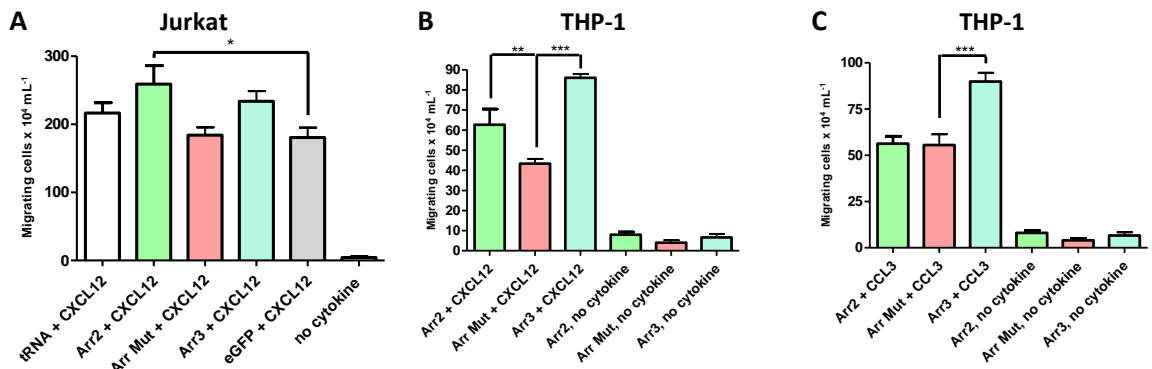


Figure 5.33: Chemotaxis assays 24 hours after transfection with arrestin-eGFP plasmids. (A) Chemotaxis of Jurkat cells transfected with Arrestin-2 eGFP or Arrestin-3 eGFP plasmids to CXCL12. (B) THP-1 cells transfected with Arrestin-2 or -3 eGFP plasmids to CCL3 and (C) to CXCL12. Means  $\pm$  SEM, one-way ANOVA, post-hoc Bonferroni,  $n \geq 3$  independent experiments, \*\*\*= $p < 0.001$ , \*\*= $p < 0.01$ .

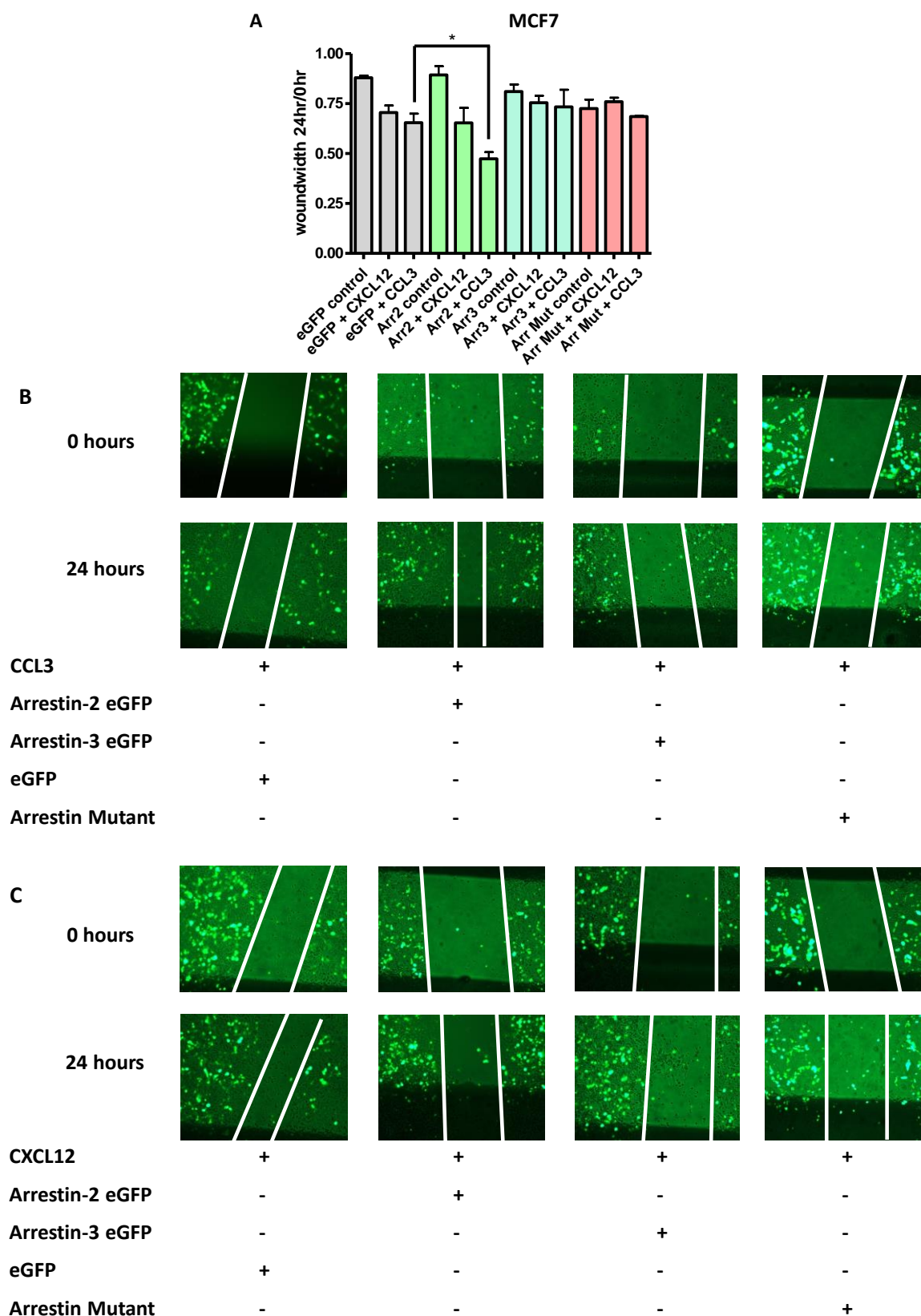


Figure 5.34: MCF7 wound-healing assays (A) supported by 10 nM CCL3 or CXCL12 undertaken 24 hours after transfection with eGFP (control), Mutant Arrestin eGFP, Arrestin-2 eGFP or Arrestin-3 eGFP plasmids. Means  $\pm$  SEM, one-way ANOVA, post-hoc Bonferroni,  $n \geq 3$ ,  $*=p < 0.05$ . (B and C) wound-healing images UV inverted microscopy (Leica DMII Fluorescence microscope 500x Ex 490 nm, Em 520 nm).



### 5.2.11: Focal adhesion kinases play a role in chemokine chemotaxis

The family of Focal adhesion kinases including FAK and Proline rich tyrosine kinase-2 (PYK2), a homologous kinase of FAK, play an important role in malignant cell chemotaxis and in cell cycle progression. FAK is often upregulated in human malignancies, and potent, reversible, ATP-competitive FAK and PYK2 inhibitor PF562271 has undergone phase II trials in human pancreatic, head and neck, and prostate cancers, all solid tumours. Solid tumours usually consist of healthy stromal cells (cancer-associated fibroblasts) and cancer cells. Metastasis of the cancer cells, which can include malignant leukocytes, is to some extent controlled by adhesions between the healthy stromal cells [666]. T-cells also express both PYK2 and FAK which are involved in responses to chemokines [667]. When PYK2 and FAK are absent cells' adhesion interaction with Intercellular Adhesion Molecule 1 (ICAM1) is defective and T-cell responses fall as T-cells' activation by antigen presenting cells is disrupted. PF562271 is reported to inhibit T-cell proliferation [668]. MTS assays found some inhibition of metabolism in THP-1 but not Jurkat cells from PF562271, negative effects on actin filament with concentration of actin filament to cells periphery were also apparent, figure 5.35.

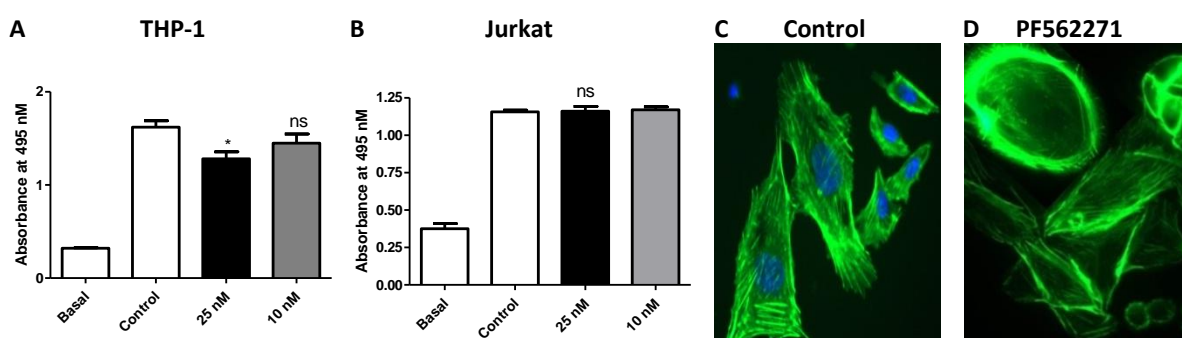
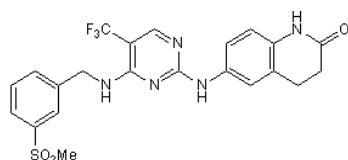


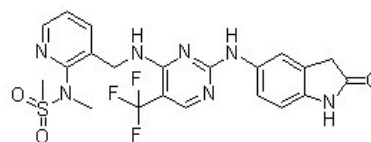
Figure 5.35: Cytotoxicity assays for PF562271. MTS assays were over 7 hours in (A) THP-1 and (B) Jurkat. Basal absorbance occurs in presence of medium after MTS treatment in the absence of cells. Means  $\pm$  SEM, one-way ANOVA, post-hoc Bonferroni,  $n \geq 3$  independent experiments,  $*=p < 0.05$ ,  $ns=p > 0.05$ . (C and D) Filament actin stains of CHO.CCR5 following PF562271 25 nM or control (1 hr, 37°C). Alexa-488 Phalloidin (green) and DAPI nuclear stains (blue). Imaged UV inverted microscopy (Leica DMII Fluorescence microscope 500x Ex 490 nm, Em 520 nm).

FAK phosphorylation on Tyr<sup>397</sup> creates a Src binding site, the Src/FAK complex can then phosphorylate focal adhesion components that influence cell adhesion dynamics, initiate signalling cascades and contribute to scaffolding [668]. Here the effects of FAK inhibitor-2 (aka PF-573228) and PF562271 which both inhibit FAK Tyr<sup>397</sup> phosphorylation and so activation, were explored in THP-1 and Jurkat chemotaxis assays. PF562271 also inhibits ATP phosphorylation of PYK2 directly possibly explaining its increased potency, although PF562271 and PF-573228 are sulphonamides and have structural similarities, figures 5.36-5.38.



### FAK inhibitor 2

3,4-Dihydro-6-[[4-[[[3-(methylsulfonyl)phenyl]methyl]amino]-5-(trifluoromethyl)-2-pyrimidinyl]amino]-2(1*H*)-quinolinone



### PF562271

N-methyl-N(3-((2-(2-oxo-2,3-dihydro-1*H*-indol-5-yl)-amino)-5-(trifluoromethyl)pyrimidin-4-yl)amino)methyl)pyridine-2-yl)

Figure 5.36 Structures of FAK Inhibitor-2 (PF-573228) and PF562271.

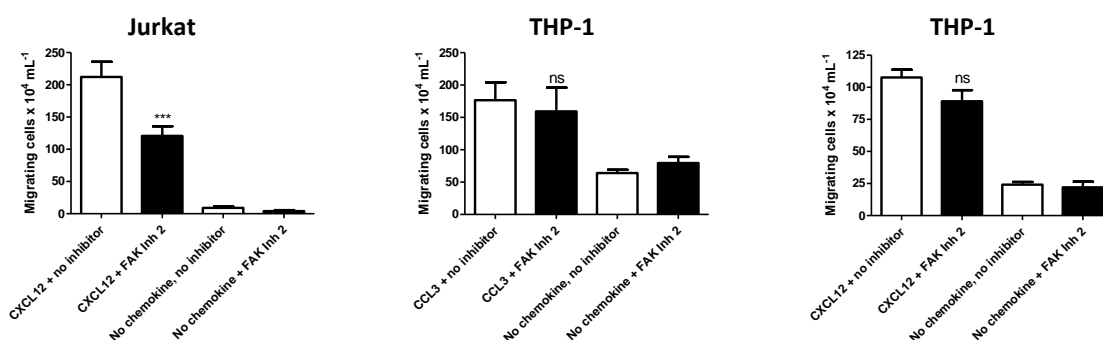


Figure 5.37: Chemotaxis assays following pre-treatment with 10  $\mu$ M FAK inhibitor-2 or control (DMSO). (A) Chemotaxis of Jurkat to 1 nM CXCL12. (B) THP-1 chemotaxis to 1 nM CXCL12. (C) THP-1 chemotaxis to 1 nM CCL3. Means  $\pm$  SEM, one-way ANOVA, post-hoc Bonferroni,  $n \geq 3$  independent experiments, \*\*\*= $p < 0.001$ , ns= $p > 0.05$ .

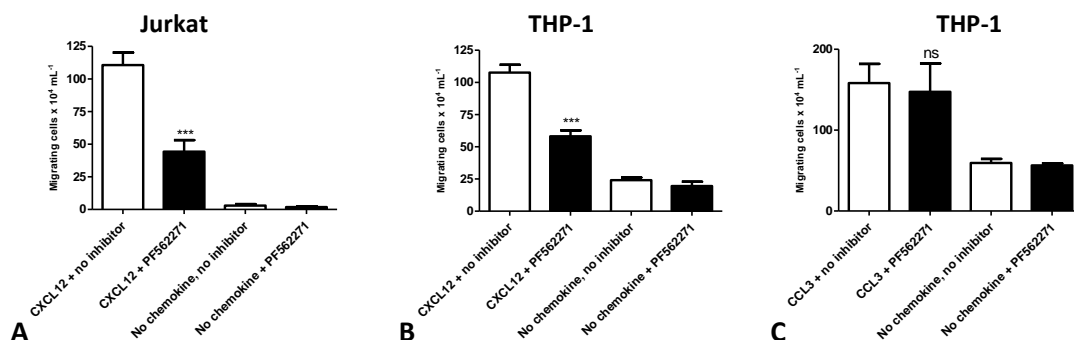


Figure 5.38: Chemotaxis assays following pre-treatment with 25 nM PF562271 or control (DMSO). (A) Chemotaxis of Jurkat to 1 nM CXCL12. (B) THP-1 chemotaxis to 1 nM CXCL12. (C) THP-1 chemotaxis to 1 nM CCL3. Means  $\pm$  SEM, one-way ANOVA, post-hoc Bonferroni,  $n \geq 3$  independent experiments, \*\*\*= $p < 0.001$ , ns= $p > 0.05$ .

Both FAK inhibitors produced significant inhibition of CXCL12-induced chemotaxis in Jurkat and had no effect on CCL3-induced migration in THP-1, however PF562271 also inhibited CXCL12-induced chemotaxis in THP-1 whereas FAK inhibitor 2 did not. PF562271 also slightly increased overall CXCL12-induced but not CCL3-triggered calcium flux, figures 5.39.



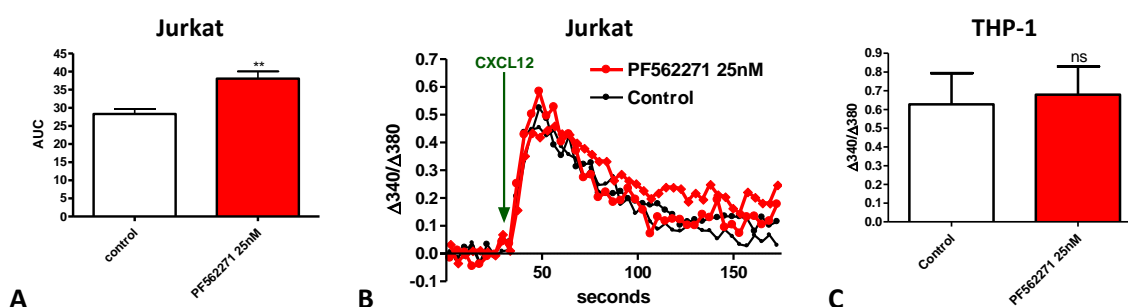


Figure 5.39: Fura2  $\text{Ca}^{2+}$  assay in (A and B) Jurkat and (C) THP-1 following 25 nM PF562271 or control (DMSO). Data expressed as fluorescence ratio change ( $\Delta 340/\Delta 380$  nm) i.e. peak fluorescence following (A and B) 10 nM CXCL12 and (C) 10 nM CCL3 addition minus basal fluorescence (prior to chemokine). (A and C) Means  $\pm$  SEM, Student t-test,  $n \geq 3$  independent experiments, \*\*= $p < 0.01$ , ns= $p > 0.05$ .

Inhibiting FAK allows PYK2 to increase Rho GTPase activation and macrophage motility, and cell survival via PYK2 regulation of p53 gene. Hence FAK-selective inhibitors may increase tyrosine phosphorylation by PYK2 [669], and inhibition of both proteins may be advantageous to hamper metastasis. FAK inhibition with PF562271 was found to inactivate (phosphorylate) cofilin in presence and absence of CXCL12 or CCL3, figure 5.40.

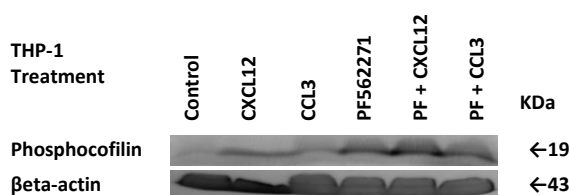


Figure 5.40: Western Blot with total-cofilin and phosphocofilin (Ser3) antibodies reveals cofilin phosphorylation levels in THP-1 following pre-treatment with 25 nM PF562271 (37°C, 30 mins) in presence and absence of CXCL12 or CCL3 (5 nM, 15 mins before lysis).  $\beta$ -actin loading control.

These results show in THP-1 and Jurkat that FAK/PYK2 inhibition inhibits chemotaxis, but specifically to CXCL12 not CCL3, and that in THP-1 FAK/PYK2 inhibition causes cofilin phosphorylation in the presence and absence of CXCL12 or CCL3.

### 5.2.12: Rho Proteins

Rho proteins are small GTPases of the Ras superfamily, including Rho A, B, C, D and E. Rho regulates actin stress fibres in cell-cell and cell-extracellular matrix environments. Cytoplasmic Rho switches between the active GTP-bound and inactive GDP-bound forms. Guanine nucleotide exchange factors (GEFs) activate Rho GTPase activating proteins, promoting GTP hydrolysis to GDP. Rho can also be maintained in its inactive form by nucleotide dissociation inhibitors. Rho targets Rho activated coiled-coil kinases (ROCKs). ROCK1 is a serine-threonine isomer, whose C-

terminus and N-terminal kinase sandwich an alpha-helical coiled-coil domain that binds Rho. When Rho binds ROCK it activates ROCK which in turn then phosphorylates and so activates its substrates, one of which is LIMK. Rho is activated by many mediators including cytokines, and ROCK can also be activated by arachidonic acid [670-672], discussed in chapter seven.

#### 5.2.12.1: Rho activated coiled-coil kinase (ROCK)

ROCK is found in a cell's uropodium and lamellipodium. ROCK aids contractions of the uropodia and ROCK inhibition impedes migration by removing the myosin light chain contractions stimulated by RhoA [673, 674]. ROCK co-locates with the microtubule organising centres in the uropodia. Depolymerizing microtubules e.g. with Nocodazole, upregulates RhoA activity and interferes with cell polarity. Antimitotic Nocodazole, which disrupts microtubules by binding to  $\beta$ -tubulin and activates the JNK signalling pathway, was found to significantly inhibit chemotaxis of both THP-1 and Jurkat to CXCL12, but not THP-1 to CCL3, figure 5.41.

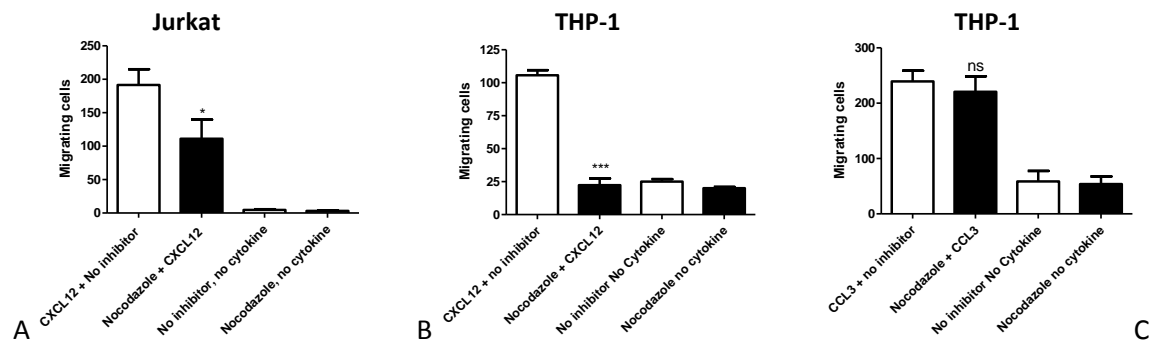


Figure 5.41: Chemotaxis assays following pre-treatment with 7.5  $\mu$ M Nocodazole or control. (A) Chemotaxis of Jurkat to 1 nM CXCL12. (B) THP-1 chemotaxis to 1 nM CXCL12. (C) THP-1 chemotaxis to 1 nM CCL3. Means  $\pm$  SEM, one-way ANOVA, post-hoc Bonferroni,  $n \geq 3$  independent experiments, \*\*\*= $p < 0.001$ , \*= $p < 0.05$ , ns= $p > 0.05$ .

Inhibitors of ROCK such as Y27632 are reported to inhibit uropodia retraction in monocytes [675]. Cofilin controls actin depolarisation; Rac and Rho activate ROCK and PAK kinases that phosphorylate LIMK which then phosphorylates and inactivates cofilin [676]. Reportedly ROCK can activate LIMK 2, by phosphorylating a LIMK2 'activation segment' on residue threonine-505. LIMK2 can then phosphorylate cofilin. LIMK 1 activation may follow signalling through Rac1 and Pac1, so LIMK1 and 2 are modulated by different kinases regulated by Rho GTPases [677, 678].

However, in malignant cells ROCK may be mutated. Shortened constitutively active ROCK may be able to activate both LIMK1 and LIMK2 whereas full-length un-mutated ROCK specifically phosphorylates LIMK2 but not LIMK1. This phosphorylation of LIMK2 by ROCK has been shown to be inhibited in COS-7 cells by 10  $\mu$ M Y27632 [678], reportedly a highly selective inhibitor of ROCK.

Inhibition of ROCK activation, using Y27632 at 10  $\mu\text{M}$  for 1 hour, inhibited cofilin phosphorylation in THP-1 cells both before and after treatment with CCL3, figures 5.42.

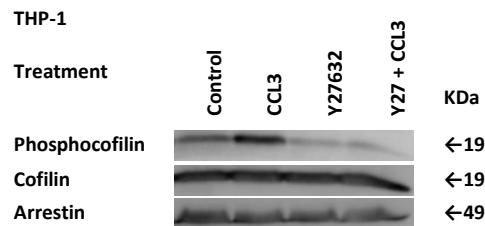


Figure 5.42: Western blot with total-cofilin and phosphocofilin (Ser3) antibodies reveals cofilin phosphorylation levels in THP-1 following pre-treatment with 10  $\mu\text{M}$  Y27632 (37°C, 30 mins) in presence and absence of CCL3 (5 nM, 15 mins before lysis). Arrestin-2 loading control.

Thus in THP-1 ROCK activity appears needed for cofilin to exist in a phosphorylated state. Y27632 at concentrations between 1 and 5  $\mu\text{M}$  dose dependently inhibited chemotaxis in Jurkat cells, and at 2.5  $\mu\text{M}$  inhibited chemotaxis in THP-1. The observed effects on chemotaxis were not due to toxicity, figures 5.43 and 5.44. Previous reports state that ROCK1 inhibition of NIH313 cells over 16 hours did not cause cofilin dephosphorylation [644], however results may be cell-type or time specific. ROCK phosphorylates LIMK, which phosphorylates cofilin; therefore inhibition of ROCK with Y27632 would be expected to prevent chemokines triggering cofilin phosphorylation.

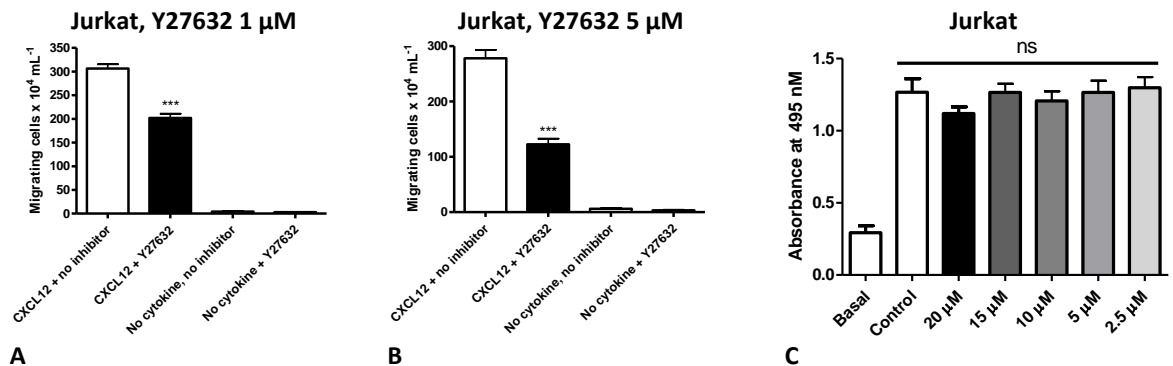


Figure 5.43: Chemotaxis assays following pre-treatment with Y27632 or control. (A and B) Chemotaxis of Jurkat to 1 nM CXCL12. (C) Cytotoxicity assay for Y27632. MTS assays were over 7 hours in Jurkat. Basal absorbance occurs in presence of medium after MTS treatment in the absence of cells. Means  $\pm$  SEM, one-way ANOVA, post-hoc Bonferroni,  $n \geq 3$  independent experiments, \*\*\*= $p < 0.001$ , ns= $p > 0.05$ .

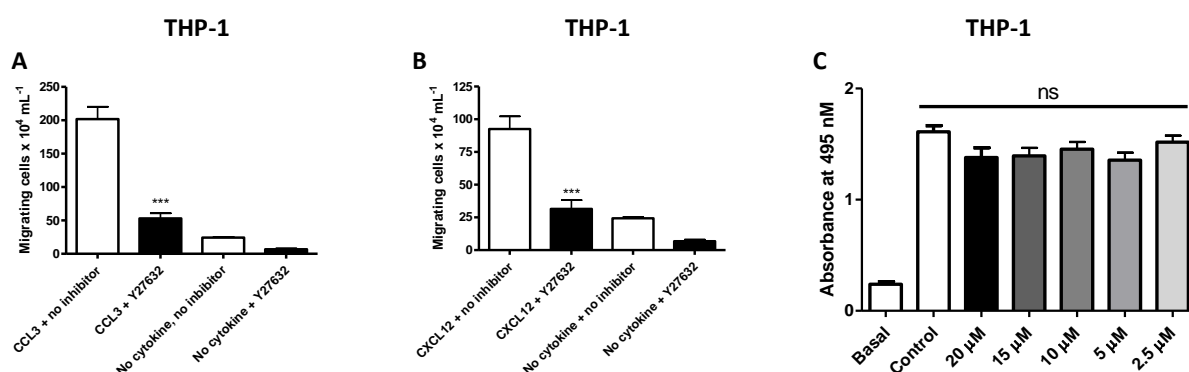


Figure 5.44: Chemotaxis assays following pre-treatment with Y27632 2.5  $\mu$ M or control. (A) Chemotaxis of THP-1 to 1 nM CCL3. (B) Chemotaxis of THP-1 to 1 nM CXCL12 (C) Cytotoxicity assay for Y27632. MTS assays were over 7 hours in THP-1. Basal absorbance occurs in presence of medium after MTS treatment in the absence of cells. Means  $\pm$  SEM, one-way ANOVA, post-hoc Bonferroni,  $n \geq 3$  independent experiments, \*\*\*= $p < 0.001$ , ns= $p > 0.05$ .

### 5.2.13: Mitogen extracellular signal regulated kinase (MAPKK) (MEK) and Src

In untransformed T-lymphocytes both PI3K and MEK are reportedly required to allow cofilin dephosphorylation [647]. This invited exploration to see if MEK was involved in CCL3 or CXCL12 signalling that modifies the cofilin phosphorylation state in THP-1 cells. Incubation with MEK inhibitor  $\alpha$ -[Amino[(4-aminophenyl)thio]methylene]-2-(trifluoromethyl) benzeneacetonitrile (SL327) even at a low concentration, 2  $\mu$ M, increased cofilin phosphorylation compared to control, more than 5 nM of CCL3 or CXCL12, figure 5.45.

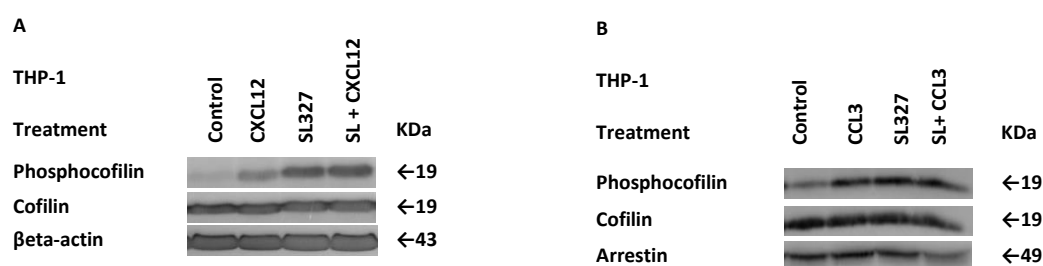


Figure 5.45: A & B. Western Blot with total-cofilin and phosphocofilin (Ser3) antibodies reveals cofilin phosphorylation levels in THP-1 following pre-treatment with 2  $\mu$ M SL327 (37°C, 30 mins) in presence and absence of CXCL12 or CCL3 (5 nM, 15 mins before lysis).  $\beta$ -actin or Arrestin-2 loading controls.

The results suggest MEK inhibition alone can influence cofilin phosphorylation in THP-1. MTS assays were used to check SL327 for toxicity in THP-1 and Jurkat, then the effects of MEK inhibition with SL327 on chemotaxis in THP-1 and Jurkat were explored, MTS assays found no evidence of SL327 inhibiting cell metabolism in THP-1 and Jurkat but inhibition of MEK very significantly inhibited chemotaxis to CXCL12 and CCL3, figures 5.46 and 5.47.

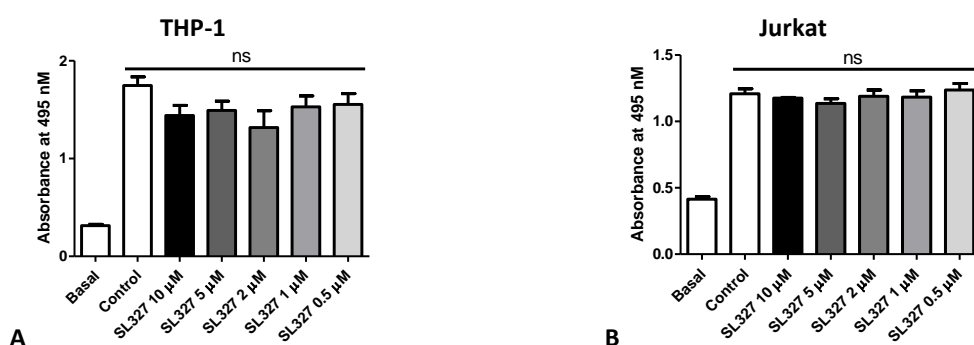


Figure 5.46: Cytotoxicity assays for SL327. MTS assays were over 7 hours in (A) THP-1 and (B) Jurkat. Basal absorbance occurs in presence of medium after MTS treatment in the absence of cells. Means  $\pm$  SEM, one-way ANOVA, post-hoc Bonferroni,  $n \geq 3$  independent experiments, ns =  $p > 0.05$ .

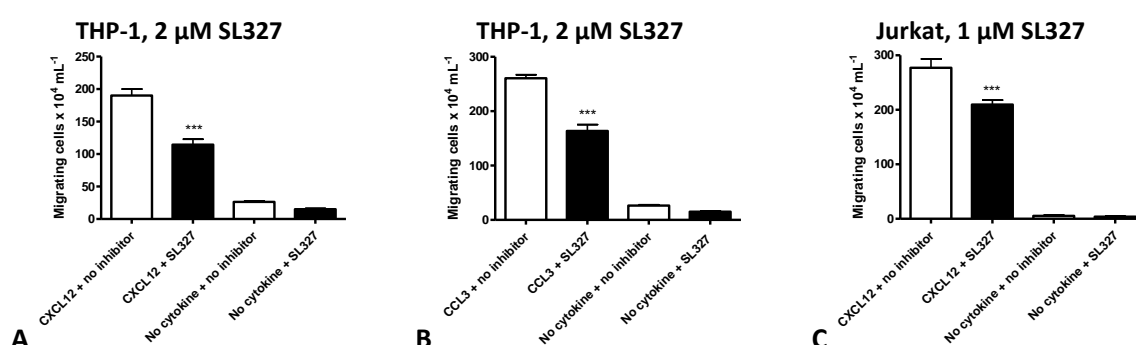


Figure 5.47: Chemotaxis assays following pre-treatment with SL327 or control. (A) Chemotaxis of THP-1 to 1 nM CXCL12. (B) THP-1 chemotaxis to 1 nM CCL3. (C) Jurkat chemotaxis to 1 nM CXCL12. Means  $\pm$  SEM, one-way ANOVA, post-hoc Bonferroni,  $n \geq 3$  independent experiments, \*\*\* =  $p < 0.001$ .

The above investigations show CXCL12, CCL3 and some other chemokines can increase cofilin phosphorylation in monocyte model THP-1, and also that phosphorylation levels can be modified by some small molecule inhibitors. CXCL12 triggered cofilin phosphorylation can be altered by PI3K, ROCK and MEK inhibition. ROCK has been shown to phosphorylate and activate LIMK [633]. These results support the premise that  $G_i$ -induced activation of MEK, PI3K and ROCK signalling pathways are involved in the control of cofilin activity. Results with Gallein,  $\beta\gamma$  G-protein inhibitor, and GRK inhibitor Ipyrimidine suggest these upstream pathway proteins are also involved. Src activation can cause loss of actin stress fibres, focal contacts and loss of cofilin phosphorylation these changes can support metastasis [679]. Inhibiting Src with Bosutinib 5  $\mu\text{M}$  in THP-1 only slightly increased cofilin phosphorylation responses to CXCL12, figure 5.48. Whereas inhibiting MEK was found to consistently increase cofilin phosphorylation, possibly because cofilin dephosphorylation may require both active MEK and PI3K.

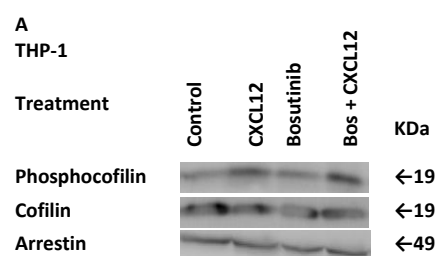


Figure 5.48: Western Blot with total-cofilin and phosphocofilin (Ser3) antibodies reveals cofilin phosphorylation levels in THP-1 following pre-treatment with 5  $\mu$ M Bosutinib (37°C, 30 mins) in presence and absence of CXCL12 (5 nM, 15 mins before lysis). Arrestin-2 loading control.

These responses appear cell type specific as in Jurkat cells baseline phosphocofilin levels are not significantly increased in the presence of CXCL12 except in the presence of some inhibitors, for example ROCK inhibitor Y27632 or PYK2/FAK inhibitor PF562271, where reduced baseline phosphorylation is increased by CXCL12, figure 5.49.

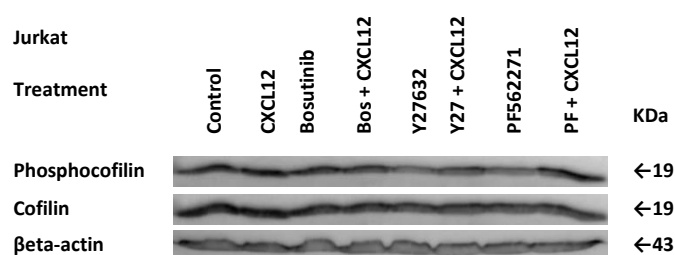


Figure 5.49: Western Blot with total-cofilin and phosphocofilin (Ser3) antibodies reveals cofilin phosphorylation levels in Jurkat following pre-treatment with Bosutinib 5  $\mu$ M, Y27632 5  $\mu$ M, or PF562291 25 nM (37°C, 30 mins) in presence and absence of CXCL12 (5 nM, 15 mins before lysis).  $\beta$ -actin loading control.

### 5.3: Discussion

This chapter examined if the signal transduction resulting in cofilin activation following CXCL12 stimulation of CXCR4, or CCL3, variant 2-70 D26A [680], stimulation of CCR1 or CCR5 receptors involved  $\beta\gamma$ , Pi3K, GRK, MEK, Src or ROCK1 or  $\beta$ -arrestin, all proteins previously connected with leading edge signalling and/or chemotaxis. To achieve this  $\beta$ -arrestin plasmid transfection and the various small molecule inhibitors shown with targets in figure 5.50 were employed.

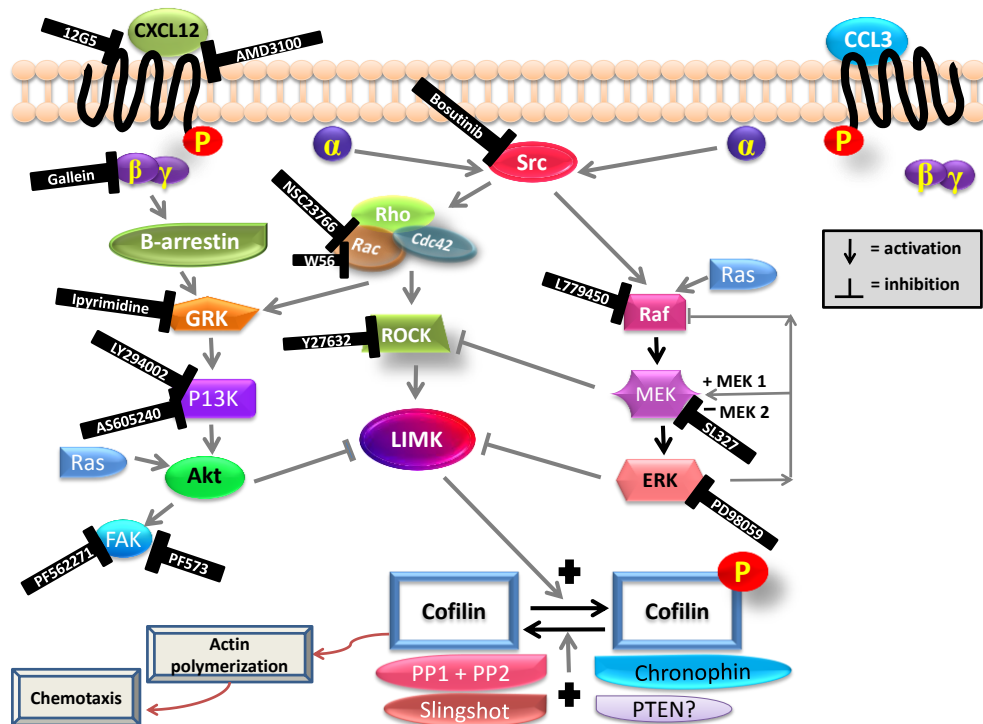


Figure 5.50: Major purported signalling pathways that modulate cofilin phosphorylation with inhibitors and protein targets.

### 5.3.1: Cofilin phosphorylation and chemokinesis

The above results indicate a relationship between cofilin Ser3 phosphorylation and chemokine stimulation of the cell-lines. Cofilin Ser3 dephosphorylation has been shown to occur seconds after chemotactic receptor activation in leukocytes [372, 681] and in cytokine receptor stimulation re-phosphorylation can occur in 3-5 minutes [371]. Several investigations show active dephosphorylated cofilin translocates in leukocytes to their leading edge, supporting actin polymerization in lamellipodia. Cofilin inhibition using siRNA can inhibit formation of free actin barbed ends and monomers. In Jurkat actin dynamics at the leading edge appear heavily influenced by cofilin controlled by SSH and LIMK [370, 682, 683]. Here siRNA knockdown of cofilin was found to inhibit MCF7 chemokinesis supported by CCL3 and CXCL12, figure 5.3.

Reduced Jurkat migration and lamellipodium formation has been shown to follow inhibition of LIMK cofilin phosphorylation and inhibition of SSH resulted in several lamellipodia formation and loss of directional migration; hence cofilin activity appears essential to maintain a single directional leading edge, i.e. to support chemotaxis. In leukocytes and mammary tumour cells investigations show cofilin is an essential team player along with ARP2/3 complex and Formins (Rho GTPase effector proteins supporting actin polymerization at barbed ends) to enable actin polymerization and facilitate chemotaxis [370, 372, 684]. Here a clear relationship between chemokine stimulation in THP-1 and cofilin phosphorylation was demonstrated, figure 5.4, and

the possibility that the degree of phosphorylation relates to the ability of a chemokine to induce chemotaxis in THP-1 was introduced, figure 5.5.

**5.3.2: Additive or inhibitory effects can occur when chemotactic chemokines are used in tandem**

Jurkat chemotaxis to CXCL12 increases steadily with concentrations from 0.1 nM to 1 nM but then plateaus, figure 5.6, whereas in THP-1 chemotaxis decreases at concentrations above and below 1-2.5 nM, figure 5.5, both for CCL3 and CXCL12. CXCL12 has previously been shown to synergise with CCL3, increasing chemotaxis in dendritic cells possibly by augmenting CCL3-triggered Akt or ERK 1/2 phosphorylation [685]. Results here in THP-1 show CCL3 and CXCL12 produced additive effects on chemotaxis, figure 5.7. CXCL11 is an agonist for CXCR3, CCL11 also binds CXCR3 acting as an antagonist. CXCR3 may act as a decoy receptor for CCL11 mopping up excess chemokine. CCL11 is an agonist at CCR3, and CXCL11 acts as antagonist at CCR3. CCL11 and CXCL11 may share overlapping binding sites on CCR3 extracellular loops; this interplay may be essential for homeostasis fine tuning chemotactic responses [686]. The results here, figures 5.8-5.9, suggest CXCL11 acts as an antagonist at CXCR4 with respect to calcium release in MCF7 and chemotaxis in THP-1 and Jurkat.

**5.3.3: *Pi3K*, Phosphatidylinositol 3,4,5 triphosphate (PIP<sub>3</sub>), Gβγ signalling and GEFs**

Pi3K is a key signalling protein mediating cell metabolism, growth, apoptosis as well as influencing actin-induced polarisation and changes in cytoskeleton arrangement [643]. Pi3K phosphorylates phosphatidylinositol 4,5-bisphosphate (PI(4,5)P<sub>2</sub>) aka PIP<sub>2</sub> producing phosphatidylinositol 3,4,5-triphosphate (PI(3,4,5)P<sub>3</sub>) aka PIP<sub>3</sub>. Guanine nucleotide exchange factors (GEFs) are also involved; GEFs activate small GTPases by catalysing GTPase-GDP to GTPase-GTP, figure 5.51.



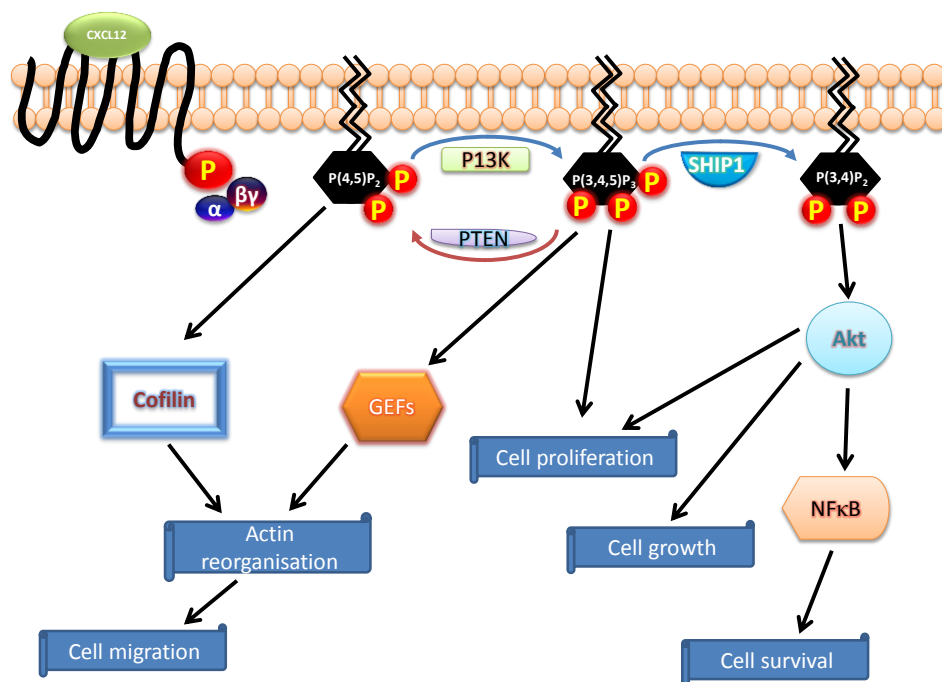


Figure 5.51: P13K and phosphatidylinositol-3,4,5-triphosphate signalling [638, 643, 646, 687, 688].

In immune cells the key controllers of levels of PIP<sub>3</sub> include Pi3K and the phosphatases, Phosphatase and Tensin homolog (PTEN), which is a tumour suppressor, and SH2-containing inositol 5-phosphatase (SHIP1). PTEN is usually constantly active, but is often deleted or mutated in cancers [687], whereas SHIP1 is activated by cell stimulation. In malignant cells PTEN may suppress cell proliferation whereas SHIP1 may reduce cell migration and activation. PTEN can downregulate Pi3K, Akt activity and SHIP1, by degrading PIP<sub>3</sub> producing PIP<sub>2</sub>. Genes coding Pi3K/Akt pathway proteins can be mutated in cancers, including in breast malignancies and lymphomas, producing constitutively active Pi3K, this appears to be the case with Jurkat [646, 688]. Also Jurkat are reported deficient in SHIP1 and PTEN, but express the substrate for both these phosphatases, PIP<sub>3</sub>, in high levels [688]. Such differences in phosphatase expression levels may be one reason why Pi3K inhibition, with Pi3K small molecule inhibitors AS605240 and LY294002, produced very significant inhibition on CXCL12 chemotaxis in Jurkat but have a lesser effect in THP-1 especially on CCL3-induced chemotaxis, figures 5.12-5.13. This may be because CXCL12- but not CCL3-triggered signalling is through G $\beta\gamma$  [638]. This was demonstrated here using the small molecule inhibitor Gallein which interrupts the interaction of G $\beta\gamma$  with Pi3K, figure 5.10. Although small molecule inhibitors suggest signalling through Pi3K may be more relevant for CXCL12 than CCL3 stimulation of chemotaxis. Cofilin phosphorylation and siRNA knockdown in cell-lines suggested Pi3K is just as important in CCL3 chemokinesis, figures 5.15-5.19. Indeed in

THP-1 cofilin phosphorylation was slightly increased in the presence of Gallein, figure 5.11, possibly suggesting constitutively active signalling in THP-1 through  $\beta\gamma$ , but the expected chemokine induced increased cofilin phosphorylation from CCL3 and CCL2, seen in figure 5.4, was reduced by pre-treatment with Gallein supporting the findings of the siRNA knockdown.

Cofilin phosphorylation was explored in THP-1 in the presence and absence of Pi3K inhibitors LY294002 and AS605240 and different concentrations of CXCL12 or CCL3. Phosphorylation of cofilin was increased with both inhibitors compared to control at low levels of chemokine (0.5 and 1 nM), however low levels of chemokine alone were insufficient alone to cause cofilin phosphorylation to controls, figures 5.18A and 5.18B. Inhibition of Pi3K may reduce the concentration of chemokine necessary to cause cofilin phosphorylation as Pi3K/Akt signalling inhibits LIMK, which phosphorylates cofilin. Treatment with LY294002 or AS605240, followed by CCL3 or CXCL12 at 5 nM produced the usual phosphorylation in controls, which was increased further by AS605240 but reduced by LY294002 figure 5.18C. Hence like the siRNA knockdown these results suggest Pi3K signalling may be equally important in both CCL3 and CXCL12 signalling in THP-1 cells, but may also be Pi3K subtype specific.

#### ***5.3.4: Cofilin links to mitogenic signalling networks***

The Ras-Raf-MEK-ERK signalling pathway can carry the signal from a chemokine stimulation of a GPCR to the cell's nucleus. MEK is a tyrosine and threonine kinase also known as MAPKK. CXCL12 stimulation of G $\alpha$ i through CXCR4 is thought to trigger Ras signals to MEK. LIMK1 downstream of MEK is then inhibited and cofilin dephosphorylation (activation) occurs [689]. Here inhibition of MEK with SL327 strongly inhibited chemotaxis and produced cofilin phosphorylation in presence and absence of CCL3 and CXCL12, figures 5.45 and 5.47. Inhibition of MEK may only inhibit leukocyte migration through three-dimensional (3D) not two-dimensional (2D) environments, possibly as on 2D surfaces leukocyte migration is based on the cells "walking" i.e. after extending a leading edge, the "back" of the cell then arches as the trailing edge or uropodia moves forward, resulting in movement similar to that seen in soft-bodied insect larva. Leukocytes migrate as single cells through many different tissues; their mode of motility has considerable plasticity depending on their extracellular environment, for example movement along 2D endothelial linings compared to through 3D interstitial spaces. Leukocytes can switch motility mode rapidly [690, 691]. Such 2D movement may not need actin tread-milling. Actin polymerization is needed for pseudopodia formation at the leading edge; actin's barbed ends push the cell membrane forward and cell adhesion between linker proteins Shootin1 and LI-CAM, and also between F-actin

and N-Cadherin, allow grip between cell and surface [691]. If these contracting cycles are inhibited, but cofilin is not, cells have been shown to produce lamellipodia to migrate. The lower the level of G-actin the more cells may depend on cofilin to move, thus MEK and active cofilin appear important in 3D migration, and cells can adapt their migratory mode to suit their external environment [633]. Neuro Probe ChemoTx<sup>®</sup> plates as used here to explore chemotactic responses may represent a useful model of a 3D system as the cells need to squeeze through the 5  $\mu$ M pores. This is a similar situation to T-cells protrusions pushing through interstitial meshes and in both cases movement is towards a chemokine attractant.

#### **5.3.5: GRKs and $\beta$ -arrestin in chemokinesis**

GRK2 is a serine threonine kinase with three key domains, a Regulator of G-protein Signalling Homology (RH) domain, a Central Catalytic domain and a lipid-binding Pleckstrin Homology (PH). GRK2 can promote  $\beta$ -arrestin binding agonist-activated GPCRs halting the receptors' activation of G-proteins [17, 692] but also interact with many cytosolic and nuclear oncogenic signalling proteins such as Mdm2, MEK, AKT and RhoA, [693], for example GRK2 has been shown to inactivate p38 MAPK [694]. GRK2's N-terminal and PH domains interact with G $\beta$ /G $\gamma$  subunits [695, 696], and its C-terminal interacts with lipids or membrane proteins [652]. GRKs are also involved in G-protein independent signalling, such as GRK2/ $\beta$ -arrestin signalling producing ERK activation [697]. Inhibition of ERK inhibits chemotaxis [698] which may explain why inhibiting GRK2 inhibitor  $\beta$ -ARK-1 and Ipyrimidine both strongly inhibited CCL3 and CXCL12 chemotaxis, figures 5.21 and 5.23.

Different chemokines binding the same chemokine receptor can activate different GRKs promoting biased signalling, through either G-proteins or GRK/ $\beta$ -arrestin [699], as different chemokines produce specific conformational changes that selectively recruit specific GRK subtype/s [700]. Different GRKs then phosphorylate differing serine/threonine residues on the GPCR. The phosphorylation pattern selects the response, either receptor desensitisation or signalling [701]. GRKs also interact directly with non-GPCR proteins [702] including cytosolic and nuclear proteins involved with cell migration [703]; for example GRK2 interacts with MEK to negatively regulate ERK activated by CCL2 [704]. ERK triggered phosphorylation of GRK2 allows GRK2 location in mitochondria [705] and interaction with mitochondrial chaperone HSP90 [706] where it mediates the effects of cellular Ca<sup>2+</sup> fluxes on mitochondria [707]. GRK2 also phosphorylates tubulin [708] and is itself phosphorylated by CDK-2 and can affect cell cycle

progression [709]. This may explain the cytotoxicity issues observed with both GRK inhibitors, figures 5.22 and 5.24.

#### **5.3.6: *$\beta$ -arrestin mediation of signalling leading to chemotaxis and chemokinesis***

Agonist phosphorylation of GPCRs by GRKs reportedly triggers arrestin binding which sterically discourages G-protein interactions with GPCR, and thus uncouples G-proteins from the GPCR and terminates signalling [710]. Arrestin-2 and Arrestin-3 may facilitate GPCR internalisation through clathrin-mediated endocytosis, a pathway that can lead to receptors recycling back to the membrane rather than degradation [711-713]. However arrestin is reported to associate with E3 ubiquitin ligase which favours ubiquitination and degradation [714]; such association has been demonstrated for CXCR4 [715, 716]. Plasmid overexpression of Arrestin-2 and Arrestin-3 has been used by others to explore any preferences for receptors for arrestin-2 or -3 in this process, which purportedly involves  $\beta$ -arrestin binding to clathrin and AP2 proteins as well as other components of clathrin coated pits. Many early studies have shown  $\beta$ -arrestins can move with associated GPCR into early endosomes. Arrestin also hinders phosphatase access to GPCRs phosphorylated C-termini, and hence influences receptor re-sensitisation [493, 717].

$\beta$ -arrestins facilitate GPCR signalling via Src, ERK and p38 MAPK pathways [718]. MAPK signalling purportedly supports metastasis [719]. GPCRs can be classified as class A and B receptors, CCR5 is a class A and CXCR4 is a class B. Class A GPCRs preferentially associate with Arrestin-3 over Arrestin-2, whereas class B receptors show no preference [710, 720, 721]. Results here in THP-1 and Jurkat support these factors; showing Arrestin-3 may be more relevant for CCL3-induced chemotaxis, likely to be mediated by CCR5 figure 5.33C, whereas both Arrestin-2 and -3 are relevant for CXCL12-induced chemotaxis likely to be mediated by CXCR4, figures 5.33A and 5.33B. However in MCF7 cells only Arrestin-2 appears to support CXCL12 wound-healing, transfection with Arrestin-3 or Arrestin-mutant plasmids may even impeded migration, figure 5.34, suggesting cell-type specificity. For CCR5-arrestin interactions to occur certain phosphorylation sites must be available [722]. CCR5 may only loosely bind  $\beta$ -arrestins whereas CXCR4 may bind more tightly [720]. This may modulate receptor fate [723], potentially giving CCR5 a better chance of recycling and CXCR4 of degradation. However over-expression of Arrestin-2 may be a negative biomarker in lung carcinoma [724].

#### **5.3.7: ROCK and MEK are key mediators of cofilin phosphorylation**

Ras proteins are a family of small GTPases. Signalling from Ras proteins is involved in cell differentiation, survival and growth, hence over-expression of Ras is common in cancer; the three Ras proteins in mammals N-Ras, H-Ras and K-Ras are all powerful oncogenes. Ras can signal to Raf, and to Pi3K. Src can also signal to Raf and Pi3K which can also be stimulated by G protein-coupled receptor kinase (GRK). MEK can in turn inhibit Rho activated kinase (ROCK), all these signalling cascades may be involved with cofilin phosphorylation [725]. ROCK inhibitor Y27632 was found to inhibit both chemotaxis and chemokine induced cofilin phosphorylation, figures 5.42-5.43. Hence when MEK is inhibited cofilin is phosphorylated, figure 5.45, and when ROCK is inhibited cofilin phosphorylation is prevented, figure 5.42, suggesting both ROCK and MEK are key in chemokine induced cofilin phosphorylation. Further complexity is added to the picture by many other signalling pathways including those influencing the activity of LIMK1 and LIMK2.

#### **5.3.8: FAK inhibition may support haematological malignancies**

FAK inhibition produced cofilin phosphorylation and inhibited chemotaxis. Others have noted that FAK inhibition can inhibit chemotaxis but support invadopodia formation in melanoma [726]. Invadopodia are actin-based protrusions that would require cofilin phosphorylation and f-actin formation. Hence although FAK/PYK2 inhibition with PF562271 was found to inhibit CXCL12-induced directional migration, figure 5.38, it produces cofilin phosphorylation, figure 5.40, suggesting it potentially could support tissue invasion by haematological cancers in a similar way to that observed for melanoma.

### **5.4: Conclusions**

Although Jurkat were only found to migrate to CXCL12; CCL2, CCL3, CCL4, CCL5, CCL23, CXCL9, CXCL11 and CXCL12 were shown to induce chemotaxis in THP-1. A Gaussian distribution chemokine concentration response curve was seen with THP-1 to CCL3 and CXCL12, and Jurkat to CXCL12. In THP-1 CCL3 with CXCL12 were found together to produce additive chemotactic responses whereas CCL2 with CXCL11 did not; suggesting that chemokine chemotactic responses may be modulated by chemokine co-operation or antagonism. Western blot and immunofluorescence confirmed cofilin expression in THP-1, MCF7 and Jurkat. Chemokines CCL3, CCL2 and CXCL12 were shown to increase cofilin phosphorylation in THP-1, and siRNA cofilin

knockdown confirmed cofilin is important in MCF7 chemokinesis. Results in THP-1 support the conclusion that if a chemokine produces cofilin phosphorylation it may also be chemotactic. Also that cofilin phosphorylation can indicate the presence of a chemokines cognate receptor within a cell-line.

Immunofluorescence and Western Blots demonstrated Arrestin-2's presence in THP-1 macrophages Jurkat and MCF7. Arrestin-2 over-expression, compared to eGFP control, increased migration of Jurkat. Arrestin-2 and Arrestin-3 plasmids were seen to locate to cell cytoplasm, and possibly associate with organelles; whereas Mutant-arrestin plasmids may target cell nuclei, possibly causing cytotoxicity. Chemokine addition produced plasmid aggregation possibly indicating Arrestin-2 and 3 plasmids associate with receptors on endocytosis. In THP-1 Arrestin-3, but not Arrestin-2, plasmid transfection increased chemotaxis to CCL3, and both Arrestin-2 and Arrestin-3 plasmids increased chemotaxis to CXCL12. However this was compared to dominant negative mutant plasmids which may themselves reduce migration. eGFP plasmid controls would have been better. In Jurkat Arrestin-2 plasmid transfection, compared to eGFP plasmid controls, modestly increased chemotaxis to CXCL12. In MCF7 only Arrestin-2, not Arrestin-3, plasmid transfection increased chemokinesis in presence of CCL3. Overall arrestin results suggest cell and chemokine biases in Arrestin-2 and Arrestin-3 activity.

GRK inhibition inhibited chemotaxis to both CXCL12 and CCL3. GRK2 inhibitor,  $\beta$ -ARK-1, is a chromophore that is toxic to Jurkat and THP-1 at higher concentrations over longer timescales, whereas GRK inhibitor Ipyrimidine lacks toxicity, but still inhibits chemotaxis to CCL3 and CXCL12 and cofilin phosphorylation, suggesting GRKs play a role in cofilin supported chemokinesis.

siRNA knockdown and small molecule inhibition confirmed the importance of Pi3K to CXCL12 migration in all cell-lines and to a lesser extent CCL3-induced chemokinesis in MCF7 and chemotaxis in THP-1. Indeed Pi3K inhibition in THP-1 and Jurkat may increase cofilin phosphorylation in presence and absence of CXCL12 or CCL3. FAK/PYK2 inhibition repressed chemotaxis to CXCL12 but not CCL3 in THP-1, and inhibited Jurkat chemotaxis to CXCL12. It also caused cofilin phosphorylation in THP-1 that was unaffected by CCL3 or CXCL12, and modulated CXCL12 but not CCL3 calcium flux. Overall suggesting FAK/PYK2 play a key role in CXCL12 signalling and cofilin activity.

ROCK co-locates with microtubule organising centres; Nocodazole, which depolymerizes microtubules, inhibits chemotaxis to CXCL12 but not CCL3; whereas ROCK inhibitor Y27632 strongly inhibits chemotaxis to both chemokines as well as preventing cofilin phosphorylation in THP-1. MEK1/2 inhibitor SL327 has the opposite effect increasing cofilin phosphorylation, but still significantly inhibiting chemotaxis to CXCL12 and CCL3. Overall results suggested differential chemokine signalling through key cellular proteins such as Gβγ, Pi3K, FAK, MEK, Src and ROCK may modulate cofilin phosphorylation to influence chemotaxis.

Having established above that phosphocofilin levels can be a useful readout tool in CXCL12 and CCL3 signalling, and that phosphocofilin levels can be modified by inhibiting proteins known to mediate CXCR4/CXCL12 pathways; next in chapter 6 cofilin phosphorylation along with chemotaxis assays were used to help to elucidate the somewhat controversial role of JAK2 and STAT3 proteins in CXCL12/CXCR4 signalling.

## Chapter 6: JAK2 and STAT3 play role in chemokine-induced chemotaxis and cofilin phosphorylation

### 6.1: Introduction

CXCL12 binding CXCR4 can trigger G $\alpha$ i signalling. This may involve signalling proteins termed 'JAKs' phosphorylating firstly the CXCR4 receptors tyrosines and then JAKs phosphorylating 'STATs' which are transcription factors which dimerize before translocating into the nucleus [323, 727, 728]. JAK2 gene mutations are common in malignancies [324, 328]; JAK2 mutations can enhance oncogenic responses to CXCR4/CXCL12 signalling aiding cancer progression and metastasis; by, for example, facilitating Pi3K signalling supporting chemotaxis [328]. Here the effects of JAK2 and STAT3 inhibition, with small molecule inhibitors, on chemokine induced chemotaxis were examined along with STAT3 phosphorylation in the context of cofilin activation. Active Rho GTPases, including Rac1 may be important for STAT3 transcriptional activity [729-731]. Phosphorylation by LIMK inactivates cofilin. LIMK may also negatively regulate STAT3, through mediation of Myc expression [732], overall suggesting chemokine triggered phosphorylation of cofilin may correlate with STAT3 phosphorylation. This piece of research elucidates the effects of JAK2 and STAT3 inhibition on cofilin and STAT3 phosphorylation induced by chemokines and the effects of JAK2 and STAT3 inhibition on cAMP production mediated by Forskolin, figure 6.1.

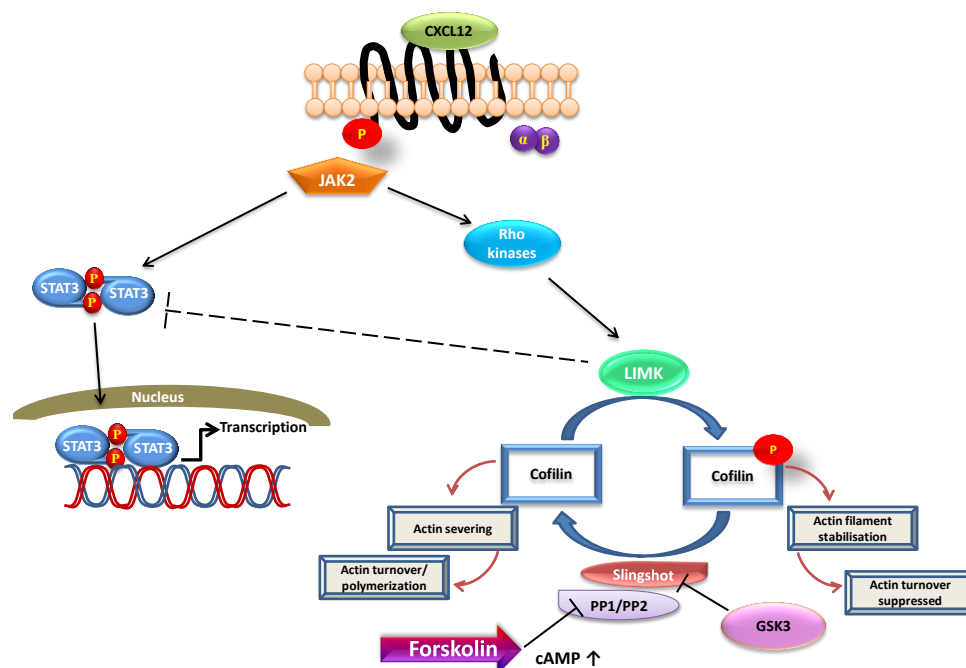


Figure 6.1: The effects of JAK signalling, through Rho GTPases, and Forskolin on cofilin phosphorylation.



**Hypothesis:** JAK2 and STAT3 signalling supports metastasis including through mediation of cofilin phosphorylation.

**Aim:** To discover if JAK2 and STAT3 inhibition affects MCF7 chemokinesis or THP-1 chemotaxis to CCL2 or CXCL12, then explore if any effects observed relate to phosphocofilin or cAMP levels in cells.

**Objectives:**

- (i) Check small molecule inhibitors of JAK2 and STAT3 for cytotoxicity
- (ii) Explore the effects of JAK2 and STAT3 inhibition on THP-1 chemotaxis to CXCL12 and CCL2.
- (iii) Discover if inhibition of JAK2 or STAT3 modulates MCF7 chemokinesis supported by CCL2 or CXCL12
- (iv) Investigate if JAK2 or STAT3 inhibition affects calcium dynamics in cell-lines
- (v) Use Forskolin to explore the effects of increased cAMP levels in MCF7 chemokinesis and THP-1 chemotaxis and cofilin phosphorylation
- (vi) Examine the effects of JAK2 and STAT3 inhibition on cellular cAMP levels
- (vii) Examine the effects of JAK2 and STAT3 inhibition on cofilin and STAT3 phosphorylation in THP-1

## **6.2: Results**

Here the roles of JAK2 and STAT3 in chemokine induced chemotaxis or wound-healing, along with calcium responses in THP-1 or MCF7 are explored along with the involvement of JAK2 and STAT3 in the temporally complex cofilin phosphorylation dynamics following CXCL12 stimulation; also possible links between cofilin and STAT3 phosphorylation are examined. Next the roles of Forskolin and PKA inhibitor H89HCl individually on chemokine-induced chemotaxis and wound-healing are covered before using Forskolin as a tool in cAMP assays exploring the effects of JAK2 and STAT3 mediation of cAMP responses to CCL2.

Small molecule inhibitors employed here include JAK2 inhibitor II, Hexabromocyclohexane (HBC), which binds a pocket adjacent to JAK2's activation loop preventing JAK2 autophosphorylation [733]; STAT3 inhibitor III, WP1066, an AG490 tyrphostin analog that inhibits the STAT3 pathway, and STAT3 inhibitor VIII, 5,15-Diphenylporphyrin (5,15-DPP), which inhibits STAT3 dimerization via STAT3 SH2 domain and prevents STAT3 nuclear translocation. Blocking STAT3 phosphorylation consequently inhibits STAT3 c-myc promotor binding, reducing cellular c-myc protein levels [734], figure 6.2.

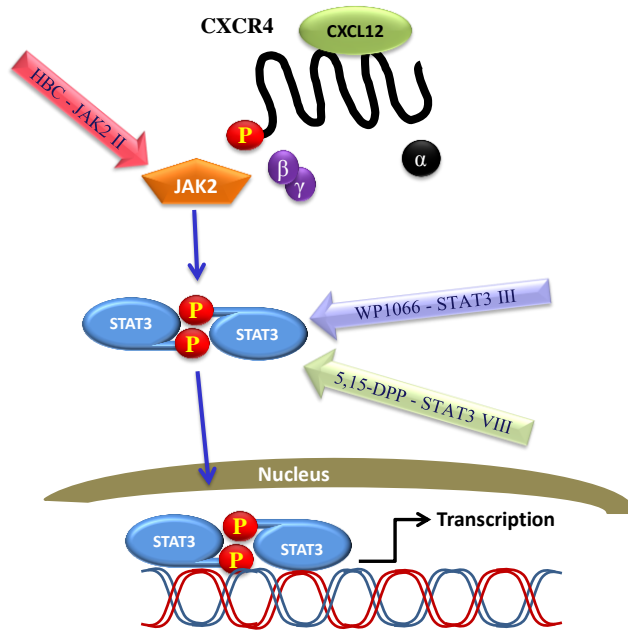


Figure 6.2: JAK2/STAT3 signalling from CXCR4, and targets of inhibitors used.

### 6.2.1: JAK2 and STAT3 inhibitors were examined for effects on cell metabolism and actin polymerisation

MTS assays were used to establish inhibitor effects on cell metabolism in MCF7 and THP-1, figure 6.3.

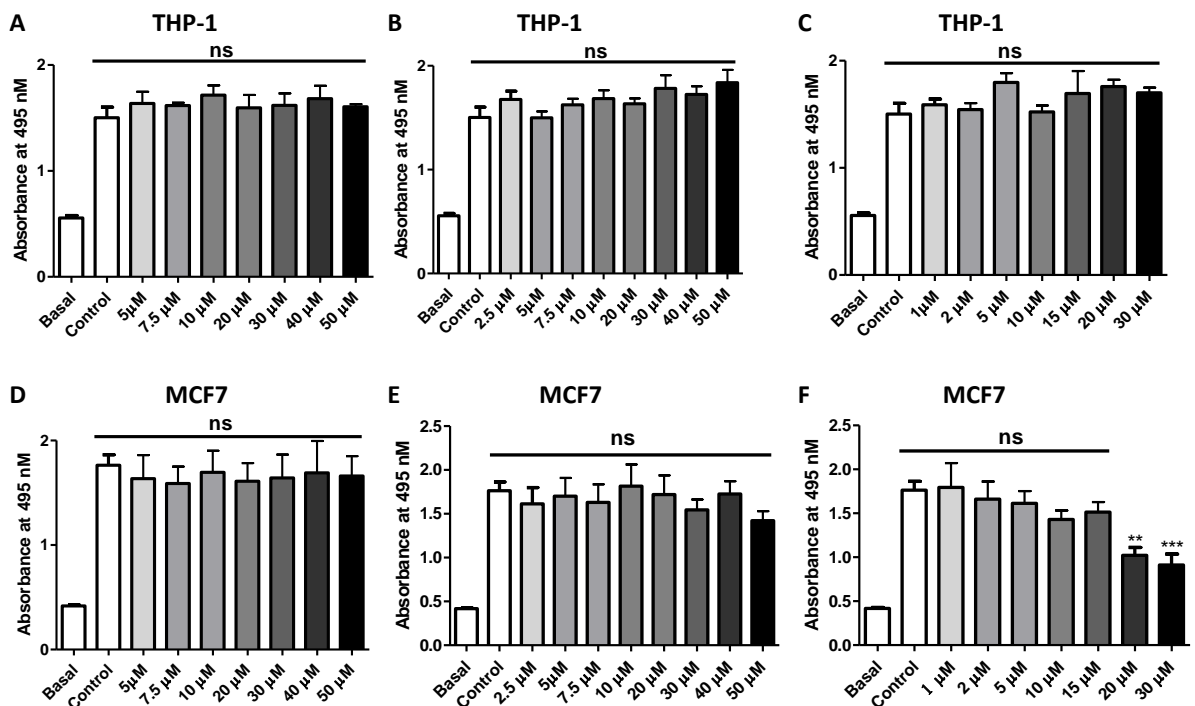


Figure 6.3: Cytotoxicity assays in THP-1 over 7 hours using a range of concentrations of (A) HBC, (B) 5,15 DPP and (C) WP1066 and in MCF7 over 26 hours using (D) HBC, (E) 5,15 DPP and (F) WP1066. Basal absorbance occurs in presence of medium after MTS treatment in the absence of cells. Means  $\pm$  SEM, one-way ANOVA, post-hoc Bonferroni,  $n \geq 3$  independent experiments, ns= $p > 0.05$ .

No evidence of toxicity was seen from any of the inhibitors in THP-1 cells over 7 hours. In MCF7 significant inhibition of metabolism occurred with WP1066, but at the concentration of 2  $\mu$ M used in all assays here no toxicity was apparent.

Next the effects of the JAK2 and STAT3 inhibitors on actin polymerisation, essential for cell migration was examined in MCF7 cells, figure 6.4. Some loss of filament actin and fine actin surface protrusions were apparent with STAT3 inhibitor 5,15-DPP.

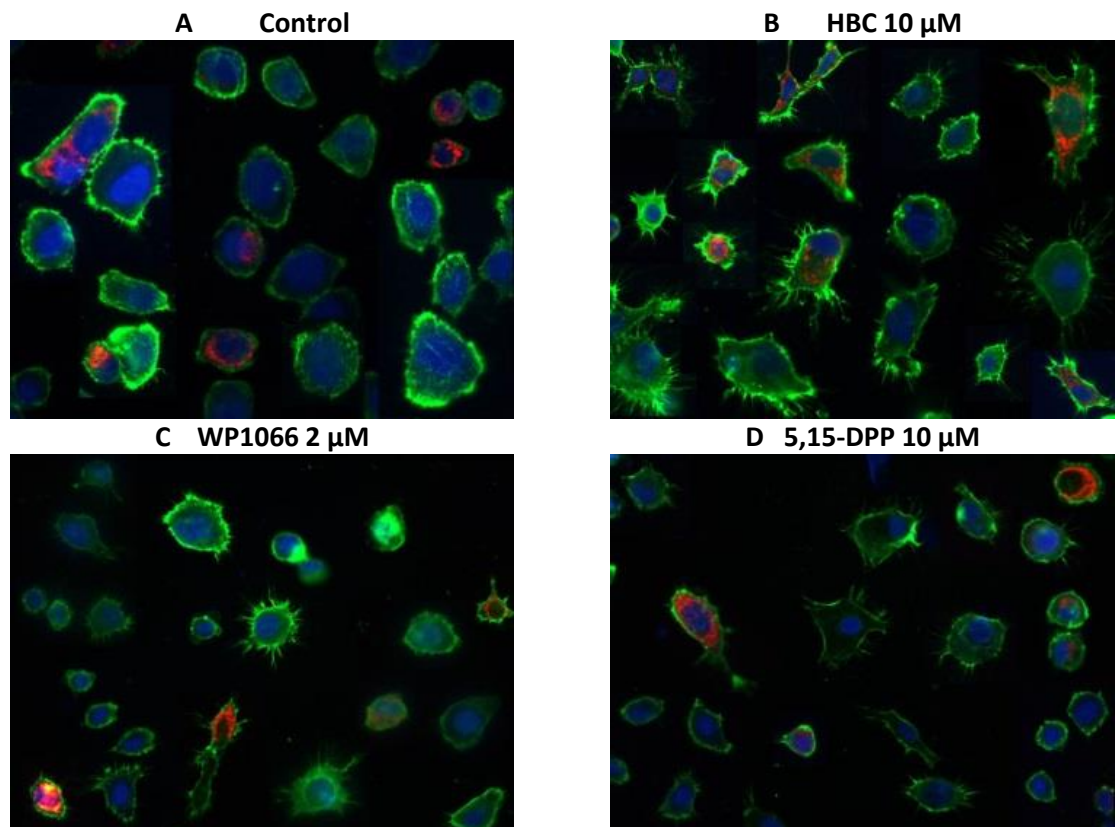


Figure 6.4: Filament actin stains following JAK2 or STAT3 inhibition. Alexa-488 Phalloidin (green) and DAPI nuclear stains (blue) of MCF7, previously transfected with DsRed Mitochondrial Plasmids, following pre-treatment with (A) DMSO control (B) 10  $\mu$ M HBC (1 hr, 37°C), (C) 2  $\mu$ M WP1066 (D) 10  $\mu$ M 5,15-DPP. Imaged UV inverted microscopy (Leica DMII Fluorescence microscope 500x Ex 490 nm, Em 520 nm).

### **6.2.2. JAK2 and STAT3 role in chemotactic cell migration and chemokinesis.**

The effects of HBC, WP1066 and 5,15-DPP on THP-1 cell migration using chemotaxis assays, figure 6.5, and then MCF7 wound-healing, figure 6.6, was examined.

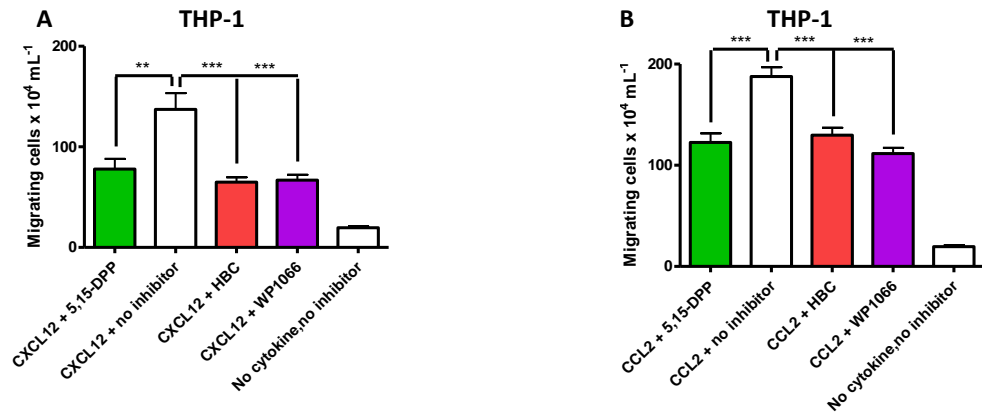


Figure 6.5: Chemotaxis assays following pre-treatment with WP1066 2  $\mu\text{M}$ , HBC 10  $\mu\text{M}$  or 5,15-DPP 10  $\mu\text{M}$  or control (DMSO). (A) Chemotaxis of THP-1 to 1 nM CXCL12. (B) THP-1 chemotaxis to 1 nM CCL2. Means  $\pm$  SEM, one-way ANOVA, post-hoc Bonferroni,  $n \geq 3$  independent experiments, \*\*\*= $p < 0.001$ .

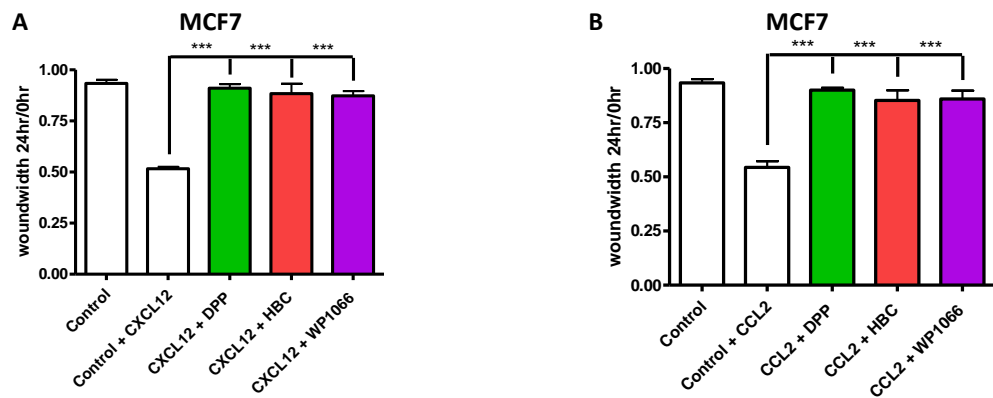


Figure 6.6: MCF7 wound-healing assays following pre-treatment with 2  $\mu\text{M}$  WP1066, 10  $\mu\text{M}$  HBC, 10  $\mu\text{M}$  5,15-DPP or DMSO control. Analysis 24 hours after (A) 10 nM CCL2, or (B) 10 nM CXCL12, (C-E) wound-healing images, see overleaf. Means  $\pm$  SEM, one-way ANOVA, post-hoc Bonferroni,  $n \geq 3$ , \*\*\*= $p < 0.001$ .

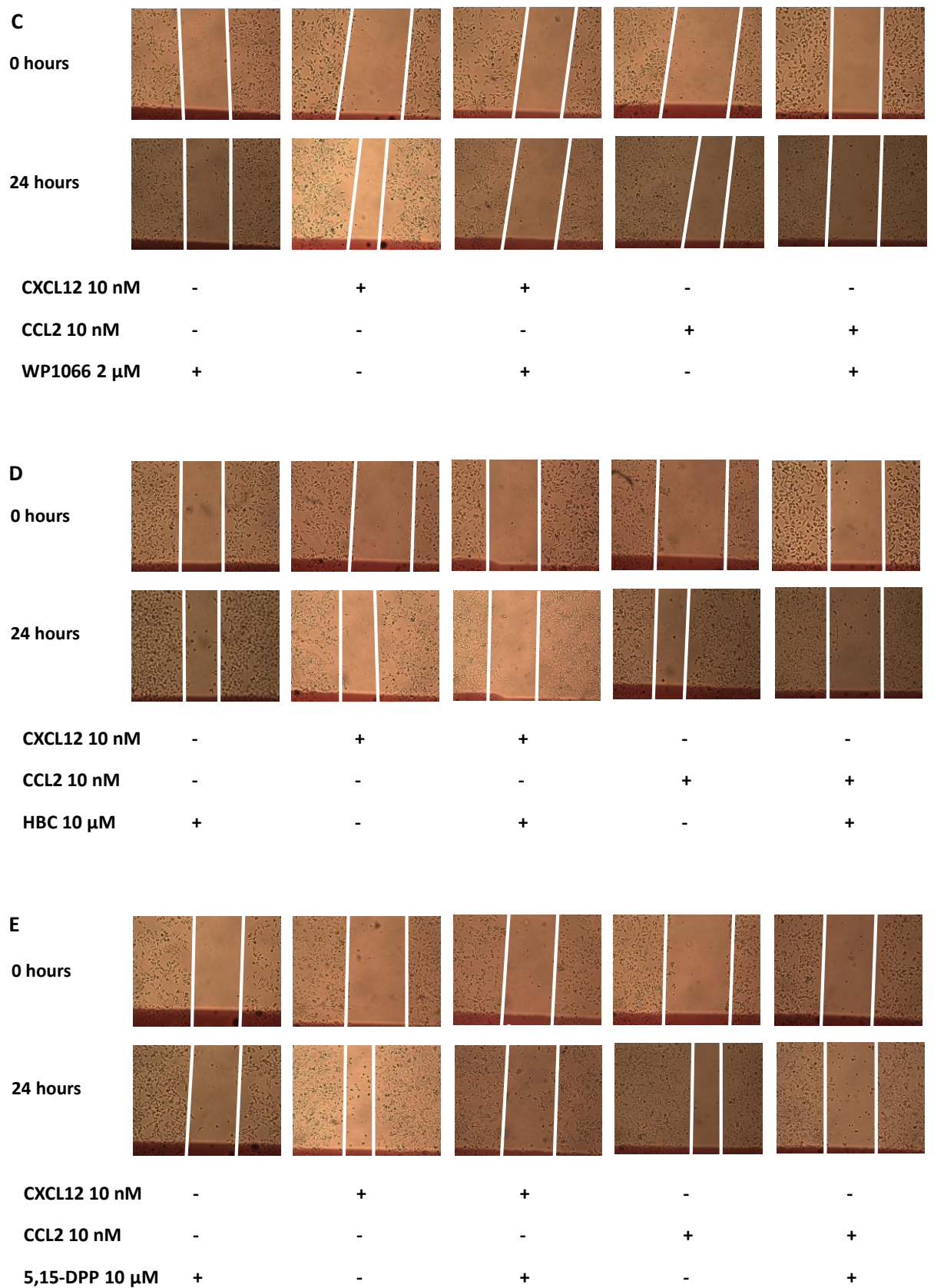


Figure 6.6C-E: Wound-healing images from 6.6A and B above.

WP1066 2  $\mu$ M, HBC 10  $\mu$ M and 5,15-DPP 10  $\mu$ M all very significantly reduced THP-1 migration to CXCL12 and CCL2 and MCF7 wound-healing induced by CXCL12. However Jurkat chemotaxis to CXCL12 was found not to be influenced by these three inhibitors, figure 6.7, suggesting JAK and STAT3 involvement in chemotaxis has cell type specificity.

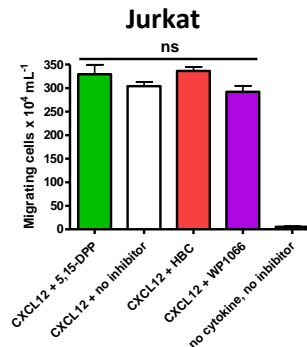


Figure 6.7: Chemotaxis assays following pre-treatment with HBC 10  $\mu$ M, WP1066 2  $\mu$ M, 5,15-DPP 10  $\mu$ M or control (DMSO). (A) Chemotaxis of Jurkat to 1 nM CXCL12. Means  $\pm$  SEM, one-way ANOVA, post-hoc Bonferroni,  $n \geq 3$  independent experiments, ns= $p > 0.05$ .

### 6.2.3: The roles of JAK2 and STAT3 in calcium dynamics

The effects on calcium release in THP-1, MCF7 and Jurkat of JAK2 II, STAT3 III and STAT3 VIII inhibition was examined using calcium flux stimulated by CXCL12, figures 6.8 and 6.9.

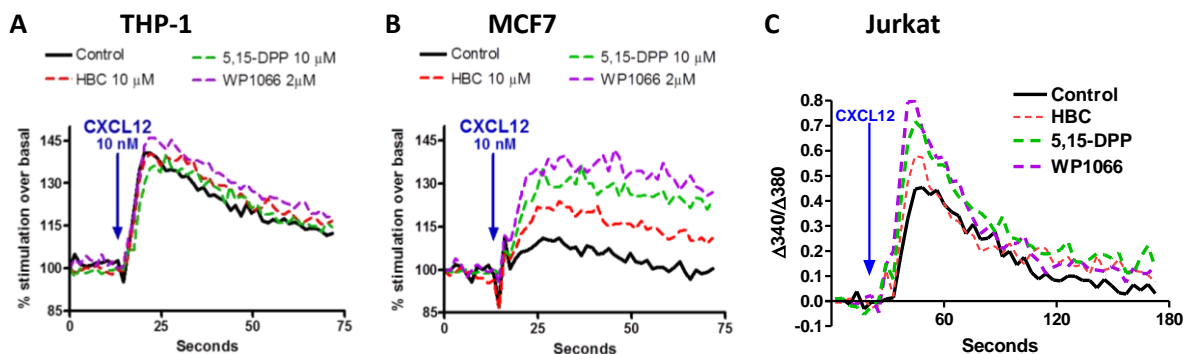


Figure 6.8: Fura2  $\text{Ca}^{2+}$  assay in THP-1 following HBC 10  $\mu$ M, WP1066 2  $\mu$ M, 5,15-DPP 10  $\mu$ M or control (DMSO). Data expressed as fluorescence ratio change ( $\Delta 340/\Delta 380$  nm) i.e. peak fluorescence following 10 nM CXCL12 addition minus basal fluorescence (prior to chemokine), traces  $n=1$ .

JAK2 and STAT3 inhibition had little effect on THP-1 cells but appeared to stimulate CXCL12-induced calcium release in MCF7 and Jurkat. Total calcium release was significantly greater in Jurkat, figure 6.9, thus as with chemotaxis, the effect of the inhibitors on calcium dynamics was found to be cell-type specific.

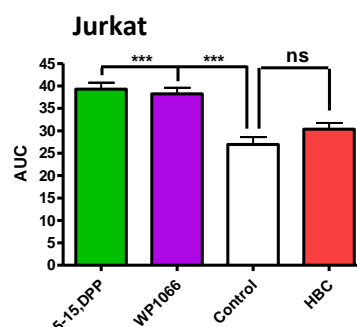


Figure 6.9: In Jurkat both STAT3 inhibitors highly significant ( $p < 0.001$ ) increased total calcium responses (AUC) but JAK2 inhibition had no significant effect.

#### 6.2.4: cAMP and JAK STAT signalling

Raised cAMP levels can either directly or via cross-talk inhibit cell proliferation in immune cells [735], possibly through inhibition of proliferative JAK/STAT signalling [736], although other pathways such as MEK and ERK may be involved [737]. Rodriguez *et al.* (2013) found PKA promoted JAK3 serine phosphorylation negatively regulating its catalytic activity and that 3-isobutyl-1-methylxanthine (IBMX) had the same effect. IBMX is a broad spectrum phosphodiesterase inhibitor that prevents the breakdown of cAMP and cGMP [738]. Hence the effects on chemotaxis of manipulating cellular cAMP levels were assessed, followed by looking at JAK2 and STAT3 inhibition wrt intercellular cAMP levels.

##### 6.2.4.1: cAMP modulator Forskolin and PKA inhibitor H89HCL inhibit chemotaxis and chemokinesis

Forskolin, a direct reversible activator of cAMP, is a diterpene derivative originally from the *Coleus forskohlii* plant and a useful tool for exploring the role of cAMP in cellular signalling. Forskolin induces a conformational change in the adenylyl cyclase ATP binding site, located close to the  $G_{\alpha s}$  subunit binding site, and results in more efficient cAMP synthesis [739]. Forskolin and phosphodiesterase inhibitors such as IBMX can elevate intracellular cAMP levels [740]. Forskolin increases intracellular cAMP levels several fold above baseline, this can interfere with expression of cell cycle regulatory genes [741, 742], so potentially inhibits cell proliferation and produces cell type specific responses. In the following investigations Forskolin and the PKA inhibitor H89 HCL were employed to explore the effects of modulation of cAMP and PKA levels on chemotaxis and wound-healing in THP-1 and MCF7 respectively. PKA was of interest as cAMP negative regulation can occur through PKA [743, 744], and PKA may phosphorylate JAK2 [745].

No significant effects on cell proliferation, as measured by MTS assay, were seen with H89 HCL or Forskolin in THP-1 or MCF7 cells, figures 6.10 and 6.11.



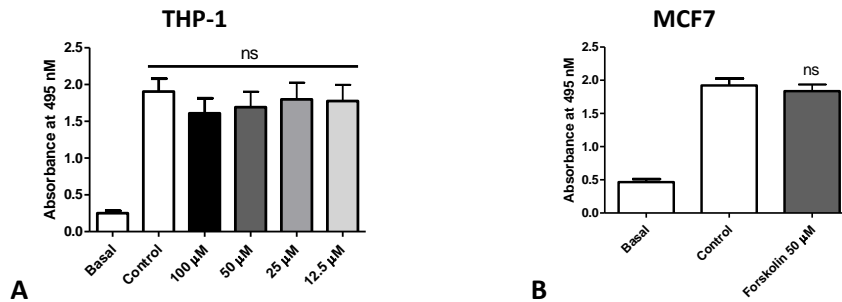


Figure 6.10: Cytotoxicity assays for Forskolin. MTS assays were over 7 hours in (A) THP-1 and over 24 hours in (B) MCF7 cells. Basal absorbance occurs in presence of medium after MTS treatment in the absence of cells. Means  $\pm$  SEM, one-way ANOVA, post-hoc Bonferroni,  $n \geq 3$  independent experiments,  $ns = p > 0.05$ .

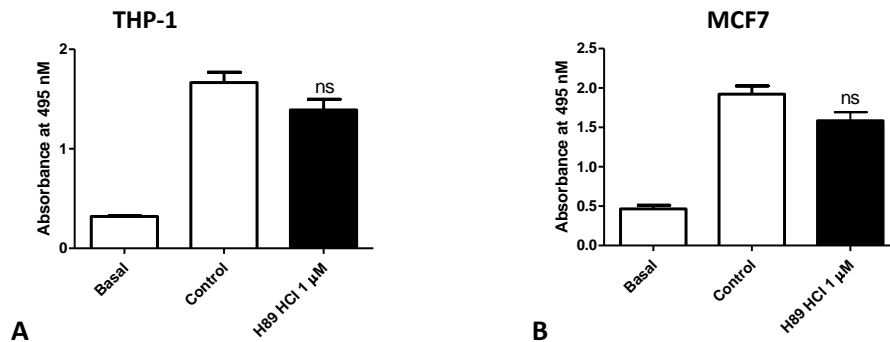
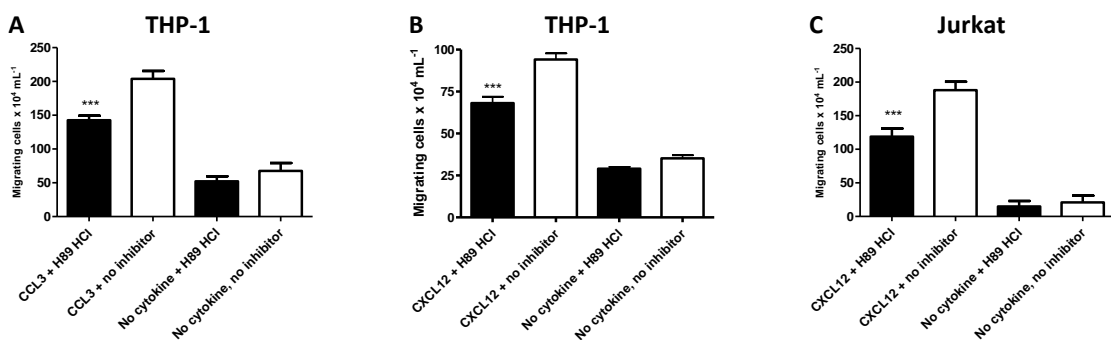


Figure 6.11: Cytotoxicity assays for H89 HCL. MTS assays were over 7 hours in (A) THP-1 and over 24 hours in (B) MCF7 cells. Basal absorbance occurs in presence of medium after MTS treatment in the absence of cells. Means  $\pm$  SEM, one-way ANOVA, post-hoc Bonferroni,  $n \geq 3$  independent experiments,  $ns = p > 0.05$ .

As Forskolin and H89 HCL did not cause toxicity their effects on chemotaxis alone and in combination in THP-1, and individually in MCF7 wound-healing were explored, figures 6.12-6.15.



Figures 6.12: Chemotaxis assays following pre-treatment with 1  $\mu$ M H89 HCL or control. (A) Chemotaxis of THP-1 to 1 nM CCL3. (B) THP-1 chemotaxis to 1 nM CXCL12. (C) Jurkat chemotaxis to 1 nM CXCL12. Means  $\pm$  SEM, one-way ANOVA, post-hoc Bonferroni,  $n \geq 3$  independent experiments, \*\*\*= $p < 0.001$ .

At 1  $\mu$ M H89 HCL significantly inhibits chemotaxis THP-1 and Jurkat, so experiments were repeated with lower concentrations of H89 HCL alone and in combination with Forskolin, figure 6.13. At 0.5



$\mu\text{M}$  H89 HCl alone did not significantly inhibit THP-1 chemotaxis and instead of opposing worked synergistically with Forskolin to potentiate inhibition of chemotaxis to CCL3 and CXCL12 in THP-1. (C) Forskolin 50  $\mu\text{M}$  very significantly inhibits Jurkat chemotaxis to CXCL12.

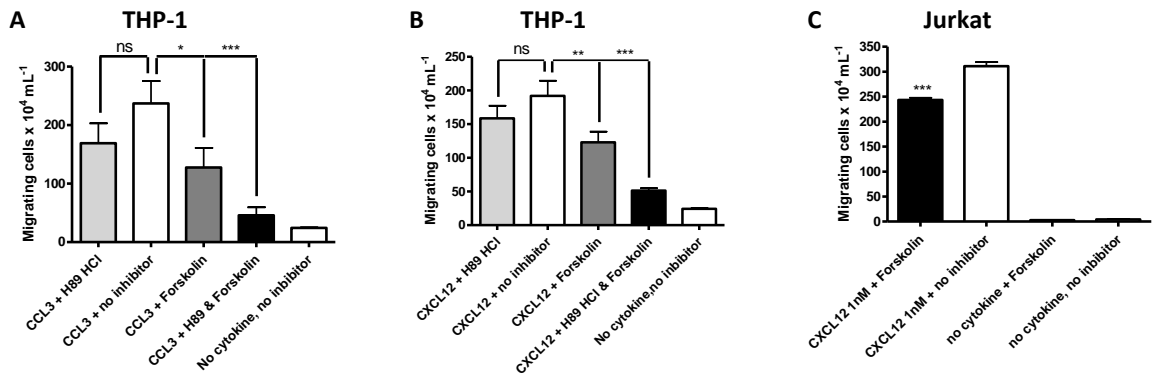


Figure 6.13: Chemotaxis assays following pre-treatment with 0.5  $\mu\text{M}$  H89 HCl and Forskolin 50  $\mu\text{M}$  alone or combined. (A) Chemotaxis of THP-1 to 1 nM CCL3. (B) THP-1 chemotaxis to 1 nM CXCL12. (C) Jurkat chemotaxis to 1 nM CXCL12. Means  $\pm$  SEM, one-way ANOVA, post-hoc Bonferroni,  $n \geq 3$  independent experiments, \*\*\*= $p < 0.001$ , \*\*= $p < 0.01$ , \*= $p < 0.05$ , ns= $p > 0.05$ .

These results show H89 HCl inhibition of chemotaxis is dose dependent, possibly due to off target effects of the inhibitor, as H89 HCl should inhibit Forskolin-induced protein phosphorylation. One possible off target effect of H89 HCl, which has an  $\text{IC}_{50}$  of 135 nM for PKA, is ROCKII ( $\text{IC}_{50} \sim 270$  nM) [606].

In MCF7 Forskolin significantly reduced wound-healing stimulated by CXCL12, whereas H89 HCl had no significant inhibitory effects. Both inhibitors have a small inhibitory effect on CCL3-stimulated chemokinesis, figures 6.14 and 6.15.

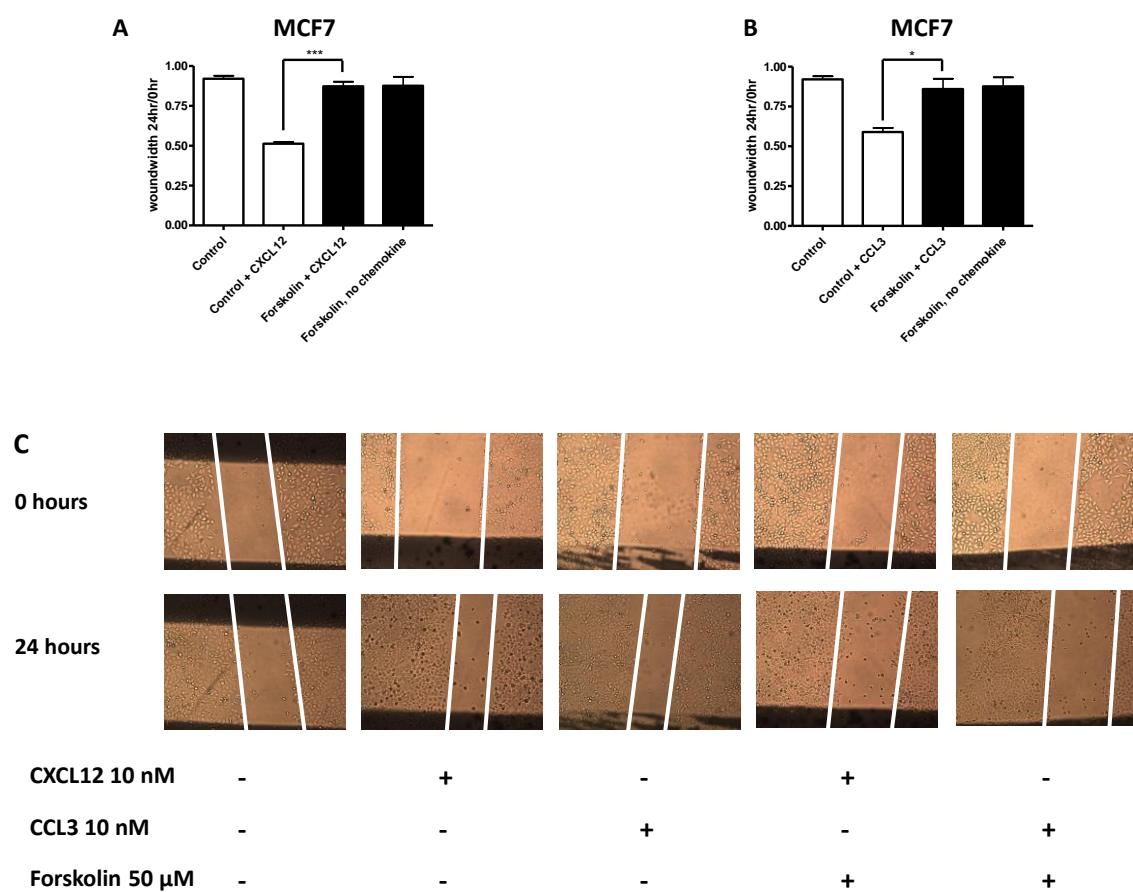


Figure 6.14: MCF7 wound-healing assays following pre-treatment with 50  $\mu$ M Forskolin or DMSO control. Analysis 24 hours after (A and C) 10 nM CXCL12, or (B and C) 10 nM CCL3. Means  $\pm$  SEM, one-way ANOVA, post-hoc Bonferroni,  $n \geq 3$ ,  $*=p < 0.05$ ,  $***=p < 0.001$ .

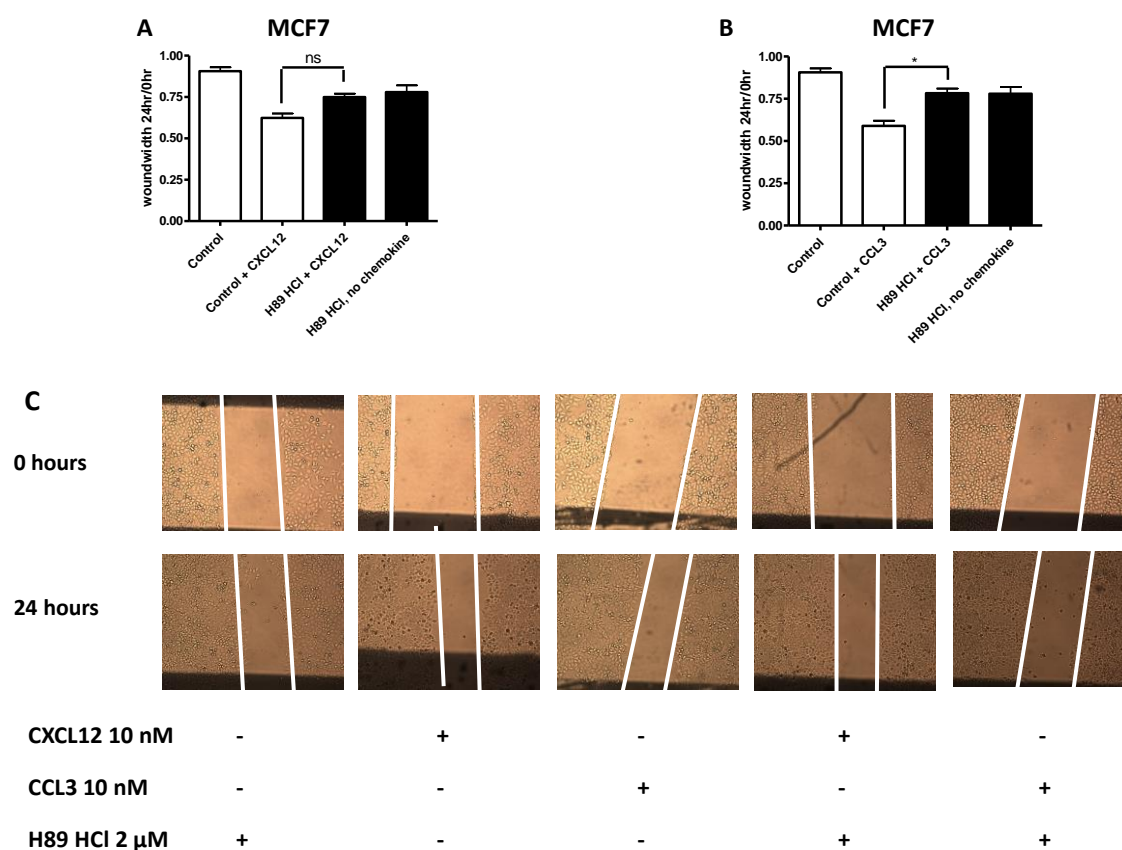
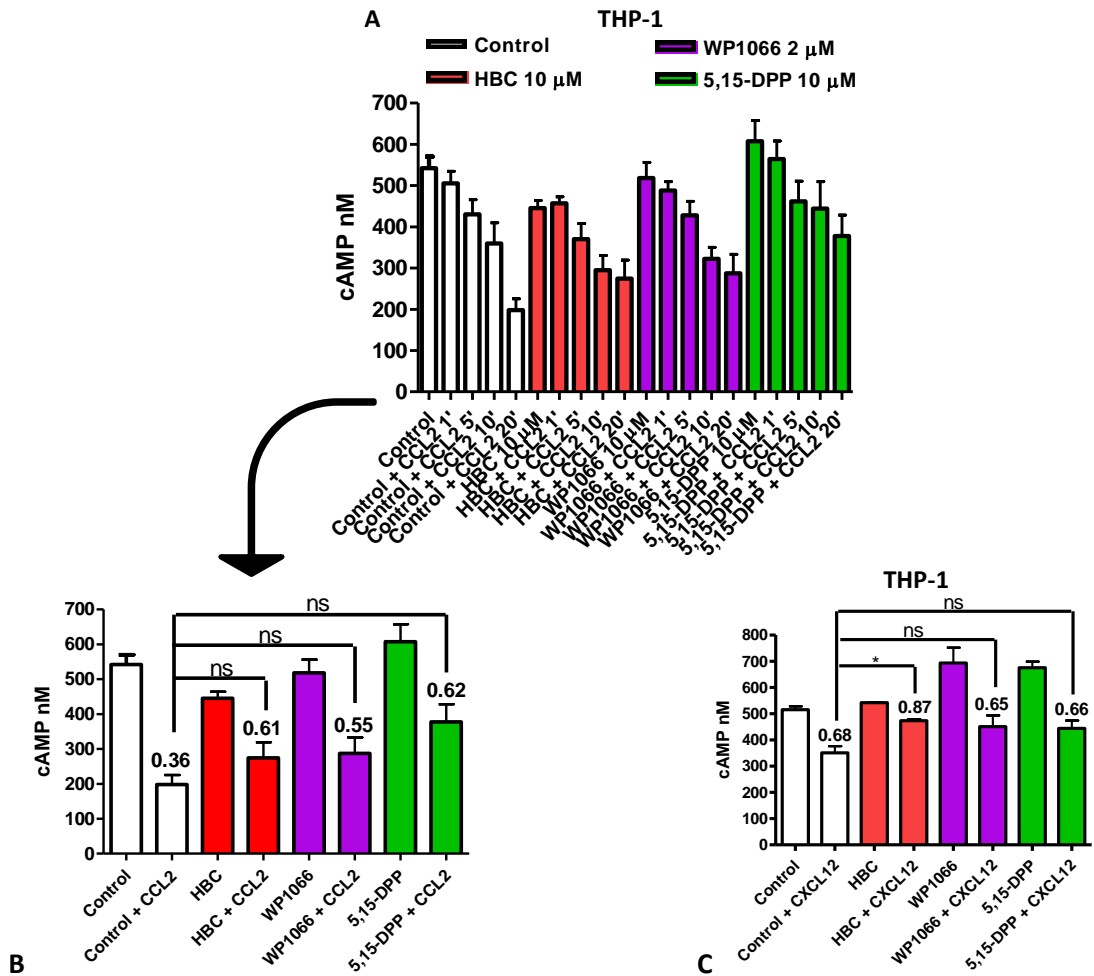


Figure 6.15: MCF7 wound-healing assays following pre-treatment with 2  $\mu$ M H89 HCl or control. Analysis 24 hours after (A and C) 10 nM CXCL12, or (B and C) 10 nM CCL3. Means  $\pm$  SEM, one-way ANOVA, post-hoc Bonferroni,  $n \geq 3$ ,  $*$ = $p < 0.05$ , ns= $p > 0.05$ .

#### 6.2.4.2: JAK2 and STAT3 inhibition did not statistically significantly increase cAMP levels

Having seen some effects on chemotaxis and chemokinesis that may be due to altered cAMP levels next the effect of JAK2 and STAT3 inhibition on cAMP production in response to CCL2 and CXCL12 was examined. THP-1 cells were treated with Jak2 inhibitor HBC, STAT3 III inhibitor WP1066 or STAT3 VIII inhibitor 5,15-DPP in presence of phosphodiesterase inhibitor IBMX (0.75mM) and Forskolin (20  $\mu$ M) with or without 10 nM CCL2 stimulation for periods varying from 1 to 20 minutes. Similarly THP-1 cells were treated with the same inhibitors, IBMX and Forskolin concentrations then CXCL12 10 nM for 20 minutes, figure 6.16.



**Figure 6.16:** cAMP production in THP-1 following 10 μM HBC, 2 μM WP1066, 10 μM 5,15-DPP or control (DMSO), (A) cAMP levels before or after 1, 5, 10 or 20 minutes CCL2 stimulation (cells pre-treated with IBMX 0.75 mM & Forskolin 20 μM). (B) 20 minute CCL2 data only, (C) cAMP levels before or after 20 minutes CXCL12 stimulation. Numbers are ratio of cAMP levels after chemokine treatment compared to levels in inhibitor treated control. Means ± SEM, one-way ANOVA, post-hoc Bonferroni, n≥3 independent experiments, \* $p < 0.05$ , ns= $p > 0.05$ .

JAK2 or STAT3 inhibition may reduce the steady fall in cAMP levels seen with controls following stimulation by CCL2, the most prominent effects were recorded 20 minutes after stimulation but this did not reach significance. However the ratios of cAMP level with inhibitor treatment compared to cAMP levels after inhibitor and 20' of CCL2 treatment illustrate that inhibition with HBC, WP1066 or 5,15 DPP all reduced the usual response to CCL2 compared to untreated control cells by nearly two fold. However with CXCL12 stimulation only JAK2 inhibitor HBC produced any significant loss in cAMP responses, figure 6.16B.

#### 6.2.4.3: cAMP levels may modulate actin filaments

Most cell signalling is governed by reversible phosphorylation often via kinases. There are hundreds of protein kinases each phosphorylating many proteins, and any individual protein

activated or inactivated by phosphorylation may be phosphorylated by several different kinases. Although H89 HCl is marketed as a selective inhibitor of PKA, H89 HCl has been shown to inhibit at least eight other kinases including ROCKII where H89 HCl was recorded as having an  $IC_{50}$  of 0.27  $\mu$ M in Sf9 cell transfects [606]. The effects of H89 HCl seen here may well therefore be off-target effects. ROCK inhibitor Y27632, also inhibited CXCL12 induced migration in THP-1 (see Chapter 5, figure 5.44). ROCK is known to be involved in leading edge dynamics [746] possibly upstream of cAMP, hence the effects on actin fibres in the presence of Forskolin, H89 HCL and Y27632 and CCL3 or CXCL12 were explored.

First the direct effect of Forskolin and H89 HCl on actin was examined using CHO.CCR5, figure 6.17.

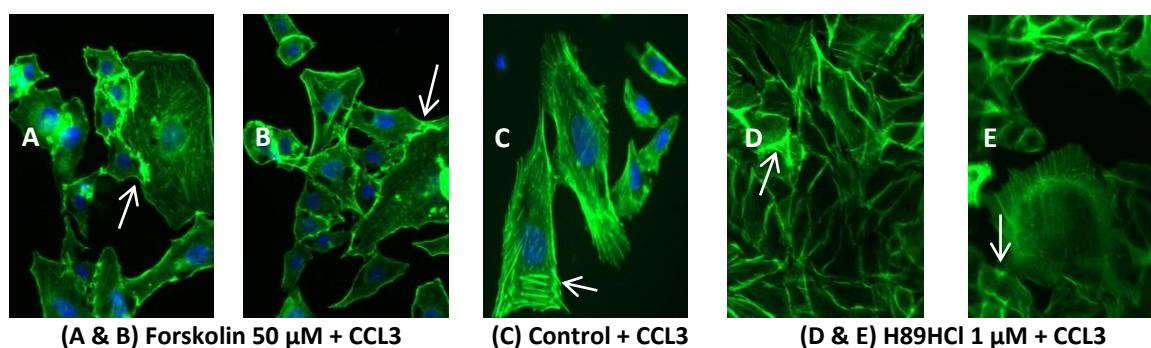


Figure 6.17: Filament actin stains. Alexa-488 Phalloidin (green) and DAPI nuclear stains (blue) of CHO.CCR5 following pre-treatment with Forskolin, DMSO control, or H89 HCl (1 hr, 37°C) followed by CCL3 5 nM (15 mins, 37°C). Imaged UV inverted microscopy (Leica DMII Fluorescence microscope 500x Ex 490 nm, Em 520 nm).

In CHO.CCR5 Forskolin produces considerable actin derangement of actin stress fibre responses to CCL3 treatment both at the cell boundary and intracellularly, H89HCl also caused actin clumping. cAMP addition itself has been observed in CHO cells to produce similar effects and loss of membrane architecture [747]. Phalloidin and DAPI stain in MCF7 pre-treated with Forskolin and H89HCl along with ROCK inhibitor Y27632 supported above findings in CHO.CCR5, figure 6.18.

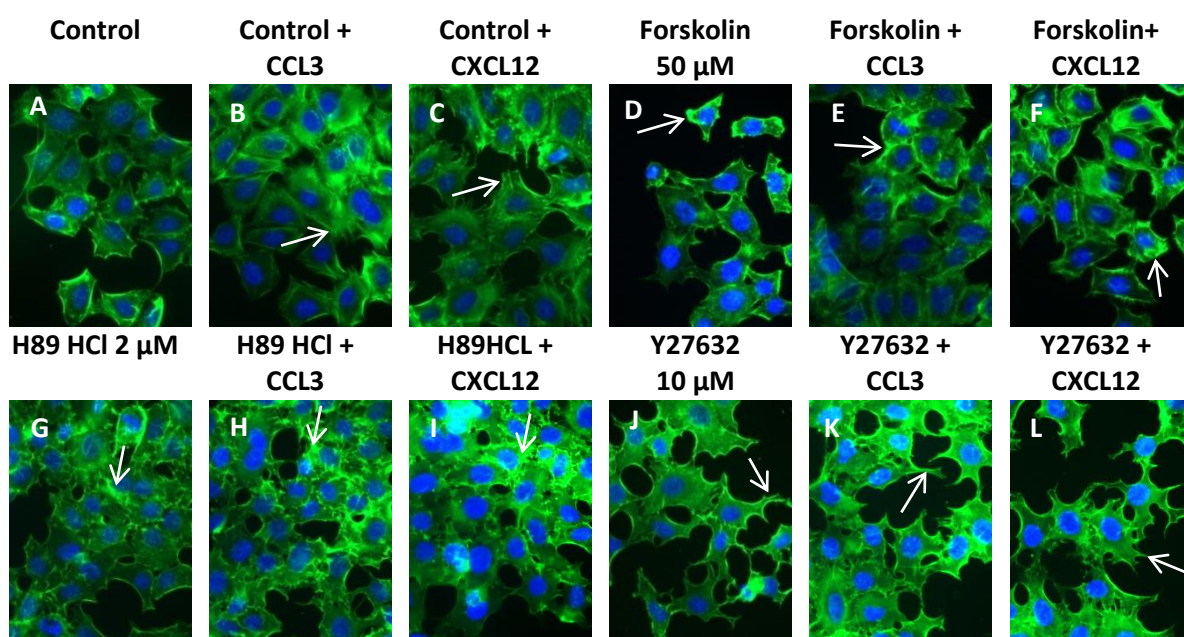


Figure 6.18: Filament actin stains. Alexa-488 Phalloidin (green) and DAPI nuclear stains (blue) of MCF7 following pre-treatment with (A-C) DMSO control, (D-F) Forskolin, (G-I) H89 HCl, or (J-L) Y27632 (1 hr, 37°C) followed by CCL3 or CXCL12 (5 nM, 15 mins, 37°C). Imaged UV inverted microscopy (Leica DMII Fluorescence microscope 500x Ex 490 nm, Em 520 nm).

The distinctive fine filaments and protrusions produced by chemokine stimulation in controls are mostly lost in the presence of Forskolin. MCF7 treated with Forskolin produced concentrated clumps of f-actin in the cytoplasm often near the cell boundary, which are modified by CCL3 or CXCL12 stimulation of cells. In H89 HCl treated MCF7 some actin bundles are apparent. ROCK inhibition with Y27632 again modifies the fine actin filament formation and as with Forskolin and H89 HCl treatment produced actin clumping but also encouraged the formation of long processes on the MCF7 in presence and absence of chemokines.

PC3 are a prostate cancer cell-line, used here to compare cytoskeletal responses to pre-treatment with Y27632, again ROCK inhibition produced elongation of cells, figure 6.19.

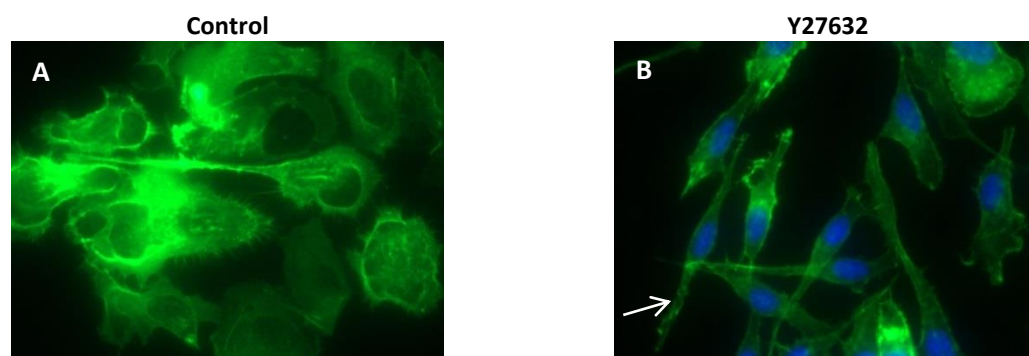


Figure 6.19: Filament actin stains. Alexa-488 Phalloidin (green) and DAPI nuclear stains (blue) of CHO.CCR5 following pre-treatment with (A) DMSO or (B) Y27632 10 μM (1 hr, 37°C). Imaged UV inverted microscopy (Leica DMII Fluorescence microscope 500x Ex 490 nm, Em 520 nm).

These results suggest the ROCK inhibitor does not destroy actin filament integrity but may modify ability of actin to branch and re-arrangement. Migration requires the maintenance of a polarized cell; chemokines may trigger Rho GTPase signalling so modulation of actin and/or microtubules in the cytoskeleton. ROCK activity elevates stress fibre Myosin-II and affects microtubule assembly dynamics [748]. Y27632 by inhibiting ROCK and thus Myosin-II produces loss of stress fibres, and actin filaments at the leading edge, causes the cell edges to appear smooth, figures 6.18J-L. ROCK inhibition upsets cell polarization in these epithelial cell-lines causing cells to develop one, figure 6.19B, or multiple processes, this may explain how Y27632 inhibits cell migration.

Forskolin and H89 HCl can be seen to disrupt the directional F-actin responses to chemokines, cAMP may be responsible. The inhibitory effects of cAMP on cell migration have also been observed in murine embryonic fibroblasts and murine breast tumour cells [749]. Overall Forskolin induced increases in cAMP were found to inhibit lamellipodia and membrane protrusion formation in MCF7, and inhibit cell migration towards CXCL12 and CCL3 in THP-1, Jurkat and MCF7, hence the effects of Forskolin on cofilin phosphorylation, a key player in leading edge dynamics was investigated next.

### 6.2.5: Forskolin increases cofilin phosphorylation

Forskolin is reported elsewhere to modulate profilin-1, which like cofilin is an actin-modulating protein, through PKA [750] and prevent agonist stimulated changes in cofilin phosphorylation [751]. Here the effects of THP-1 pre-treatment with Forskolin 50  $\mu$ M on cofilin phosphorylation in response to chemokine stimulation was examined, figure 6.20. Forskolin was found to increased cofilin phosphorylation in the presence or absence of CCL3 or CXCL12.

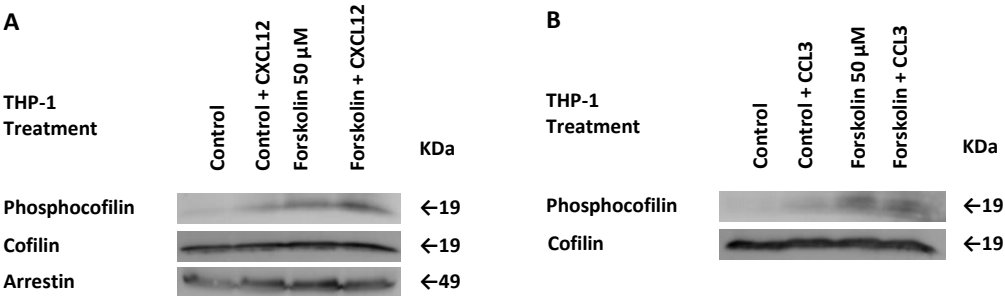


Figure 6.20: Total-cofilin and phosphocofilin (Ser3) antibodies reveals cofilin phosphorylation levels in THP-1 following pre-treatment with 50  $\mu$ M Forskolin or DMSO control (37°C, 30 mins) in presence and absence of CXCL12 or CCL3 (5 nM, 15 mins before lysis). Arrestin-2 loading control.

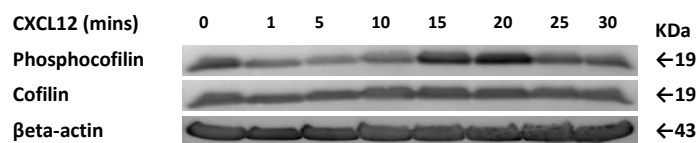


### 6.2.6: Cofilin phosphorylation in the presence of JAK2 and STAT3 VIII inhibition

The effect of JAK2 and STAT3 inhibition on cofilin phosphorylation at Ser3 in THP-1 cells was then examined using western blot. Cofilin phosphorylation in response to CXCL12 stimulation was recorded over a period of 30 minutes. In THP-1 cofilin phosphorylation was found to be modified by CXCL12 over time, this temporal response was further modified by JAK2 and STAT3 inhibition. STAT3 III inhibition eliminated the phosphorylation seen in controls whereas JAK2 II inhibition reduced phosphorylation to a brief early response, and STAT3 VIII inhibition concentrated early phosphorylation responses to 5 minutes after cell stimulation, figure 6.21.

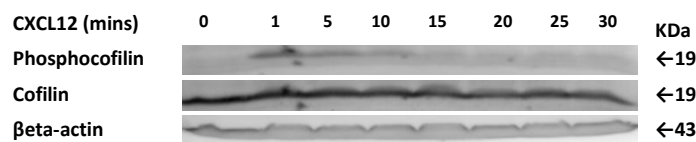
#### A Control (DMSO)

##### THP-1



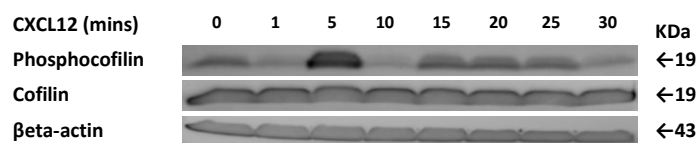
#### B HBC 10 μM (JAK2 II inhibitor)

##### THP-1



#### C DPP 10 μM (STAT3 VIII inhibitor)

##### THP-1



#### D WP1066 2 μM (STAT3 III inhibitor)

##### THP-1

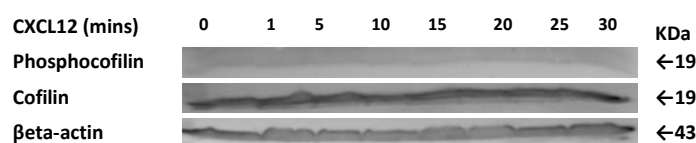


Figure 6.21: Western Blot with total-cofilin and phosphocofilin (Ser3) antibodies reveals cofilin phosphorylation levels in THP-1 following pre-treatment with (A) DMSO (control), (B) 10 μM HBC, (C) 10 μM 5,15-DPP or (D) 2 μM WP1066 (37°C, 30 mins) in presence and absence of CXCL12 (5 nM, zero to 30 mins before lysis). β-actin loading control.

#### 6.2.6.1: CXCL12 induce cofilin phosphorylation and STAT3 phosphorylation

The literature discussed above suggests there may be a relationship between the phosphorylation of STAT3 and cofilin phosphorylation, hence possible correlation was explored by comparing



cofilin and STAT3 phosphorylation in the presence and absence of JAK2 II and STAT3 VIII and STAT3 III inhibitors and CXCL12, using western blot. STAT3 phosphorylation was seen in response to CXCL12 treatment after 10 and 30 minutes in control cells and in presence of STAT3 inhibition with WP1066, this phosphorylation was completely lost in presence of 5,15-DPP, and HBC. Cofilin phosphorylation was not altered by WP1066 but was lost with HBC whereas 5,15-DPP produced cofilin phosphorylation after 10 minutes CXCL12, figure 6.22A, similar to control in figure 6.22B.

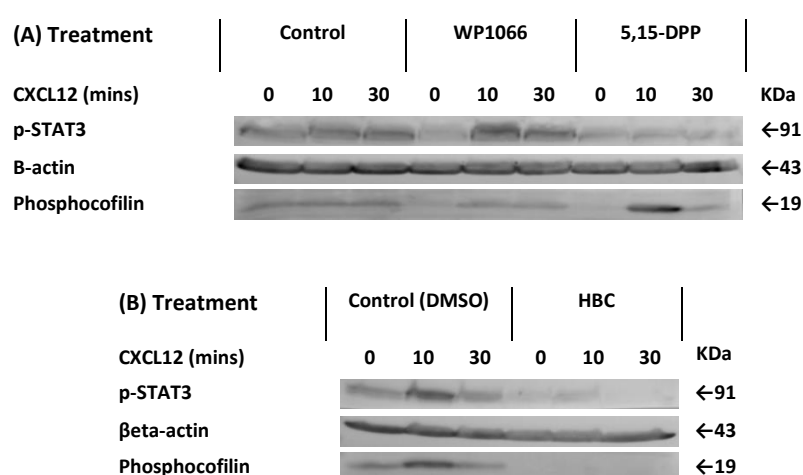


Figure 6.22: Western Blot with phospho-STAT3 (B-7) and phosphocofilin (Ser3) antibodies reveals STAT3 and cofilin phosphorylation levels in THP-1 following pre-treatment with (A) DMSO control or 2  $\mu$ M WP1066 or 10  $\mu$ M 5,15-DPP (37°C, 30 mins) in presence and absence of CXCL12 (5 nM, zero, 15 or 30 mins before lysis), (B) Control or 10  $\mu$ M HBC (37°C, 30 mins) in presence and absence of CXCL12 (5 nM, zero, 15 or 30 mins before lysis).  $\beta$ -actin loading control.

STAT3 and JAK2 phosphorylation was also examined using ELISA, figure 6.23. ELISA suggested that STAT3 phosphorylation initially rapidly decreases in THP-1 stimulated by CXCL12 and that 5,15-DPP and HBC significantly reduced basal phosphorylated STAT3 levels and non-significantly to CXCL12 responses at 10 minutes, concurring with Western blot, figure 6.22.

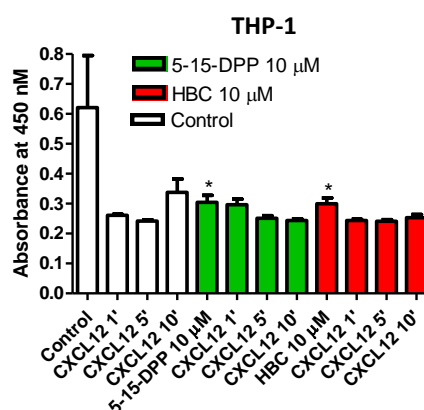


Figure 6.23: ELISA analysis of STAT3 phosphorylation. THP-1 were treated with DMSO (control), 10 μM 5,15-DPP or 10 μM HBC (37°C, 15 mins) then CXCL12 5 nM (37°C, 0, 1, 5 or 10 mins), n≥3.

### 6.3: Discussion

Research suggests that chemokine triggered receptor dimerization, precedes JAK and Gαi association and activation [752], but both JAK and Gαi activation can be prevented with JAK inhibitor AG490 [727]. JAK activation is required for Gαi association with GPCR upstream of PLC stimulated  $\text{Ca}^{2+}$  mobilization, which itself is independent of Pi3K [728]. CXCL12 binds CXCR4 triggering receptor dimerization; however JAK2 may have to be activated by autophosphorylation prior to docking with the GPCRs' dimers. This docking involves JAK2 kinase phosphorylation of receptor tyrosines, and then Gαi-independent JAK2 activation by transphosphorylation, followed by the recruitment and tyrosine phosphorylation of STATs including STAT3. Also Gαi activation of tyrosine phosphatases, including Shp1, may terminate CXCL12 stimulation of JAK/STAT signalling, but further tyrosine kinases may bind CXCR4 after JAK dissociation to extend CXCR4 signalling [323, 753]. Soriano *et al.* (2003) concluded that JAK/STAT activation was essential for CXCL12-induced G-protein activation, specifically JAK for Gαi activation and phospholipase-β (PLC-β) for calcium flux [728].

Mueller and Strange (2004) showed CCL3 triggered interaction of JAK2 with CCR5 in THP-1 cells, and using HEK.CCR5 transfects found CCR5 ligand CCL3 could transiently enhance JAK2 phosphorylation and this was unaffected by PTX inhibition of Gαi or U73122 inhibition of phospholipase C. They also demonstrated Gαi, CCR5 and JAK2 protein association in inactive receptor complexes [754]. Mellado *et al.* (1998) examined the effects of MCP-1 (CCL2) in a monocytic cell line and concluded that CCL2 causes JAK2 to phosphorylate CCR2 tyrosine<sup>139</sup> triggering JAK2/STAT3 Gαi-independent receptor association upstream of Gαi signalling [727]. Mellado then explored the relationship of JAK2 and CCR5, concluding JAK and heterotrimeric G

protein activation is JAK activation dependent [755]. Rodriguez-Frade *et al.* (1999) concluded the same sequence of events with a RANTES/CCR5 model, and suggested chemokine receptor dimerization and then internalisation were common features of JAK/STAT signalling [756].

The above research shows that JAK/STAT signalling is important for CXCL12 and CCL2 chemokinesis in MCF7 and chemotaxis in THP-1, but not in Jurkat, figures 6.5-6.7. Interestingly Khabbazi *et al.* (2013) found no effect of JAK2 or STAT3 inhibition on CCL3 induced chemotaxis in THP-1 and that only STAT3 inhibitor III not STAT3 inhibitor VIII induced cell death [757]. Further experiments with the inhibitors used by Khabbazi *et al.* (2013) in THP-1 and MCF7 cells were undertaken using CCL2 and CXCL12 to further elucidate JAK/STAT signalling complexities. Direct inhibition of STAT3 may induce cytotoxicity in a range of cancer cells suggesting these cells depend on STAT3 activation to thrive. JAK/STAT signalling is upregulated in some cancers including those of haematopoietic cells, with JAK inhibition sometimes the chosen therapeutic option [324].

### **6.3.1: JAK2, STAT3 and cofilin phosphorylation**

Cytokines may trigger reactive oxygen species (ROS) production by membrane NADPH oxidase complexes in some cell types. ROS may activate JAK/STAT pathway, Rac1 can regulate NADPH oxidase and active Rho GTPases and may be essential for STAT3 transcription activity [729-731, 758]. More recent research also demonstrates a Rac1 pathway link to STAT3. Inhibition of Rac1 using NSC23766 (an inhibitor discussed in depth in chapter 8) or JAK2 using AG490 both reportedly reduced phosphorylation of STAT3, this may be attributed to Rac1 inducing STAT3 activation through IL-6 [759]. However Rac1 downregulates Myc via PAK2 phosphorylation, Myc is a multifunctional transcription factor, responsive to mitogenic signals, that activates expression of many genes [760]. Downregulation of Myc can be inhibited by ROCK inhibition using Y27632, and downregulation of Myc increases cofilin phosphorylation, hence ROCK inhibition with Y27632 decreases cofilin phosphorylation and increases Myc. ROCK inhibition also reportedly upregulates STAT3 activity. Src and JAK2 kinases bind to and activate STAT3, this has been inhibited with JAK2 and Src inhibitors, suggesting ROCK and LIMK negatively affect STAT3 via Src and JAK2 [732]. Here JAK2 and STAT3 inhibition was shown to disrupt cofilin phosphorylation in response to CXCL12 stimulation of THP-1, figure 6.21, and have similar effects on STAT3 and cofilin phosphorylation following CXCL12 stimulation of THP-1, figure 6.22.

Cofilin orchestrates actin monomer and filament dynamics, and so cell motility, in response to chemotactic chemokines [761]. However chemotactic responses, and cofilin phosphorylation,

may be modified by metabolic environment stresses such as raised glucose or lipids. This has been shown to be the case for THP-1. In the presence of normal glucose and lipid levels the addition of CCL2 produced a gradual increase in cofilin phosphorylation, although total cofilin levels were unaffected [384]. The cofilin phosphorylation responses shown here, to CXCL12 in THP-1, similarly increase but in a wave-like temporal fashion, figure 6.21A. This phosphorylation can be disrupted by JAK2 or STAT3 inhibition supporting the hypothesis that both may be relevant to cofilin's function in THP-1 cell migration to CXCL12. In a metabolic stress environment of raised cholesterol and glucose THP-1 are reported to become sensitised to CCL2; a decrease in filament to globular actin ratio occurs, along with enhanced actin turnover, and decreased cofilin phosphorylation, producing increased migration of THP-1 towards CCL2 [384]. Although it is possible that the inhibitors used here could cause cellular stress, this seems unlikely as they decrease migration towards CCL2 not increase it, figures 6.5-6.6.

### **6.3.2: cAMP involvement with JAK2 and STAT3 signalling**

cAMP is a second messenger that can be produced in response to stimulation of receptors, including chemokine receptors, via membrane associated adenylyl cyclase's. Human cells can contain one soluble and up to nine adenylyl cyclase isoforms. These are purportedly variably expressed in different tissues and cellular compartments [739]. Adenylyl cyclase enzymatically converts ATP to pyrophosphate and 3'5' cAMP [762]. cAMP then undergoes bond hydrolysis by phosphodiesterase's to 5'AMP [763]. cAMP transfers signals from receptors to intracellular downstream effectors. cAMP is a negative regulator in immune cells through the protein kinase A (PKA) pathway. Protein phosphorylation is a fundamental regulatory mechanism in signalling and enzymes catalysing protein phosphorylation, protein kinases, are key in signal transduction, PKA is one such protein kinase. PKA is a serine/threonine kinase containing a four subunits, two catalytic and two regulatory [743, 744].

PKA has been shown to phosphorylate JAK2, this may occur via Src and Rac1, and STAT3 via Pi3K [745]. PKA inhibition itself, with H89 HCl, was shown to inhibit chemotaxis, figures 6.12-6.13, but little or no effect on chemokinesis, figure 6.15. cAMP may produce responses in four ways; (i) activation of exchange factors Epac1 and Epac2; (ii) cAMP gated ion channels; (iii) cAMP-mediated phosphodiesterase's; and (iv) via catalytic PKA activation, which affects a range of cellular processes. In some cell types the balance between RAS/RAF/MEK/ERK and cAMP signalling maintains healthy homeostasis between cell differentiation and proliferation [735, 743, 764].

Forskolin reportedly may negatively regulate JAK3 or PKA activity, PKA may directly phosphorylate and inactivate JAK3 [735]. JAK/STAT signalling can be negatively regulated by (i) suppressing cytokine signalling, (ii) protein kinase phosphatases and (iii) by protein inhibitors of activated STATs inhibiting JAK/STAT signalling directly [765]. Other signalling proteins and pathways such as MAPK, Pi3K and cAMP are also involved [766]. ATP is converted to 3'5'-cAMP and pyrophosphate by membrane enzyme adenylate cyclase [762]. Phosphodiesterases then hydrolyse the phosphodiester linkage producing 5'AMP [763]. cAMP acts through several mediators including the serine/threonine kinase PKA [744]. Forskolin and phosphodiesterase inhibitors such as IBMX increase levels of cAMP [767] and cAMP levels may affect JAK/STAT signalling [768] hence Forskolin activation of adenylate cyclase, cAMP and PKA may inhibit JAK/STAT signalling [735]. Forskolin can increase intracellular cAMP several fold above normal. This may antagonise expression of cell cycle regulatory and checkpoint genes [741, 769] so potentially inhibit cell proliferation, however this may not be applicable to cancer cell lines where cell cycle checkpoints may no longer be functional. Certainly Forskolin did not show any obvious toxicity in above assays, figure 6.10, but inhibited chemotaxis and chemokinesis, figures 6.13-6.14.

Rodriguez *et al.* (2013) concluded JAK3 could be inhibited by a Forskolin-cAMP-PKA pathway through serine residues negatively regulating JAK3 catalytic activity. Also that treatment with non-specific phosphodiesterase IBMX may trap cells in G<sub>0</sub> phase and prevent JAK3 catalysing the phosphorylation of STAT5 [735]. Calcium mobilisation purportedly activates adenylate cyclase that produces cAMP [770-772]. The results here indicate cross talk may occur between cAMP/PKA and JAK2/STAT3 signalling, suggesting that Forskolin's negative effect on CXCL12 chemotaxis may be through interfering with JAK-mediated stability of CXCR4 receptor dimerization or that PKA could phosphorylate JAK serine residues and negatively regulate its catalytic functions.

The inhibitory effects of Forskolin on chemotaxis and wound-healing, may be due to the increased cAMP levels. Others have noted in breast cancer cell line MDA-MD-231 that increasing cAMP inhibits wound-healing. Research shows this can be attributed to abrogated STAT3 and ERK1/2 activation, along with inhibition of FAK phosphorylation. FAK is a tyrosine kinase scaffolding and phosphorylating protein that acts, along with integrins, in focal adhesion complexes [773]. FAK inhibition itself was shown to inhibit CXCL12-induced cell migration (chapter 5 figure 5.37 and 5.38). FAK expression may be upregulated in malignant cells [774] such as MCF7. An invasive phenotype can be produced by Src-FAK-p130<sup>CAS</sup> complex formation. p130<sup>CAS</sup> is a docking protein regulating FAK signalling to Rac1. FAK may signal through p130<sup>CAS</sup> to Rac1, Rac1 activation inhibits Rho signalling. Inhibiting Rho kinase (ROCK) with Y27632 may allow FAK stimulation of Rac1

signalling to predominate [775]. Rho activation can cause bundling of actin filaments into stress fibres, whereas activation of Rac can cause formation of long slender filopodia and lamellipodia [776] as seen in figure 6.18.

PP2A is a serine-threonine phosphatase that may be present in malignant cells in lower levels than normal cells, present at normal levels, or present in a hyper-phosphorylated state. Hyper-phosphorylation makes PP2A inactive by preventing it forming the active phosphatase an heterotrimeric catalytic complex. PP2A in addition to catalysing cofilin dephosphorylation and activation can also act as a tumour suppressor reducing AKT and ERK phosphorylation and signalling. In addition to raising cellular cAMP levels Forskolin can dephosphorylate PP2A. If hyper-phosphorylated PP2 is dephosphorylated, it is activated [777]. PP1 and PP2 purportedly dephosphorylate cofilin. However these results indicate that at the concentrations used (50  $\mu$ M) Forskolin has effectively increased cofilin phosphorylation, suggesting that PP2A if present in THP-1 cells it is not hyper-phosphorylated and may have been inactivated by the Forskolin treatment, figures 6.20 and 6.24.

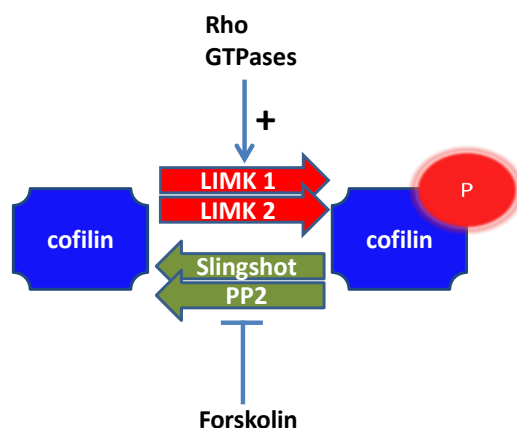


Figure 6.24: Forskolin may produce cofilin phosphorylation in THP-1 by inhibiting PP2 [777].

Overall results point to a relationship between the phosphorylation of cofilin in response to CXCL12 and JAK2/STAT3 signalling. LIMKs are modulated by Rho GTPases, they receive signalling from RhoA and RhoC and are phosphorylated and activated by ROCK producing linear actin, whereas actin branching, and lamellipodia, are mediated by Rac GTPases via p21-activated kinases (PAK). Rac1 activates LIMKs, including LIMK1 and LIMK2. LIMK can reportedly negative regulates not only cofilin but also STAT3 and Myc [732, 778]. Downstream of ROCK, LIMK and Rac1 negatively regulate Myc, Rac1 through PAK2-mediated phosphorylation and LIMK via cofilin phosphorylation [779]. Rho GTPases can mediate Myc, and Myc down-regulation negatively correlates with cofilin phosphorylation. Also cofilin knockdown with siRNA can reduce Myc expression [732]. Hence ROCK, LIMK and cofilin can reduce Myc levels, and ROCK can increase phosphorylation of cofilin via downregulation of Myc. Src and JAK2 kinases bind and activate

STAT3; STAT3 also targets Myc [780, 781]. ROCK and LIMK can decrease levels of phosphorylated (active) STAT3 by decreasing Myc, but this decrease can be dependent on Src or JAK2 [732]. Overall this suggests the phosphorylation of cofilin may relate to or correlate with STAT3 phosphorylation, figure 6.25.

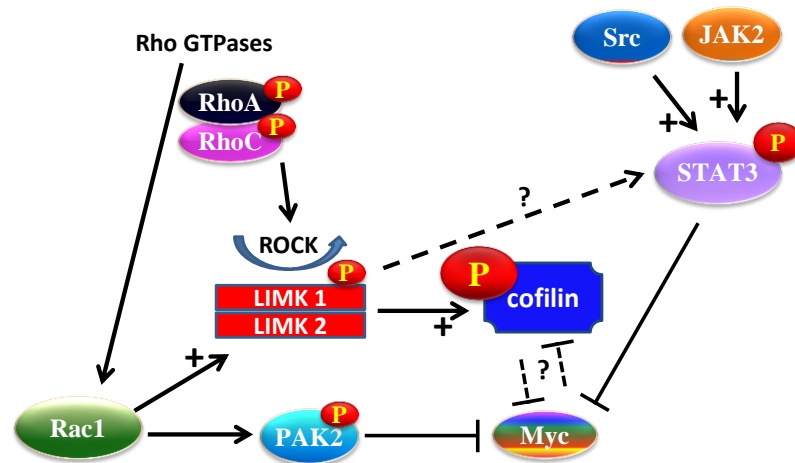


Figure 6.25: Signalling that may link STAT3, JAK2 and cofilin phosphorylation [732, 780, 781].

The involvement of JAK2 in chemokine signalling has produced diametrically opposed debate [782], and has indicated that JAK2 is not essential in CCL3-induced chemotaxis [757]. However JAK/STAT signalling may be cell type or chemokine specific. Research by others has also shown CXCL12 to induce JAK-STAT signalling, and that inhibition of JAK2 may block CXCL12-stimulated JAK2 tyrosine phosphorylation and prevent the binding of GTP to RhoA stimulated by CXCL12 [783].

The inhibitor HBC binds the kinase domain of JAK2 inhibiting tyrosine kinase auto-phosphorylation. WP1066 inhibits the STAT3 pathway but also JAK2, although WP1066 inhibition of JAK2 may be less than that achieved by the specific JAK2 II inhibitor HBC. HBC and WP1066 causes a dramatic change in cofilin phosphorylation compared to control, figure 6.21, that is not seen with the STAT3 VIII inhibitor DPP, suggesting JAK2 may directly or indirectly influence LIMK activity to stimulate cofilin phosphorylation. This may be through Rho associated protein kinase, as inhibition of ROCK using Y27632 also inhibits cofilin phosphorylation, (chapter 5, figure 5.42). Rac1 may also activate STAT3, as inhibition of Rac1 using NSC23766, (an inhibitor discussed in chapter 8) and JAK2 with AG490 both reportedly reduced phosphorylation of STAT3; IL-6 stimulating Rac1 to activate STAT3 [759]. JAK2 inhibitor HBC also eliminated STAT3 phosphorylation, figure 6.22.

CXCL12/CXCR4 signalling and JAK2 and one of its downstream targets STAT3 signalling may cross-talk in THP-1 monocytes. Others have also concluded cross-talk between JAK2 and the CXCR4/CXCL12 co-operate to increase chemotactic responses in malignant hematopoietic cells through Pi3K signalling, and that chemotaxis is reduced in JAK2 inhibition [328]. Here results in THP-1 and MCF7 cells support their findings and further demonstrate that STAT3 may be involved. Perez-Rivero *et al.* (2013) also implicated JAK2 signalling in CXCL12 chemotaxis in leukocytes (in mice) and linked this to F-actin polymerization [784]. Early work implicated JAK/STAT signalling in EMT, concluding G $\alpha$ i association with GPCR is JAK activation dependent and that phospholipase C activity is downstream of JAKs [728]. Here results further elucidate the relationships between cofilin phosphorylation and JAK2/STAT3 signalling.

#### **6.4: Conclusions**

In THP-1 JAK2 and STAT3 inhibition can modify the usual temporal cofilin phosphorylation responses to CXCL12, this appeared not due to inhibitor cytotoxicity. JAK2 and STAT3 inhibition can in a cell- and chemokine-specific manner significantly reduce chemotaxis and chemokinesis. Increasing cAMP levels appear to inhibit both CXCL12 and CCL3 chemotaxis in THP-1 and chemokinesis in MCF7. Also JAK2 may support intracellular cAMP falls in responses to CXCL12 signalling in THP-1. Overall results provide considerable evidence of JAK2 and STAT3 involvement in CXCL12 and CCL2 supported cell migration in both cell-lines.

With CCL3-induced migration in THP-1 higher concentrations of H89 HCl were required to significantly inhibit migration, at this higher concentration H89 HCl may also be inhibiting ROCK11 kinase as well as PKA. Both H89 HCl and ROCK inhibitor Y27632 were found to disrupt actin filament formation, with Y27632 especially producing elongated lamellipodia, possibly due to ROCK inhibition producing Rac over Rho signalling predominance. Forskolin also disrupted the fine actin filaments produced in response to chemokines, instead actin bundles were present. Forskolin also inhibited chemotaxis and chemokinesis, plus produced increased phosphorylation of cofilin, suggesting cAMP levels influence lamellipodia and membrane protrusion formation and so cell migration in THP-1 and MCF7.

Some tenuous correlation was observed between early STAT3 phosphorylation and cofilin phosphorylation produced in response to CXCL12 in THP-1. Both were somewhat similarly modified by JAK2 or STAT3 inhibition, further work is needed to clarify if STAT3 and cofilin



phosphorylation are related, if both involve JAK2 or STAT3, and if this phosphorylation occurs in a cell- or chemokine-specific manner.

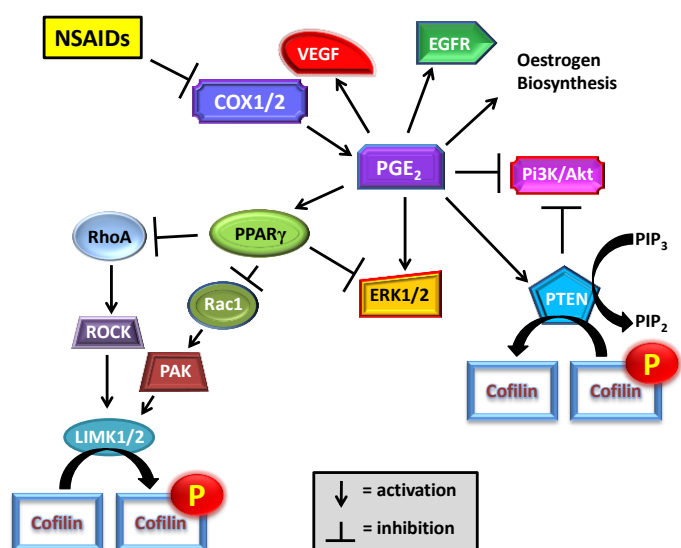
Cofilin may mediate inflammatory factors through the JAK/STAT pathway [785] thus posing the question do anti-inflammatories such as COX inhibitors mediate cofilin phosphorylation, or indeed CXCL12 or CCL3 chemotaxis, answering these questions was the challenge addressed in chapter 7.

## Chapter 7: Direct and indirect effects of NSAIDs in chemotactic metastasis

### 7.1: Introduction

The NSAIDs Ibuprofen, Naproxen and Celecoxib along with Paracetamol and Aspirin, are widely prescribed analgesics. NSAIDs inhibit cyclooxygenase enzymes COX1 or COX2 that catalyse the production of prostaglandins, including prostaglandin E<sub>2</sub> (PGE<sub>2</sub>) [414]. Aspirin, Ibuprofen and Naproxen inhibit both COX enzymes whereas Paracetamol has diverse modes of action including COX2 inhibition [419-421]. Celecoxib is a specific COX2 inhibitor; the inflammation that accompanies cancer can induce COX2 activity [411]. PGE<sub>2</sub> can suppress leucocyte activity causing immunosuppression [438]. PGE<sub>2</sub> may stimulate cancer initiation, proliferation survival and metastatic spread [439]. NSAID therapy may reduce cancer incidence for example by inhibiting progression of dysplasia to cancer [786], which some chemokines support [787]. COX2-produced PGE<sub>2</sub> expressed by tumours can inhibit apoptosis, promote proliferation and support metastasis [453, 464, 465]. NSAIDs' off-target effects can also be therapeutic in malignancy. Celecoxib can cause cell cycle arrest [478] and activate apoptosis [480, 481]. NSAIDs can also modulate calcium ATPases and Ca<sup>2+</sup> dynamics so favourably inhibiting EGFR, Pi3K-Akt and Raf-MEK-ERK signalling often corrupted in cancer [467-469, 487, 788-790]. Chapters 4 and 5 of this thesis show that CXCL12- and CCL3-induced chemotaxis also involves Pi3K-Akt and Raf-MEK-ERK signalling. This suggested NSAIDs may affect chemotaxis and even cofilin phosphorylation. This chapter reports investigations into the effects of various NSAIDs and Paracetamol on CCL3 and CXCL12-induced cell migration in THP-1, Jurkat and MCF7, and some preliminary work on NSAID mediation of cofilin phosphorylation in THP-1, figure 7.1.

Figure 7.1: How NSAIDs interact with signalling pathways influencing cofilin phosphorylation [409, 458, 791-794].



**Hypothesis:** NSAIDs can inhibit anti-apoptotic and proliferative signalling through Pi3K/Akt, EGFR and Raf/MEK/ERK pathways, and may inhibit LIMK phosphorylation of cofilin and metastasis.

**Aim:** To investigate if NSAIDs affect CCL3 or CXCL12-stimulated THP-1 or Jurkat chemotaxis or MCF7 chemokinesis, and if effects can be related to cellular levels of cAMP or phosphorylated cofilin.

**Objectives:**

- (i) Select a range of NSAIDs and check for cytotoxicity
- (ii) Examine NSAIDs for effects on CXCL12-chemotaxis in THP-1 and Jurkat and CCL3-chemotaxis in THP-1
- (iii) Investigate if NSAIDs mediate CCL3 or CXCL12-supported chemokinesis in MCF7
- (iv) Use Phalloidin stains to probe NSAIDs effects on actin filaments
- (v) Explore the effects of NSAIDs on cellular cAMP levels following chemokine stimulation
- (vi) Observe if NSAIDs effect cofilin phosphorylation following CCL3 or CXCL12 stimulation

## **7.2: Results**

Here the effects of Ibuprofen, Naproxen and Celecoxib along Paracetamol and Aspirin on chemokine induced migration, cAMP release and calcium responses was explored in THP-1 and/or Jurkat and cofilin phosphorylation in THP-1. Concentrations of the drugs used are those reached by therapeutic doses [795, 796].

Please note controls are common between graphs where experiments were conducted simultaneously; results for each inhibitor have been displayed separately for ease of description of results, this applies to: figures 7.7B and 6.17C; 7.6B and C; 7.10B and C; 7.11A and 5.27A; 7.12B and C; 7.18C and 4.11A; 7.21A and 6.16A.

### **7.2.1: Aspirin and Naproxen**

Aspirin, which has been attributed with cancer preventative properties [797], very significantly inhibited chemotaxis to CXCL12 in THP-1 ( $p < 0.001$ ), and to a lesser extent in Jurkat ( $p < 0.05$ ). Whereas Aspirin had no significant effect on CCL3-induced chemotaxis in THP-1, figures 7.2.

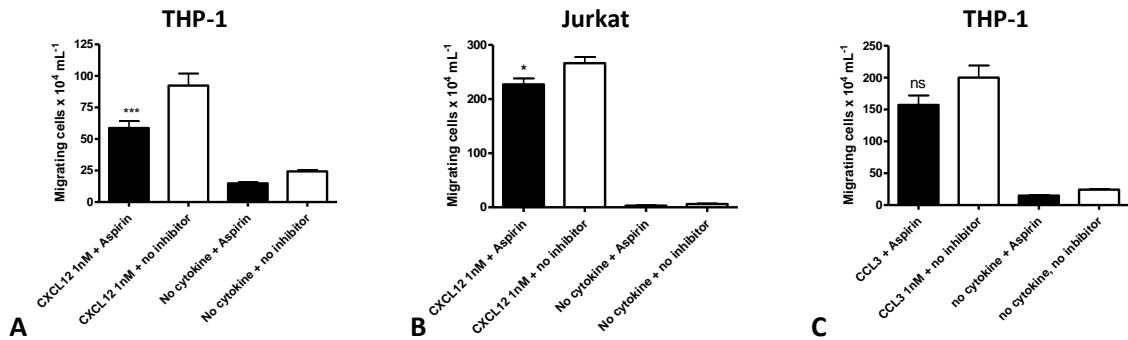


Figure 7.2: Chemotaxis assays following pre-treatment with Aspirin 555  $\mu\text{M}$  or control. (A) Chemotaxis of THP-1 to 1 nM CXCL12. (B) Jurkat chemotaxis to 1 nM CXCL12. (C) THP-1 chemotaxis to 1 nM CCL3. Means  $\pm$  SEM, one-way ANOVA, post-hoc Bonferroni,  $n \geq 3$  independent experiments, \*\*\*= $p < 0.001$ , \*= $p < 0.05$ , ns= $p > 0.05$ .

This effect on migration could not be explained by toxicity, as MTS assays showed aspirin at 555  $\mu\text{M}$  and even up to 1.11 mM did not inhibit cell metabolism in either cell line, figure 7.3.

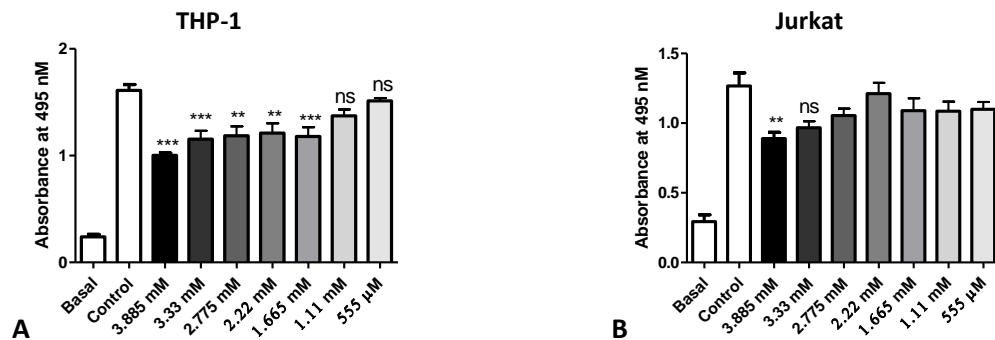


Figure 7.3: Cytotoxicity assays for Aspirin. MTS assays were over 7 hours in (A) THP-1 and (B) Jurkat. Basal absorbance occurs in presence of medium after MTS treatment in the absence of cells. Means  $\pm$  SEM, one-way ANOVA, post-hoc Bonferroni,  $n \geq 3$  independent experiments, \*\*\*= $p < 0.001$ , \*\*= $p < 0.01$ , ns= $p > 0.05$ .

The effects of Naproxen were then examined on chemokine-induced chemotaxis in THP-1 and Jurkat cells and on wound-healing in MCF7 cells after first checking the drug for toxicity using MTS assays, figures 7.4-7.6.

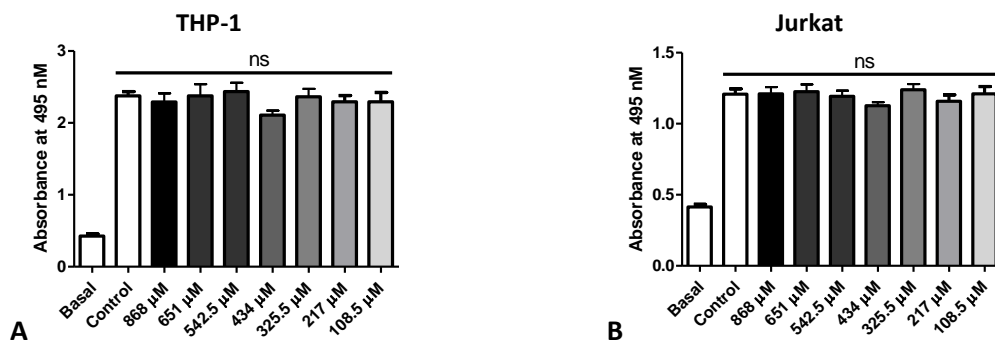


Figure 7.4: Cytotoxicity assays for Naproxen. MTS assays were over 7 hours in (A) THP-1 and (B) Jurkat. Basal absorbance occurs in presence of medium after MTS treatment in the absence of cells. Means  $\pm$  SEM, one-way ANOVA, post-hoc Bonferroni,  $n \geq 3$  independent experiments, \*\*\*= $p < 0.001$ , \*\*= $p < 0.01$ , ns= $p > 0.05$ .

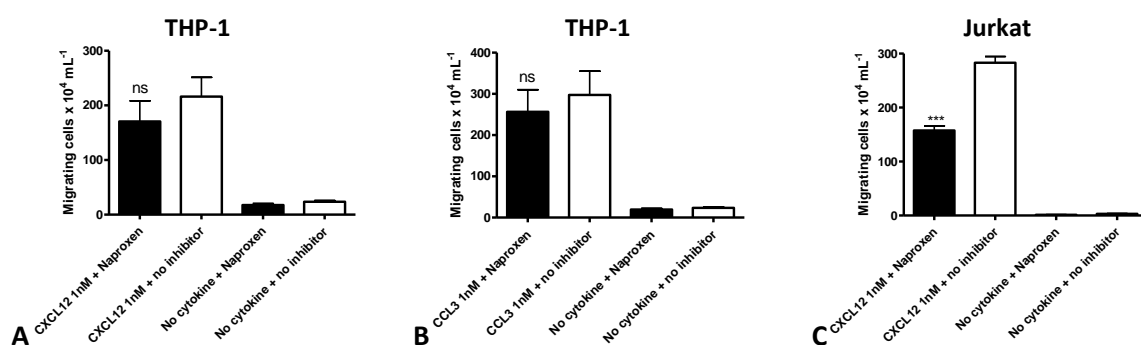


Figure 7.5: Chemotaxis assays following pre-treatment with Naproxen 217  $\mu\text{M}$  or control. (A) Chemotaxis of THP-1 to 1 nM CXCL12. (B) THP-1 chemotaxis to 1 nM CCL3. (C) Jurkat chemotaxis to 1 nM CXCL12. Means  $\pm$  SEM, one-way ANOVA, post-hoc Bonferroni,  $n \geq 3$  independent experiments, \*\*\*= $p < 0.001$ , ns= $p > 0.05$ .

MTS assays confirmed Naproxen treatment had no toxic effects on cell metabolism in THP-1, Jurkat or MCF7. However Naproxen at 217  $\mu\text{M}$  significantly inhibited Jurkat chemotaxis to CXCL12, figure 7.5, and MCF7 wound-healing induced by both CCL3 and CXCL12, figure 7.6.

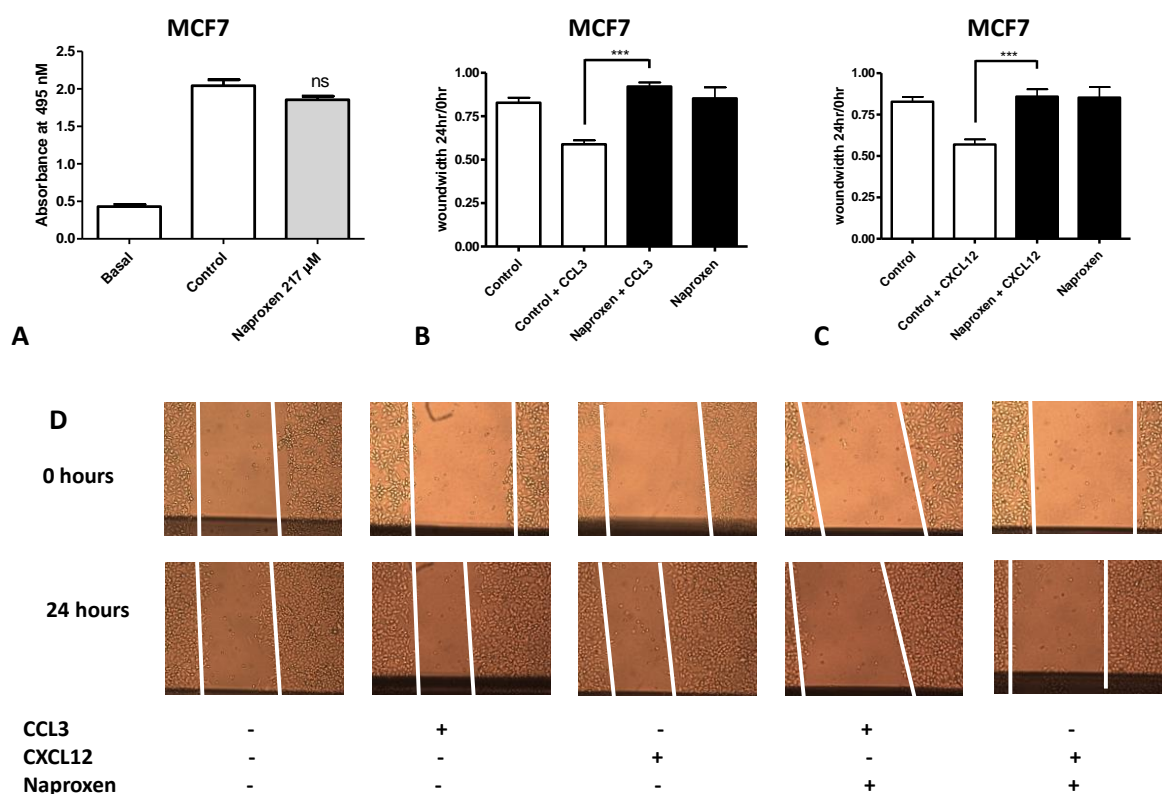


Figure 7.6: (A) Cytotoxicity assay for Naproxen 217  $\mu\text{M}$  over 24 hours in MCF7. Basal absorbance occurs in presence of medium after MTS treatment in the absence of cells. (B) MCF7 wound-healing assays following transfection with Naproxen 217  $\mu\text{M}$  or control, analysis 24 hours after 10 nM CCL3, or (C) 10 nM CXCL12. Means  $\pm$  SEM, one-way ANOVA, post-hoc Bonferroni,  $n \geq 3$  independent experiments, \*\*\*= $p < 0.001$ , ns= $p > 0.05$ .

The effects of Aspirin and Naproxen on actin fibres in CHO.CCR5 cells was also examined. Aspirin appeared to concentrate the F-actin fibres in the cells' periphery and cause some distortion of cell morphology compared to control. Whereas Naproxen caused some loss of clearly defined F-actin filaments, reduced cell size and produced cell rounding, figure 7.7.

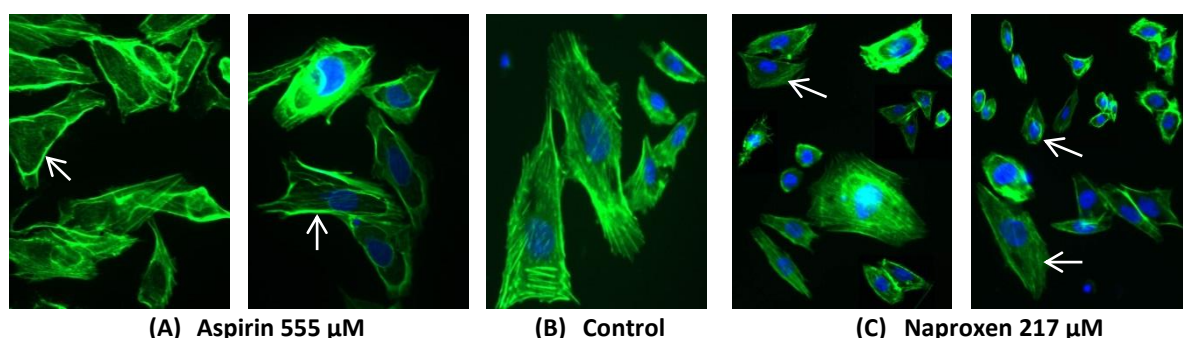


Figure 7.7: Filament actin stain. Alexa-488 Phalloidin (green) and DAPI nuclear stains (blue) of CHO.CCR5 following pre-treatment with (A) Aspirin 555 µM, (B) Control and (C) Naproxen 217 µM (1 hr, 37°C). Imaged UV inverted microscopy (Leica DMII Fluorescence microscope 500x Ex 490 nm, Em 520 nm).

### 7.2.2: Ibuprofen

MTS assay showed ibuprofen very significantly inhibited cell metabolism of both Jurkat ( $IC_{50}$  = 1.16 mM), and THP-1 ( $IC_{50}$  = 690 µM), although at the experimental concentration used (290 µM) no evidence of toxicity was apparent over 7 hours in THP-1 or Jurkat, figures 7.8.

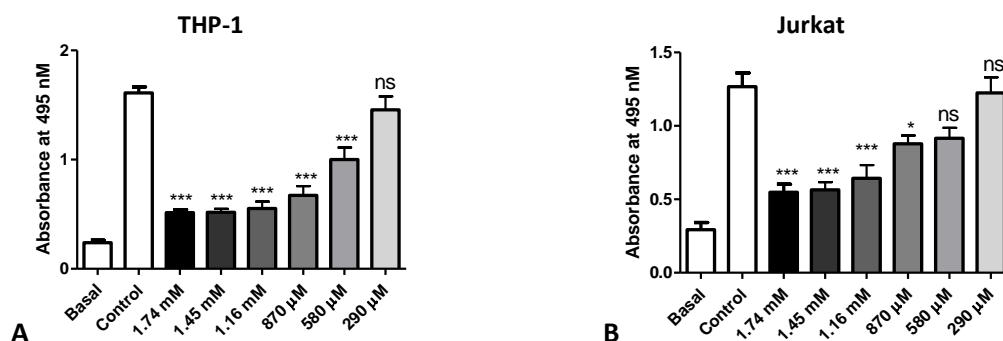


Figure 7.8: Cytotoxicity assays for Ibuprofen. MTS assays were over 7 hours in (A) THP-1 and (B) Jurkat. Basal absorbance occurs in presence of medium after MTS treatment in the absence of cells. Means  $\pm$  SEM, one-way ANOVA, post-hoc Bonferroni,  $n \geq 3$  independent experiments, \*\*\*= $p < 0.001$ , \*= $p < 0.05$ , ns= $p > 0.05$ .

Others have examined the  $IC_{50}$  of ibuprofen by other methods, for example Akrami *et al.* (2015), using an adenocarcinoma gastric cell line, found an  $IC_{50}$  of 630 µM by trypan blue staining and 456 µM by neutral red uptake assays over 24 hours; these values fell to 549 µM and 408 µM respectively over 48 hours [798]. Ibuprofen is a racemic mix, *in vivo* the R-enantiomer is extensively converted to the S-enantiomer which is more pharmacologically active [799]. It is not clear if this conversion occurs in THP-1, Jurkat or MCF7 *in vitro*. However both enantiomers are

reported to COX2-independently down-regulate cyclin A and B and cause a G0/G1 phase block [800].

Ibuprofen's reported therapeutic benefits in cancer may partly relate to its inhibition of cell migration [801], and so the effects of Ibuprofen on chemotaxis in Jurkat and THP-1 and wound-healing in MCF7 were explored, figures 7.9.

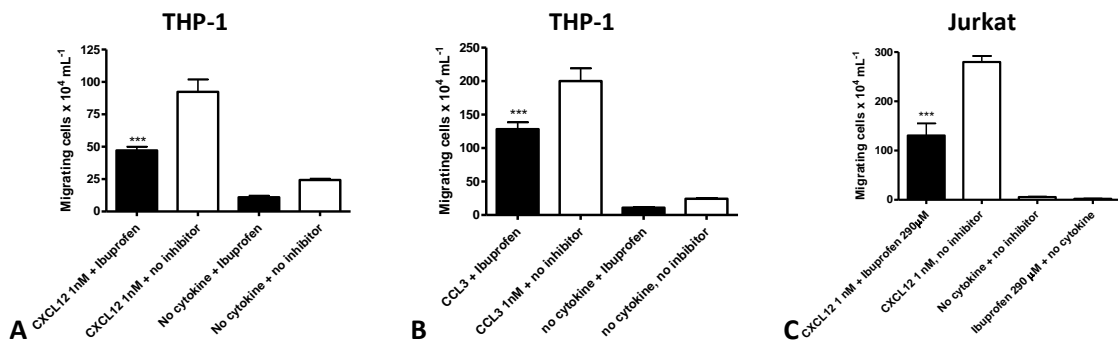


Figure 7.9: Chemotaxis assays following pre-treatment with Ibuprofen 290 µM or control (DMSO). (A) Chemotaxis of THP-1 to 1 nM CXCL12. (B) THP-1 chemotaxis to 1 nM CCL3. (C) Jurkat chemotaxis to 1 nM CXCL12. Means ± SEM, one-way ANOVA, post-hoc Bonferroni, n≥3 independent experiments, \*\*\*=p<0.001.

Monocytes are reported to express EP receptors, mainly EP2 and EP4, these may modulate monocyte responses via CCR5 to CCL3 and via CXCR4 to CXCL12 respectively as EP2 and EP4 agonists are reported to increase chemotaxis to CCL3 and CXCL12 [802]; this may be why NSAIDs inhibit chemotaxis to these two chemokines in monocyte cell-line THP-1.

Ibuprofen may exert its anti-tumour effects through inhibiting cell apoptosis or proliferation. Assays in MCF7 undertaken in the absence of serum to prevent proliferation demonstrated significant inhibition of migration-induced wound-healing produced by CXCL12 and CCL3 in cells exposed to ibuprofen 290 µM. MTS assays in MCF7 over 26 hours at 290 µM did show significant inhibition of cell metabolism, although wound-healing imaging revealed no evidence of cell death, figure 7.10.

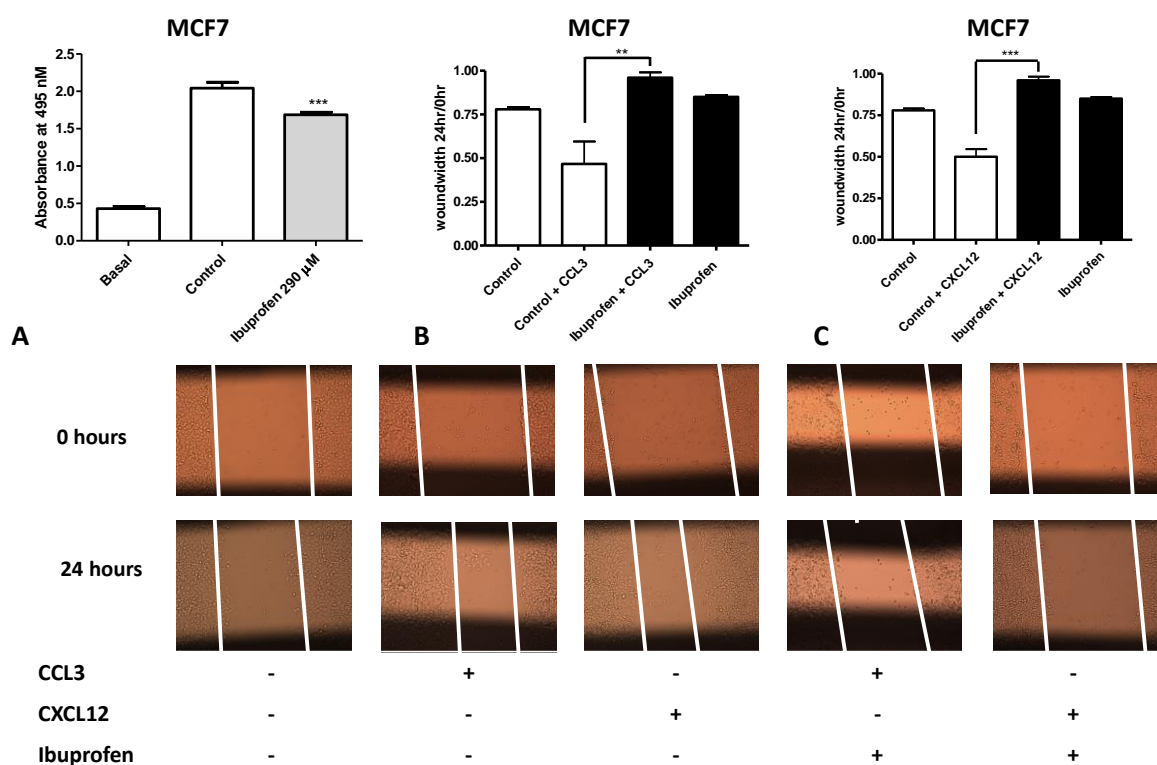


Figure 7.10: (A) Cytotoxicity assay for Ibuprofen 290  $\mu$ M over 24 hours in MCF7. Basal absorbance occurs in presence of medium after MTS treatment in the absence of cells. (B) MCF7 wound-healing assays following transfection with Ibuprofen 290  $\mu$ M or DMSO control, analysis 24 hours after 10 nM CCL3, or (C) 10 nM CXCL12. Means  $\pm$  SEM, one-way ANOVA, post-hoc Bonferroni,  $n \geq 3$  independent experiments, \*\*\*= $p < 0.001$ , ns= $p > 0.05$ .

Chemotaxis employs actin dynamics, pre-treatment of monocytes with PGE<sub>2</sub> is reported to aid conversion of globulin to filamentous actin when cells were stimulated with CCL3 or CXCL12 [802]. Here pre-treatment of CHO.CCR5 cells with ibuprofen caused loss of stress fibres, and actin fibre distortion in the presence of CCL3, figure 7.11.

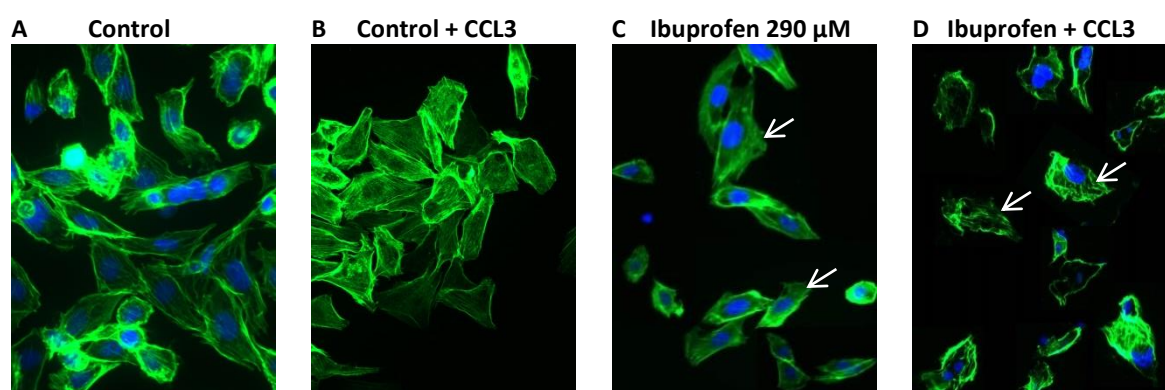


Figure 7.11: Filament actin stain. Alexa-488 Phalloidin (green) and DAPI nuclear stains (blue) of CHO.CCR5 following pre-treatment with (A) DMSO control (1 hr, 37°C) (B) Control then CCL3 (10 nM, 15 mins 37°C) (C) 290  $\mu$ M Ibuprofen (1 hr, 37°C) (D) 290  $\mu$ M Ibuprofen then then CCL3 (10 nM, 15 mins 37°C). Imaged UV inverted microscopy (Leica DMII Fluorescence microscope 500x Ex 490 nm, Em 520 nm).



Ibuprofen, Naproxen and Aspirin all reportedly inhibit both COX1 and COX2 enzymes, so next celecoxib a specific COX2 inhibitor's ability to influence chemotaxis and chemokinesis were investigated [414].

### **7.2.3: Celecoxib**

Celecoxib is a commonly prescribed COX2 inhibitor which has many on- and off-target cellular effects. Celecoxib can modulate the expression of many genes involved in cell metabolism, proliferation, energetics, and apoptosis [803]. Celecoxib at low concentrations (10  $\mu\text{M}$ ) is reported to work synergistically with calcitrol (vitamin D) to inhibit proliferation of MCF7 *in vitro*, both drugs were thought to be targeting COX2 [804]. Celecoxib is also reported to inhibit 3-phosphoinositide-dependent kinase 1 (PDK-1), one of the proteins that phosphorylate Akt [805]. Celecoxib but not Rofecoxib, another COX2 inhibitor, can at nanomolar concentrations, cause inhibition of some carbonic anhydrase isoforms [806]. Carbonic anhydrases support pH and  $\text{CO}_2$  homeostasis by catalysing the conversion of  $\text{CO}_2$  to the bicarbonate ion and hence mediate transport of  $\text{CO}_2/\text{HCO}_3^-$  between lungs and metabolising/respiring tissues. Many cellular processes are influenced including bone reabsorption and calcification, gluconeogenesis, lipogenesis and tumourigenicity [807]. Certain carbonic anhydrases such as tumour-associated isoform hCA 1X are implicated in cancer cell development and invasion [808].

MTS assays indicated Celecoxib at 50  $\mu\text{M}$  very significantly inhibits MCF7 cell proliferation, this cytotoxicity could explain the inhibition of wound-healing induced by CCL3 or CXCL12 in MCF7, figure 7.12.

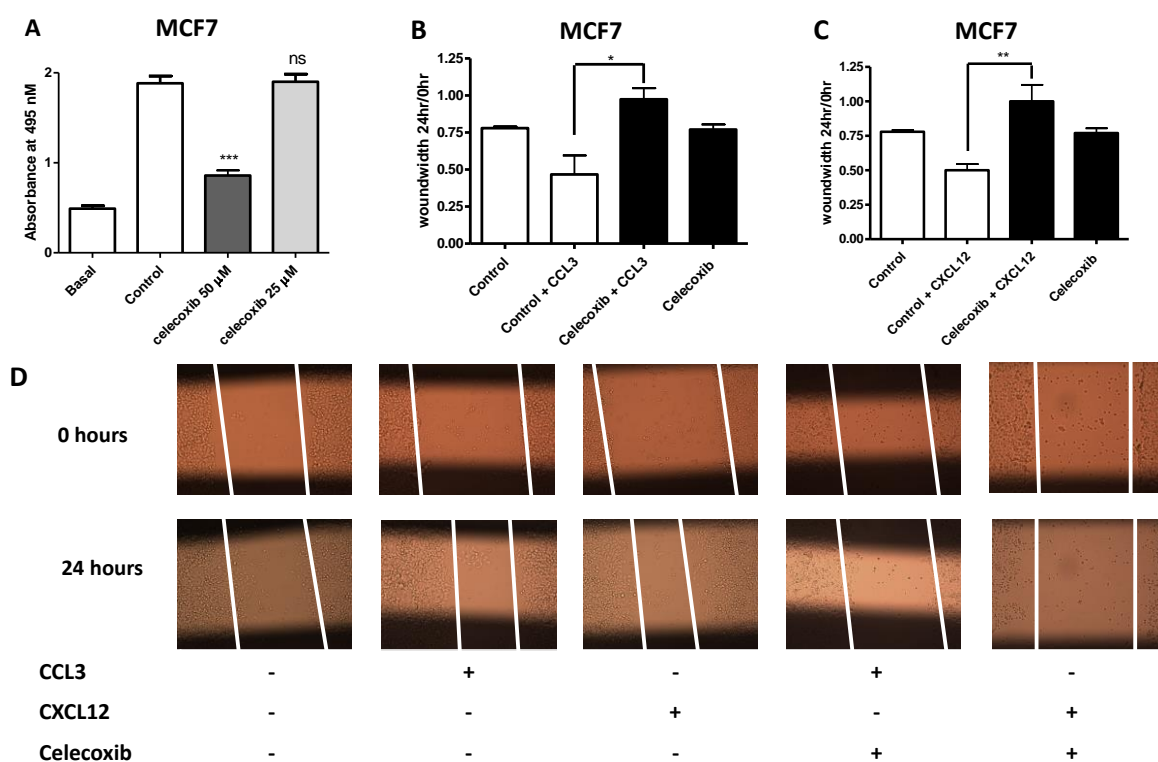


Figure 7.12: (A) Cytotoxicity assays for Celecoxib. MTS assays were over 24 hours in MCF7 cells. Basal absorbance occurs in presence of medium after MTS treatment in the absence of cells. (B) MCF7 wound-healing assays following 50  $\mu$ M Celecoxib or DMSO control. Analysis 24 hours after 10 nM CCL3, or (C) 10 nM CXCL12, (D) wound-healing images. Means  $\pm$  SEM, one-way ANOVA, post-hoc Bonferroni,  $n \geq 3$  independent experiments, \*\*\*= $p < 0.001$ , \*\*= $p < 0.01$ , \*= $p < 0.05$ , ns= $p > 0.05$ .

MTS assays allowed calculation of Celecoxib's  $IC_{50}$  in THP-1 (54  $\mu$ M) and Jurkat (48  $\mu$ M), figure 7.13, yet even at 50  $\mu$ M celecoxib did not inhibit chemotaxis of THP-1 to CXCL12 or CCL3 or Jurkat to CXCL12, figure 7.14.

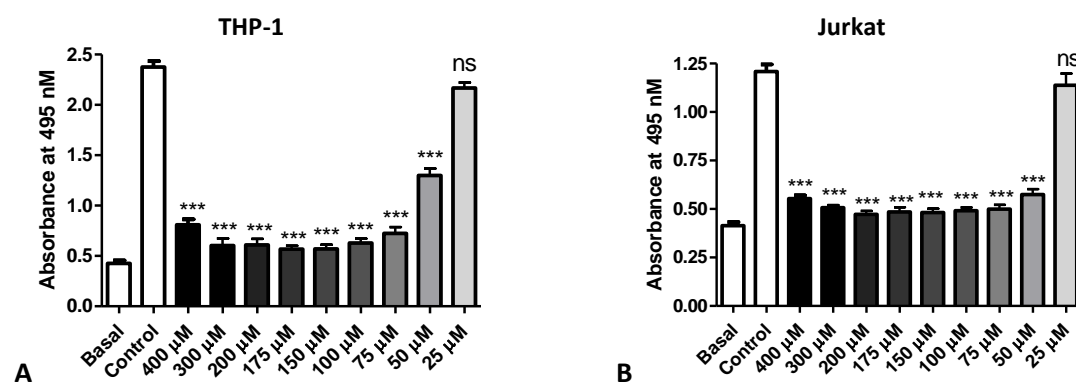


Figure 7.13: Cytotoxicity assays for Celecoxib. MTS assays were over 7 hours in (A) THP-1 and (B) Jurkat. Basal absorbance occurs in presence of medium after MTS treatment in the absence of cells. Means  $\pm$  SEM, one-way ANOVA, post-hoc Bonferroni,  $n \geq 3$  independent experiments, \*\*\*= $p < 0.001$ , ns= $p > 0.05$ .

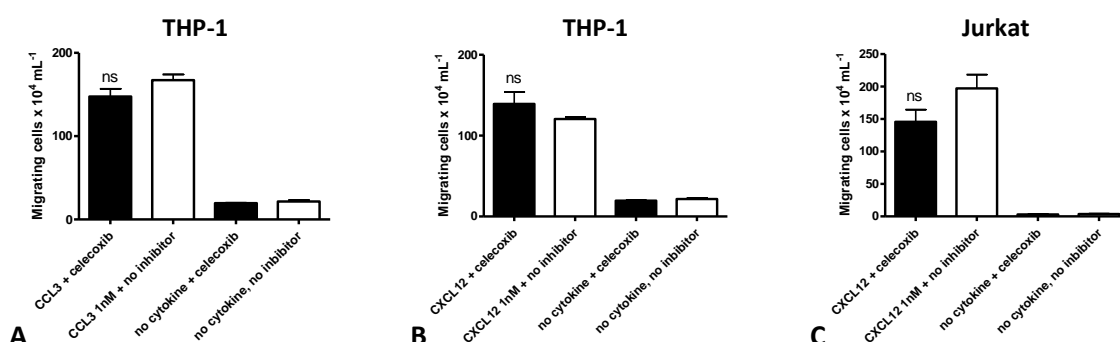


Figure 7.14: Chemotaxis assays following pre-treatment with Celecoxib 50  $\mu\text{M}$  or control (DMSO). (A) Chemotaxis of THP-1 to 1 nM CCL3. (B) THP-1 chemotaxis to 1 nM CXCL12. (C) Jurkat chemotaxis to 1 nM CXCL12. Means  $\pm$  SEM, one-way ANOVA, post-hoc Bonferroni,  $n \geq 3$  independent experiments, \*\*\*= $p < 0.001$ , \*\*= $p < 0.01$ , \*= $p < 0.05$ , ns= $p > 0.05$ .

The effect of Celecoxib on actin fibres was examined in CHO.CCR5 and MCF7 cells. 30 minutes pre-treatment with Celecoxib followed by Phalloidin stain revealed cell shrinkage and lack of actin filament definition in both cell types, total disorganisation of f-actin formation after CCL3 (10 nM) treatment was more easily seen in CHO.CCR5, figure 7.15.

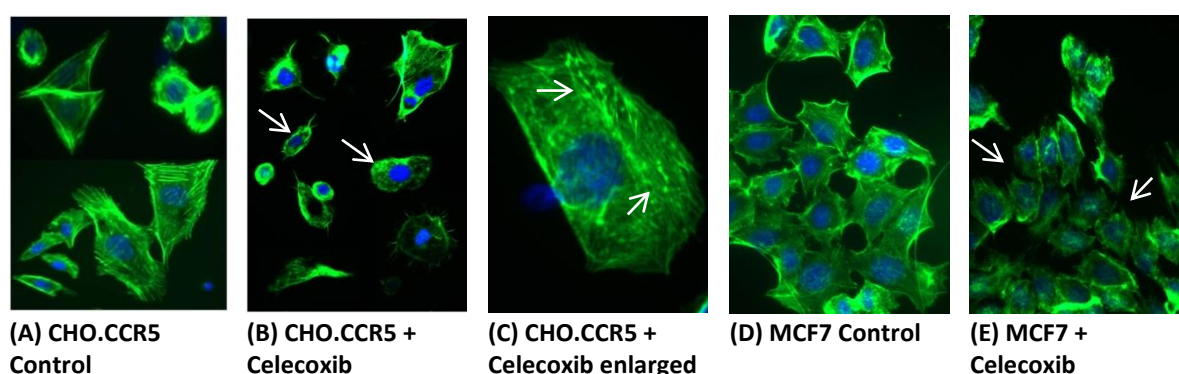


Figure 7.15: Filament actin stain following Celecoxib. Alexa-488 Phalloidin (green) and DAPI nuclear stains (blue) of (A-C) CHO.CCR5 or (D-E) MCF7 following pre-treatment with 50  $\mu\text{M}$  Celecoxib or control (DMSO) (30 mins, 37°C). Imaged UV inverted microscopy (Leica DMII Fluorescence microscope 500x Ex 490 nm, Em 520 nm).

One of the most commonly used analgesics in the UK is paracetamol [809]. Paracetamol inhibits COX2 more than COX1, and may reduce COX2 activity by 80% in monocytes [422, 423] so its effects on chemotaxis in THP-1 and Jurkat were explored.

#### 7.2.4: Paracetamol

Paracetamol is reported to have increased apoptosis, possibly through both the death receptor and mitochondrial pathways, and decreased caspase 9 expression in two colon-cancer cell lines [810]. However in Jurkat, THP-1 and MCF7 cell lines MTS assays indicated no significant effect on

cell metabolism, although at concentrations well above safe therapeutic levels THP-1 metabolism fell, figure 7.16.

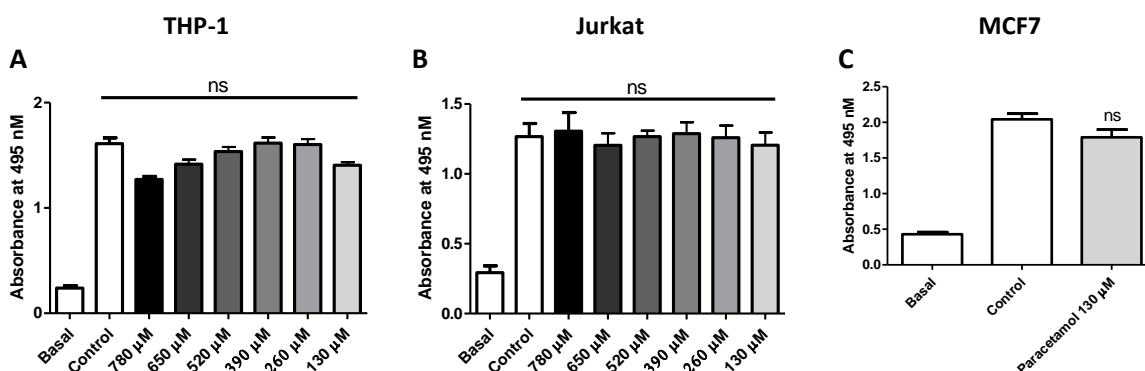


Figure 7.16: Cytotoxicity assays for Paracetamol. MTS assays were over 7 hours in (A) THP-1 and (B) Jurkat and over 24 hours in (C) MCF7. Basal absorbance occurs in presence of medium after MTS treatment in the absence of cells. Means  $\pm$  SEM, one-way ANOVA, post-hoc Bonferroni,  $n \geq 3$  independent experiments, ns= $p > 0.05$ .

Chemotaxis assays explored the effects of Paracetamol at 130  $\mu$ M on chemotaxis with THP-1 to CCL3 and CXCL12 along with Jurkat assays to CXCL12. Paracetamol had no significant effect on chemotaxis in Jurkat or THP-1, figure 7.17, or wound-healing in MCF7 (data not shown).

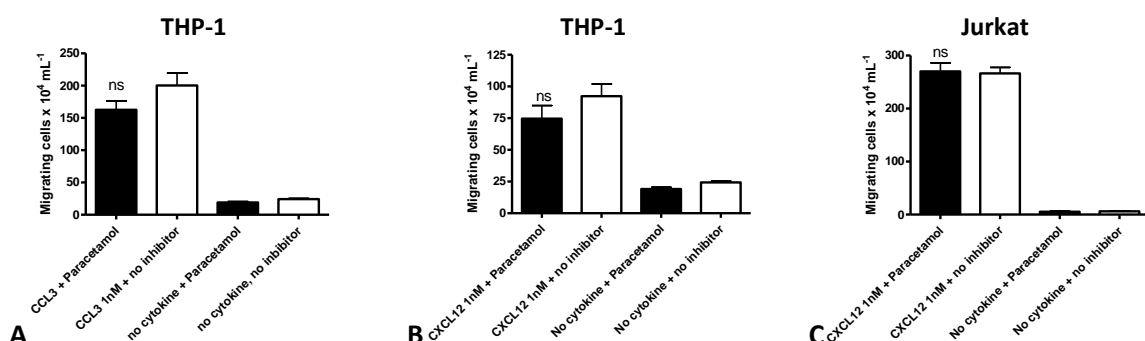


Figure 7.17: Chemotaxis assays following pre-treatment with Paracetamol 130  $\mu$ M or control. (A) Chemotaxis of THP-1 to 1 nM CCL3. (B) THP-1 chemotaxis to 1 nM CXCL12. (C) Jurkat chemotaxis to 1 nM CXCL12. Means  $\pm$  SEM, one-way ANOVA, post-hoc Bonferroni,  $n \geq 3$  independent experiments, ns= $p > 0.05$ .

### 7.2.5: Paracetamol, Aspirin and NSAID's effects on cellular calcium dynamics

Calcium acts as a second messenger. Calcium dynamics are central to the oncogenesis, deregulation, proliferation and resistance to apoptosis that defines malignancy, as cellular  $\text{Ca}^{2+}$  concentrations and fluctuations can modulate signalling pathways [811]. Expression of calcium v1.2 L-type calcium channels, Voltage Gated Calcium Channels (VGCC) in THP-1 is increased by their differentiation into macrophages [812], although THP-1 also operate via receptor and Store Operated Calcium Channels (SOCC) [813]. Whereas Jurkat also express  $\text{Ca}^{2+}$  permeable non-

selective cation channels termed TRPs [814]. TRPV1 channels reportedly contribute to  $\text{Ca}^{2+}$  signalling triggered proliferation in MCF7 [815].

Calcium levels in cell cytosol are approximately 10,000 times lower in resting conditions than levels in the ER and other  $\text{Ca}^{2+}$  stores. This gradient is created by  $\text{Ca}^{2+}$  pumps in the stores' plasma membranes. Both VGCC on calcium store membranes and cell Receptor-Operated Calcium Channels (ROCC) can potentially respond to signalling causing cytosol calcium influx [816].  $\text{Ca}^{2+}$  fluctuation can themselves trigger other calcium release channels controlled by inositol-1,4,5-triphosphate and ryanodine receptors located on the ER membrane. This generates further  $\text{Ca}^{2+}$  movements [817, 818].

Here the effects of Paracetamol treatment of THP-1, CHO.CCR5 and Jurkat on calcium dynamics induced by CCL3 and CXCL12 were explored, figure 7.18.

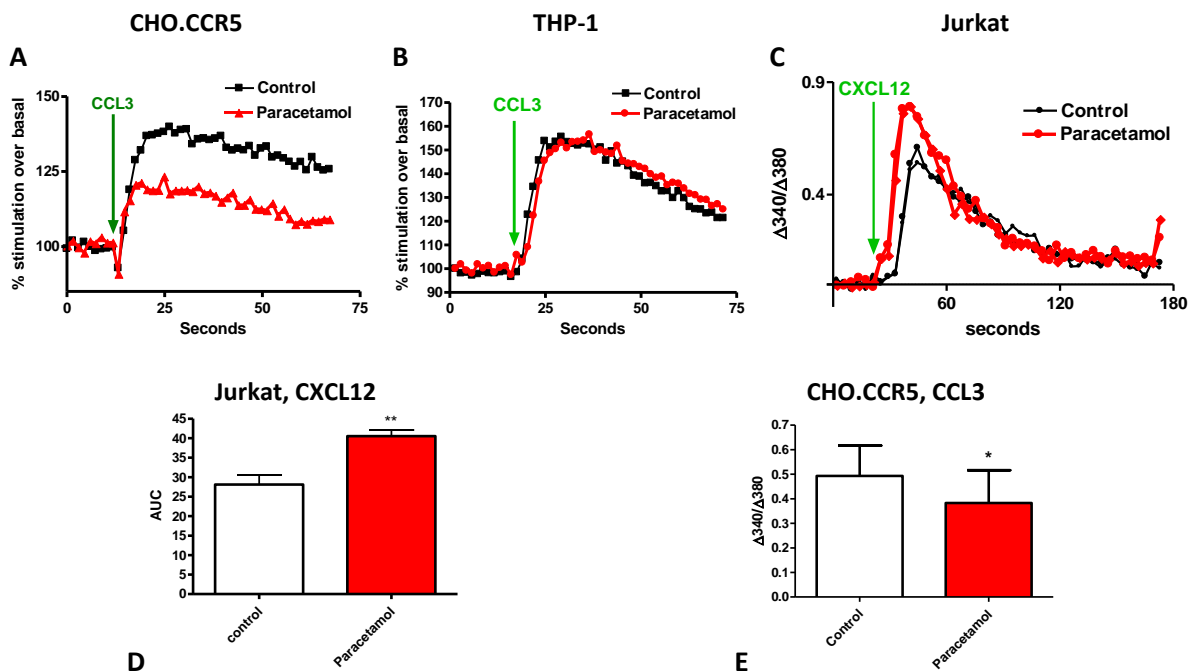


Figure 7.18: Fura2  $\text{Ca}^{2+}$  assay following 130  $\mu\text{M}$  Paracetamol or control. Traces for (A) CHO.CCR5 following 10 nM CCL3, (B) THP-1 following 10 nM CCL3 and (C) Jurkat following 10 nM CXCL12, all  $n=1$ . (D) Jurkat AUC following 10 nM CXCL12, (E) CHO.CCR5 following 10 nM CCL3. Means  $\pm$  SEM, Student t-test,  $n \geq 3$  independent experiments,  $**=p < 0.01$ ,  $*=p < 0.05$ . Data: Fluorescence ratio change ( $\Delta 340/\Delta 380$  nm) i.e. peak fluorescence following 10 nM chemokine additions minus basal fluorescence (prior to chemokine).

Paracetamol at 130  $\mu\text{M}$  was found to significantly decrease calcium responses to CCL3 in CHO.CCR5 cells, and conversely to significantly increase calcium release in response to CXCL12 in Jurkat. The effects observed with Paracetamol suggest cell type and chemokine specific responses. Others have observed a slight increase in calcium responses in Jurkat after treatment

with Paracetamol metabolite AM404 [819]. THP-1, like HEK cells [820], may express FAAH, or other enzymes that degrade Paracetamol's active metabolites, so calcium flux was not affected.

Next the effects of Ibuprofen and Celecoxib on chemokine-induced calcium flux were explored, figure 7.19.

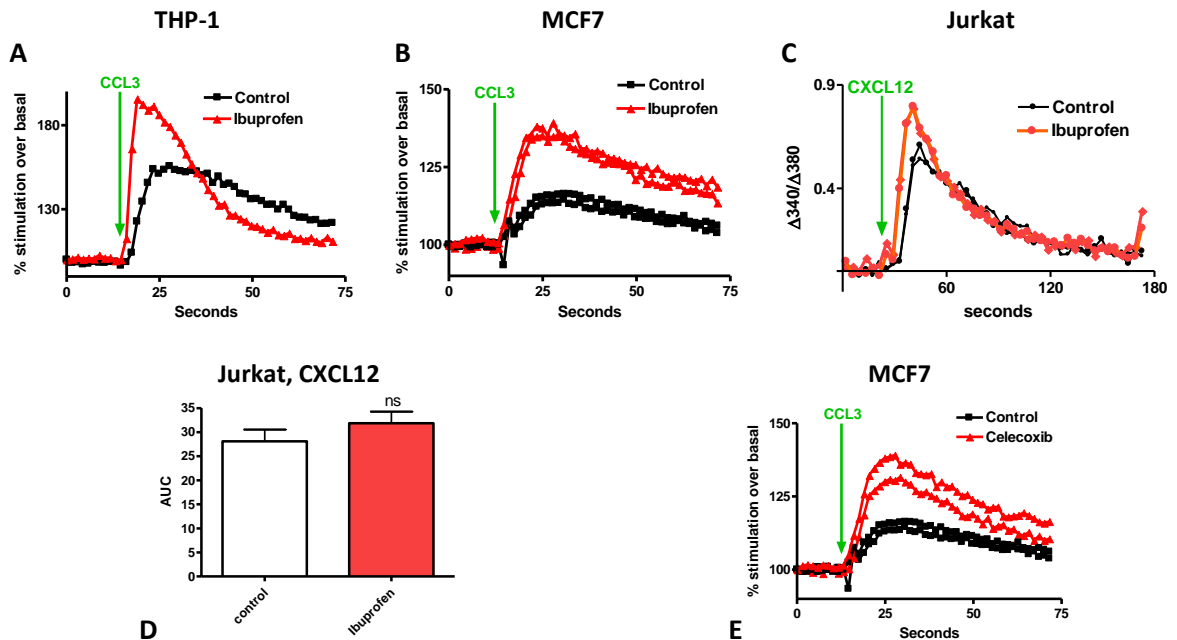


Figure 7.19: Fura2  $\text{Ca}^{2+}$  assays following Ibuprofen, celecoxib or control (DMSO). Traces following Ibuprofen 290  $\mu\text{M}$  pre-treatment (A) THP-1 response to 10 nM CCL3, (B) MCF7 response to 10 nM CCL3 (C) Jurkat response to 10 nM CXCL12, all  $n=1$ . (D) Jurkat, AUC following 10 nM CXCL12, Means  $\pm$  SEM, Student t-test,  $n \geq 3$  independent experiments,  $ns=p>0.05$ . (E) Celecoxib 50  $\mu\text{M}$  pre-treatment of MCF7 response to 10 nM CCL3,  $n=1$ . Data: Fluorescence ratio change ( $\Delta 340/\Delta 380$  nm) i.e. peak fluorescence following chemokine addition minus basal fluorescence (prior to chemokine).

Rather than reduce calcium flux Ibuprofen significantly increased both the speed and peak levels reach in all three cell types, although the smaller increase seen in Jurkat was not statistically significant. Celecoxib also increased calcium flux. Some NSAIDs may mediate apoptosis in malignant cells partly through effects on intracellular calcium concentrations. Celecoxib inhibits both calcium uptake and  $\text{Ca}^{2+}$  ATPases (aka SERCAs). Calcium enters the endoplasmic reticulum (ER) through  $\text{Ca}^{2+}$  ATPases, and Celecoxib inhibits this calcium uptake causing calcium mobilisation and elevation [487]. Calcium levels can affect apoptosis. Celecoxib may trigger apoptosis via inhibiting signalling via ERK and Akt, both pathways support cell survival [821].  $\text{Ca}^{2+}$  rise may activate calcium-dependent proteases, endonucleases and calcineurin, all of which can induce apoptosis. Raised  $\text{Ca}^{2+}$  levels facilitate  $\text{Ca}^{2+}$  infiltration of mitochondria, causing cytochrome C release, which activates caspases causing apoptosis [822, 823].

In contrast Aspirin was found to have a small negative effect on CCL3 calcium dynamics in THP-1, but significantly increased calcium flux in Jurkat in response to CXCL12. Whereas Naproxen blunted peak calcium release but prolonged the time of release, hence overall did not significantly reduce the total AUC, figures 7.20.

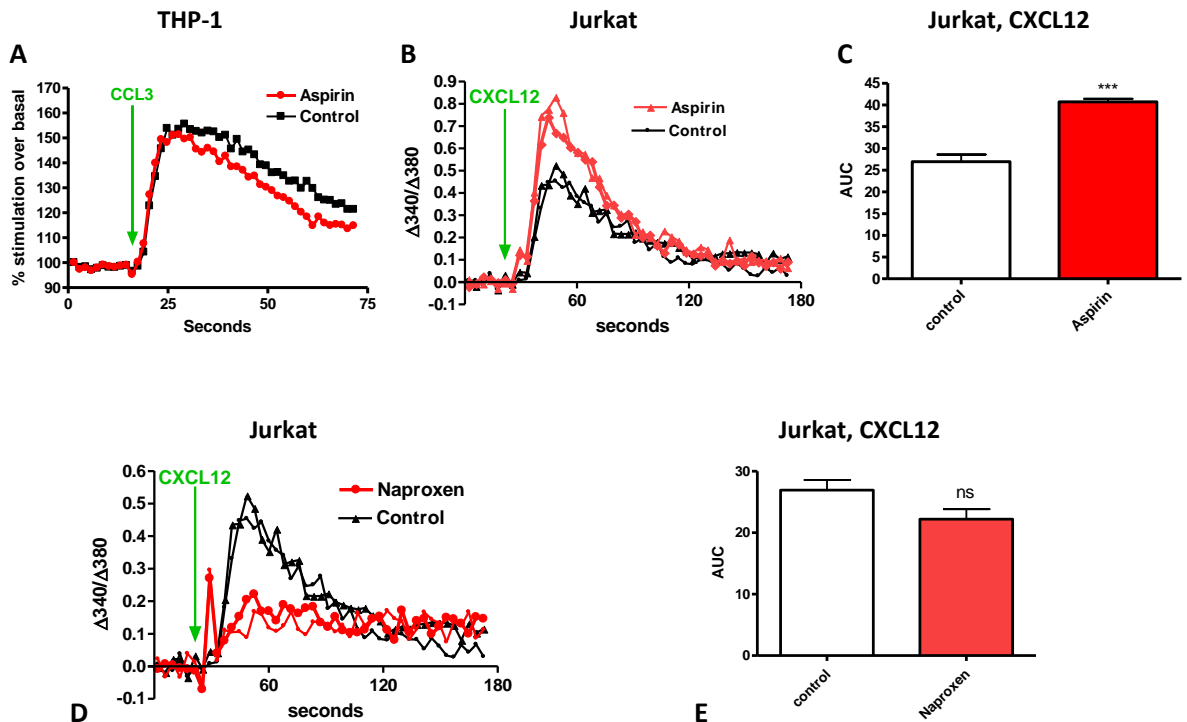
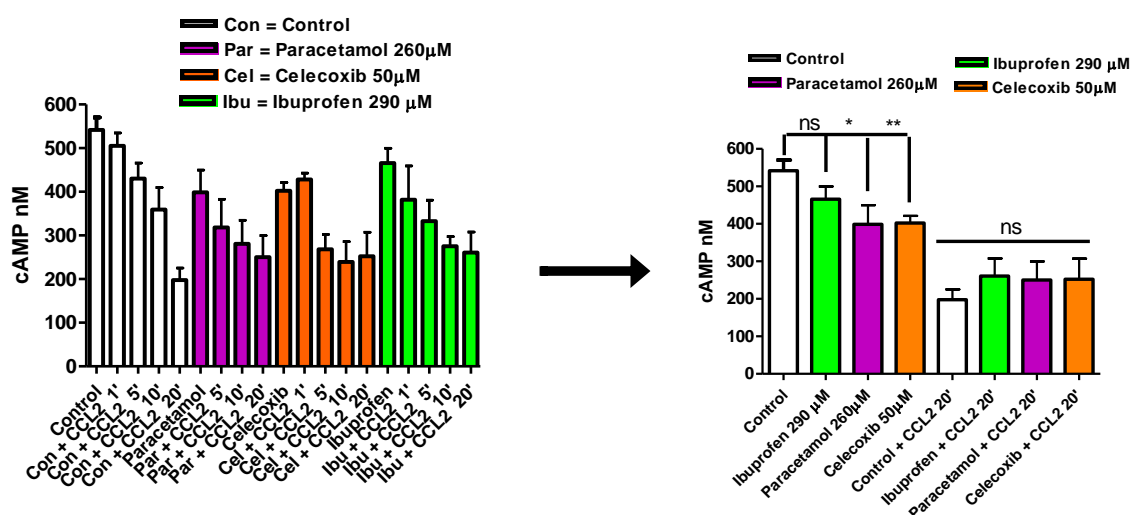


Figure 7.20: Fura2  $\text{Ca}^{2+}$  assays following Aspirin, Naproxen or control. Traces following Aspirin 555  $\mu\text{M}$  pre-treatment (A) THP-1 response to 10 nM CCL3, (B) Jurkat response to 10 nM CXCL12, both  $n=1$ , (C) Jurkat AUC response to 10 nM CXCL12. (D) Naproxen 217  $\mu\text{M}$  pre-treatment of Jurkat trace response to 10 nM CXCL12,  $n=1$ , and (E) Jurkat AUC following 10 nM CXCL12, Means  $\pm$  SEM, Student t-test,  $n \geq 3$  independent experiments, ns= $p > 0.05$ . Data: Fluorescence ratio change ( $\Delta 340/\Delta 380$  nm) i.e. peak fluorescence following chemokine addition minus basal fluorescence (prior to chemokine).

#### 7.2.6: COX2-inhibition may modulate basal cAMP levels

cAMP is a second messenger that can be produced in response to stimulation of receptors including chemokine receptors, via membrane associated adenylyl cyclases converting ATP to cAMP. cAMP is then degraded by phosphodiesterases. cAMP transfers signals from receptors to intracellular downstream effectors, and is a negative regulator in immune cells through the protein kinase A (PKA) pathway [743].

Here the effects of Celecoxib, Ibuprofen and Paracetamol on cAMP levels before and after CCL2 treatment were examined. THP-1 cells were treated with the drugs in the presence of phosphodiesterase inhibitor IBMX 0.75 mM with or without 10 nM CCL2 stimulation for periods varying from 1 to 20 minutes, figure 7.21.



**A** **B**

Figure 7.21: THP-1 cAMP levels before and following treatment with CCL2 10 nM. (A) THP-1 in presence of IBMX 0.75 mM, were pre-treated with control (DMSO), Celecoxib 50  $\mu$ M, Ibuprofen 290  $\mu$ M or Paracetamol 260  $\mu$ M (30 mins, 37°C) before Forskolin 20  $\mu$ M then CCL2 for timed periods (1, 5, 10 and 20 minutes). Cells were then lysed and cAMP levels recorded. (B) Analysis of data selected from (A). Means  $\pm$  SEM, one-way ANOVA, post-hoc Bonferroni,  $n \geq 3$  independent experiments, \*\*= $p < 0.01$ , \*= $p < 0.05$ , ns= $p > 0.05$ .

Paracetamol and Celecoxib reduced basal cAMP levels, but not the fall in cAMP levels over 1 to 20 minutes in THP-1 subject to 10 nM CCL2 stimulation, figure 7.21B. Reduction in basal cAMP levels were statistically significantly with Celecoxib ( $p < 0.01$ ) and Paracetamol ( $p < 0.05$ ) but not with Ibuprofen ( $p > 0.05$ ), suggesting observed effects may relate more to COX2 than COX1 inhibition. Although cAMP levels at 20 minutes post CCL2 treatment were slightly higher than control in the presence of all three drugs, the increases did reach statistical significance.

### 7.2.7: NSAIDs and Paracetamol modulated cofilin phosphorylation

Cofilin phosphorylation in response to CCL3 and CXCL12 was examined in THP-1 cells pre-treated for 30 minutes with Celecoxib, Aspirin, Naproxen, Paracetamol or Ibuprofen, figure 7.22.



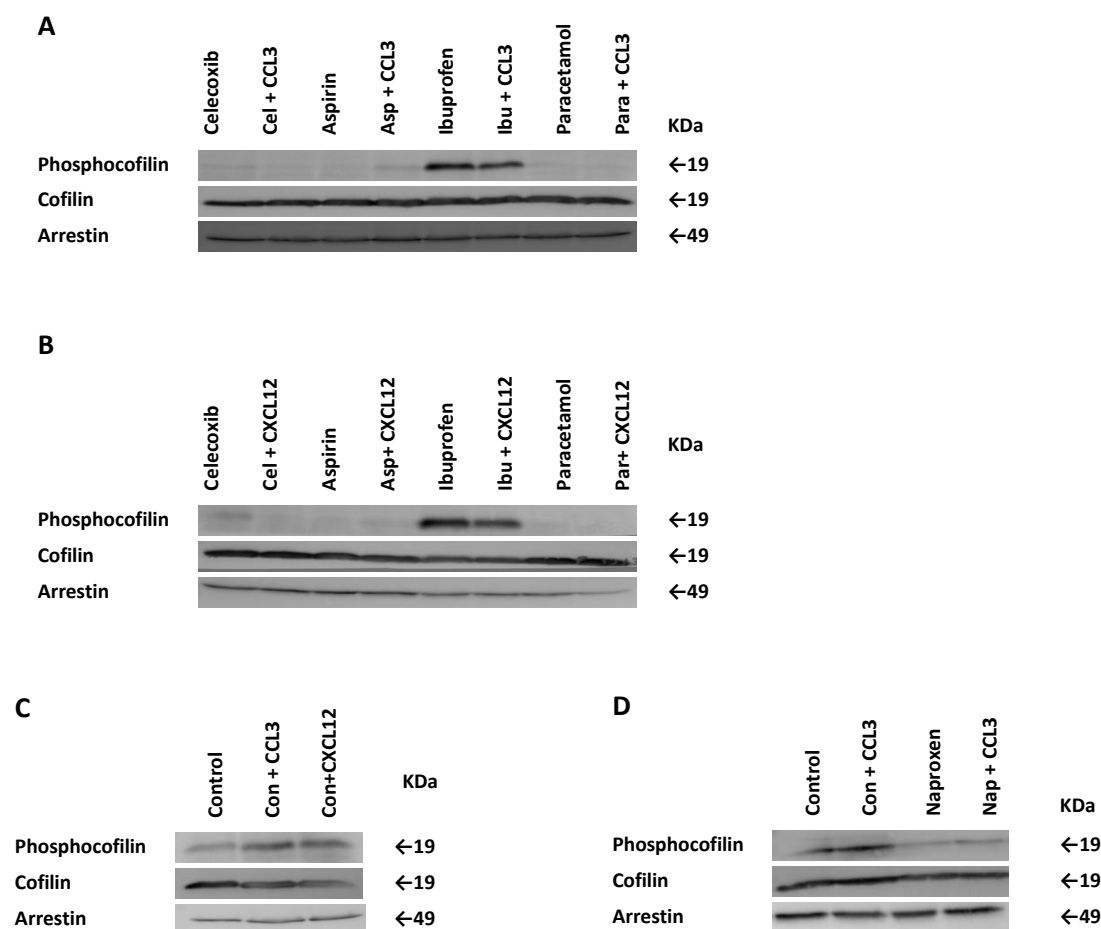


Figure 7.22: Total-cofilin and phosphocofilin (Ser3) antibodies reveals cofilin phosphorylation levels in THP-1 following pre-treatment with Celecoxib 25  $\mu$ M, Aspirin 555  $\mu$ M, Ibuprofen 290  $\mu$ M or Paracetamol 130  $\mu$ M (37°C, 30 mins) in presence and absence of (A) CCL3 or (B) CCL3 (5 nM, 15 mins before lysis). (C) THP-1 pre-treatment with control (DMSO) (37°C, 30 mins) then CCL3 or CXCL12 (5 nM, 15 mins). (D) THP-1 pre-treated with Naproxen 217  $\mu$ M (37°C, 30 mins) then CCL3 (5 nM, 15 mins). Arrestin-2 loading controls.

Cofilin phosphorylation usually follows treatment with CCL3 or CXCL12 in THP-1, as discussed in chapter five, see figure 5.4. Celecoxib, Naproxen, Aspirin and Paracetamol eliminated the expected phosphorylation from CCL3 or CXCL12 treatment whereas Ibuprofen consistently produced cofilin phosphorylation in presence and absence of CCL3 or CXCL12, figure 7.22.

### **7.3: Discussion**

Aspirin, Paracetamol and NSAIDs Ibuprofen, Naproxen and Celecoxib were found to have drug and/or cell-line specific effects on chemotaxis, chemokinesis, calcium flux, cAMP production and cofilin phosphorylation in response to chemokines.

#### **7.3.1: Ibuprofen may have PGE<sub>2</sub>-independent effects on cell viability and migration**

Ibuprofen was used here at 290  $\mu$ M a concentration that did not cause cytotoxicity, well below the IC<sub>50</sub>s found of 690  $\mu$ M in THP-1 and 1.16 mM in Jurkat, figure 7.8, and below IC<sub>50</sub>'s reported by others [798]. In other cancer cell-lines exposed to growth-supporting media and conditions ibuprofen is reported to have caused apoptosis and/or inhibited proliferation, including in human malignant colorectal, gastric adenocarcinoma, human cutaneous and prostate cancer cells [801, 824, 825]. Ibuprofen may produce a concentration-dependent effect over 24-72 hours inhibiting cell proliferation, decreasing cell size and inducing cell rounding with loss of detachment but not direct cytotoxicity [801]. Akrami *et al.* (2014) found Ibuprofen at 500  $\mu$ M upregulated apoptosis supporting proteins p53 and Bax, and down-regulated angiogenesis supporter VEGF-A along with stemness markers OCT3/4 and CDC44 [798]. Others concur that ibuprofen increases p53 and BAX expression [799].

At 600  $\mu$ M Ibuprofen is reported to upregulate MDM2, p53, p21 and caspase-3 along with caspase-6 to caspase-9, while down regulating cell cycle related proteins E2F2, CDC25A and PCNA. Detailed examination of the effects of ibuprofen on cell cycle genes showed, in a gastric cancer cell-line, that at 600  $\mu$ M ibuprofen caused cells to move from S and G2/M phases to G0/G1 and cause G1 arrest [801]. Similar effects have been reported for another NSAID, Indomethacin [446]. Ibuprofen appeared to block cells in G1, by decreasing cyclins and cyclin-dependent kinase expression and increasing cell cycle inhibition by protein p21. Ibuprofen at 800  $\mu$ M also increased Reactive Oxygen Species levels inducing p21/p53-dependent apoptosis [801].

Ibuprofen at 290  $\mu$ M was found to inhibit chemotaxis and chemokinesis supported by CCL3 and/or CXCL12 in THP-1, Jurkat and MCF7, figures 7.9-7.10. The mechanism may involve Akt. Ibuprofen is reported to inhibit Akt and hence Pi3K-Akt signalling [798]. The Akt pathway regulates cell survival, migration and angiogenesis, and Akt inhibition by NSAIDs may induce apoptosis in some cell types [826]. Akt is pivotal in cancer development. Akt activation requires direct interaction of Akt's PH domain with PIP<sub>3</sub>, at the plasma membrane. Phosphorylation by kinases PDK1 and mTORC2 activate Akt which can inactivate cell cycle inhibitors p27 and p21 thus facilitating G1/S phase progression [618, 827]. Akt may also interact with Cyclin A2 which activates Cyclin-Dependent Kinase-2 (CDK2) [828].

Ibuprofen was found to cause loss and distortion of actin filaments and stress fibres, figure 7.11. Others have examined the effects of NSAIDs *in vitro* on A549 lung cancer cell morphology. Indomethacin but not Aspirin (3 mM), or NSAIDs Diclofenac (300  $\mu$ M) or Sulindac (300  $\mu$ M) caused exposure time-dependent reversible loss of actin stress fibres along with cell elongation and shrinkage. PGE<sub>2</sub> levels were equally reduced by around 70% by all four NSAIDs, but morphology was not restored in Indomethacin-treated cells by PGE<sub>2</sub> supplementation. However, only Indomethacin was found to have reduced cellular levels of adhesion molecules, E-cadherin and collagen IV, by upregulating matrix metalloprotease 9 (MMP9), molecular scissors that support epithelial mesenchymal transition (EMT). Indomethacin's effects on cell morphology were all reversible by treatment with PPAR $\gamma$  agonist troglitazoneb [829].

Ibuprofen has been found to activate transcription factor PPAR $\gamma$  [830], which is expressed in a very wide range of cancers [831], neuronal, and adipocyte cells [830, 832]. PPAR $\gamma$  activation inhibits RhoA and Rac1 activation essential for cell migration [671], blocks P13K/Akt and Erk1/2 signalling [833, 834], and stimulates transcription of PTEN tumour suppressor [835]. PTEN can dephosphorylate PIP<sub>3</sub> and so inhibit the activation of Akt and also induce mitochondrial translocation of cofilin [792, 793, 836], although PTEN can be mutated in cancer [687]. Thus while Indomethacin could potentially aid epithelial-mesenchymal transition from primary tumour and mesenchymal-epithelial transition at a secondary (seeding) site [829], Ibuprofen by activating PPAR $\gamma$  would not. This may be one factor why the effects of different NSAIDs in cancer are inconsistent.

Ibuprofen ability to inhibit cell migration, figures 7.9-7.10, invites further investigation as potentially may translate to Ibuprofen *in vivo* inhibiting chemokine-supported metastasis. Other potential therapeutic benefits of Ibuprofen on signalling in cancer include evidence that VEGF, a key mediator of angiogenesis in cancer which induces growth factor release from its target tissues, and fibroblast growth factor production, may be reduced by NSAID inhibition of COX1 and COX2 [837, 838]. For Ibuprofen these effects may be concentration dependent. Ibuprofen has been shown to reduce hypoxia-inducible factors HIF-1 $\alpha$  and HIF-2 $\alpha$ , along with HIF-regulated proteins Glut-1 and VEGF, in cells not expressing COX2 [839]. Some NSAIDs may inhibit hypoxia-induced angiogenesis by increasing the expression of tumour suppressor VHL so reducing HIF $\alpha$  levels and consequently reducing VEGF secretion [840]. HIF support tumour survival, aggressiveness and angiogenesis [841]. Many tissues may produce VEGF including neutrophils, platelets and endothelium [842]. Ibuprofen may also reduce the production of fibroblast growth factor which supports PGE<sub>2</sub> and PGI<sub>2</sub> inflammation and angiogenesis [843].

Ibuprofen has been shown to inhibit ovarian and breast cancer growth and tumour PGE<sub>2</sub> levels [844], possibly partly through an anti-oestrogenic effect [845]. Overall Ibuprofen is attributed with many off-target effects, figure 7.23, the drug may even partly reduce pain by inhibiting the excitatory neurotransmitter, Acid Sensing Ion Channel 1a which is involved in pain sensation and inflammation [846].

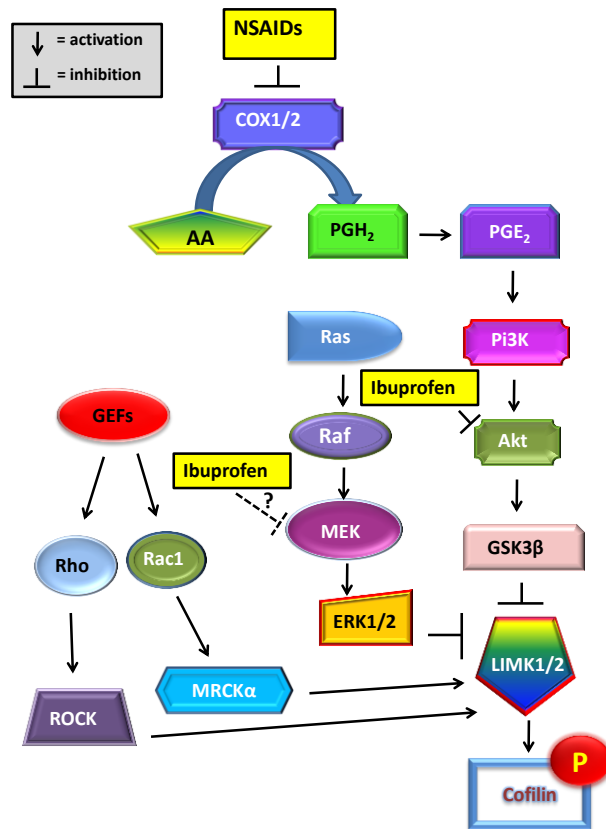


Figure 7.23: Ibuprofen's possible off target effect, and links to cofilin phosphorylation [830, 833].

### 7.3.2: NSAIDS effects on calcium fluctuations

Receptor stimulation by physiological agonists such as chemokines can trigger Ca<sup>2+</sup> oscillations [847], which then affect gene expression [848]. Chemokine-stimulated Ca<sup>2+</sup> signalling can stimulate PIP<sub>2</sub> hydrolysis to DAG and Inositol trisphosphate (InsP<sub>3</sub>) which then binds InsP<sub>3</sub> receptors, which are calcium release channels in the ER [849]. The calcium release that follows can stimulate calmodulin [850] which binds and activates calcineurin, a protein phosphatase, (and other targets) which themselves activate transcription factors including NFκB and Nuclear Factor of Activated T-cells (NFAT), and hence Ca<sup>2+</sup> dynamics can regulate gene expression [811, 851, 852]. This can produce proliferation, progression of cell cycle and mediate apoptosis [853]. Inhibiting T-type Ca<sup>2+</sup> channels can reduce proliferation and support apoptosis in cancer cells [854]. Also targeting ORAL1, a plasma membrane pore structure, and STIM1, an ER calcium

sensor, (see annotated illustration chapter 8, figure 8.36) which both mediate store operated calcium re-entry following stimulation, may inhibit malignant cell growth [855].

Here Aspirin, but not Naproxen, was observed to significantly increase overall CXCL12-stimulated  $\text{Ca}^{2+}$  responses in Jurkat but not to affect THP-1  $\text{Ca}^{2+}$  oscillations following CCL3, figure 7.20. Conversely Celecoxib and Ibuprofen consistently increased peak calcium stimulation levels following CCL3 or CXCL12 in Jurkat MCF7 and THP-1, figure 7.19. Overall results suggest calcium responses are chemokine and cell-type specific. Aspirin and some NSAIDs may inhibit  $\text{Ca}^{2+}$  uptake by mitochondria which support  $\text{Ca}^{2+}$  oscillations by importing  $\text{Ca}^{2+}$  after influx effectively acting as  $\text{Ca}^{2+}$  buffers [856]. NSAIDs and Aspirin have for many years been reported as having inhibitory effects on malignant cell proliferation [857, 858], as has Phenacetin which is converted to Paracetamol *in vivo* [857]. Proposed mechanisms include modulation of calcium dynamics that support migration. This may be via modulation of focal adhesions; by inhibiting store-operated calcium influx focal adhesion turnover is stalled, inhibiting cell migration [859, 860].

The crosstalk between the immune and nervous systems contributes to inflammation in cancer [861]. The transient receptor potential (TRP) proteins are a family of cation proteins implicated in pro-inflammatory immune cells including macrophages and T-cells [862]. Important TRPs include TRPV1 and TRPA1; both play key roles in neurogenic inflammation. Both are  $\text{Ca}^{2+}$  permeable non-selective cation channels that can depolarise plasma membranes allowing  $\text{Ca}^{2+}$  influx. Activation of TRPV1 produces anti-tumour activity in many breast cancer types [863] and may be therapeutic in other cancers including bladder and endometrial [864, 865]. However  $\text{Ca}^{2+}$  influx through another TRP cation channel, Transient Receptor Potential Melanostatine-2 (TRPM2), is reported to contribute to Paracetamol toxic effects in overdose [866].

Many inflammatory mediators, including prostaglandins and cytokines, act as TRP channel agonists, for example CCL3 has been shown to sensitize TRPs and activate TRPV2  $\text{Ca}^{2+}$  channels [867] and TRPA1 agonists include a metabolite of  $\text{PGD}_2$  called 15-deoxy- $\delta(12,14)\text{-PGJ}_2$  [868]. The actions of agonists at TRPA1 and TRPV1 and channel activation are dependent on both agonist combinations and concentrations, plus intracellular  $\text{Ca}^{2+}$  concentrations [869, 870].  $\text{PGE}_2$  can increase cytosolic free calcium in monocytes treated with 10 nM CCL3 or CXCL12 [802].

Paracetamol also produced specific chemokine and cell-type calcium responses, figure 7.18. The mode of action of Paracetamol, discussed in chapter one section 1.9.2, includes increasing levels of anandamide, which can act as a T-type calcium channel blocker [871] and inhibits  $\text{Ca}_v3.2$  channels [872]. Paracetamol *in vivo* is metabolized to p-aminophenol in the liver then to N-(4-

hydroxyphenyl)-5,8,11,14-eicosatetraenamide (AM404) by fatty acid amide hydrolase in the brain [421]. AM404 can activate TRPV1 channels. TRPV1 may interact with  $\text{Ca}_v3.2$  channels found in the dorsal horn and dorsal root ganglion, two key pain pathway areas [820, 873]. Therefore *in vitro* investigations into Paracetamol's effects on calcium responses may not accurately reflect *in vivo* reality.

### **7.3.3: NSAIDs and basal cAMP levels**

The cAMP/PKA pathway must be tightly regulated to prevent excessive immunological activation. NSAIDs negatively regulate the cAMP/PKA pathway by inhibiting COX1 and COX2. Inhibition of these enzymes with NSAIDs blocks  $\text{PGE}_2$  synthesis, which subsequently, via EP3 receptors and  $\text{G}_i$  responses, downregulates cAMP levels in some immune cells including T-cells, see figure 7.24. This may enhance anti-tumour responses in cancer [874-877]. Although neither Ibuprofen, Paracetamol or Celecoxib had any significant effect on cAMP falls following CCL2 stimulation, figure 7.21, results suggest that COX2 inhibition with Paracetamol and Celecoxib may downregulate basal cAMP levels in THP-1 monocytes, this may deserve further investigation for anti-cancer effects. COX2 is expressed in adenoma and malignant tissues but colon cancer initiation appears connected with COX2 expression in macrophages within mildly dysplastic adenoma tissues [878]. Inhibition of COX2 appears therapeutic in preventing progression of dysplasia to cancer [786], possibly as COX2 expression in macrophages supports angiogenesis. Colon tumours have high macrophage density as CCL2 recruits circulating monocytes which differentiate to macrophages. In macrophages CCL2 stimulates both COX2 expression and, via a COX2/ $\text{PGE}_2$  autocrine/paracrine pathway, Vascular Endothelium Growth Factor (VEGF) release [787].

### **7.3.4: The Prostaglandin Cascade, cAMP and Cofilin**

$\text{PGE}_2$  is produced through COX metabolism of membrane arachidonic acid.  $\text{PGE}_2$  can produce effects through the E-series Prostanoid GPCRs [879] which through  $\text{G}\alpha_s$  G-proteins increase cAMP activity stimulating PAK and Epac1/2 which acting via PTEN [791] inhibit macrophage phagocytosis [880]. PTEN can dephosphorylate  $\text{PIP}_3$  and inhibit Akt [791, 881]. The  $\text{PGE}_2$  triggered cAMP signalling through PKA and PTEN can activate cofilin-1 preventing effective actin polymerization [409] so NSAIDs may, through inhibition of  $\text{PGE}_2$  production, influence phosphorylation of cofilin and hence cell migration. Prostanoids can coordinate autocrine and paracrine signalling by binding GPCRs EP1-4 [882]. COX1 and COX2 are regulated by arachidonate and peroxide availability. The lower levels of substrate peroxide activate COX2 more than COX1 [883]. Tissue-specific synthases then control the pathway from  $\text{PGH}_2$  onwards [459], figure 7.24.

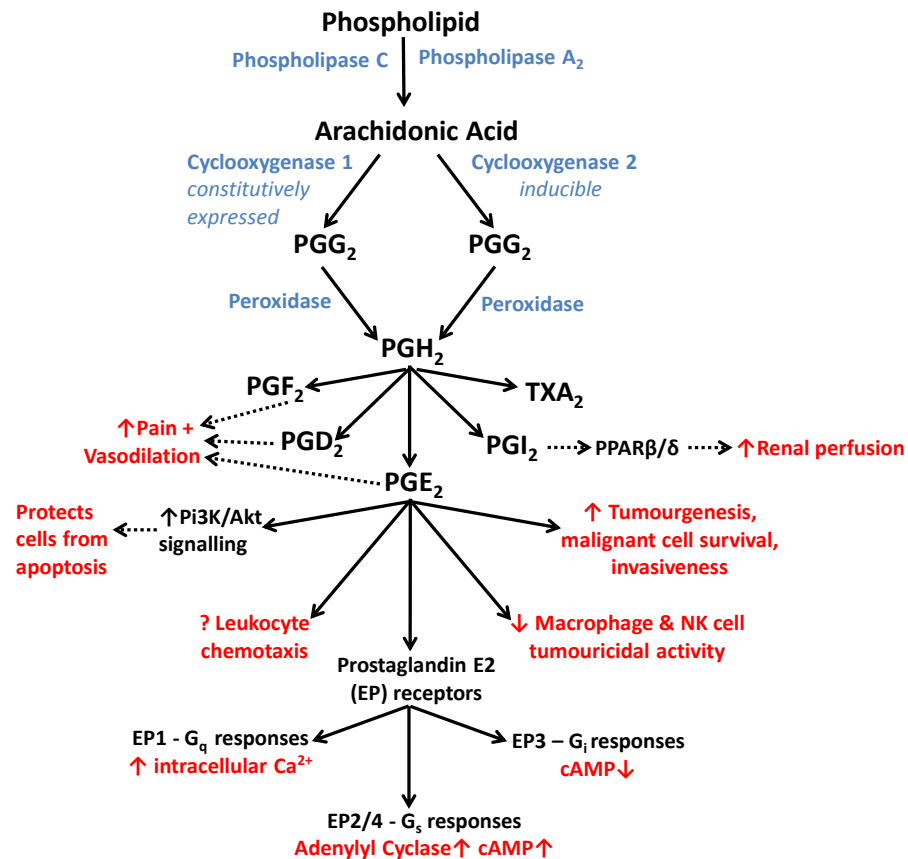


Figure 7.24: Hydrolysis of the ester linkage in phospholipid by phospholipases C and A2 releases arachidonic acid which COX1 & COX2 along with peroxidases oxidise to  $\text{PGH}_2$ . Specific prostaglandin synthases then produce products including prostanoid  $\text{PGE}_2$ .  $\text{PGE}_2$  binds prostaglandin  $\text{E}_2$  receptors 1 – 4. Leukocytes carry EP2 and EP4 receptors, stimulation of which activate Adenylyl Cyclase (AC) and increases cAMP. EP4 signals via  $\text{G}_{\alpha i}$ , Pi3K,  $\beta$ -arrestin, and  $\beta$ -catenin [884-886].

Celecoxib, Aspirin, Naproxen and Paracetamol were all found to reduce cofilin phosphorylation, figure 7.22, an expected response from drugs which reduce  $\text{PGE}_2$  levels. However pre-treatment with Ibuprofen consistently caused cofilin phosphorylation in the presence and absence of CCL3 or CXCL12. Ibuprofen can decrease RhoA activation and ROCK-1 expression [794, 887]. Ibuprofen enhances axonal sprouting and regeneration [888] possibly as activation of Rho contributes to lack of nerve regeneration [889]. So logically Ibuprofen should inhibit  $\text{PGE}_2$  and possibly directly RhoA-ROCK-LIMK-cofilin phosphorylation, but as the above blots show this was not found to be the case.

Ibuprofen is also reported to mediate cytoskeletal  $\text{Ca}^{2+}$  binding protein Swiprosin-1 aka EFHD2 [890], which is present in monocytes [891], and both buffers intracellular  $\text{Ca}^{2+}$  and regulates

cofilin's access to filament actin [892]. Here Ibuprofen was shown to increase peak calcium flux levels in response to chemokines, figure 7.19. Raised  $\text{Ca}^{2+}$  may enhance Calcineurin's activation of Slingshot, hence dephosphorylation of cofilin [893], conversely here Ibuprofen increased phosphocofilin levels, figure 7.22. Amplification of Swiprosin-1, which lies upstream of Cdc42, Rac and Rho, has been shown to increase the effects of CXCL12 on Jurkat. When inhibited Swiprosin-1 may amplify Rho and PAK signalling stimulating cofilin phosphorylation through LIMK [894]. Ibuprofen mediation of Swiprosin-1 may contribute to Ibuprofen's effects on cofilin phosphorylation, calcium flux, actin filaments, figure 7.11, and chemokinesis, figures 7.9-7.10. Also Ibuprofen is reported to inhibit MEK-ERK signalling [895]. The MEK small molecule inhibitor SL327 also consistently strongly induces cofilin phosphorylation (chapter 5, figure 5.45) possibly suggesting that Ibuprofen may have some anti-cancer effects through strongly inhibiting MEK signalling and chemotaxis.

#### **7.4: Conclusions**

Only Ibuprofen amongst the drugs investigated here inhibited chemotaxis or chemokinesis to both chemokines in all three cell-lines. Naproxen inhibited CXCL12 migration in Jurkat and THP-1 but not CCL3-induced migration in THP-1 or chemokinesis in MCF7. Whereas Aspirin inhibited CXCL12 but not CCL3-chemotaxis and Celecoxib and Paracetamol had no effect on chemotaxis although Celecoxib did inhibit MCF7 chemokinesis. These results were not explain by cytotoxicity as for example Celecoxib appeared more cytotoxic,  $\text{IC}_{50}$  54  $\mu\text{M}$  in THP-1 and 48  $\mu\text{M}$  in Jurkat, than Ibuprofen,  $\text{IC}_{50}$  1.16 mM in Jurkat and 690  $\mu\text{M}$  in THP-1. Thus Aspirin and NSAIDs but not Paracetamol appear able to inhibit chemotaxis and/or chemokinesis but they may do so in a chemokine and cell-type specific fashion.

All the drugs tested here modulated calcium oscillations in a cell- or chemokine-specific manor. In THP-1, Paracetamol and Celecoxib but not Ibuprofen significantly reduced basal cAMP levels but not cAMP level reduction produced by CCL2 suggesting signalling involving calcium channels or cAMP may be involved in some of NSAIDs off-target effects.

Aspirin, Naproxen, Ibuprofen and Celecoxib all adversely influenced actin filament formation. Also Celecoxib, Aspirin, Naproxen and Paracetamol eliminated, but Ibuprofen increased, THP-1 basal phosphorylation of cofilin, and that following treatment with CCL3 or CXCL12.

The results suggest the effects of Ibuprofen, Naproxen, Celecoxib and Aspirin, on cancer initiation and progression should be assessed individually, as each produced contrasting responses to chemokines. Ibuprofen appears the most consistent and potent inhibitor of chemotaxis and



chemokinesis and Ibuprofens eliciting of cofilin phosphorylation suggest its reported antineoplastic effects may be PGE2-independent; possibly acting through inhibiting MEK signalling or modulation of cytoskeletal protein cytoskeletal  $\text{Ca}^{2+}$  buffering protein Swiprosin-1.

Fascinatingly the R-enantiomer of Naproxen, which is marketed as a racemic mix, has been found to inhibit Rho GTPase Rac1 and act in a similar way to popular Rac1 inhibitor NSC23766 [896]. Also Rac1 overexpression in bowel cancer may be prevented by NSAIDS [897]. These factors raised the questions; what effects does Rac1 inhibition have on CXCL12- and CCL3-chemotaxis, and cofilin phosphorylation? Investigations exploring these questions are reported in chapter 8.

## **Chapter 8: Rac1 mediates chemotaxis to CXCL12 but not CCL3, in leukaemic and breast cancer cell-lines, and Rac1 GEF inhibitor NSC23766 may have off-target effects on CXCR4/CXCR7 axis**

### ***8.1: Introduction***

The CXCR4/CXCL12 axis is complex, as CXCR4 variants and oligomerization along with CXCL12 functioning in monomeric and dimeric forms adds to the challenge of understanding CXCL12-induced chemotaxis in cancers [142, 145, 148]. The illumination of how CXCR4 ligands, such as CXCL12 and AMD3100, bind has taken extensive research over decades [147, 149]. CXCR4 ligands have the potential to mitigate metastasis [135]. Ras family Rho GTPases, co-ordinate actin polymerization, cell adhesion and cytoskeletal dynamics. They are molecular switches which can be activated by chemokines to trigger downstream signalling pathways [330, 336]. Rho GTPases are controlled by three sets of proteins Rho GDIs which can sequester and inactivate RhoGTPases [337]; Rho GAPs which facilitate switching 'off' Rho GTPases [341, 342]; and Rho GEFs which promote switching Rho GTPase 'on'. There are many Rho GEFs, most are controlled by phosphorylation [330, 338, 343]. One important Rho GTPase, Rac1, is key in the formulation of lamellipodia and overall cell motility [334], figure 8.1. Rac1 is activated, i.e. bound GDP is replaced by GTP, by Rho GEFs including Tiam1 and TrioN. In some cell-lines Rac1 supports chemotaxis through signalling also involving Akt and PKC [344, 346-350]. Here the aim was to elucidate the role of Rac1 in CXCL12- and CCL3-induced chemotaxis and wound-healing using small molecule inhibitor NSC23766 which purportedly selectively inhibits Rac1 interactions with Rho GEFs Tiam1 and TrioN [346], direct Rac1 inhibitor EHT1864, and Rac1-inhibiting peptide W56.

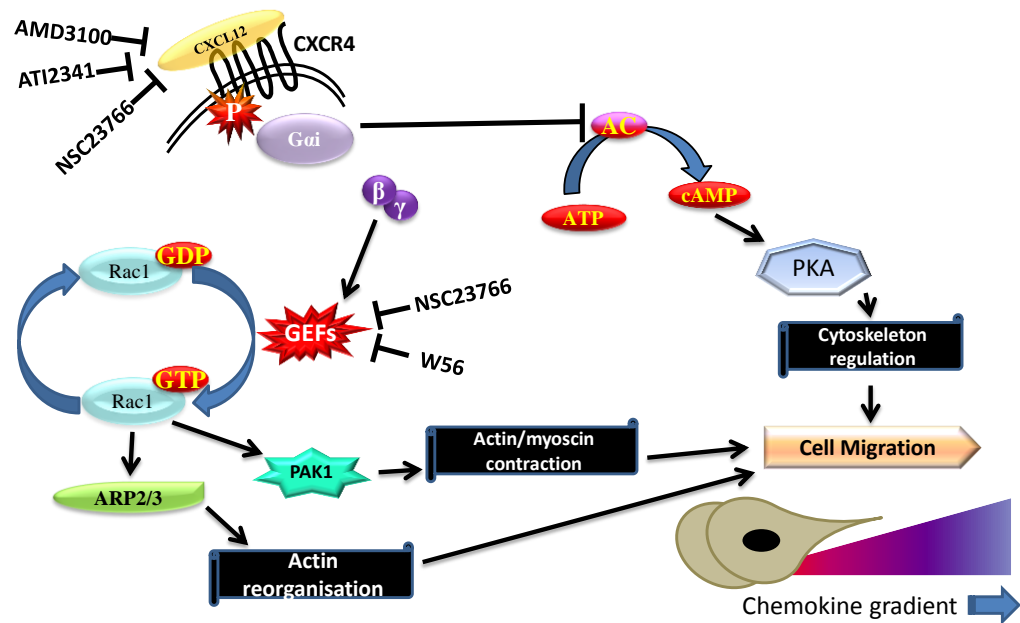


Figure 8.1: CXCL12-induced signalling can be modified by CXCR4 inhibition, for example with AMD3100 or ATI2341, and by Rac1 inhibition with W56 or NSC23766.

**Hypothesis:** Rac1 signalling is important for chemokine-supported cell migration of both haematopoietic and epithelial cancers.

**Aim:** To elucidate the role of Rac1 in THP-1 and Jurkat chemotaxis, MCF7 chemokinesis, cofilin phosphorylation, cAMP responses and calcium flux stimulated by chemokines CXCL12 and CCL3.

**Objectives:**

- (i) Explore the role of Rac1 in THP-1 and Jurkat chemotaxis and MCF7 wound-healing using small molecule inhibitor NSC23766, and Rac1-inhibiting peptide W56.
- (ii) Examine the effect of CXCR4 small molecule inhibition on Rac1 activation.
- (iii) Investigate if Rac1 inhibition interacts positively or negatively with CXCR4-binding antibody or small molecule inhibitors using chemotaxis assays and flow cytometry.
- (iv) Explore the effect of Rac1 and CXCR4 inhibition on cAMP modulation by CXCL12.
- (v) Elucidate the effect of PKC $\zeta$  siRNA knockdown on Jurkat chemotaxis and MCF7 chemokinesis.
- (vi) Explore the effects of Rac1 inhibition in THP-1 and Jurkat on calcium mobilisation triggered by chemokine stimulation.
- (vii) Examine if inhibition of Cdc42 or PLC affects chemotaxis, calcium flux or cAMP levels in THP-1 and Jurkat.
- (viii) Investigate if Rac1 inhibition modulates actin filament formation or cofilin phosphorylation in response to CXCL12 in THP-1.
- (ix) Discover if NSC23766 or W56 affect THP-1 chemotaxis to other CXC and CC chemokines.

## 8.2: Results

Please note controls are common between graphs where experiments were conducted simultaneously; results for each inhibitor have been displayed separately for ease of description of results, this applies to: figures 8.6A and B; 8.25A and 4.24C; 8.30A and B.

The tools used to achieve the chapter aims included small molecule inhibitors of Rac, NSC23766 and EHT1864, along with a peptide that binds a region of the human Rac1 protein between its two Switch regions. Rac1 residues 45-60 appear critical for specific Rac1 guanine nucleotide exchange factors (GEF's) recognition and activation, with Trp56 located in the Rac1 Switch II region being key for specificity between Rac1 and Cdc42 binding. These 15 residues, (see chapter one, figure 1.16), have been found to act as a very specific inhibitor preventing Rac1–GEF interactions [898]. Two 15 amino acid peptides were synthesised: active peptide W56 sequence VDGKPVNLGLWDTAG, and inactive control F56 sequence VDGKPVNLGLFDTAG where the key amino acid Trp56 was replaced by Phe56 to inactivate the peptide.

### 8.2.1: NSC23766 inhibits chemotaxis to CXCL12 but not CCL3

NSC23766 is a small molecule inhibitor that binds to the surface of Rac1 at the location where Rac1 specific GEFs Tiam1 and TrioN bind [899]. Hence NSC23766 inhibits TrioN and Tiam1 binding and activating Rac1. NSC23766 effects on Jurkat, THP-1 and MCF7 chemotaxis or chemokinesis in response to CCL3 and CXCL12 were examined, figure 8.2.

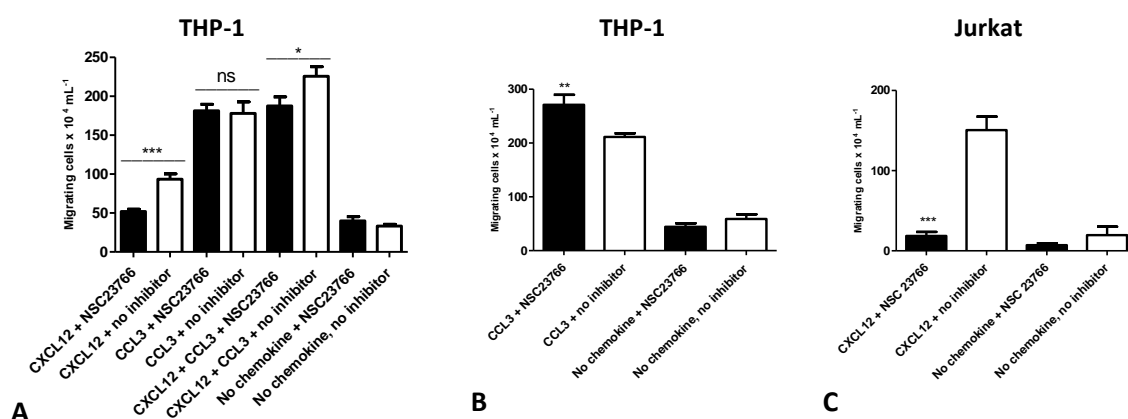


Figure 8.2: Chemotaxis assays following pre-treatment with NSC23766 100  $\mu$ M or control (A) Chemotaxis of THP-1 to 1 nM CXCL12, 1 nM CCL3 or 1 nM CCL3 + 1 nM CXCL12. (B) THP-1 chemotaxis to 1 nM CCL3. (C) Jurkat chemotaxis to 1 nM CXCL12. Means  $\pm$  SEM, one-way ANOVA, post-hoc Bonferroni,  $n \geq 3$  independent experiments, \*\*\*= $p < 0.001$ , \*\*= $p < 0.01$ , \*= $p < 0.05$ , ns= $p > 0.05$ .

In THP-1 the effects of 100  $\mu$ M NSC23766 on CXCL12 chemotaxis were dramatic, figure 8.2, yet on CCL3-induced chemotaxis 100  $\mu$ M NSC23766 either had no inhibitory effects, or in some THP-1

CCL3 assays 100  $\mu$ M NSC23766 was seen to statistically significantly increase chemotaxis. Combining chemokines CXCL12 1 nM and CCL3 1 nM increased migration further, but not in the presence of NSC23766, suggesting either a direct effect of NSC23766 on CXCR4 or that Rac1 specifically supports CXCL12-induced chemotaxis. In Jurkat CXCL12 assays 100  $\mu$ M NSC23766 consistently highly significantly inhibited chemotaxis.

AMD3100 inhibits CXCR4 so its effect on THP-1 chemotaxis to CXCL12 but also CCL3 was investigated. AMD3100 was found to produce a small ( $p < 0.05$ ) inhibitory effect on CCL3 chemotaxis, while very significantly inhibiting chemotaxis to CXCL12 ( $p < 0.001$ ), figure 8.3, suggesting CXCR4 may play a role in CCL3/CCR5 or CCL3/CCR1 chemotaxis or that AMD3100 has some off target effects.

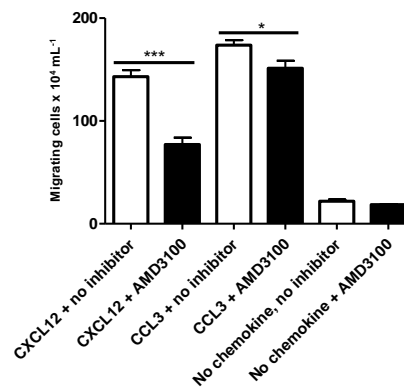


Figure 8.3: Chemotaxis assay of THP-1 following pre-treatment with AMD3100 1  $\mu$ M or control to 1 nM CXCL12 or 1 nM CCL3. Means  $\pm$  SEM, one-way ANOVA, post-hoc Bonferroni,  $n \geq 3$  independent experiments, \*\*\*= $p < 0.001$ , \*= $p < 0.05$ .

Cell viability assays using NSC23766 at 100  $\mu$ M in THP-1, Jurkat and MCF7 were conducted to confirm that the effects seen were not just from toxicity, figure 8.4.

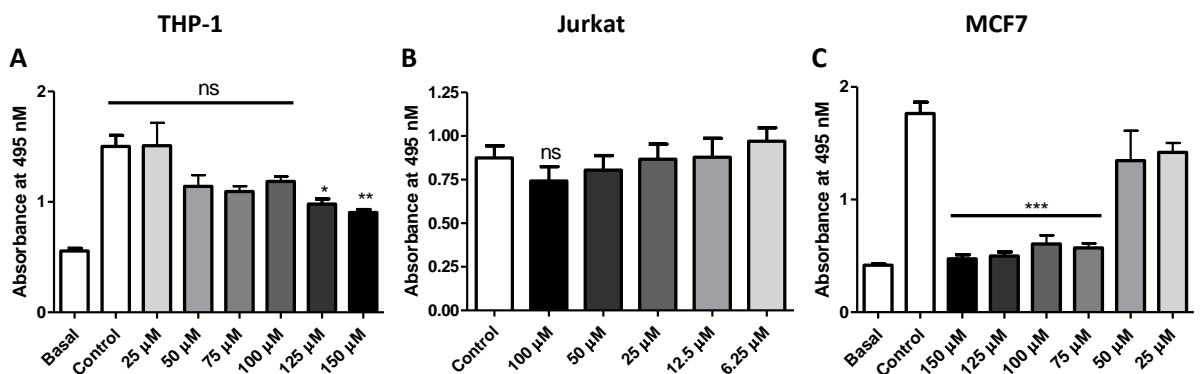


Figure 8.4: Cytotoxicity assays for NSC23766. MTS assays were over 7 hours in (A) THP-1 and (B) Jurkat and over 24 hours in (C) MCF7 cells. Basal absorbance occurs in presence of medium after MTS treatment in the absence of cells. Means  $\pm$  SEM, one-way ANOVA, post-hoc Bonferroni,  $n \geq 3$  independent experiments, \*\*\*= $p < 0.001$ , ns= $p > 0.05$ .

MTS assays showed NSC23766 produced no significant inhibition to metabolism over 7 hours in THP-1 or Jurkat at concentrations up to 100  $\mu$ M but produced toxicity above 100  $\mu$ M, whereas in MCF7 over 24 hours toxicity was apparent over 50  $\mu$ M.

### 8.2.2: *Rac1* inhibiting peptide W56 inhibits chemotaxis to CXCL12 but not CCL3

The effects of Rac1 inhibiting peptide W56, and control peptide F56, on chemotaxis in THP-1 and Jurkat were examined, figure 8.5.

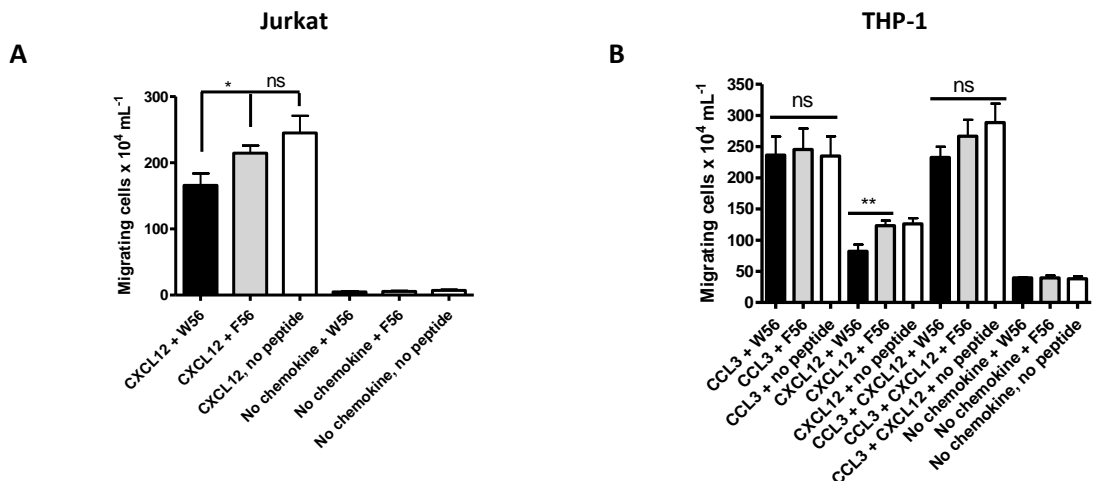


Figure 8.5: Chemotaxis assays following pre-treatment with Active Rac1 inhibiting peptide (W56) or Control peptide (F56) at 280  $\mu$ M. (A) Chemotaxis of Jurkat to 1 nM CXCL12. (B) Chemotaxis of THP-1 to 1 nM CXCL12, 1 nM CCL3 or 1 nM CCL3 + 1 nM CXCL12. Means  $\pm$  SEM, one-way ANOVA, post-hoc Bonferroni,  $n \geq 3$  independent experiments,  $**=p < 0.01$ ,  $*=p < 0.05$ ,  $ns=p > 0.05$ .

Active peptide (W56) significantly inhibited chemotaxis to CXCL12 of Jurkat and THP-1 but not THP-1 to CCL3. Control peptide (F56) at 280  $\mu$ M had no significant effect compared to untreated controls in either cell-line. MTS assays demonstrated W56 and F56 peptides had no effect on metabolism in THP-1, Jurkat or MCF7 (data not shown).

### 8.2.3: *NSC23766* and W56 inhibit CXCL12-induced but not CCL3-induced wound-healing in MCF7

Assays examined the effects of 50  $\mu$ M NSC23766, 280  $\mu$ M W56 and 280  $\mu$ M F56 on MCF7 wound-healing induced by CCL3 and CXCL12, figure 8.6.

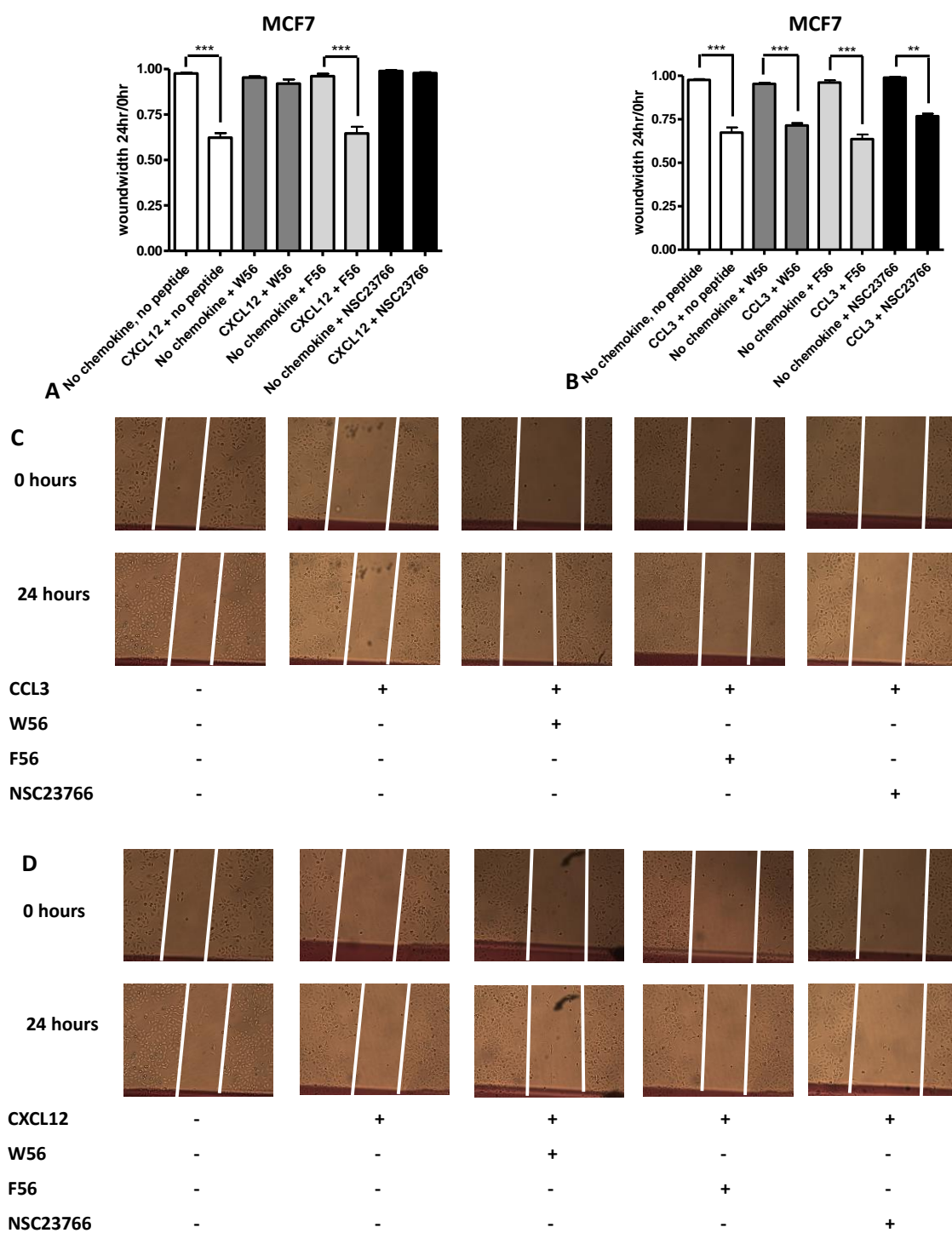


Figure 8.6: MCF7 wound-healing following pre-treatment (30 mins, 37°C) with 50  $\mu$ M NSC23766, 280  $\mu$ M W56, or 280  $\mu$ M F56. Analysis 24 hours after (A) 10 nM CXCL12, or (B) 10 nM CCL3. (C and D) representative images. Means  $\pm$  SEM, one-way ANOVA, post-hoc Bonferroni,  $n \geq 3$  independent experiments, \*\*\*= $p < 0.001$ , \*\*= $p < 0.01$ .

MCF7 chemokinesis in presence of CXCL12 but not CCL3 was significantly inhibited by both NSC23766 and W56, whereas control F56 had no effect.

#### 8.2.4: NSC23766, AMD3100 and ATI2341 inhibit CXCL12-induced Rac1 activation in MCF7

The above results suggested that in all three cell-lines Rac1 was important for CXCL12-induced migration and had little effect on CCL3-induced migration. However the dramatic effect on Jurkat migration to CXCL12 did stand out. Unfortunately Jurkat fail to migrate to other chemokines in any numbers so the effects of CXCL12 on Rac activation were explored using a Rac1 activation pull-down assay, and western blotting. Rac1 activation signal was clear in MCF7 but not detected in THP-1 or Jurkat; possibly this is not surprising as only 5-10% of Rac1 may be activated by extracellular stimulation [900]. In MCF7 NSC23766 and two CXCR4 inhibitors, AMD3100 and ATI2341, clearly inhibited Rac1 activation by CXCL12, figure 8.7.

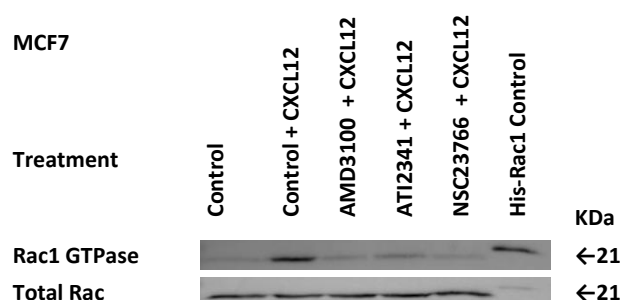


Figure 8.7: Western Blot of Rac1 activation pull-down assay, MCF7 were serum starved for 24 hours, treated with 25  $\mu$ M NSC23766, 5  $\mu$ M ATI2341 or 1  $\mu$ M AMD3100 (30 mins, 37°C) then with 10 nM CXCL12 (15 mins, 37°C), loading confirmed using total Rac.

#### 8.2.5: NSC23766 competes with CXCL12 for CXCR4 binding.

These results suggested that the responses seen with NSC23766 treatment on CXCL12-induced chemotaxis in Jurkat and THP-1 may not be predominantly due to the effects of the inhibitor on Rac1 GEFs Tiam1 or TrioN. Published research suggests NSC23766 may have off target affinity for NMDA and mACh receptors [901, 902], so investigations into NSC23766's effect on CXCR4 signalling were undertaken. Firstly chemotaxis assays to CXCL12 at a range of concentrations were conducted with NSC23766 at lower than concentrations, 25  $\mu$ M and 50  $\mu$ M, than previously used in Jurkat chemotaxis. The results suggested CXCL12 and NSC23766 may be competing for CXCR4, and/or that NSC23766 by interacting with CXCR7, is modulating CXCL12's effect on CXCR4, figure 8.8.



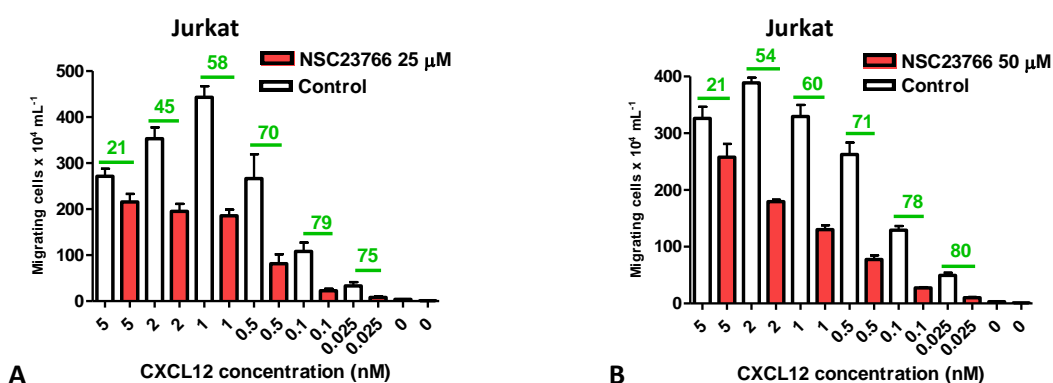


Figure 8.8: Chemotaxis assays of Jurkat treated with NSC23766 (A) 25  $\mu$ M or (B) 50  $\mu$ M to reducing concentrations of CXCL12, the ratio of treated to untreated cells migrating, at each concentration of CXCL12, are shown in green. Means  $\pm$  SEM, one-way ANOVA, post-hoc Bonferroni,  $n \geq 3$  independent experiments.

Figure 8.8 shows that the inhibitory effect of a set concentration of NSC23766 increased as the concentration of CXCL12 decreased. For example with CXCL12 at 1 nM and NSC23766 at 50  $\mu$ M the ratio of inhibition was 60; and with CXCL12 at 0.5 nM, 70. This indicated a concentration response towards CXCL12, suggesting the inhibitor and the chemokine may be competing for CXCR4. The data from the above chemotaxis assays translates to the concentration response curves below, figure 8.9.

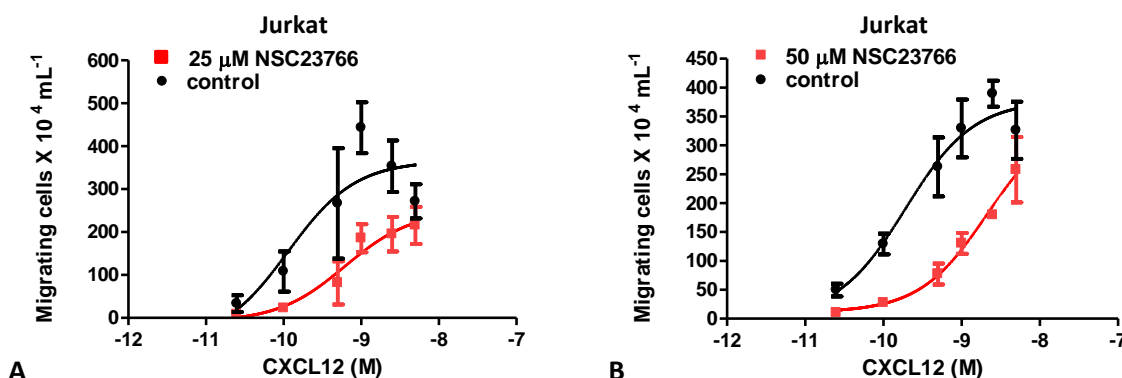


Figure 8.9: Data from figure 8.8 shown as concentration response curves towards CXCL12 comparing control or NSC23766 treatment at (A) 25  $\mu$ M or (B) 50  $\mu$ M. Means  $\pm$  SEM, one-way ANOVA, post-hoc Bonferroni,  $n \geq 3$  independent experiments.

The sigmoidal dose response curve indicates a reduction in CXCL12 potency in the presence of NSC23766. The CXCL12  $EC_{50}$  calculates as 0.19 nM in absence of NSC23766 25  $\mu$ M and as 2 nM in presence of 50  $\mu$ M NSC23766, however the efficacy of CXCL12 remains the same. This suggests NSC23766 may have been acting as a competitive antagonist of CXCR4 in these migration assays.

### 8.2.6: NSC23766 competes with CXCR4 antibody 12G5 and CXCL12

Next the effects of NSC23766 in competition with the CXCR4 antibody 12G5 were explored. 12G5 was used at saturating concentrations 10  $\mu\text{g/mL}$ , 12G5  $\text{EC}_{50}$  is reportedly  $1.9 \pm 0.5 \mu\text{g/mL}$  [903], figure 8.10.

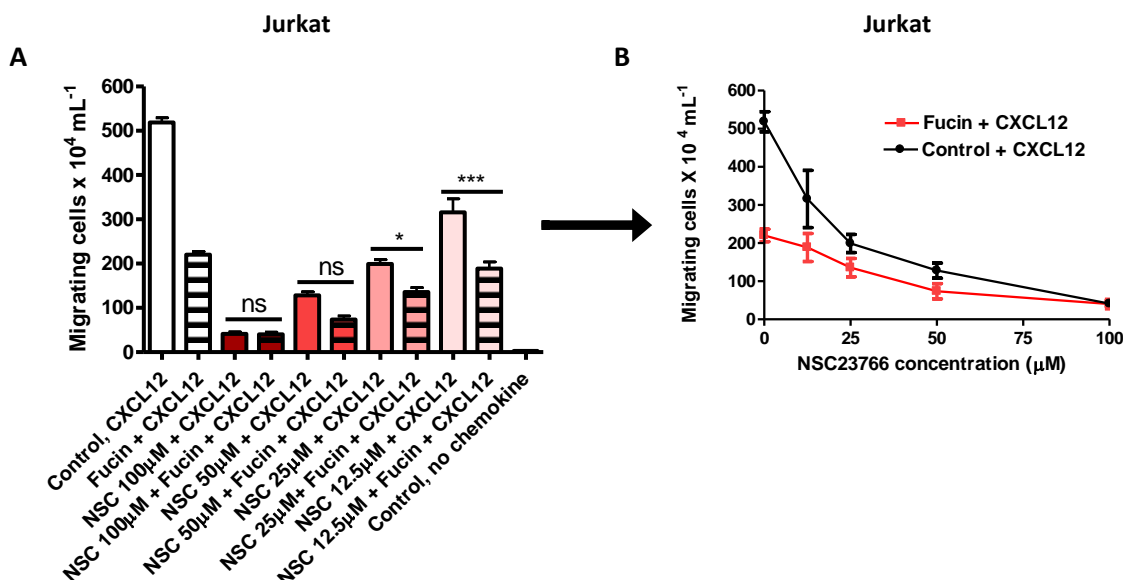


Figure 8.10: (A) Jurkat cells were treated with 10  $\mu\text{g/mL}$  12G5 and/or with NSC23766 at various concentrations before CXCL12 1nM chemotaxis assays. Means  $\pm$  SEM, one-way ANOVA, post-hoc Bonferroni,  $n \geq 3$  independent experiments, \*\*\*= $p < 0.001$ , \*=  $p < 0.05$ , ns= $p > 0.05$ . (B) Data from (A) illustrating that with CXCL12 1 nM the combined inhibitory effects on chemotaxis of NSC23766 and 12G5 reached a maximal at NSC23766 100  $\mu\text{M}$ .

Figure 8.10 illustrates that 12.5  $\mu\text{M}$  NSC23766 does not add greatly to 12G5 inhibitory effects on chemotaxis but that 25  $\mu\text{M}$  or 50  $\mu\text{M}$  NSC23766 has an additive inhibitory effect to 12G5; and at 100  $\mu\text{M}$  NSC23766 the presence or absence of 12G5 makes no difference, inhibition is at a maximum, yet compared to the absence of CXCL12 some chemotaxis to CXCL12 still occurs. This suggests CXCR4 activity is not completely abrogated by either NSC23766 100  $\mu\text{M}$  or 12G5, or the combination, hence neither is totally blocking CXCL12 stimulation. These results may suggest NSC23766 binds the same or similar sites to 12G5 and that these sites impact CXCL12 binding but do not completely abrogate the chemokine activating CXCR4. However results do not exclude the possibility that NSC23766 could be acting as an allosteric modulator, or is binding CXCR7 so modulating CXCR4/CXCR7 dimerization which could also partly but not completely inhibit chemotaxis to CXCL12.

### 8.2.7: ATI2341, AMD3100 and NSC23766 are not chemotactic to Jurkat

The small molecule CXCR4 inhibitors AMD3100 and ATI2341 were then employed to establish what response they would have in Jurkat and THP-1 chemotaxis assays to CXCL12. ATI2341 is an allosteric ligand, a pepducin. ATI2341 has a long palmitate lipidic tail to facilitate cell penetration

and a peptidic moiety derived from a 16-amino acid stretch of CXCR4 ICL1, the location it is thought to bind, figure 8.11A. None of the inhibitors used here had any chemotactic effects in Jurkat, figure 8.11B.

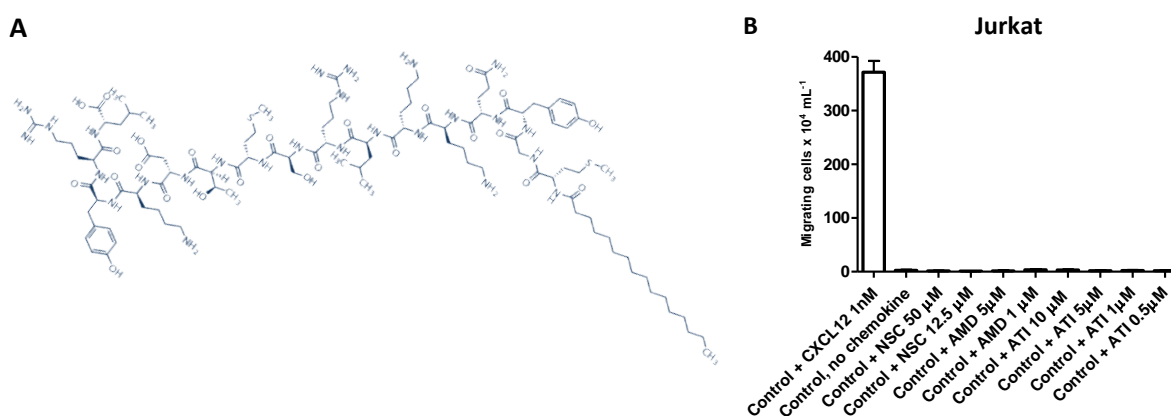


Figure 8.11: (A) Structure of ATI2341 C<sub>104</sub>H<sub>178</sub>N<sub>26</sub>O<sub>25</sub>S<sub>2</sub> (Pal-Met-Gly-Tyr-Gln-Lys-Lys-Leu-Arg-Ser-Met-Thr-Asp-Lys-Tyr-Arg-Leu), modification Met1 = N-terminal palmotoyl, Mol Wt: 2256.82. (B) Inhibitors NSC23766, AMD3100 or ATI2341 did not show any chemotactic properties towards Jurkat. Means ± SEM, n≥3 independent experiments.

Allosteric ligands bind to spatially distinct sites away from the orthosteric site, but are capable of modifying the orthosteric site conformation. Allosteric ligands can have higher receptor isoform selectivity and often have limited or subtle effects on normal spatiotemporal signalling, also their maximal effect may be determined by co-operation with endogenous ligand/s. If they affect orthosteric signalling an allosteric ligand can produce positive or negative modulation of orthosteric agonism. But equally allosteric ligands may themselves act as agonists or inverse agonists. An agonist can shift a receptor from an inactive conformation to an active one, an inverse agonist moves a receptor to an inactive state. An agonist's efficacy is a measure of the shift to an active state [904].

#### 8.2.8: CXCR4 inhibition in presence of NSC23766

MTS assays found no evidence of toxicity for AMD3100 or ATI2341 up to 10 μM, in MCF7, THP-1 or Jurkat (data not shown). The effects of ATI2341 5 μM and various concentrations of AMD3100 in combination and alone with 25 μM, 50 μM and 100 μM NSC23766 were first explored in Jurkat chemotaxis, figure 8.12.

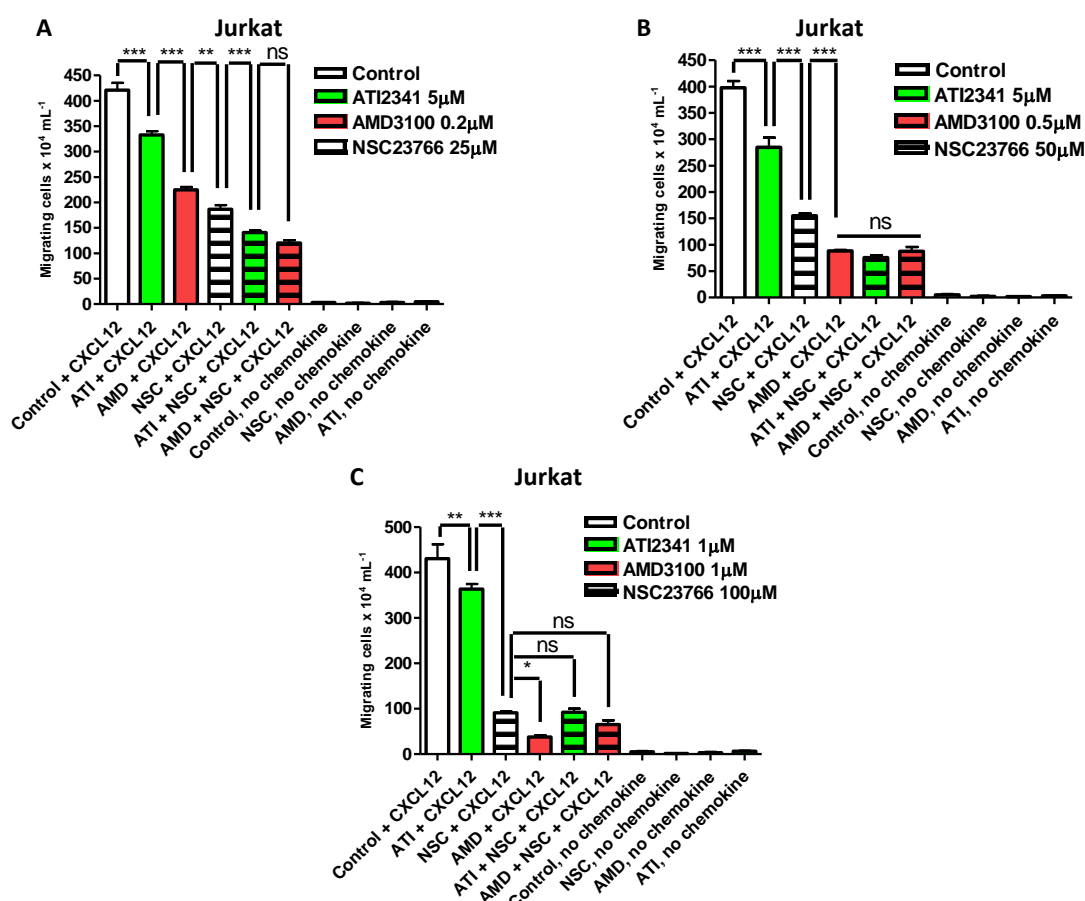


Figure 8.12: Jurkat chemotaxis following pre-treatment with AMD3100, ATI2341 and various concentrations of NSC23766 in combination. (A) Chemotaxis to 1 nM CXCL12 following 25  $\mu$ M NSC23766, 0.2  $\mu$ M AMD3100 or 5  $\mu$ M ATI2341 and in combination. (B) Chemotaxis to 1 nM CXCL12 following 50  $\mu$ M NSC23766, 0.5  $\mu$ M AMD3100 or 5  $\mu$ M ATI2341 and in combination. (C) Chemotaxis to 1 nM CXCL12 following 100  $\mu$ M NSC23766, 1  $\mu$ M AMD3100 or 1  $\mu$ M ATI2341 and in combination. Means  $\pm$  SEM, one-way ANOVA, post-hoc Bonferroni,  $n \geq 3$  independent experiments, \*\*\*= $p < 0.001$ , \*\*= $p < 0.01$ , \*= $p < 0.05$ , ns= $p > 0.05$ .

At 25  $\mu$ M NSC23766, both 0.2  $\mu$ M AMD3100 and 5  $\mu$ M ATI2341 added to inhibition of chemotaxis. At 50  $\mu$ M NSC23766 and above inhibition of chemotaxis was increased by allosteric inhibition with 5  $\mu$ M ATI2341 but the combined inhibitory effect of NSC23766 and 0.5  $\mu$ M AMD3100 was not any greater than 0.5  $\mu$ M AMD3100 alone. At 100  $\mu$ M NSC23766 neither AMD3100, nor ATI2341 added to inhibition, figure 8.12. These results support the above suggestion that in Jurkat NSC23766 may act as a competitive antagonist in CXCL12-induced chemotaxis.

#### 8.2.9: Flow cytometry demonstrated NSC23766 was displacing CXCR4 antibody 12G5

Flow cytometry was used to explore the effects of NSC23766 with Rac1-inhibiting peptide W56, and then with ATI2341, AMD3100 CXCR4 inhibitors, on CXCR4 expression in presence and absence of CXCL12, figures 8.13-8.14.

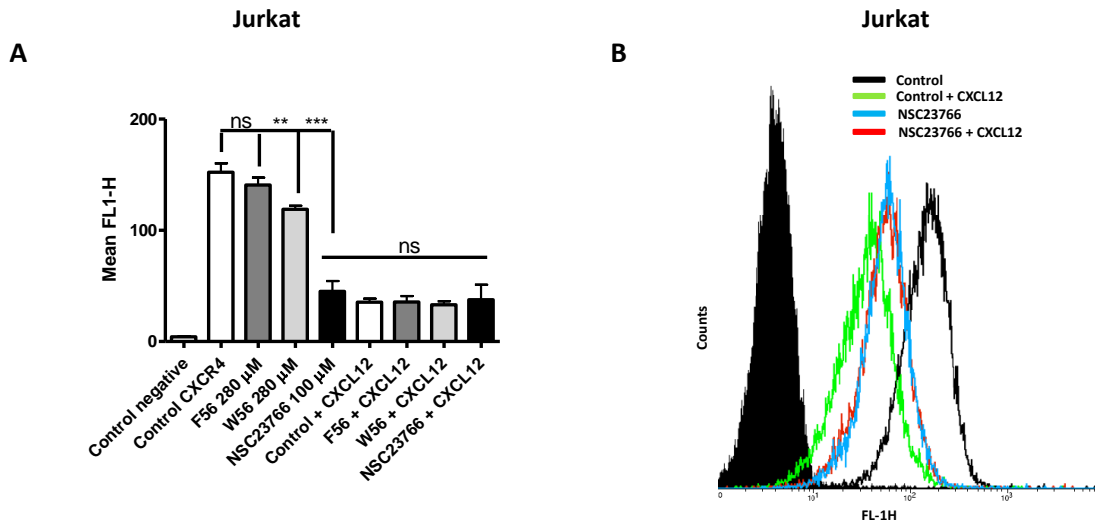


Figure 8.13: (A) Flow cytometry measurement of CXCR4 expression in Jurkat treated with NSC23766 100  $\mu$ M, F56 peptide 280  $\mu$ M or W56 peptide 280  $\mu$ M (30 mins, 37°C), followed by CXCL12 15 nM (15', 37°C) then 12G5/mouse FITC staining (both 1 hr, 4°C). Means  $\pm$  SEM, 20,000 events, one-way ANOVA, post-hoc Bonferroni,  $n \geq 3$  independent experiments, \*\*=  $p < 0.01$ , \*\*\*=  $p < 0.001$ , ns =  $p > 0.05$ . (B) Representative trace illustrating position of NSC23766 with and without CXCL12 15 nM trace compared to negative control (solid black) and control + CXCL12 15 nM.

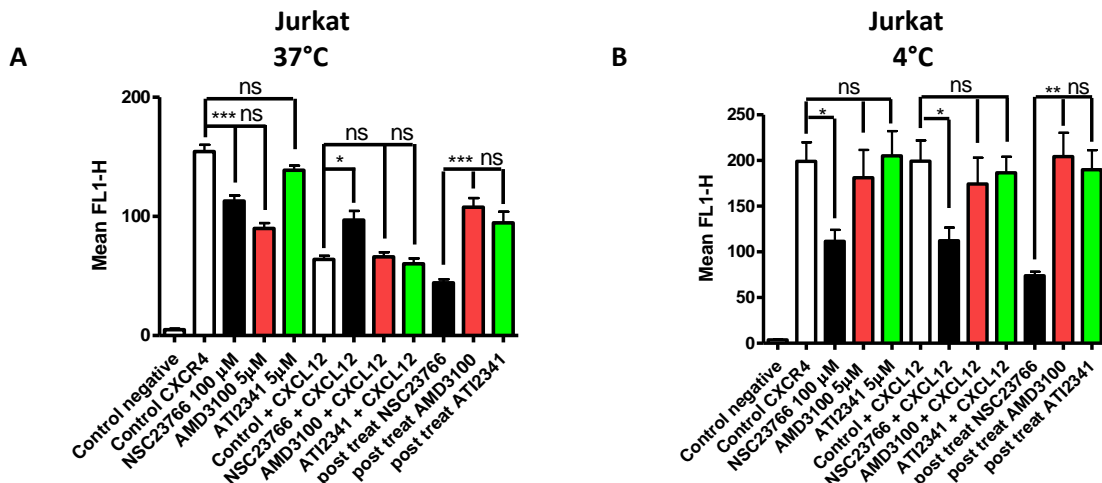


Figure 8.14: Flow cytometry measurement of CXCR4 expression in Jurkat treated with NSC23766 100  $\mu$ M, AMD3100 5  $\mu$ M or ATI2341 5  $\mu$ M (30 mins, 37°C) followed by CXCL12 15 nM for 15 minutes at (A) 37°C and (B) 4°C, in both cases followed by 12G5/mouse FITC staining (both 1 hour, 4°C). Post treatment is control with inhibitors added after 12G5/FITC at (A) 37°C, 30 minutes or (B) 4°C, 30 minutes. Means  $\pm$  SEM, 20,000 events, one-way ANOVA, post-hoc Bonferroni,  $n \geq 3$  independent experiments, \* =  $p < 0.05$ , \*\* =  $p < 0.01$ , \*\*\* =  $p < 0.001$ , ns =  $p > 0.05$ .

The flow cytometry clearly shows CXCL12 causes internalisation of CXCR4 in Jurkat, this internalisation is prevented when the system is kept at 4°C, figure 8.14. The Rac peptide W56 did cause some loss of receptor from the cell surface compared to F56 control but this was marginal compared to the effect of NSC23766 100  $\mu$ M, figure 8.13. It can be seen that NSC23766 controls

the CXCR4 signal loss in presence and absence of CXCL12, and NSC23766 activity is not substantially affected by temperature, figure 8.14.

#### 8.2.10: Rac1 inhibitor ETH1864 does not modify 12G5 binding or CXCL12-triggered CXCR4 internalisation

To explore if the NSC23766 flow cytometry results could be due to Rac1 inhibition the experiment was repeated using 10  $\mu$ M ETH1864 which binds and directly inhibits Rac1, Rac2 and Rac3, figure 8.15.

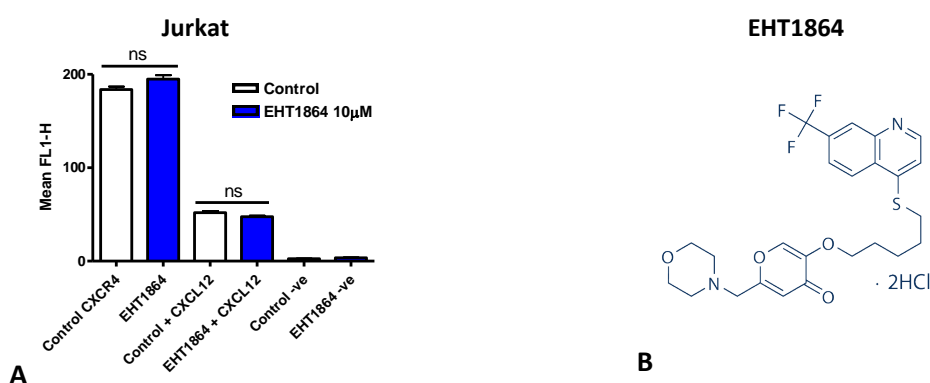


Figure 8.15: (A) Flow cytometry measurement of CXCR4 expression in Jurkat pre-treated with ETH1864 10  $\mu$ M (30', 37°C) followed by CXCL12 15 nM (15', 37°C) followed by 12G5/mouse FITC staining (both 1 hr, 4°C). Means  $\pm$  SEM, 20,000 events, one-way ANOVA, post-hoc Bonferroni,  $n \geq 3$  independent experiments, ns =  $p > 0.05$ . (B) Structure of ETH1864.

The ETH1864 had no effect on CXCR4 internalisation indicating that direct Rac inhibition did not explain results.

#### 8.2.11: Sucrose and sodium azide pre-treatment does not stop NSC23766 causing CXCR4 internalisation

Endocytosis is a process that requires energy so to further examine if NSC23766 was causing endocytosis the flow cytometry with AMD3100 and NSC23766 was repeated in the presence of sodium azide at 9 mM to deplete cellular ATP [905] and sucrose at 0.4 M which can inhibit endocytosis, figure 8.16.

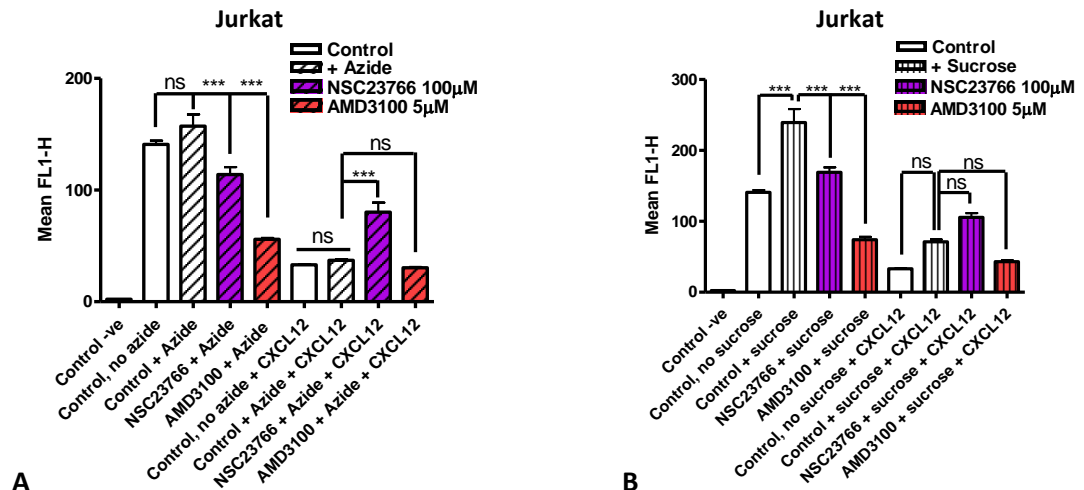


Figure 8.16: (A) Flow cytometry measurement of CXCR4 expression in Jurkat pre-treated with (A) sodium azide 9 mM (30', 37°C) or (B) Sucrose 0.4 M (30', 37°C) then NSC23766 100  $\mu$ M or AMD3100 5 $\mu$ M (30', 37°C) followed by CXCL12 15 nM (15', 37°C) followed by 12G5/mouse FITC staining (both 1 hr, 4°C). Means  $\pm$  SEM, 20,000 events, one-way ANOVA, post-hoc Bonferroni,  $n \geq 3$  independent experiments, ns= $p > 0.05$

Flow cytometry showed that NSC23766 and AMD3100 continued to influence endocytosis in response to CXCL12 after pre-treatment of Jurkat with sodium azide or sucrose, figure 8.16. Sodium azide non-significantly increased CXCR4 expression, in control, in absence but not presence of CXCL12. AMD3100 and NSC23766 both reduced CXCR4 basal signal. In presence of sodium azide NSC23766 but not AMD3100 very significantly increased CXCR4 expression after CXCL12 stimulation. Sucrose very significantly increased CXCR4 basal signal before but not after CXCL12 stimulation, so in the absence of CXCL12 sucrose does hinder CXCR4 internalisation. AMD3100 and NSC23766 reduced CXCR4 basal signal similarly in the presence of sucrose before CXCL12 stimulation but neither significantly changed CXCR4 signal after CXCL12 treatment.

#### 8.2.12: NSC23766 may act as a biased antagonist with respect to cAMP signalling

The CXCR4 receptor couples to heterotrimeric G-proteins, including  $G_{\alpha_i}$ ;  $G_{\alpha_i}$  responses include reduction of cellular second messenger cAMP levels, figure 8.17.

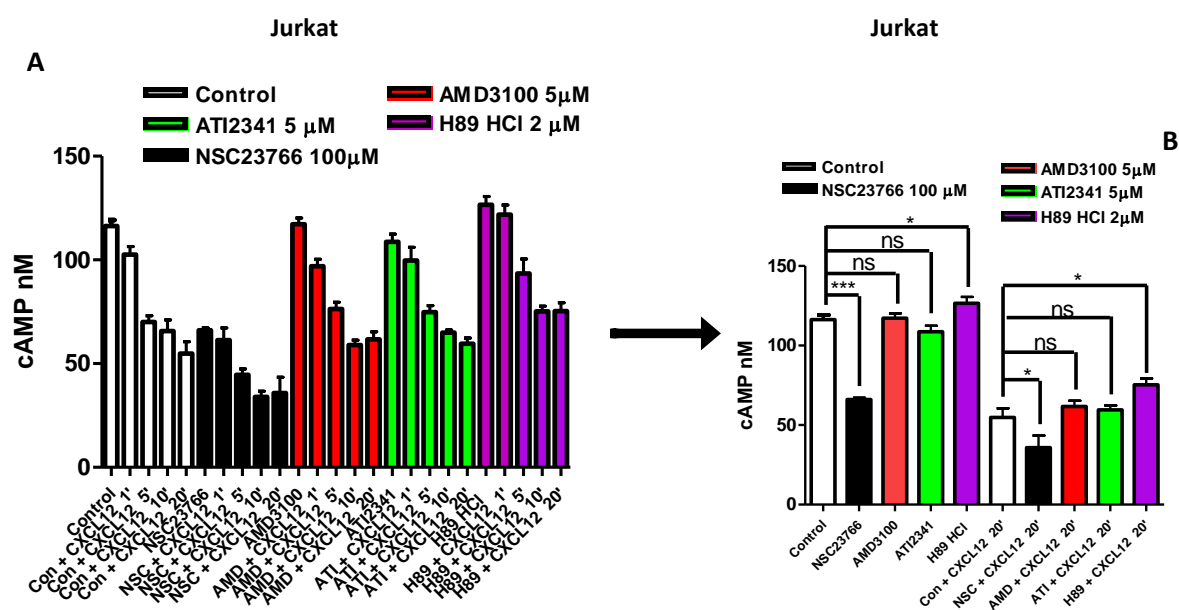


Figure 8.17: (A) Jurkat cAMP production following NSC23766 100 μM, AMD3100 5 μM, ATI2341 5 μM, PKA inhibitor H89 HCl 2 μM or control (30 mins, 37°C) measured before or after 1, 5, 10 or 20 minutes CXCL12 stimulation (10 nM, 37°C) (cells pre-treated with IBMX 0.75 mM & Forskolin 20 μM). (B) Control and 20 minute data from A. Means ± SEM, one-way ANOVA, post-hoc Bonferroni,  $n \geq 3$  independent experiments, \*\*\* =  $p < 0.001$ , \*\* =  $p < 0.01$ , \* =  $p < 0.05$ , ns =  $p > 0.05$ .

Compared to control NSC23766 very significantly reduced basal cAMP levels and significantly reduce cAMP levels after CXCL12 stimulation. AMD3100, ATI2341 did not significantly change basal levels or those after CXCL12 treatment, and H89 HCl statistically significantly increased cAMP levels both before and after 20 minutes CXCL12 treatment, figure 8.17.

### 8.2.13: cAMP levels may modulate PKCζ signalling

The RhoGEF Tiam1 has been reported to sit in a feedback loop involving cAMP, Rac1, PKCζ and CXCR4. Increasing cAMP levels has been shown to increase the presence of membrane CXCR4, by both reducing CXCR4 endocytosis, prolonging CXCR4's stay at the membrane, and increasing the speed of recycling CXCR4 back to the membrane from endosomes [906]. Increasing cAMP also antagonises CXCL12-induced receptor internalisation [907].

The effects of siRNA inhibition of PKCζ on CXCL12 chemotaxis in Jurkat, along with CXCL12 and CCL3 wound-healing in MCF7 cells confirmed the involvement of PKCζ in the CXCL12 and CCL3 signalling pathways, figure 8.18.



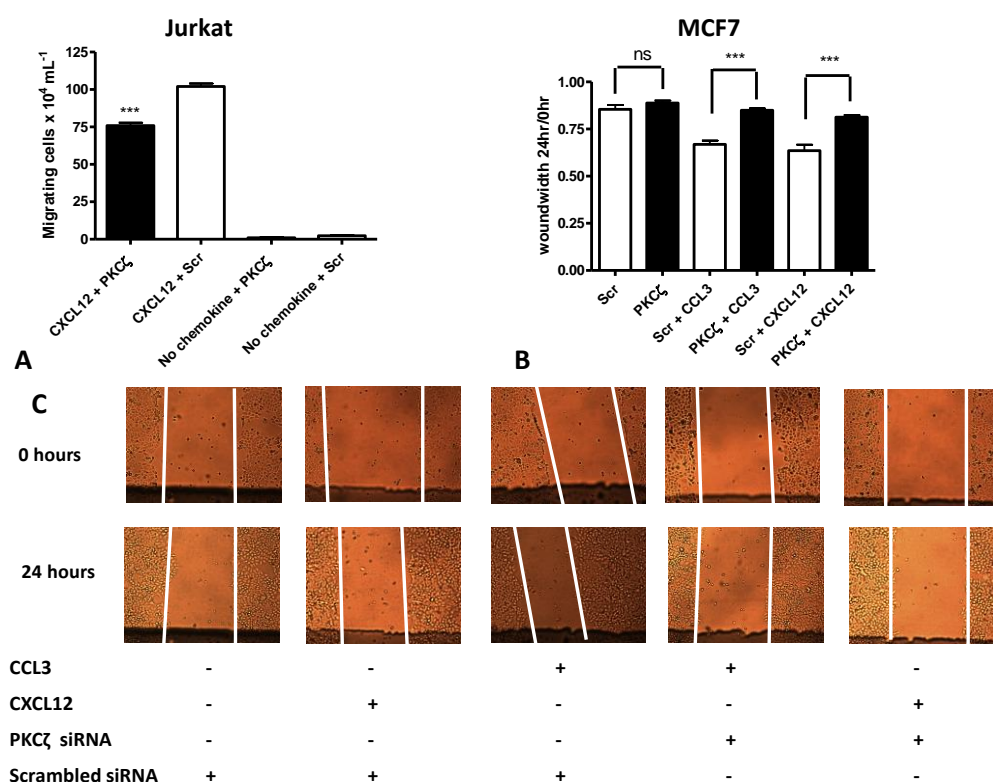


Figure 8.18: Transfection with 50 nM PKC $\zeta$  siRNA or nonsense siRNA (Scr) control. (A) Jurkat chemotaxis to CXCL12 (B) MCF7 wound-healing, analysis 24 hours after 10 nM CCL3, or CXCL12 Means  $\pm$  SEM, one-way ANOVA, post-hoc Bonferroni,  $n \geq 3$  independent experiments, \*\*\*= $p < 0.001$ , ns= $p > 0.05$ . (C) Wound-healing images.

The success of the PKC zeta siRNA 50 nM (PRKCZ6) knockdown was confirmed by western blotting, knockdown was very successful in MCF7, figure 8.19.

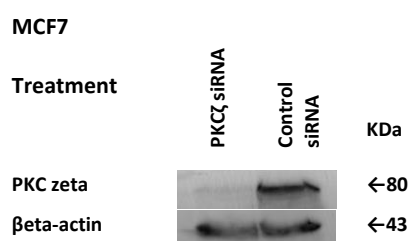


Figure 8.19: Western Blot and PKC $\zeta$  antibody reveals PKC $\zeta$  expression in MCF7 24 hours after siRNA knockdown,  $\beta$ -actin loading control.

#### 8.2.14: Effects of NSC23766 on intracellular calcium

Tiam1 does not have a calcium-calmodulin binding site but can be phosphorylated, and so activated, by calcium-calmodulin-dependent protein kinase II [908]. Hence Rac activation may be influenced by intracellular calcium levels. This is thought to occur via disruption of Rac-Rho-GDI complex orchestrated by PKC and translocation of Rac to the membrane where it is activated by GEFs [909]. To help understand the relationship of intracellular calcium signalling and Rac-1

inhibition with NSC23766, THP-1 were pre-treated with NSC23766 and Fura2-AM then stimulated by CXCL12 10 nM or CCL3 100 nM, figure 8.20.

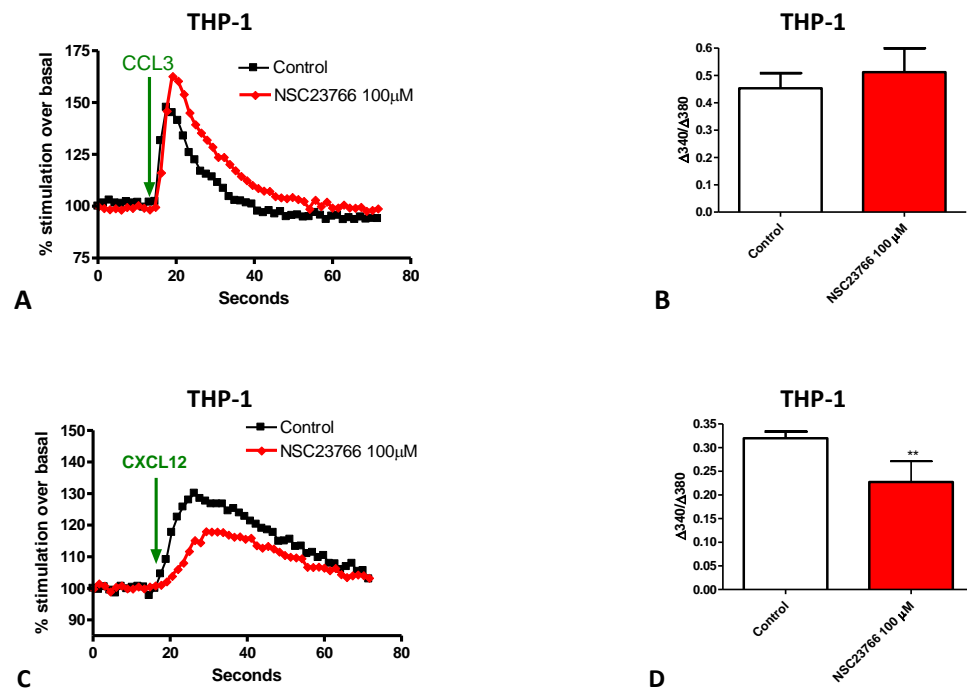


Figure 8.20: Fura2  $\text{Ca}^{2+}$  assay in THP-1 following 100  $\mu\text{M}$  NSC23766 or control. Data expressed as fluorescence ratio change ( $\Delta 340/\Delta 380$  nm) i.e. peak fluorescence following CCL3 or CXCL12 addition minus basal fluorescence (prior to chemokine). (A & B) THP-1 responses to CCL3 10 nM (C & D) responses to CXCL12 10 nM (B & D) Means  $\pm$  SEM, Student t-test,  $n \geq 3$  independent experiments, \*\*= $p < 0.01$ .

NSC23766 produced opposite effects on calcium signalling in THP-1 in response to CXCL12 and CCL3, figure 8.20, again suggesting it may be having a direct effect on CXCR4 or a modulator of CXCR4 and CCR5. It also dramatically reduced calcium signalling in response to CXCL12 in Jurkat, and dose dependently in MCF7, figure 8.21.

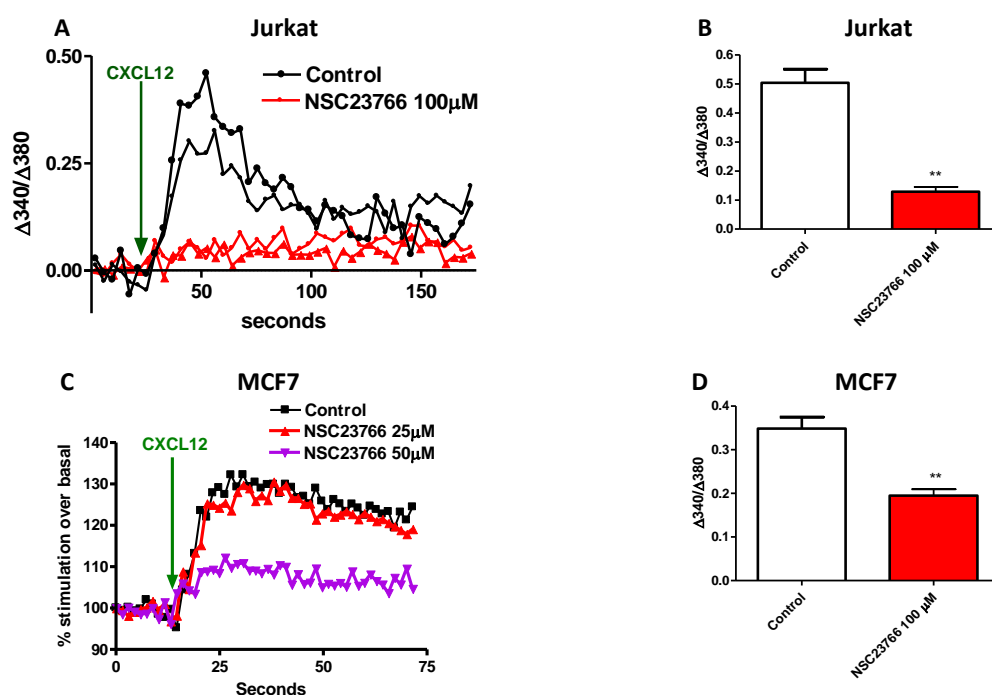


Figure 8.21: Fura2  $\text{Ca}^{2+}$  assay in Jurkat and MCF7 following NSC23766 or control. Data expressed as fluorescence ratio change ( $\Delta 340/\Delta 380$  nm) i.e. peak fluorescence following CXCL12 10 nM addition minus basal fluorescence (prior to chemokine). (A & B) Jurkat (C & D) MCF7 (B & D) Means  $\pm$  SEM, Student t-test,  $n \geq 3$  independent experiments,  $**=p < 0.01$ .

NSC23766 produces very significant inhibition of calcium release in response to CXCL12 in both Jurkat and MCF7. As expected both chemokines produced a rapid but transient rise in calcium release. The biased effects of NSC23766 suggested either that Rac1 activation relates to CXCL12-induced but not CCL3-induced calcium signalling, or that NSC23766 is having a direct or indirect effect on CXCR4. CXCL12 was found to trigger calcium release in Jurkat dose dependently up to 10 nM, figure 8.22, and NSC23766 at 100  $\mu\text{M}$  was found to inhibit this calcium release, but this inhibition was eroded as CXCL12 dose increased to 100 nM. NSC23766 and CXCL12 appeared to be competing for CXCR4.

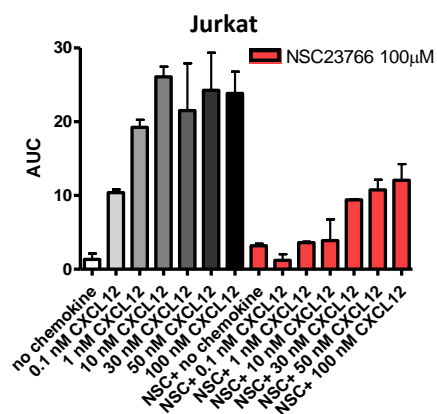


Figure 8.22: Fura2  $\text{Ca}^{2+}$  assay in Jurkat following 100  $\mu\text{M}$  NSC23766 or control. Data expressed as AUC following CXCL12 addition when peak release is normalised to stimulation over basal ( $\Delta 340/\Delta 380$ ). Means  $\pm$  SEM, Student t-test,  $n \geq 3$  independent experiments.

Further investigations compared the effects of NSC23766 and CXCR4 inhibitors AMD3100 and ATI2341 on calcium release in Jurkat, figure 8.23.

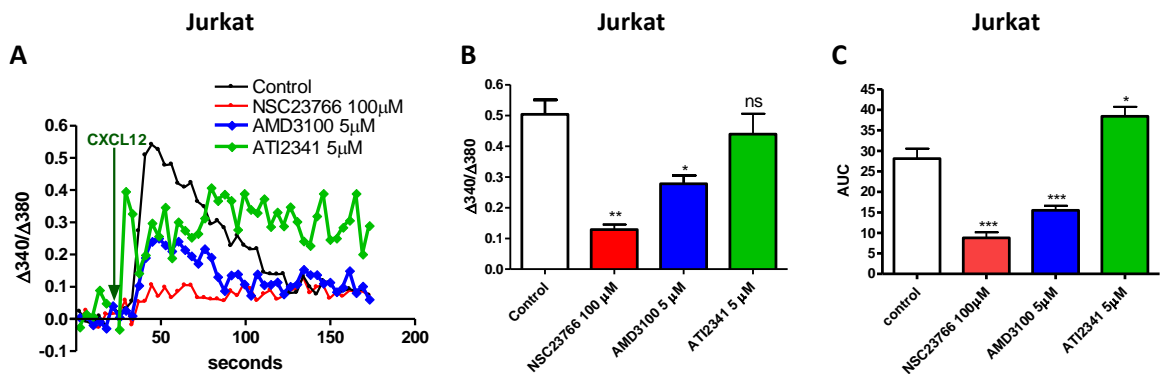


Figure 8.23: Fura2  $\text{Ca}^{2+}$  assay in Jurkat treated with NSC23766 100  $\mu\text{M}$ , ATI2341 5  $\mu\text{M}$  or AMD3100 5  $\mu\text{M}$ . (A) Fluorescence ratio change ( $\Delta 340/\Delta 380$  nm) i.e. peak fluorescence following 10 nM CXCL12 addition minus basal fluorescence (prior to chemokine). (B) Means  $\pm$  SEM, one-way ANOVA, post-hoc Bonferroni,  $n \geq 3$  independent experiments, (C) Area under curve from B, \*\*\*= $p < 0.001$ , \*\*= $p < 0.01$ , \*= $p < 0.05$ ,  $ns = p > 0.05$ .

NSC23766 and AMD3100 caused very significant inhibition of calcium release in Jurkat, figure 8.23, whereas ATI2341 has no significant effect on peak release but when the trace is analysed as area under curve it is apparent that ATI2341 causes a significant ( $p < 0.05$ ) increase in the overall calcium release.

### 8.2.15: U73122 inhibits PLC signalling

$\text{IP}_3$  receptors can be influenced by many intracellular signals including phosphorylation by PKC and Rho kinases [910]. If the signalling effects above are due to NSC23766 inhibiting Rac1 then inhibiting U73122 should modestly mirror NSC23766 inhibition to CCL3 and CXCL12 chemotaxis and calcium flux and cAMP responses, figures 8.24-8.26.

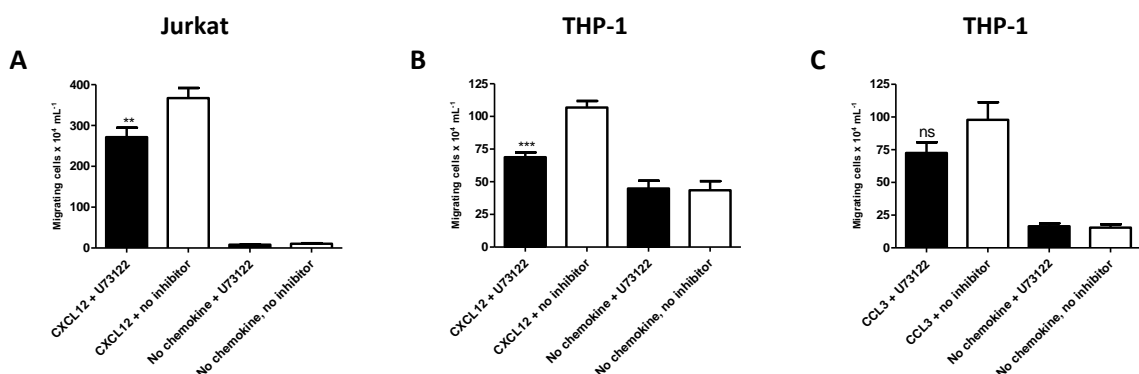


Figure 8.24: Chemotaxis assays following pre-treatment with U73122 10 nM or control. (A) Chemotaxis of Jurkat to 1 nM CXCL12. (B) THP-1 chemotaxis to 1 nM CXCL12. (C) THP-1 chemotaxis to 1 nM CCL3. Means  $\pm$  SEM, one-way ANOVA, post-hoc Bonferroni,  $n \geq 3$  independent experiments, \*\*\*= $p < 0.001$ , \*\*= $p < 0.01$ ,  $ns = p > 0.05$ .

U73122 at very low concentration significantly inhibited chemotaxis to CXCL12 in both Jurkat and THP-1, but failed to statistically significantly inhibit chemotaxis to CCL3 in THP-1.

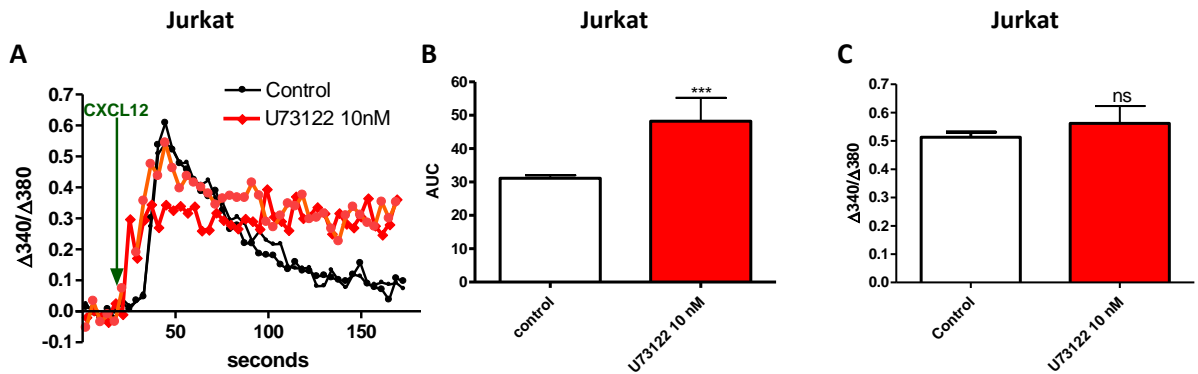


Figure 8.25: Fura2  $\text{Ca}^{2+}$  assay in Jurkat following 10 nM U73122 or control. Data expressed as fluorescence ratio change ( $\Delta 340/\Delta 380$  nm) i.e. peak fluorescence following 10 nM CXCL12 addition minus basal fluorescence (prior to chemokine). (A) Trace  $n=1$ , (B & C) Means  $\pm$  SEM, Student t-test,  $n \geq 3$  independent experiments, \*\*\*= $p < 0.001$ , \*\*= $p < 0.01$ , \*= $p < 0.05$ , ns = $p > 0.05$ .

U73122 10 nM also caused changes in calcium responses in Jurkat to CXCL12 which were apparent from the trace and AUC, figure 8.25.

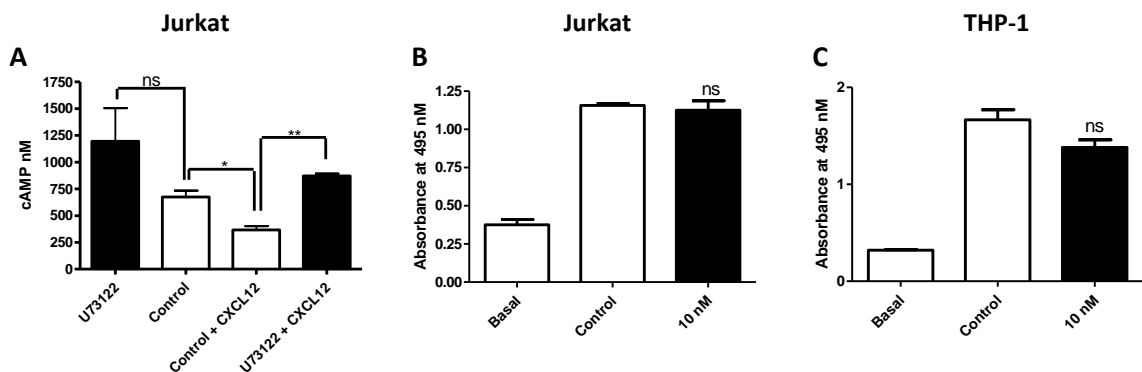


Figure 8.26: (A) cAMP production in Jurkat following 10 nM U73122 or control measured before or after 20 minutes CXCL12 10 nM stimulation (cells pre-treated with IBMX 0.75 mM & Forskolin 20  $\mu\text{M}$ ). (B & C) Cytotoxicity assays for U73122. MTS assays were over 7 hours in (B) Jurkat and (C) THP-1. Basal absorbance occurs in presence of medium after MTS treatment in the absence of cells. Means  $\pm$  SEM, one-way ANOVA, post-hoc Bonferroni,  $n \geq 3$  independent experiments, \*\*= $p < 0.01$ , \*= $p < 0.05$ , ns= $p > 0.05$ .

cAMP production in Jurkat following CXCL12 10 nM stimulation showed U73122 significantly increased levels reached in response to CXCL12. MTS assays confirmed observed effects were not due to U73122 toxicity. Although figures 8.25-8.27 above show there was some correlation

between Jurkat responses to NSC23766 and U73122 with respect to inhibition of CXCL12 and not CCL3 chemotaxis, the inhibitors had opposite effects on calcium release and cAMP levels in Jurkat.

#### 8.2.16: Inhibiting Cdc42 reduced migration towards CCL3 and CXCL12

Rac 1 regulates actin polymerization through WAVE complex proteins. WAVE activates ARP2/3 triggering actin polymerization [911]. Cdc42 working through WASP proteins also produces ARP2/3 actin nucleation [912]. Additionally Cdc42 contributes to polarized cell migration [746], and aids transmigration by causing filopodia extensions into the epithelium [911]. Cdc42 also supports cells' polarity by inhibiting lamellipodium formation in uropodium [913]. Inhibition of Cdc42 with ZCL278 was found to inhibit both CCL3 and CXCL12 chemotaxis, figure 8.27. ZCL278 and NSC23766 do appear to hinder F-actin polymerization, figure 8.28.

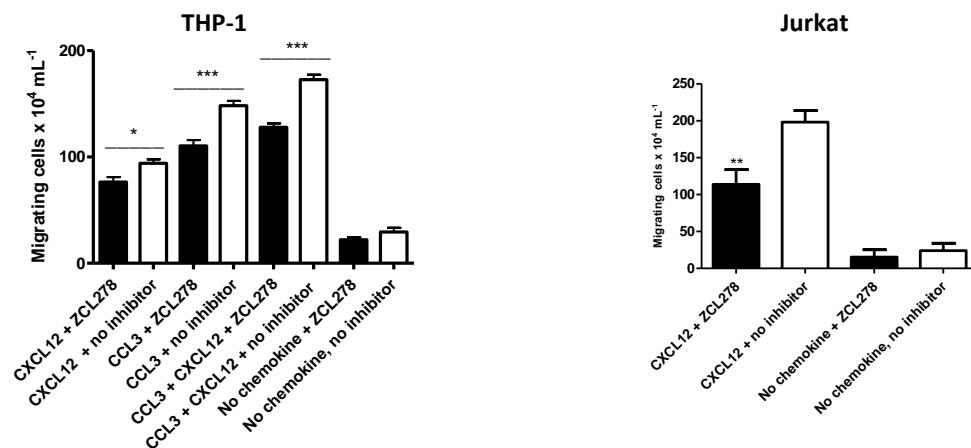


Figure 8.27: Chemotaxis assays following pre-treatment with ZCL278 or control. (A) Chemotaxis of THP-1 to 1 nM CCL3 or CXCL12 or both. (B) Jurkat chemotaxis to 1 nM CXCL12. Means  $\pm$  SEM, one-way ANOVA, post-hoc Bonferroni,  $n \geq 3$  independent experiments, \*\*\*= $p < 0.001$ , \*\*= $p < 0.01$ , \*= $p < 0.05$ .

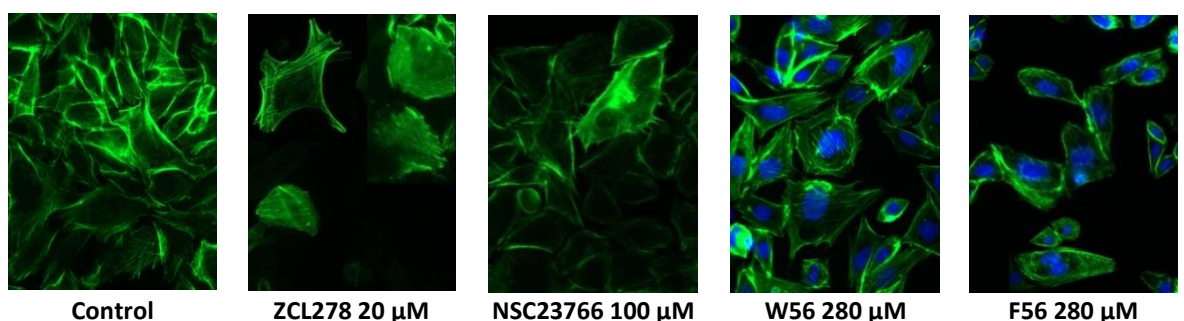


Figure 8.28: Filament actin stains. Alexa-488 Phalloidin (green) and DAPI nuclear stains (blue) of CHO.CCR5 following pre-treatment with ZCL278, W56, F56 or NSC23766 (1 hr, 37°C). Imaged UV inverted microscopy (Leica DMII Fluorescence microscope 500x Ex 490 nm, Em 520 nm).

### 8.2.17: W56 and NSC23766 both inhibit CXCL12- but not CCL3-induced cofilin phosphorylation

Rac1 regulation of lamellipodia also involves cofilin, reviewed in chapter five, therefore the effects of Rac1 inhibitors W56 and NSC23766 on cofilin phosphorylation triggered by CXCL12 were explored, figure 8.29.

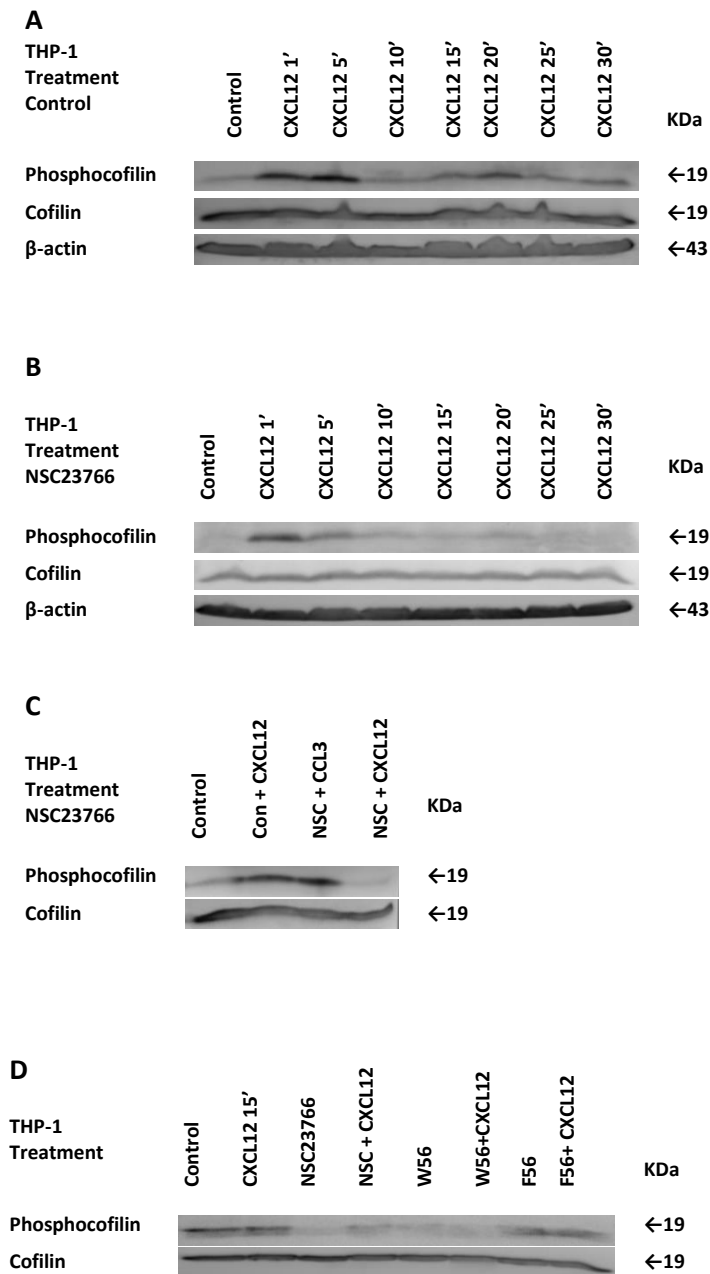


Figure 8.29: Total-cofilin and phosphocofilin (Ser3) antibodies reveals cofilin phosphorylation levels in THP-1 (A) Control treated with CXCL12 5 nM over 1, 5, 10, 15, 20, 25, or 30 minutes at 37°C. (B) Treated with NSC23766 100 μM (30', 37°C) then CXCL12 5 nM over 1, 5, 10, 15, 20, 25, or 30 minutes (37°C) (C) Control or treated with NSC23766 100 μM (30', 37°C) then CXCL12 5 nM or CCL3 5 nM (15', 37°C) (D) Control or treated with NSC23766 100 μM, W56 280 μM, or F56 280 μM (all 30', 37°C) then CXCL12 5 nM (15', 37°C). β-actin loading control.

Cofilin phosphorylation in THP-1 was observed to occur in response to CXCL12 in two waves, figure 8.29, initially as a response detectable at 1 and 5 minutes, which is lost by 10 minutes and returns at 15 minutes onwards. Treatment with NSC23766 inhibited the early and eliminated the later phosphorylation.

#### 8.2.18: NSC23766 also inhibits chemotaxis of THP-1 to CXCL11 but not to CXCL9 or CCL2

The effect of NSC23766 and W56 and F56 was explored on CXCL11, CXCL9 and CCL2 chemotaxis in THP-1 cells, figure 8.30.

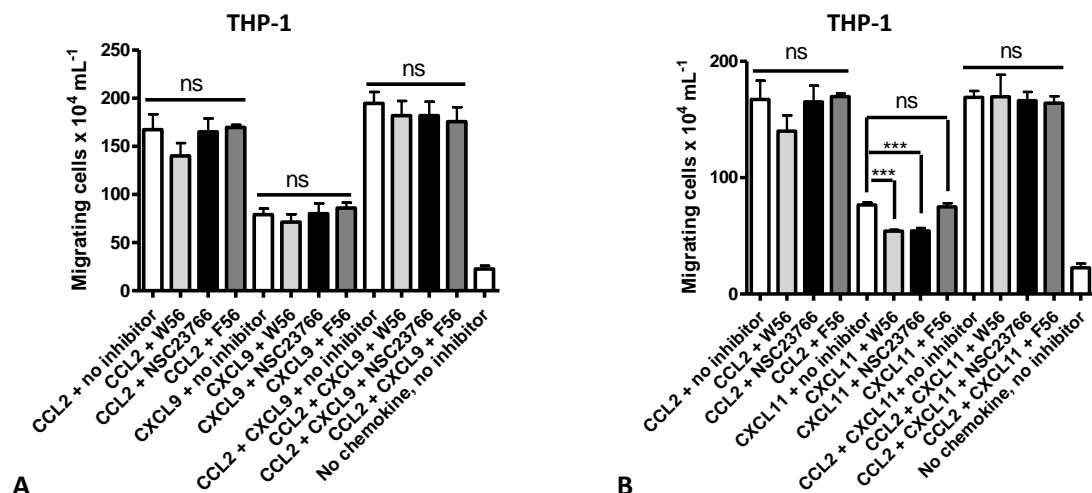


Figure 8.30: Chemotaxis assays following pre-treatment with 100μM NSC23766, 280μM F56 or W56, or control. (A) Chemotaxis of THP-1 to 1 nM CCL2 and/or 1 nM CXCL9. (B) THP-1 chemotaxis to 1 nM CCL2 and/or 1 nM CXCL11. Means ± SEM, one-way ANOVA, post-hoc Bonferroni, n≥3 independent experiments, \*\*\*=p<0.001, ns=p>0.05.

THP-1 migration towards CCL2 or CXCL9 was not reduced by either NSC2376, W56 or F56 whereas both NSC23766 and W56 reduced migration towards CXCL11, figure 8.30.

#### 8.2.19: CXCL14 modulates CXCR4/CXCL12 signalling in Jurkat

CXCL14 is a non ELR CXC chemokine with similarities in structure to CXCL12. The N-terminus of a chemokine interacts with its receptor, in CXCL14 this NH<sub>2</sub> tail is shorter than in CXCL12 or CXCL11 [914], and contains a unique amino acid sequence which appears to be CXCL14's 'Achilles heel' in cancer. The sequence allows CXCL14 to be targeted for ubiquitination and degraded by proteasomes, but this may occur only in malignant and immortalised cells. Destroying CXCL14 may help cancer cells hide from the immune system [915]. High expression of CXCL14 is linked to improved overall and event free survival in some cancers [916]. This may explain why responses to CXCL14 dramatically differ in various primary and malignant cell-lines, for example in cells that express CXCL14, like monocytes and THP-1, CXCL14 is chemotactic, *in vivo* this may support CXCL14's role in immune surveillance, however CXCL14 can also inhibit endothelial cell migration, proliferation and be angiostatic [917]. Jurkat do not express CXCL14 [918]. Although CXCL14 alone



in some cells expressing CXCR4 will not induce chemotaxis, calcium responses, or trigger Rac1 signalling alone, it may potentiate or antagonise CXCL12 responses and affect cell-surface distribution of CXCR4 [919]. Hence the effects of CXCL14 on Jurkat chemotaxis and calcium responses to CXCL12 and CXCR4 internalisation in presence of NSC23766 and W56 were investigated, figures 8.31-8.33.

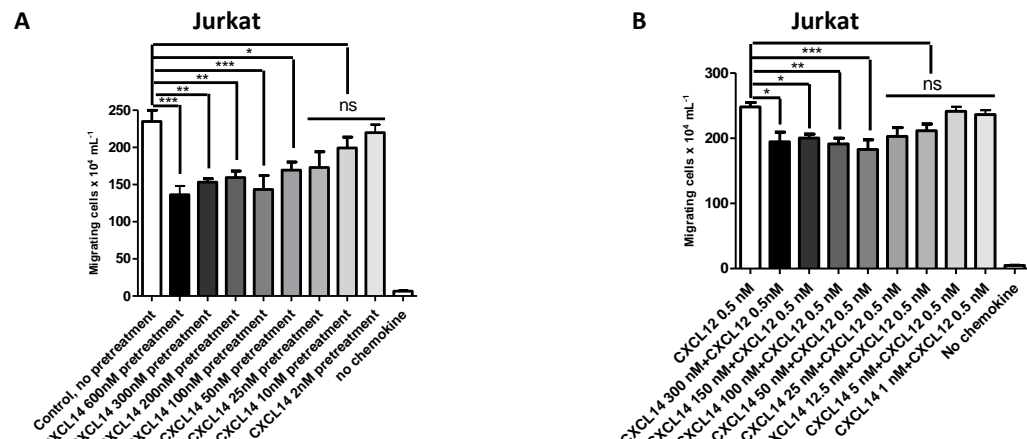


Figure 8.31: CXCL14 inhibits Jurkat chemotaxis to CXCL12. (A) Chemotaxis to 1 nM CXCL12 following pre-treatment with 2 nM to 600 nM of CXCL14 (30 mins, 37°C). (B) Chemotaxis to 0.5 nM CXCL12 and 1 to 300 nM CXCL14, no pre-treatment. Means  $\pm$  SEM, one-way ANOVA, post-hoc Bonferroni,  $n \geq 3$  independent experiments, \*\*\*= $p < 0.001$ , \*\*= $p < 0.01$ , \*= $p < 0.05$ , ns= $p > 0.05$ .

Figure 8.31 illustrates that even high concentrations of CXCL14, either as pre-treatment or mixed with CXCL12 as chemoattractant, inhibited but did not completely prevent chemotaxis of Jurkat to CXCL12. CXCL14 pre-treatment was found to dose-dependently inhibit chemotaxis to CXCL12 1 nM by up to about ~45%, whereas in the presence of 0.5 nM CXCL12, CXCL14 at concentrations above 50 nM reduce chemotaxis by ~25%, suggesting concentration of these two chemokines is key.

The effects of CXCL14 on calcium flux in Jurkat were also explored, figure 8.32.

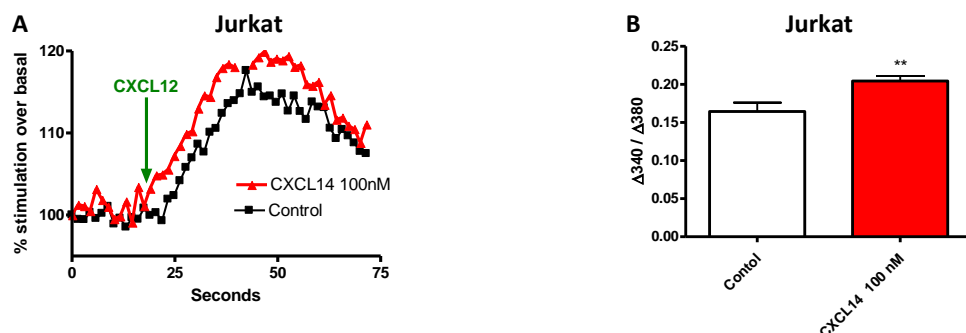


Figure 8.32: Fura2 Ca<sup>2+</sup> assay in Jurkat following pre-treatment with 100 nM CXCL14 or control. Data expressed as fluorescence ratio change ( $\Delta 340 / \Delta 380$ ) i.e. peak fluorescence following 10 nM CXCL12 addition minus basal fluorescence (prior to chemokine). (A) Trace (B) Means  $\pm$  SEM, Student t-test,  $n \geq 3$  independent experiments, \*\*= $p < 0.01$ .

Figure 8.32 demonstrated that in Jurkat CXCL14 pre-treatment significantly increased both the speed and volume of calcium response to CXCL12. Finally flow cytometry experiments were undertaken to establish the effect of CXCL14 on CXCR4 internalization triggered by CXCL12 in presence and absence of NSC23766 and W56, figure 8.33.

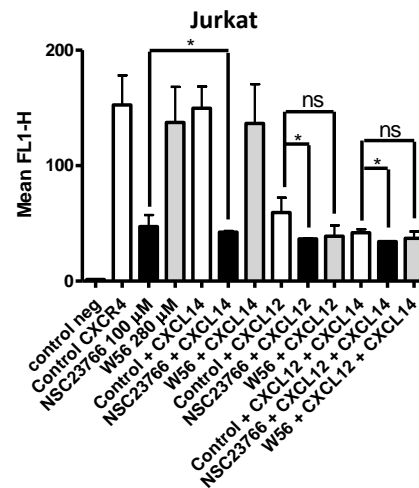


Figure 8.33: Flow cytometry measurement of CXCR4 expression in Jurkat pre-treated with NSC23766 100 μM, W56 280 μM or control (30 mins 37°C) followed by CXCL12 15 nM or CXCL14 100 nM (15 mins, 37°C) followed by 12G5/mouse FITC staining (both 1 hour, 4°C). Means ± SEM, 20,000 events, one-way ANOVA, post-hoc Bonferroni, n=2 independent experiments, \*=p<0.05, ns=p>0.05.

NSC23766 but not W56 was found to significantly reduce the expression of CXCR4 in the presence of CXCL14 and in the presence of CXCL12 and CXCL14, figure 8.33, both chemokines reputedly bind and cause internalisation of CXCR4, NSC23766 at 100 μM potentiated their effects.

### 8.3: Discussion

Results indicate specific Rac1 signalling differences in CCL3- and CXCL12-induced cell migration and suggest a surprising role for NSC23766 as a allosteric modulator of CXCR4.

#### 8.3.1: Rac1 inhibitor produces chemokine specific responses

Figures 8.2, 8.5 and 8.6 indicate Rac1 inhibition specifically inhibits migration to CXCL12 but not CCL3. In contrast Cdc42 inhibition equally inhibits both CCL3 and CXCL12 chemotaxis, figure 8.27. Serine palmitoyltransferase (SPT) is an enzyme consisting of two components, SPT long chain base subunit 1 (SPTLC1) and SPTLC2. SPTLC1 interacts with Par3, a scaffolding factor, which recruits proteins such as atypical PKC and Cdc42 into PAR complexes required for directional migration. SPTLC1 is expressed in THP-1 cells. Loss of Par3 in THP-1 is reported to inhibit their migration to

inflammatory chemokine CCL2 [920]. NSC23766 inhibits Tiam1 which promotes tight junction assembly through Rac activation and the Par complex. Inhibition of Tiam1 could conversely therefore promote migration through a transwell plate 5  $\mu$ M pore, if clumping of cells was inhibiting them moving through the pores towards the chemokine. This may be what is apparent in figure 8.2(B).

Atypical PKC $\zeta$  is reported to phosphorylate Tiam1, stabilising its interaction with Par3. The Par complex is reportedly crucial for cell polarity and chemotaxis [347]. CCL3 may phosphorylate Tiam1, which may be dependent on PKC as well as Par3 for activity. Tiam1 phosphorylation may be required for Rac1 activation, although this can be a transient effect depending on cell type and balance between phosphatases and kinases. 14-3-3 regulatory proteins can bind Tiam-1 N-terminal PEST sequences triggering Tiam1 degradation. Tiam1 needs to be bound to membrane Phosphatidylinositol 5-phosphate (PtdIns5P) to be active; PtdIns5P can potentiate Tiam1 activity. Tiam1 has a myristoylation motif at its N-terminal which favours plasma membrane binding. Binding of Tiam1 to PtdIns5P can restrict Rac1 activation, causing active Tiam1 and Rac1 to relocate to early endosomes and membrane ruffles. Whereas treatment with NSC23766 is reported to restore F-actin polymerization [921]. So the dramatic differences seen in NSC23766's effects on CCL3 and CXCL12 in the THP-1 may be differences in Rac1 signalling between CCL3 and CXCL12. This theory was supported by the inhibitory actions of NSC23766 on CXCL12 chemotaxis in Jurkat, but results seen were also the first indication that the NSC23766 was having some off-target effects on CXCR4.

### 8.3.2: Rac GEF inhibitor NSC23766

The investigations undertaken with Rac GEF inhibitor NSC23766 reported here revealed some surprising results, suggesting NSC23766 modulates CXCR4 signalling either directly or allosterically as well as producing Rac1 inhibition. NSC23766, figure 8.34, is a nitrogen rich molecule with many rotatable bonds, making it a flexible molecule that could potentially bind into several sites on many receptors including CXCR4.

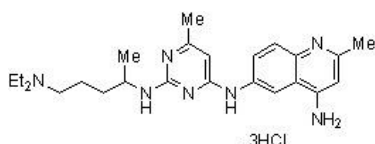


Figure 8.34: Structure of Rac1 GEF inhibitor NSC23766

NSC23766 contains primary, secondary and tertiary amines, a methylpyrimidine ring, a base weakened by the inductive effect of the second nitrogen, and a substituted quinoline ring, 6-methyl-4,6-quinolinediamine. NSC23766 has a methylated butyl amine tail which may, like CXCR4

inhibitor AMD11070, interact with Asp97 in TM2. NSC23766 also has a plentiful supply of amines in common with CXCR4/CXCL12 signalling inhibitors AMD3100, AMD11070 and AMD3465. Testing NSC23766 with CXCR4 Glu288 (TM7) and Asp97 mutants, along with several ECL2 residue mutants, could provide evidence of if, and where, NSC23766 binds CXCR4, which would explain its ability to so effectively block CXCL12 activation in Jurkat, and less dramatically THP-1. There are several orientation options for computer modelling of NSC23766 onto CXCR4. NSC23766 has basic nitrogens so can form ionic bonds, and electronegative nitrogens so can form H-bonds. For example further research could investigate if NSC23766 forms ionic interactions with negatively charged amino acids Asp97, Asp171 (TM4), Glu179, Asp181, Asp182 (ECL2), Asp262 (TM6) and Glu288, cationic  $\pi$ -interactions with Trp94 (TM2), or aromatic interactions with Tyr45 (TM1) or Trp94 (TM2), or if NSC23766 binding disrupts the essential Cys186 (ECL2) – Cys109 (ECL1) disulphide bond.

Interestingly NSC23766 has been found to act as a competitive antagonist at muscarinic acetylcholine receptors (mAChRs) and at the NMDA receptor [901, 902]. NSC23766 was found to inhibit carbachol responses in human-derived HEK293 cells expressing M<sub>1</sub>, M<sub>2</sub> and M<sub>3</sub> mAChRs and act as a non-selective mAChR competitive antagonist. Computer modelling, which was not backed by mutant studies and so is speculative, suggested NSC23766 could theoretically bind M<sub>2</sub> and M<sub>3</sub> AChRs orthosteric binding pocket on the receptor extracellular surface. The suggestion was that NSC23766's diethylamine group's positively charged tertiary amine nitrogen could have electrostatic interactions with Asp, Tyr, or Trp residues. This would position NSC23766's butyl chain methyl group sitting in a hydrophobic pocket in M<sub>2</sub> AChRs formed of Ala, Tyr, Phe and Trp residues; the methylpyrimidine position 3 nitrogen acting as hydrogen acceptor to a Tyr residue in M<sub>2</sub> AChR and the methylquinolinediamine ring with hydrophobic interactions with Tyr, Trp and Thr residues [901]. NSC23766 binding on NMDA receptor was not computer modelled by Hou *et al.* (2014), but it would be interesting to examine the mAChRs, NMDA and CXCR4 receptors using computer modelling looking for similar pockets where NSC23766 could theoretically bind.

### **8.3.3: NSC23766 competes with CXCL12 and 12G5**

Rac1 activation can be prevented by CXCR4 inhibitors but also by NSC23766, figure 8.7, suggesting NSC23766 may be interacting with CXCR4. NSC23766 also competes with CXCL12 and 12G5, figures 8.8-8.10. 12G5 CXCR4 binding has been extensively researched. CXCR4 antibodies are reported to predominantly target CXCR4's extracellular domains, ECL1, ECL2, ECL3 and N-terminal region [903], see figure 1.5, chapter 1. Western blots with 12G5 failed to show any specific binding (data not shown) suggesting that 12G5 binding is conformational dependent, hence NSC23766 just changing CXCR4 conformation could explain FACS results, figures 8.13-8.14. The

failure of 12G5 to completely prevent chemotaxis may be attributed to CXCR4 conformational heterogeneity, as has been identified in both CD4<sup>+</sup> and CD4<sup>-</sup> Jurkat cells, indicating that Jurkat may carry two or more CXCR4 conformations. Whereas CXCL12 may bind all conformations of CXCR4, 12G5 may not, also receptor dimerization or position in lipid rafts may influence 12G5 binding [903]. Conformation of CXCR4 ECL2, which contains residues 176 to 202, has been found essential for 12G5 binding in Jurkat, with residues Asp176, Glu179 and Asp181 essential, and N-terminal residues 1-23 unimportant. G-protein phosphorylation or activation and N-linked glycosylation or sulfation appears not to affect 12G5 binding [903, 922]. ECL2 residue Cys186 which forms disulphide bonds with Cys109 (ECL1) are needed for CXCR4 tertiary structure, and if broken weaken 12G5 binding [923]. Cys186, Asp187 and Tyr190 mutations either disrupt the conformation of ECL2 or are directly involved in 12G5 binding [151, 153]. Asp171 on TM4 close to ECL2 also appears to influence 12G5 binding [924]. 12G5 binding reportedly requires two disulphide bonds to be intact, not for binding but for CXCR4 conformation, between Cys28 (N-terminal) and Cys274 (ECL3), plus Cys186 (ECL2) and Cys109 (ECL1) [922]. Signoret *et al.* (1997) exquisitely demonstrated that CXCL12 only modestly completes for 12G5 binding in T-cells [279]. Another explanation for the observed results in figures 8.8-8.10 are that NSC23766 is modulating CXCR4/CXCR7 heterodimer or oligomer formation. Certainly neither NSC23766, ATI2341 nor AMD3100 produced chemotaxis in Jurkat, figure 8.11.

#### **8.3.4: CXCR7 receptor in cancer**

CXCR7, aka RDC-1, a receptor which binds CXCL11 and CXCL12, is deemed pro-tumorigenic in malignancy and is upregulated in many cancers and cell-lines. CXCR7 is a highly conserved receptor across mammalian species and is now accepted as a major player in CXCR4-CXCL12 signalling. Interestingly the affinity of CXCR7 for CXCL12 exceeds that of CXCR4 [106, 656, 925]. Like CXCR4, CXCR7 is induced by hypoxia, and is associated with poor prognosis and metastasis in cancers [926, 927, 928]. CXCR7 may also aid angiogenesis [929]. 12G5 has been shown not to inhibit CXCL12-induced chemotaxis in a T-cell-line expressing CXCR7 but not CXCR4 [106], suggesting CXCR7 could be influencing results reported here.

#### **8.3.5: NSC23766 can displace CXCR4 antibody 12G5**

Various explanations for the chemotaxis and flow cytometry results with NSC23766, AMD3100 and ATI2341 are plausible, figures 8.12 and 8.14. However NSC23766 is unlikely to be triggering internalisation as results at 37°C and 4°C are similar; 4°C should prevent active internalisation. NSC23766 may be causing a conformation change of the receptor acting through Rac1, and so cause a loss of 12G5 binding, as has been suggested by others [930], but then a greater effect of W56 would be expected and Rac direct inhibitor ETH1864 has no effect, figure 8.15. The effects of

NSC23766 are similar at 37°C and 4°C, this suggests NSC23766 is displacing 12G5 from the receptor; also treatment with NSC23766 after 12G5 and FITC staining causes greater effects than pre-treatment of cells. This may suggest that NSC23766 rapidly binds or allosterically modulates CXCR4, but its affinity weakens over the 2 hours of primary and secondary antibody staining, suggesting if it binds CXCR4 directly affinity is much lower than that of CXCL12 or 12G5.

ATI2341 5  $\mu$ M produces non-significant effects at 37°C or 4°C. AMD3100 5  $\mu$ M however causes greater loss of CXCR4 in absence of CXCL12 than NSC23766, but does not hinder CXCL12 internalisation like NSC23766 at 37°C, and AMD3100 does not cause any significant internalisation at 4°C, suggesting AMD3100 and NSC23766 have very different modes of action and that NSC23766 is not simply acting as a CXCR4 antagonist or a Rac1 GEF inhibitor. The promiscuity of NSC23766 has been previously reported. Examples include: acting as an antagonist at NMDA and Muscarinic acetylcholine receptors [901, 902]; acting to modulate p21-activated kinase (PAK)1 and PAK2, and inhibiting activation and glycoprotein 1b signalling in Rac1(-/-) platelets [931]; and acting to inhibit the phosphorylation of NF- $\kappa$ B and cyclin D<sub>1</sub> in prostate cancer cells and directly inhibiting the phosphorylation of Rac1, albeit at 200  $\mu$ M [932]. NSC23766 and EHT1864, figures 8.34 and 8.15B, can also both modulate glucose-stimulated insulin secretion [933].

#### ***8.3.6: Endocytosis inhibitors do not prevent NSC23766 triggered CXCR4 internalisation***

Sucrose treatment significantly increased CXCR4 expression in control, 8.16B, but did not prevent the NSC23766, AMD3100 or CXCL12 causing CXCR4 signal loss. Hyperosmotic sucrose at 0.4 M reportedly non-selectively inhibits GPCR internalisation, causes strong ERK activation [934] and may induce phosphorylation of p38MAPK causing pathway activation [935, 936]. Cell surface receptors can be internalised via clathrin-dependent or clathrin-independent, lipid raft and calveolae-dependent endocytosis. With the former the clathrin-coated pit is pinched off by dynamin and other proteins to form clathrin-coated vesicles which then fuse with early endosomes and recycle back to the surface or via late endosomes are degraded in lysosomes. Alternatively lipid raft/calveolae-dependent endocytosis occurs [937]. Binding of CXCL12 to CXCR4 is reported to cause ubiquitination of receptor followed by degradation in lysosomes [715, 938]. Sucrose at 0.4 M appears unable to prevent this process in presence of 15 nM CXCL12, but did very significantly ( $p < 0.001$ ) increase CXCR4 expression in absence of CXCL12..

Sodium azide failed to modify CXCR4 expression in Jurkat, figure 8.16A. Sodium Azide reportedly inhibits ATP hydrolysis by inhibiting oxidative phosphorylation in mitochondria, the major source of ATP production in eukaryotes. Mitochondria contribute to gluconeogenesis, heme synthesis and the urea cycle, and are the location of the tricarboxylic acid cycle,  $\beta$ -oxidation of fatty acids,

ketogenesis and oxidative phosphorylation. Oxidative phosphorylation involves electrons being passed down a chain of enzyme complexes in a series of redox reactions that release energy [939]. Sodium azide reportedly blocks cytochrome C oxidase (aka Complex IV) the last enzyme of respiratory electron transport chain; sodium azide binds between iron and copper ions in the cytochrome C oxidase's oxygen reduction site [940]. Cytochrome C oxidase receives and then transfers electrons to oxygen to make water and transport protons into the mitochondria intermembrane space. ATP synthase (aka F-ATPase and Complex V) then uses the proton gradient between the intermembrane space and the matrix to drive ATP production from ADP and inorganic phosphate [941].

However this experiment was completed using Jurkat, a cancer T-cell line. Mitochondrial metabolism has been shown to provide the necessary reactive oxygen species for antigen-specific T-cell activation in non-transformed cells [942]. Jurkat are a rapidly proliferating cell line. Proliferating cells have vastly increased metabolic requirements to quiescent ones. When activated non-transformed (healthy) T-cells increase glucose metabolism, they take up large amounts of glucose from their environment while also producing lactate. That is, they are primarily glycolytic via aerobic glycolysis [943-945]. Hence glycolysis provides ATP and fuels the pentose phosphate pathway generating NADPH and nucleotides. Activated non-transformed T-cells also increase glutamine metabolism to fuel the mitochondrial tricarboxylic acid cycle via glutaminolysis to  $\alpha$ -ketoglutarate [946, 947]. Cancer cells can flourish in conditions that would cause apoptosis of non-transformed healthy cells, for example in conditions of low pH or oxygen tension [948], this is because they preferentially generate ATP by glycolysis followed by cytosolic lactic acid fermentation rather than oxidative phosphorylation; oxygen can actually inhibit this process, which is known as the Warburg effect [949]. Tumour cells run glycolysis, which does not use oxygen, at much higher rates than normal cells to acquire the necessary ATP for rapid proliferation. If they used mitochondrial production to generate the required levels of ATP they would also generate levels of reactive oxygen species (ROS), a normal by-product of oxidative phosphorylation that would be toxic to the cells. Normally oxygen and ATP would inhibit phosphofructokinase-1, the enzyme controlling the rate of glycolysis. But the Warburg effect allows the tumour cell (i) to accelerate glycolysis in presence of oxygen and (ii) to convert the end product of glycolysis, pyruvate, to lactate even in the presence of normal levels of oxygen. Lactate production then allows the necessary regeneration of  $\text{NAD}^+$ . Lactate itself may stimulate signalling that stimulates tumour growth [950].

Hence the FAC results obtained following sodium azide pre-treatment, figure 8.16A, suggest the Jurkat were predominantly generating energy via glycolysis, not oxidative phosphorylation, as may be expected with a fast replicating cancer cell-line.

#### **8.3.7: cAMP levels are reduced by NSC23766 but not by AMD3100**

AMD3100 can act as a competitive orthosteric unbiased antagonist of CXCR4, figure 8.3 shows 1  $\mu$ M can strongly inhibit chemotaxis to CXCL12. AMD3100 can inhibit CXCR4 endocytosis and both  $\beta$ -arrestin and  $G_{\alpha i}$  signalling [951] but can over time promote CXCR4 upregulation of CXCR4 so drug resistance and even increased responses to CXCL12 [952]. Here surprisingly 5  $\mu$ M AMD3100 failed to significantly modify cAMP production in Jurkat, pre-treated with 20  $\mu$ M Forskolin plus IBMX, and stimulated by 10 nM CXCL12, figure 8.17. Hitchinson *et al.* (2018) also investigated the effects of AMD3100 on Jurkat cAMP production triggered by CXCL12. They used 100  $\mu$ M Forskolin, 30 nM CXCL12 and AMD3100 (strength not stated) and saw a small ( $p < 0.05$ ) loss of reduction of cAMP in AMD3100/CXCL12 treated cells compared to control [953]. Mechanisms for the discrepancies include that AMD3100 at low concentrations (0.1-1  $\mu$ M) may act as a weak partial agonist [954], and/or that other receptors were playing a role. However the artificial nature of Forskolin activation of adenylyl cyclase and IBMX phosphodiesterase inhibition of cAMP breakdown, noted by others as obvious possible sources of error [955] may have obscured AMD3100 responses.

NSC23766 produced a very significant ( $p < 0.001$ ) reduction in basal cAMP levels, figure 8.17. Basal levels of cAMP may relate to numbers of receptors on the cell surface [956]. CXCL12 binds CXCR4 but also CXCR7, Jurkat express CXCR7 at high levels as well as CXCR4 [957]. CXCL12 binding CXCR4 activates canonical  $G_{\alpha i}$  signalling, reducing cAMP levels. CXCR7 activation does not. However CXCR7/CXCR4 heterodimer formation prioritises activation of  $\beta$ -arrestins over  $G_{\alpha i}$  signalling [958], suggesting CXCR7 can regulate coupling of CXCR4 to  $G_{\alpha i}$  and thus cAMP levels [928]. If NSC23766 prevents CXCR4/CXCR7 heterodimer formation, increasing CXCR4 monomers on the cell surface it could increase basal CXCR4  $G_{\alpha i}$  signalling, and cAMP levels would fall, this could explain results. If both CXCR4 and CXCR7 are expressed then  $Ca^{2+}$  mobilisation may be greater than if just CXCR4 are present, as CXCR7 may enable CXCR4- $G_{\alpha i}$  conformational rearrangements supporting both CXCL12-induced chemotaxis and calcium flux [958], possibly explaining figures 8.20-8.22. Interestingly NSC23766 more strongly inhibited  $Ca^{2+}$  flux than the CXCR4 inhibitors ATI2341 or AMD3100, figure 8.23. These results therefore do not preclude that NSC23766 is binding CXCR7 rather than CXCR4 or acting as a biased ligand.



### **8.3.8: Biased signalling**

Different ligands binding the same receptor can produce specific conformations that trigger initiation of only a specific subset of the receptor's many possible signalling cascades. This is termed biased agonism or functional selectivity. Equally allosteric ligands can produce biased modulation of biased agonism [959, 960]. The underlying molecular basis for biased agonism is complex and not fully understood [961]. *In vivo* other biases may add to the complexities; circadian rhythms and pathology including cancer affect natural ligand/receptor stoichiometry and may for example change cell expression of G-protein  $\gamma$  subunits [962, 963]. Therefore computer modelling analysis of binding sites based on assays in any one cell-line or transfected system are unlikely to be universally applicable, and could mislead future research.

### **8.3.9: cAMP levels may modulate PKC $\zeta$ signalling**

Unlike AMD3100 or ATI2341, NSC23766 reduced both basal and post-CXCL12 stimulation cAMP levels compared to control, figure 8.17. Increasing cAMP levels increases Ras GTPase Rap1-GTP, hence Rap-1 activation [964]. Inhibiting Rap-1 decreases CXCR4 expression at the membrane so Rap-1-GTP appears to be required for cAMP-induced CXCR4-increased membrane expression. PKA inhibitor H89 was found here to significantly increase cAMP production, figure 8.17. Others note H89 failed to prevent CXCR4 expression [906].

PKC $\zeta$  is involved in cAMP signalling, as increasing cAMP increases PKC $\zeta$  phosphorylation and activation [965]. Rap1 affects signalling upstream of PKC $\zeta$  translocation to the membrane [906]. Rap1 recruits Rac1 GEFs including Tiam1. Active Rac1 triggers translocation and activation of PKC $\zeta$ . Blocking Rac1 by NSC23766 can inhibit cAMP-induced PKC $\zeta$  phosphorylation, suggesting Rac1 is required for PKC $\zeta$  activation by cAMP [964, 966]. Thus PKC $\zeta$  has a role in cAMP-activated CXCR4 expression. Inhibiting PKC $\zeta$  activity inhibits CXCR4 expression at the membrane; upregulating PKC $\zeta$  increases CXCR4 expression. Inhibiting Rac1 activation has the same effect as blocking PKC $\zeta$  activity, suggesting Rac1 and PKC $\zeta$  are in the same signalling pathway influencing CXCR4 membrane expression, possibly by reducing CXCR4 endocytosis. Hence in the absence of CXCL12 cAMP prolongs CXCR4's stay at the membrane, and increasing cAMP levels increases CXCR4 recycling back to the membrane [906]. PKC $\zeta$  is activated by binding to the Par activity complex containing Par6, Par3 and Cdc42; Rac1 binds Par6 to activate PKC $\zeta$  [967]. Therefore there appears to be a feedback loop between PKC $\zeta$  activation by cAMP causing elevated CXCR4 expression which itself increases PKC $\zeta$  activity, figure 8.35.

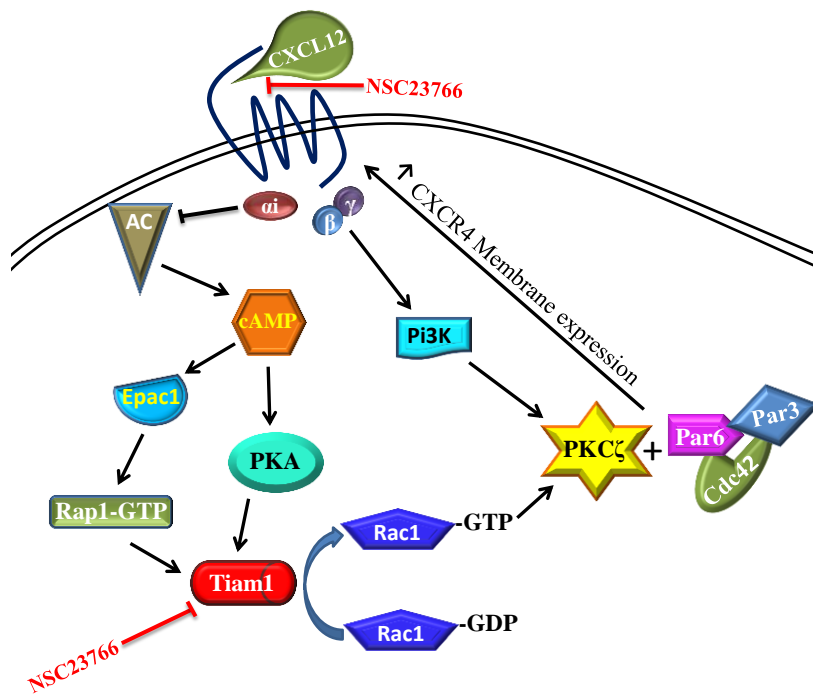


Figure 8.35: Schematic representation of cAMP, PKC $\zeta$ , Rac1 and CXCR4 expression feedback loop [906, 964].

#### 8.3.9.1: PKC $\zeta$ knockdown inhibits CCL3 and CXCL12 MCF7 wound-healing and Jurkat chemotaxis to CXCL12

The cAMP results, figure 8.17, suggest that NSC23766 is stimulating G $\alpha_i$  signalling from CXCR4, which is inhibiting adenylyl cyclase hence reducing cAMP levels. The addition of CXCL12 increases the G $\alpha_i$  signal, reducing cAMP levels further. If NSC23766 was purely inhibiting Tiam1 it would be expected to reduce Rac1 activation of PKC $\zeta$ /Par3/Par6/Cdc42 complex and possibly reduce CXCR4 membrane expression and G $\alpha_i$  inhibitory signalling, increasing cAMP levels. The signalling may be complicated by the reported constitutively active signalling of Pi3K in Jurkat cells [647, 968, 969], so any effect on Tiam1 by NSC23766, figure 8.35, may be mitigated, but direct effects of NSC23766 on CXCR4 would not.

#### 8.3.9.2: Both PKC $\zeta$ over-expression and inactivation can support malignancies

PKC $\zeta$  knockdown was found to inhibit both CXCL12 supported chemotaxis in Jurkat and chemokinesis in MCF7, confirming the proteins role in promoting CXCR4 signalling in these cell-lines, figures 8.18-8.19. PKC $\zeta$ 's roles in cancers are complex. PKC $\zeta$  down-regulation has been found to promote malignancy in pancreatic [970], lung [971], and prostate cancers [972]. However PKC $\zeta$  deletion increases prostate cancer invasiveness if Phosphatase and Tensin Homolog (PTEN) is lacking [973]. Possibly as PKC $\zeta$  silencing can also promote invasion and growth in some cell-lines as PKC $\zeta$  may conversely act as a tumour suppressor in some breast cancers, PKC $\zeta$  may through IL-6 modulation counteracting adverse transformed Ras-signalling [971].

PKC $\zeta$  can be inactive in colon cancers resulting in poor prognosis [974] but PKC $\zeta$  loss in colon cancer can increase transcription of  $\beta$ -catenin in crypt stem cells leading to malignancy [975]. LOF of PKC $\zeta$  is also found in some breast cancers, and PKC $\zeta$  appears essential for stem cell homeostasis. These contradictory findings may be due to effects of PDPK1, an upstream regulator of all PKCs. Rapamycin (sirolimus), temsirolimus and everolimus inhibit mTOR signalling, which is involved in activation of all novel and conventional PKCs. PDPK1 and mTOR phosphorylate all PKCs on conserved sequences [976]. Inhibiting mTOR can inhibit breast cancer growth yet these drugs are also immunosuppressants inhibiting cytokine-responsive T-lymphocyte activation and proliferation, and so resistance develops [262].

### **8.3.10: Intracellular calcium, PLC and Rac1**

Intracellular calcium can act as a second messenger in signalling cascades. Resting intracellular calcium concentrations are usually far lower than extracellular levels. This is achieved by pumping calcium from the cytosol into the extracellular space and into the endoplasmic reticulum (ER), also by proteins and organelles in the cytosol sequestering Ca<sup>2+</sup>. GPCR stimulation can indirectly trigger opening of ion channels allowing Ca<sup>2+</sup> to flood into the cytosol from the ER and/or extracellular space, triggering signalling cascades [977].

In T-cells phospholipase C (PLC) gamma can be activated by GPCR triggered Ca<sup>2+</sup> signalling. PLC hydrolyses membrane phosphatidylinositol biphosphate (PIP<sub>2</sub>) forming inositol 1,4,5 triphosphate (IP<sub>3</sub>) and diacylglycerol (DAG). DAG can then recruit PKC to the cell membrane while IP<sub>3</sub> binds IP<sub>3</sub> receptors opening Ca<sup>2+</sup> channels on the ER. This activates STIM1, an ER Ca<sup>2+</sup> sensor, and finally Orai1 channels, the main T-cell SOCC, open. The IP<sub>3</sub> channels opening and releasing ER Ca<sup>2+</sup> may trigger PKC activation, and intracellular Ca<sup>2+</sup> may activate calcium-calmodulin kinase pathways which can trigger dephosphorylation and activation of transcription factors [977]. Intracellular calcium signalling is accepted as a cellular second messenger system that links to chemokine receptor activation, and to the activation of Rho GTPases [978].

Relationships between Rac and calcium signalling are thought to be dependent on cell type, and signalling trigger. For example in neutrophils Rac activation triggered by chemokines can be independent of intracellular calcium [979], and T-cells carry several varieties of calcium channels at the cell and/or ER membrane [977].

NSC23766 may be acting via inhibiting Tiam1, which activates Rac1 and so influences the PLC-IP<sub>3</sub> pathway explained above, or via direct inhibition of CXCL12/CXCR4 activation. NSC23766 was found to increase Ca<sup>2+</sup> flux in THP-1 triggered by CCL3 but reduce response from CXCL12, figure 8.20. In Jurkat and MCF7 NSC23766 dose-dependently competed with CXCL12 inhibiting Ca<sup>2+</sup> flux,

figures 8.21 and 8.22. These results suggest NSC23766 has a direct effect on CXCL12/CXCR4 but not CCL3 signalling. Indeed it more effectively inhibited  $\text{Ca}^{2+}$  production than either CXCR4 inhibitor AMD3100 or ATI2341, figure 8.23.

PLC inhibition was achieved using U73122, figures 8.24 and 8.25. U73122 inhibits PLC so can reduce  $\text{IP}_3$  production in neutrophils [980, 981], although U73122 has also been found to potentiate  $\text{IP}_3$ -mediated  $\text{Ca}^{2+}$  release [982], figure 8.36. Here it statistically increases  $\text{Ca}^{2+}$  production in Jurkat, figure 8.25.

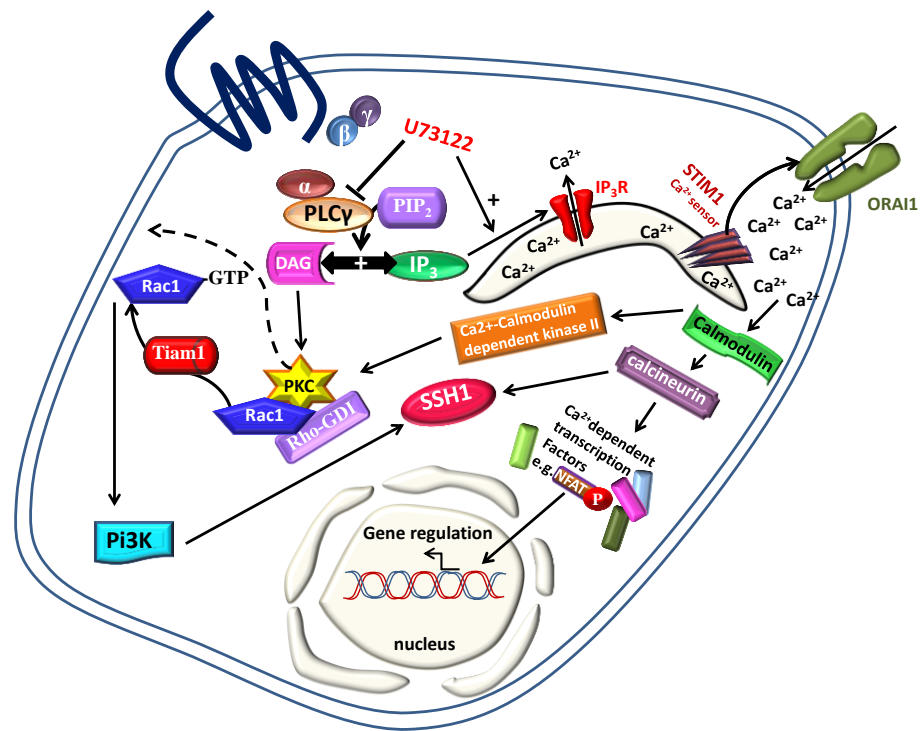


Figure 8.36: Involvement of Rac1, PLC, PKC and Slingshot (SSH1) in GPCR calcium signalling. SSH1 can be activated by two routes, rapidly through calcineurin and more slowly through Rac1-Pi3K. SSH1 phosphatase phosphorylates cofilin [977, 983].

U73122 behaved similarly in THP-1 and Jurkat chemotaxis to NSC23766, reinforcing evidence for specificity of Rac1 signalling in CXCL12 but not CCL3 chemotaxis, figures 8.2 and 8.24, however U73122 produced opposite effects on cAMP responses both before and after CXCL12 compared to NSC23766, figures 8.26A and 8.17, suggesting NSC23766 off-targets effects.

### 8.3.11: NSC23766 inhibits both early and late cofilin phosphorylation events in response to CXCL12

The temporal early responses of cofilin phosphorylation observed, figure 8.29, may be attributable to  $\text{Ca}^{2+}$  dependent cofilin re-phosphorylation, and the later ones to Rho-kinase/LIMK signalling. Rac1 inhibition was shown above to inhibit CXCL12-induced calcium flux, figures 8.20-

8.22, indicating Rac1 activation may be calcium-dependent. Cofilin phosphorylation in other cells has been reported as calcium dependent, mediated through PAKs; phosphatase Slingshot can be activated by calcineurin [893]. PKC may function upstream, and Pi3K downstream of Rac1, Pi3K can stimulate SSH1 activity, figure 8.36. PKC can phosphorylate Tiam1 activating Rac1, however both PKC-independent and dependent pathways may trigger cofilin phosphorylation [643, 984]. Early changes in cofilin phosphorylation may also be involved with cell secretion; cofilin inactivation may reduce the constraints of actin cytoskeleton on monocyte secretion as vesicle-membrane fusions involves actin polymerization [985, 986].

**8.3.12: Rac1 may be involved in CXCL11 but not CCL2 or CXCL9 chemotaxis**

CCL2 aka Monocyte chemoattractant protein-1 (MCP-1) has both chemotactic and activating properties [987]. Rac1 is important for membrane ruffles formation as well as lamellipodia. Ruffles are instrumental in the formation of the phagocytic cup employed when macrophages phagocytose apoptotic cells, a process known as efferocytosis. CCL2 is reported to enhance efferocytosis through a CCL2/Rac1/Pi3K pathway in acute inflammation, and NSC23766 at 50  $\mu$ M can inhibit this in mouse macrophages [988]. Others have implicated Rac1 activation in CCL2 chemotaxis in CHO cells [989]. However, here in THP-1 neither NSC23766 at 100  $\mu$ M or W56 at 280  $\mu$ M significantly inhibited chemotaxis to CCL2. However both inhibitors significantly reduced chemotaxis induced by CXCL11 but not CXCL9, suggesting Rac1 activation is involved in CXCL11-triggered chemotaxis in THP-1, or NSC23766 may be having off target effects on CXCR7, which also binds CXCL11. CXCL11, aka I-TAC, and CXCL9 are both ligands for CXCR3, but CXCL11 binds with higher affinity [990]. The different ligands trigger different downstream pathways and receptor locations; CXCR9 activation involves serine/threonine residues on CXCR3 C-terminus whereas CXCL11 involves CXCR3 ICL3 [991]. CXCL11/CXCR3 signalling involves p70 kinase/mTOR STAT3 and STAT6 whereas CXCL9/CXCR3 signals via STAT1 and STAT5, an example of ligand-biased signalling [992].

The receptor CXCR3 is known to have two isoforms termed CXCR3-A and CXCR3-B. In malignancy CXCL11 binding CXCR3-A or CXCR7 triggers proliferation, but CXCL11 binding CXCR3-B inhibits tumour growth [993]. Ligands for CXCR3, CXCR4 and CXCR7 can be expressed by malignant cells, although only CXCR4 is accepted as a cancer stem cell marker [994, 995]. What is more complex to analyse is the outcome of signalling cross-talk and reported dimerization of CXCR4 and CXCR7 [958], which may involve G-proteins or biased signalling through  $\beta$ -arrestin [996, 997], or CXCL14 [919]. CXCL12 can be secreted by cells as monomers or dimers, and can dimerize once secreted. Monomeric CXCL12 may preferentially activate CXCR4 signalling via G $\alpha$ i and Akt whereas dimeric

CXCL12 signals via  $\beta$ -arrestin-2 recruitment to CXCR4. CXCR7 may only bind monomeric CXCL12 [998].

Although CXCR7 binds both CXCL11 and CXCL12 neither partnership produces classical heterotrimeric G-protein signalling [113], but they have been shown to stimulate signalling via the recruitment of  $\beta$ -arrestin, and produce ERK1/2 phosphorylation. The presence of CXCR7 on immune cells such as monocytes was initially reported using an antibody approach, then challenged due to suggested limitations of the antibody, before being confirmed by proteomic evidence [999-1001]. CXCR7 has been shown to dimerize with CXCR4, modulating CXCR4-CXCL12 signalling [958], and to play a role in murine haematopoietic stem cell development and so may also do so in humans [1002]. CXCR7 may also act as a sponge for CXCL11 and CXCL12 maintaining the gradient essential for chemotaxis [41, 1003]. Figure 8.30B may provide evidence that CXCR3 is involved in THP-1 migration stimulated by CXCL11, or that CXCL11 binding CXCR7 in monocytes can stimulate migration, and that NSC23766 may be inhibiting the actions of CXCR7.

#### **8.3.13: NSC23766 may potentiate CXCL14 inhibition of Jurkat chemotaxis to CXCL12**

CXCL14 is found in and produced by healthy epithelial tissues and macrophages, its expression can be reduced by inflammation, and malignancy [916, 1004]. Although chemotactic to most types of white blood cells, T-cells are not attracted to CXCL14 [1005]. CXCL14 appears to be an indirect [1006] or direct ligand for CXCR4 [1005] but reportedly also interacts with other proteins/receptors [914]. Collins *et al.* (2017) found that CXCL14 can displace bound CXCL12, but CXCL12 is less efficient at displacing CXCL14 [919], this may explain why here in figure 8.31A pre-treatment with CXCL14 had more of a dose-dependent effect than the same concentrations of CXCL14 combined with CXCL12 as chemoattractant, figure 8.31B. Research suggests 300 nM CXCL14 can potentiate chemotaxis to 0.1-1 nM CXCL12 in PMBC's [919]. PMBC's include NK-cells and monocytes which migrate to CXCL14, as well as pre-B and T-cells which may not. Conversely Collins *et al.* found CXCR4 inhibitor AMD3100 (10  $\mu$ M) pre-treatment did not prevent monocyte migration to a high concentration (1  $\mu$ M) CXCL14, and that CXCL14 did not activate CXCR4-associated signalling events [919], suggesting CXCL14-induced chemotaxis in monocytes employs a receptor, protein or chemokine partner other than CXCR4.

The effects of CXCL14 on metastasis may depend on the degree of mitochondrial dysfunction present in malignant cells. Dysfunction in mitochondrial respiration has been shown to promote CXCL14 expression. CXCL14 binding inositol 1,4,5-trisphosphate receptors on the endoplasmic reticulum producing elevation of intracellular  $\text{Ca}^{2+}$  may promote cell motility and invasion [1007]. Explaining how CXCL14 could perform a useful role in immune surveillance but also promote

metastases. Here CXCL14 100 nM pre-treatment significantly increased responses to CXCL12/CXCR4 coupling to G $\alpha$ i, producing elevation of intracellular calcium in Jurkat, figure 8.32. Others saw similar Ca<sup>2+</sup> responses to CXCL12/CXCL14 combinations, along with elevation of Rac-GTP in murine CXCR4-transfected cells [919]. Here using flow cytometry and Jurkat, figure 8.33, Rac1 inhibition with W56 did not modulate CXCL14 responses, but NSC23766 significantly did, again suggesting NSC23766 can allosterically modulate CXCR4 or a receptor forming dimers with CXCR4. Collins *et al.* (2017) concluded that synergism between CXCL12 and CXCL14 is dependent on CXCR4 dimer/oligomerization, CXCL14 binding one CXCR4 partner facilitating CXCL12 binding other. However their cells only expressed CXCR4, so could only form CXCR4 homodimers. THP-1 and healthy monocytes express little CXCR7 [1008], whereas Jurkat highly express CXCR7 [957], so Jurkat may express more CXCR4/CXCR7 heterodimers or oligomers than CXCR4 homodimers or oligomers. CXCL14 binding the CXCR4 component of a CXCR4/CXCR7 dimer would block CXCL12 binding, so inhibit migration, which is what figure 8.31 illustrates. Whereas in monocytes, CXCL14 binding one component of a CXCR4 homodimer could then facilitate CXCL12 binding other CXCR4 and thus expedite chemotaxis, *in vitro* concentration of the two chemokines and cell-line appears key.

#### **8.4: Conclusions**

THP-1 express CXCR4 but possibly little CXCR7 [1008], this may explain why NSC23766 had less effect on CXCL12 chemotaxis in THP-1 than in Jurkat where CXCR7 is highly expressed [957]. Here THP-1 were shown to also express CCR5, chapter 3, figure 3.3. Overall NSC23766 was shown to inhibit CXCL12-induced chemotaxis, chemokinesis and calcium mobilisation in Jurkat, THP-1 and MCF7, figures 8.2, 8.6, 8.20-8.23; also to significantly reduce basal cAMP levels in Jurkat, figure 8.17. One explanation for these results is that NSC23766 may be allosterically inhibiting CXCR4 by binding and inactivating CXCR7. Contrastingly NSC23766 increased THP-1 chemotaxis and calcium mobilisation to CCL3, acting as a partial agonist, figures 8.2B and 8.20A. Possible mechanisms include acting on CXCR4 affecting CXCR4/CCR5 dimers or by acting on CXCR7. CXCR4-CCR5 modulate T-cell functions but recent research suggesting CXCR7-targeting may block HIV entry into cells [1009]. This raises the question could CXCR7 also modulate CCL3/CCR5 induced chemotaxis?

NSC23766 had significantly different effects to AMD3100 and ATI2341 on cAMP basal levels and those following CXCL12 suggesting it was not targeting CXCR4 but either preventing CXCR4/CXCR7 dimerization or targeting CXCR7. CXCR7 is upregulated in cancer cells and present in Jurkat [957].

NSC23766 targeting CXCR7 may explain not only cAMP results but also results from the chemotaxis, calcium, and internalisation assays. As CXCR7 has been shown to signal through G $\alpha$ i in some cell types [110], so may do in others, and to produce hetero-oligomers with CXCR4 [1010]. Such hetero-oligomers may, depending on conditions and cell type, increase or decrease Ca<sup>2+</sup> flux following CXCL12 stimulation and alter ERK activation and chemotaxis. Mechanisms may include CXCR7 altering CXCR4-G $\alpha$ i interactions and/or sequestering CXCL12; *in vivo* CXCR7 sequestering appears to maintain CXCR4 sensitivity to CXCL12 supporting metastasis [958, 1011]. The CXCR7 ligand CX771 has been found to more potentially inhibit CXCL12 migration than AMD3100 [1010], similarly here AMD3100, at the concentration used failed to inhibit cAMP responses as much as NSC23766. Others have seen little effect of AMD3100 on cAMP production boosted by Forskolin [953]. CXCR7/CXCR4 co-expression can decrease CXCL12 stimulated G $\alpha$ i-mediated cAMP reduction [928] therefore if NSC23766 either inactivates CXCR7 or prevents CXCR4/CXCR7 dimer or oligomer formation this would explain why NSC23766 was able to reduce basal cAMP levels and those in the presence of CXCL12, figure 8.17. NSC23766 also reduced CXCL12 chemotaxis, when CXCR7 is inhibited so would  $\beta$ -arrestin responses that have been shown here, chapter 5, figure 5.33 and by others [1012] to significantly increase chemotaxis to CXCL12.

Overall Rac1 was found important for CXCL12 chemotaxis but less essential for chemotaxis to CCL3, figure 8.2 and results hint receptor oligomerisation involving CXCR7 may mediate chemotaxis to CCL3.

CXCR7 purportedly sequesters CXCL12, so CXCR7 may function to modify chemokine concentrations during *in vitro* assays. Also inhibition of a signalling protein may modify the concentration of chemokine needed to produce chemotaxis, chemokinesis or calcium flux. Thus figure 8.22 may illustrate an inhibitor simply modifying the concentration of a chemokine needed to achieve calcium flux.

The balance of CXCR4/CXCR4 homodimers or CXCR4/CXCR7 heterodimers may influence whether CXCL14 inhibits or expedites chemotaxis to CXCL12, the high expression of CXCR7 in Jurkat [957] may explain why CXCL14 inhibits their chemotaxis to CXCL12, figure 8.31. Also CXCL14 may be synergistic to CXCL12-induced Ca<sup>2+</sup> responses by mediating by endoplasmic reticulum inositol 1,4,5-trisphosphate receptors [1007], explaining figure 8.32. Flow cytometry in Jurkat demonstrated CXCL14 significantly increase CXCR4 signal loss produced by NSC23766, figure 8.33, this could be explained by CXCL14 binding CXCR4 and NSC23766 binding CXCR7 component of CXCR4/CXCR7 dimers.



## 9: General Conclusions

These are some of the many interesting conclusions that can be drawn from the research reported in this thesis.

THP-1 and MCF7 were found to express both CCR5 and CXCR4. THP-1 migrated towards many CC and CXC chemokines; Jurkat only to CXCL12. In both cases numbers of cells migrating to a range of chemokine concentrations produced Gaussian distributions, with modest concentrations of chemokines being the most chemotactic. Spaks (2017) reports that chemokine concentrations can correlate with both the numbers of immune cells infiltrating a tumour's microenvironment and chemokine receptor expression [1013]. This thesis contributes towards a better understanding of the chemokine concentrations that attract immune and cancer cells, knowledge necessary to enable therapeutic manipulation of the chemotactic responses that support metastases.

In THP-1, CCL3 plus CXCL12 produced additive chemotactic responses, whereas CCL2 plus CXCL11 does not, suggesting CCR5 and CXCR4 may dimerize to support migration but CCR2 and CXCR3 do not. When different chemokines bind the same chemokine receptor the specific receptor conformation changes may direct the GRK subtype recruited, and which serine/threonine receptor residues it phosphorylates and so directing resultant biased signalling through G-proteins or  $\beta$ -arrestins. GRK2 was identified as important to both CCL3- and CXCL12-induced migration; Arrestin-2 as more important for CXCL12-induced migration and Arrestin-3 for migration to CCL3, depending on cell type. Gahbauer *et al.* (2018) and many others report that biased agonism and receptor dimerization relate to the agonist molecular structure, as different agonists may stabilise different GPCR conformations and consequent cellular responses [1014, 1015]. This thesis provides further evidence for links between GPCR class and  $\beta$ -arrestin isotype, but also cell-type specific factors. It also adds evidence for the involvement of receptor dimerization and co-operation in chemokine-induced chemotaxis and hence contributes to a better understanding of chemokine receptor interplay in malignancies.

Dynamin is a key protein in endocytosis. Dynamin was visualised in the cytoplasm and nucleus; knockdown of Dynamin-2 and small molecule inhibitors demonstrated Dynamin's significance in cytokinesis and cell migration. Different Dynamin domains were found important for migration to different chemokines, the GTPase domain for migration to CCL3 and the PH domain for migration to CXCL12. Bazzani *et al.* (2018) has established that both clathrin and caveolin-mediated endocytosis depends on Dynamin, and that blocking endocytosis with Dynamin inhibitors can prevent receptor endocytosis that would enhance malignant cell proliferation [1016]. Results here suggest cell type and chemokine specific control over which ligand/receptor pairs undergo

endocytosis may be achieved by using different Dynamin inhibitors, a novel option to explore further.

PKC's role in cell migration was found to be isoform, cell type and chemokine specific. Results with small molecule PKC inhibitors were deceptive, suggesting only PKC $\mu$  was important, but siRNA knockdown of PKC isoforms clarified the importance of PKC $\alpha$  and PKC $\delta$ , and to a lesser extent of PKC $\epsilon$  and PKC $\zeta$ . Each isoform's importance was resolved along with chemokine and/or cell type specificities. Isakov (2017) reviewed how many tumours have altered PKC expression or mutation of PKC isoform/s [262]. Results here show how this links to chemokine signalling through two important chemokines implicated in cancers, CXCL12 and CCL3, information which may help open windows for therapeutic exploitation.

Extensive use of small molecule inhibitors established that both CCL3 and CXCL12 signalling employs Src and the Raf/MEK/ERK pathway. Research by others has recognised Src's importance in CXCL12-supported malignancy [555, 576]. Results in this thesis suggest it may also be important in responses of cancer cells to CCL3. Investigations also discovered synergism between inhibition of ROCK and Raf, and also between MEK and Raf. Pi3K and FAK appear key in CXCL12- but not CCL3-signal transduction leading to cell migration, whereas ROCK and MEK are important in both CCL3 and CXCL12-induced migration; all three proteins influence cofilin phosphorylation. This demonstrates that CXCL12- and CCL3-signalling uses diverse pathways to trigger chemotaxis, but also that signalling protein use by a specific receptor/chemokine pair can be very individual to the chemokine and cell-type. This lack of generalisation needs further investigations but suggests opportunities for the further development of synergistic chemotherapies.

In MCF7 siRNA knockdown of actin binding protein Cofilin established its importance to cell migration. In THP-1 Cofilin phosphorylation showed positive correlation with the ability of a chemokine to induce migration. Also this phosphorylation can be modified by inhibition of cytosolic signalling proteins, and so can confirm the relevance of any individual signalling protein to a signalling pathway triggered by a specific chemokine. This offers a novel readout method that can be used alongside other assays to clarify chemokine signalling pathway components.

JAK2 and STAT3 were found to support CXCL12-induced wound-healing in MCF7 and chemotaxis to CCL2 and CXCL12 in THP-1 but not migration to CXCL12 in Jurkat. Inhibition of JAK2 and STAT3 potentiated calcium flux in all three cell types and blunted cAMP falls in THP-1 in response to CCL2 stimulation. Forskolin, employed in cAMP assays, also independently inhibited cell migration and wound-healing to CXCL12 and produced cofilin phosphorylation. In THP-1 JAK2 and STAT3

inhibitors were found to alter the temporal cofilin phosphorylation pattern produced between one and thirty minutes after CXCL12 stimulation, this cofilin phosphorylation pattern correlated with STAT3 phosphorylation responses to CXCL12. Roussos *et al.* (2011) described the role of cofilin in the amoeboid migration mode of adherent breast cancer cells [1017], the results here show how temporal phosphorylation of cofilin operates in the chemotaxis of leukaemic cells to chemokines. This research also suggests Forskolin shows promise as an anti-metastatic adjunctive treatment in chemotherapy, and further elucidates JAK2 and STAT3 signalling in both leukaemic and breast cancer cell-lines.

The NSAIDs ibuprofen, naproxen and celecoxib, along with Aspirin and Paracetamol, were found to have varying effects on cell migration, cAMP levels and calcium dynamics. COX1 inhibitors Ibuprofen, Naproxen and Aspirin inhibited migration to CXCL12, whereas COX2 inhibitors Paracetamol and Celecoxib did not. Ibuprofen dramatically increased cofilin phosphorylation, whereas the other drugs all eliminated CXCL12-induced phosphorylation, possibly as Ibuprofen may have off-target inhibitory effects on Akt or MEK. Often in population and retrospective cohort studies the effects of NSAIDs and Aspirin on cancer initiation and progression is assessed by grouping the drugs into one study [1018-1020], this thesis shows why such a strategy may give unclear outcomes, as each can produce contrasting drug-specific effects on factors that may influence metastasis.

Rac1 GEF inhibitor NSC23766 was found to compete with 12G5 for CXCR4. This was confirmed by flow cytometry, where NSC23766 displaced CXCR4 antibody 12G5. NSC23766 also dose-dependently inhibited calcium flux triggered by CXCL12, and reduced cAMP levels in presence and absence of CXCL12, whereas CXCR4 ligands AMD3100 and ATI2341 did not. Rho GTPases include Cdc42 and Rac1. Results here show Cdc42 is involved in CXCL12- and CCL3-induced chemotaxis whereas Rac1 is involved in migration to CXCL12 but not CCL3, this was confirmed by use of a Rac-inhibiting peptide. Inhibition of CXCR4, using NSC23766, AMD3100 and ATI2341 was shown to impede both cell-migration to CXCL12 and Rac1 activation. This may relate to Rac1 signalling through PKC $\zeta$ , as knockdown of PKC $\zeta$  also inhibited CXCL12-induced chemotaxis. Additionally Rac1 inhibition by NSC23766 was found to inhibit THP-1 migration to CXCL11 but not CCL2, suggesting NSC23766's target could be CXCR7, and/or its effect on CXCL12/CXCR4 may be through modulating CXCR4/CXCR7 dimerization. Cofilin phosphorylation in presence of CXCL12 was reduced by both NSC23766 and Rac1-inhibiting peptide W56, demonstrating that NSC23766 inhibits Rac1 signalling and also has off-target effects as a CXCR4-biased antagonist. Chemotaxis and flow cytometry assays using CXCL14 with CXCL12 in Jurkat supported this conclusion.

## **10: Future Work**

**Chapter 3:** Future investigations could establish if CCL3/CCR1 and CCL3/CCR5 respond in similar ways to dynamin inhibitors, and if chemokine concentration influences responses to inhibitors.

**Chapter 4:** GSK3 $\alpha/\beta$  are proteins with oncogenic (through promoting  $\beta$ -catenin) and tumour suppressing abilities [1021]. Small molecule GSK3 inhibitors are available e.g. StemMACSTM CHIR99021. Establishing the role GSK3 plays in chemotaxis would facilitate further interpretation of the results above.

**Chapter 5:** Cofilin phosphorylation dynamics in adherent cell-lines such as MCF7 and PC3 could be investigated hence establish if chemokine-responses reported above in THP-1 are general or cell-type specific.

**Chapter 6:** Like many transcription factors STAT3 can translocate to mitochondria where it may influence function of complexes in the electron transport chain to modulate ATP levels and energy dynamics [1022]. Mitochondrial STAT3 may also influence ROS production, cell growth and transformation [1023] all factors thought important in malignancy. MCF7 were transfected with mito-DS Red plasmids then treated with JAK2/STAT3 inhibitors, figure 6.4; however transfection levels were not sufficient to analyse if there were any visual changes in mitochondria appearance/location from control in cells treated with JAK2 or STAT3 inhibitors. This would be interesting to establish.

**Chapter 7:** The next steps could include using Western Blot analysis of the effects of a range of NSAIDs along with Aspirin and Paracetamol on phosphorylation, i.e. activation or inhibition, of signalling proteins which purportedly are implicated in malignancies such as Akt, MEK, ERK and JAK.

**Chapter 8:** Next all papers which have used NSC23766 as a selective Rac1 inhibitor could be reviewed in the light of this and research by others [901, 902] showing NSC23766 has off target effects. Also chemotaxis assays using NSC23766 with CXCR7 inhibitor CCX771 combinations could be done to see if they produce similar or additive effects. Then Flow cytometry and chemotaxis assays could be undertaken to see if AMD3100 competes with NSC23766 for CXCR4 or just has additive effect, if so this provides additional evidence that NSC23766 is binding CXCR7, preventing CXCR4/CXCR7 dimerization or hitting another cellular target to modulate CXCR4 expression. Finally treatment with pertussis toxin informs if signalling is Gai linked, so further investigations could explore if NSC23766 effects are modulated by pertussis toxin.

## 11: References

1. Ward, P.S. and C.B. Thompson, *Metabolic reprogramming: a cancer hallmark even warburg did not anticipate*. Cancer Cell, 2012. 21(3):297-308.
2. Pavlova, N.N. and C.B. Thompson, *The Emerging Hallmarks of Cancer Metabolism*. Cell Metab, 2016. 23(1):27-47.
3. Balkwill, F., *Cancer and the chemokine network*. Nat Rev Cancer, 2004. 4(7):540-50.
4. Ananthakrishnan, R. and A. Ehrlicher, *The forces behind cell movement*. Int J Biol Sci, 2007. 3(5):303-17.
5. Roden, R.B.S. and P.L. Stern, *Opportunities and challenges for human papillomavirus vaccination in cancer*. Nat Rev Cancer, 2018. 18(4):240-254.
6. Vander Heiden, M.G. and R.J. DeBerardinis, *Understanding the Intersections between Metabolism and Cancer Biology*. Cell, 2017. 168(4):657-669.
7. Nussinov, R. and H. Jang, *Dynamic multiprotein assemblies shape the spatial structure of cell signaling*. Prog Biophys Mol Biol, 2014. 116(0):158-164.
8. Brucher, B.L. and I.S. Jamall, *Cell-cell communication in the tumor microenvironment, carcinogenesis, and anticancer treatment*. Cell Physiol Biochem, 2014. 34(2):213-43.
9. Miller, M.C. and K.H. Mayo, *Chemokines from a Structural Perspective*. Int J Mol Sci, 2017. 18(10):2088.
10. Baggiolini, M., *Chemokines and leukocyte traffic*. Nature, 1998. 392(6676):565-8.
11. de The, H., *Differentiation therapy revisited*. Nat Rev Cancer, 2017. 1(103):103.
12. Carruthers, C. and V. Suntzeff, *The Role of Calcium in Carcinogenesis Summary*. Science, 1944. 99(2569):245-7.
13. Marchi, S. and P. Pinton, *The mitochondrial calcium uniporter complex: molecular components, structure and physiopathological implications*. J Physiol, 2014. 592(5):829-39.
14. Galluzzi, L., et al., *Essential versus accessory aspects of cell death: recommendations of the NCCD 2015*. Cell Death Differ, 2015. 22(1):58-73.
15. O'Hayre, M., et al., *The Emerging Mutational Landscape of G-proteins and G-protein Coupled Receptors in Cancer*. Nat Rev Cancer, 2013. 13(6):412-424.
16. Pento, J.T., *Monoclonal Antibodies for the Treatment of Cancer*. Anticancer Res, 2017. 37(11):5935-5939.
17. Gurevich, V.V. and E.V. Gurevich, *Molecular Mechanisms of GPCR Signaling: A Structural Perspective*. Int J Mol Sci, 2017. 18(12):E2519.

18. Cotton, M. and A. Claing, *G protein-coupled receptors stimulation and the control of cell migration*. Cell Signal, 2009. 21(7):1045-53.
19. Ferguson, S.S., *Evolving concepts in G protein-coupled receptor endocytosis: the role in receptor desensitization and signaling*. Pharmacol Rev, 2001. 53(1):1-24.
20. Kohout, T.A. and R.J. Lefkowitz, *Regulation of G protein-coupled receptor kinases and arrestins during receptor desensitization*. Mol Pharmacol, 2003. 63(1):9-18.
21. Park, J.Y., et al., *Structural mechanism of GPCR-arrestin interaction: recent breakthroughs*. Arch Pharm Res, 2016. 39(3):293-301.
22. Proudfoot, A.E., *The chemokine family. Potential therapeutic targets from allergy to HIV infection*. Eur J Dermatol, 1998. 8(3):147-57.
23. Vlahopoulos, S.A., et al., *Dynamic aberrant NF-kappaB spurs tumorigenesis: a new model encompassing the microenvironment*. Cytokine Growth Factor Rev, 2015. 26(4):389-403.
24. Moser, B., et al., *Chemokines: multiple levels of leukocyte migration control*. Trends Immunol, 2004. 25(2):75-84.
25. Zlotnik, A., O. Yoshie, and H. Nomiya, *The chemokine and chemokine receptor superfamilies and their molecular evolution*. Genome Biol, 2006. 7(12):243.
26. Griffith, J.W., C.L. Sokol, and A.D. Luster, *Chemokines and chemokine receptors: positioning cells for host defense and immunity*. Annu Rev Immunol, 2014. 32:659-702.
27. Loetscher, P., et al., *The ligands of CXC chemokine receptor 3, I-TAC, Mig, and IP10, are natural antagonists for CCR3*. J Biol Chem, 2001. 276(5):2986-91.
28. Sallusto, F. and A. Lanzavecchia, *Understanding dendritic cell and T-lymphocyte traffic through the analysis of chemokine receptor expression*. Immunol Rev, 2000. 177:134-40.
29. Bernhagen, J., et al., *MIF is a noncognate ligand of CXC chemokine receptors in inflammatory and atherogenic cell recruitment*. Nat Med, 2007. 13(5):587-96.
30. Saini, V., A. Marchese, and M. Majetschak, *CXC chemokine receptor 4 is a cell surface receptor for extracellular ubiquitin*. J Biol Chem, 2010. 285(20):15566-76.
31. Schiraldi, M., et al., *HMGB1 promotes recruitment of inflammatory cells to damaged tissues by forming a complex with CXCL12 and signaling via CXCR4*. J Exp Med, 2012. 209(3):551-63.
32. Simon, M.I., M.P. Strathmann, and N. Gautam, *Diversity of G proteins in signal transduction*. Science, 1991. 252(5007):802-8.
33. Wilkie, T.M., et al., *Evolution of the mammalian G protein alpha subunit multigene family*. Nat Genet, 1992. 1(2):85-91.

34. Tang, W., et al., *A PLCbeta/PI3Kgamma-GSK3 signaling pathway regulates cofilin phosphatase slingshot2 and neutrophil polarization and chemotaxis*. Dev Cell, 2011. 21(6):1038-50.
35. Kiefer, F. and A.F. Siekmann, *The role of chemokines and their receptors in angiogenesis*. Cell Mol Life Sci, 2011. 68(17):2811-30.
36. Charo, I.F. and R.M. Ransohoff, *The many roles of chemokines and chemokine receptors in inflammation*. N Engl J Med, 2006. 354(6):610-21.
37. Mantovani, A., R. Bonecchi, and M. Locati, *Tuning inflammation and immunity by chemokine sequestration: decoys and more*. Nat Rev Immunol, 2006. 6(12):907-18.
38. Ulvmar, M.H., E. Hub, and A. Rot, *Atypical chemokine receptors*. Exp Cell Res, 2011. 317(5):556-68.
39. Nomiyama, H., N. Osada, and O. Yoshie, *A family tree of vertebrate chemokine receptors for a unified nomenclature*. Dev Comp Immunol, 2011. 35(7):705-15.
40. Maksym, R.B., et al., *The role of stromal-derived factor-1--CXCR7 axis in development and cancer*. Eur J Pharmacol, 2009. 625(1-3):31-40.
41. Boldajipour, B., et al., *Control of chemokine-guided cell migration by ligand sequestration*. Cell, 2008. 132(3):463-73.
42. Broxmeyer, H.E., et al., *Rapid mobilization of murine and human hematopoietic stem and progenitor cells with AMD3100, a CXCR4 antagonist*. J Exp Med, 2005. 201(8):1307-18.
43. Zlotnik, A., A.M. Burkhardt, and B. Homey, *Homeostatic chemokine receptors and organ-specific metastasis*. Nat Rev Immunol, 2011. 11(9):597-606.
44. Belperio, J.A., et al., *CXC chemokines in angiogenesis*. J Leukoc Biol, 2000. 68(1):1-8.
45. Arenberg, D.A., et al., *Improved survival in tumor-bearing SCID mice treated with interferon-gamma-inducible protein 10 (IP-10/CXCL10)*. Cancer Immunol Immunother, 2001. 50(10):533-8.
46. Sgadari, C., et al., *Mig, the monokine induced by interferon-gamma, promotes tumor necrosis in vivo*. Blood, 1997. 89(8):2635-43.
47. Luster, A.D. and P. Leder, *IP-10, a -C-X-C- chemokine, elicits a potent thymus-dependent antitumor response in vivo*. J Exp Med, 1993. 178(3):1057-65.
48. Lasagni, L., et al., *An Alternatively Spliced Variant of CXCR3 Mediates the Inhibition of Endothelial Cell Growth Induced by IP-10, Mig, and I-TAC, and Acts as Functional Receptor for Platelet Factor 4*. J Exp Med, 2003. 197(11):1537-1549.
49. Billottet, C., C. Quemener, and A. Bikfalvi, *CXCR3, a double-edged sword in tumor progression and angiogenesis*. Biochim Biophys Acta Rev Cancer, 2013. 1836(2):287-295.

50. Walker, G.M., et al., *Effects of flow and diffusion on chemotaxis studies in a microfabricated gradient generator*. Lab Chip, 2005. 5(6):611-8.
51. Pages, F., et al., *Effector memory T cells, early metastasis, and survival in colorectal cancer*. N Engl J Med, 2005. 353(25):2654-66.
52. Sato, E., et al., *Intraepithelial CD8+ tumor-infiltrating lymphocytes and a high CD8+/regulatory T cell ratio are associated with favorable prognosis in ovarian cancer*. Proc Natl Acad Sci U S A, 2005. 102(51):18538-43.
53. Wang, W., et al., *Effector T Cells Abrogate Stroma-Mediated Chemoresistance in Ovarian Cancer*. Cell, 2016. 165(5):1092-1105.
54. Sica, A., et al., *Tumour-associated macrophages are a distinct M2 polarised population promoting tumour progression: potential targets of anti-cancer therapy*. Eur J Cancer, 2006. 42(6):717-27.
55. Taniguchi, M., et al., *Discovery of NKT cells and development of NKT cell-targeted anti-tumor immunotherapy*. Proc Jpn Acad Ser B Phys Biol Sci, 2015. 91(7):292-304.
56. Swiecki, M. and M. Colonna, *The multifaceted biology of plasmacytoid dendritic cells*. Nat Rev Immunol, 2015. 15(8):471-85.
57. Annunziato, F., et al., *Main features of human T helper 17 cells*. Ann N Y Acad Sci, 2013:12075.
58. Acosta-Rodriguez, E.V., et al., *Surface phenotype and antigenic specificity of human interleukin 17-producing T helper memory cells*. Nat Immunol, 2007. 8(6):639-46.
59. Kryczek, I., et al., *Human TH17 cells are long-lived effector memory cells*. Sci Transl Med, 2011. 3(104):3002949.
60. Kryczek, I., et al., *CXCL12 and vascular endothelial growth factor synergistically induce neoangiogenesis in human ovarian cancers*. Cancer Res, 2005. 65(2):465-72.
61. Martin-Orozco, N., et al., *T helper 17 cells promote cytotoxic T cell activation in tumor immunity*. Immunity, 2009. 31(5):787-98.
62. Mathan, T., C. Figdor, and S. Buschow, *Human Plasmacytoid Dendritic Cells: From Molecules to Intercellular Communication Network*. Front Immunol, 2013. 4(372).
63. Guery, L. and S. Hugues, *Th17 Cell Plasticity and Functions in Cancer Immunity*. Biomed Res Int, 2015. 314620(10):25.
64. Nicholas, N.S., B. Apollonio, and A.G. Ramsay, *Tumor microenvironment (TME)-driven immune suppression in B cell malignancy*. Biochim Biophys Acta, 2016. 3:471-482.
65. Zou, L., et al., *Bone marrow is a reservoir for CD4+CD25+ regulatory T cells that traffic through CXCL12/CXCR4 signals*. Cancer Res, 2004. 64(22):8451-5.



66. Pierini, A., et al., *Foxp3(+) regulatory T cells maintain the bone marrow microenvironment for B cell lymphopoiesis*. Nat Commun, 2017. 8(15068).
67. Kim, C.H., B. Johnston, and E.C. Butcher, *Trafficking machinery of NKT cells: shared and differential chemokine receptor expression among V alpha 24(+)V beta 11(+) NKT cell subsets with distinct cytokine-producing capacity*. Blood, 2002. 100(1):11-6.
68. Metelitsa, L.S., et al., *Natural killer T cells infiltrate neuroblastomas expressing the chemokine CCL2*. J Exp Med, 2004. 199(9):1213-21.
69. Tangye, S.G. and D.M. Tarlinton, *Memory B cells: effectors of long-lived immune responses*. Eur J Immunol, 2009. 39(8):2065-75.
70. Schmidt, M., et al., *The humoral immune system has a key prognostic impact in node-negative breast cancer*. Cancer Res, 2008. 68(13):5405-13.
71. Ten Hacken, E. and J.A. Burger, *Microenvironment interactions and B-cell receptor signaling in Chronic Lymphocytic Leukemia: Implications for disease pathogenesis and treatment*. Biochim Biophys Acta, 2016. 3:401-413.
72. Germain, C., S. Gnjatic, and M.C. Dieu-Nosjean, *Tertiary Lymphoid Structure-Associated B Cells are Key Players in Anti-Tumor Immunity*. Front Immunol, 2015. 6(67).
73. Labidi-Galy, S.I., et al., *Plasmacytoid dendritic cells infiltrating ovarian cancer are associated with poor prognosis*. Oncoimmunology, 2012. 1(3):380-382.
74. Lombardi, V.C., S.F. Khaiboullina, and A.A. Rizvanov, *Plasmacytoid dendritic cells, a role in neoplastic prevention and progression*. Eur J Clin Invest, 2015. 1:1-8.
75. Qian, B.Z., et al., *CCL2 recruits inflammatory monocytes to facilitate breast-tumour metastasis*. Nature, 2011. 475(7355):222-5.
76. Pollard, J.W., *Tumour-educated macrophages promote tumour progression and metastasis*. Nat Rev Cancer, 2004. 4:71.
77. Noy, R. and J.W. Pollard, *Tumor-associated macrophages: from mechanisms to therapy*. Immunity, 2014. 41(1):49-61.
78. DeNardo, D.G., et al., *Leukocyte complexity predicts breast cancer survival and functionally regulates response to chemotherapy*. Cancer Discov, 2011. 1(1):54-67.
79. Kitamura, T., et al., *CCL2-induced chemokine cascade promotes breast cancer metastasis by enhancing retention of metastasis-associated macrophages*. J Exp Med, 2015. 212(7):1043-59.
80. Asano, K., et al., *CD169-positive macrophages dominate antitumor immunity by crosspresenting dead cell-associated antigens*. Immunity, 2011. 34(1):85-95.
81. De Palma, M. and C.E. Lewis, *Macrophage regulation of tumor responses to anticancer therapies*. Cancer Cell, 2013. 23(3):277-86.

82. Gordon, S.R., et al., *PD-1 expression by tumour-associated macrophages inhibits phagocytosis and tumour immunity*. Nature, 2017. 545(7655):495-499.
83. Mantovani, A., et al., *Macrophage polarization: tumor-associated macrophages as a paradigm for polarized M2 mononuclear phagocytes*. Trends Immunol, 2002. 23(11):549-55.
84. Ueno, T., et al., *Significance of macrophage chemoattractant protein-1 in macrophage recruitment, angiogenesis, and survival in human breast cancer*. Clin Cancer Res, 2000. 6(8):3282-9.
85. Pahler, J.C., et al., *Plasticity in tumor-promoting inflammation: impairment of macrophage recruitment evokes a compensatory neutrophil response*. Neoplasia, 2008. 10(4):329-40.
86. Saji, H., et al., *Significant correlation of monocyte chemoattractant protein-1 expression with neovascularization and progression of breast carcinoma*. Cancer, 2001. 92(5):1085-91.
87. Bonapace, L., et al., *Cessation of CCL2 inhibition accelerates breast cancer metastasis by promoting angiogenesis*. Nature, 2014. 515(7525):130-3.
88. Pienta, K.J., et al., *Phase 2 study of carlumab (CNTO 888), a human monoclonal antibody against CC-chemokine ligand 2 (CCL2), in metastatic castration-resistant prostate cancer*. Invest New Drugs, 2013. 31(3):760-8.
89. Squadrito, M.L. and M. De Palma, *Macrophage regulation of tumor angiogenesis: implications for cancer therapy*. Mol Aspects Med, 2011. 32(2):123-45.
90. Swierczak, A., et al., *The promotion of breast cancer metastasis caused by inhibition of CSF-1R/CSF-1 signaling is blocked by targeting the G-CSF receptor*. Cancer Immunol Res, 2014. 2(8):765-76.
91. Wolf, M.J., et al., *Endothelial CCR2 signaling induced by colon carcinoma cells enables extravasation via the JAK2-Stat5 and p38MAPK pathway*. Cancer Cell, 2012. 22(1):91-105.
92. Fang, W.B., et al., *CCL2/CCR2 chemokine signaling coordinates survival and motility of breast cancer cells through Smad3 protein- and p42/44 mitogen-activated protein kinase (MAPK)-dependent mechanisms*. J Biol Chem, 2012. 287(43):36593-608.
93. Long, H., et al., *CD133+ ovarian cancer stem-like cells promote non-stem cancer cell metastasis via CCL5 induced epithelial-mesenchymal transition*. Oncotarget, 2015. 6(8):5846-59.
94. Lee, J.M., et al., *The epithelial-mesenchymal transition: new insights in signaling, development, and disease*. J Cell Biol, 2006. 172(7):973-81.
95. Fridlender, Z.G., et al., *CCL2 blockade augments cancer immunotherapy*. Cancer Res, 2010. 70(1):109-18.
96. Noel, M.S., et al., *Orally administered CCR2 selective inhibitor CCX872-b clinical trial in pancreatic cancer*. J Clin Oncol, 2017. 35(4\_suppl):276-276.

97. Gilbert, J., et al., *Effect of CC chemokine receptor 2 CCR2 blockade on serum C-reactive protein in individuals at atherosclerotic risk and with a single nucleotide polymorphism of the monocyte chemoattractant protein-1 promoter region*. Am J Cardiol, 2011. 107(6):906-11.
98. Schoenborn, J.R. and C.B. Wilson, *Regulation of interferon-gamma during innate and adaptive immune responses*. Adv Immunol, 2007. 96:41-101.
99. Cambien, B., et al., *Organ-specific inhibition of metastatic colon carcinoma by CXCR3 antagonism*. Br J Cancer, 2009. 100(11):1755-64.
100. Ohmori, Y., et al., *Tumor necrosis factor-alpha induces cell type and tissue-specific expression of chemoattractant cytokines in vivo*. Am J Pathol, 1993. 142(3):861-70.
101. Tokunaga, R., et al., *CXCL9, CXCL10, CXCL11/CXCR3 axis for immune activation - A target for novel cancer therapy*. Cancer Treat Rev, 2017. 63:40-47.
102. Xanthou, G., et al., *CCR3 functional responses are regulated by both CXCR3 and its ligands CXCL9, CXCL10 and CXCL11*. Eur J Immunol, 2003. 33(8):2241-50.
103. Scotton, C.J., et al., *Multiple actions of the chemokine CXCL12 on epithelial tumor cells in human ovarian cancer*. Cancer Res, 2002. 62(20):5930-8.
104. Darash-Yahana, M., et al., *Role of high expression levels of CXCR4 in tumor growth, vascularization, and metastasis*. Faseb J, 2004. 18(11):1240-2.
105. Goffart, N., et al., *CXCL12 mediates glioblastoma resistance to radiotherapy in the subventricular zone*. Neuro Oncol, 2017. 19(1):66-77.
106. Balabanian, K., et al., *The chemokine SDF-1/CXCL12 binds to and signals through the orphan receptor RDC1 in T lymphocytes*. J Biol Chem, 2005. 280(42):35760-6.
107. Kumar, R., et al., *CXCR7 mediated Gialpha independent activation of ERK and Akt promotes cell survival and chemotaxis in T cells*. Cell Immunol, 2012. 272(2):230-41.
108. Hao, M., et al., *Role of chemokine receptor CXCR7 in bladder cancer progression*. Biochem Pharmacol, 2012. 84(2):204-214.
109. Spranger, S., R. Bao, and T.F. Gajewski, *Melanoma-intrinsic beta-catenin signalling prevents anti-tumour immunity*. Nature, 2015. 523(7559):231-5.
110. Odemis, V., et al., *The presumed atypical chemokine receptor CXCR7 signals through G(i/o) proteins in primary rodent astrocytes and human glioma cells*. Glia, 2012. 60(3):372-81.
111. Luker, K.E., et al., *Constitutive and chemokine-dependent internalization and recycling of CXCR7 in breast cancer cells to degrade chemokine ligands*. Oncogene, 2010. 29(32):4599-610.
112. Wang, J., et al., *The role of CXCR7/RDC1 as a chemokine receptor for CXCL12/SDF-1 in prostate cancer*. J Biol Chem, 2008. 283(7):4283-94.

113. Burns, J.M., et al., *A novel chemokine receptor for SDF-1 and I-TAC involved in cell survival, cell adhesion, and tumor development*. J Exp Med, 2006. 203(9):2201-13.
114. Singh, R.K. and B.L. Lokeshwar, *The IL-8-regulated chemokine receptor CXCR7 stimulates EGFR signaling to promote prostate cancer growth*. Cancer Res, 2011. 71(9):3268-77.
115. Miao, Z., et al., *CXCR7 (RDC1) promotes breast and lung tumor growth in vivo and is expressed on tumor-associated vasculature*. Proc Natl Acad Sci U S A, 2007. 104(40):15735-40.
116. Cully, M., *Lung disease: CXCR7 activation overrides lung fibrosis*. Nat Rev Drug Discov, 2016. 15(3):26.
117. Ribas, R., et al., *Identification of chemokine receptors as potential modulators of endocrine resistance in oestrogen receptor-positive breast cancers*. Breast Cancer Res, 2014. 16(5):014-0447.
118. Peng, D., et al., *Epigenetic silencing of TH1-type chemokines shapes tumour immunity and immunotherapy*. Nature, 2015. 527(7577):249-53.
119. Barbee, M.S., et al., *Current status and future directions of the immune checkpoint inhibitors ipilimumab, pembrolizumab, and nivolumab in oncology*. Ann Pharmacother, 2015. 49(8):907-37.
120. Ierano, C., et al., *A point mutation (G574A) in the chemokine receptor CXCR4 detected in human cancer cells enhances migration*. Cell Cycle, 2009. 8(8):1228-37.
121. Libura, J., et al., *CXCR4-SDF-1 signaling is active in rhabdomyosarcoma cells and regulates locomotion, chemotaxis, and adhesion*. Blood, 2002. 100(7):2597-606.
122. Ceradini, D.J., et al., *Progenitor cell trafficking is regulated by hypoxic gradients through HIF-1 induction of SDF-1*. Nat Med, 2004. 10(8):858-64.
123. Mojsilovic-Petrovic, J., et al., *Hypoxia-inducible factor-1 (HIF-1) is involved in the regulation of hypoxia-stimulated expression of monocyte chemoattractant protein-1 (MCP-1/CCL2) and MCP-5 (Ccl12) in astrocytes*. J Neuroinflammation, 2007. 4(12):1742-2094.
124. Semenza, G.L., *Targeting HIF-1 for cancer therapy*. Nat Rev Cancer, 2003. 3(10):721-32.
125. Semaan, A., et al., *CXCL12 expression and PD-L1 expression serve as prognostic biomarkers in HCC and are induced by hypoxia*. Virchows Arch, 2017. 470(2):185-196.
126. Schioppa, T., et al., *Regulation of the chemokine receptor CXCR4 by hypoxia*. J Exp Med, 2003. 198(9):1391-402.
127. Tarnowski, M., et al., *Regulation of expression of stromal-derived factor-1 receptors: CXCR4 and CXCR7 in human rhabdomyosarcomas*. Mol Cancer Res, 2010. 8(1):1-14.
128. Ruiz, A., et al., *Pharmacological blockage of the CXCR4-CXCL12 axis in endometriosis leads to contrasting effects in proliferation, migration and invasion*. Biol Reprod, 2017. 17(4638520).

129. Janssens, R., S. Struyf, and P. Proost, *The unique structural and functional features of CXCL12*. Cell Mol Immunol, 2017. 30(10):107.
130. de Lourdes Perim, A., et al., *CXCL12/CXCR4 axis in the pathogenesis of acute lymphoblastic leukemia (ALL): a possible therapeutic target*. Cell Mol Life Sci, 2015. 72(9):1715-23.
131. Hinton, C.V., S. Avraham, and H.K. Avraham, *Role of the CXCR4/CXCL12 signaling axis in breast cancer metastasis to the brain*. Clin Exp Metastasis, 2010. 27(2):97-105.
132. Guo, F., et al., *CXCL12/CXCR4: a symbiotic bridge linking cancer cells and their stromal neighbors in oncogenic communication networks*. Oncogene. 2015. 35(7):816-26.
133. Shen, P., et al., *IL-35-producing B cells are critical regulators of immunity during autoimmune and infectious diseases*. Nature, 2014. 507(7492):366-370.
134. Nakai, A., et al., *Control of lymphocyte egress from lymph nodes through beta2-adrenergic receptors*. J Exp Med, 2014. 211(13):2583-98.
135. Burger, J.A. and T.J. Kipps, *CXCR4: a key receptor in the crosstalk between tumor cells and their microenvironment*. Blood, 2006. 107(5):1761-7.
136. Teicher, B.A. and S.P. Fricker, *CXCL12 (SDF-1)/CXCR4 Pathway in Cancer*. Clin Cancer Res, 2010. 16(11):2927-2931.
137. Lombardi, L., et al., *Chemokine receptor CXCR4: role in gastrointestinal cancer*. Crit Rev Oncol Hematol, 2013. 88(3):696-705.
138. Poznansky, M.C., et al., *Active movement of T cells away from a chemokine*. Nat Med, 2000. 6(5):543-8.
139. Fearon, D.T., *The carcinoma-associated fibroblast expressing fibroblast activation protein and escape from immune surveillance*. Cancer Immunol Res, 2014. 2(3):187-93.
140. Zboralski, D., et al., *Increasing Tumor-Infiltrating T Cells through Inhibition of CXCL12 with NOX-A12 Synergizes with PD-1 Blockade*. Cancer Immunol Res, 2017. 5(11):950-956.
141. Bachelierie, F., et al., *International Union of Basic and Clinical Pharmacology. [corrected]. LXXXIX. Update on the extended family of chemokine receptors and introducing a new nomenclature for atypical chemokine receptors*. Pharmacol Rev, 2013. 66(1):1-79.
142. Ferre, S., et al., *G protein-coupled receptor oligomerization revisited: functional and pharmacological perspectives*. Pharmacol Rev, 2014. 66(2):413-34.
143. Bleul, C.C., et al., *The lymphocyte chemoattractant SDF-1 is a ligand for LESTR/fusin and blocks HIV-1 entry*. Nature, 1996. 382(6594):829-33.
144. Balabanian, K., et al., *Proper desensitization of CXCR4 is required for lymphocyte development and peripheral compartmentalization in mice*. Blood, 2012. 119(24):5722-30.

145. Wu, B., et al., *Structures of the CXCR4 chemokine GPCR with small-molecule and cyclic peptide antagonists*. *Science*, 2010. 330(6007):1066-71.
146. Qin, L., et al., *Structural biology. Crystal structure of the chemokine receptor CXCR4 in complex with a viral chemokine*. *Science*, 2015. 347(6226):1117-22.
147. Roumen, L., et al., *C(X)CR in silico: Computer-aided prediction of chemokine receptor-ligand interactions*. *Drug Discov Today Technol*, 2012. 9(4):002.
148. Cutolo, P., et al., *Interaction of chemokine receptor CXCR4 in monomeric and dimeric state with its endogenous ligand CXCL12: coarse-grained simulations identify differences*. *J Biomol Struct Dyn*, 2017. 35(2):399-412.
149. Wong, R.S., et al., *Comparison of the potential multiple binding modes of bicyclam, monocyclam, and noncyclam small-molecule CXC chemokine receptor 4 inhibitors*. *Mol Pharmacol*, 2008. 74(6):1485-95.
150. Doranz, B.J., et al., *Identification of CXCR4 domains that support coreceptor and chemokine receptor functions*. *J Virol*, 1999. 73(4):2752-61.
151. Brelot, A., et al., *Identification of residues of CXCR4 critical for human immunodeficiency virus coreceptor and chemokine receptor activities*. *J Biol Chem*, 2000. 275(31):23736-44.
152. Tian, S., et al., *Distinct functional sites for human immunodeficiency virus type 1 and stromal cell-derived factor 1alpha on CXCR4 transmembrane helical domains*. *J Virol*, 2005. 79(20):12667-73.
153. Zhou, N., et al., *Structural and functional characterization of human CXCR4 as a chemokine receptor and HIV-1 co-receptor by mutagenesis and molecular modeling studies*. *J Biol Chem*, 2001. 276(46):42826-33.
154. Kufareva, I., et al., *Status of GPCR modeling and docking as reflected by community-wide GPCR Dock 2010 assessment*. *Structure*, 2011. 19(8):1108-26.
155. Ballesteros, J.A. and H. Weinstein, [19] *Integrated methods for the construction of three-dimensional models and computational probing of structure-function relations in G protein-coupled receptors*. *Methods Neurosci*, 1995. 25:366-428.
156. Drury, L.J., et al., *Monomeric and dimeric CXCL12 inhibit metastasis through distinct CXCR4 interactions and signaling pathways*. *Proc Natl Acad Sci U S A*, 2011. 108(43):17655-60.
157. Veldkamp, C.T., et al., *The monomer-dimer equilibrium of stromal cell-derived factor-1 (CXCL12) is altered by pH, phosphate, sulfate, and heparin*. *Protein Sci*, 2005. 14(4):1071-81.
158. Veldkamp, C.T., et al., *Structural basis of CXCR4 sulfotyrosine recognition by the chemokine SDF-1/CXCL12*. *Sci Signal*, 2008. 1(37):1160755.
159. Crump, M.P., et al., *Solution structure and basis for functional activity of stromal cell-derived factor-1; dissociation of CXCR4 activation from binding and inhibition of HIV-1*. *Embo J*, 1997. 16(23):6996-7007.

160. Kofuku, Y., et al., *Structural basis of the interaction between chemokine stromal cell-derived factor-1/CXCL12 and its G-protein-coupled receptor CXCR4*. J Biol Chem, 2009. 284(50):35240-50.
161. Heveker, N., et al., *Dissociation of the signalling and antiviral properties of SDF-1-derived small peptides*. Curr Biol, 1998. 8(7):369-76.
162. Murphy, J.W., et al., *Structural and functional basis of CXCL12 (stromal cell-derived factor-1 alpha) binding to heparin*. J Biol Chem, 2007. 282(13):10018-27.
163. Ferguson, S.M. and P. De Camilli, *Dynamin, a membrane remodelling GTPase*. Nat Rev Mol Cell Biol, 2012. 13(2):75-88.
164. Shpetner, H.S. and R.B. Vallee, *Identification of dynamin, a novel mechanochemical enzyme that mediates interactions between microtubules*. Cell, 1989. 59(3):421-32.
165. Praefcke, G.J. and H.T. McMahon, *The dynamin superfamily: universal membrane tubulation and fission molecules?* Nat Rev Mol Cell Biol, 2004. 5(2):133-47.
166. Cao, H., F. Garcia, and M.A. McNiven, *Differential distribution of dynamin isoforms in mammalian cells*. Mol Biol Cell, 1998. 9(9):2595-609.
167. Bodmer, D., M. Ascano, and R. Kuruvilla, *Isoform-specific dephosphorylation of dynamin1 by calcineurin couples neurotrophin receptor endocytosis to axonal growth*. Neuron, 2011. 70(6):1085-99.
168. Gray, N.W., et al., *Dynamin 3 is a component of the postsynapse, where it interacts with mGluR5 and Homer*. Curr Biol, 2003. 13(6):510-5.
169. Liu, Y.W., et al., *Differential curvature sensing and generating activities of dynamin isoforms provide opportunities for tissue-specific regulation*. Proc Natl Acad Sci U S A, 2011. 108(26):13.
170. Westermann, B., *Mitochondrial fusion and fission in cell life and death*. Nat Rev Mol Cell Biol, 2010. 11(12):872-84.
171. Schmid, S.L., *Reciprocal regulation of signaling and endocytosis: Implications for the evolving cancer cell*. J Cell Biol, 2017. 216(9):2623-2632.
172. Ferguson, K.M., et al., *Crystal structure at 2.2 Å resolution of the pleckstrin homology domain from human dynamin*. Cell, 1994. 79(2):199-209.
173. Ford, M.G., S. Jenni, and J. Nunnari, *The crystal structure of dynamin*. Nature, 2011. 477(7366):561-6.
174. Chappie, J.S., et al., *G domain dimerization controls dynamin's assembly-stimulated GTPase activity*. Nature, 2010. 465(7297):435-40.
175. Stowell, M.H., et al., *Nucleotide-dependent conformational changes in dynamin: evidence for a mechanochemical molecular spring*. Nat Cell Biol, 1999. 1(1):27-32.

176. Zheng, J., et al., *Identification of the binding site for acidic phospholipids on the pH domain of dynamin: implications for stimulation of GTPase activity*. J Mol Biol, 1996. 255(1):14-21.
177. Roux, A., et al., *Membrane curvature controls dynamin polymerization*. Proc Natl Acad Sci U S A, 2010. 107(9):4141-6.
178. Lee, A., et al., *Dominant-negative inhibition of receptor-mediated endocytosis by a dynamin-1 mutant with a defective pleckstrin homology domain*. Curr Biol, 1999. 9(5):261-4.
179. Ramachandran, R., et al., *Membrane insertion of the pleckstrin homology domain variable loop 1 is critical for dynamin-catalyzed vesicle scission*. Mol Biol Cell, 2009. 20(22):4630-9.
180. Shpetner, H.S., J.S. Herskovits, and R.B. Vallee, *A binding site for SH3 domains targets dynamin to coated pits*. J Biol Chem, 1996. 271(1):13-6.
181. Damke, H., et al., *Induction of mutant dynamin specifically blocks endocytic coated vesicle formation*. J Cell Biol, 1994. 127(4):915-34.
182. Marks, B., et al., *GTPase activity of dynamin and resulting conformation change are essential for endocytosis*. Nature, 2001. 410(6825):231-5.
183. Chappie, J.S., et al., *A pseudoatomic model of the dynamin polymer identifies a hydrolysis-dependent powerstroke*. Cell, 2011. 147(1):209-22.
184. Morlot, S. and A. Roux, *Mechanics of dynamin-mediated membrane fission*. Annu Rev Biophys, 2013. 42:629-49.
185. Bashkirov, P.V., et al., *GTPase cycle of dynamin is coupled to membrane squeeze and release, leading to spontaneous fission*. Cell, 2008. 135(7):1276-86.
186. Byrnes, L.J. and H. Sondermann, *Structural basis for the nucleotide-dependent dimerization of the large G protein atlastin-1/SPG3A*. Proc Natl Acad Sci U S A, 2011. 108(6):2216-21.
187. Low, H.H. and J. Lowe, *Dynamin architecture--from monomer to polymer*. Curr Opin Struct Biol, 2010. 20(6):791-8.
188. Taylor, M.J., D. Perrais, and C.J. Merrifield, *A high precision survey of the molecular dynamics of mammalian clathrin-mediated endocytosis*. PLoS Biol, 2011. 9(3):22.
189. Sever, S., H. Damke, and S.L. Schmid, *Dynamin:GTP controls the formation of constricted coated pits, the rate limiting step in clathrin-mediated endocytosis*. J Cell Biol, 2000. 150(5):1137-48.
190. Neumann, S. and S.L. Schmid, *Dual role of BAR domain-containing proteins in regulating vesicle release catalyzed by the GTPase, dynamin-2*. J Biol Chem, 2013. 288(35):25119-28.
191. Clayton, E.L., et al., *Dynamin I phosphorylation by GSK3 controls activity-dependent bulk endocytosis of synaptic vesicles*. Nat Neurosci, 2010. 13(7):845-51.



192. Reis, C.R., et al., *Crosstalk between Akt/GSK3beta signaling and dynamin-1 regulates clathrin-mediated endocytosis*. *Embo J*, 2015. 34(16):2132-46.
193. Di Fiore, P.P. and M. von Zastrow, *Endocytosis, signaling, and beyond*. *Cold Spring Harb Perspect Biol*, 2014. 6(8):a016865.
194. Grandal, M.V. and I.H. Madhus, *Epidermal growth factor receptor and cancer: control of oncogenic signalling by endocytosis*. *J Cell Mol Med*, 2008. 12(5A):1527-34.
195. Platta, H.W. and H. Stenmark, *Endocytosis and signaling*. *Curr Opin Cell Biol*, 2011. 23(4):393-403.
196. Reis, C.R., et al., *TRAIL-death receptor endocytosis and apoptosis are selectively regulated by dynamin-1 activation*. *Proc Natl Acad Sci U S A*, 2017. 114(3):504-509.
197. Puthenveedu, M.A. and M. von Zastrow, *Cargo regulates clathrin-coated pit dynamics*. *Cell*, 2006. 127(1):113-24.
198. Mellman, I. and Y. Yarden, *Endocytosis and cancer*. *Cold Spring Harb Perspect Biol*, 2013. 5(12):a016949.
199. Barbieri, E., P.P. Di Fiore, and S. Sigismund, *Endocytic control of signaling at the plasma membrane*. *Curr Opin Cell Biol*, 2016. 39:21-7.
200. Garay, C., et al., *Epidermal growth factor-stimulated Akt phosphorylation requires clathrin or ErbB2 but not receptor endocytosis*. *Mol Biol Cell*, 2015. 26(19):3504-19.
201. Grove, J., et al., *Flat clathrin lattices: stable features of the plasma membrane*. *Mol Biol Cell*, 2014. 25(22):3581-94.
202. Martinez-Outschoorn, U.E., F. Sotgia, and M.P. Lisanti, *Caveolae and signalling in cancer*. *Nat Rev Cancer*, 2015. 15(4):225-37.
203. Di Guglielmo, G.M., et al., *Compartmentalization of SHC, GRB2 and mSOS, and hyperphosphorylation of Raf-1 by EGF but not insulin in liver parenchyma*. *Embo J*, 1994. 13(18):4269-77.
204. Vieira, A.V., C. Lamaze, and S.L. Schmid, *Control of EGF receptor signaling by clathrin-mediated endocytosis*. *Science*, 1996. 274(5295):2086-9.
205. Schenck, A., et al., *The endosomal protein Appl1 mediates Akt substrate specificity and cell survival in vertebrate development*. *Cell*, 2008. 133(3):486-97.
206. Moore, C.A., S.K. Milano, and J.L. Benovic, *Regulation of receptor trafficking by GRKs and arrestins*. *Annu Rev Physiol*, 2007. 69:451-82.
207. Thomsen, A.R.B., et al., *GPCR-G Protein-beta-Arrestin Super-Complex Mediates Sustained G Protein Signaling*. *Cell*, 2016. 166(4):907-919.

208. Tsvetanova, N.G., R. Irannejad, and M. von Zastrow, *G protein-coupled receptor (GPCR) signaling via heterotrimeric G proteins from endosomes*. J Biol Chem, 2015. 290(11):6689-96.
209. Mayor, S., R.G. Parton, and J.G. Donaldson, *Clathrin-independent pathways of endocytosis*. Cold Spring Harb Perspect Biol, 2014. 6(6):a016758.
210. Henry, A.G., et al., *Regulation of endocytic clathrin dynamics by cargo ubiquitination*. Dev Cell, 2012. 23(3):519-32.
211. Struckhoff, A.P., et al., *PDZ-RhoGEF is essential for CXCR4-driven breast tumor cell motility through spatial regulation of RhoA*. J Cell Sci, 2013. 126(19):4514-4526.
212. Delhay, M., et al., *Identification of a postendocytic sorting sequence in CCR5*. Mol Pharmacol, 2007. 72(6):1497-507.
213. Lamaze, C., et al., *Regulation of receptor-mediated endocytosis by Rho and Rac*. Nature, 1996. 382(6587):177-9.
214. Pearse, B.M., *Clathrin and coated vesicles*. Embo J, 1987. 6(9):2507-12.
215. Robinson, M.S., *Forty Years of Clathrin-coated Vesicles*. Traffic, 2015. 16(12):1210-38.
216. Antonny, B., et al., *Membrane fission by dynamin: what we know and what we need to know*. Embo J, 2016. 35(21):2270-2284.
217. Kalaidzidis, I., et al., *APPL endosomes are not obligatory endocytic intermediates but act as stable cargo-sorting compartments*. J Cell Biol, 2015. 211(1):123-44.
218. Mettlen, M., et al., *Dissecting dynamin's role in clathrin-mediated endocytosis*. Biochem Soc Trans, 2009. 37(Pt 5):1022-6.
219. Zoncu, R., et al., *A phosphoinositide switch controls the maturation and signaling properties of APPL endosomes*. Cell, 2009. 136(6):1110-21.
220. Ringstad, N., Y. Nemoto, and P. De Camilli, *The SH3p4/Sh3p8/SH3p13 protein family: binding partners for synaptojanin and dynamin via a Grb2-like Src homology 3 domain*. Proc Natl Acad Sci U S A, 1997. 94(16):8569-74.
221. Boucrot, E., et al., *Endophilin marks and controls a clathrin-independent endocytic pathway*. Nature, 2015. 517(7535):460-5.
222. Renard, H.F., et al., *Endophilin-A2 functions in membrane scission in clathrin-independent endocytosis*. Nature, 2015. 517(7535):493-6.
223. Song, M.S., L. Salmena, and P.P. Pandolfi, *The functions and regulation of the PTEN tumour suppressor*. Nat Rev Mol Cell Biol, 2012. 13(5):283-96.
224. Xie, J., C. Erneux, and I. Pirson, *How does SHIP1/2 balance PtdIns(3,4)P2 and does it signal independently of its phosphatase activity?* Bioessays, 2013. 35(8):733-43.

225. Vehlow, A., et al., *Endophilin, Lamellipodin, and Mena cooperate to regulate F-actin-dependent EGF-receptor endocytosis*. *Embo J*, 2013. 32(20):2722-34.
226. Eppinga, R.D., et al., *Increased expression of the large GTPase dynamin 2 potentiates metastatic migration and invasion of pancreatic ductal carcinoma*. *Oncogene*, 2012. 31(10):1228-41.
227. Ezratty, E.J., M.A. Partridge, and G.G. Gundersen, *Microtubule-induced focal adhesion disassembly is mediated by dynamin and focal adhesion kinase*. *Nat Cell Biol*, 2005. 7(6):581-90.
228. Kruchten, A.E. and M.A. McNiven, *Dynamin as a mover and pincher during cell migration and invasion*. *J Cell Sci*, 2006. 119(Pt 9):1683-90.
229. Razidlo, G.L., et al., *Dynamin 2 potentiates invasive migration of pancreatic tumor cells through stabilization of the Rac1 GEF Vav1*. *Dev Cell*, 2013. 24(6):573-85.
230. Ridley, A.J., *Life at the leading edge*. *Cell*, 2011. 145(7):1012-22.
231. Gomez, T.S., et al., *Dynamin 2 regulates T cell activation by controlling actin polymerization at the immunological synapse*. *Nat Immunol*, 2005. 6(3):261-70.
232. Lopez-Lago, M., et al., *Tyrosine phosphorylation mediates both activation and downmodulation of the biological activity of Vav*. *Mol Cell Biol*, 2000. 20(5):1678-91.
233. Katzav, S., *Vav1: a hematopoietic signal transduction molecule involved in human malignancies*. *Int J Biochem Cell Biol*, 2009. 41(6):1245-8.
234. Bartolome, R.A., et al., *Activation of Vav/Rho GTPase signaling by CXCL12 controls membrane-type matrix metalloproteinase-dependent melanoma cell invasion*. *Cancer Res*, 2006. 66(1):248-58.
235. Tanwar, D.K., et al., *Crosstalk between the mitochondrial fission protein, Drp1, and the cell cycle is identified across various cancer types and can impact survival of epithelial ovarian cancer patients*. *Oncotarget*, 2016. 7(37):60021-60037.
236. Ferreira-da-Silva, A., et al., *Mitochondrial dynamics protein Drp1 is overexpressed in oncocyctic thyroid tumors and regulates cancer cell migration*. *PLoS One*, 2015. 10(3).
237. Cipolat, S., et al., *OPA1 requires mitofusin 1 to promote mitochondrial fusion*. *Proc Natl Acad Sci U S A*, 2004. 101(45):15927-32.
238. de Brito, O.M. and L. Scorrano, *Mitofusin 2 tethers endoplasmic reticulum to mitochondria*. *Nature*, 2008. 456(7222):605-10.
239. Meyer, J.N., T.C. Leuthner, and A.L. Luz, *Mitochondrial fusion, fission, and mitochondrial toxicity*. *Toxicology*, 2017. 5(17):30225-1.
240. Archer, S.L., *Mitochondrial dynamics--mitochondrial fission and fusion in human diseases*. *N Engl J Med*, 2013. 369(23):2236-51.

241. Patergnani, S., et al., *Calcium signaling around Mitochondria Associated Membranes*. Cell Commun Signal, 2011. 9(19):9-19.
242. Szabadkai, G., et al., *Drp-1-dependent division of the mitochondrial network blocks intraorganellar Ca<sup>2+</sup> waves and protects against Ca<sup>2+</sup>-mediated apoptosis*. Mol Cell, 2004. 16(1):59-68.
243. Han, X.J., et al., *CaM kinase I alpha-induced phosphorylation of Drp1 regulates mitochondrial morphology*. J Cell Biol, 2008. 182(3):573-85.
244. Tolkovsky, A.M., *Mitophagy*. Biochim Biophys Acta, 2009. 9(15):13.
245. Cribbs, J.T. and S. Strack, *Functional characterization of phosphorylation sites in dynamin-related protein 1*. Methods Enzymol, 2009. 457:231-53.
246. Zhu, P.P., et al., *Intra- and intermolecular domain interactions of the C-terminal GTPase effector domain of the multimeric dynamin-like GTPase Drp1*. J Biol Chem, 2004. 279(34):35967-74.
247. Evan, G.I. and K.H. Vousden, *Proliferation, cell cycle and apoptosis in cancer*. Nature, 2001. 411(6835):342-8.
248. Bonnet, S., et al., *A mitochondria-K<sup>+</sup> channel axis is suppressed in cancer and its normalization promotes apoptosis and inhibits cancer growth*. Cancer Cell, 2007. 11(1):37-51.
249. Mitra, K., et al., *A hyperfused mitochondrial state achieved at G1-S regulates cyclin E buildup and entry into S phase*. Proc Natl Acad Sci U S A, 2009. 106(29):11960-5.
250. Kashatus, D.F., et al., *RALA and RALBP1 regulate mitochondrial fission at mitosis*. Nat Cell Biol, 2011. 13(9):1108-15.
251. Marsboom, G., et al., *Dynamin-related protein 1-mediated mitochondrial mitotic fission permits hyperproliferation of vascular smooth muscle cells and offers a novel therapeutic target in pulmonary hypertension*. Circ Res, 2012. 110(11):1484-97.
252. Rehman, J., et al., *Inhibition of mitochondrial fission prevents cell cycle progression in lung cancer*. Faseb J, 2012. 26(5):2175-86.
253. Redmann, M., et al., *Mitophagy mechanisms and role in human diseases*. Int J Biochem Cell Biol, 2014. 53:127-133.
254. Lyons, S.M., et al., *Changes in cell shape are correlated with metastatic potential in murine and human osteosarcomas*. Biol Open, 2016. 5(3):289-299.
255. Falkenburger, B.H., E.J. Dickson, and B. Hille, *Quantitative properties and receptor reserve of the DAG and PKC branch of G(q)-coupled receptor signaling*. J Gen Physiol, 2013. 141(5):537-555.

256. Balasubramanian, N., S.H. Advani, and S.M. Zingde, *Protein kinase C isoforms in normal and leukemic neutrophils: altered levels in leukemic neutrophils and changes during myeloid maturation in chronic myeloid leukemia*. Leuk Res, 2002. 26(1):67-81.
257. Boyle, G.M., et al., *Intra-lesional injection of the novel PKC activator EBC-46 rapidly ablates tumors in mouse models*. PLoS One, 2014. 9(10).
258. Han, Z.T., et al., *Effect of intravenous infusions of 12-O-tetradecanoylphorbol-13-acetate (TPA) in patients with myelocytic leukemia: preliminary studies on therapeutic efficacy and toxicity*. Proc Natl Acad Sci U S A, 1998. 95(9):5357-61.
259. Antal, C.E., et al., *Cancer-associated protein kinase C mutations reveal kinase's role as tumor suppressor*. Cell, 2015. 160(3):489-502.
260. Mauro, L.V., et al., *PKCdelta promotes tumoral progression of human ductal pancreatic cancer*. Pancreas, 2010. 39(1):e31-41.
261. Newton, A.C., *Protein kinase C as a tumor suppressor*. Semin Cancer Biol, 2017. 2(17):30116-5.
262. Isakov, N., *Protein kinase C (PKC) isoforms in cancer, tumor promotion and tumor suppression*. Semin Cancer Biol, 2017. 29(17):30108-6.
263. Carrasco, S. and I. Merida, *Diacylglycerol, when simplicity becomes complex*. Trends Biochem Sci, 2007. 32(1):27-36.
264. Johnson, J.E., J. Giorgione, and A.C. Newton, *The C1 and C2 domains of protein kinase C are independent membrane targeting modules, with specificity for phosphatidylserine conferred by the C1 domain*. Biochemistry, 2000. 39(37):11360-9.
265. Dries, D.R., L.L. Gallegos, and A.C. Newton, *A single residue in the C1 domain sensitizes novel protein kinase C isoforms to cellular diacylglycerol production*. J Biol Chem, 2007. 282(2):826-30.
266. Giorgione, J.R., et al., *Increased membrane affinity of the C1 domain of protein kinase Cdelta compensates for the lack of involvement of its C2 domain in membrane recruitment*. J Biol Chem, 2006. 281(3):1660-9.
267. Ivey, R.A., M.P. Sajan, and R.V. Farese, *Requirements for pseudosubstrate arginine residues during autoinhibition and phosphatidylinositol 3,4,5-(PO<sub>4</sub>)(3)-dependent activation of atypical PKC*. J Biol Chem, 2014. 289(36):25021-30.
268. Fox, T.E., et al., *Ceramide recruits and activates protein kinase C zeta (PKC zeta) within structured membrane microdomains*. J Biol Chem, 2007. 282(17):12450-7.
269. Muller, G., et al., *PKC zeta is a molecular switch in signal transduction of TNF-alpha, bifunctionally regulated by ceramide and arachidonic acid*. Embo J, 1995. 14(9):1961-9.
270. Lamark, T., et al., *Interaction codes within the family of mammalian Phox and Bem1p domain-containing proteins*. J Biol Chem, 2003. 278(36):34568-81.

271. Moscat, J., et al., *Cell signaling and function organized by PB1 domain interactions*. Mol Cell, 2006. 23(5):631-40.
272. Wilson, M.I., et al., *PB1 domain-mediated heterodimerization in NADPH oxidase and signaling complexes of atypical protein kinase C with Par6 and p62*. Mol Cell, 2003. 12(1):39-50.
273. Joberty, G., et al., *The cell-polarity protein Par6 links Par3 and atypical protein kinase C to Cdc42*. Nat Cell Biol, 2000. 2(8):531-9.
274. Qiu, R.G., A. Abo, and G. Steven Martin, *A human homolog of the C. elegans polarity determinant Par-6 links Rac and Cdc42 to PKC $\zeta$  signaling and cell transformation*. Curr Biol, 2000. 10(12):697-707.
275. Pitcher, J.A., N.J. Freedman, and R.J. Lefkowitz, *G protein-coupled receptor kinases*. Annu Rev Biochem, 1998. 67:653-92.
276. Ong, S.T., et al., *Phosphorylation of Rab5a protein by protein kinase C is crucial for T-cell migration*. J Biol Chem, 2014. 289(28):19420-34.
277. Huang, S., et al., *HGF-induced PKC $\zeta$  activation increases functional CXCR4 expression in human breast cancer cells*. PLoS One, 2012. 7(1):5.
278. Mueller, W., et al., *Hierarchical organization of multi-site phosphorylation at the CXCR4 C terminus*. PLoS One, 2013. 8(5).
279. Signoret, N., et al., *Phorbol esters and SDF-1 induce rapid endocytosis and down modulation of the chemokine receptor CXCR4*. J Cell Biol, 1997. 139(3):651-64.
280. Luo, J., et al., *G Protein-Coupled Receptor Kinase 3 and Protein Kinase C Phosphorylate the Distal C-Terminal Tail of the Chemokine Receptor CXCR4 and Mediate Recruitment of beta-Arrestin*. Mol Pharmacol, 2017. 91(6):554-566.
281. Poole, A.W., et al., *PKC-interacting proteins: from function to pharmacology*. Trends Pharmacol Sci, 2004. 25(10):528-35.
282. Corbalan-Garcia, S., et al., *A new phosphatidylinositol 4,5-bisphosphate-binding site located in the C2 domain of protein kinase C $\alpha$* . J Biol Chem, 2003. 278(7):4972-80.
283. Evans, J.H., et al., *Specific translocation of protein kinase C $\alpha$  to the plasma membrane requires both Ca<sup>2+</sup> and PIP2 recognition by its C2 domain*. Mol Biol Cell, 2006. 17(1):56-66.
284. Tobias, I.S., et al., *Protein kinase C $\zeta$  exhibits constitutive phosphorylation and phosphatidylinositol-3,4,5-triphosphate-independent regulation*. Biochem J, 2016. 473(4):509-23.
285. Graybill, C., et al., *Partitioning-defective protein 6 (Par-6) activates atypical protein kinase C ( $\alpha$ PKC) by pseudosubstrate displacement*. J Biol Chem, 2012. 287(25):21003-11.
286. Soriano, E.V., et al.,  *$\alpha$ PKC Inhibition by Par3 CR3 Flanking Regions Controls Substrate Access and Underpins Apical-Junctional Polarization*. Dev Cell, 2016. 38(4):384-98.

287. Hoque, M., et al., *Annexins - scaffolds modulating PKC localization and signaling*. Cell Signal, 2014. 26(6):1213-25.
288. Rosse, C., et al., *PKC and the control of localized signal dynamics*. Nat Rev Mol Cell Biol, 2010. 11(2):103-12.
289. Mochly-Rosen, D., K. Das, and K.V. Grimes, *Protein kinase C, an elusive therapeutic target?* Nat Rev Drug Discov, 2012. 11(12):937-57.
290. Gallegos, L.L., M.T. Kunkel, and A.C. Newton, *Targeting protein kinase C activity reporter to discrete intracellular regions reveals spatiotemporal differences in agonist-dependent signaling*. J Biol Chem, 2006. 281(41):30947-56.
291. Goode, N.T., M.A. Hajibagheri, and P.J. Parker, *Protein kinase C (PKC)-induced PKC down-regulation. Association with up-regulation of vesicle traffic*. J Biol Chem, 1995. 270(6):2669-73.
292. Brenner, W., et al., *Protein kinase C eta is associated with progression of renal cell carcinoma*. Anticancer Res, 2003. 23(5A):4001-6.
293. Bae, K.M., et al., *Protein kinase C epsilon is overexpressed in primary human non-small cell lung cancers and functionally required for proliferation of non-small cell lung cancer cells in a p21/Cip1-dependent manner*. Cancer Res, 2007. 67(13):6053-63.
294. Corbit, K.C., et al., *Activation of Raf-1 signaling by protein kinase C through a mechanism involving Raf kinase inhibitory protein*. J Biol Chem, 2003. 278(15):13061-8.
295. Garcia-Paramio, P., et al., *The broad specificity of dominant inhibitory protein kinase C mutants infers a common step in phosphorylation*. Biochem J, 1998. 333(Pt 3):631-6.
296. Prevostel, C., et al., *The natural protein kinase C alpha mutant is present in human thyroid neoplasms*. Oncogene, 1995. 11(4):669-74.
297. Zhang, L.L., et al., *The protein kinase C (PKC) inhibitors combined with chemotherapy in the treatment of advanced non-small cell lung cancer: meta-analysis of randomized controlled trials*. Clin Transl Oncol, 2015. 17(5):371-7.
298. Hunter, T., N. Ling, and J.A. Cooper, *Protein kinase C phosphorylation of the EGF receptor at a threonine residue close to the cytoplasmic face of the plasma membrane*. Nature, 1984. 311(5985):480-3.
299. Santiskulvong, C. and E. Rozengurt, *Protein kinase Calpha mediates feedback inhibition of EGF receptor transactivation induced by Gq-coupled receptor agonists*. Cell Signal, 2007. 19(6):1348-57.
300. Ouyang, X., T. Gulliford, and R.J. Epstein, *The duration of phorbol-inducible ErbB2 tyrosine dephosphorylation parallels that of receptor endocytosis rather than threonine-686 phosphorylation: implications for the physiological role of protein kinase C in growth factor receptor signalling*. Carcinogenesis, 1998. 19(11):2013-9.

301. Namkung, Y. and D.R. Sibley, *Protein kinase C mediates phosphorylation, desensitization, and trafficking of the D2 dopamine receptor*. J Biol Chem, 2004. 279(47):49533-41.
302. Bivona, T.G., et al., *PKC regulates a farnesyl-electrostatic switch on K-Ras that promotes its association with Bcl-XL on mitochondria and induces apoptosis*. Mol Cell, 2006. 21(4):481-93.
303. D'Costa, A.M., et al., *The proapoptotic tumor suppressor protein kinase C-delta is lost in human squamous cell carcinomas*. Oncogene, 2006. 25(3):378-86.
304. Okhrimenko, H., et al., *Roles of tyrosine phosphorylation and cleavage of protein kinase Cdelta in its protective effect against tumor necrosis factor-related apoptosis inducing ligand-induced apoptosis*. J Biol Chem, 2005. 280(25):23643-52.
305. Symonds, J.M., et al., *PKCdelta regulates integrin alphaVbeta3 expression and transformed growth of K-ras dependent lung cancer cells*. Oncotarget, 2016. 7(14):17905-19.
306. Griner, E.M. and M.G. Kazanietz, *Protein kinase C and other diacylglycerol effectors in cancer*. Nat Rev Cancer, 2007. 7(4):281-94.
307. Basu, A. and D. Pal, *Two faces of protein kinase Cdelta: the contrasting roles of PKCdelta in cell survival and cell death*. ScientificWorldJournal, 2010. 10:2272-84.
308. Gyorffy, B., et al., *Online survival analysis software to assess the prognostic value of biomarkers using transcriptomic data in non-small-cell lung cancer*. PLoS One, 2013. 8(12).
309. Reno, E.M., et al., *Analysis of protein kinase C delta expression in endometrial tumors*. Hum Pathol, 2008. 39(1):21-9.
310. Garg, R., et al., *Protein kinase C and cancer: what we know and what we do not*. Oncogene, 2014. 33(45):5225-37.
311. Hafeez, B.B., et al., *Genetic ablation of PKC epsilon inhibits prostate cancer development and metastasis in transgenic mouse model of prostate adenocarcinoma*. Cancer Res, 2011. 71(6):2318-27.
312. Aaronson, D.S. and C.M. Horvath, *A road map for those who don't know JAK-STAT*. Science, 2002. 296(5573):1653-5.
313. Levy, D.E. and J.E. Darnell, *STATs: transcriptional control and biological impact*. Nat Rev Mol Cell Biol, 2002. 3(9):651-662.
314. Buettner, R., L.B. Mora, and R. Jove, *Activated STAT signaling in human tumors provides novel molecular targets for therapeutic intervention*. Clin Cancer Res, 2002. 8(4):945-54.
315. Schroeder, A., et al., *Loss of androgen receptor expression promotes a stem-like cell phenotype in prostate cancer through STAT3 signaling*. Cancer Res, 2014. 74(4):1227-37.
316. Burger, M., et al., *KSHV-GPCR and CXCR2 transforming capacity and angiogenic responses are mediated through a JAK2-STAT3-dependent pathway*. Oncogene, 2005. 24(12):2067-75.



317. Germain, D. and D.A. Frank, *Targeting the cytoplasmic and nuclear functions of signal transducers and activators of transcription 3 for cancer therapy*. Clin Cancer Res, 2007. 13(19):5665-9.
318. Johnston, P.A. and J.R. Grandis, *STAT3 signaling: anticancer strategies and challenges*. Mol Interv, 2011. 11(1):18-26.
319. Roskoski, R., Jr., *Janus kinase (JAK) inhibitors in the treatment of inflammatory and neoplastic diseases*. Pharmacol Res, 2016. 111:784-803.
320. O'Shea, J.J., M. Gadina, and R.D. Schreiber, *Cytokine signaling in 2002: new surprises in the Jak/Stat pathway*. Cell, 2002. 109(31):S121-31.
321. Wang, D., et al., *Phospholipase Cgamma2 is essential in the functions of B cell and several Fc receptors*. Immunity, 2000. 13(1):25-35.
322. Mangmool, S. and H. Kurose, *G(i/o) protein-dependent and -independent actions of Pertussis Toxin (PTX)*. Toxins, 2011. 3(7):884-99.
323. Vila-Coro, A.J., et al., *The chemokine SDF-1alpha triggers CXCR4 receptor dimerization and activates the JAK/STAT pathway*. Faseb J, 1999. 13(13):1699-710.
324. Furqan, M., et al., *Dysregulation of JAK-STAT pathway in hematological malignancies and JAK inhibitors for clinical application*. Biomark Res, 2013. 1(1):2050-7771.
325. Wang, X., et al., *Spleens of myelofibrosis patients contain malignant hematopoietic stem cells*. J Clin Invest, 2012. 122(11):3888-99.
326. Devi, S., et al., *Neutrophil mobilization via plerixafor-mediated CXCR4 inhibition arises from lung demargination and blockade of neutrophil homing to the bone marrow*. J Exp Med, 2013. 210(11):2321-36.
327. Rosti, V., et al., *The expression of CXCR4 is down-regulated on the CD34+ cells of patients with myelofibrosis with myeloid metaplasia*. Blood Cells Mol Dis, 2007. 38(3):280-6.
328. Abdelouahab, H., et al., *CXCL12/CXCR4 pathway is activated by oncogenic JAK2 in a PI3K-dependent manner*. Oncotarget, 2016. 22(10):10789.
329. Vainchenker, W., et al., *JAK inhibitors for the treatment of myeloproliferative neoplasms and other disorders*. F1000Res, 2018. 7:82-82.
330. Hodge, R.G. and A.J. Ridley, *Regulating Rho GTPases and their regulators*. Nat Rev Mol Cell Biol, 2016. 17(8):496-510.
331. Nobes, C.D. and A. Hall, *Rho, rac, and cdc42 GTPases regulate the assembly of multimolecular focal complexes associated with actin stress fibers, lamellipodia, and filopodia*. Cell, 1995. 81(1):53-62.
332. Michaelson, D., et al., *Differential localization of Rho GTPases in live cells: regulation by hypervariable regions and RhoGDI binding*. J Cell Biol, 2001. 152(1):111-26.

333. Schaefer, A., N.R. Reinhard, and P.L. Hordijk, *Toward understanding RhoGTPase specificity: structure, function and local activation*. Small GTPases, 2014. 5(2):968004.
334. Donnelly, S.K., J.J. Bravo-Cordero, and L. Hodgson, *Rho GTPase isoforms in cell motility: Don't fret, we have FRET*. Cell Adh Migr, 2014. 8(6):526-34.
335. Navarro-Lerida, I., et al., *A palmitoylation switch mechanism regulates Rac1 function and membrane organization*. Embo J, 2012. 31(3):534-51.
336. Wyse, M.M., et al., *mDia2 and CXCL12/CXCR4 chemokine signaling intersect to drive tumor cell amoeboid morphological transitions*. Biochem Biophys Res Commun, 2017. 484(2):255-261.
337. Garcia-Mata, R., E. Boulter, and K. Burridge, *The 'invisible hand': regulation of RHO GTPases by RHOGDIs*. Nat Rev Mol Cell Biol, 2011. 12(8):493-504.
338. Cherfils, J. and M. Zeghouf, *Regulation of small GTPases by GEFs, GAPs, and GDIs*. Physiol Rev, 2013. 93(1):269-309.
339. Longenecker, K., et al., *How RhoGDI binds Rho*. Acta Crystallogr D Biol Crystallogr, 1999. 55(Pt 9):1503-15.
340. Scheffzek, K., et al., *The Rac-RhoGDI complex and the structural basis for the regulation of Rho proteins by RhoGDI*. Nat Struct Biol, 2000. 7(2):122-6.
341. Sun, Z., et al., *Forkhead box P3 regulates ARHGAP15 expression and affects migration of glioma cells through the Rac1 signaling pathway*. Cancer Sci, 2017. 108(1):61-72.
342. Hara, A., et al., *The role of FilGAP, a Rac-specific Rho-GTPase-activating protein, in tumor progression and behavior of astrocytomas*. Cancer Med, 2016. 5(12):3412-3425.
343. Laurin, M. and J.F. Cote, *Insights into the biological functions of Dock family guanine nucleotide exchange factors*. Genes Dev, 2014. 28(6):533-47.
344. O'Toole, T.E., et al., *Tiam1 is recruited to beta1-integrin complexes by 14-3-3zeta where it mediates integrin-induced Rac1 activation and motility*. J Cell Physiol, 2011. 226(11):2965-78.
345. Mertens, A.E., et al., *The Rac activator Tiam1 controls tight junction biogenesis in keratinocytes through binding to and activation of the Par polarity complex*. J Cell Biol, 2005. 170(7):1029-37.
346. Mertens, A.E., D.M. Pegtel, and J.G. Collard, *Tiam1 takes PART in cell polarity*. Trends Cell Biol, 2006. 16(6):308-16.
347. Pegtel, D.M., et al., *The Par-Tiam1 complex controls persistent migration by stabilizing microtubule-dependent front-rear polarity*. Curr Biol, 2007. 17(19):1623-34.
348. Morrison Joly, M., et al., *Two distinct mTORC2-dependent pathways converge on Rac1 to drive breast cancer metastasis*. Breast Cancer Res, 2017. 19(1):017-0868.

349. Wang, S., et al., *Tiam1 interaction with the PAR complex promotes talin-mediated Rac1 activation during polarized cell migration*. J Cell Biol, 2012. 199(2):331-45.
350. Fukui, Y., et al., *Haematopoietic cell-specific CDM family protein DOCK2 is essential for lymphocyte migration*. Nature, 2001. 412(6849):826-31.
351. Chang, F., et al., *Tyrosine phosphorylation of Rac1: a role in regulation of cell spreading*. PLoS One, 2011. 6(12):6.
352. Kwon, T., et al., *Akt protein kinase inhibits Rac1-GTP binding through phosphorylation at serine 71 of Rac1*. J Biol Chem, 2000. 275(1):423-8.
353. Cuadrado, A., et al., *Transcription factors NRF2 and NF-kappaB are coordinated effectors of the Rho family, GTP-binding protein RAC1 during inflammation*. J Biol Chem, 2014. 289(22):15244-58.
354. Jamieson, C., et al., *Rac1 augments Wnt signaling by stimulating beta-catenin-lymphoid enhancer factor-1 complex assembly independent of beta-catenin nuclear import*. J Cell Sci, 2015. 128(21):3933-46.
355. Navarro-Lerida, I., et al., *Rac1 nucleocytoplasmic shuttling drives nuclear shape changes and tumor invasion*. Dev Cell, 2015. 32(3):318-34.
356. Tong, J., et al., *Phosphorylation of Rac1 T108 by extracellular signal-regulated kinase in response to epidermal growth factor: a novel mechanism to regulate Rac1 function*. Mol Cell Biol, 2013. 33(22):4538-51.
357. Weiner, O.D., *Regulation of cell polarity during eukaryotic chemotaxis: the chemotactic compass*. Curr Opin Cell Biol, 2002. 14(2):196-202.
358. Ridley, A.J., et al., *Cell migration: integrating signals from front to back*. Science, 2003. 302(5651):1704-9.
359. Campbell, I.D. and M.J. Humphries, *Integrin structure, activation, and interactions*. Cold Spring Harb Perspect Biol, 2011. 3(3):a004994
360. Webb, D.J., et al., *FAK-Src signalling through paxillin, ERK and MLCK regulates adhesion disassembly*. Nat Cell Biol, 2004. 6(2):154-61.
361. Margadant, C., et al., *Mechanisms of integrin activation and trafficking*. Curr Opin Cell Biol, 2011. 23(5):607-14.
362. Maritzen, T., H. Schachtner, and D.F. Legler, *On the move: endocytic trafficking in cell migration*. Cell Mol Life Sci, 2015. 72(11):2119-34.
363. Coly, P.M., et al., *The Autophagy Machinery: A New Player in Chemotactic Cell Migration*. Front Neurosci, 2017. 11:78.
364. Serebryanny, L.A., et al., *The Effects of Disease Models of Nuclear Actin Polymerization on the Nucleus*. Front Physiol, 2016. 7:454.

365. Ishikawa-Ankerhold, H.C., et al., *Actin-Interacting Protein 1 Contributes to Intranuclear Rod Assembly in Dictyostelium discoideum*. Sci Rep, 2017. 7:40310.
366. Satoh, M., et al., *Immune-complex level of cofilin-1 in sera is associated with cancer progression and poor prognosis in pancreatic cancer*. Cancer Sci, 2017. 4(10):13181.
367. Haibo, W., et al., *Cofilin 1 induces the epithelial-mesenchymal transition of gastric cancer cells by promoting cytoskeletal rearrangement*. Oncotarget, 2017. 27(10):16608.
368. Keshamouni, V.G., et al., *Differential protein expression profiling by iTRAQ-2DLC-MS/MS of lung cancer cells undergoing epithelial-mesenchymal transition reveals a migratory/invasive phenotype*. J Proteome Res, 2006. 5(5):1143-54.
369. Nebl, G., S.C. Meuer, and Y. Samstag, *Dephosphorylation of serine 3 regulates nuclear translocation of cofilin*. J Biol Chem, 1996. 271(42):26276-80.
370. Nishita, M., et al., *Spatial and temporal regulation of cofilin activity by LIM kinase and Slingshot is critical for directional cell migration*. J Cell Biol, 2005. 171(2):349-59.
371. Hirayama, A., et al., *Cofilin plays a critical role in IL-8-dependent chemotaxis of neutrophilic HL-60 cells through changes in phosphorylation*. J Leukoc Biol, 2007. 81(3):720-8.
372. Sun, C.X., M.A. Magalhaes, and M. Glogauer, *Rac1 and Rac2 differentially regulate actin free barbed end formation downstream of the fMLP receptor*. J Cell Biol, 2007. 179(2):239-45.
373. Bamburg, J.R., *Proteins of the ADF/cofilin family: essential regulators of actin dynamics*. Annu Rev Cell Dev Biol, 1999. 15:185-230.
374. Bernard, O., *Lim kinases, regulators of actin dynamics*. Int J Biochem Cell Biol, 2007. 39(6):1071-6.
375. Moriyama, K., K. Iida, and I. Yahara, *Phosphorylation of Ser-3 of cofilin regulates its essential function on actin*. Genes Cells, 1996. 1(1):73-86.
376. Huang, T.Y., C. DerMardirossian, and G.M. Bokoch, *Cofilin phosphatases and regulation of actin dynamics*. Curr Opin Cell Biol, 2006. 18(1):26-31.
377. Samstag, Y., I. John, and G.H. Wabnitz, *Cofilin: a redox sensitive mediator of actin dynamics during T-cell activation and migration*. Immunol Rev, 2013. 256(1):30-47.
378. Han, L., et al., *Direct stimulation of receptor-controlled phospholipase D1 by phospho-cofilin*. Embo J, 2007. 26(19):4189-202.
379. van Rheenen, J., J. Condeelis, and M. Glogauer, *A common cofilin activity cycle in invasive tumor cells and inflammatory cells*. J Cell Sci, 2009. 122(Pt 3):305-11.
380. Nagata-Ohashi, K., et al., *A pathway of neuregulin-induced activation of cofilin-phosphatase Slingshot and cofilin in lamellipodia*. J Cell Biol, 2004. 165(4):465-71.

381. Barišić, S., et al., *Phosphorylation of Ser 402 impedes phosphatase activity of slingshot 1*. EMBO Rep, 2011. 12(6):527-533.
382. Oser, M. and J. Condeelis, *The cofilin activity cycle in lamellipodia and invadopodia*. J Cell Biochem, 2009. 108(6):1252-62.
383. Eiseler, T., et al., *Protein Kinase D1 regulates Cofilin mediated F-actin reorganization and cell motility via Slingshot*. Nat Cell Biol, 2009. 11(5):545-556.
384. Kim, H.S., et al., *Redox regulation of 14-3-3zeta controls monocyte migration*. Arterioscler Thromb Vasc Biol, 2014. 34(7):1514-21.
385. Edwards, D.C., et al., *Activation of LIM-kinase by Pak1 couples Rac/Cdc42 GTPase signalling to actin cytoskeletal dynamics*. Nat Cell Biol, 1999. 1(5):253-9.
386. Arber, S., et al., *Regulation of actin dynamics through phosphorylation of cofilin by LIM-kinase*. Nature, 1998. 393(6687):805-9.
387. Ohashi, K., et al., *Rho-associated kinase ROCK activates LIM-kinase 1 by phosphorylation at threonine 508 within the activation loop*. J Biol Chem, 2000. 275(5):3577-82.
388. Amano, T., et al., *LIM-kinase 2 induces formation of stress fibres, focal adhesions and membrane blebs, dependent on its activation by Rho-associated kinase-catalysed phosphorylation at threonine-505*. Biochem J, 2001. 354(Pt 1):149-59.
389. Scott, R.W. and M.F. Olson, *LIM kinases: function, regulation and association with human disease*. J Mol Med, 2007. 85(6):555-68.
390. Mizuno, K., *Signaling mechanisms and functional roles of cofilin phosphorylation and dephosphorylation*. Cell Signal, 2013. 25(2):457-69.
391. Chua, B.T., et al., *Mitochondrial translocation of cofilin is an early step in apoptosis induction*. Nat Cell Biol, 2003. 5(12):1083-9.
392. Song, X., et al., *Initiation of cofilin activity in response to EGF is uncoupled from cofilin phosphorylation and dephosphorylation in carcinoma cells*. J Cell Sci, 2006. 119(Pt 14):2871-81.
393. Wang, W., R. Eddy, and J. Condeelis, *The cofilin pathway in breast cancer invasion and metastasis*. Nat Rev Cancer, 2007. 7(6):429-40.
394. Pendleton, A., et al., *Latrunculin B or ATP depletion induces cofilin-dependent translocation of actin into nuclei of mast cells*. J Biol Chem, 2003. 278(16):14394-400.
395. Abe, H., R. Nagaoka, and T. Obinata, *Cytoplasmic localization and nuclear transport of cofilin in cultured myotubes*. Exp Cell Res, 1993. 206(1):1-10.
396. Yokoo, T., et al., *p57Kip2 regulates actin dynamics by binding and translocating LIM-kinase 1 to the nucleus*. J Biol Chem, 2003. 278(52):52919-23.

397. Kapoor, P. and X. Shen, *Mechanisms of nuclear actin in chromatin-remodeling complexes*. Trends Cell Biol, 2014. 24(4):238-46.
398. Philimonenko, V.V., et al., *Nuclear actin and myosin I are required for RNA polymerase I transcription*. Nat Cell Biol, 2004. 6(12):1165-72.
399. Balcer, H.I., et al., *Coordinated regulation of actin filament turnover by a high-molecular-weight Srv2/CAP complex, cofilin, profilin, and Aip1*. Curr Biol, 2003. 13(24):2159-69.
400. Gorbatyuk, V.Y., et al., *Mapping the phosphoinositide-binding site on chick cofilin explains how PIP2 regulates the cofilin-actin interaction*. Mol Cell, 2006. 24(4):511-22.
401. Ojala, P.J., V. Paavilainen, and P. Lappalainen, *Identification of yeast cofilin residues specific for actin monomer and PIP2 binding*. Biochemistry, 2001. 40(51):15562-9.
402. Peterburs, P., et al., *Protein kinase D regulates cell migration by direct phosphorylation of the cofilin phosphatase slingshot 1 like*. Cancer Res, 2009. 69(14):5634-8.
403. Yin, H.L. and P.A. Janmey, *Phosphoinositide regulation of the actin cytoskeleton*. Annu Rev Physiol, 2003. 65:761-89.
404. Ghosh, M., et al., *Cofilin promotes actin polymerization and defines the direction of cell motility*. Science, 2004. 304(5671):743-6.
405. Mouneimne, G., et al., *Phospholipase C and cofilin are required for carcinoma cell directionality in response to EGF stimulation*. J Cell Biol, 2004. 166(5):697-708.
406. Frantz, C., et al., *Cofilin is a pH sensor for actin free barbed end formation: role of phosphoinositide binding*. J Cell Biol, 2008. 183(5):865-79.
407. Maimaiti, Y., et al., *Overexpression of cofilin correlates with poor survival in breast cancer: A tissue microarray analysis*. Oncol Lett, 2017. 14(2):2288-2294.
408. Leu, J.D., et al., *Enhanced cellular radiosensitivity induced by cofilin-1 over-expression is associated with reduced DNA repair capacity*. Int J Radiat Biol, 2013. 89(6):433-44.
409. Serezani, C.H., et al., *PTEN directly activates the actin depolymerization factor cofilin-1 during PGE2-mediated inhibition of phagocytosis of fungi*. Sci Signal, 2012. 5(210):2002448.
410. Klasen, C., et al., *LPS-mediated cell surface expression of CD74 promotes the proliferation of B cells in response to MIF*. Cell Signal, 2018. 46:32-42.
411. Shebl, F.M., et al., *Non-steroidal anti-inflammatory drugs use is associated with reduced risk of inflammation-associated cancers: NIH-AARP study*. PLoS One, 2014. 9:12.
412. Cuzick, J., *Preventive therapy for cancer*. Lancet Oncol, 2017. 18(8):e472-e482.
413. Rothwell, P.M., et al., *Long-term effect of aspirin on colorectal cancer incidence and mortality: 20-year follow-up of five randomised trials*. Lancet, 2010. 376(9754):1741-50.

414. Nissen, S.E., et al., *Cardiovascular Safety of Celecoxib, Naproxen, or Ibuprofen for Arthritis*. N Engl J Med, 2016. 375(26):2519-29.
415. Kispert, S., T. Schwartz, and J. McHowat, *Cigarette Smoke Regulates Calcium-Independent Phospholipase A2 Metabolic Pathways in Breast Cancer*. Am J Pathol, 2017. 187(8):1855-1866.
416. Ricciotti, E. and G.A. FitzGerald, *Prostaglandins and Inflammation*. Arterioscler Thromb Vasc Biol, 2011. 31(5):986-1000.
417. Mantovani, A. and A. Sica, *Macrophages, innate immunity and cancer: balance, tolerance, and diversity*. Curr Opin Immunol, 2010. 22(2):231-7.
418. Moore, U.J., R.A. Seymour, and M.D. Rawlins, *The efficacy of locally applied aspirin and acetaminophen in postoperative pain after third molar surgery*. Clin Pharmacol Ther, 1992. 52(3):292-6.
419. Dani, M., et al., *The local antinociceptive effects of paracetamol in neuropathic pain are mediated by cannabinoid receptors*. Eur J Pharmacol, 2007. 573(1-3):214-5.
420. Liu, J., A.R. Reid, and J. Sawynok, *Antinociception by systemically-administered acetaminophen (paracetamol) involves spinal serotonin 5-HT7 and adenosine A1 receptors, as well as peripheral adenosine A1 receptors*. Neurosci Lett, 2013. 536:64-8.
421. Mallet, C., et al., *TRPV1 in brain is involved in acetaminophen-induced antinociception*. PLoS One, 2010. 5(9):0012748.
422. Graham, G.G. and K.F. Scott, *Mechanism of action of paracetamol*. Am J Ther, 2005. 12(1):46-55.
423. Hinz, B. and K. Brune, *Paracetamol and cyclooxygenase inhibition: is there a cause for concern?* Ann Rheum Dis, 2012. 71(1):20-5.
424. Pickering, G., et al., *Acetaminophen reinforces descending inhibitory pain pathways*. Clin Pharmacol Ther, 2008. 84(1):47-51.
425. Pickering, G., et al., *Analgesic effect of acetaminophen in humans: first evidence of a central serotonergic mechanism*. Clin Pharmacol Ther, 2006. 79(4):371-8.
426. Nakamura, K., et al., *Prostaglandin EP3 receptor protein in serotonin and catecholamine cell groups: a double immunofluorescence study in the rat brain*. Neurosci, 2001. 103(3):763-75.
427. Ohashi, N., et al., *Acetaminophen Metabolite N-Acylphenolamine Induces Analgesia via Transient Receptor Potential Vanilloid 1 Receptors Expressed on the Primary Afferent Terminals of C-fibers in the Spinal Dorsal Horn*. Anesthesiology, 2017. 127(2):355-371.
428. Hogestatt, E.D., et al., *Conversion of acetaminophen to the bioactive N-acylphenolamine AM404 via fatty acid amide hydrolase-dependent arachidonic acid conjugation in the nervous system*. J Biol Chem, 2005. 280(36):31405-12.

429. Caterina, M.J., *Transient receptor potential ion channels as participants in thermosensation and thermoregulation*. Am J Physiol Regul Integr Comp Physiol, 2007. 292(1):14.
430. Bley, K.R., *Recent developments in transient receptor potential vanilloid receptor 1 agonist-based therapies*. Expert Opin Investig Drugs, 2004. 13(11):1445-56.
431. Beltramo, M., et al., *Functional role of high-affinity anandamide transport, as revealed by selective inhibition*. Science, 1997. 277(5329):1094-7.
432. Păunescu, H., et al., *Cannabinoid system and cyclooxygenases inhibitors*. J Med Life, 2011. 4(1):11-20.
433. Umathe, S.N., et al., *Endocannabinoids mediate anxiolytic-like effect of acetaminophen via CB1 receptors*. Prog Neuropsychopharmacol Biol Psychiatry, 2009. 33(7):1191-9.
434. Bertolini, A., et al., *Paracetamol: new vistas of an old drug*. CNS Drug Rev, 2006. 12(3-4):250-75.
435. Bujalska, M., *Effect of nitric oxide synthase inhibition on antinociceptive action of different doses of acetaminophen*. Pol J Pharmacol, 2004. 56(5):605-10.
436. Graham, G.G., et al., *The modern pharmacology of paracetamol: therapeutic actions, mechanism of action, metabolism, toxicity and recent pharmacological findings*. Inflammopharmacology, 2013. 21(3):201-32.
437. Krishnan, K., et al., *Colonic mucosal prostaglandin E2 and cyclooxygenase expression before and after low aspirin doses in subjects at high risk or at normal risk for colorectal cancer*. Cancer Epidemiol Biomarkers Prev, 2001. 10(5):447-53.
438. Ballinger, M.N., et al., *Critical role of prostaglandin E2 overproduction in impaired pulmonary host response following bone marrow transplantation*. J Immunol, 2006. 177(8):5499-508.
439. Madrigal-Martinez, A., A.B. Fernandez-Martinez, and F.J. Lucio Cazana, *Intracrine prostaglandin E2 pro-tumoral actions in prostate epithelial cells originate from non-canonical pathways*. J Cell Physiol, 2018. 233(4):3590-3602.
440. Giroux, M. and A. Descoteaux, *Cyclooxygenase-2 expression in macrophages: modulation by protein kinase C-alpha*. J Immunol, 2000. 165(7):3985-91.
441. Serezani, C.H., et al., *Prostaglandin E2 suppresses bacterial killing in alveolar macrophages by inhibiting NADPH oxidase*. Am J Respir Cell Mol Biol, 2007. 37(5):562-70.
442. Eferl, R. and E.F. Wagner, *AP-1: a double-edged sword in tumorigenesis*. Nat Rev Cancer, 2003. 3(11):859-68.
443. Yakar, I., et al., *Prostaglandin e(2) suppresses NK activity in vivo and promotes postoperative tumor metastasis in rats*. Ann Surg Oncol, 2003. 10(4):469-79.



444. Barrios-Rodiles, M. and K. Chadee, *Novel regulation of cyclooxygenase-2 expression and prostaglandin E2 production by IFN-gamma in human macrophages*. J Immunol, 1998. 161(5):2441-8.
445. Agarwal, S., et al., *Inhibition of 12-LOX and COX-2 reduces the proliferation of human epidermoid carcinoma cells (A431) by modulating the ERK and PI3K-Akt signalling pathways*. Exp Dermatol, 2009. 18(11):939-46.
446. Eli, Y., et al., *Comparative effects of indomethacin on cell proliferation and cell cycle progression in tumor cells grown in vitro and in vivo*. Biochem Pharmacol, 2001. 61(5):565-71.
447. Harris, R.E., *Cyclooxygenase-2 (cox-2) and the inflammogenesis of cancer*. Subcell Biochem, 2007. 42:93-126.
448. Garcia-Rodriguez, L.A. and C. Huerta-Alvarez, *Reduced risk of colorectal cancer among long-term users of aspirin and nonaspirin nonsteroidal antiinflammatory drugs*. Epidemiology, 2001. 12(1):88-93.
449. Harris, R.E., J. Beebe-Donk, and G.A. Alshafie, *Similar reductions in the risk of human colon cancer by selective and nonselective cyclooxygenase-2 (COX-2) inhibitors*. BMC Cancer, 2008. 8(237):1471-2407.
450. Ristimaki, A., et al., *Induction of cyclooxygenase-2 by interleukin-1 alpha. Evidence for post-transcriptional regulation*. J Biol Chem, 1994. 269(16):11769-75.
451. Buchanan, F.G., et al., *Prostaglandin E2 regulates cell migration via the intracellular activation of the epidermal growth factor receptor*. J Biol Chem, 2003. 278(37):35451-7.
452. Accioly, M.T., et al., *Lipid bodies are reservoirs of cyclooxygenase-2 and sites of prostaglandin-E2 synthesis in colon cancer cells*. Cancer Res, 2008. 68(6):1732-40.
453. Leone, V., et al., *PGE2 inhibits apoptosis in human adenocarcinoma Caco-2 cell line through Ras-PI3K association and cAMP-dependent kinase A activation*. Am J Physiol Gastrointest Liver Physiol, 2007. 293(4):19.
454. Manoukian, A.S. and J.R. Woodgett, *Role of glycogen synthase kinase-3 in cancer: regulation by Wnts and other signaling pathways*. Adv Cancer Res, 2002. 84:203-29.
455. Smalley, W., et al., *Use of nonsteroidal anti-inflammatory drugs and incidence of colorectal cancer: a population-based study*. Arch Intern Med, 1999. 159(2):161-6.
456. Williamson, T., et al., *Mebendazole and a non-steroidal anti-inflammatory combine to reduce tumor initiation in a colon cancer preclinical model*. Oncotarget, 2016. 7(42):68571-68584.
457. Gunjal, P.M., et al., *Evidence for induction of a tumor metastasis-receptive microenvironment for ovarian cancer cells in bone marrow and other organs as an unwanted and underestimated side effect of chemotherapy/radiotherapy*. J Ovarian Res, 2015. 8(20):015-0141.
458. Wang, J.Y., et al., *STIM1 overexpression promotes colorectal cancer progression, cell motility and COX-2 expression*. Oncogene, 2015. 34(33):4358-67.

459. FitzGerald, G.A. and C. Patrono, *The coxibs, selective inhibitors of cyclooxygenase-2*. N Engl J Med, 2001. 345(6):433-42.
460. Patrono, C., *The PGH-synthase system and isozyme-selective inhibition*. J Cardiovasc Pharmacol, 2006. 47(1):S1-6.
461. Yona, D. and N. Arber, *Coxibs and cancer prevention*. J Cardiovasc Pharmacol, 2006. 47(1):S76-81.
462. Takeuchi, K., et al., *Roles of COX inhibition in pathogenesis of NSAID-induced small intestinal damage*. Clin Chim Acta, 2010. 411(7-8):459-66.
463. Rolland, P.H., et al., *Prostaglandin in human breast cancer: Evidence suggesting that an elevated prostaglandin production is a marker of high metastatic potential for neoplastic cells*. J Natl Cancer Inst, 1980. 64(5):1061-70.
464. Coussens, L.M. and Z. Werb, *Inflammation and cancer*. Nature, 2002. 420(6917):860-7.
465. Macarthur, M., G.L. Hold, and E.M. El-Omar, *Inflammation and Cancer II. Role of chronic inflammation and cytokine gene polymorphisms in the pathogenesis of gastrointestinal malignancy*. Am J Physiol Gastrointest Liver Physiol, 2004. 286(4):G515-20.
466. Wang, D., et al., *Prostaglandin E(2) promotes colorectal adenoma growth via transactivation of the nuclear peroxisome proliferator-activated receptor delta*. Cancer Cell, 2004. 6(3):285-95.
467. Grosch, S., et al., *Cyclooxygenase-2 (COX-2)-independent anticarcinogenic effects of selective COX-2 inhibitors*. J Natl Cancer Inst, 2006. 98(11):736-47.
468. Fushimi, K., et al., *Prostaglandin E2 downregulates TNF-alpha-induced production of matrix metalloproteinase-1 in HCS-2/8 chondrocytes by inhibiting Raf-1/MEK/ERK cascade through EP4 prostanoid receptor activation*. J Cell Biochem, 2007. 100(3):783-93.
469. Husain, S.S., et al., *MAPK (ERK2) kinase--a key target for NSAIDs-induced inhibition of gastric cancer cell proliferation and growth*. Life Sci, 2001. 69(25-26):3045-54.
470. Uefuji, K., T. Ichikura, and H. Mochizuki, *Cyclooxygenase-2 expression is related to prostaglandin biosynthesis and angiogenesis in human gastric cancer*. Clin Cancer Res, 2000. 6(1):135-8.
471. Gately, S. and R. Kerbel, *Therapeutic potential of selective cyclooxygenase-2 inhibitors in the management of tumor angiogenesis*. Prog Exp Tumor Res, 2003. 37:179-92.
472. Mutoh, M., et al., *Involvement of prostaglandin E receptor subtype EP(4) in colon carcinogenesis*. Cancer Res, 2002. 62(1):28-32.
473. Kawamori, T., et al., *Chemopreventive effects of ONO-8711, a selective prostaglandin E receptor EP(1) antagonist, on breast cancer development*. Carcinogenesis, 2001. 22(12):2001-4.

474. Sonoshita, M., et al., *Acceleration of intestinal polyposis through prostaglandin receptor EP2 in Apc(Delta 716) knockout mice*. Nat Med, 2001. 7(9):1048-51.
475. Thorat, M.A., et al., *Prostanoid receptor EP1 expression in breast cancer*. Mod Pathol, 2008. 21(1):15-21.
476. Zhao, Y., et al., *Estrogen biosynthesis proximal to a breast tumor is stimulated by PGE2 via cyclic AMP, leading to activation of promoter II of the CYP19 (aromatase) gene*. Endocrinology, 1996. 137(12):5739-42.
477. Prosperi, J.R. and F.M. Robertson, *Cyclooxygenase-2 directly regulates gene expression of P450 Cyp19 aromatase promoter regions plI, pl.3 and pl.7 and estradiol production in human breast tumor cells*. Prostaglandins Other Lipid Mediat, 2006. 81(1):55-70.
478. Maier, T.J., et al., *Cyclooxygenase-2 (COX-2)-dependent and -independent anticarcinogenic effects of celecoxib in human colon carcinoma cells*. Biochem Pharmacol, 2004. 67(8):1469-78.
479. Kulp, S.K., et al., *3-phosphoinositide-dependent protein kinase-1/Akt signaling represents a major cyclooxygenase-2-independent target for celecoxib in prostate cancer cells*. Cancer Res, 2004. 64(4):1444-51.
480. Dandekar, D.S., et al., *Cyclooxygenase-2 inhibitor celecoxib augments chemotherapeutic drug-induced apoptosis by enhancing activation of caspase-3 and -9 in prostate cancer cells*. Int J Cancer, 2005. 115(3):484-92.
481. Jendrossek, V., R. Handrick, and C. Belka, *Celecoxib activates a novel mitochondrial apoptosis signaling pathway*. Faseb J, 2003. 17(11):1547-9.
482. Yan, M., et al., *15-Hydroxyprostaglandin dehydrogenase, a COX-2 oncogene antagonist, is a TGF-beta-induced suppressor of human gastrointestinal cancers*. Proc Natl Acad Sci U S A, 2004. 101(50):17468-73.
483. Quidville, V., et al., *15-Hydroxyprostaglandin-dehydrogenase is involved in anti-proliferative effect of non-steroidal anti-inflammatory drugs COX-1 inhibitors on a human medullary thyroid carcinoma cell line*. Prostaglandins Other Lipid Mediat, 2006. 81(1-2):14-30.
484. Fukushima, E., et al., *Protective effects of acetaminophen on ibuprofen-induced gastric mucosal damage in rats with associated suppression of matrix metalloproteinase*. J Pharmacol Exp Ther, 2014. 349(1):165-73.
485. Zara, S., et al., *Ibuprofen and lipoic acid codrug 1 control Alzheimer's disease progression by down-regulating protein kinase C epsilon-mediated metalloproteinase 2 and 9 levels in beta-amyloid infused Alzheimer's disease rat model*. Brain Res, 2011. 15:79-87.
486. Sun, F., Y. Zhang, and Q. Li, *Therapeutic mechanisms of ibuprofen, prednisone and betamethasone in osteoarthritis*. Mol Med Rep, 2017. 15(2):981-987.

487. Johnson, A.J., et al., *The cyclo-oxygenase-2 inhibitor celecoxib perturbs intracellular calcium by inhibiting endoplasmic reticulum Ca<sup>2+</sup>-ATPases: a plausible link with its anti-tumour effect and cardiovascular risks*. *Biochem J*, 2002. 366(Pt 3):831-7.
488. Hainsworth, J.D., et al., *A Randomized, Open-Label Phase 2 Study of the CXCR4 Inhibitor LY2510924 in Combination with Sunitinib Versus Sunitinib Alone in Patients with Metastatic Renal Cell Carcinoma*. *Target Oncol*, 2016. 11(5):643-653.
489. Salgia, R., et al., *A randomized phase II study of LY2510924 and carboplatin/etoposide versus carboplatin/etoposide in extensive-disease small cell lung cancer*. *Lung Cancer*, 2017. 105:7-13.
490. Bhullar, K.S., et al., *Kinase-targeted cancer therapies: progress, challenges and future directions*. *Mol Cancer*, 2018. 17(1):018-0804.
491. Mueller, A., N.G. Mahmoud, and P.G. Strange, *Diverse signalling by different chemokines through the chemokine receptor CCR5*. *Biochem Pharmacol*, 2006. 72(6):739-748.
492. Leach, K., S.J. Charlton, and P.G. Strange, *Analysis of second messenger pathways stimulated by different chemokines acting at the chemokine receptor CCR5*. *Biochem Pharmacol*, 2007. 74(6):881-890.
493. Mundell, S.J., et al., *Arrestin isoforms dictate differential kinetics of A2B adenosine receptor trafficking*. *Biochemistry*, 2000. 39(42):12828-36.
494. Ferguson, S.S., et al., *Role of beta-arrestin in mediating agonist-promoted G protein-coupled receptor internalization*. *Science*, 1996. 271(5247):363-6.
495. Mueller, A., et al., *Pharmacological characterization of the chemokine receptor, CCR5*. *Br J Pharmacol*, 2002. 135(4):1033-43.
496. Malkinson, J.P., et al., *Solid-phase synthesis of the cyclic peptide portion of chlorofusin, an inhibitor of p53-MDM2 interactions*. *Org Lett*, 2003. 5(26):5051-4.
497. Ferguson, S.M. and P. De Camilli, *Dynamin, a membrane-remodelling GTPase*. *Nat Rev Mol Cell Biol*, 2012. 13(2):75-88.
498. Orso, G., et al., *Homotypic fusion of ER membranes requires the dynamin-like GTPase atlastin*. *Nature*, 2009. 460(7258):978-83.
499. Hill, T., et al., *Small molecule inhibitors of dynamin I GTPase activity: development of dimeric tyrphostins*. *J Med Chem*, 2005. 48(24):7781-8.
500. Hughes, C.E. and R.J.B. Nibbs, *A guide to chemokines and their receptors*. *Febs J*, 2018. 10(10):14466.
501. Harper, C.B., et al., *Targeting membrane trafficking in infection prophylaxis: dynamin inhibitors*. *Trends Cell Biol*, 2013. 23(2):90-101.

502. McCluskey, A., et al., *Building a Better Dynasore: The Dyngo Compounds Potently Inhibit Dynamin and Endocytosis*. Traffic (Copenhagen, Denmark), 2013. 14(12):1272-1289.
503. Hill, T.A., et al., *Long chain amines and long chain ammonium salts as novel inhibitors of dynamin GTPase activity*. Bioorg Med Chem Lett, 2004. 14(12):3275-8.
504. Robertson, M.J., et al., *The Rhodadyns, a New Class of Small Molecule Inhibitors of Dynamin GTPase Activity*. ACS Med Chem Lett, 2012. 3(5):352-356.
505. van Lessen, M., et al., *Intracellular uptake of macromolecules by brain lymphatic endothelial cells during zebrafish embryonic development*. eLife, 2017. 6:e25932.
506. McGeachie, A.B., et al., *Pyrimidyn compounds: dual-action small molecule pyrimidine-based dynamin inhibitors*. ACS Chem Biol, 2013. 8(7):1507-18.
507. Cassidy-Stone, A., et al., *Chemical inhibition of the mitochondrial division dynamin reveals its role in Bax/Bak-dependent mitochondrial outer membrane permeabilization*. Dev Cell, 2008. 14(2):193-204.
508. Yamada, H., et al., *Dynasore, a dynamin inhibitor, suppresses lamellipodia formation and cancer cell invasion by destabilizing actin filaments*. Biochem Biophys Res Commun, 2009. 390(4):1142-8.
509. Hua, Y., et al., *Blocking endocytosis enhances short-term synaptic depression under conditions of normal availability of vesicles*. Neuron, 2013. 80(2):343-9.
510. Pelekanos, R.A., et al., *Intracellular trafficking and endocytosis of CXCR4 in fetal mesenchymal stem/stromal cells*. BMC Cell Biol, 2014. 15(15):1471-2121.
511. Preta, G., J.G. Cronin, and I.M. Sheldon, *Dynasore - not just a dynamin inhibitor*. Cell Commun and Signal, 2015. 13:24.
512. Macia, E., et al., *Dynasore, a cell-permeable inhibitor of dynamin*. Dev Cell, 2006. 10(6):839-50.
513. Park, R.J., et al., *Dynamin triple knockout cells reveal off target effects of commonly used dynamin inhibitors*. J Cell Sci, 2013. 126(Pt 22):5305-12.
514. Douthitt, H.L., et al., *Dynasore, an inhibitor of dynamin, increases the probability of transmitter release*. Neuroscience, 2011. 172:187-95.
515. Harper, C.B., et al., *Dynamin inhibition blocks botulinum neurotoxin type A endocytosis in neurons and delays botulism*. J Biol Chem, 2011. 286(41):35966-76.
516. Reid, A.T., et al., *Dynamin regulates specific membrane fusion events necessary for acrosomal exocytosis in mouse spermatozoa*. J Biol Chem, 2012. 287(45):37659-72.
517. Joshi, S., et al., *Dynamin inhibitors induce caspase-mediated apoptosis following cytokinesis failure in human cancer cells and this is blocked by Bcl-2 overexpression*. Mol Cancer, 2011. 10(78):1476-4598.

518. Jackson, J.R., et al., *Targeted anti-mitotic therapies: can we improve on tubulin agents?* Nat Rev Cancer, 2007. 7(2):107-17.
519. Wilkinson, R.W., et al., *AZD1152, a selective inhibitor of Aurora B kinase, inhibits human tumor xenograft growth by inducing apoptosis.* Clin Cancer Res, 2007. 13(12):3682-8.
520. Joshi, S., et al., *The dynamin inhibitors MiTMAB and OcTMAB induce cytokinesis failure and inhibit cell proliferation in human cancer cells.* Mol Cancer Ther, 2010. 9(7):1995-2006.
521. Chircop, M., et al., *Calcineurin activity is required for the completion of cytokinesis.* Cell Mol Life Sci, 2010. 67(21):3725-37.
522. Weaver, B.A. and D.W. Cleveland, *Decoding the links between mitosis, cancer, and chemotherapy: The mitotic checkpoint, adaptation, and cell death.* Cancer Cell, 2005. 8(1):7-12.
523. Linares-Clemente, P., et al., *Different dynamin blockers interfere with distinct phases of synaptic endocytosis during stimulation in motoneurons.* J Physiol, 2015. 593(13):2867-88.
524. Quan, A., et al., *Myristyl trimethyl ammonium bromide and octadecyl trimethyl ammonium bromide are surface-active small molecule dynamin inhibitors that block endocytosis mediated by dynamin I or dynamin II.* Mol Pharmacol, 2007. 72(6):1425-39.
525. Midorikawa, M., Y. Okamoto, and T. Sakaba, *Developmental changes in Ca<sup>2+</sup> channel subtypes regulating endocytosis at the calyx of Held.* J Physiol, 2014. 592(16):3495-510.
526. Marks, B. and H.T. McMahon, *Calcium triggers calcineurin-dependent synaptic vesicle recycling in mammalian nerve terminals.* Curr Biol, 1998. 8(13):740-9.
527. Balaji, J., M. Armbruster, and T.A. Ryan, *Calcium control of endocytic capacity at a CNS synapse.* J Neurosci, 2008. 28(26):6742-9.
528. Zhang, J., et al., *From Spanish fly to room-temperature ionic liquids (RTILs): synthesis, thermal stability and inhibition of dynamin 1 GTPase by a novel class of RTILs.* New J Chem, 2008. 32(1):28-36.
529. Lin, H.C., et al., *Phosphatidylinositol (4,5)-bisphosphate-dependent activation of dynamins I and II lacking the proline/arginine-rich domains.* J Biol Chem, 1997. 272(41):25999-6004.
530. Masud Rana, A.Y., et al., *Dynamin contributes to cytokinesis by stabilizing actin filaments in the contractile ring.* Genes Cells, 2013. 18(8):621-35.
531. Thompson, H.M., et al., *The Large GTPase Dynamin Associates with the Spindle Midzone and Is Required for Cytokinesis.* Curr Biol, 2002. 12(24):2111-2117.
532. Townson, J.R., L.F. Barcellos, and R.J. Nibbs, *Gene copy number regulates the production of the human chemokine CCL3-L1.* Eur J Immunol, 2002. 32(10):3016-26.
533. Garcia Lopez, M.A., et al., *Inhibition of dynamin prevents CCL2-mediated endocytosis of CCR2 and activation of ERK1/2.* Cell Signal, 2009. 21(12):1748-57.

534. Cai, J., et al., *ERK/Drp1-dependent mitochondrial fission is involved in the MSC-induced drug resistance of T-cell acute lymphoblastic leukemia cells*. Cell Death Dis, 2016. 7(11):370.
535. Gao, D., et al., *Targeting Dynamin 2 as a Novel Pathway to Inhibit Cardiomyocyte Apoptosis Following Oxidative Stress*. Cell Physiol Biochem, 2016. 39(6):2121-2134.
536. Kirchhausen, T., E. Macia, and H.E. Pelish, *Use of dynasore, the small molecule inhibitor of dynamin, in the regulation of endocytosis*. Methods Enzymol, 2008. 438:77-93.
537. Wan, Y.Y., et al., *Involvement of Drp1 in hypoxia-induced migration of human glioblastoma U251 cells*. Oncol Rep, 2014. 32(2):619-26.
538. Chang, C.R. and C. Blackstone, *Dynamic regulation of mitochondrial fission through modification of the dynamin-related protein Drp1*. Ann N Y Acad Sci, 2010. 1201:34-9.
539. Venkatesan, S., et al., *Distinct mechanisms of agonist-induced endocytosis for human chemokine receptors CCR5 and CXCR4*. Mol Biol Cell, 2003. 14(8):3305-24.
540. Allen, J.A., R.A. Halverson-Tamboli, and M.M. Rasenick, *Lipid raft microdomains and neurotransmitter signalling*. Nat Rev Neurosci, 2007. 8(2):128-40.
541. Merrifield, C.J. and M. Kaksonen, *Endocytic accessory factors and regulation of clathrin-mediated endocytosis*. Cold Spring Harb Perspect Biol, 2014. 6(11):a016733.
542. Taylor, M.J., M. Lampe, and C.J. Merrifield, *A feedback loop between dynamin and actin recruitment during clathrin-mediated endocytosis*. PLoS Biol, 2012. 10(4):10.
543. McMahon, H.T. and E. Boucrot, *Molecular mechanism and physiological functions of clathrin-mediated endocytosis*. Nat Rev Mol Cell Biol, 2011. 12(8):517-33.
544. Antonescu, C.N., G. Danuser, and S.L. Schmid, *Phosphatidic acid plays a regulatory role in clathrin-mediated endocytosis*. Mol Biol Cell, 2010. 21(16):2944-52.
545. Motley, A., et al., *Clathrin-mediated endocytosis in AP-2-depleted cells*. J Cell Biol, 2003. 162(5):909-18.
546. Cocucci, E., et al., *The first five seconds in the life of a clathrin-coated pit*. Cell, 2012. 150(3):495-507.
547. Jacques, R.O., et al., *Dynamin function is important for chemokine receptor-induced cell migration*. Cell Biochem Funct, 2015. 33(6):407-14.
548. Dey, R., et al., *Regulation of impaired protein kinase C signaling by chemokines in murine macrophages during visceral leishmaniasis*. Infect Immun, 2005. 73(12):8334-44.
549. Kim, H., et al., *PKC activation induces inflammatory response and cell death in human bronchial epithelial cells*. PLoS One, 2013. 8(5):e64182.
550. Lochhead, P.A., et al., *A chaperone-dependent GSK3beta transitional intermediate mediates activation-loop autophosphorylation*. Mol Cell, 2006. 24(4):627-33.

551. Moore, S.F., et al., *Dual regulation of glycogen synthase kinase 3 (GSK3)alpha/beta by protein kinase C (PKC)alpha and Akt promotes thrombin-mediated integrin alphabeta3 activation and granule secretion in platelets*. J Biol Chem, 2013. 288(6):3918-28.
552. Kaidanovich-Beilin, O. and J.R. Woodgett, *GSK-3: Functional Insights from Cell Biology and Animal Models*. Front Mol Neurosci, 2011. 4:40.
553. Fan, G., et al., *c-Src tyrosine kinase binds the beta 2-adrenergic receptor via phospho-Tyr-350, phosphorylates G-protein-linked receptor kinase 2, and mediates agonist-induced receptor desensitization*. J Biol Chem, 2001. 276(16):13240-7.
554. Wang, J.T., et al., *Src controls neuronal migration by regulating the activity of FAK and cofilin*. Neuroscience, 2015. 292:90-100.
555. Creedon, H. and V.G. Brunton, *Src kinase inhibitors: promising cancer therapeutics?* Crit Rev Oncog, 2012. 17(2):145-59.
556. Cursons, J., et al., *Regulation of ERK-MAPK signaling in human epidermis*. BMC Syst Biol, 2015. 9(41):015-0187.
557. Marais, R. and C.J. Marshall, *Control of the ERK MAP kinase cascade by Ras and Raf*. Cancer Surv, 1996. 27:101-25.
558. Pritchard, C.A., et al., *Conditionally oncogenic forms of the A-Raf and B-Raf protein kinases display different biological and biochemical properties in NIH 3T3 cells*. Mol Cell Biol, 1995. 15(11):6430-42.
559. Hong, S.K., et al., *ERK1/2 can feedback-regulate cellular MEK1/2 levels*. Cell Signal, 2015. 27(10):1939-48.
560. Soltoff, S.P., *Rottlerin: an inappropriate and ineffective inhibitor of PKCdelta*. Trends Pharmacol Sci, 2007. 28(9):453-8.
561. Susarla, B.T. and M.B. Robinson, *Rottlerin, an inhibitor of protein kinase Cdelta (PKCdelta), inhibits astrocytic glutamate transport activity and reduces GLAST immunoreactivity by a mechanism that appears to be PKCdelta-independent*. J Neurochem, 2003. 86(3):635-45.
562. Park, S.W., et al., *Protein kinase Cdelta differentially regulates cAMP-dependent translocation of NTCP and MRP2 to the plasma membrane*. Am J Physiol Gastrointest Liver Physiol, 2012. 303(5):28.
563. Dietrich, C., et al., *Rottlerin induces a transformed phenotype in human keratinocytes*. Biochem Biophys Res Commun, 2001. 282(2):575-9.
564. Lim, J.H., et al., *Rottlerin induces apoptosis via death receptor 5 (DR5) upregulation through CHOP-dependent and PKC delta-independent mechanism in human malignant tumor cells*. Carcinogenesis, 2009. 30(5):729-36.
565. Mills, S.C., et al., *Cell migration towards CXCL12 in leukemic cells compared to breast cancer cells*. Cell Signal, 2016. 28(4):316-24.



566. Antonsson, A. and J.L. Persson, *Induction of Apoptosis by Staurosporine Involves the Inhibition of Expression of the Major Cell Cycle Proteins at the G2/M Checkpoint Accompanied by Alterations in Erk and Akt Kinase Activities*. *Anticancer Res*, 2009. 29(8):2893-2898.
567. Preta, G. and B. Fadeel, *Scythe cleavage during Fas (APO-1)-and staurosporine-mediated apoptosis*. *FEBS lett*, 2012. 586(6):747-752.
568. Sipeki, S., et al., *PKCalpha reduces the lipid kinase activity of the p110alpha/p85alpha PI3K through the phosphorylation of the catalytic subunit*. *Biochem Biophys Res Commun*, 2006. 339(1):122-5.
569. Tanaka, Y., et al., *Protein kinase C promotes apoptosis in LNCaP prostate cancer cells through activation of p38 MAPK and inhibition of the Akt survival pathway*. *J Biol Chem*, 2003. 278(36):33753-62.
570. Matsumoto, T., et al., *Am80 inhibits stromal cell-derived factor-1-induced chemotaxis in T-cell acute lymphoblastic leukemia cells*. *Leuk Lymphoma*, 2010. 51(3):507-14.
571. Sharlow, E.R., et al., *Potent and selective disruption of protein kinase D functionality by a benzoxoloazepinolone*. *J Biol Chem*, 2008. 283(48):33516-26.
572. Storz, P. and A. Toker, *Protein kinase D mediates a stress-induced NF-kappaB activation and survival pathway*. *Embo J*, 2003. 22(1):109-20.
573. Jaggi, M., et al., *E-cadherin phosphorylation by protein kinase D1/protein kinase C{mu} is associated with altered cellular aggregation and motility in prostate cancer*. *Cancer Res*, 2005. 65(2):483-92.
574. Prigozhina, N.L. and C.M. Waterman-Storer, *Protein kinase D-mediated anterograde membrane trafficking is required for fibroblast motility*. *Curr Biol*, 2004. 14(2):88-98.
575. Bieerkehazhi, S., et al., *Novel Src/Abl tyrosine kinase inhibitor bosutinib suppresses neuroblastoma growth via inhibiting Src/Abl signaling*. *Oncotarget*, 2016. 8(1):1469-1480.
576. Duda, D.G., et al., *CXCL12 (SDF1alpha)-CXCR4/CXCR7 pathway inhibition: an emerging sensitizer for anticancer therapies?* *Clin Cancer Res*, 2011. 17(8):2074-80.
577. De Luca, A., et al., *Src and CXCR4 are involved in the invasiveness of breast cancer cells with acquired resistance to lapatinib*. *Cell Cycle*, 2014. 13(1):148-56.
578. Ptasznik, A., et al., *Crosstalk between BCR/ABL oncoprotein and CXCR4 signaling through a Src family kinase in human leukemia cells*. *J Exp Med*, 2002. 196(5):667-78.
579. Berger, A., et al., *RAF Inhibition Overcomes Resistance to TRAIL-Induced Apoptosis in Melanoma Cells*. *J Invest Dermatol*, 2014. 134(2):430-440.
580. Pritchard, C.A., et al., *B-Raf acts via the ROCKII/LIMK/cofilin pathway to maintain actin stress fibers in fibroblasts*. *Mol Cell Biol*, 2004. 24(13):5937-52.

581. Juarez, J., et al., *Effects of inhibitors of the chemokine receptor CXCR4 on acute lymphoblastic leukemia cells in vitro*. Leukemia, 2003. 17(7):1294-300.
582. Cashman, J., et al., *Stromal-derived factor 1 inhibits the cycling of very primitive human hematopoietic cells in vitro and in NOD/SCID mice*. Blood, 2002. 99(3):792-9.
583. Juarez, J., et al., *Interaction of interleukin-7 and interleukin-3 with the CXCL12-induced proliferation of B-cell progenitor acute lymphoblastic leukemia*. Haematologica, 2007. 92(4):450-9.
584. Wellbrock, C. and A. Hurlstone, *BRAF as therapeutic target in melanoma*. Biochem Pharmacol, 2010. 80(5):561-7.
585. Bollag, G., et al., *Clinical efficacy of a RAF inhibitor needs broad target blockade in BRAF-mutant melanoma*. Nature, 2010. 467(7315):596-9.
586. Heidorn, S.J., et al., *Kinase-dead BRAF and oncogenic RAS cooperate to drive tumor progression through CRAF*. Cell, 2010. 140(2):209-21.
587. Gopal, Y.N., et al., *Basal and treatment-induced activation of AKT mediates resistance to cell death by AZD6244 (ARRY-142886) in Braf-mutant human cutaneous melanoma cells*. Cancer Res, 2010. 70(21):8736-47.
588. Wolf, K., et al., *Compensation mechanism in tumor cell migration: mesenchymal-amoeboid transition after blocking of pericellular proteolysis*. J Cell Biol, 2003. 160(2):267-77.
589. Brunton, V.G. and M.C. Frame, *Src and focal adhesion kinase as therapeutic targets in cancer*. Curr Opin Pharmacol, 2008. 8(4):427-32.
590. Carragher, N.O., et al., *Calpain 2 and Src dependence distinguishes mesenchymal and amoeboid modes of tumour cell invasion: a link to integrin function*. Oncogene, 2006. 25(42):5726-40.
591. Basu, A. and A. Miura, *Differential regulation of extrinsic and intrinsic cell death pathways by protein kinase C*. Int J Mol Med, 2002. 10(5):541-5.
592. Watanabe, T., et al., *Cell division arrest induced by phorbol ester in CHO cells overexpressing protein kinase C-delta subspecies*. Proc Natl Acad Sci U S A, 1992. 89(21):10159-63.
593. Churchill, E.N. and D. Mochly-Rosen, *The roles of PKCdelta and epsilon isoenzymes in the regulation of myocardial ischaemia/reperfusion injury*. Biochem Soc Trans, 2007. 35(Pt 5):1040-2.
594. Mischak, H., et al., *Phorbol ester-induced myeloid differentiation is mediated by protein kinase C-alpha and -delta and not by protein kinase C-beta II, -epsilon, -zeta, and -eta*. J Biol Chem, 1993. 268(27):20110-5.
595. Perletti, G.P., et al., *PKCdelta acts as a growth and tumor suppressor in rat colonic epithelial cells*. Oncogene, 1999. 18(5):1251-6.

596. Denning, M.F., et al., *Protein kinase Cdelta is activated by caspase-dependent proteolysis during ultraviolet radiation-induced apoptosis of human keratinocytes*. J Biol Chem, 1998. 273(45):29995-30002.
597. Denning, M.F., et al., *Activation of the epidermal growth factor receptor signal transduction pathway stimulates tyrosine phosphorylation of protein kinase C delta*. J Biol Chem, 1996. 271(10):5325-31.
598. Mandil, R., et al., *Protein kinase Calpha and protein kinase Cdelta play opposite roles in the proliferation and apoptosis of glioma cells*. Cancer Res, 2001. 61(11):4612-9.
599. Wu, B., et al., *Involvement of PKCalpha activation in TF/VIIa/PAR2-induced proliferation, migration, and survival of colon cancer cell SW620*. Tumour Biol, 2013. 34(2):837-46.
600. Gwak, J., et al., *Stimulation of protein kinase C-alpha suppresses colon cancer cell proliferation by down-regulation of beta-catenin*. J Cell Mol Med, 2009. 13(8B):2171-80.
601. Vaškovičová, K., et al., *PKCα promotes the mesenchymal to amoeboid transition and increases cancer cell invasiveness*. BMC Cancer, 2015. 15:326.
602. Pongracz, J., et al., *Expression of protein kinase C isoenzymes in colorectal cancer tissue and their differential activation by different bile acids*. Int J Cancer, 1995. 61(1):35-9.
603. Hill, K.S., et al., *Protein kinase Calpha suppresses Kras-mediated lung tumor formation through activation of a p38 MAPK-TGFbeta signaling axis*. Oncogene, 2014. 33(16):2134-44.
604. Masur, K., et al., *Norepinephrine-induced migration of SW 480 colon carcinoma cells is inhibited by beta-blockers*. Cancer Res, 2001. 61(7):2866-9.
605. Gauthier, M.L., et al., *Protein kinase Calpha negatively regulates cell spreading and motility in MDA-MB-231 human breast cancer cells downstream of epidermal growth factor receptor*. Biochem Biophys Res Commun, 2003. 307(4):839-46.
606. Davies, S.P., et al., *Specificity and mechanism of action of some commonly used protein kinase inhibitors*. Biochem J, 2000. 351(Pt 1):95-105.
607. Grandage, V.L., et al., *Go6976 is a potent inhibitor of the JAK 2 and FLT3 tyrosine kinases with significant activity in primary acute myeloid leukaemia cells*. Br J Haematol, 2006. 135(3):303-16.
608. Gschwendt, M., et al., *Inhibition of protein kinase C mu by various inhibitors. Differentiation from protein kinase c isoenzymes*. FEBS Lett, 1996. 392(2):77-80.
609. Gorin, M.A. and Q. Pan, *Protein kinase C epsilon: an oncogene and emerging tumor biomarker*. Mol Cancer, 2009. 8(9):1476-4598.
610. Mischak, H., et al., *Overexpression of protein kinase C-delta and -epsilon in NIH 3T3 cells induces opposite effects on growth, morphology, anchorage dependence, and tumorigenicity*. J Biol Chem, 1993. 268(9):6090-6.

611. Jansen, A.P., et al., *Protein kinase C-epsilon transgenic mice: a unique model for metastatic squamous cell carcinoma*. Cancer Res, 2001. 61(3):808-12.
612. Gobbi, G., et al., *Phorbol ester-induced PKCepsilon down-modulation sensitizes AML cells to TRAIL-induced apoptosis and cell differentiation*. Blood, 2009. 113(13):3080-7.
613. Sivaprasad, U., E. Shankar, and A. Basu, *Downregulation of Bid is associated with PKCepsilon-mediated TRAIL resistance*. Cell Death Differ, 2007. 14(4):851-60.
614. Basu, A. and U. Sivaprasad, *Protein kinase Cepsilon makes the life and death decision*. Cell Signal, 2007. 19(8):1633-42.
615. Lau, E., et al., *PKCepsilon promotes oncogenic functions of ATF2 in the nucleus while blocking its apoptotic function at mitochondria*. Cell, 2012. 148(3):543-55.
616. Gillespie, S., X.D. Zhang, and P. Hersey, *Variable expression of protein kinase C epsilon in human melanoma cells regulates sensitivity to TRAIL-induced apoptosis*. Mol Cancer Ther, 2005. 4(4):668-76.
617. Mayne, G.C. and A.W. Murray, *Evidence that protein kinase Cepsilon mediates phorbol ester inhibition of calphostin C- and tumor necrosis factor-alpha-induced apoptosis in U937 histiocytic lymphoma cells*. J Biol Chem, 1998. 273(37):24115-21.
618. Vivanco, I. and C.L. Sawyers, *The phosphatidylinositol 3-Kinase AKT pathway in human cancer*. Nat Rev Cancer, 2002. 2(7):489-501.
619. Pan, Q., et al., *Protein kinase C epsilon is a predictive biomarker of aggressive breast cancer and a validated target for RNA interference anticancer therapy*. Cancer Res, 2005. 65(18):8366-71.
620. Pan, Q., et al., *Targeted disruption of protein kinase C epsilon reduces cell invasion and motility through inactivation of RhoA and RhoC GTPases in head and neck squamous cell carcinoma*. Cancer Res, 2006. 66(19):9379-84.
621. Haribabu, B., et al., *Regulation of human chemokine receptors CXCR4. Role of phosphorylation in desensitization and internalization*. J Biol Chem, 1997. 272(45):28726-31.
622. Ding, Q., et al., *Erk associates with and primes GSK-3beta for its inactivation resulting in upregulation of beta-catenin*. Mol Cell, 2005. 19(2):159-70.
623. Ohgushi, M., et al., *Molecular pathway and cell state responsible for dissociation-induced apoptosis in human pluripotent stem cells*. Cell Stem Cell, 2010. 7(2):225-39.
624. Kajabadi, N.S., et al., *The Synergistic Enhancement of Cloning Efficiency in Individualized Human Pluripotent Stem Cells by Peroxisome Proliferative-activated Receptor-gamma (PPARGgamma) Activation and Rho-associated Kinase (ROCK) Inhibition*. J Biol Chem, 2015. 290(43):26303-13.
625. Orsulic, S., et al., *E-cadherin binding prevents beta-catenin nuclear localization and beta-catenin/LEF-1-mediated transactivation*. J Cell Sci, 1999. 112(Pt 8):1237-45.

626. Zoudilova, M., et al., *beta-Arrestins scaffold cofilin with chronophin to direct localized actin filament severing and membrane protrusions downstream of protease-activated receptor-2*. J Biol Chem, 2010. 285(19):14318-29.
627. Bravo-Cordero, J.J., L. Hodgson, and J. Condeelis, *Directed cell invasion and migration during metastasis*. Curr Opin Cell Biol, 2012. 24(2):277-83.
628. Nishida, E., S. Maekawa, and H. Sakai, *Cofilin, a protein in porcine brain that binds to actin filaments and inhibits their interactions with myosin and tropomyosin*. Biochemistry, 1984. 23(22):5307-13.
629. Mabuchi, I., *Purification from starfish eggs of a protein that depolymerizes actin*. J Biochem, 1981. 89(4):1341-4.
630. Samstag, Y., I. John, and G.H. Wabnitz, *Cofilin: a redox sensitive mediator of actin dynamics during T-cell activation and migration*. Immunol Rev, 2013. 256(1):30-47.
631. Chimini, G. and P. Chavrier, *Function of Rho family proteins in actin dynamics during phagocytosis and engulfment*. Nat Cell Biol, 2000. 2(10):E191-E196.
632. Scott, G.A., et al., *Plexin C1, a receptor for semaphorin 7a, inactivates cofilin and is a potential tumor suppressor for melanoma progression*. J Invest Dermatol, 2009. 129(4):954-63.
633. Klemke, M., et al., *An MEK-cofilin signalling module controls migration of human T cells in 3D but not 2D environments*. EMBO J, 2010. 29(17):2915-2929.
634. Niwa, R., et al., *Control of actin reorganization by Slingshot, a family of phosphatases that dephosphorylate ADF/cofilin*. Cell, 2002. 108(2):233-46.
635. Ohta, Y., et al., *Differential activities, subcellular distribution and tissue expression patterns of three members of Slingshot family phosphatases that dephosphorylate cofilin*. Genes Cells, 2003. 8(10):811-24.
636. Kaji, N., et al., *Cell cycle-associated changes in Slingshot phosphatase activity and roles in cytokinesis in animal cells*. J Biol Chem, 2003. 278(35):33450-5.
637. Hattermann, K., et al., *Effects of the chemokine CXCL12 and combined internalization of its receptors CXCR4 and CXCR7 in human MCF-7 breast cancer cells*. Cell Tissue Res, 2014. 357(1):253-266.
638. Khan, S.M., et al., *The Expanding Roles of G $\beta\gamma$  Subunits in G Protein–Coupled Receptor Signaling and Drug Action*. Pharmacol Rev, 2013. 65(2):545-577.
639. Sanz, G., et al., *Gallein, a G $\beta\gamma$  subunit signalling inhibitor, inhibits metastatic spread of tumour cells expressing OR51E2 and exposed to its odorant ligand*. BMC Res notes, 2017. 10(1):541-541.
640. Erdmann, T., et al., *Sensitivity to PI3K and AKT inhibitors is mediated by divergent molecular mechanisms in subtypes of DLBCL*. Blood, 2017. 130(3):310-322.

641. Harris, S.J., et al., *Phosphoinositide lipid phosphatases: natural regulators of phosphoinositide 3-kinase signaling in T lymphocytes*. J Biol Chem, 2008. 283(5):2465-9.
642. Son, K., T.C. Smith, and E.J. Luna, *Supervillin binds the Rac/Rho-GEF Trio and increases Trio-mediated Rac1 activation*. Cytoskeleton, 2015. 72(1):47-64.
643. Nishita, M., et al., *Phosphoinositide 3-kinase-mediated activation of cofilin phosphatase Slingshot and its role for insulin-induced membrane protrusion*. J Biol Chem, 2004. 279(8):7193-8.
644. Nebl, G., et al., *Dephosphorylation of cofilin is regulated through Ras and requires the combined activities of the Ras-effectors MEK and PI3K*. Cell Signal, 2004. 16(2):235-43.
645. Jung, J., et al., *Molecular mechanism of cofilin dephosphorylation by ouabain*. Cell Signal, 2006. 18(11):2033-2040.
646. Genot, E., et al., *p21ras initiates Rac-1 but not phosphatidyl inositol 3 kinase/PKB, mediated signaling pathways in T lymphocytes*. Oncogene, 1998. 17(13):1731-8.
647. Wabnitz, G.H., et al., *Phosphatidylinositol 3-kinase functions as a Ras effector in the signaling cascade that regulates dephosphorylation of the actin-remodeling protein cofilin after costimulation of untransformed human T lymphocytes*. J Immunol, 2006. 176(3):1668-74.
648. Nogues, L., et al., *G-Protein-Coupled Receptor Kinase 2 as a Potential Modulator of the Hallmarks of Cancer*. Mol Pharmacol, 2017. 91(3):220-228.
649. Gurevich, E.V., et al., *G protein-coupled receptor kinases: more than just kinases and not only for GPCRs*. Pharmacol Ther, 2012. 133(1):40-69.
650. Shenoy, S.K. and R.J. Lefkowitz, *beta-Arrestin-mediated receptor trafficking and signal transduction*. Trends Pharmacol Sci, 2011. 32(9):521-33.
651. Penela, P., et al., *The complex G protein-coupled receptor kinase 2 (GRK2) interactome unveils new physiopathological targets*. Br J Pharmacol, 2010. 160(4):821-32.
652. Watari, K., M. Nakaya, and H. Kurose, *Multiple functions of G protein-coupled receptor kinases*. J Mol Signal, 2014. 9(1):1750-2187.
653. Iino, M., et al., *Rational design and evaluation of new lead compound structures for selective betaARK1 inhibitors*. J Med Chem, 2002. 45(11):2150-9.
654. Freeburn, R.W. and S.G. Ward, *The Jurkat cell line has constitutively active PI3K/PKB Signalling: effect of inducible expression of a membrane-localised SHIP construct*. Biochem Soc Trans, 2001. 29(5):A128.
655. Salcedo, A., F. Mayor, Jr., and P. Penela, *Mdm2 is involved in the ubiquitination and degradation of G-protein-coupled receptor kinase 2*. Embo J, 2006. 25(20):4752-62.
656. Thelen, M. and S. Thelen, *CXCR7, CXCR4 and CXCL12: an eccentric trio?* J Neuroimmunol, 2008. 198(1-2):9-13.

657. Hattermann, K. and R. Mentlein, *An infernal trio: the chemokine CXCL12 and its receptors CXCR4 and CXCR7 in tumor biology*. Ann Anat, 2013. 195(2):103-10.
658. Rajagopal, S. and S.K. Shenoy, *GPCR desensitization: Acute and prolonged phases*. Cell Signal, 2017. 28(17): 024.
659. Ma, X., et al., *Acute activation of beta2-adrenergic receptor regulates focal adhesions through betaArrestin2- and p115RhoGEF protein-mediated activation of RhoA*. J Biol Chem, 2012. 287(23):18925-36.
660. Fereshteh, M., et al., *beta-Arrestin2 mediates the initiation and progression of myeloid leukemia*. Proc Natl Acad Sci U S A, 2012. 109(31):12532-7.
661. Barnes, W.G., et al., *beta-Arrestin 1 and Galphagq/11 coordinately activate RhoA and stress fiber formation following receptor stimulation*. J Biol Chem, 2005. 280(9):8041-50.
662. Li, T.T., et al., *Beta-arrestin/Ral signaling regulates lysophosphatidic acid-mediated migration and invasion of human breast tumor cells*. Mol Cancer Res, 2009. 7(7):1064-77.
663. Anthony, D.F., et al., *beta-Arrestin 1 inhibits the GTPase-activating protein function of ARHGAP21, promoting activation of RhoA following angiotensin II type 1A receptor stimulation*. Mol Cell Biol, 2011. 31(5):1066-75.
664. Guilluy, C., et al., *The Rho exchange factor Arhgef1 mediates the effects of angiotensin II on vascular tone and blood pressure*. Nat Med, 2010. 16(2):183-90.
665. Ma, X., et al., *betaArrestin1 regulates the guanine nucleotide exchange factor RasGRF2 expression and the small GTPase Rac-mediated formation of membrane protrusion and cell motility*. J Biol Chem, 2014. 289(19):13638-50.
666. Izumi, D., et al., *CXCL12/CXCR4 activation by cancer-associated fibroblasts promotes integrin beta1 clustering and invasiveness in gastric cancer*. Int J Cancer, 2016. 138(5):1207-19.
667. Bacon, K.B., et al., *RANTES induces tyrosine kinase activity of stably complexed p125FAK and ZAP-70 in human T cells*. J Exp Med, 1996. 184(3):873-82.
668. Wiemer, A.J., et al., *The focal adhesion kinase inhibitor PF-562,271 impairs primary CD4+ T cell activation*. Biochem Pharmacol, 2013. 86(6):770-81.
669. Sulzmaier, F.J., C. Jean, and D.D. Schlaepfer, *FAK in cancer: mechanistic findings and clinical applications*. Nat Rev Cancer, 2014. 14(9):598-610.
670. Fujimura, M., et al., *Inhibition of the Rho/ROCK pathway prevents neuronal degeneration in vitro and in vivo following methylmercury exposure*. Toxicol Appl Pharmacol, 2011. 250(1):1-9.
671. Ramirez, S.H., et al., *Activation of Peroxisome Proliferator-Activated Receptor gamma (PPAR $\gamma$ ) suppresses Rho GTPases in human brain microvascular endothelial cells and inhibits adhesion and transendothelial migration of HIV-1 infected monocytes*. J Immunol (Baltimore, Md.:1950), 2008. 180(3):1854-1865.

672. Schmandke, A., A. Schmandke, and S.M. Strittmatter, *ROCK and Rho: Biochemistry and Neuronal Functions of Rho-Associated Protein Kinases*. Neuroscientist, 2007. 13(5):454-469.
673. Takesono, A., et al., *Microtubules regulate migratory polarity through Rho/ROCK signaling in T cells*. PLoS One, 2010. 5(1):0008774.
674. Sanchez-Madrid, F. and J.M. Serrador, *Bringing up the rear: defining the roles of the uropod*. Nat Rev Mol Cell Biol. 2009. 10(5):353-9.
675. Worthylake, R.A., et al., *RhoA is required for monocyte tail retraction during transendothelial migration*. J Cell Biol, 2001. 154(1):147-60.
676. Kiuchi, T., et al., *Cofilin promotes stimulus-induced lamellipodium formation by generating an abundant supply of actin monomers*. J Cell Biol, 2007. 177(3):465-76.
677. Maekawa, M., et al., *Signaling from Rho to the Actin Cytoskeleton Through Protein Kinases ROCK and LIM-kinase*. Science, 1999. 285(5429):895-898.
678. Sumi, T., K. Matsumoto, and T. Nakamura, *Specific activation of LIM kinase 2 via phosphorylation of threonine 505 by ROCK, a Rho-dependent protein kinase*. J Biol Chem, 2001. 276(1):670-6.
679. Pawlak, G. and D.M. Helfman, *MEK mediates v-Src-induced disruption of the actin cytoskeleton via inactivation of the Rho-ROCK-LIM kinase pathway*. J Biol Chem, 2002. 277(30):26927-33.
680. Cardaba, C.M., J.S. Kerr, and A. Mueller, *CCR5 internalisation and signalling have different dependence on membrane lipid raft integrity*. Cell Signal, 2008. 20(9):1687-94.
681. Boldt, K., et al., *FPRL-1 induces modifications of migration-associated proteins in human neutrophils*. Proteomics, 2006. 6(17):4790-9.
682. Adachi, R., et al., *Nitric oxide induces chemotaxis of neutrophil-like HL-60 cells and translocation of cofilin to plasma membranes*. Int J Immunopharmacol, 2000. 22(11):855-64.
683. Jovceva, E., et al., *Dynamic cofilin phosphorylation in the control of lamellipodial actin homeostasis*. J Cell Sci, 2007. 120(Pt 11):1888-97.
684. DesMarais, V., et al., *Cofilin takes the lead*. J Cell Sci, 2005. 118(Pt 1): p. 19-26.
685. Gouwy, M., et al., *Chemokines and other GPCR ligands synergize in receptor-mediated migration of monocyte-derived immature and mature dendritic cells*. Immunobiology, 2014. 219(3):218-29.
686. Xanthou, G., et al., *CCR3 functional responses are regulated by both CXCR3 and its ligands CXCL9, CXCL10 and CXCL11*. Eur J Immunol, 2003. 33(8):2241-2250.
687. Ngeow, J., et al., *Detecting Germline PTEN Mutations Among At-Risk Patients With Cancer: An Age- and Sex-Specific Cost-Effectiveness Analysis*. J Clin Oncol, 2015. 33(23):2537-44.



688. Freeburn, R.W., et al., *Evidence that SHIP-1 contributes to phosphatidylinositol 3,4,5-trisphosphate metabolism in T lymphocytes and can regulate novel phosphoinositide 3-kinase effectors*. J Immunol, 2002. 169(10):5441-50.
689. Wu, Y. and A. Yoder, *Chemokine Coreceptor Signaling in HIV-1 Infection and Pathogenesis*. PLoS Pathog, 2009. 5(12):e1000520.
690. Renkawitz, J., et al., *Adaptive force transmission in amoeboid cell migration*. Nat Cell Biol, 2009. 11(12):1438-43.
691. Narumiya, S. and N. Watanabe, *Migration without a clutch*. Nat Cell Biol, 2009. 11(12):1394-1396.
692. Komolov, K.E. and J.L. Benovic, *G protein-coupled receptor kinases: Past, present and future*. Cell Signal, 2018. 41:17-24.
693. Evron, T., T.L. Daigle, and M.G. Caron, *GRK2: multiple roles beyond G protein-coupled receptor desensitization*. Trends Pharmacol Sci, 2012. 33(3):154-64.
694. Peregrin, S., et al., *Phosphorylation of p38 by GRK2 at the docking groove unveils a novel mechanism for inactivating p38MAPK*. Curr Biol, 2006. 16(20):2042-7.
695. Eichmann, T., et al., *The amino-terminal domain of G-protein-coupled receptor kinase 2 is a regulatory Gbeta gamma binding site*. J Biol Chem, 2003. 278(10):8052-7.
696. Pitcher, J.A., et al., *Pleckstrin homology domain-mediated membrane association and activation of the beta-adrenergic receptor kinase requires coordinate interaction with G beta gamma subunits and lipid*. J Biol Chem, 1995. 270(20):11707-10.
697. Kim, J., et al., *Functional antagonism of different G protein-coupled receptor kinases for beta-arrestin-mediated angiotensin II receptor signaling*. Proc Natl Acad Sci U S A, 2005. 102(5):1442-7.
698. Brahmbhatt, A.A. and R.L. Klemke, *ERK and RhoA differentially regulate pseudopodia growth and retraction during chemotaxis*. J Biol Chem, 2003. 278(15):13016-25.
699. Zidar, D.A., et al., *Selective engagement of G protein coupled receptor kinases (GRKs) encodes distinct functions of biased ligands*. Proc Natl Acad Sci U S A, 2009. 106(24):9649-54.
700. Liu, J.J., et al., *Biased signaling pathways in beta2-adrenergic receptor characterized by 19F-NMR*. Science, 2012. 335(6072):1106-10.
701. Nobles, K.N., et al., *Distinct phosphorylation sites on the beta(2)-adrenergic receptor establish a barcode that encodes differential functions of beta-arrestin*. Sci Signal, 2011. 4(185):2001707.
702. Hitoshi, K., et al., *Atypical Actions of G Protein-Coupled Receptor Kinases*. Korean Soc Appl Pharmacol, 2011. 19(4):390-397.

703. Lafarga, V., et al., *A novel GRK2/HDAC6 interaction modulates cell spreading and motility*. *Embo J*, 2012. 31(4):856-69.
704. Jimenez-Sainz, M.C., et al., *G protein-coupled receptor kinase 2 negatively regulates chemokine signaling at a level downstream from G protein subunits*. *Mol Biol Cell*, 2006. 17(1):25-31.
705. Fusco, A., et al., *Mitochondrial localization unveils a novel role for GRK2 in organelle biogenesis*. *Cell Signal*, 2012. 24(2):468-75.
706. Luo, J. and J.L. Benovic, *G protein-coupled receptor kinase interaction with Hsp90 mediates kinase maturation*. *J Biol Chem*, 2003. 278(51):50908-14.
707. Chen, M., et al., *Prodeath signaling of G protein-coupled receptor kinase 2 in cardiac myocytes after ischemic stress occurs via extracellular signal-regulated kinase-dependent heat shock protein 90-mediated mitochondrial targeting*. *Circ Res*, 2013. 112(8):1121-34.
708. Pitcher, J.A., et al., *The G protein-coupled receptor kinase 2 is a microtubule-associated protein kinase that phosphorylates tubulin*. *J Biol Chem*, 1998. 273(20):12316-24.
709. Penela, P., et al., *G protein-coupled receptor kinase 2 (GRK2) modulation and cell cycle progression*. *Proc Natl Acad Sci U S A*, 2010. 107(3):1118-23.
710. Liebick, M., et al., *Functional consequences of chemically-induced beta-arrestin binding to chemokine receptors CXCR4 and CCR5 in the absence of ligand stimulation*. *Cell Signal*, 2017. 38:201-211.
711. Krupnick, J.G., et al., *Arrestin/clathrin interaction. Localization of the clathrin binding domain of nonvisual arrestins to the carboxy terminus*. *J Biol Chem*, 1997. 272(23):15011-6.
712. Goodman, O.B., Jr., et al., *Beta-arrestin acts as a clathrin adaptor in endocytosis of the beta2-adrenergic receptor*. *Nature*, 1996. 383(6599):447-50.
713. Carman, C.V. and J.L. Benovic, *G-protein-coupled receptors: turn-ons and turn-offs*. *Curr Opin Neurobiol*, 1998. 8(3):335-44.
714. Kommaddi, R.P. and S.K. Shenoy, *Arrestins and protein ubiquitination*. *Prog Mol Biol Transl Sci*, 2013. 118:175-204.
715. Marchese, A., et al., *The E3 ubiquitin ligase AIP4 mediates ubiquitination and sorting of the G protein-coupled receptor CXCR4*. *Dev Cell*, 2003. 5(5):709-22.
716. Marchese, A., *Endocytic trafficking of chemokine receptors*. *Curr Opin Cell Biol*, 2014. 27: p. 72-7.
717. Oakley, R.H., et al., *Association of beta-arrestin with G protein-coupled receptors during clathrin-mediated endocytosis dictates the profile of receptor resensitization*. *J Biol Chem*, 1999. 274(45):32248-57.

718. Smith, J.S. and S. Rajagopal, *The beta-Arrestins: Multifunctional Regulators of G Protein-coupled Receptors*. J Biol Chem, 2016. 291(17):8969-77.
719. Urosevic, J., A.R. Nebreda, and R.R. Gomis, *MAPK signaling control of colon cancer metastasis*. Cell Cycle, 2014. 13(17):2641-2642.
720. Oakley, R.H., et al., *Differential affinities of visual arrestin, beta arrestin1, and beta arrestin2 for G protein-coupled receptors delineate two major classes of receptors*. J Biol Chem, 2000. 275(22):17201-10.
721. Hanyaloglu, A.C. and M. von Zastrow, *Regulation of GPCRs by endocytic membrane trafficking and its potential implications*. Annu Rev Pharmacol Toxicol, 2008. 48:537-68.
722. Huttenrauch, F., et al., *Beta-arrestin binding to CC chemokine receptor 5 requires multiple C-terminal receptor phosphorylation sites and involves a conserved Asp-Arg-Tyr sequence motif*. J Biol Chem, 2002. 277(34):30769-77.
723. Gurevich, V.V. and E.V. Gurevich, *The molecular acrobatics of arrestin activation*. Trends Pharmacol Sci, 2004. 25(2):105-11.
724. El-Khoury, V., et al., *Identification of beta-arrestin-1 as a diagnostic biomarker in lung cancer*. Br J Cancer, 2018. 119(5):580-590.
725. Simanshu, D.K., D.V. Nissley, and F. McCormick, *RAS Proteins and Their Regulators in Human Disease*. Cell, 2017. 170(1):17-33.
726. Kolli-Bouhafs, K., et al., *FAK competes for Src to promote migration against invasion in melanoma cells*. Cell Death Dis, 2014. 14(5):329.
727. Mellado, M., et al., *The chemokine monocyte chemotactic protein 1 triggers Janus kinase 2 activation and tyrosine phosphorylation of the CCR2B receptor*. J Immunol, 1998. 161(2):805-13.
728. Soriano, S.F., et al., *Chemokines integrate JAK/STAT and G-protein pathways during chemotaxis and calcium flux responses*. Eur J Immunol, 2003. 33(5):1328-33.
729. Simon, A.R., et al., *Activation of the JAK-STAT pathway by reactive oxygen species*. Am J Physiol, 1998. 275(6 Pt 1):C1640-52.
730. Schieffer, B., et al., *Role of NAD(P)H oxidase in angiotensin II-induced JAK/STAT signaling and cytokine induction*. Circ Res, 2000. 87(12):1195-201.
731. Pelletier, S., et al., *Rho family GTPases are required for activation of Jak/STAT signaling by G protein-coupled receptors*. Mol Cell Biol, 2003. 23(4):1316-33.
732. Honma, M., S.A. Benitah, and F.M. Watt, *Role of LIM Kinases in Normal and Psoriatic Human Epidermis*. Mol Biol Cell, 2006. 17(4):1888-1896.
733. Sandberg, E.M., et al., *Identification of 1,2,3,4,5,6-hexabromocyclohexane as a small molecule inhibitor of jak2 tyrosine kinase autophosphorylation [correction of autophosphorylation]*. J Med Chem, 2005. 48(7):2526-33.

734. Uehara, Y., et al., *Novel high-throughput screening system for identifying STAT3-SH2 antagonists*. Biochem Biophys Res Commun, 2009. 380(3):627-31.
735. Rodriguez, G., et al., *Forskolin-inducible cAMP pathway negatively regulates T-cell proliferation by uncoupling the interleukin-2 receptor complex*. J Biol Chem, 2013. 288(10):7137-46.
736. Zhang, H., et al., *Adenosine acts through A2 receptors to inhibit IL-2-induced tyrosine phosphorylation of STAT5 in T lymphocytes: role of cyclic adenosine 3',5'-monophosphate and phosphatases*. J Immunol, 2004. 173(2):932-44.
737. Derenzini, E., et al., *The JAK inhibitor AZD1480 regulates proliferation and immunity in Hodgkin lymphoma*. Blood Cancer J, 2011. 1(12):2.
738. Palmer, D., K. Tsoi, and D.H. Maurice, *Synergistic inhibition of vascular smooth muscle cell migration by phosphodiesterase 3 and phosphodiesterase 4 inhibitors*. Circ Res, 1998. 82(8):852-61.
739. Dessauer, C.W., et al., *International Union of Basic and Clinical Pharmacology. CI. Structures and Small Molecule Modulators of Mammalian Adenylyl Cyclases*. Pharmacol Rev, 2017. 69(2):93-139.
740. Ekholm, D., et al., *Cyclic nucleotide phosphodiesterases (PDE) 3 and 4 in normal, malignant, and HTLV-I transformed human lymphocytes*. Biochem Pharmacol, 1999. 58(6):935-50.
741. Zambon, A.C., et al., *Gene expression patterns define key transcriptional events in cell-cycle regulation by cAMP and protein kinase A*. Proc Natl Acad Sci U S A, 2005. 102(24):8561-6.
742. Sen Sharma, S. and S.S. Majumdar, *Transcriptional co-activator YAP regulates cAMP signaling in Sertoli cells*. Mol Cell Endocrinol, 2017. 18(17):017.
743. Arumugham, V.B. and C.T. Baldari, *cAMP: a multifaceted modulator of immune synapse assembly and T cell activation*. J Leukoc Biol, 2017. 29(10):2RU1116-474R.
744. Mosenden, R. and K. Tasken, *Cyclic AMP-mediated immune regulation--overview of mechanisms of action in T cells*. Cell Signal, 2011. 23(6):1009-16.
745. Liu, A.M., et al., *Activation of STAT3 by G alpha(s) distinctively requires protein kinase A, JNK, and phosphatidylinositol 3-kinase*. J Biol Chem, 2006. 281(47):35812-25.
746. Infante, E. and A.J. Ridley, *Roles of Rho GTPases in leucocyte and leukaemia cell transendothelial migration*. Philos Trans R Soc Lond B Biol Sci, 2013. 368:1629.
747. Osborn, M. and K. Weber, *Actin paracrystal induction by forskolin and by db-cAMP in CHO cells*. Exp Cell Res, 1984. 150(2):408-18.
748. Omelchenko, T., et al., *Mechanisms of polarization of the shape of fibroblasts and epitheliocytes: Separation of the roles of microtubules and Rho-dependent actin-myosin contractility*. Proc Natl Acad Sci U S A, 2002. 99(16):10452-7.

749. Chen, L., J.J. Zhang, and X.Y. Huang, *cAMP inhibits cell migration by interfering with Rac-induced lamellipodium formation*. J Biol Chem, 2008. 283(20):13799-805.
750. Gau, D., et al., *Threonine 89 Is an Important Residue of Profilin-1 That Is Phosphorylatable by Protein Kinase A*. PLoS One, 2016. 11(5):e0156313.
751. Hocking, K.M., et al., *Role of cyclic nucleotide-dependent actin cytoskeletal dynamics:Ca(2+)](i) and force suppression in forskolin-pretreated porcine coronary arteries*. PLoS One, 2013. 8(4):e60986.
752. Rodriguez-Frade, J.M., et al., *The chemokine monocyte chemoattractant protein-1 induces functional responses through dimerization of its receptor CCR2*. Proc Natl Acad Sci U S A, 1999. 96(7):3628-33.
753. Ali, M.S., et al., *Janus kinase 2 (Jak2) must be catalytically active to associate with the AT1 receptor in response to angiotensin II*. Biochem Biophys Res Commun, 1998. 249(3):672-7.
754. Mueller, A. and P.G. Strange, *CCL3, acting via the chemokine receptor CCR5, leads to independent activation of Janus kinase 2 (JAK2) and Gi proteins*. FEBS Lett, 2004. 570(1-3):126-32.
755. Mellado, M., et al., *Receptor dimerization: a key step in chemokine signaling*. Cell Mol Biol, 2001. 47(4):575-82.
756. Rodriguez-Frade, J.M., et al., *Similarities and differences in RANTES- and (AOP)-RANTES-triggered signals: implications for chemotaxis*. J Cell Biol, 1999. 144(4):755-65.
757. Khabbazi, S., et al., *Janus kinase 2 and signal transducer and activator of transcription 3 activation is not essential for CCL3-, CCL5- or CCL8-induced chemotaxis*. Cell Biochem Funct, 2013. 31(4):312-8.
758. Bokoch, G.M., *Regulation of the human neutrophil NADPH oxidase by the Rac GTP-binding proteins*. Curr Opin Cell Biol, 1994. 6(2):212-8.
759. Kim, H. and J.K. Sonn, *Rac1 promotes chondrogenesis by regulating STAT3 signaling pathway*. Cell Biol Int, 2016. 40(9):976-83.
760. Benitah, S.A., et al., *Stem cell depletion through epidermal deletion of Rac1*. Science, 2005. 309(5736):933-5.
761. Ohashi, K., et al., *Damnacanthal, an effective inhibitor of LIM-kinase, inhibits cell migration and invasion*. Mol Biol Cell, 2014. 25(6):828-40.
762. Vandamme, J., D. Castermans, and J.M. Thevelein, *Molecular mechanisms of feedback inhibition of protein kinase A on intracellular cAMP accumulation*. Cell Signal, 2012. 24(8):1610-8.
763. Houslay, M.D., *Underpinning compartmentalised cAMP signalling through targeted cAMP breakdown*. Trends Biochem Sci, 2010. 35(2):91-100.
764. Kumar, N., et al., *Role of exchange protein directly activated by cAMP (EPAC1) in breast cancer cell migration and apoptosis*. Mol Cell Biochem, 2017. 16(10):017-2959.

765. Ross, J.A., et al., *Regulation of T cell homeostasis by JAKs and STATs*. Arch Immunol Ther Exp, 2007. 55(4):231-45.
766. Tasken, K. and E.M. Aandahl, *Localized effects of cAMP mediated by distinct routes of protein kinase A*. Physiol Rev, 2004. 84(1):137-67.
767. Yamada, T., et al., *Involvement of intracellular cAMP in epirubicin-induced vascular endothelial cell injury*. J Pharmacol Sci, 2016. 130(1):33-7.
768. Lee, I.H., et al., *Inhibition of interleukin 2 signaling and signal transducer and activator of transcription (STAT)5 activation during T cell receptor-mediated feedback inhibition of T cell expansion*. J Exp Med, 1999. 190(9):1263-74.
769. Stork, P.J. and J.M. Schmitt, *Crosstalk between cAMP and MAP kinase signaling in the regulation of cell proliferation*. Trends Cell Biol, 2002. 12(6):258-66.
770. Sadana, R. and C.W. Dessauer, *Physiological roles for G protein-regulated adenylyl cyclase isoforms: insights from knockout and overexpression studies*. Neurosignals, 2009. 17(1):5-22.
771. Steegborn, C., *Structure, mechanism, and regulation of soluble adenylyl cyclases - similarities and differences to transmembrane adenylyl cyclases*. Biochim Biophys Acta, 2014. 12(47):2.
772. Tasken, K. and A.J. Stokka, *The molecular machinery for cAMP-dependent immunomodulation in T-cells*. Biochem Soc Trans, 2006. 34(Pt 4):476-9.
773. Spina, A., et al., *cAMP Elevation Down-Regulates  $\beta 3$  Integrin and Focal Adhesion Kinase and Inhibits Leptin-Induced Migration of MDA-MB-231 Breast Cancer Cells*. BioRes Open Access, 2012. 1(6):324-332.
774. McLean, G.W., et al., *The role of focal-adhesion kinase in cancer - a new therapeutic opportunity*. Nat Rev Cancer, 2005. 5(7):505-15.
775. Gu, J., et al., *Laminin-10/11 and fibronectin differentially regulate integrin-dependent Rho and Rac activation via p130(Cas)-CrkII-DOCK180 pathway*. J Biol Chem, 2001. 276(29):27090-7.
776. Hall, A., *Rho GTPases and the actin cytoskeleton*. Science, 1998. 279(5350):509-14.
777. Cristobal, I., et al., *Hyperphosphorylation of PP2A in colorectal cancer and the potential therapeutic value showed by its forskolin-induced dephosphorylation and activation*. Biochim Biophys Acta, 2014. 9(9):2.
778. Bhardwaj, A., et al., *CXCL12/CXCR4 signaling counteracts docetaxel-induced microtubule stabilization via p21-activated kinase 4-dependent activation of LIM domain kinase 1*. Oncotarget, 2014. 5(22):11490-11500.
779. Misra, U.K., R. Deedwania, and S.V. Pizzo, *Binding of activated alpha2-macroglobulin to its cell surface receptor GRP78 in 1-LN prostate cancer cells regulates PAK-2-dependent activation of LIMK*. J Biol Chem, 2005. 280(28):26278-86.

780. Bowman, T., et al., *Stat3-mediated Myc expression is required for Src transformation and PDGF-induced mitogenesis*. Proc Natl Acad Sci U S A, 2001. 98(13):7319-24.
781. Levy, D.E. and J.E. Darnell, Jr., *Stats: transcriptional control and biological impact*. Nat Rev Mol Cell Biol, 2002. 3(9):651-62.
782. Moriguchi, M., et al., *CXCL12 signaling is independent of Jak2 and Jak3*. J Biol Chem, 2005. 280(17):17408-14.
783. Montresor, A., et al., *JAK2 tyrosine kinase mediates integrin activation induced by CXCL12 in B-cell chronic lymphocytic leukemia*. Oncotarget, 2015. 6(33):34245-34257.
784. Perez-Rivero, G., et al., *Janus kinases 1 and 2 regulate chemokine-mediated integrin activation and naive T-cell homing*. Eur J Immunol, 2013. 43(7):1745-57.
785. Alhadidi, Q. and Z.A. Shah, *Cofilin Mediates LPS-Induced Microglial Cell Activation and Associated Neurotoxicity Through Activation of NF-kappaB and JAK-STAT Pathway*. Mol Neurobiol, 2018. 55(2):1676-1691.
786. Oshima, M., et al., *Chemoprevention of intestinal polyposis in the Apcdelta716 mouse by rofecoxib, a specific cyclooxygenase-2 inhibitor*. Cancer Res, 2001. 61(4):1733-40.
787. Tanaka, S., et al., *Monocyte chemoattractant protein 1 and macrophage cyclooxygenase 2 expression in colonic adenoma*. Gut, 2006. 55(1):54-61.
788. Bardia, A., et al., *Effect of aspirin and other NSAIDs on postmenopausal breast cancer incidence by hormone receptor status: results from a prospective cohort study*. Breast Cancer Res Treat, 2011. 126(1):149-55.
789. Pangburn, H.A., D.J. Ahnen, and P.L. Rice, *Sulindac metabolites induce proteosomal and lysosomal degradation of the epidermal growth factor receptor*. Cancer Prev Res, 2010. 3(4):560-72.
790. Howe, L.R., et al., *Celecoxib, a selective cyclooxygenase 2 inhibitor, protects against human epidermal growth factor receptor 2 (HER-2)/neu-induced breast cancer*. Cancer Res, 2002. 62(19):5405-7.
791. Canetti, C., et al., *Activation of phosphatase and tensin homolog on chromosome 10 mediates the inhibition of FcgammaR phagocytosis by prostaglandin E2 in alveolar macrophages*. J Immunol, 2007. 179(12):8350-6.
792. Gai, W.T., et al., *Anti-cancer effect of ursolic acid activates apoptosis through ROCK/PTEN mediated mitochondrial translocation of cofilin-1 in prostate cancer*. Oncol Lett, 2016. 12(4):2880-2885.
793. Davies, E.M., et al., *Differential SKIP expression in PTEN-deficient glioblastoma regulates cellular proliferation and migration*. Oncogene, 2015. 34(28):3711-27.
794. Patel, P., et al., *Inhibition of RhoA/Rho kinase by ibuprofen exerts cardioprotective effect on isoproterenol induced myocardial infarction in rats*. Eur J Pharmacol, 2016. 791:91-98.

795. Davies, N.M., *Clinical Pharmacokinetics of Ibuprofen*. Clin Pharmacokinet, 1998. 34(2):101-154.
796. Moore, R.A., et al., *Effects of food on pharmacokinetics of immediate release oral formulations of aspirin, dipyrrone, paracetamol and NSAIDs - a systematic review*. Br J Clin Pharmacol, 2015. 80(3):381-8.
797. Strawson, J., *Nonsteroidal anti-inflammatory drugs and cancer pain*. Curr Opin Support Palliat Care, 2018. 12(2):102-107.
798. Akrami, H., S. Aminzadeh, and H. Fallahi, *Inhibitory effect of ibuprofen on tumor survival and angiogenesis in gastric cancer cell*. Tumour Biol, 2015. 36(5):3237-43.
799. Janssen, A., et al., *p53 is important for the anti-proliferative effect of ibuprofen in colon carcinoma cells*. Biochem Biophys Res Commun, 2008. 365(4):698-703.
800. Janssen, A., et al., *Evidence of COX-2 independent induction of apoptosis and cell cycle block in human colon carcinoma cells after S- or R-ibuprofen treatment*. Eur J Pharmacol, 2006. 540(1-3):24-33.
801. Bonelli, P., et al., *Changes in the gene expression profile of gastric cancer cells in response to ibuprofen: a gene pathway analysis*. Pharmacogenomics J, 2011. 11(6):412-28.
802. Panzer, U. and M. Ugucioni, *Prostaglandin E2 modulates the functional responsiveness of human monocytes to chemokines*. Eur J Immunol, 2004. 34(12):3682-9.
803. Cervello, M., et al., *COX-2-dependent and COX-2-independent mode of action of celecoxib in human liver cancer cells*. Omics, 2011. 15(6):383-92.
804. Friedrich, M., et al., *Effects of Combined Treatment with Vitamin D and COX2 Inhibitors on Breast Cancer Cell Lines*. Anticancer Res, 2018. 38(2):1201-1207.
805. de Groot, D.J., et al., *Non-steroidal anti-inflammatory drugs to potentiate chemotherapy effects: from lab to clinic*. Crit Rev Oncol Hematol, 2007. 61(1):52-69.
806. Dogne, J.M., et al., *Dual carbonic anhydrase--cyclooxygenase-2 inhibitors*. Curr Top Med Chem, 2007. 7(9):885-91.
807. Supuran, C.T., A. Scozzafava, and A. Casini, *Carbonic anhydrase inhibitors*. Med Res Rev, 2003. 23(2):146-89.
808. Nocentini, A., et al., *Synthesis and biological evaluation of novel pyrazoline-based aromatic sulfamates with potent carbonic anhydrase isoforms II, IV and IX inhibitory efficacy*. Bioorg Chem, 2018. 77:633-639.
809. O'Neil, C.K., J.T. Hanlon, and Z.A. Marcum, *Adverse effects of analgesics commonly used by older adults with osteoarthritis: focus on non-opioid and opioid analgesics*. Am J Geriatr Pharmacother, 2012. 10(6):331-42.



810. Bundscherer, A.C., et al., *Acetaminophen and Metamizole Induce Apoptosis in HT 29 and SW 480 Colon Carcinoma Cell Lines In Vitro*. *Anticancer Res*, 2018. 38(2):745-751.
811. Berridge, M.J., P. Lipp, and M.D. Bootman, *The versatility and universality of calcium signalling*. *Nat Rev Mol Cell Biol*, 2000. 1(1):11-21.
812. Komoda, H., et al., *Azelnidipine Inhibits the Differentiation and Activation of THP-1 Macrophages through the L-Type Calcium Channel*. *J Atheroscler Thromb*, 2018. 3(10):41798.
813. Lin, M., M.X. Zhu, and Y. Rikihisa, *Rapid activation of protein tyrosine kinase and phospholipase C-gamma2 and increase in cytosolic free calcium are required by Ehrlichia chaffeensis for internalization and growth in THP-1 cells*. *Infect Immun*, 2002. 70(2):889-98.
814. Gasser, A., et al., *Activation of T cell calcium influx by the second messenger ADP-ribose*. *J Biol Chem*, 2006. 281(5):2489-96.
815. Deveci, H.A., M. Naziroglu, and G. Nur, *5-Fluorouracil-induced mitochondrial oxidative cytotoxicity and apoptosis are increased in MCF-7 human breast cancer cells by TRPV1 channel activation but not Hypericum perforatum treatment*. *Mol Cell Biochem*, 2018. 439(1-2):189-198.
816. Rink, T.J., *Receptor-mediated calcium entry*. *FEBS Lett*, 1990. 268(2):381-5.
817. Patterson, R.L., D. Boehning, and S.H. Snyder, *Inositol 1,4,5-trisphosphate receptors as signal integrators*. *Annu Rev Biochem*, 2004. 73:437-65.
818. Lanner, J.T., et al., *Ryanodine receptors: structure, expression, molecular details, and function in calcium release*. *Cold Spring Harb Perspect Biol*, 2010. 2(11):20.
819. Caballero, F.J., et al., *The acetaminophen-derived bioactive N-acylphenolamine AM404 inhibits NFAT by targeting nuclear regulatory events*. *Biochem Pharmacol*, 2007. 73(7):1013-23.
820. Kerckhove, N., et al., *Ca(v)3.2 calcium channels: the key protagonist in the supraspinal effect of paracetamol*. *Pain*, 2014. 155(4):764-72.
821. Frolov, R.V. and S. Singh, *Celecoxib and ion channels: a story of unexpected discoveries*. *Eur J Pharmacol*, 2014. 730:61-71.
822. Berridge, M.J., M.D. Bootman, and P. Lipp, *Calcium - a life and death signal*. *Nature*, 1998. 395:645.
823. Humeau, J., et al., *Calcium signaling and cell cycle: Progression or death*. *Cell Calcium*, 2018. 70:3-15.
824. Andrews, J., et al., *Superior effectiveness of ibuprofen compared with other NSAIDs for reducing the survival of human prostate cancer cells*. *Cancer Chemother Pharmacol*, 2002. 50(4):277-84.
825. Redpath, M., et al., *Ibuprofen and hydrogel-released ibuprofen in the reduction of inflammation-induced migration in melanoma cells*. *Br J Dermatol*, 2009. 161(1):25-33.

826. Lincova, E., et al., *Multiple defects in negative regulation of the PKB/Akt pathway sensitise human cancer cells to the antiproliferative effect of non-steroidal anti-inflammatory drugs*. *Biochem Pharmacol*, 2009. 78(6):561-72.
827. Sarbassov, D.D., et al., *Phosphorylation and regulation of Akt/PKB by the rictor-mTOR complex*. *Science*, 2005. 307(5712):1098-101.
828. Liu, P., et al., *Cell-cycle-regulated activation of Akt kinase by phosphorylation at its carboxyl terminus*. *Nature*, 2014. 508(7497):541-5.
829. Kato, T., et al., *Indomethacin induces cellular morphological change and migration via epithelial-mesenchymal transition in A549 human lung cancer cells: a novel cyclooxygenase-inhibition-independent effect*. *Biochem Pharmacol*, 2011. 82(11):1781-91.
830. Dill, J., et al., *A molecular mechanism for ibuprofen-mediated RhoA inhibition in neurons*. *J Neurosci*, 2010. 30(3):963-72.
831. Veliceasa, D., F.T. Schulze-Hoepfner, and O.V. Volpert, *PPARgamma and Agonists against Cancer: Rational Design of Complementation Treatments*. *PPAR Res*, 2008. 945275(10):18.
832. Lehmann, J.M., et al., *Peroxisome proliferator-activated receptors alpha and gamma are activated by indomethacin and other non-steroidal anti-inflammatory drugs*. *J Biol Chem*, 1997. 272(6):3406-10.
833. Goetze, S., et al., *PPAR activators inhibit endothelial cell migration by targeting Akt*. *Biochem Biophys Res Commun*, 2002. 293(5):1431-7.
834. Hsueh, W.A., S. Jackson, and R.E. Law, *Control of vascular cell proliferation and migration by PPAR-gamma: a new approach to the macrovascular complications of diabetes*. *Diabetes Care*, 2001. 24(2):392-7.
835. Teresi, R.E., et al., *Regulation of the PTEN promoter by statins and SREBP*. *Hum Mol Genet*, 2008. 17(7):919-28.
836. Ma, B., et al., *RIG-like Helicase Regulation of Chitinase 3-like 1 Axis and Pulmonary Metastasis*. *Sci Rep*, 2016. 6:26299.
837. Goren, I., et al., *Inhibition of cyclooxygenase-1 and -2 activity in keratinocytes inhibits PGE2 formation and impairs vascular endothelial growth factor release and neovascularisation in skin wounds*. *Int Wound J*, 2017. 14(1):53-63.
838. Carmeliet, P., *VEGF as a key mediator of angiogenesis in cancer*. *Oncology*, 2005. 3:4-10.
839. Palayoor, S.T., P.J. Tofilon, and C.N. Coleman, *Ibuprofen-mediated reduction of hypoxia-inducible factors HIF-1alpha and HIF-2alpha in prostate cancer cells*. *Clin Cancer Res*, 2003. 9(8):3150-7.
840. Gallelli, L., et al., *The effects of nonsteroidal anti-inflammatory drugs on clinical outcomes, synovial fluid cytokine concentration and signal transduction pathways in knee osteoarthritis. A randomized open label trial*. *Osteoarthr Cartilage*, 2013. 21(9):1400-1408.

841. Ognibene, M., et al., *Immunohistochemical analysis of PDK1, PHD3 and HIF-1alpha expression defines the hypoxic status of neuroblastoma tumors*. PLoS One, 2017. 12(11):e0187206.
842. Johnson, K.E. and T.A. Wilgus, *Vascular Endothelial Growth Factor and Angiogenesis in the Regulation of Cutaneous Wound Repair*. Adv Wound Care, 2014. 3(10):647-661.
843. Wiktorowska-Owczarek, A., M. Namiecinska, and J. Owczarek, *The effect of Ibuprofen on bFGF, VEGF secretion and cell proliferation in the presence of LPS in HMEC-1 cells*. Acta Pol Pharm, 2015. 72(5):889-94.
844. Dandah, O., et al., *Aspirin and ibuprofen, in bulk and nanoforms: Effects on DNA damage in peripheral lymphocytes from breast cancer patients and healthy individuals*. Mutat Res, 2018. 826:41-46.
845. Ezechias, M., et al., *Widely used pharmaceuticals present in the environment revealed as in vitro antagonists for human estrogen and androgen receptors*. Chemosphere, 2016. 152:284-91.
846. Lynagh, T., et al., *Molecular Basis for Allosteric Inhibition of Acid-Sensing Ion Channel 1a by Ibuprofen*. J Med Chem, 2017. 60(19):8192-8200.
847. Villalobos, C. and J. Garcia-Sancho, *Capacitative Ca<sup>2+</sup> entry contributes to the Ca<sup>2+</sup> influx induced by thyrotropin-releasing hormone (TRH) in GH3 pituitary cells*. Pflugers Arch, 1995. 430(6):923-35.
848. Nunez, L., et al., *The relationship between pulsatile secretion and calcium dynamics in single, living gonadotropin-releasing hormone neurons*. Endocrinology, 2000. 141(6):2012-7.
849. Vervloessem, T., et al., *The type 2 inositol 1,4,5-trisphosphate receptor, emerging functions for an intriguing Ca(2)(+)-release channel*. Biochim Biophys Acta, 2015. 9(10):10.
850. Chin, D. and A.R. Means, *Calmodulin: a prototypical calcium sensor*. Trends Cell Biol, 2000. 10(8):322-8.
851. Crabtree, G.R., *Generic signals and specific outcomes: signaling through Ca<sup>2+</sup>, calcineurin, and NF-AT*. Cell, 1999. 96(5):611-4.
852. Trushin, S.A., et al., *Protein kinase C and calcineurin synergize to activate I $\kappa$ B kinase and NF-kappaB in T lymphocytes*. J Biol Chem, 1999. 274(33):22923-31.
853. See, V., et al., *Calcium-dependent regulation of the cell cycle via a novel MAPK--NF-kappaB pathway in Swiss 3T3 cells*. J Cell Biol, 2004. 166(5):661-72.
854. Huang, W., et al., *T-type calcium channel antagonists, mibefradil and NNC-55-0396 inhibit cell proliferation and induce cell apoptosis in leukemia cell lines*. J Exp Clin Cancer Res, 2015. 34(54):015-0171.

855. Ong, H.L. and I.S. Ambudkar, *STIM-TRP Pathways and Microdomain Organization: Contribution of TRPC1 in Store-Operated Ca(2+) Entry: Impact on Ca(2+) Signaling and Cell Function*. *Adv Exp Med Biol*, 2017. 993:159-188.
856. Rizzuto, R., et al., *Mitochondria as sensors and regulators of calcium signalling*. *Nat Rev Mol Cell Biol*, 2012. 13(9):566-78.
857. Hial, V., et al., *Antiproliferative activity of anti-inflammatory drugs in two mammalian cell culture lines*. *J Pharmacol Exp Ther*, 1977. 202(2):446-54.
858. Bayer, B.M. and M.A. Beaven, *Evidence that indomethacin reversibly inhibits cell growth in the G1 phase of the cell cycle*. *Biochem Pharmacol*, 1979. 28(3):441-3.
859. Schafer, C., et al., *Role of molecular determinants of store-operated Ca(2+) entry (Orai1, phospholipase A2 group 6, and STIM1) in focal adhesion formation and cell migration*. *J Biol Chem*, 2012. 287(48):40745-57.
860. Villalobos, C., et al., *Calcium remodeling in colorectal cancer*. *Biochim Biophys Acta*, 2017. 6:843-849.
861. Murphy, P.M. and L. Heusinkveld, *Multisystem multitasking by CXCL12 and its receptors CXCR4 and ACKR3*. *Cytokine*, 2018. 1(17):30393-9.
862. Omari, S.A., M.J. Adams, and D.P. Geraghty, *TRPV1 Channels in Immune Cells and Hematological Malignancies*. *Adv Pharmacol*, 2017. 79:173-198.
863. Weber, L.V., et al., *Expression and functionality of TRPV1 in breast cancer cells*. *Breast Cancer*, 2016. 8:243-252.
864. Mistretta, F., et al., *Bladder cancer and urothelial impairment: the role of TRPV1 as potential drug target*. *Biomed Res Int*, 2014. 987149(10):8.
865. Fonseca, B.M., G. Correia-da-Silva, and N.A. Teixeira, *Cannabinoid-induced cell death in endometrial cancer cells: involvement of TRPV1 receptors in apoptosis*. *J Physiol Biochem*, 2018. 13(10):018-0611.
866. Kheradpezhough, E., et al., *TRPM2 channels mediate acetaminophen-induced liver damage*. *Proc Natl Acad Sci U S A*, 2014. 111(8):3176-81.
867. Zhang, N., et al., *A proinflammatory chemokine, CCL3, sensitizes the heat- and capsaicin-gated ion channel TRPV1*. *Proc Natl Acad Sci U S A*, 2005. 102(12):4536-41.
868. Taylor-Clark, T.E., et al., *Prostaglandin-induced activation of nociceptive neurons via direct interaction with transient receptor potential A1 (TRPA1)*. *Mol Pharmacol*, 2008. 73(2):274-81.
869. Karashima, Y., et al., *Modulation of the transient receptor potential channel TRPA1 by phosphatidylinositol 4,5-bisphosphate manipulators*. *Pflugers Arch*, 2008. 457(1):77-89.
870. Alpizar, Y.A., et al., *Bimodal effects of cinnamaldehyde and camphor on mouse TRPA1*. *Pflugers Arch*, 2013. 465(6):853-64.

871. Chemin, J., J. Nargeot, and P. Lory, *Chemical determinants involved in anandamide-induced inhibition of T-type calcium channels*. J Biol Chem, 2007. 282(4):2314-23.
872. Barbara, G., et al., *T-type calcium channel inhibition underlies the analgesic effects of the endogenous lipoamino acids*. J Neurosci, 2009. 29(42):13106-14.
873. Talley, E.M., et al., *Differential distribution of three members of a gene family encoding low voltage-activated (T-type) calcium channels*. J Neurosci, 1999. 19(6):1895-911.
874. Sharma, S., et al., *Tumor cyclooxygenase-2/prostaglandin E2-dependent promotion of FOXP3 expression and CD4+ CD25+ T regulatory cell activities in lung cancer*. Cancer Res, 2005. 65(12):5211-20.
875. Sharma, S., et al., *Cyclooxygenase 2 inhibition promotes IFN-gamma-dependent enhancement of antitumor responses*. J Immunol, 2005. 175(2):813-9.
876. Yaqub, S., et al., *Regulatory T cells in colorectal cancer patients suppress anti-tumor immune activity in a COX-2 dependent manner*. Cancer Immunol Immunother, 2008. 57(6):813-21.
877. Brudvik, K.W., et al., *Protein kinase A antagonist inhibits beta-catenin nuclear translocation, c-Myc and COX-2 expression and tumor promotion in Apc(Min/+) mice*. Mol Cancer, 2011. 10(149):1476-4598.
878. Chapple, K.S., et al., *Localization of cyclooxygenase-2 in human sporadic colorectal adenomas*. Am J Pathol, 2000. 156(2):545-53.
879. Alexanian, A. and A. Sorokin, *Cyclooxygenase 2: protein-protein interactions and posttranslational modifications*. Physiol Genomics, 2017. 49(11):667-681.
880. Aronoff, D.M., et al., *Cutting edge: macrophage inhibition by cyclic AMP (cAMP): differential roles of protein kinase A and exchange protein directly activated by cAMP-1*. J Immunol, 2005. 174(2):595-9.
881. Ooms, L.M., et al., *The role of the inositol polyphosphate 5-phosphatases in cellular function and human disease*. Biochem J, 2009. 419(1):29-49.
882. Thun, M.J., S.J. Henley, and C. Patrono, *Nonsteroidal anti-inflammatory drugs as anticancer agents: mechanistic, pharmacologic, and clinical issues*. J Natl Cancer Inst, 2002. 94(4):252-66.
883. Chen, W., T.R. Pawelek, and R.J. Kulmacz, *Hydroperoxide dependence and cooperative cyclooxygenase kinetics in prostaglandin H synthase-1 and -2*. J Biol Chem, 1999. 274(29):20301-6.
884. Fujino, H., W. Xu, and J.W. Regan, *Prostaglandin E2 induced functional expression of early growth response factor-1 by EP4, but not EP2, prostanoid receptors via the phosphatidylinositol 3-kinase and extracellular signal-regulated kinases*. J Biol Chem, 2003. 278(14):12151-6.
885. Yokoyama, U., et al., *The prostanoid EP4 receptor and its signaling pathway*. Pharmacol Rev, 2013. 65(3):1010-52.

886. Jones, R.L., M.A. Giembycz, and D.F. Woodward, *Prostanoid receptor antagonists: development strategies and therapeutic applications*. Br J Pharmacol, 2009. 158(1):104-45.
887. Scheiblich, H. and G. Bicker, *Regulation of Microglial Phagocytosis by RhoA/ROCK-Inhibiting Drugs*. Cell Mol Neurobiol, 2017. 37(3):461-473.
888. Kopp, M.A., et al., *Small-molecule-induced Rho-inhibition: NSAIDs after spinal cord injury*. Cell Tissue Res, 2012. 349(1):119-32.
889. Madura, T., K. Tomita, and G. Terenghi, *Ibuprofen improves functional outcome after axotomy and immediate repair in the peripheral nervous system*. J Plast Reconstr Aesthet Surg, 2011. 64(12):1641-6.
890. Matsuura, K., et al., *The influence of chronic ibuprofen treatment on proteins expressed in the mouse hippocampus*. Eur J Pharmacol, 2015. 752:61-8.
891. Brachs, S., et al., *Monoclonal antibodies to discriminate the EF hand containing calcium binding adaptor proteins EFhd1 and EFhd2*. Monoclon Antib Immunodiagn Immunother, 2013. 32(4):237-45.
892. Mielenz, D. and F. Gunn-Moore, *Physiological and pathophysiological functions of Swiprosin-1/EFhd2 in the nervous system*. Biochem J, 2016. 473(16):2429-2437.
893. Wang, Y., F. Shibasaki, and K. Mizuno, *Calcium signal-induced cofilin dephosphorylation is mediated by Slingshot via calcineurin*. J Biol Chem, 2005. 280(13):12683-9.
894. Kwon, M.S., et al., *Swiprosin-1 is a novel actin bundling protein that regulates cell spreading and migration*. PLoS One, 2013. 8(8):e71626.
895. Markworth, J.F., et al., *Ibuprofen treatment blunts early translational signaling responses in human skeletal muscle following resistance exercise*. J Appl Physiol, 1985. 117(1):20-8.
896. Oprea, T.I., et al., *Novel Activities of Select NSAID R-Enantiomers against Rac1 and Cdc42 GTPases*. PLoS One, 2015. 10(11):e0142182.
897. Matos, P., et al., *Ibuprofen inhibits colitis-induced overexpression of tumor-related Rac1b*. Neoplasia, 2013. 15(1):102-11.
898. Gao, Y., et al., *Trp(56) of rac1 specifies interaction with a subset of guanine nucleotide exchange factors*. J Biol Chem, 2001. 276(50):47530-41.
899. Gao, Y., et al., *Rational design and characterization of a Rac GTPase-specific small molecule inhibitor*. Proc Natl Acad Sci U S A, 2004. 101(20):7618-23.
900. Ridley, A.J., et al., *The small GTP-binding protein rac regulates growth factor-induced membrane ruffling*. Cell, 1992. 70(3):401-10.
901. Levay, M., et al., *NSC23766, a widely used inhibitor of Rac1 activation, additionally acts as a competitive antagonist at muscarinic acetylcholine receptors*. J Pharmacol Exp Ther, 2013. 347(1):69-79.

902. Hou, H., et al., *The Rac1 inhibitor NSC23766 suppresses CREB signaling by targeting NMDA receptor function*. J Neurosci, 2014. 34(42):14006-12.
903. Baribaud, F., et al., *Antigenically distinct conformations of CXCR4*. J Virol, 2001. 75(19):8957-67.
904. Lane, J.R., et al., *A kinetic view of GPCR allostery and biased agonism*. Nat Chem Biol, 2017. 13(9):929-937.
905. Schmid, S.L. and L.L. Carter, *ATP is required for receptor-mediated endocytosis in intact cells*. J Cell Biol, 1990. 111(6 Pt 1):2307-18.
906. Goichberg, P., et al., *cAMP-induced PKC $\zeta$  activation increases functional CXCR4 expression on human CD34+ hematopoietic progenitors*. Blood, 2006. 107(3):870-9.
907. Cole, S.W., B.D. Jamieson, and J.A. Zack, *cAMP up-regulates cell surface expression of lymphocyte CXCR4: implications for chemotaxis and HIV-1 infection*. J Immunol, 1999. 162(3):1392-400.
908. Fleming, I.N., et al., *Ca<sup>2+</sup>/calmodulin-dependent protein kinase II regulates Tiam1 by reversible protein phosphorylation*. J Biol Chem, 1999. 274(18):12753-8.
909. Price, L.S., et al., *Calcium signaling regulates translocation and activation of Rac*. J Biol Chem, 2003. 278(41):39413-21.
910. Vanderheyden, V., et al., *Regulation of inositol 1,4,5-trisphosphate-induced Ca<sup>2+</sup> release by reversible phosphorylation and dephosphorylation*. Biochim Biophys Acta, 2009. 6:959-70.
911. Rougerie, P. and J. Delon, *Rho GTPases: masters of T lymphocyte migration and activation*. Immunol Lett, 2012. 142(1-2):1-13.
912. Harris, K.P. and U. Tepass, *Cdc42 and vesicle trafficking in polarized cells*. Traffic, 2010. 11(10):1272-9.
913. Ratner, S., M.P. Piechocki, and A. Galy, *Role of Rho-family GTPase Cdc42 in polarized expression of lymphocyte appendages*. J Leukoc Biol, 2003. 73(6):830-40.
914. Lu, J., et al., *CXCL14 as an emerging immune and inflammatory modulator*. J Inflamm, 2016. 13(1):015-0109.
915. Peterson, F.C., et al., *Structural determinants involved in the regulation of CXCL14/BRAK expression by the 26 S proteasome*. J Mol Biol, 2006. 363(4):813-22.
916. Sand, L.G., et al., *CXCL14, CXCR7 expression and CXCR4 splice variant ratio associate with survival and metastases in Ewing sarcoma patients*. Eur J Cancer, 2015. 51(17):2624-33.
917. Witte, A., et al., *Platelets as a Novel Source of Pro-Inflammatory Chemokine CXCL14*. Cell Physiol Biochem, 2017. 41(4):1684-1696.

918. Cao, X., et al., *Molecular cloning and characterization of a novel CXC chemokine macrophage inflammatory protein-2 gamma chemoattractant for human neutrophils and dendritic cells*. J Immunol, 2000. 165(5):2588-95.
919. Collins, P.J., et al., *Epithelial chemokine CXCL14 synergizes with CXCL12 via allosteric modulation of CXCR4*. Faseb J, 2017. 31(7):3084-3097.
920. Tamehiro, N., et al., *Cell polarity factor Par3 binds SPTLC1 and modulates monocyte serine palmitoyltransferase activity and chemotaxis*. J Biol Chem, 2009. 284(37):24881-90.
921. Viaud, J., et al., *Phosphatidylinositol 5-phosphate regulates invasion through binding and activation of Tiam1*. Nat Commun, 2014. 5:4080.
922. Carnec, X., et al., *Anti-CXCR4 monoclonal antibodies recognizing overlapping epitopes differ significantly in their ability to inhibit entry of human immunodeficiency virus type 1*. J Virol, 2005. 79(3):1930-3.
923. Ray-Saha, S., T. Huber, and T.P. Sakmar, *Antibody epitopes on G protein-coupled receptors mapped with genetically encoded photoactivatable cross-linkers*. Biochemistry, 2014. 53(8):1302-10.
924. Hatse, S., et al., *Mutation of Asp(171) and Asp(262) of the chemokine receptor CXCR4 impairs its coreceptor function for human immunodeficiency virus-1 entry and abrogates the antagonistic activity of AMD3100*. Mol Pharmacol, 2001. 60(1):164-73.
925. Broberg, K., et al., *Fusion of RDC1 with HMGA2 in lipomas as the result of chromosome aberrations involving 2q35-37 and 12q13-15*. Int J Oncol, 2002. 21(2):321-6.
926. Sun, X., et al., *CXCL12 / CXCR4 / CXCR7 chemokine axis and cancer progression*. Cancer Metastasis Rev, 2010. 29(4):709-22.
927. Hernandez, L., et al., *Opposing roles of CXCR4 and CXCR7 in breast cancer metastasis*. Breast Cancer Res, 2011. 13(6):9.
928. Decaillot, F.M., et al., *CXCR7/CXCR4 heterodimer constitutively recruits beta-arrestin to enhance cell migration*. J Biol Chem, 2011. 286(37):32188-97.
929. Maishi, N., et al., *CXCR7: a novel tumor endothelial marker in renal cell carcinoma*. Pathol Int, 2012. 62(5):309-17.
930. Zoughlami, Y., et al., *Regulation of CXCR4 conformation by the small GTPase Rac1: implications for HIV infection*. Blood, 2012. 119:2024-2032.
931. Dutting, S., et al., *Critical off-target effects of the widely used Rac1 inhibitors NSC23766 and EHT1864 in mouse platelets*. J Thromb Haemost, 2015. 13(5):827-38.
932. Suzuki, S., et al., *Apocynin, an NADPH oxidase inhibitor, suppresses progression of prostate cancer via Rac1 dephosphorylation*. Exp Toxicol Pathol, 2013. 65(7-8):1035-41.



933. Sidarala, V., et al., *EHT 1864, a small molecule inhibitor of Ras-related C3 botulinum toxin substrate 1 (Rac1), attenuates glucose-stimulated insulin secretion in pancreatic beta-cells*. *Cell Signal*, 2015. 27(6):1159-67.
934. Guo, S., et al., *Selectivity of commonly used inhibitors of clathrin-mediated and caveolae-dependent endocytosis of G protein-coupled receptors*. *Biochimica et Biophysica Acta-Biomembranes*, 2015. 1848(10, Part A):2101-2110.
935. Frasch, S.C., et al., *p38 mitogen-activated protein kinase-dependent and -independent intracellular signal transduction pathways leading to apoptosis in human neutrophils*. *J Biol Chem*, 1998. 273(14):8389-97.
936. Creed, T.M., et al., *Endocytosis is required for exocytosis and priming of respiratory burst activity in human neutrophils*. *Inflamm Res*, 2017. 21(10):017-1070.
937. Otero, C., M. Groettrup, and D.F. Legler, *Opposite fate of endocytosed CCR7 and its ligands: recycling versus degradation*. *J Immunol*, 2006. 177(4):2314-23.
938. Marchese, A. and J.L. Benovic, *Agonist-promoted ubiquitination of the G protein-coupled receptor CXCR4 mediates lysosomal sorting*. *J Biol Chem*, 2001. 276(49):45509-12.
939. San-Millan, I. and G.A. Brooks, *Reexamining cancer metabolism: lactate production for carcinogenesis could be the purpose and explanation of the Warburg Effect*. *Carcinogenesis*, 2017. 38(2):119-133.
940. Fei, M.J., et al., *X-ray structure of azide-bound fully oxidized cytochrome c oxidase from bovine heart at 2.9 Å resolution*. *Acta Crystallogr D Biol Crystallogr*, 2000. 56(Pt 5):529-35.
941. Alvarez-Paggi, D., U. Zitare, and D.H. Murgida, *The role of protein dynamics and thermal fluctuations in regulating cytochrome c/cytochrome c oxidase electron transfer*. *Biochim Biophys Acta*, 2014. 7(207):3.
942. Sena, L.A., et al., *Mitochondria are required for antigen-specific T cell activation through reactive oxygen species signaling*. *Immunity*, 2013. 38(2):225-36.
943. Jones, R.G. and C.B. Thompson, *Revving the engine: signal transduction fuels T cell activation*. *Immunity*, 2007. 27(2):173-8.
944. Krauss, S., M.D. Brand, and F. Buttgerit, *Signaling takes a breath--new quantitative perspectives on bioenergetics and signal transduction*. *Immunity*, 2001. 15(4):497-502.
945. Pearce, E.L., *Metabolism in T cell activation and differentiation*. *Curr Opin Immunol*, 2010. 22(3):314-20.
946. Carr, E.L., et al., *Glutamine uptake and metabolism are coordinately regulated by ERK/MAPK during T lymphocyte activation*. *J Immunol*, 2010. 185(2):1037-44.
947. DeBerardinis, R.J., et al., *Beyond aerobic glycolysis: transformed cells can engage in glutamine metabolism that exceeds the requirement for protein and nucleotide synthesis*. *Proc Natl Acad Sci U S A*, 2007. 104(49):19345-50.

948. Rossignol, R., et al., *Energy substrate modulates mitochondrial structure and oxidative capacity in cancer cells*. Cancer Res, 2004. 64(3):985-93.
949. Liberti, M.V. and J.W. Locasale, *The Warburg Effect: How Does it Benefit Cancer Cells?* Trends Biochem Sci, 2016. 41(3):211-8.
950. Ristic, B., Y.D. Bhutia, and V. Ganapathy, *Cell-surface G-protein-coupled receptors for tumor-associated metabolites: A direct link to mitochondrial dysfunction in cancer*. Biochim Biophys Acta, 2017. 13(1):246-257.
951. Hatse, S., et al., *Chemokine receptor inhibition by AMD3100 is strictly confined to CXCR4*. FEBS Lett, 2002. 527(1-3):255-62.
952. Sison, E.A., et al., *Plerixafor as a chemosensitizing agent in pediatric acute lymphoblastic leukemia: efficacy and potential mechanisms of resistance to CXCR4 inhibition*. Oncotarget, 2014. 5(19):8947-58.
953. Hitchinson, B., et al., *Biased antagonism of CXCR4 avoids antagonist tolerance*. Sci Signal, 2018. 11:552.
954. Zhang, W.B., et al., *A point mutation that confers constitutive activity to CXCR4 reveals that T140 is an inverse agonist and that AMD3100 and ALX40-4C are weak partial agonists*. J Biol Chem, 2002. 277(27):24515-21.
955. Hill, S.J., C. Williams, and L.T. May, *Insights into GPCR pharmacology from the measurement of changes in intracellular cyclic AMP; advantages and pitfalls of differing methodologies*. Br J Pharmacol, 2010. 161(6):1266-75.
956. Lefkowitz, R.J., et al., *Constitutive activity of receptors coupled to guanine nucleotide regulatory proteins*. Trends Pharmacol Sci, 1993. 14(8):303-7.
957. Melo, R.C.C., et al., *CXCR7 is highly expressed in acute lymphoblastic leukemia and potentiates CXCR4 response to CXCL12*. PLoS One, 2014. 9(1):e85926.
958. Levoe, A., et al., *CXCR7 heterodimerizes with CXCR4 and regulates CXCL12-mediated G protein signaling*. Blood, 2009. 113(24):6085-93.
959. Shonberg, J., et al., *Biased agonism at G protein-coupled receptors: the promise and the challenges--a medicinal chemistry perspective*. Med Res Rev, 2014. 34(6):1286-330.
960. Dror, R.O., et al., *Structural basis for modulation of a G-protein-coupled receptor by allosteric drugs*. Nature, 2013. 503(7475):295-9.
961. Onfroy, L., et al., *G protein stoichiometry dictates biased agonism through distinct receptor-G protein partitioning*. Sci Rep, 2017. 7(1):017-07392.
962. Doi, M., et al., *Gpr176 is a Gz-linked orphan G-protein-coupled receptor that sets the pace of circadian behaviour*. Nat Commun, 2016. 7:10583.

963. Yajima, I., et al., *Reduced GNG2 expression levels in mouse malignant melanomas and human melanoma cell lines*. Am J Cancer Res, 2012. 2(3):322-9.
964. Schlegel, N. and J. Waschke, *cAMP with other signaling cues converges on Rac1 to stabilize the endothelial barrier- a signaling pathway compromised in inflammation*. Cell Tissue Res, 2014. 355(3):587-96.
965. McConkey, M., et al., *Cross-talk between protein kinases Czeta and B in cyclic AMP-mediated sodium taurocholate co-transporting polypeptide translocation in hepatocytes*. J Biol Chem, 2004. 279(20):20882-8.
966. Arthur, W.T., L.A. Quilliam, and J.A. Cooper, *Rap1 promotes cell spreading by localizing Rac guanine nucleotide exchange factors*. J Cell Biol, 2004. 167(1):111-22.
967. Noda, Y., et al., *Human homologues of the Caenorhabditis elegans cell polarity protein PAR6 as an adaptor that links the small GTPases Rac and Cdc42 to atypical protein kinase C*. Genes Cells, 2001. 6(2):107-19.
968. Cani, A., et al., *Triple Akt inhibition as a new therapeutic strategy in T-cell acute lymphoblastic leukemia*. Oncotarget, 2015. 6(9):6597-610.
969. Lonetti, A., et al., *Activity of the pan-class I phosphoinositide 3-kinase inhibitor NVP-BKM120 in T-cell acute lymphoblastic leukemia*. Leukemia, 2014. 28(6):1196-206.
970. Laudanna, C., et al., *Motility analysis of pancreatic adenocarcinoma cells reveals a role for the atypical zeta isoform of protein kinase C in cancer cell movement*. Lab Invest, 2003. 83(8):1155-63.
971. Galvez, A.S., et al., *Protein kinase Czeta represses the interleukin-6 promoter and impairs tumorigenesis in vivo*. Mol Cell Biol, 2009. 29(1):104-15.
972. Yao, S., et al., *PRKC-zeta Expression Promotes the Aggressive Phenotype of Human Prostate Cancer Cells and Is a Novel Target for Therapeutic Intervention*. Genes Cancer, 2010. 1(5):444-64.
973. Kim, J.Y., et al., *c-Myc phosphorylation by PKCzeta represses prostate tumorigenesis*. Proc Natl Acad Sci U S A, 2013. 110(16):6418-23.
974. Ma, L., et al., *Control of nutrient stress-induced metabolic reprogramming by PKCzeta in tumorigenesis*. Cell, 2013. 152(3):599-611.
975. Llado, V., et al., *Repression of Intestinal Stem Cell Function and Tumorigenesis through Direct Phosphorylation of beta-Catenin and Yap by PKCzeta*. Cell Rep, 2015. 4(15):007.
976. Facchinetti, V., et al., *The mammalian target of rapamycin complex 2 controls folding and stability of Akt and protein kinase C*. Embo J, 2008. 27(14):1932-43.
977. Robert, V., et al., *Calcium signalling in T-lymphocytes*. Biochimie, 2011. 93(12):2087-2094.

978. Feske, S., *Calcium signalling in lymphocyte activation and disease*. Nat Rev Immunol, 2007. 7(9):690-702.
979. Geijsen, N., et al., *Regulation of p21rac activation in human neutrophils*. Blood, 1999. 94(3):1121-30.
980. Smith, R.J., et al., *Receptor-coupled signal transduction in human polymorphonuclear neutrophils: effects of a novel inhibitor of phospholipase C-dependent processes on cell responsiveness*. J Pharmacol Exp Ther, 1990. 253(2):688-97.
981. Bleasdale, J.E., et al., *Selective inhibition of receptor-coupled phospholipase C-dependent processes in human platelets and polymorphonuclear neutrophils*. J Pharmacol Exp Ther, 1990. 255(2):756-68.
982. Mogami, H., C. Lloyd Mills, and D.V. Gallacher, *Phospholipase C inhibitor, U73122, releases intracellular Ca<sup>2+</sup>, potentiates Ins(1,4,5)P<sub>3</sub>-mediated Ca<sup>2+</sup> release and directly activates ion channels in mouse pancreatic acinar cells*. Biochem J, 1997. 324(Pt 2):645-51.
983. Stewart, T.A., K.T. Yapa, and G.R. Monteith, *Altered calcium signaling in cancer cells*. Biochim Biophys Acta, 2015. 10(11):20.
984. Djafarzadeh, S. and V. Niggli, *Signaling pathways involved in dephosphorylation and localization of the actin-binding protein cofilin in stimulated human neutrophils*. Exp Cell Res, 1997. 236(2):427-35.
985. Porat-Shliom, N., et al., *Multiple roles for the actin cytoskeleton during regulated exocytosis*. Cell Mol Life Sci, 2013. 70(12):2099-121.
986. Isgandarova, S., et al., *Stimulation of actin polymerization by vacuoles via Cdc42p-dependent signaling*. J Biol Chem, 2007. 282(42):30466-75.
987. Matsushima, K., et al., *Purification and characterization of a novel monocyte chemotactic and activating factor produced by a human myelomonocytic cell line*. J Exp Med, 1989. 169(4):1485-90.
988. Tanaka, T., et al., *Monocyte chemoattractant protein-1/CC chemokine ligand 2 enhances apoptotic cell removal by macrophages through Rac1 activation*. Biochem Biophys Res Commun, 2010. 399(4):677-82.
989. Terashima, Y., et al., *Pivotal function for cytoplasmic protein FROUNT in CCR2-mediated monocyte chemotaxis*. Nat Immunol, 2005. 6(8):827-35.
990. Zohar, Y., et al., *CXCL11-dependent induction of FOXP3-negative regulatory T cells suppresses autoimmune encephalomyelitis*. J Clin Invest, 2014. 124(5):2009-22.
991. Colvin, R.A., et al., *Intracellular domains of CXCR3 that mediate CXCL9, CXCL10, and CXCL11 function*. J Biol Chem, 2004. 279(29):30219-27.
992. Karin, N., G. Wildbaum, and M. Thelen, *Biased signaling pathways via CXCR3 control the development and function of CD4<sup>+</sup> T cell subsets*. J Leukoc Biol, 2016. 99(6):857-62.

993. Lasagni, L., et al., *An alternatively spliced variant of CXCR3 mediates the inhibition of endothelial cell growth induced by IP-10, Mig, and I-TAC, and acts as functional receptor for platelet factor 4*. J Exp Med, 2003. 197(11):1537-49.
994. Hermann, P.C., et al., *Distinct populations of cancer stem cells determine tumor growth and metastatic activity in human pancreatic cancer*. Cell Stem Cell, 2007. 1(3):313-23.
995. Williams, K.M., et al., *FLT3 Ligand regulates thymic precursor cells and hematopoietic stem cells through interactions with CXCR4 and the marrow niche*. Exp Hematol, 2017. 52:40-49.
996. Rajagopal, S., et al., *Beta-arrestin- but not G protein-mediated signaling by the "decoy" receptor CXCR7*. Proc Natl Acad Sci U S A, 2010. 107(2):628-32.
997. Rajagopal, S., K. Rajagopal, and R.J. Lefkowitz, *Teaching old receptors new tricks: biasing seven-transmembrane receptors*. Nat Rev Drug Discov, 2010. 9(5):373-86.
998. Ray, P., et al., *Secreted CXCL12 (SDF-1) forms dimers under physiological conditions*. Biochem J, 2012. 442(2):433-42.
999. Berahovich, R.D., et al., *CXCR7 protein is not expressed on human or mouse leukocytes*. J Immunol, 2010. 185(9):5130-9.
1000. Berahovich, R.D., M.E. Penfold, and T.J. Schall, *Nonspecific CXCR7 antibodies*. Immunol Lett. 2010. 133(2):112-4.
1001. Humpert, M.L., et al., *Complementary methods provide evidence for the expression of CXCR7 on human B cells*. Proteomics, 2012. 12(12):1938-48.
1002. Lis, R., et al., *Conversion of adult endothelium to immunocompetent haematopoietic stem cells*. Nature, 2017. 545(7655):439-445.
1003. Naumann, U., et al., *CXCR7 functions as a scavenger for CXCL12 and CXCL11*. PLoS One, 2010. 5(2):e9175.
1004. Meuter, S. and B. Moser, *Constitutive expression of CXCL14 in healthy human and murine epithelial tissues*. Cytokine, 2008. 44(2):248-55.
1005. Tanegashima, K., et al., *CXCL14 is a natural inhibitor of the CXCL12-CXCR4 signaling axis*. FEBS Lett, 2013. 587(12):1731-5.
1006. Otte, M., et al., *CXCL14 is no direct modulator of CXCR4*. FEBS Lett, 2014. 588(24):4769-75.
1007. Pelicano, H., et al., *Mitochondrial dysfunction and reactive oxygen species imbalance promote breast cancer cell motility through a CXCL14-mediated mechanism*. Cancer Res, 2009. 69(6):2375-83.
1008. Tripathi, A., et al., *CXC chemokine receptor 4 signaling upon co-activation with stromal cell-derived factor-1alpha and ubiquitin*. Cytokine, 2014. 65(2):121-5.

1009. D'Huys, T., et al., *CXCR7/ACKR3-targeting ligands interfere with X7 HIV-1 and HIV-2 entry and replication in human host cells*. Heliyon, 2018. 4(3):e00557.
1010. Zabel, B.A., et al., *Elucidation of CXCR7-mediated signaling events and inhibition of CXCR4-mediated tumor cell transendothelial migration by CXCR7 ligands*. J Immunol, 2009. 183(5):3204-11.
1011. Sierro, F., et al., *Disrupted cardiac development but normal hematopoiesis in mice deficient in the second CXCL12/SDF-1 receptor, CXCR7*. Proc Natl Acad Sci U S A, 2007. 104(37):14759-64.
1012. Lagane, B., et al., *CXCR4 dimerization and beta-arrestin-mediated signaling account for the enhanced chemotaxis to CXCL12 in WHIM syndrome*. Blood, 2008. 112(1):34-44.
1013. Spaks, A., *Role of CXC group chemokines in lung cancer development and progression*. J Thorac Dis, 2017. 9(Suppl 3):S164-S171.
1014. Kenakin, T. and A. Christopoulos, *Signalling bias in new drug discovery: detection, quantification and therapeutic impact*. Nat Rev Drug Discov, 2013. 12(3):205-16.
1015. Gahbauer, S., K. Pluhackova, and R.A. Bockmann, *Closely related, yet unique: Distinct homo- and heterodimerization patterns of G protein coupled chemokine receptors and their fine-tuning by cholesterol*. PLoS Comput Biol, 2018. 14(3):e1006062.
1016. Bazzani, L., et al., *PGE2 mediates EGFR internalization and nuclear translocation via caveolin endocytosis promoting its transcriptional activity and proliferation in human NSCLC cells*. Oncotarget, 2018. 9(19):14939-14958.
1017. Roussos, E.T., J.S. Condeelis, and A. Patsialou, *Chemotaxis in cancer*. Nat Rev Cancer, 2011. 11(8):573-87.
1018. Piazuelo, E. and A. Lanas, *NSAIDS and gastrointestinal cancer*. Prostaglandins Other Lipid Mediat, 2015. 120:91-6.
1019. Wysong, A., et al., *Non-melanoma skin cancer and NSAID use in women with a history of skin cancer in the Women's Health Initiative*. Prev Med, 2014. 69:8-12.
1020. Kuo, C.N., et al., *Association between Nonsteroidal Anti-inflammatory Drugs and Colorectal Cancer: a Population-based Case-control Study*. Cancer Epidemiol Biomarkers Prev, 2018. 25:1055-9965.
1021. Maqbool, M. and N. Hoda, *GSK3 Inhibitors in the Therapeutic Development of Diabetes, Cancer and Neurodegeneration: Past, Present and Future*. Curr Pharm Des, 2017. 23(29): p. 4332-4350.
1022. Gough, D.J., et al., *Mitochondrial STAT3 supports Ras-dependent oncogenic transformation*. Science (New York), 2009. 324(5935):1713-1716.
1023. Meier, J.A. and A.C. Lerner, *Toward a new STATE: the role of STATs in mitochondrial function*. Semin Immunol, 2014. 26(1):20-28.

## **Appendix 1 - List of Tables**

### ***Chapter 2: Materials and Methodology***

- 2.1: Small molecule Inhibitors
- 2.2: Small molecule inhibitors and receptor antagonists
- 2.3: Peptide inhibitors
- 2.4: Chemokines
- 2.5: Bacterial Plasmids
- 2.6: Primary Antibodies
- 2.7: Secondary Antibodies
- 2.8: siRNAs
- 2.9: SMARTpool siRNAs
- 2.10: Imaging Stains
- 2.11: Activation Kits
- 2.12: Cell-lines
- 2.13: Cell Culture Mediums

### ***Chapter 3: Exploring the intricacies of dynamin function in malignant cell migration***

- 3.1: Small molecule inhibitors of dynamin, their target region/s and IC<sub>50</sub>'s.

## **Appendix 2 - List of Figures**

### ***Chapter 1: Introduction***

- 1.1: Differences between normal and cancerous cells.
- 1.2: Examples of (A) CC and (B) CXC chemokine receptors and their ligands.
- 1.3: Immune cells can be recruited into the tumour microenvironment by chemokines
- 1.4: CXCR4/CXCL12 signalling supports tumour cell spread
- 1.5: Basic goblet structure of the CXCR4 receptor.
- 1.6: Structures of CXCR4 inhibitors AMD3100 and AMD11070.
- 1.7: CXCR4 sequence with key binding residues for CXCL12.
- 1.8: Dynamics of dynamin and dynamin-like proteins (DLPs) in a migrating cell.
- 1.9: Regions of the crystal structure of a dynamin dimer.
- 1.10: Structural elements of Dynamin and Dynamin-Like Proteins.
- 1.11: Mechanism of dynamin-mediated vesicle and membrane fission
- 1.12: Dynamin contributes to both clathrin-dependent and endophilin-mediated endocytosis.
- 1.13: Drp-1 influences mitochondria fission/fusion dynamics during the cell cycle.
- 1.14: PKC isoenzymes, domains and activators.
- 1.15: PKC isoenzymes interact with scaffolding proteins.
- 1.16: Human Rac1 sequence.
- 1.17: Some of the many signalling pathways producing LIMK activation.
- 1.18: Signalling resulting in phospholipid PIP<sub>2</sub> sequestering cofilin.
- 1.19: Modes of action of paracetamol, ibuprofen, naproxen and celecoxib.

### ***Chapter 3: Exploring the intricacies of dynamin function in malignant cell migration***

- 3.1: Conformation of CXCR4 expression.
- 3.2: CCR5 and CXCR4 Immunofluorescence.
- 3.3: Conformation of CCR5 expression.
- 3.4: J113863 and Maraviroc in CCL3-chemotaxis.
- 3.5: Immunofluorescent staining of Dynamin-2.



- 3.6: Dynamin-2 siRNA knockdown in CCL3- and CXCL12-chemotaxis.
- 3.7: Dynamin-2 siRNA knockdown in CCL3 and CXCL12 wound-healing.
- 3.8: Dynasore cytotoxicity assays.
- 3.9: Dynasore in Phalloidin actin stains.
- 3.10: Dynasore 80  $\mu$ M in CCL3- and CXCL12-chemotaxis.
- 3.11: Dynasore 60  $\mu$ M in CCL3- and CXCL12-chemotaxis.
- 3.12: Dynasore 40  $\mu$ M in CCL3- and CXCL12-chemotaxis.
- 3.13: Dynasore in Fura2 calcium assays.
- 3.14: Dyngo-4a in CCL3- and CXCL12-chemotaxis.
- 3.15: Dyngo-4a cytotoxicity assays.
- 3.16: MitMAB cytotoxicity assays.
- 3.17: MitMAB in CCL3- and CXCL12-chemotaxis.
- 3.18: OcTMAB in CCL3- and CXCL12-chemotaxis.
- 3.19: OcTMAB cytotoxicity assays.
- 3.20: Rhododyn-C10<sup>TM</sup> in CCL3- and CXCL12-chemotaxis.
- 3.21: RTIL-13 in CCL3- and CXCL12-chemotaxis.
- 3.22: RTIL-13 in Phalloidin actin stains.
- 3.23: RTIL-13 cytotoxicity assays.
- 3.24: Pyrimidyn-7<sup>TM</sup> cytotoxicity assays
- 3.25: Pyrimidyn-7<sup>TM</sup> in CCL3- and CXCL12-chemotaxis.
- 3.26: Dynasore interrupts cytokinesis.
- 3.27: Dynasore and RTIL-13 interrupt cytokinesis.
- 3.28A: Caveolae invaginations and CCR5 signalling
- 3.28B: Clathrin-mediated endocytosis and CXCR4 endocytosis
- 3.29: Dynamin domains in CCL3- and CXCL12-chemotaxis.

***Chapter 4: PKC and other key signalling proteins in cell migration towards CXCL12 and CCL3 in leukemic cells compared to breast cancer cells.***

- 4.1: PKC and other key signalling proteins involved in chemotaxis and metastasis.

- 4.2: PKC $\delta$  siRNA knockdown and Rottlerin in CCL3- and CXCL12-chemokinesis.
- 4.3: Rottlerin in cAMP and Fura2 calcium assays.
- 4.4: Staurosporine in CXCL12-chemotaxis, cAMP and Fura2 calcium assays.
- 4.5: GF109203X cytotoxicity assays.
- 4.6: GF109203X in CXCL12-chemotaxis, cAMP and Fura2 calcium assays.
- 4.7: PKC $\alpha$  and PKC $\epsilon$  siRNA knockdown in CXCL12-chemotaxis.
- 4.8: PKC $\alpha$  and PKC $\epsilon$  siRNA knockdown in CCL3- and CXCL12 wound-healing.
- 4.9: Western Blot confirming PKC $\alpha$  siRNA knockdown.
- 4.10: CID755673 in CXCL12-chemotaxis and cytotoxicity assays.
- 4.11: CID755673 in CCL3- and CXCL12-chemotaxis and Fura2 calcium assays.
- 4.12: CID75673 cAMP assays
- 4.13: FH535 in CCL3- and CXCL12-chemotaxis and cytotoxicity assays.
- 4.14: GF109203X, CID755673, Staurosporine and Rottlerin Fura2 calcium assays.
- 4.15: Bosutinib in CCL3- and CXCL12-chemotaxis.
- 4.16: Bosutinib cytotoxicity assays.
- 4.17: Bosutinib in cAMP and calcium assays plus Phalloidin actin stains.
- 4.18: Src siRNA knockdown in CCL3- and CXCL12-chemotaxis.
- 4.19: Src siRNA knockdown in CCL3- and CXCL12 wound-healing.
- 4.20: Western Blot confirming Src siRNA knockdown.
- 4.21: Inhibitors and feedback affecting the mitogenic Ras/Raf/MEK/ERK and ROCK signalling pathways.
- 4.22: L779450 in CCL3- and CXCL12-chemotaxis.
- 4.23: L779450 cAMP and cytotoxicity assays.
- 4.24: L779450 in Fura2 calcium assays.
- 4.25: SB203580 cytotoxicity assays.
- 4.26: PD98059 cytotoxicity assays.
- 4.27: SB203580 in CCL3- and CXCL12-chemotaxis.
- 4.28: PD98059 in CCL3- and CXCL12-chemotaxis and cAMP assays.

- 4.29: PD98059 in Fura2 calcium assays
- 4.30: L779450 and/or PD98059 in CCL3- and CXCL12-chemotaxis.
- 4.31: L779450 and/or SL327 in CCL3- and CXCL12-chemotaxis.
- 4.32: L779450 and/or Y27632 in CCL3- and CXCL12-chemotaxis.
- 4.33: L779450 and/or LY294002 in CCL3- and CXCL12-chemotaxis
- 4.34: AS605240 and/or LY2940025 in CCL3- and CXCL12-chemotaxis
- 4.35: Bosutinib and/or L779450 in CXCL12-chemotaxis.
- 4.36: Many proteins activate or inactivate GSK3 including PKC.
- 4.37: Effects of ROCK inhibition on  $\beta$ -catenin signalling.
- 4.38: PKC signalling through GSK3, Slingshot and cofilin.

***Chapter 5: CXCL12 and CCL3 chemokine-induced migration can involve cofilin phosphorylation, Pi3K and  $\beta$ -arrestins in leukaemic and breast cancer cells.***

- 5.1: Summary of actin remodelling and the involvement of cofilin.
- 5.2: Western Blot, CXCL12 effect on cofilin phosphorylation in Jurkat.
- 5.3: Cofilin siRNA knockdown in CCL3- and CXCL12 wound-healing with Western Blot and immunofluorescence.
- 5.4: Western Blot, CC and CXC chemokines effect on cofilin phosphorylation in THP-1.
- 5.5: Chemotactic responses to CC and CXC chemokines in THP-1.
- 5.6: Chemotactic dose-responses to CXCL12 in Jurkat.
- 5.7: Chemotactic responses to combined CC and CXC chemokines.
- 5.8: Chemotactic responses to CC and CXC chemokines following 12G5 or CXCL11.
- 5.9: Fura2 calcium CXCL12 responses following CXCL11.
- 5.10: Gallein cytotoxicity assay and in CCL3- and CXCL12-chemotaxis.
- 5.11: Western Blot cofilin phosphorylation following Gallein.
- 5.12: AS605240 and LY294002 in THP-1 CCL3- and CXCL12-chemotaxis
- 5.13: LY294002 and AS605240 in Jurkat CXCL12-chemotaxis.
- 5.14: AS605240 and LY294002 cytotoxicity assays.
- 5.15: Pi3K siRNA knockdown in CXCL12- and CCL3-chemotaxis.

5.16: Pi3K siRNA knockdown in CXCL12- and CCL3 wound-healing.

5.17: Western blot confirming Pi3K siRNA knockdown.

5.18: Western Blot, THP-1 cofilin phosphorylation following LY294002 or AS605240.

5.19: Western Blot, Jurkat cofilin phosphorylation following LY294002 or AS605240.

5.20: AS605240 and LY294002 in Phalloidin actin stains.

5.21:  $\beta$ -ARK-1 in CCL3- and CXCL12-chemotaxis and Phalloidin actin stain.

5.22:  $\beta$ -ARK-1 cytotoxicity assays.

5.23: Ipyrimidine in CCL3- and CXCL12-chemotaxis.

5.24: Ipyrimidine cytotoxicity assays.

5.25: Ipyrimidine chemical structure.

5.26: Western blot, cofilin phosphorylation following Ipyrimidine.

5.27: Ipyrimidine in Phalloidin actin stains.

5.28: Arrestin-2 immunofluorescent stain.

5.29:  $\beta$ -arrestin CHO.CCR5 transfects.

5.30:  $\beta$ -arrestin MCF7 transfects.

5.31: Arrestin-3 and Arrestin-2 MCF7 transfects.

5.32: Transfection efficiency was checked using immunofluorescence imaging

5.33: Arrestin-2 and arrestin-3 transfects in CCL3- and CXCL12-chemotaxis.

5.34: Arrestin-2 and arrestin-3 transfects in CCL3- and CXCL12 wound-healing.

5.35: PF562271 in actin filament stain and cytotoxicity assays.

5.36: FAK Inhibitor-2 and PF562271 chemical structures.

5.37: FAK inhibitor 2 in CCL3- and CXCL12-chemotaxis.

5.38: PF562271 in CCL3 and CXCL12 chemotaxis.

5.39: PF562271 in Fura2 Calcium Assay.

5.40: Western blot, cofilin phosphorylation following PF562271.

5.41: Nocodazole in CCL3- and CXCL12-chemotaxis.

5.42: Western blot, cofilin phosphorylation following Y27632.

- 5.43: Y27632 in Jurkat CXCL12 chemotaxis and cytotoxicity assays.
- 5.44: Y27632 in THP-1 CCL3- and CXCL12-chemotaxis and cytotoxicity assays
- 5.45: Western blot, cofilin phosphorylation following SL327.
- 5.46: SL327 cytotoxicity assays.
- 5.47: SL327 in CCL3- and CXCL12-chemotaxis.
- 5.48: Western Blot THP-1, cofilin phosphorylation following Bosutinib.
- 5.49: Western Blot Jurkat, cofilin phosphorylation following Bosutinib, Y27632, or PF562291.
- 5.50: Major signalling pathways that modulate cofilin phosphorylation with inhibitors and protein targets.
- 5.51: P13K and phosphatidylinositol-3,4,5-triphosphate signalling.

***Chapter 6: JAK2 and STAT3 play role in chemokine induced chemotaxis and cofilin phosphorylation***

- 6.1: The effects of JAK signalling, through Rho GTPases, and Forskolin on cofilin phosphorylation.
- 6.2: JAK2/STAT3 signalling from CXCR4, and targets of inhibitors used.
- 6.3: HBC, 5,15 DPP and WP1066 cytotoxicity assays.
- 6.4: HBC, 5,15 DPP and WP1066 Phalloidin actin stains.
- 6.5: HBC, 5,15 DPP and WP1066 in THP-1 CCL2- and CXCL12-chemotaxis
- 6.6: HBC, 5,15 DPP and WP1066 in CCL2- and CXCL12 wound-healing.
- 6.7: HBC, 5,15 DPP and WP1066 in Jurkat CXCL12-chemotaxis.
- 6.8: HBC, 5,15 DPP and WP1066 in Fura2 calcium assays.
- 6.9: HBC, 5,15 DPP and WP1066 in Fura2 AUC calcium assays.
- 6.10: Forskolin cytotoxicity assays.
- 6.11: H89 cytotoxicity assays.
- 6.12: H89 in chemotaxis to CCL3- and CXCL12.
- 6.13: H89 and/or Forskolin in CCL3- and CXCL12-chemotaxis.
- 6.14: Forskolin in CCL3- and CXCL12 wound-healing.
- 6.15: H89 in CCL3- and CXCL12 wound-healing.

- 6.16: HBC, 5,15 DPP and WP1066 in cAMP assays.
- 6.17: Forskolin and H89 in Phalloidin CHO.CCR5 actin stains.
- 6.18: Forskolin, H89 and Y27632 in Phalloidin MCF7 actin stains.
- 6.19: Y27632 in Phalloidin PC3 actin stains.
- 6.20: Western blot, cofilin phosphorylation following Forskolin.
- 6.21: Western blot, cofilin phosphorylation following HBC, 5,15-DPP or WP1066..
- 6.22: Western blot, STAT3 phosphorylation and cofilin phosphorylation following WP1066, 5,15-DPP or HBC.
- 6.23: ELIZA, STAT3 phosphorylation following 5,15-DPP or HBC.
- 6.24: Forskolin may produce cofilin phosphorylation in THP-1 by inhibiting PP2.
- 6.25: Signalling linking STAT3, JAK2 and cofilin phosphorylation.

***Chapter 7: Direct and indirect effects of NSAIDs in chemotactic metastasis***

- 7.1: How NSAIDs interact with signalling pathways influencing cofilin phosphorylation.
- 7.2: Aspirin in CCL3- and CXCL12-chemotaxis.
- 7.3: Aspirin cytotoxicity assays.
- 7.4: Naproxen cytotoxicity assays.
- 7.5: Naproxen in CCL3- and CXCL12-chemotaxis.
- 7.6: Naproxen in CCL3- and CXCL12 wound-healing and cytotoxicity assays.
- 7.7: Aspirin and Naproxen in Phalloidin actin stains.
- 7.8: Ibuprofen cytotoxicity assays.
- 7.9: Ibuprofen in CCL3- and CXCL12-chemotaxis.
- 7.10: Ibuprofen in CCL3- and CXCL12 wound-healing and cytotoxicity assays.
- 7.11: Ibuprofen in Phalloidin actin stains.
- 7.12: Celecoxib in CCL3- and CXCL12 MCF7 wound-healing and cytotoxicity assays.
- 7.13: Celecoxib THP-1 and Jurkat cytotoxicity assays.
- 7.14: Celecoxib in CCL3- and CXCL12-chemotaxis.
- 7.15: Celecoxib in Phalloidin actin stains.
- 7.16: Paracetamol cytotoxicity assays.

- 7.17: Paracetamol in CCL3- and CXCL12-chemotaxis.
- 7.18: Paracetamol in Fura2 calcium assays.
- 7.19: Ibuprofen and Celecoxib in Fura2 calcium assays.
- 7.20: Aspirin and Naproxen in Fura2 calcium assays.
- 7.21: Celecoxib, Ibuprofen and Paracetamol in cAMP assays.
- 7.22: Western blot, cofilin phosphorylation following Celecoxib, Aspirin, Ibuprofen, Paracetamol and Naproxen.
- 7.23: Ibuprofen's possible off target effect, and links to cofilin phosphorylation.
- 7.24: Phospholipid hydrolysis pathway to the production of prostaglandins.

***Chapter 8: Rac1 mediates chemotaxis to CXCL12, but not CCL3, in leukaemic and breast cancer cell-lines, and Rac1 GEF inhibitor NSC23766 may have off-target effects on CXCR4/CXCR7 axis.***

- 8.1: CXCL12-induced signalling can be modified by CXCR4 inhibition.
- 8.2: NSC23766 in CCL3- and CXCL12-chemotaxis.
- 8.3: AMD3100 in CCL3- and CXCL12-chemotaxis.
- 8.4: NSC23766 cytotoxicity assays.
- 8.5: W56 and F56 in CCL3- and CXCL12-chemotaxis.
- 8.6: NSC23766, W56 and F56 in CCL3- and CXCL12 wound-healing.
- 8.7: Western Blot, Rac1 activation pull down assay following NSC23766, ATI2341 and AMD3100.
- 8.8: NSC23766 dose-dependence in CXCL12-chemotaxis.
- 8.9: NSC23766 concentration-response curve towards CXCL12 (using data from figure 8.8).
- 8.10: NSC23766 and 12G5 competition in CXCL12-chemotaxis.
- 8.11: ATI2341 chemical structure and combination with NSC23766 or AMD3100 in CXCL12-chemotaxis.
- 8.12: ATI2341, AMD3100 and/or NSC23766 concentration-dependent effect on CXCL12-chemotaxis.
- 8.13: Flow cytometry, CXCR4 expression following NSC23766, F56 or W56.
- 8.14: Flow cytometry, CXCR4 expression following NSC23766, AMD3100 and ATI2341.

- 8.15: Flow cytometry, CXCR4 expression following EHT1864 and EHT1864 chemical structure.
- 8.16: Flow cytometry, CXCR4 expression following Sodium Azide or Sucrose, then NSC23766 and AMD3100.
- 8.17: NSC23766, AMD3100, ATI2341 and H89 in cAMP assays.
- 8.18: PKC $\zeta$  siRNA knockdown in CXCL12-chemotaxis and CCL3- and CXCL12 wound-healing assays.
- 8.19: Western blot PKC zeta expression in MCF7 following PKC $\zeta$  siRNA 50 nM.
- 8.20: NSC23766 in THP-1 Fura2 calcium assays.
- 8.21: NSC23766 in Jurkat and MCF7 Fura2 calcium assays.
- 8.22: NSC23766 CXCL12-dose dependent Fura2 calcium assay.
- 8.23: NSC23766, AMD3100 and ATI2341 in Fura2 calcium assays.
- 8.24: U73122 in CCL3- and CXCL12-chemotaxis.
- 8.25: U73122 in Fura2 calcium assays.
- 8.26: U73122 in cAMP assay.
- 8.27: ZCL278 in CCL3- and CXCL12-chemotaxis.
- 8.28: NSC23766, ZCL278, W56 or F56 in Phalloidin actin stains.
- 8.29: Western blot, cofilin phosphorylation following NSC23766, W56, and F56.
- 8.30: NSC23766, W56 or F56 in CCL2-, CXCL9-, and CXCL11-chemotaxis.
- 8.31: CXCL14 in CXCL12-chemotaxis.
- 8.32: CXCL14 in Fura2 calcium assays.
- 8.33: Flow cytometry, CXCR4 expression following NSC23766, W56 and CXCL14.
- 8.34: NSC23766 chemical structure.
- 8.35: Schematic representation of cAMP, PKC $\zeta$ , Rac1 and CXCR4 expression feedback loop.
- 8.36: Involvement of Rac1, PLC, PKC and SSH1 in GPCR calcium signalling.



## Appendix 3 - List of Abbreviations

**Table A3** – Abbreviations

Abbreviation	Full name
AA	Arachidonic acid
AC	Adenylyl Cyclase
ACKR3	Atypical chemokine receptor 3 aka CXCR7
ACKRs	Atypical chemokine receptors
ADP	Adenosine diphosphate
Aip1	Actin-interacting protein 1
AKAPs	A-kinase-anchoring proteins
Akt	AKT serine/threonine kinase 1 aka AKT and Protein kinase B ( <b>PKB</b> ),
ANOVA	Analysis of Variance
AP1, AP2	Adaptor Protein Complex -1, Adaptor Protein Complex-2
APL	Acute Promyelocytic Leukaemia
APPL1	Adaptor protein, phosphotyrosine interacting with PH domain and leucine zipper 1
ARP2/3	Actin-related protein 2/3
Arf6	ADP-ribosylation factor 6
ATF2	Activating Transcription Factor 2
ATP	Adenosine triphosphate
AUC	Area Under Curve
BAR	Bin-amphiphysin-Rvs proteins
β-ARK	Beta-adrenergic receptor kinase
BCR-ABL	BCR-ABL oncogene aka Philadelphia chromosome causing CML
BRAF	serine/threonine-protein kinase B-Raf
BSE	Bundle Signalling Element
cAMP	Cyclic adenosine 3',5'-monophosphate
CAP	Adenylyl cyclase-associated protein
CCL2	C-C Motif Chemokine Ligand 2 aka MCP-1
CCL3	C-C Motif Chemokine Ligand 3 aka MIP-1α
CCR1	C-C motif chemokine receptor 1 aka MIP-1α receptor
CCR2	C-C chemokine receptor type 2 aka CD192
CCR5	C-C chemokine receptor type 5 aka CD195

Abbreviation	Full name
CD4 <sup>+</sup>	Cells expressing surface protein Cluster of Differentiation 4
CD8 <sup>+</sup>	Cells expressing surface protein Cluster of Differentiation 8
CDC25A	cell division cycle 25 homolog A aka M-phase inducer phosphatase 1
Cdc42	Cell division control protein 42
CDK1, CDK2	Cyclin-dependent kinase-1, Cyclin-dependent kinase-2
CHO.CCR5	Chinese Hamster Ovary Cells transfected with CCR5 receptor
CLTA-4	Cytotoxic T-Lymphocyte Associated Antigen-1
CML	Chronic myelogenous Leukemia
COX1 & COX2	Cyclooxygenase-1, cyclooxygenase-2
c-Src	Proto-oncogene tyrosine-protein kinase Src aka proto-oncogene c-Src
CXCL10	C-X-C motif chemokine ligand 10 aka IP-10
CXCL11	C-X-C motif chemokine ligand 11 aka ITAC
CXCL12	C-X-C Motif Chemokine Ligand 12 aka Stromal Cell-Derived Factor 1
CXCL9	C-X-C Motif Chemokine Ligand 9 aka MIG
CXCR3	C-X-C Motif Chemokine Receptor 3 aka CD183
CXCR4	C-X-C Motif Chemokine Receptor 4
CXCR7	Atypical chemokine receptor 3 aka ACKR3
DAG	Diacylglycerol
DBL family	Diffuse B-cell lymphoma family of guanine nucleotide exchange factors
DHR1	DOCK homology region 1
DLP	Dynamin-Like Proteins
DMSO	Dimethyl sulfoxide (solvent)
Drp-1	Dynamin related protein 1
DRY motif	Asp-Arg-Tyr
E2F2	E2F Transcription Factor 2
EC <sub>50</sub>	Half maximal effective concentration, measures a drug's potency
ECL	Extracellular loop
ECM	Extracellular matrix
EEA1	Early Endosome Antigen 1
EGFR	Epidermal Growth Factor Receptor
EMT	Epithelial mesenchymal transition

Abbreviation	Full name
ER	Endoplasmic reticulum
ERK	Extracellular signal-regulated kinase 2 aka MAPK
FAAH	Fatty acid amide hydrolase
FACS	Fluorescence-activated cell sorting
FAK	Focal Adhesion Kinase
FITC	Fluorescein isothiocyanate
FKHR	Forkhead box O1 transcription factor
FOXO3	Forkhead box protein O3 transcription factor
FOXO4	Forkhead box protein O4 transcription factor
GAPs	GTPase Activating Proteins
G-CSF	Granulocyte-colony Stimulating Factor
G-domain	guanosine triphosphate-binding domain
GDP	guanosine diphosphate
GED	GTPase Effector Domain
GEF	Guanine nucleotide Exchange Factor
GOF	Gain of function
GPCR	G-protein coupled receptor
Grb2	Growth factor receptor-bound protein-2
GRK	G-protein receptor Kinase aka GPCR kinases
GSK3 $\beta$	Glycogen synthase kinase 3 beta
GTP	guanosine triphosphate
GTPase	Enzyme that hydrolyses guanosine triphosphate
G $\alpha$	heterotrimeric guanine nucleotide-binding proteins alpha subunit
G $\beta$	heterotrimeric guanine nucleotide-binding protein beta subunit
G $\gamma$	heterotrimeric guanine nucleotide-binding protein gamma subunit
HBC	Hexabromocyclohexane
HIF1	Hypoxia-inducible factor 1
HIV	Human Immunodeficiency Virus
HSP	Heat Shock Protein
IBMX	3-Isobutyl-1-methylxanthine
IC <sub>50</sub>	The half maximal inhibitory concentration
ICL	Intracellular loop
ICL1	Intracellular Loop One

Abbreviation	Full name
IFN $\gamma$	Interferon gamma
IP	Immunoprecipitation
IP-10	Interferon gamma-induced protein 10 aka CXCL10
IP <sub>3</sub>	Inositol 1,4,5-triphosphatase
ITAC	Interferon Inducible T-cell $\alpha$ Chemokine aka CXCL11
JAK2	Janus Kinase 2
JNK	Jun amino-terminal kinases (MAPK family member)
kDa	Kilo Dalton
LIMK	LIM Domain Kinase
LOF	Loss of function
MAPK	Mitogen-Activated Protein Kinase
MCF7	Michigan Cancer Foundation-7 cell line
MHC	Major Histocompatibility Complex
MCP-1	monocyte chemoattractant protein 1 aka CCL2
MEK	Mitogen-activated protein kinase kinase aka MAP2K, MAPKK
Mfn	Mitofusin
MIF	Macrophage migration inhibitory factor
MIG	Monokine induced by gamma interferon aka CXCL9
MIP-1 $\alpha$	Macrophage Inflammatory Protein 1 alpha aka CCL3
MIP-1 $\beta$	Macrophage inflammatory protein 1-beta aka CCL4
MiTMAB	Myristyltrimethylammonium Bromide
MLS	Mitochondrial Leader Sequence
mM	Millimolar concentration
MMP	Matrix metalloproteases
mTORC2 / mTOR	Mammalian Target of Rapamycin Complex 2
MTS Assay	3-(4,5-dimethylthiazol-2-yl)-5-(3-carboxymethoxyphenyl)-2-(4-sulfophenyl)-2H-tetrazolium Cell Proliferation Assay
NADPH	Nicotinamide Adenine Dinucleotide Phosphate + Hydrogen
NFAT	Nuclear Factor of Activated T-cells
NF $\kappa$ B	Nuclear factor kappaB
NK cells	Natural Killer cells
nM	Nano molar concentration
NMDA receptors	N-methyl-D-aspartate receptor

Abbreviation	Full name
NMR	Nuclear Magnetic Resonance
NO	Nitric oxide
NRAS	Neuroblastoma RAS Viral (V-Ras) Oncogene Homolog aka NRAS Proto-Oncogene, GTPase
NSAIDs	Non–Steroidal Anti–Inflammatory Drugs
Nuclear protein HMGB1	Nuclear protein High mobility group box 1
OctMAB	Octadecyltrimethyl ammonium bromide
OPA1	Optic Atrophy protein 1
ORAL1	Calcium release-activated calcium channel protein 1
p38 MAPK	p38 Mitogen activated protein kinase
PAK	P21-activated kinases
PAK	P21-activated kinase
Par3	Partition Defective Protein 3
PAX3	Paired box (PAX) 3 transcription factor
PC3	Human prostate cancer cell-line 3
PCNA	Proliferating cell nuclear antigen
PD-1	Programmed Death Protein 1
pDC cells	Plasmacytoid dendritic cell
PDK-1 / PDPK1	3-phosphoinositide-dependent protein kinase 1
PD-L1	Programmed death-ligand 1
PGE <sub>2</sub>	Prostaglandin E2
PGH <sub>2</sub> , PGE <sub>2</sub> , PGF <sub>2</sub>	Prostaglandin H2, Prostaglandin E2, Prostaglandin F2
PGI <sub>2</sub>	Prostacyclin
PH domain	Pleckstrin homology <b>domain</b>
Pi3K	Phosphoinositide-3 kinase
PIP <sub>2</sub>	Phosphatidylinositol 4,5-bisphosphate
PIP <sub>3</sub>	Phosphatidylinositol (3,4,5)-trisphosphate
PKA	Protein Kinase A
PKC	Protein Kinase C
PKD aka PKC $\mu$	Protein Kinase D aka Protein Kinase C Mu
PLC $\beta$	Phospholipase-beta
PLC $\gamma$	Phospholipase C gamma

Abbreviation	Full name
PMA	Phorbol 12-myristate 13-acetate
PP2A	Protein Phosphatase 2A
PPAR $\beta$	Peroxisome-Proliferator-Activated Receptor beta
PRD	Proline-Rich Domain
PTD	Predicted Transmembrane Domain
PtdIns(3,4,5)P <sub>3</sub> aka PIP <sub>3</sub>	Phosphatidylinositol (3,4,5)-trisphosphate
PtdIns(4,5)P <sub>2</sub> aka PIP <sub>2</sub>	Phosphatidylinositol 4,5-bisphosphate
PTEN	Phosphatase and tensin homolog (a tumour suppressor)
PTX	Pertussis toxin
Rac1	Ras-related C3 botulinum toxin substrate 1,
RACKs	Receptors for activated C-kinase
RANTES	Regulated on activation, normal T cell expressed and secreted (CCL5)
Ras	Rat Sarcoma gene
RH	Regulator of G-protein signalling homology
Rho	Ras homolog family member
Rho GDIs	Rho-specific Guanine Nucleotide Dissociation Inhibitors
ROCC	Receptor operated calcium channels
ROS	Reactive oxygen species
RTIL	Room Temperature Ionic Liquid
SAPK	Stress-activated protein kinases/( MAPK family member)
SDF-1	Stromal Cell-Derived Factor 1 aka CXCL12
SEM	Standard Error of the Mean
SERCAs	Sarco/endoplasmic reticulum Ca <sup>2+</sup> ATPase
SHIP1	SH2 domain containing inositol 5-phosphatase
SIM1	Stromal interaction molecule 1
siRNA	Small interfering Ribonucleic Acid
SOCC	Store Operated Calcium Channels
SOS	Son of Sevenless
SPT	Serine Palmitoyltransferase
SSH	Slingshot
STAT3	Signal transducer and activator of transcription 3
TAM	Tumour associated macrophages
TGF $\alpha$	Transforming Growth Factor alpha

Abbreviation	Full name
THP-1	Human monocytic cell line from acute monocytic leukaemia
Tiam1	T cell lymphoma invasion and metastasis 1
TIMP-1	Tissue inhibitor of metalloproteinase-1
TM3	Transmembrane helix 3
TNF $\alpha$	Tumor Necrosis Factor- $\alpha$
T-reg cells	Regulatory T cells aka Suppressor T cells
Trion	Trio N-terminal DH-PH domains, a Guanine nucleotide Exchange Factor
TRPM2	Transient Receptor Potential Melanostatine-2
TRPs	Transient receptor potential channels
TRPV1	Transient receptor potential vanilloid subtype 1
TXA2, TXB2	Thromboxane A2, Thromboxane B2.
UV	Ultra violet
VEGF	Vascular endothelial growth factor
VGCC	Voltage Gated Calcium Channels
WASp	Wiskott-Aldrich syndrome <b>protein</b> (actin-regulatory <b>protein</b> )
WAVE	WASp family Verprolin-homologous <b>protein</b> (actin-regulatory <b>protein</b> )
WHIM Syndrome	Warts Hypoammaglobulinemia Immunodeficiency and Myelokathexis Syndrome
$\mu$ M	Micromolar concentration
$^{\circ}$ C	Degrees centigrade
15-PGDH	15-Hydroxyprostaglandin dehydrogenase
2D	Two-dimensional
3D	Three-dimensional
5,15-DPP	5,15-Diphenylporphyrin

## Appendix 4 - Small Molecule Inhibitor and Receptor Antagonist structures

**Table A4** - Small Molecule Inhibitor and Receptor Antagonist structures

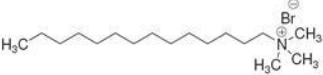

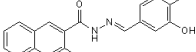
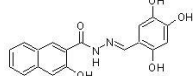
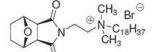
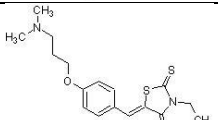
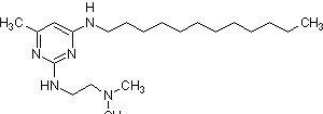
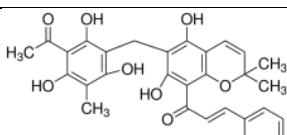
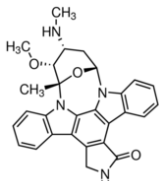
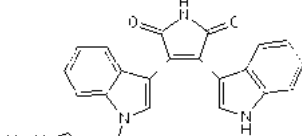
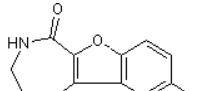
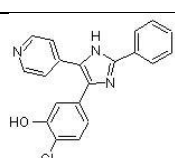
Small molecule Inhibitor	Structure
<b>Dynamin Inhibitors</b>	
MitMAB	
OctMAB	
Dynasore	
Dyngo 4a	
RTIL-13™	
RhodadynC10™	
Pyrimidyn-7™	
<b>PKC Inhibitors</b>	
Rottlerin	
Staurosporine	
GF109203X	
<b>PKD Inhibitor</b>	
CID755673	
<b>Raf-1 Inhibitor</b>	
L779450	



Table A4 continued: Small Molecule Inhibitors and Receptor Antagonists structures

Small molecule Inhibitor	Structure
<b>cAMP Activator</b>	
Forskolin	
<b>ERK/MEK Inhibitors</b>	
SL327	
PD98059	
<b>Rac Inhibitors</b>	
NSC23766	
EHT1864	
<b>FAK/Pyk2 Inhibitors</b>	
PF562271	
FAK Inhibitor PF-228	

Table A4 continued: Small Molecule Inhibitors and Receptor Antagonists structures

Small molecule Inhibitor	Structure
<b>Kinase Inhibitors</b>	
SB203580	
$\beta$ -ARK-1	
Bosutinib	
H89 2HCL	
Y27632	
<b>Pi3K Inhibitors</b>	
AS605240	
LY294002	
<b>GRK Inhibitor</b>	
lpyrimidine (4-Amino-5-ethoxymethyl-2-methylpyrimidine)	
<b>JAK2 Inhibitor</b>	
Hexabromocyclohexane (HBC)	
<b>STAT3 Inhibitors</b>	
WP1066	
5,15-Diphenylporphyrin (5,15-DPP)	

Table A4 continued: Small Molecule Inhibitors and Receptor Antagonists structures

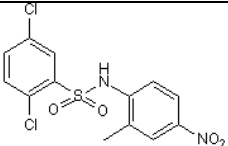
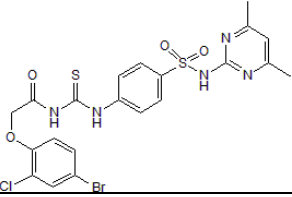
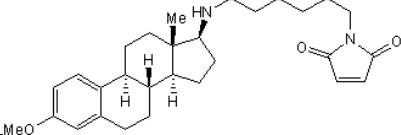
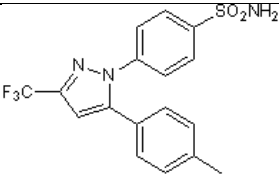
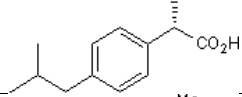
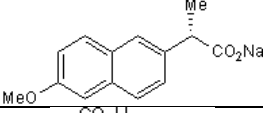
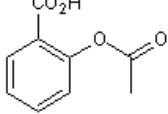
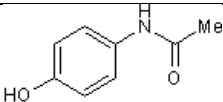
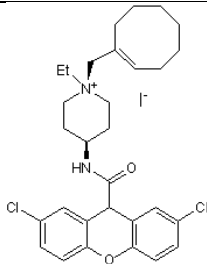
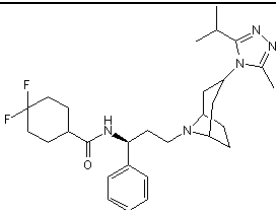
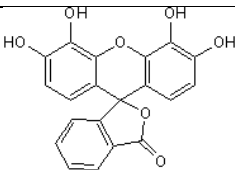
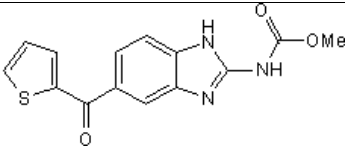
Small molecule Inhibitor	Structure
<b><math>\beta</math>-catenin Inhibitor</b>	
FH535	
<b>Cdc 42 Inhibitor</b>	
ZCL278	
<b>Phospholipase C Inhibitor</b>	
U73122	
<b>NSAIDs</b>	
Celecoxib	
Ibuprofen	
Naproxen	
Aspirin	
Paracetamol	
<b>CXCR4 antagonist</b>	
ATI2341	Pal-Met-Gly-Tyr-Gln-Lys-Lys-Leu-Arg-Ser-Met-Thr-Asp-Lys-Tyr-Arg-Leu
<b>CCR1/CCR3 antagonist</b>	
J113863	

Table A4 continued: Small Molecule Inhibitors and Receptor Antagonists structures

Small molecule Inhibitor	Structure
<b>CCR5 Antagonist</b>	
Maraviroc	
<b>Gβγ Inhibitor</b>	
Gallein	
<b>Cytoskeletal Inhibitor</b>	
Nocodazole	

## Appendix 5 - Published Abstracts, Posters and Oral Presentations

### 2014

**Poster:** *Chemokine receptor-induced cell migration: distinct signalling networks are used by different receptors.* Jacques R O, Zerwes P, Fagade F, Green J, Roberts-Dalton H, Downham S, Mills S C, Sexton D and Mueller A. Presented: 28<sup>th</sup> – 29<sup>th</sup> April 2014, British Pharmacology Society (BPS) 5<sup>th</sup> Focused Meeting on Cell Signalling, British Society for Immunology (BSI) Leukocyte Migration Affinity Group Meeting, University of Leicester.

### 2015

**Abstract and Poster:** *The importance of signalling pathway proteins differ in CC and CXC chemokine-induced chemotaxis.* Mills S C, Jacques R O, Zerwes P, Sexton D, and Mueller A. **Presented:** 9<sup>th</sup> – 11<sup>th</sup> February 2015, BSI Leukocyte Migration Affinity Group Meeting, “Leukocyte Migration in Health and Disease” at Medical School Birmingham University. **Also presented:** 17<sup>th</sup> September 2015, Annual Pharmacy Research Colloquium, John Innes Conference Centre, Norwich Research Park.

**Abstract and Poster:** *Signalling Pathway Proteins in CC and CXC Chemokine-induced Chemotaxis.* Mills S C. **Presented:** 15<sup>th</sup> – 17<sup>th</sup> December 2015, BPS, Pharmacology 2015, at QEII Conference Centre, London.

### 2016

**Abstract and Poster:** *Signalling Pathway Proteins in CC and CXC Chemokine-induced Chemotaxis.* Mills S C. **Presented:** 18<sup>th</sup>-19<sup>th</sup> April 2016, BPS 6<sup>th</sup> Focused Meeting on Cell Signalling, BSI Leukocyte Migration Affinity Group Meeting, University of Leicester.

**Abstract and Poster:** *Cofilin: a key protein in chemokine-induced cell migration in metastasis.* Mills S C and Mueller A. **Presented:** 29<sup>th</sup> May – 3<sup>rd</sup> June 2016, From Molecular Mechanisms of Chemokine Biology and Pathophysiology to Progress and Challenges in the Development of Therapeutics, Chemotactic Cytokine Gordon Research Conference, Girona, Spain. **Also presented:** 13<sup>th</sup> – 15<sup>th</sup> December 2016, BPS, Pharmacology 2016, at QEII Conference Centre, London.

**Abstract and Poster:** *Signalling Pathway Proteins in CC and CXC Chemokine-induced Chemotaxis.* Mills S C. **Presented:** 15<sup>th</sup> June 2016, School of Pharmacy Research Day, Thomas Paine Study Centre UEA. (won Best Pharmacology Poster Prize).

## **Oral Presentations**

**3 Minute Thesis Competition**, 15<sup>th</sup> June 2016, *Does chemokine signalling hold the elusive silver bullet to beat metastasis?* Single PowerPoint Slide and 3 minute oral presentation.

**School of Pharmacy Seminar**, 19<sup>th</sup> September 2016, Thirty minute PowerPoint presentation and questions covering my research entitled: *"Manipulating Chemokine Signalling to Prevent Metastasis"*.

## **Appendix 6 - Contributions to and Copies of Published Papers**

**Published 9<sup>th</sup> September 2015:** Jacques R O, Mills S C, Zerwes P, Fagade F O, Green J E, Downham S, Sexton D W, Mueller A. *Dynamin function is important for chemokine receptor-induced cell migration*. Cell Biochem Funct 2015 33(6):407-414.

I contributed to writing and proof reading of paper, and undertook investigations and analysed data to supply figure 1 (a), (b) and (e); figure 2 (a), (c), (d); figure 3 (e), (f), (g), (h); figure 4 (a), (b).

**Published 21<sup>st</sup> January 2016:** Mills S C, Goh P H, Kudatsih J, Ncube S, Gurung R, Maxwell W, Mueller A. *Cell migration towards CXCL12 in leukaemic cells compared to breast cancer cells*. Cell Signal 2016 28(4):316-324

I contributed to writing the paper with Dr Mueller and influenced the story line. Proof read paper and undertook investigations and analysed data to supply following: figure 1 (g); figure 2 (a), (b), (c), (d), (e), (f), (g); figure 4 (a), (b), (c); figure 5 (a), (b), (c), (d), (e), (f), (g); figure 6 (a), (b), (c), (d), (g).

**Published 16<sup>th</sup> October 2017:** Mills S C, Howell L, Beekman A, Stokes L, Mueller A. *Rac1 plays a role in CXCL12 but not CCL3-induced chemotaxis and Rac1 GEF inhibitor NSC23766 has off target effects on CXCR4*. Cell Signal 2018 42:88-96

I discovered and contributed paper's story, wrote the paper with Dr Mueller, undertook investigations and analysed data to supply following: figure 1 (a), (b), (c), (f), (g), (h); figure 2 (a), (b), (c), (d), (e); figure 3 (a), (b), (c), (d); figure 4 (a), (b), (c); figure 5 (a), (b), (except EHT1864 chemotaxis data) (c); figure 6 (a), (b), (c); figure 7(a), (b).

## Dynamin function is important for chemokine receptor-induced cell migration

Richard O. Jacques<sup>1</sup>, Shirley C. Mills<sup>1</sup>, Paula Cazonatto Zerwes<sup>1</sup>, Feyisope O. Fagade<sup>1</sup>, John E. Green<sup>1</sup>, Scott Downham<sup>1</sup>, Darren W. Sexton<sup>2,3</sup> and Anja Mueller<sup>1\*</sup>

<sup>1</sup>School of Pharmacy, University of East Anglia, Norwich Research Park, Norwich, UK

<sup>2</sup>Norwich Medical School, University of East Anglia, Norwich Research Park, Norwich, UK

<sup>3</sup>School of Pharmacy and Biomolecular Science, Liverpool John Moores University, Liverpool, UK

The HIV viral entry co-receptors CCR5 and CXCR4 function physiologically as typical chemokine receptors. Activation leads to cytosolic signal transduction that results in a variety of cellular responses such as cytoskeletal rearrangement and chemotaxis (CTX). Our aim was to investigate the signalling pathways involved in CC and CXC receptor-mediated cell migration. Inhibition of dynamin I and II GTPase with dynasore completely inhibited CCL3-stimulated CTX in THP-1 cells, whereas the dynasore analogue Dyngo-4a, which is a more potent inhibitor, showed reduced ability to inhibit CC chemokine-induced CTX. In contrast, dynasore was not able to block cell migration via CXCR4. The same activation/inhibition pattern was verified in activated T lymphocytes for different CC and CXC chemokines. Cell migration induced by CC and CXC receptors does not rely on active internalization processes driven by dynamin because the blockade of internalization does not affect migration, but it might rely on dynamin interaction with the cytoskeleton. We identify here a functional difference in how CC and CXC receptor migration is controlled, suggesting that specific signalling networks are being employed for different receptor classes and potentially specific therapeutic targets to prevent receptor migration can be identified. Copyright © 2015 John Wiley & Sons, Ltd.

KEY WORDS—chemokine receptor; chemotaxis; dynamin; signalling; internalization

### INTRODUCTION

Cellular migration can be activated by chemokine receptors, which are part of the G protein-coupled receptor (GPCR) family.<sup>1</sup> In different disease settings and different cancer types, it has been shown that chemokine receptors play a crucial role in promoting cell migration and even cancer growth.<sup>2,3</sup> Several chemokines (CCL5 and CCL8) act as agonists for CCR1, CCR3 and CCR5, whereas a few chemokines, like CCL2, only activate CCR2 and CCR4, but not CCR5.<sup>4,5</sup> It has been shown that chemokine receptor activation leads to activation of heterotrimeric G proteins and phosphorylation of the receptor via GPCR kinases, which in turn leads to binding of  $\beta$ -arrestins to the receptor and is followed by receptor internalization.<sup>4</sup> Activation is also followed by actin polymerization, but the signalling networks that allowed this to happen have yet to be fully defined.

In recent years, it has become clear that GPCRs do not signal solely via G proteins.<sup>6</sup> The so-called receptosome of these receptors, which includes  $\beta$ -arrestins and other associating proteins, makes signalling of GPCRs comparatively

complex.  $\beta$ -Arrestins can associate directly with a range of proteins including ERK1/2, cofilin, filamin and Jnk3 and therefore activate a variety of cellular responses without the involvement of G proteins.<sup>7</sup> Ligand-biased signalling is important for chemokine receptors, and it allows different ligands to activate different signalling cascades by encouraging specific ligand–receptor conformations. Receptors adopting such ligand-dependent conformations then display specificity or bias towards certain signalling pathways dependent on which ligand binds to the receptor<sup>8</sup> and which receptor class is involved. There is also a marked difference in the regulation of CXC receptor and CC receptor expression on the cell surfaces. Whereas CCR5, CCR2 and CCR4 internalize via clathrin-coated pits and caveolae, CXCR3 and CXCR4 use only clathrin-coated pits.<sup>9–13</sup> Similarly, CCR5 recycles back to the cell surface, whereas CXCR3 and CXCR4 are targeted to the late endosomes and lysosomes.<sup>10,12,13</sup>

Traditionally, it is thought that  $\beta\gamma$ -subunits of the G proteins induce migration via activation of phosphoinositide 3-kinase (PI3K);<sup>14</sup> however, we have recently shown that this seems not to be the case for CCL3-induced migration in THP-1 cells.<sup>15</sup> For CXCR4, it has been shown that migration under certain circumstances is dependent on  $\beta$ -arrestins as well as filamin A, a protein that can bind actin

\*Correspondence to: Anja Mueller, School of Pharmacy, University of East Anglia, Norwich Research Park, Norwich NR4 7TJ, UK.  
E-mail: anja.mueller@uea.ac.uk

and interacts with  $\beta$ -arrestins.<sup>16,17</sup> This raises the possibility that  $\beta$ -arrestin-interacting and actin-interacting proteins are activated downstream of different types of chemokine receptors. One of these actin-interacting proteins is dynamin. Several groups have shown that dynamin, an enzyme that has traditionally been linked to internalization of receptors via clathrin-coated pits, is important for the integral structure of actin polymers.<sup>18–20</sup> Dynamins are large multi-domain proteins (~100 kDa) that constitute an N-terminal GTPase domain, a middle domain, a pleckstrin homology (PH) domain, a GTPase effector domain and a C-terminal proline-rich domain, which interacts with proteins that contain SH3 domains,<sup>21</sup> and there are several types of the protein: Dynamin I is primarily found in neurones where it is involved in synaptic vesicle endocytosis,<sup>22,23</sup> and it has been linked with several neurological processes such as long-term memory formation<sup>24</sup>. Dynamin II is ubiquitously expressed and is found in all cell types, and dynamin III is primarily found in the testis. Dynamin II interacts with numerous GPCRs as well as non-GPCRs, including the chemokine receptor CCR5<sup>25</sup> and various cytokine receptors,<sup>26</sup> and is, therefore, an interesting target protein to investigate chemokine receptor-triggered migration.

Here, we analysed different small-molecule inhibitors for their effects on chemokine receptor-induced migration and release of intracellular calcium. We investigated whether dynamin plays a role for both CC receptor-induced and CXC receptor-induced migration or whether distinct signalling pathways are activated by different subsets of receptors.

## METHODS

### Cells and materials

Culture conditions for THP-1 cells have previously been described.<sup>9</sup> Jurkat cells were obtained from ATCC and grown in Roswell Park Memorial Institute containing 10% foetal calf serum and 2 mM L-glutamine. Blood was sampled from healthy normal subjects according to a protocol approved by a local ethics committee (reference number 2008042). Peripheral blood mononuclear cells were subsequently isolated as previously described by Sabroe *et al.*<sup>27</sup> Lymphocytes were separated from monocytes by allowing the latter to adhere to a tissue culture flask for 2 h at 37 °C and 5% CO<sub>2</sub> and were activated by culture in the presence of interleukin-2 (200 mg ml<sup>-1</sup>) and concanavalin A (30 mg ml<sup>-1</sup>) for at least 10 days. The chemokine used for CCR5/CCR1 activation was human CCL3 (D26A) and has been described before.<sup>9,28</sup> CXCL11 and CXCL12 were from PeproTech (UK). Dynamin inhibitors dynasore, Dyngo-4a, MiTMAB, OcTMAB, Dynole-34-2, Dynole-31-2 (negative control), Iminodyn-22 and Iminodyn-17 (negative control) and Pyrimidin-7 were purchased from Abcam (for an overview of dynamin inhibitors, see Table 1). Clathrin-mediated endocytosis inhibitor Pitstop 2 and the corresponding negative control were from Abcam. All other chemicals were from Fisher Scientific.

### Chemotaxis assays

Cells were harvested and washed twice with pre-warmed, sterile phosphate-buffered saline and then resuspended in serum-free Roswell Park Memorial Institute 1640, which contained 0.1% bovine serum albumin. The concentration of cells was adjusted to  $6.25 \times 10^7$  cells ml<sup>-1</sup>. Chemoattractants were loaded in a final volume of 31  $\mu$ l at indicated concentrations in the lower compartment, and 20  $\mu$ l of resuspended cells was loaded onto the upper compartment of a microchemotaxis chamber (Receptor Technologies, Adderbury, UK). The two compartments were separated by a polyvinylpyrrolidone-free polycarbonate filter with 5- $\mu$ m pores. For inhibitor treatment, cells were incubated for 30 min with the inhibitor or with vehicle control before being loaded onto the upper compartment of the chamber. Chambers were incubated at 37 °C and 5% CO<sub>2</sub> for 4 h before cells were counted. Data were analysed as previously described.<sup>15</sup>

### Analysis of data

Data were analysed using GRAPHPAD PRISM 5 (GraphPad software). Statistical analyses were performed using a one-way ANOVA with a Bonferroni multiple-comparison test as *post hoc* test with a *p* value <0.05 deemed significant. In all figures, data represent the mean  $\pm$  standard error of the mean of at least three independent experiments.

## RESULTS

Chemokine receptors are expressed on different cell types, and THP-1 cells express naturally CCR1, CCR2 and CCR5 as well as CXCR4 and migrate towards stimuli with CCL2, CCL3, CCL8, CCL23 and CXCL12, whereas Jurkat cells express CXCR4 and migrate towards stimuli with CXCL12, but not towards CCL3. Activated T cells have been shown to express functional CXCR3 and CCR5 and migrate towards CXCL11 and CCL3.<sup>29</sup> We therefore used these different cells to investigate the effect of dynamin inhibitors on cell migration with the view to differentiate between CC receptor and CXC receptor family behaviour. In our hands, Jurkat cells do not migrate towards CCL3, and hence, we used THP-1 cells for both CCL3 and CXCL12. Dynasore blocks migration towards CCL3 in THP-1 cells in a dose-dependent manner (Figure 1a). At a concentration where dynasore clearly blocks CCL3-induced migration (40  $\mu$ M), it does not affect CXCL12-induced migration in THP-1 (Figure 1b). To rule out any ambiguities, we used the higher concentration of dynasore (80  $\mu$ M) in activated T cells. Dynasore does not block migration of activated T cells towards CXCL11, whereas there is a clear trend of inhibition towards CCL3-induced migration (Figure 1c, d), showing a distinct difference in the activation pattern of CXC and CC receptors. Confirming the differences between CC and CXC receptors are results with CXCL12 in Jurkat cells, where dynasore has no effect at all on migration, even at 80  $\mu$ M (Figure 1e). At the concentration used, none of the



Table 1. Overview of dynamin inhibitors

Inhibitor	Mode of action	IC <sub>50(SVE)</sub> * (μM)	Specificity, dynamin I versus II (μM)	References
Dyngo-4a <sup>TM</sup>	G domain: allosteric site	16 ± 1.2	Dynamin I selective, 0.38 ± 0.05 vs 2.6 ± 0.12	30,35
Dynasore	Unknown: non-competitive inhibition	79.3 ± 1.3	Non-selective	35
Dynole-34-2 <sup>TM</sup>	G domain: uncompetitive with GTP	105	Non-selective	36
Iminodyn-22 <sup>TM</sup>	G domain: uncompetitive with GTP	99.5 ± 1.7	Non-selective	33
Pyrimidin-7 <sup>TM</sup>	Competitively inhibits both GTP and phospholipid binding	Not reported	Non-selective, 1.1 vs 1.8	32
MiTMAB <sup>TM</sup>	PH domain: competitive with lipid and non-competitive with GTP	105	Non-selective	36
OcTMAB <sup>TM</sup>	PH domain: competitive with lipid and non-competitive with GTP	Not reported	Non-selective	36

IC<sub>50</sub>, half maximal inhibitory concentration; GTP, guanosine triphosphate; PH, pleckstrin homology.

\*FM4-64 uptake in synaptosomes.

dynamin inhibitors showed any cytotoxic effects in the experimental set-up, as shown by MTS assays (data not shown).

The dynasore analogue Dyngo-4a, which is more potent than dynasore (Dyngo-4a half maximal inhibitory concentration 16 ± 1.2 μM versus dynasore 79.3 ± 1.3 μM),<sup>30</sup> blocks migration towards CCL3 in THP-1 cells to a lesser degree than does dynasore. Remarkably, Dyngo-4a blocks migration towards CXCL11 in activated T cells and CXCL12 in THP-1 and Jurkat cells (Figure 2). Dyngo-4a shows selectivity towards dynamin I versus dynamin II, whereas dynasore is non-selective, and therefore, these results might reflect a different usage of the dynamin isoforms by different receptors (Table 1). We further investigated which domains of the dynamin proteins are essential for cell migration and whether they are equally important for different receptor families. In the first instance, we used Iminodyn-22 and Dynole-34-2, which are both non-selective dynamin I and II inhibitors, and their negative controls, which are Iminodyn-17 and Dynole-31-2. Neither Iminodyn-22 nor Dynole-34-2 blocks migration in THP-1 cells towards CCL3 or in Jurkat cells towards CXCL12 (Figure 3a–d). However, there is a distinct difference between CCL3-induced and CXCL12-induced chemotaxis for the non-selective MiTMAB and OcTMAB inhibitors, which bind to the dynamin PH domain<sup>30</sup> and completely block any migration in Jurkat cells towards CXCL12 (Figure 3f) but have no significant effect on CCL3-induced migration in THP-1 cells (Figure 3e, g) but still affect CXCL12 migration in THP-1, even though with less of an effect than in Jurkat cells (Figure 3h). Again, these data show a clear difference in the reliance of CC and CXC receptors on dynamin usage. We also used Pyrimidin-7, which competitively inhibits both guanosine triphosphate and phospholipid binding and is the only inhibitor available up to now that targets two distinct domains of dynamin. There is no effect on CCL3-induced migration in THP-1 cells (Figure 4a), but CXCL12-induced migration is significantly blocked in THP-1 cells (Figure 4b) as well as in Jurkat cells (data not shown).

Dynamin is classically known as being of importance for clathrin-coated pit-triggered internalization of receptors,

even though recently its importance for actin dynamics has become more apparent.<sup>19</sup> We previously showed that CCR5 can use clathrin-coated pits for internalization,<sup>9,31</sup> and indeed dynamin inhibition via dynasore completely abrogates internalization on CHO.CCR5 as well as THP-1 cells as analysed via immunofluorescence (data not shown). To investigate whether it is the prohibition of internalization that prevents cell migration, we used another clathrin-coated pit endocytosis inhibitor, Pitstop 2, and its negative control analogue in THP-1 cells for CCL3 activation as well as in Jurkat cells for CXCL12 activation. Pitstop 2 does not block cell migration (Figure 4c, d). The concentration of Pitstop 2 used for migration assays actually inhibits internalization of CCR5 receptor in THP-1 cells (data not shown). An increase of the concentration of Pitstop 2 used in THP-1 cells in fact increased the number of migrating cells by a small but significant amount.

## DISCUSSION

In this study, we investigated the role of dynamin in the signalling events that occur after the activation of CC and CXC receptors. Dynamin involvement in cell migration is related to its role as a focal adhesion regulator, and it has been shown that inhibition of dynamin II inhibits focal adhesion disassembly and impairs cell migration. We, therefore, used different dynamin inhibitors, which either have a higher potency for dynamin I over II (Dyngo-4a) or are non-selective dynamin I and II inhibitors (dynasore, Dynole-34-2, MiTMAB, OcTMAB, Iminodyn-22 and Pyrimidin-7).<sup>30,32,33</sup> Dynasore has been shown previously to block endocytosis via clathrin-coated pits,<sup>34–36</sup> and indeed, it blocks CCL3-induced endocytosis of CCR5 in CHO.CCR5 cells. Dynasore blocks CCL3-induced migration in THP-1 cells and activated T lymphocytes, but it has no effect on either CXCL12-induced migration of THP-1 or Jurkat cells or CXCL11-induced migration of activated T lymphocytes. These results point towards a significant difference between CC and CXC receptor-activated signalling networks. Dyngo-4a, a close analogue of dynasore, which is more potent than dynasore and has a higher potency for

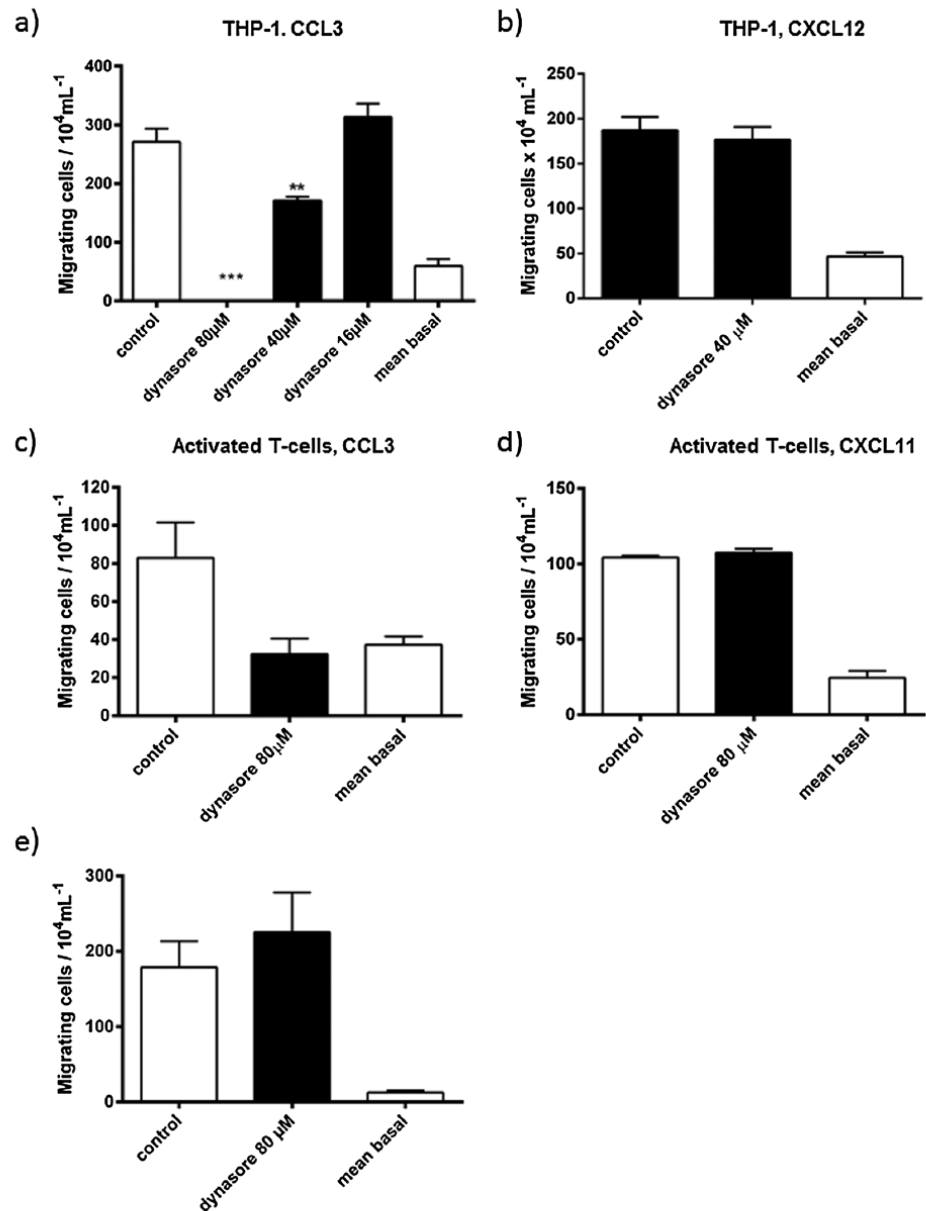


Figure 1. Cell migration towards CCL3 but not towards CXCL11 or CXCL12 is blocked by dynasore. (a) THP-1 cells were treated with 16, 40 or 80 μM of dynasore. (b) THP-1 cells were treated with 40 μM of dynasore. Migration was induced with 1 nM CXCL12. (c) Activated T lymphocytes were treated with 80 μM of dynasore, and migration was induced with 20 nM CCL3. (d) Activated T lymphocytes were treated with 80 μM of dynasore, and migration was induced with 1 nM CXCL11. (e) Jurkat cells were treated with 80 μM of dynasore, and migration was induced with 1 nM CXCL12. Base level of migration was determined in the absence of chemokines. Statistical analysis was performed using a one-way ANOVA with a Bonferroni multiple-comparison test as post-test, with \*\**p* value < 0.01 and \*\*\**p* value < 0.001. Data represent the mean ± standard error of the mean of at least three independent experiments

dynamins I over dynamins II,<sup>30</sup> is less effective in blocking CCL3-induced migration in THP-1 cells; however, it blocks CXCL11-induced and CXCL12-induced migration in activated T lymphocytes and Jurkat cells, respectively.

Similarly, dynasore can significantly reduce CCL2-induced migration in THP-1 cells, whereas Dyno-4a shows a trend to inhibit migration but does not reach significance. The functional differences between dynasore and Dyno-4a

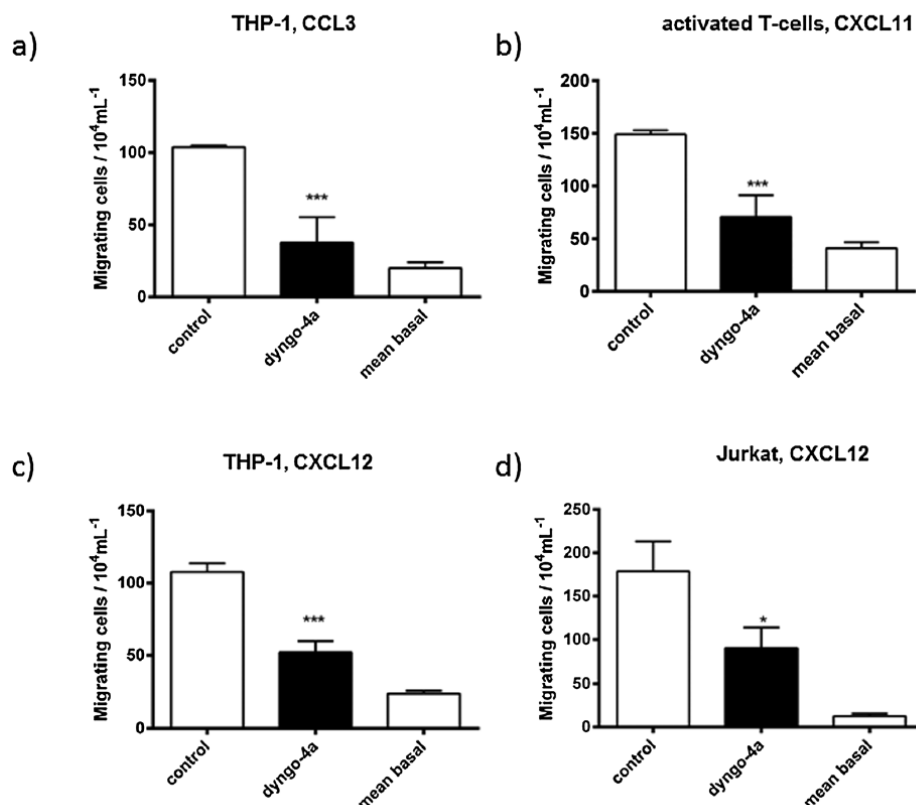


Figure 2. Cell migration towards CCL3, CXCL11 and CXCL12 is blocked by Dyngo-4a. (a) THP-1 cells were treated with 80  $\mu$ M of Dyngo-4a. Migration was induced with 1 nM CCL3. (b) Activated T lymphocytes were treated with 80  $\mu$ M of Dyngo-4a, and migration was induced with 20 nM CXCL11. (c) THP-1 cells were treated with 80  $\mu$ M of Dyngo-4a, and migration was induced with 1 nM CXCL12. (d) Jurkat cells were treated with 80  $\mu$ M of Dyngo-4a, and migration was induced with 1 nM CXCL12. Statistical analysis was performed using a one-way ANOVA with a Bonferroni multiple-comparison test as post-test, with \**p* value < 0.05, \*\**p* value < 0.01 and \*\*\**p* value < 0.001. Data represent the mean  $\pm$  standard error of the mean of at least three independent experiments

have not been fully analysed yet, but with the knowledge available today, our data point towards either a different usage of dynamin isoforms by chemokine receptor subtypes or the usage of a varying set of dynamin-interacting protein by different receptor subfamilies. This difference between CC and CXC receptors was further highlighted by the use of Dynole-34-2, MiTMAB, OcTMAB, Iminodyn-22 and Pyrimidyn-7. None of those blocked CCL3-induced migration in THP-1 cells, but Pyrimidyn-7, MiTMAB and OcTMAB block CXCL12-induced migration in THP-1 and Jurkat cells. Unlike MiTMAB and OcTMAB, which block dynamin recruitment to the membranes, Dynole-34-2, Dyngo-4a and dynasore block dynamin function after its recruitment.<sup>30</sup> MiTMAB and OcTMAB also bind to the PH domain of the dynamin molecule, unlike the other inhibitors, which bind to the G domain. An obvious reason for the prevention of migration after the use of dynamin inhibitors is the potential importance of internalization for receptor activation and ultimately signal transduction. We, therefore, employed a different clathrin-coated pit endocytosis

inhibitor, Pitstop 2, and its negative control compound to analyse whether internalization is a prerequisite for migration. In both THP-1 cells and Jurkat cells, Pitstop 2 did not prevent CCL3-induced and CXCL12-induced migration, respectively, which is evidence that receptor internalization is not necessary to activate cell migration as had been described already for the CCR2b receptor.<sup>37</sup>

In our study, we detect distinct differences between the CC and CXC receptors. Traditionally, it has been shown that CXCR4 activation leads to chemotaxis in a manner dependent on  $\beta$ -arrestin 2, ERK1/2 and  $G\beta\gamma$  and is PI3K dependent.<sup>38,39</sup> Therefore, the implication of the dynamin PH domain in cell migration for CXCL12 is in line with the already published signalling networks, whereas the PH domain is not necessary for CCL3-induced migration, as this migration is independent of PI3K activation.<sup>15</sup> Overall, our study showed that there are distinct differences in signalling networks used by CC receptors compared with CXC receptors, which will yield novel therapeutic targets to prevent cell migration triggered by specific receptors.

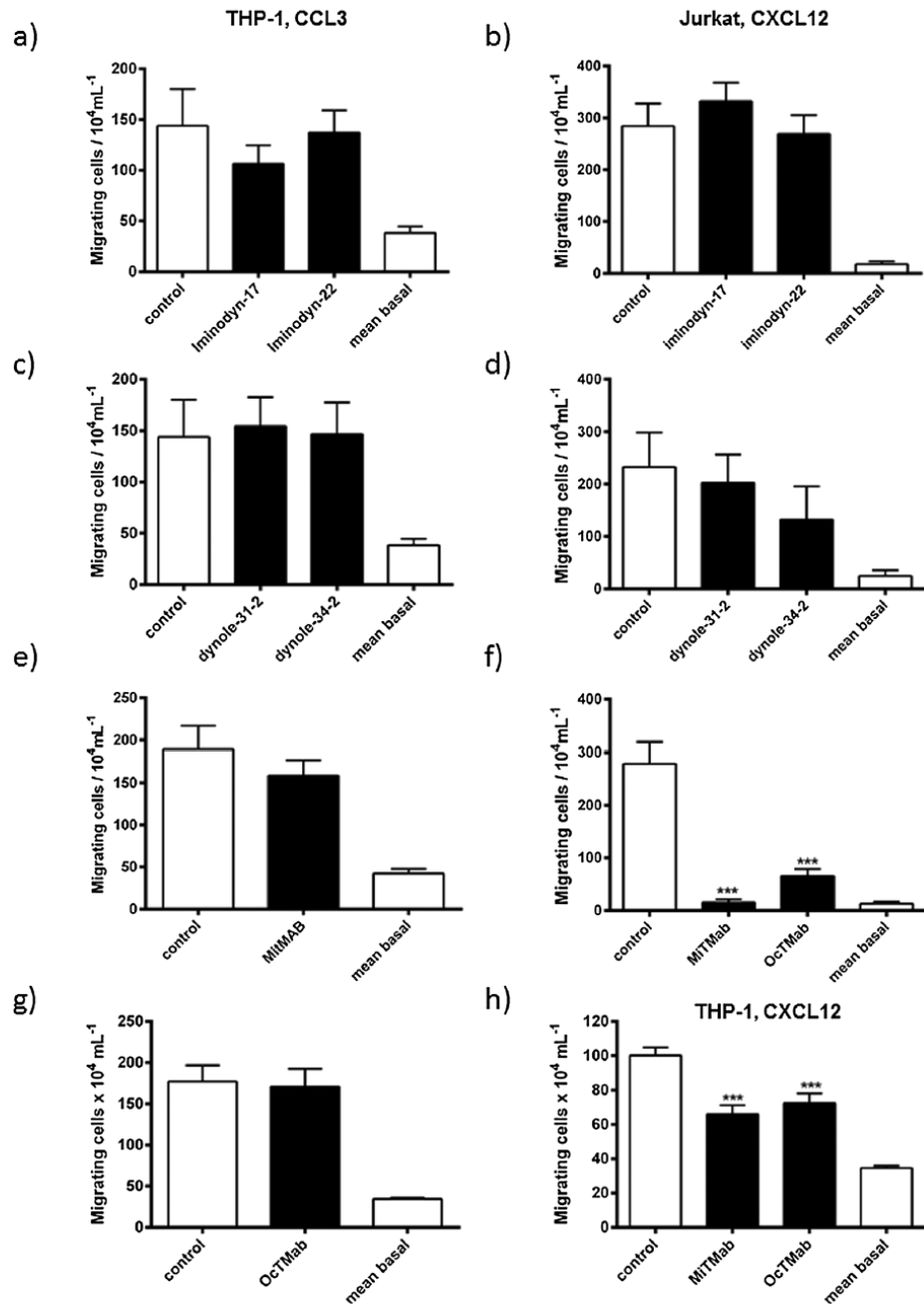


Figure 3. Effect of different dynamin inhibitors on migration towards CCL3 and CXCL12. (a) THP-1 cells were treated with 1  $\mu\text{M}$  of Iminodan-17 and 1  $\mu\text{M}$  of Iminodan-22. Migration was induced with 1 nM CCL3. (b) Jurkat cells were treated with 1  $\mu\text{M}$  of Iminodan-17 and 1  $\mu\text{M}$  of Iminodan-22. Migration was induced with 1 nM CXCL12. (c) THP-1 cells were treated with 15  $\mu\text{M}$  of Dynole-31-2 and 15  $\mu\text{M}$  of Dynole-34-2, and migration was induced with 1 nM CCL3. (d) Jurkat cells were treated with 15  $\mu\text{M}$  of Dynole-31-2 and 15  $\mu\text{M}$  of Dynole-34-2, and migration was induced with 1 nM CXCL12. (e) THP-1 cells were treated with 10  $\mu\text{M}$  of MiTMAB, and migration was induced with 1 nM CCL3. (f) Jurkat cells were treated with 10  $\mu\text{M}$  of MiTMAB and 5  $\mu\text{M}$  of OcTMAB. Migration was induced with 1 nM CXCL12. (g) THP-1 cells were treated with 5  $\mu\text{M}$  of OcTMAB. Migration was induced with 1 nM CCL3. (h) THP-1 cells were treated with 10  $\mu\text{M}$  of MiTMAB and 5  $\mu\text{M}$  of OcTMAB. Migration was induced with 1 nM CXCL12. Statistical analysis was performed using a one-way ANOVA with a Bonferroni multiple-comparison test as post-test, with \*\*\* $p$  value < 0.001. Data represent the mean  $\pm$  standard error of the mean of at least three independent experiments.

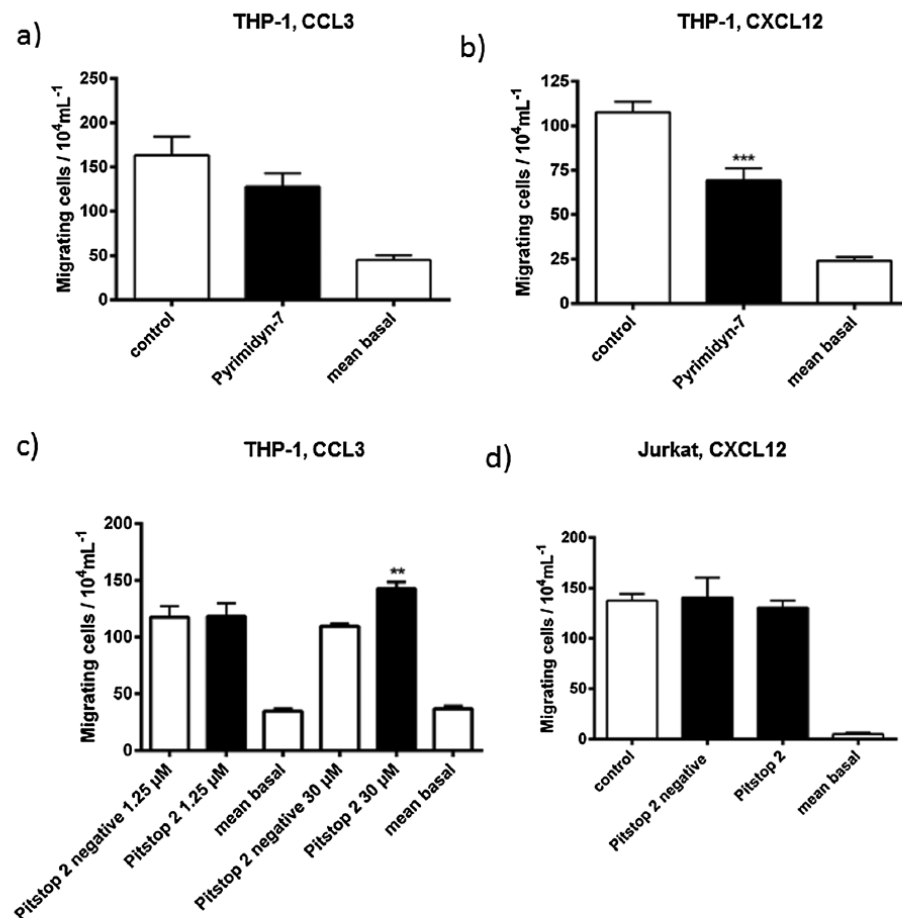


Figure 4. Effect of endocytosis inhibitors on migration towards CCL3 and CXCL12. (a) THP-1 cells were treated with 10  $\mu$ M of Pyrimidyn-7. Migration was induced with 1 nM CCL3. (b) THP-1 cells were treated with 10  $\mu$ M of Pyrimidyn-7. Migration was induced with 1 nM CXCL12, and migrated cells were counted after 4 h. (c) THP-1 cells were treated with 1.25  $\mu$ M of Pitstop 2 and Pitstop 2 negative control compound and 30  $\mu$ M of Pitstop 2 and Pitstop 2 negative control compound. Migration was induced with 1 nM CCL3. (d) Jurkat cells were treated with 30  $\mu$ M of Pitstop 2 and Pitstop 2 negative control compound, and migration was induced with 1 nM CXCL12. Statistical analysis was performed using a one-way ANOVA with a Bonferroni multiple-comparison test as post-test, with \*\* $p$  value < 0.01 and \*\*\* $p$  value < 0.001. Data represent the mean  $\pm$  standard error of the mean of at least three independent experiments

#### CONFLICT OF INTEREST

The authors have declared that there is no conflict of interest.

#### ACKNOWLEDGEMENTS

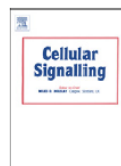
We thank the UEA for providing a studentship for R. O. J., and we acknowledge the support for S. C. M. from the Novartis studentship fund.

#### REFERENCES

- Thelen M. Dancing to the tune of chemokines. *Nat Immunol* 2001; **2**: 129–134.
- Homey B, Muller A, Zlotnik A. Chemokines: agents for the immunotherapy of cancer? *Nat Rev Immunol* 2002; **2**: 175–184.
- Zlotnik A. Chemokines and cancer. *Ernst Schering Res Found Workshop* 2004; **45**: 53–58.
- Bachelier F, Ben-Baruch A, Burkhardt AM, *et al.* International Union of Pharmacology. LXXXIX. Update on the extended family of chemokine receptors and introducing a new nomenclature for atypical chemokine receptors. *Pharmacol Rev* 2014; **66**: 1–79.
- Zlotnik A, Yoshie O. The chemokine superfamily revisited. *Immunity* 2012; **36**: 705–716.
- Magalhaes AC, Dunn H, Ferguson SS. Regulation of GPCR activity, trafficking and localization by GPCR-interacting proteins. *Br J Pharmacol* 2012; **165**: 1717–1736.
- Rajagopal S, Rajagopal K, Lefkowitz RJ. Teaching old receptors new tricks: biasing seven-transmembrane receptors. *Nat Rev Drug Discov* 2010; **9**: 373–386.
- Rajagopal S, Bassoni DL, Campbell JJ, Gerard NP, Gerard C, Wehrman TS. Biased agonism as a mechanism for differential



- signaling by chemokine receptors. *J Biol Chem* 2013; **288**: 35039–35048.
9. Mueller A, Kelly E, Strange PG. Pathways for internalization and recycling of the chemokine receptor CCR5. *Blood* 2002; **99**: 785–791.
  10. Meiser A, Mueller A, Wise EL, McDonagh EM, Petit SJ, Saran N, Clark PC, Williams TJ, Pease JE. The chemokine receptor CXCR3 is degraded following internalization and is replenished at the cell surface by *de novo* synthesis of receptor. *J Immunol* 2008; **180**: 6713–6724.
  11. Mariani M, Lang R, Binda E, Panina-Bordignon P, D'Ambrosio D. Dominance of CCL22 over CCL17 in induction of chemokine receptor CCR4 desensitization and internalization on human Th2 cells. *Eur J Immunol* 2004; **34**: 231–240.
  12. Borroni EM, Mantovani A, Locati M, Bonecchi R. Chemokine receptors intracellular trafficking. *Pharmacol Ther* 2010; **127**: 1–8.
  13. Zhang Y, Foudi A, Geay JF, et al. Intracellular localization and constitutive endocytosis of CXCR4 in human CD34+ hematopoietic progenitor cells. *Stem Cells* 2004; **22**: 1015–1029.
  14. Gernena G, Hirsch E. PI3Ks and small GTPases in neutrophil migration: two sides of the same coin. *Mol Immunol* 2013; **55**: 83–86.
  15. Kerr JS, Jacques RO, Moyano Cardaba C, Tse T, Sexton D, Mueller A. Differential regulation of chemotaxis: role of G $\beta\gamma$  in chemokine receptor-induced cell migration. *Cell Signal* 2013; **25**: 729–735.
  16. Lagane B, Chow KY, Balabanian K, et al. CXCR4 dimerization and beta-arrestin-mediated signaling account for the enhanced chemotaxis to CXCL12 in WHIM syndrome. *Blood* 2008; **112**: 34–44.
  17. Scott MG, Pierotti V, Storez H, et al. Cooperative regulation of extracellular signal-regulated kinase activation and cell shape change by filamin A and beta-arrestins. *Mol Cell Biol* 2006; **26**: 3432–3445.
  18. Ferguson SM, Raimondi A, Paradise S, et al. Coordinated actions of actin and BAR proteins upstream of dynamin at endocytic clathrin-coated pits. *Dev Cell* 2009; **17**: 811–822.
  19. Chua J, Rikhy R, Lippincott-Schwartz J. Dynamin 2 orchestrates the global actomyosin cytoskeleton for epithelial maintenance and apical constriction. *Proc Natl Acad Sci U S A* 2009; **106**: 20770–20775.
  20. Gallo G. More than one ring to bind them all: recent insights into the structure of the axon. *Dev Neurobiol* 2013; **73**: 799–805.
  21. Shpetner HS, Vallee RB. Dynamin is a GTPase stimulated to high levels of activity by microtubules. *Nature* 1992; **355**: 733–735.
  22. De Camilli P, Takei K, McPherson PS. The function of dynamin in endocytosis. *Curr Opin Neurobiol* 1995; **5**: 559–565.
  23. Tomizawa K, Sunada S, Lu YF. Cophosphorylation of amphiphysin I and dynamin I by Cdk5 regulates clathrin-mediated endocytosis of synaptic vesicles. *J Cell Biol* 2003; **163**: 813–824.
  24. Casoli T, Di Stefano G, Fattoretti P, et al. Dynamin binding protein gene expression and memory performance in aged rats. *Neurobiology of Aging* 2012; **33**(618): e615–619.
  25. Tadagaki K, Tudor D, Gbahou F, et al. Human cytomegalovirus-encoded UL33 and UL78 heteromerize with host CCR5 and CXCR4 impairing their HIV coreceptor activity. *Blood* 2012; **119**: 4908–4918.
  26. Kawada K, Upadhyay G, Ferandon S, et al. Cell migration is regulated by platelet-derived growth factor receptor endocytosis. *Mol Cell Biol* 2009; **29**: 4508–4518.
  27. Sabroe I, Hartnell A, Jopling LA, et al. Differential regulation of eosinophil chemokine signaling via CCR3 and non-CCR3 pathways. *J Immunol* 1999; **162**: 2946–2955.
  28. Mueller A, Mahmoud NG, Strange PG. Diverse signalling by different chemokines through the chemokine receptor CCR5. *Biochem Pharmacol* 2006; **72**: 739–748.
  29. Loetscher M, Gerber B, Loetscher P. Chemokine receptor specific for IP10 and mig: structure, function, and expression in activated T-lymphocytes. *J Exp Med* 1996; **184**: 963–969.
  30. Harper CB, Popoff MR, McCluskey A, Robinson PJ, Meunier FA. Targeting membrane trafficking in infection prophylaxis: dynamin inhibitors. *Trends Cell Biol* 2013; **23**: 90–101.
  31. Mueller A, Strange PG. Mechanisms of internalization and recycling of the chemokine receptor, CCR5. *Eur J Biochem* 2004; **271**: 243–252.
  32. McGeachie AB, Odell LR, Quan A, et al. Pyrimidin compounds: dual-action small molecule pyrimidine-based dynamin inhibitors. *ACS Chem Biol* 2013; **8**: 1507–1518.
  33. Hill TA, Mariana A, Gordon CP, et al. Iminochromene inhibitors of dynamins I and II GTPase activity and endocytosis. *J Med Chem* 2010; **53**: 4094–4102.
  34. Lee S, Jung KY, Park J, Cho JH, Kim YC, Chang S. Synthesis of potent chemical inhibitors of dynamin GTPase. *Bioorg Med Chem Lett* 2010; **20**: 4858–4864.
  35. Harper CB, Martin S, Nguyen TH, et al. Dynamin inhibition blocks botulinum neurotoxin type A endocytosis in neurons and delays botulism. *J Biol Chem* 2011; **286**: 35966–35976.
  36. McCluskey A, Daniel JA, Hadzic G, et al. Building a better dynasore: the dyngo compounds potentially inhibit dynamin and endocytosis. *Traffic* 2013; **14**: 1272–1289.
  37. Arai H, Tsou CL, Charo IF. Chemotaxis in a lymphocyte cell line transfected with C-C chemokine receptor 2B: evidence that directed migration is mediated by  $\beta\gamma$  dimers released by activation of G $\alpha_i$ -coupled receptors. *Proc Natl Acad Sci U S A* 1997; **94**: 14495–14499.
  38. Drury LJ, Ziarek JJ, Gravel S, et al. Monomeric and dimeric CXCL12 inhibit metastasis through distinct CXCR4 interactions and signaling pathways. *Proc Natl Acad Sci U S A* 2011; **108**: 17655–17660.
  39. Delgado-Martin C, Escribano C, Pablos JL, Riol-Blanco L, Rodriguez-Fernandez JL. Chemokine CXCL12 uses CXCR4 and a signaling core formed by bifunctional Akt, extracellular signal-regulated kinase (ERK)1/2, and mammalian target of rapamycin complex 1 (mTORC1) proteins to control chemotaxis and survival simultaneously in mature dendritic cells. *J Biol Chem* 2011; **286**: 37222–37236.



## Cell migration towards CXCL12 in leukemic cells compared to breast cancer cells



Shirley C. Mills, Poh Hui Goh, Jossie Kudatsih, Sithembile Ncube, Renu Gurung, Will Maxwell, Anja Mueller \*

School of Pharmacy, University of East Anglia, Norwich Research Park, Norwich NR4 7TJ, UK

### ARTICLE INFO

#### Article history:

Received 20 August 2015

Received in revised form 19 January 2016

Accepted 19 January 2016

Available online 21 January 2016

#### Keywords:

Chemokine receptor

Chemotaxis

Protein kinase

Src

### ABSTRACT

Chemotaxis or directed cell migration is mediated by signalling events initiated by binding of chemokines to their cognate receptors and the activation of a complex signalling cascade. The molecular signalling pathways involved in cell migration are important to understand cancer cell metastasis. Therefore, we investigated the molecular mechanisms of CXCL12 induced cell migration and the importance of different signalling cascades that become activated by CXCR4 in leukemic cells versus breast cancer cells. We identified Src kinase as being essential for cell migration in both cancer types, with strong involvement of the Raf/MEK/ERK1/2 pathway. We did not detect any involvement of Ras or JAK2/STAT3 in CXCL12 induced migration in Jurkat cells. Preventing PKC activation with inhibitors does not affect migration in Jurkat cells at all, unlike in the adherent breast cancer cell line MCF-7 cells. However, in both cell lines, knock down of PKC $\alpha$  prevents migration towards CXCL12, whereas the expression of PKC $\zeta$  is less crucial for migration. PI3K activation is essential in both cell types, however LY294002 usage in MCF-7 cells does not block migration significantly. These results highlight the importance of verifying specific signalling pathways in different cell settings and with different approaches.

Crown Copyright © 2016 Published by Elsevier Inc. All rights reserved.

### 1. Introduction

Tumour metastasis is the major cause of death in cancer patients who have suffered a primary solid tumour or haematological malignancy. The chemokine CXCL12 along with Src and PI3K/Akt signalling appears to be implicated in both breast cancer metastatic progression to bone and other tissues, and leukaemia recurrence [1–4]. Metastasis results from a sequential series of processes, in which tumour cells undergo epithelial-mesenchymal transition. Cells detach from the original tumour tissue, intravasate into blood vessels, survive and travel along the circulation, extravasate to secondary organs, transform back to the epithelial state, and proliferate at their new location [5–7]. Recent data indicates that chemotactic signalling plays a crucial role in tumour invasion and spreading [8–14]. Chemotaxis is mediated by signalling events initiated by binding of chemokines to their cognate receptors, and involves re-arrangement of the actin cytoskeleton. CXCL12 can bind the G-protein coupled receptor CXCR4 causing G $\alpha$ i triggered adenylate cyclase inhibition and hence a reduction in cAMP levels in the cell. This

mediates the Src kinase phosphorylation cascade, which leads to ERK activation, Rho triggered actin rearrangement, cell polarisation and finally migration down a chemokine gradient [15]. Chemokine induced chemotaxis is key in homeostasis; for example CXCL12 is essential in lymph tissues and for movement of haematopoietic cells between blood and bone marrow [15,16]. CXCR4 has been the subject of much scrutiny, since it has been implicated in the metastasis of various cancers [1,7,8]. For example, CXCL12 has been shown to be detrimental in the movement of blasts in leukaemia [17] and CXCL12 + cells are implicated in the formation of bone metastasis following breast cancer [18]. However, the signal networks that are important for chemokine receptor triggered cell migration and metastasis are not yet completely understood due to their complexity. Nevertheless, for CXCR4 signalling, concentrations and gradients of CXCL12 are purportedly important. Excess CXCL12 may further damage tissues suffering insult from ischaemia, toxins, chemotherapeutic agents and atherosclerosis [15]. CXCL12 levels tend to rise with age [19] and excess concentrations may inhibit metastasis [20]. Many chemokines bind several chemokine receptors and CXCL12 binds CXCR4 and CXCR7. It appears that CXCR7 activities include acting as a scavenger, modulating the levels of CXCL12 in the vicinity of cells carrying the receptor, and that binding of CXCL12 to CXCR7 may cause internalisation of the receptor without resulting in downstream signalling [21–23]. Over the years various signalling molecules that are involved in CXCR4 triggered migration have been identified, however there is still some uncertainty about which pathways are directly involved in cell migration.

**Abbreviations:** DMEM, Dulbecco's Modified Eagle's Medium; EDTA, ethylenediaminetetraacetic acid; FCS, foetal calf serum; GPCR, G protein coupled receptor; mAb, monoclonal antibody; n.s., non-significant; PBS, phosphate buffered saline; PKC, Protein Kinase C; S.E.M., standard error of means.

\* Corresponding author.

E-mail address: [anja.mueller@uea.ac.uk](mailto:anja.mueller@uea.ac.uk) (A. Mueller).

<http://dx.doi.org/10.1016/j.cellsig.2016.01.006>

0898-6568/Crown Copyright © 2016 Published by Elsevier Inc. All rights reserved.

For CXCR4 it has been shown that migration under certain circumstances is dependent on  $\beta$ -arrestins as well as filamin-A, a protein, which can bind actin and interacts with  $\beta$ -arrestins [24–26]. Several groups have shown that ERK1/2 or p38 MAPK activation is important for cell migration as well [13,27]. Similarly, Protein Kinase C $\epsilon$  (PKC $\epsilon$ ) activation has been shown to be implicated in the movement of T cells [28] and atypical Protein Kinase C $\zeta$  (PKC $\zeta$ ) is directly involved in CXCL12 signalling in immature human CD34<sup>+</sup>-enriched cells and in leukemic pre-B Acute Lymphocytic Leukaemia (ALL) G2 cells [29]. There is still some discussion whether JAK kinase activity is needed for migration or not, with some reports showing that in murine neural progenitor cells JAK activation is not necessary [30] whereas in metastatic T-lymphoma JAK activation is essential for migration [31]. Of particular interest in this respect is a study by Pfeiffer et al. [32] where the JAK2 inhibitor AG490 only inhibited CXCL12 induced adhesion in NCI-H82 and not in NCI-H69 cells. These data show that the signalling networks which are used by CXCL12 and its receptor CXCR4 probably vary between different species and cell types. Subsequently, we determined in this study whether the pharmacological blockade of different signalling cascades like the MEK/ERK1/2 kinase cascade or JAK/STAT differentially block CXCL12 induced cell migration in leukemic cells versus adherent breast cancer cells.

## 2. Materials and methods

### 2.1. Cells and materials

The leukemic cell line Jurkat was obtained from the ATCC and grown in RPMI containing 10% FCS and 2 mM L-glutamine. The breast cancer cell line MCF-7 was obtained from the ATCC and grown in DMEM containing 10% FCS and 2 mM L-glutamine. The chemokine CXCL12 was obtained from Peprotech. JAK inhibitor 2 (1,2,3,4,5,6-Hexabromocyclohexane, JAK-2) and STAT3 inhibitor VIII, 5,15-DPP (STAT3 VIII) were from Calbiochem. LY294002, AG490, Bosutinib, Rottlerin, GF109203X, Staurosporine and CID755673 were purchased from Tocris. Farnesyl thiosalicylic acid (FTS), SB203580, PD98059, L775450, FH535 and SL327 were from Abcam. Cells were treated with 10  $\mu$ M LY294002, 50  $\mu$ M JAK2, 50  $\mu$ M STAT3 VIII, 5  $\mu$ M GF109203X, 10 nM Staurosporine, 11  $\mu$ M CID755673, 10  $\mu$ M AG490, 5  $\mu$ M Bosutinib, 12.5  $\mu$ M FTS, 10  $\mu$ M SB203580, 12.5  $\mu$ M & 25  $\mu$ M PD98059, 0.5 & 1  $\mu$ M L775450, 1  $\mu$ M FH535, 1  $\mu$ M SL327 and 4  $\mu$ M Rottlerin for 30 min before induction of chemotaxis. Anti-CXCR4 antibody 12G5 was from Santa Cruz and the corresponding goat anti-mouse FITC labelled secondary antibody came from Sigma Aldrich. Anti-PKC $\alpha$  (H-7), anti-PKC $\zeta$  and  $\beta$ -actin antibodies were purchased from Santa Cruz. Anti-Src and anti-Pi3K p85 were

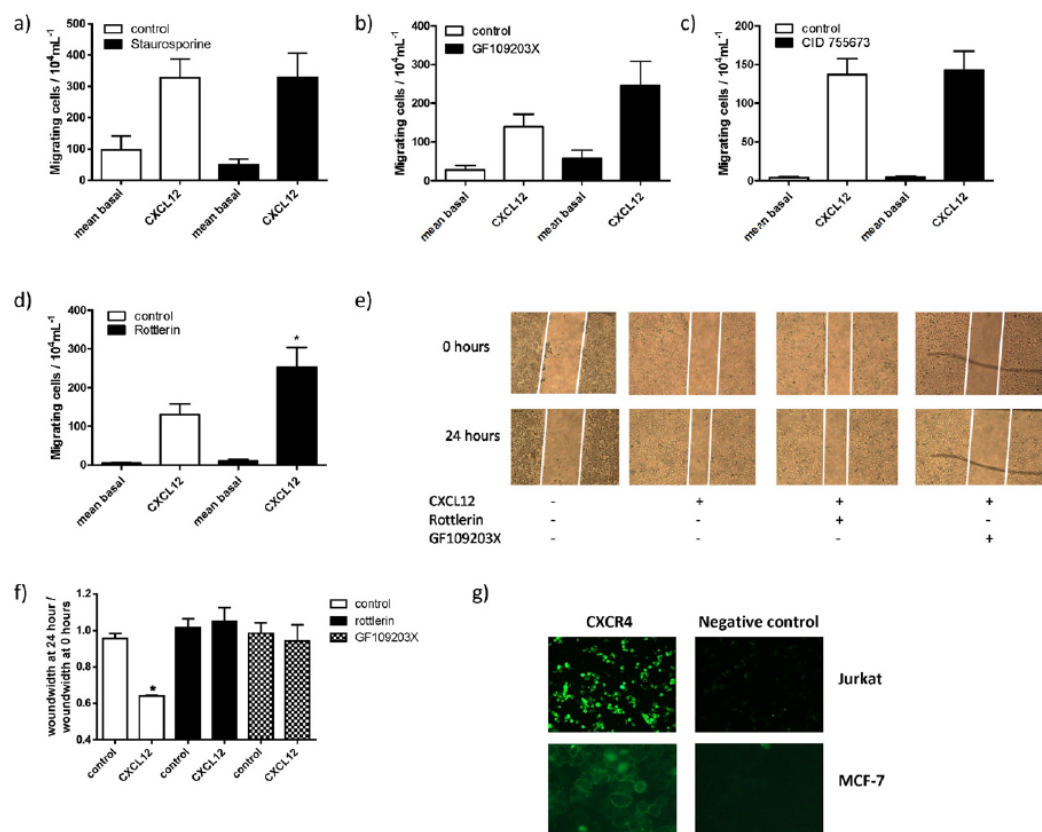


Fig. 1. PKC and PKD activation is not essential for CXCL12 induced migration. a) Shows migratory response of Jurkat cells towards 1 nM CXCL12 in untreated control cells or Staurosporine pre-treated cells. b) Cell migration towards 1 nM CXCL12 in untreated control cells or GF109203x pre-treated cells. c) Cell migration towards 1 nM CXCL12 in untreated control cells or CID755673 pre-treated cells. d) Cell migration towards 1 nM CXCL12 in untreated control cells or Rottlerin pre-treated cells. e) Wound healing assay on MCF-7 cells in the presence or absence of Rottlerin or GF109203X. Cell migration was induced with 10 nM CXCL12 and measured after 24 h. f) Quantification of migration of cells into the wound. A number 1 denotes no migration occurred whereas a number <1 denotes cell migration. \* denotes a significant difference towards to corresponding control ( $p \leq 0.05$ , One-way ANOVA with a Bonferroni Multiple Comparison test as post-test). g) CXCR4 was visualised on Jurkat and MCF-7 cells by 12G5 mAb staining. Data shown are the mean  $\pm$  S.E.M. of at least 3 independent experiments.



from Biotechne and the mouse peroxidase labelled secondary antibodies were from Sigma Aldrich. All other chemicals were obtained from Fisher Scientific.

## 2.2. Chemotaxis assays

Cells were harvested and then resuspended at a concentration of  $25 \times 10^4$  cells  $\text{mL}^{-1}$  in serum-free RPMI 1640 containing 0.1% BSA. Cells were loaded in a total volume of 20  $\mu\text{L}$  into the upper compartment of a microchemotaxis chamber (Receptor Technologies, Adderbury, UK). For inhibitor treatment, cells were incubated for 30 min with the relevant inhibitors or vehicle control before loading onto the membrane. Chemoattractants at a concentration of 1 nM were loaded in a final volume of 31  $\mu\text{L}$  at indicated concentrations in the lower compartment. The two compartments were separated by a polyvinylpyrrolidone-free polycarbonate filter with 5  $\mu\text{m}$  pores. The chemotaxis chamber was incubated at 37 °C, 100% humidity, and 5%  $\text{CO}_2$  for 4 h. The filter was then removed, and the number of cells migrating into each bottom compartment was counted using a haemocytometer. In all experiments, each data point was performed in duplicate.

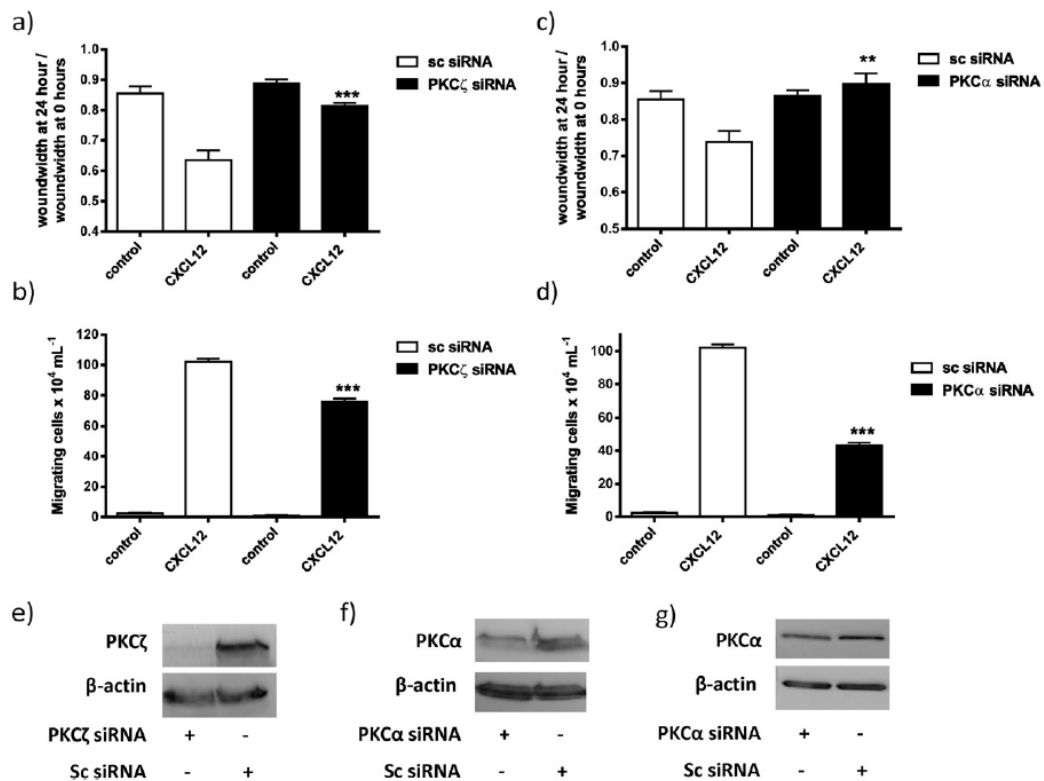
## 2.3. Wound healing assays

MCF-7 cells were seeded onto 24 well plates overnight. After 24 h, the cells were washed once in DMEM without supplements and

incubated in DMEM without supplements. A scratch was introduced to the monolayer with 200  $\mu\text{L}$  pipette tips (time point 0). Inhibitors were added to the cells and incubated for 30 min at 37 °C, 100% humidity, and 5%  $\text{CO}_2$ . Chemokines or vehicle controls were added to the cells and pictures were taken at time point 0 and after 24 h using an inverted Leica microscope. Images were analysed and the width of the wound was measured for control and with inhibitor treatment (with and without chemokine) at 0 h and 24 h. The ratio of the width of the wound after 24 h divided by the width of the wound at 0 h can then be used to compare the effectiveness of treatments in preventing migration, where a number 1 denotes no migration and a number smaller than 1 denotes migration of cells.

## 2.4. Cell viability studies

MTS assays were performed using a CellTiter 96® Aqueous Non-Radioactive Cell Proliferation Assay (Promega). 100  $\mu\text{L}$  wells containing  $5 \times 10^5$  cells  $\text{mL}^{-1}$  in complete RPMI supplemented with the test compounds at working concentrations were maintained at 37 °C and 5%  $\text{CO}_2$  for 2 h in a humidified atmosphere. After incubation, cell viability was assessed using the CellTiter 96® Aqueous One Solution Cell Proliferation Assay. The 3-(4,5-dimethylthiazol-2-yl)-5-(3-carboxymethoxyphenyl)-2-(4-sulfophenyl)-2H-tetrazolium (MTS) tetrazolium compound is bioreduced by cells into a coloured formazan product that is soluble in tissue culture medium [33]. This conversion is presumably



**Fig. 2.** siRNA transfection into MCF-7 cells and Jurkat cells. a) Wound healing assay on MCF-7 cells after transfection with scrambled control siRNA (sc siRNA) or PKCζ siRNA. Cell migration was induced with 10 nM CXCL12 and measured after 24 h. b) Cell migration towards 1 nM CXCL12 in Jurkat cells after transfection with scrambled control siRNA (sc siRNA) or PKCζ siRNA. c) Wound healing assay on MCF-7 cells after transfection with scrambled control siRNA (sc siRNA) or PKCα siRNA. Cell migration was induced with 10 nM CXCL12 and measured after 24 h. d) Cell migration towards 1 nM CXCL12 in Jurkat cells after transfection with scrambled control siRNA (sc siRNA) or PKCα siRNA. e, f) Western blot analysis of PKCζ and PKCα expression in MCF-7 after knockdown, β-actin acts as loading control. g) Western blot analysis of PKCα expression in Jurkat cells after knockdown, β-actin acts as loading control. Quantification of migration of cells into the wound. A number 1 denotes no migration occurred whereas a number <1 denotes cell migration. \*\* denotes a significant difference towards the corresponding control (\*\* =  $p \leq 0.01$ , \*\*\* =  $p \leq 0.001$ , One-way ANOVA with a Bonferroni Multiple Comparison test as post-test). Data shown are the mean  $\pm$  S.E.M. of at least 3 independent experiments.

accomplished by NADPH or NADH produced by dehydrogenase enzymes in metabolically active cells [34]. Aliquots of 20  $\mu\text{L}$  of the CellTiter 96® Aqueous One Solution Reagent were added directly to the wells and the plates were incubated for 4 h at 37 °C in a humidified atmosphere, 5%  $\text{CO}_2$  and then absorbance at 490 nm was read with a 96-well plate reader. The quantity of formazan product as measured by the absorbance at 490 nm is directly proportional to the number of living cells in culture. The inhibitors were used at concentrations which did not show any toxic effects over a 6 h incubation period.

## 2.5. Immunofluorescence staining

The Jurkat cell line was washed in PBS and re-suspended at a concentration of  $5 \times 10^6$  cells  $\text{mL}^{-1}$  in PBS and were incubated at 4 °C with CXCR4 mAb 12G5 or isotype control for 1 h. Cells were washed twice in cold PBS staining was performed using fluorescein isothiocyanate (FITC) labelled donkey anti-mouse immunoglobulin secondary antibodies (1:100, Sigma Aldrich) for 1 h at 4 °C. Cells were then washed in PBS and dropped onto a glassslide and pictures taken with an inverted Leica DMII fluorescence microscope. MCF-7 cells were seeded on coverslips overnight, washed with PBS and stained with 12G5 or isotype control as described above.

## 2.6. siRNA transfection

PKC $\alpha$ , PKC $\zeta$  siRNA and scrambled siRNA were obtained from Qiagen (Hilden, Germany), PI3K and Src siRNA were obtained from GE Healthcare (UK) and diluted to working concentrations in RNase free water. Jurkat cells were transfected with 50 nM scrambled siRNA, 50 nM PKC $\alpha$  or PKC $\zeta$  siRNA or vehicle, respectively, using the Amaxa Nucleofector according to the manufacturer's instructions. In short  $3 \times 10^6$  cells per cuvette were used for the transfection and after 48 h a chemotaxis assay was performed. The MCF-7 cells were transfected using Lipofectamine RNAi (ThermoFisher Scientific) according to the manufacturer's instruction.

## 2.7. SDS-PAGE and Western blot

Cells were harvested and then resuspended in Mammalian Protein Extraction Buffer (GE Healthcare) at 4 °C for 30 min with gentle mixing. Analysis of the proteins on SDS-PAGE was done as described [35]. Antibodies were removed from the membrane before a second stain by incubation with Millipore Stripping Solution (Millipore, Temecula California) at room temperature for 15 min before blocking and reprobing.

## 2.8. Analysis of data

Data were analysed using GraphPad Prism (GraphPad Software). Statistical analyses were performed using a One-way ANOVA with a *post-hoc* Bonferroni Multiple Comparison test with a *p* value <0.05. Data represent the mean  $\pm$  S.E.M. of at least three independent experiments.

## 3. Results

### 3.1. PKC activation is vital for cell migration in breast cancer cell, but less so in leukemic cells

CXCR4 induced cell migration is depending on a plethora of intracellular proteins, which need to become activated to allow the cell to move towards the chemokine stimulus. Here we investigated different signalling cascades and whether they are implicated in CXCR4 migration in suspension cells versus adherent cells. We have recently shown that PKC activation is not essential for CCL3 induced migration of the suspension cell line THP-1 [36]. In a similar fashion, we used two PKC inhibitors which block a wide variety of PKC isoforms (Staurosporine and GF109203X) as well as the more specific PKD inhibitor CID755673 and Rottlerin, which has been described as a selective PKC $\delta$ , but has since been found to block other kinases and to uncouple mitochondria [37]. All four inhibitors used did not block migration in Jurkat cells induced by CXCL12 (Fig. 1a–d). The only significant effect was observed

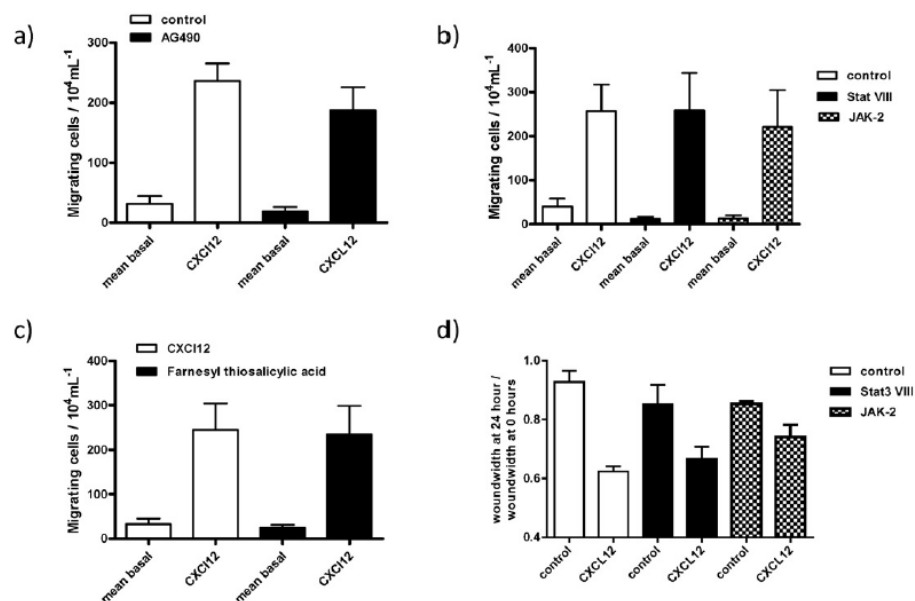


Fig. 3. Jak/STAT activation is not essential for CXCL12 induced migration. a) Shows migratory response of Jurkat cells towards 1 nM CXCL12 in untreated control cells or AG490 pre-treated cells, there is no significant differences between the inhibitor treated cells and control cells in the presence of CXCL12. b) Cell migration towards 1 nM CXCL12 in untreated control cells or Stat VIII or Jak-2 pre-treated cells. c) Cell migration towards 1 nM CXCL12 in untreated control cells or farnesyl thiosalicylic acid pre-treated cells. Data shown are the mean  $\pm$  SEM of at least 3 experiments.

with Rotterlin, which actually increases the number of cells migrating. However, in wound healing assays on the breast cancer cell line MCF-7, both Rotterlin and GFI09203X exhibit the opposite effect. In these cells, they prevent migration of cells into the wound effectively after 24 h (Fig. 1e, f). Expression of CXCR4 in both cell lines was confirmed using a monoclonal antibody against CXCR4 (Fig. 1g). siRNA knockdown of PKC $\alpha$  and PKC $\zeta$  proteins in MCF-7 cells confirmed the importance of PKC for migration in these cells (Fig. 2a, c), where the loss of PKC $\alpha$  and PKC $\zeta$  completely abolishes any migration towards CXCL12. Whereas transfection of PKC $\alpha$  and PKC $\zeta$  siRNA into Jurkat cells allows us to differentiate between the use of different PKC isoforms. PKC $\alpha$  knockdown leads to a loss of about half the migratory response, whereas the PKC $\zeta$  knockdown has less impact. In both cases, there are still a robust number of cells migrating, even though the migration is significantly lower than in control cells (transfected with scrambled siRNA) (Fig. 2b, d), unlike the MCF-7 cells (Fig. 2a, c), where the knockdown of PKC $\alpha$  and PKC $\zeta$  completely prevents movement of cells into the wound. The success of knockdown was confirmed by Western blot analysis (Fig. 2e, f, g).

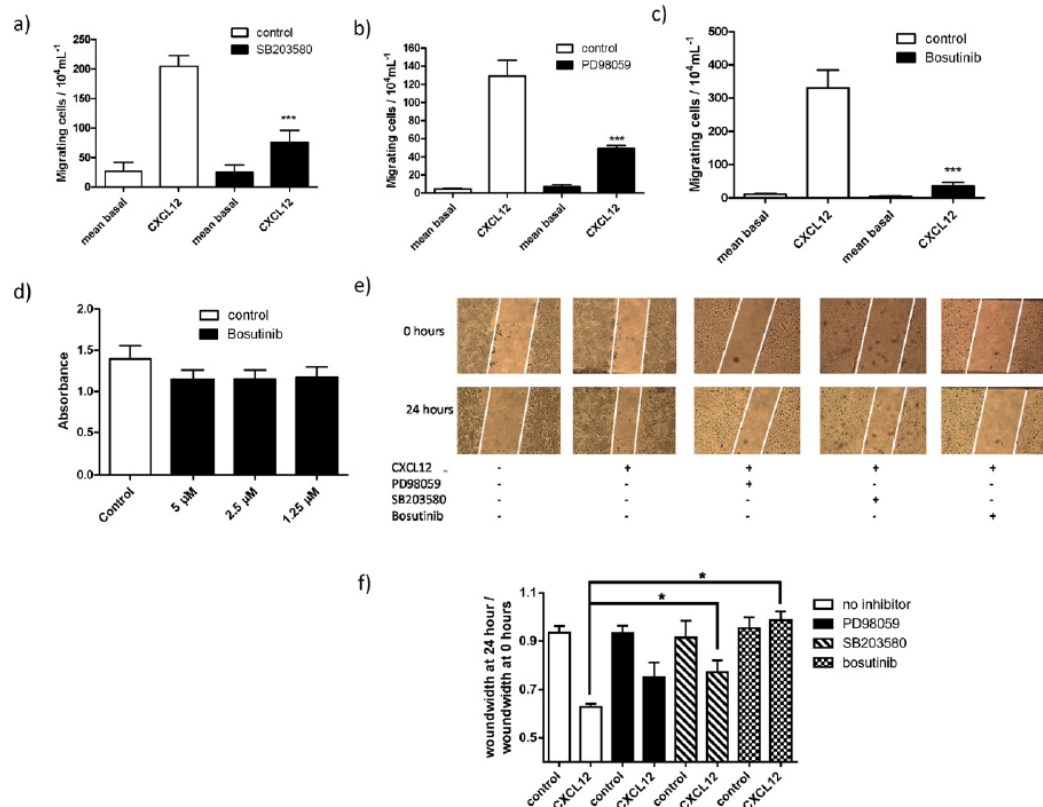
### 3.2. JAK2 and STAT3 activation is not necessary for migration of leukemic cells

We then investigated whether there are other pathways that are important in cell migration. We used inhibitors to block JAK2 and STAT3

activation (Fig. 3a, b), but none blocked CXCL12 induced migration in Jurkat cells. Similarly, a Ras inhibitor, Farnesylthiosalicylic acid, did not affect Jurkat migration towards CXCL12 (Fig. 3c). The Ras inhibitor shows toxicity in MCF-7 cells after 24 h (data not shown) and is therefore not suitable for wound healing assays, even at lowered concentrations. Similarly, the JAK2 and STAT3 inhibitors affect cell viability over 24 h at 10  $\mu$ M, at the lower concentration of 1  $\mu$ M both inhibitors do not show any toxicity. Whereas the STAT3 inhibitor does not affect cell migration into the wound, the effect of the JAK2 inhibitor is less clear; there seems to be a slight trend to block migration, but it was not significant (Fig. 3d).

### 3.3. Src activation is vital for both breast cancer cell as well as leukemic cell migration

Another signalling cascade, which has been highlighted as being involved in CXCR4 induced migration, is the Raf/MEK/ERK network. Cells were pre-treated with SB203580, an inhibitor of p38 MAPK, PD98059, a small molecule inhibitor targeting MEK specifically or Bosutinib, a Src inhibitor. Blocking p38 MAPK, MEK and Src resulted in around 50% reduction in migration (Fig. 4). This reduction in migrating cells is not a consequence of any toxicity of Bosutinib, as shown by MTS assays (Fig. 4d). Again, there are significant differences in MCF-7 cells. Even though the Src inhibitor Bosutinib completely blocked any migration



**Fig. 4.** CXCL12 induced migration depends on Src, p38 MAPK and MEK activation. a) Shows migratory response of Jurkat cells towards 1 nM CXCL12 in untreated control cells or SB203580 pre-treated cells. b) Cell migration towards 1 nM CXCL12 in untreated control cells or 25  $\mu$ M PD98059 pre-treated cells. c) Cell migration towards 1 nM CXCL12 in untreated control cells or 2.5  $\mu$ M Bosutinib pre-treated cells. Statistical analyses were performed using a one-way ANOVA with a Bonferroni multiple comparison test as post-test with \*\*\* showing a p value of  $\leq 0.001$ . d) MTS assay in Jurkat cells with different concentrations of Bosutinib, as indicated. e) Wound healing assay on MCF-7 cells in the presence or absence of PD98059, SB203580 or Bosutinib. Cell migration was induced with 10 nM CXCL12 and measured after 24 h. f) Quantification of migration of cells into the wound. 1 denotes no migration occurred whereas a number  $< 1$  denotes cell migration. \* denotes a significant difference towards to inhibitor treated/untreated cells in the presence of CXCL12 ( $p \leq 0.05$ , One-way ANOVA with a Bonferroni Multiple Comparison test as post-test). Data shown are the mean  $\pm$  S.E.M. of at least 3 experiments.



of MCF-7 cells into the wound, both the ERK1/2 inhibitor PD98059 and the p38 MAPK inhibitor SB203580 did not show a pronounced blocking of cell migration, however the wound in the SB203580 treated cells remained significantly larger than in the control cells (Fig. 4e, f). We verified the results obtained with Bosutinib with a siRNA approach. A knock down of Src prevents migration of Jurkat cells as well as the migration of MCF-7 cells in a wound-healing assay (Fig. 5a, b). The efficiency of knockdown was confirmed by Western blot analysis (Fig. 5e).

#### 3.4. PI3K activation is important for leukemic cell migration but not in wound-healing assays

To further evaluate which signalling partners are involved in transducing receptor activation to cell migration, we used a second MEK inhibitor (SL327) as well as the well-established PI3K inhibitor (LY294002), Raf (L779450) and  $\beta$ -catenin (FH535) inhibitors and we also knocked down p85 PI3K using a siRNA approach (Fig. 5c, d, e, f). Whereas the knock down of PI3K in Jurkat and MCF-7 cells prevented migration significantly, the results with a small molecule antagonist LY294002 were less clear. The blockade of PI3K completely abolishes any migration in Jurkat cells and the other inhibitors led to a small, but significant decrease of migrating suspension cells (Fig. 6). In the adherent MCF-7 cells there are some differences. Whereas the effect of blocking migration by L775450 is much more pronounced, LY294002

fails to show a significant effect on these cells (Fig. 6e). We verified that in Jurkat cells the migration towards CXCL12 is in response to CXCR4 with the use of a monoclonal antibody directed against CXCR4 which blocks migration (Fig. 6g).

#### 4. Discussion

Chemokine receptor induced cell migration is a crucial step in metastasis of cancer as well as the inflammatory response [23]. Understanding the mechanisms of migration therefore can potentially provide novel therapeutic targets to prevent undesirable cell migration. The chemokine receptor CXCR4 has been of interest for a number of years, as it has been shown to be up-regulated in several cancers and its activation can lead to cancer cell metastasis [23,38–41]. Although numerous studies have investigated different aspects of the signalling cascades which are involved in the cell migration, some questions still remain unanswered. Furthermore, there is conflicting evidence in the literature about the importance or involvement of downstream signalling partners in different systems [11,27–29,38,42–44]. One problem is that most studies only characterised a small number of signalling molecules at any one time and since a whole variety of cell types/read-out systems and approaches were used, it can be expected that some of the data may contradict each other. We therefore set out to investigate the main signalling molecules that are thought to be of importance in

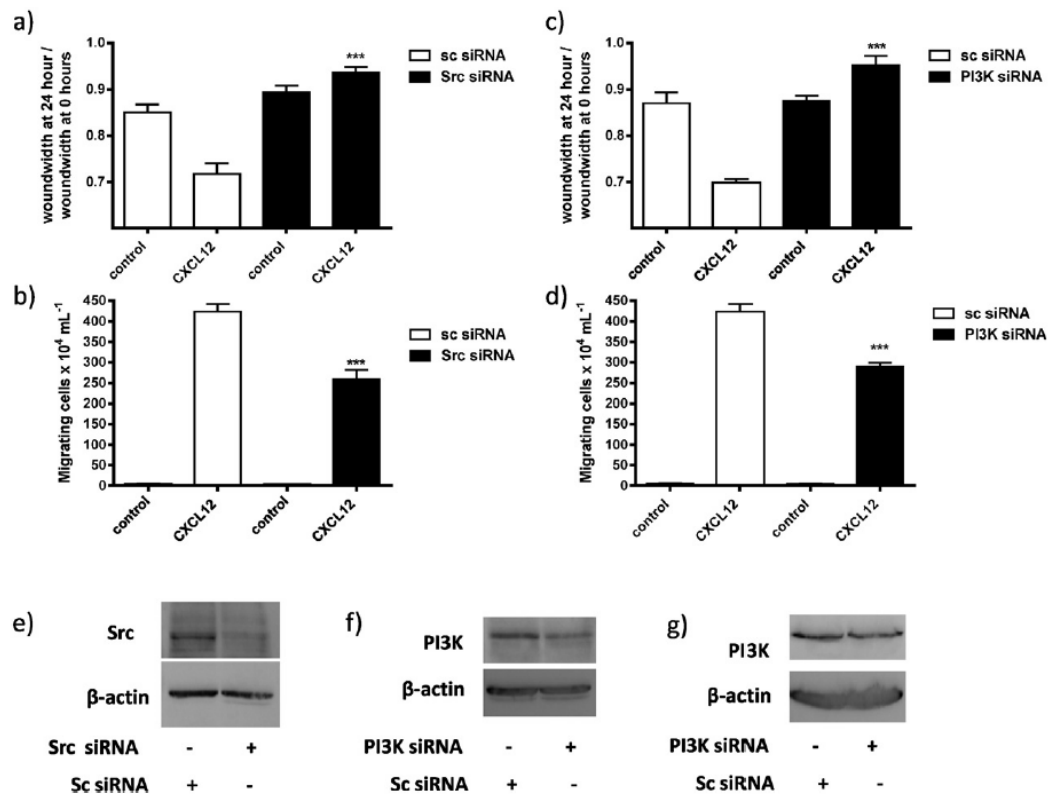


Fig. 5. siRNA transfection into MCF-7 cells and Jurkat cells. a) Wound healing assay on MCF-7 cells after transfection with scrambled control siRNA (sc siRNA) or Src siRNA. Cell migration was induced with 10 nM CXCL12 and measured after 24 h. b) Cell migration towards 1 nM CXCL12 in Jurkat cells after transfection with scrambled control siRNA (sc siRNA) or Src siRNA. c) Wound healing assay on MCF-7 cells after transfection with scrambled control siRNA (sc siRNA) or PI3K siRNA. Cell migration was induced with 10 nM CXCL12 and measured after 24 h. d) Cell migration towards 1 nM CXCL12 in Jurkat cells after transfection with scrambled control siRNA (sc siRNA) or PI3K siRNA. e, f) Western blot analysis of Src and PI3K expression in MCF-7 after knockdown,  $\beta$ -actin acts as loading control. g) Western blot analysis of PI3K expression in Jurkat cells after knockdown,  $\beta$ -actin acts as loading control. Quantification of migration of cells into the wound. A number 1 denotes no migration occurred whereas a number <1 denotes cell migration. \*\* denotes a significant difference towards the corresponding control (\*\* =  $p \leq 0.01$ , \*\*\* =  $p \leq 0.001$ , One-way ANOVA with a Bonferroni Multiple Comparison test as post-test). Data shown are the mean  $\pm$  S.E.M. of at least 3 independent experiments.



of a CXCR4 specific antibody prevents migration of cells, showing that CXCR4 is the main receptor, if not the only one on these cells to induce migration in response to CXCL12 (see Fig. 7 for overview).

Protein Kinase C (PKC) has been shown to have central roles in signalling in response to many extracellular ligands, and can influence many aspects of cell behaviour. Several groups have shown that receptor desensitisation is not necessarily based only on phosphorylation of agonist-occupied receptors by G-protein coupled receptor kinases (GRK) but also can be caused by phosphorylation of receptors by second messenger-activated kinases such as Protein Kinase C, to attenuate receptor interaction with G-proteins. Oppermann et al. [45] have shown the equivalence in importance of both GRK and second messengers PKC in phosphorylation of receptors. Second messenger-activated kinases, Protein Kinase A (PKA) and PKC potentially phosphorylate both the ligand bound GPCR and multiple other receptors in a heterologous manner [46]. There are a variety of studies that show that PKC isoforms are also important for cancer cell migration [10,47] and indeed, a pan PKC inhibitor GF109203X completely blocks breast cancer cell migration towards CXCL12; however at the same concentration there is no effect on the migration of the leukemic suspension cells towards CXCL12. Instead, GF109203X leads to a slight, if not significant, increase in migration. This agrees with a previous study of our lab, where we showed that the same PKC inhibitor does not block CCL3 induced migration in the suspension cells THP-1 [36]. We used a siRNA approach to confirm the results obtained with the small molecule antagonists, and indeed, a knock down of PKC $\alpha$  and PKC $\zeta$  in MCF-7 cells completely abrogates any movement of the cells into the wound, confirming the results obtained with the PKC inhibitors. The picture in Jurkat cells is slightly more complicated. Both PKC $\alpha$  and PKC $\zeta$  knockdowns result in a significant loss of migratory cells which is in stark contrast to the PKC inhibitor studies. We therefore speculate that there is a difference in usage of PKC in the two cell types. Whereas the MCF-7 cells need the catalytic activity of PKC (hence a small molecule antagonist as well as knock down prevents migration) in Jurkat cells it seems plausible, that it is not the kinase activity of PKC which is implicated in cell migration, it is rather the functionality of the other PKC domains. For example PKCs localise in cells with cytoskeletal proteins (such as actin and tubulin) and true scaffolding proteins (such as caveolin) and might therefore be implicated in migration. It has also been shown that PKCs can be cleaved by caspases, generating a catalytically active kinase domain and a freed regulatory domain fragment that can act both as an inhibitor of the full-length enzyme and as an activator of certain signalling responses [48]. Altogether the data in Jurkat cells are more complex, but they show a difference towards PKC use in MCF-7 cells and warrant further investigation.

The JAK/STAT pathway has been implicated for being an essential pathway in cell migration for some time [49], however recent studies showed that some of the results could be due to the effects some inhibitors have on actin dynamics in cells [50,51] or that JAK activation is not important for chemokine induced activation after all [30]. Using a variety of different JAK2/STAT3 inhibitors, we did not detect a significant effect of JAK2/STAT3 inhibition on migration in both leukemic or breast cancer cells.

In keeping with the findings of other groups studying aspects of CXCL12 signalling in a variety of cell types [42,52] Src kinase activation is critical migration in both leukemic and breast cancer cells. We have also confirmed that the Raf/MEK/ERK1/2 pathway plays an important role in leukemic cell migration with a somewhat diminished importance in breast cancer cells. Unlike Sobolik et al., who showed that in a 3D model, inhibition of PI3K reversed the aggressive phenotype of MCF-7 [53], we did not observe a significant effect of PI3K inhibition on wound-healing in a 2D model when using LY294002. Knock down of PI3K p85 expression in MCF-7 cells, abrogates any migration towards CXCL12 in the wound healing assay, confirming published studies. In Jurkat cells, PI3K inhibition significantly reduces cell migration, whether it is the use of LY294002 or the knock down of protein expression.

Our study highlights that the cellular background can be important for the distinct signalling pathways used by the CXCR4 receptor and therefore a generalisation of how CXCR4 induces migration in different cell types and species should be avoided. There are quite a few similarities between the different cell types, however some subtle differences mean that there is the potential to block migration of specific cancer cell types when targeting metastases.

## Acknowledgments

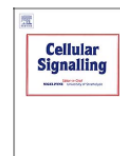
We acknowledge the support for SCM from the Novartis studentship fund (3890392RA1) and we thank the Government of His Majesty The Sultan and Yang Di-Pertuan Negara Brunei Darussalam and the Ministry of Education, Negara Brunei Darussalam for providing a studentship for PHG (3753182RA1).

## References

- [1] X.H.F. Zhang, Q. Wang, W. Gerald, C.A. Hudis, L. Norton, M. Smid, J.A. Foekens, J. Massague, *Cancer Cell* 16 (2009) 67–78.
- [2] S.E. Wang, J. Signal Transduct. 2011 (2011) 804236.
- [3] A. de Lourdes Perim, M.K. Amarante, R.L. Guembarovski, C.E.C. de Oliveira, M.A.E. Watanabe, *Cell. Mol. Life Sci.* 72 (2015) 1715–1723.
- [4] H. Reikvam, M. Hauge, A.K. Brenner, K.J. Hatfield, Ø. Bruserud, *Expert. Rev. Hematol.* (2015) 1–15.
- [5] D. Hanahan, R.A. Weinberg, *Cell* 144 (2011) 646–674.
- [6] K. Polyak, R.A. Weinberg, *Nat. Rev. Cancer* 9 (2009) 265–273.
- [7] M.W. Klymkowsky, P. Savagner, *Am. J. Pathol.* 174 (2009) 1588–1593.
- [8] A. Zlotnik, *Int. J. Cancer* 119 (2006) 2026–2029.
- [9] J. Vandercappellen, J. Van Damme, S. Struyf, *Cancer Lett.* 267 (2008) 226–244.
- [10] J.Y. Chuang, W.H. Yang, H.T. Chen, C.Y. Huang, T.W. Tan, Y.T. Lin, C.J. Hsu, Y.C. Fong, C.H. Tang, *J. Cell. Physiol.* 220 (2009) 418–426.
- [11] J.K. Kirui, Y. Xie, D.W. Wolff, H. Jiang, P.W. Abel, Y. Tu, J. Pharmacol. Exp. Ther. 333 (2010) 393–403.
- [12] D. Raman, T. Sobolik-Delmaire, A. Richmond, *Exp. Cell Res.* 317 (2011) 575–589.
- [13] L.J. Drury, J.J. Ziarek, S. Gravel, C.T. Veldkamp, T. Takekoshi, S.T. Hwang, N. Heveker, B.F. Volkman, M.B. Dwinell, *Proc. Natl. Acad. Sci. U. S. A.* 108 (2011) 17655–17660.
- [14] S. Konoplev, P. Lin, C.C. Yin, E. Lin, G.M. Nogueras Gonzalez, H.M. Kantarjian, M. Andreeff, L.J. Medeiros, M. Konopleva, *Clin. Lymphoma Myeloma Leuk.* 13 (2013) 686–692.
- [15] B.A. Teicher, S.P. Fricker, *Clin. Cancer Res.* 16 (2010) 2927–2931.
- [16] L. Patrussi, N. Capitani, E. Cannizzaro, F. Finetti, O.M. Lucherini, P.G. Pellicci, C.T. Baldari, *Cell Death Dis.* 5 (2014) e1068.
- [17] E.A.R. Sison, D. Magoon, L. Li, C.E. Annesley, R.E. Rau, D. Small, P. Brown, *Oncotarget* 5 (2014) 8947–8958.
- [18] T. Masuda, M. Endo, Y. Yamamoto, H. Odagiri, T. Kadomatsu, T. Nakamura, H. Tanoue, H. Ito, M. Yugami, K. Miyata, J. Morinaga, H. Horiguchi, I. Motokawa, K. Terada, M.S. Morioka, I. Manabe, H. Iwase, H. Mizuta, Y. Oike, *Sci. Rep.* 5 (2015) 9170.
- [19] S. Cane, S. Ponnappan, U. Ponnappan, *Aging Cell* 11 (2012) 651–658.
- [20] I. Roy, N.P. Zimmerman, A.C. Mackinnon, S. Tsai, D.B. Evans, M.B. Dwinell, *PLoS One* 9 (2014) e90400.
- [21] R.J.B. Nibbs, G.J. Graham, *Nat. Rev. Immunol.* 13 (2013) 815–829.
- [22] B. Boldajipour, H. Mahabaleswar, E. Kardash, M. Reichman-Fried, H. Blaser, S. Minina, D. Wilson, Q. Xu, E. Raz, *Cell* 132 (2008) 463–473.
- [23] F. Bachelier, A. Ben-Baruch, A.M. Burkhardt, C. Combadiere, J.M. Farber, G.J. Graham, R. Horuk, A.H. Sparre-Ulrich, M. Locati, A.D. Luster, A. Mantovani, K. Matsushima, P.M. Murphy, R. Nibbs, H. Nomiyama, C.A. Power, A.E. Proudfoot, M.M. Rosenkilde, A. Rot, S. Sozzani, M. Thelen, O. Yoshie, A. Zlotnik, *Pharmacol. Rev.* 66 (2014) 1–79.
- [24] N.L. Coggins, D. Trakimas, S.L. Chang, A. Ehrlich, P. Ray, K.E. Luker, J.J. Linderman, G.D. Luker, *PLoS One* 9 (2014) e98328.
- [25] B. Lagane, K.Y. Chow, K. Balabanian, A. Levoye, J. Harriague, T. Planchenault, F. Baleux, N. Gunera-Saad, F. Arenzana-Seisdedos, F. Bachelier, *Blood* 112 (2008) 34–44.
- [26] Y. Sun, Z. Cheng, L. Ma, G. Pei, *J. Biol. Chem.* 277 (2002) 49212–49219.
- [27] I. Delgado-Martin, C. Escibano, J.L. Pablos, L. Riol-Blanco, J.L. Rodriguez-Fernandez, *J. Biol. Chem.* 286 (2011) 37222–37236.
- [28] S.T. Ong, M. Freeley, J. Skubis-Zegadlo, M.H. Fazil, D. Kelleher, F. Fresser, G. Baier, N.K. Verma, A. Long, *J. Biol. Chem.* 289 (2014) 19420–19434.
- [29] I. Petit, P. Goichberg, A. Spiegel, A. Peled, C. Brodie, R. Seger, A. Nagler, R. Alon, T. Lapidot, *J. Clin. Invest.* 115 (2005) 168–176.
- [30] B.L. Holgado, L. Martinez-Munoz, J.A. Sanchez-Alcaniz, P. Lucas, V. Perez-Garcia, G. Perez, J.M. Rodriguez-Frade, M. Nieto, O. Marin, Y.R. Carrasco, A.C. Carrera, M. Alvarez-Dolado, M. Mellado, *Mol. Neurobiol.* 48 (2013) 217–231.
- [31] F.J. Opdam, M. Kamp, R. de Bruijn, E. Roos, *Oncogene* 23 (2004) 6647–6653.
- [32] M. Pfeiffer, T.N. Hartmann, M. Leick, J. Catusse, A. Schmitt-Graeff, M. Burger, *Br. J. Cancer* 100 (2009) 1949–1956.
- [33] A.H. Cory, T.C. Owen, J.A. Barltrop, J.G. Cory, *Cancer Commun.* 3 (1991) 207–212.
- [34] M.V. Berridge, A.S. Tan, *Arch. Biochem. Biophys.* 303 (1993) 474–482.



- [35] A. Mueller, N.G. Mahmoud, M.C. Goedecke, J.A. McKeating, P.G. Strange, Br. J. Pharmacol. 135 (2002) 1033–1043.
- [36] C. Moyano Cardaba, R.O. Jacques, J.E. Barrett, K.M. Hassell, A. Kavanagh, F.C. Remington, T. Tse, A. Mueller, Biochem. Biophys. Res. Commun. 418 (2012) 17–21.
- [37] S.P. Soltoff, Trends Pharmacol. Sci. 28 (2007) 453–458.
- [38] P. Dillenburg-Pilla, V. Patel, C.M. Mikelis, C.R. Zarate-Blades, C.L. Doci, P. Amornphimoltham, Z. Wang, D. Martin, K. Leelahavanichkul, R.T. Dorsam, A. Masedunskas, R. Weigert, A.A. Molinolo, J.S. Gutkind, FASEB J. 29 (2015) 1056–1068.
- [39] Y. Sun, X. Mao, C. Fan, C. Liu, A. Guo, S. Guan, Q. Jin, B. Li, F. Yao, F. Jin, Tumour Biol. 35 (2014) 7765–7773.
- [40] D. Mukherjee, J. Zhao, Am. J. Cancer Res. 3 (2013) 46–57.
- [41] D.M. Ramsey, S.R. McAlpine, Bioorg. Med. Chem. Lett. 23 (2013) 20–25.
- [42] M. Cheng, K. Huang, J. Zhou, D. Yan, Y.L. Tang, T.C. Zhao, R.J. Miller, R. Kishore, D.W. Losordo, G. Qin, J. Mol. Cell. Cardiol. 81 (2015) 49–53.
- [43] Z. Wang, Q. Ma, Med. Hypotheses 69 (2007) 816–820.
- [44] M. Vicente-Manzanares, J.R. Cabrero, M. Rey, M. Perez-Martinez, A. Ursa, K. Itoh, F. Sanchez-Madrid, J. Immunol. 168 (2002) 400–410.
- [45] M. Oppermann, N.J. Freedman, R.W. Alexander, R.J. Lefkowitz, J. Biol. Chem. 271 (1996) 13266–13272.
- [46] B. Pollok-Kopp, K. Schwarze, V.K. Baradari, M. Oppermann, J. Biol. Chem. 278 (2003) 2190–2198.
- [47] J. Kim, S.H. Thorne, L. Sun, B. Huang, D. Mochly-Rosen, Oncogene 30 (2011) 323–333.
- [48] S.F. Steinberg, Physiol. Rev. 88 (2008) 1341–1378.
- [49] S. Brown, M.P. Zeidler, J.E. Hombria, Dev. Dyn. 235 (2006) 958–966.
- [50] D.A. Knecht, R.A. LaFleur, A.W. Kahsai, C.E. Argueta, A.B. Beshir, G. Fenteany, PLoS One 5 (2010) e14039.
- [51] S. Khabbazi, R.O. Jacques, C. Moyano Cardaba, A. Mueller, Cell Biochem. Funct. 31 (2013) 312–318.
- [52] A. De Luca, A. D'Alessio, M. Gallo, M.R. Maiello, A.M. Bode, N. Normanno, Cell Cycle 13 (2014) 148–156.
- [53] T. Sobolik, Y.J. Su, S. Wells, G.D. Ayers, R.S. Cook, A. Richmond, Mol. Biol. Cell 25 (2014) 566–582.



## Rac1 plays a role in CXCL12 but not CCL3-induced chemotaxis and Rac1 GEF inhibitor NSC23766 has off target effects on CXCR4



Shirley C. Mills, Lesley Howell<sup>1</sup>, Andrew Beekman, Leanne Stokes, Anja Mueller\*

School of Pharmacy, University of East Anglia, Norwich Research Park, Norwich NR4 7TJ, UK

### ARTICLE INFO

**Keywords:**  
Chemokine receptor  
Chemotaxis  
Antagonist  
Rac1  
Ligand bias

### ABSTRACT

Cell migration towards a chemotactic stimulus relies on the re-arrangement of the cytoskeleton, which is triggered by activation of small G proteins RhoA, Rac1 and Cdc42, and leads to formation of lamellipodia and actin polymerisation amongst other effects. Here we show that Rac1 is important for CXCR4 induced chemotaxis but not for CCR1/CCR5 induced chemotaxis. For CXCL12-induced migration via CXCR4, breast cancer MCF-7 cells are reliant on Rac1, similarly to THP-1 monocytes and Jurkat T-cells. For CCL3-induced migration via CCR1 and/or CCR5, Rac1 signalling does not regulate cell migration in either suspension or adherent cells. We have confirmed the involvement of Rac1 with the use of a specific Rac1 blocking peptide. We also used a Rac1 inhibitor EHT 1864 and a Rac1-GEF inhibitor NSC23766 to probe the importance of Rac1 in chemotaxis. Both inhibitors did not block CCL3-induced chemotaxis, but they were able to block CXCL12-induced chemotaxis. This confirms that Rac1 activation is not essential for CCL3-induced migration, however NSC23766 might have secondary effects on CXCR4. This small molecule exhibits agonistic features in internalisation and cAMP assays, whereas it acts as an antagonist for CXCR4 in migration and calcium release assays. Our findings strongly suggest that Rac1 activation is not necessary for CCL3 signalling, and reveal that NSC23766 could be a novel CXCR4 receptor ligand.

### 1. Introduction

Chemokines are small proteins produced by cells that can trigger cellular migration activated by G protein-coupled receptors (GPCRs), called chemokine receptors [1]. Particularly in cancer, it has been shown that these chemokine receptors play a critical role in inducing the migration of cancer cells to different parts of the body [2,3]. Several chemokine receptors are highly expressed on cancer cells, including CXCR4, CCR5 and CCR1 [4–10]. Chemokine receptors may initiate signalling through binding a ligand, a specific chemokine or a chemical. CXCL12 binds to and activates the CXCR4 and CXCR7 receptors, but it is thought that only CXCR4 activation leads to chemotaxis of cells [11]. CCL3 is a ligand for both CCR5 and CCR1; it can activate both receptors and lead to a migratory response in cells [12]. Several other ligands can also bind to either CCR1 or CCR5 or both [12,13]. In general, chemokine receptor activation leads to an activation of heterotrimeric G proteins and phosphorylation of the receptors via GRKs (G protein-coupled receptor kinases) or PKC (protein kinase c). This leads to the binding of arrestins to the phosphorylated form of the receptor and

causes receptor internalisation [12,14]. Traditionally it is thought that  $\beta\gamma$ -subunits of the G proteins induce migration via activation of PI3K [15], however we have recently shown that this seems not to be the case for CCL3-induced chemotaxis in THP-1 cells [16] whereas PI3K is important for CXCL12-induced migration [5]. Both CXCL12 and CCL3-induced migration relies on the activation of Src, whereas the involvement of PKC seems to be cell type dependant [5].

Re-arrangement of the actin cytoskeleton is of major importance for chemotaxis, and the small G proteins of the rho family (rho, rac and cdc42) play important roles in this [17]. Actin filament reorganization is a dynamic process that requires both actin polymerizing and depolymerizing factors [18]. Specifically, Cdc42 and Rac1 regulate filopodia and lamellipodia formation, respectively, while RhoA regulates stress fibres and focal adhesion [19]. It has been well documented that activation of chemokine receptors leads to the occurrence of actin stress fibres and membrane ruffling [20–22]. It has also been shown that the blocking of RhoA or ROCK (rho-activated kinase) prevents migration of cells [16]. However, it is not known how chemokines and their receptors regulate the actin cytoskeleton leading to metastasis of cancer

**Abbreviations:** AUC, Area under Curve; EDTA, Ethylenediaminetetraacetic acid; FCS, Foetal calf serum; FSC, Forward scatter; GPCR, G protein-coupled receptor; PBS, Phosphate buffered saline; SEM, Standard Error of Means; SSC, Side scatter

\* Corresponding author.

E-mail address: [anja.mueller@uea.ac.uk](mailto:anja.mueller@uea.ac.uk) (A. Mueller).

<sup>1</sup> Current address: School of Biological and Chemical Sciences, Queen Mary, Mile End Road, London, E1 4NS.

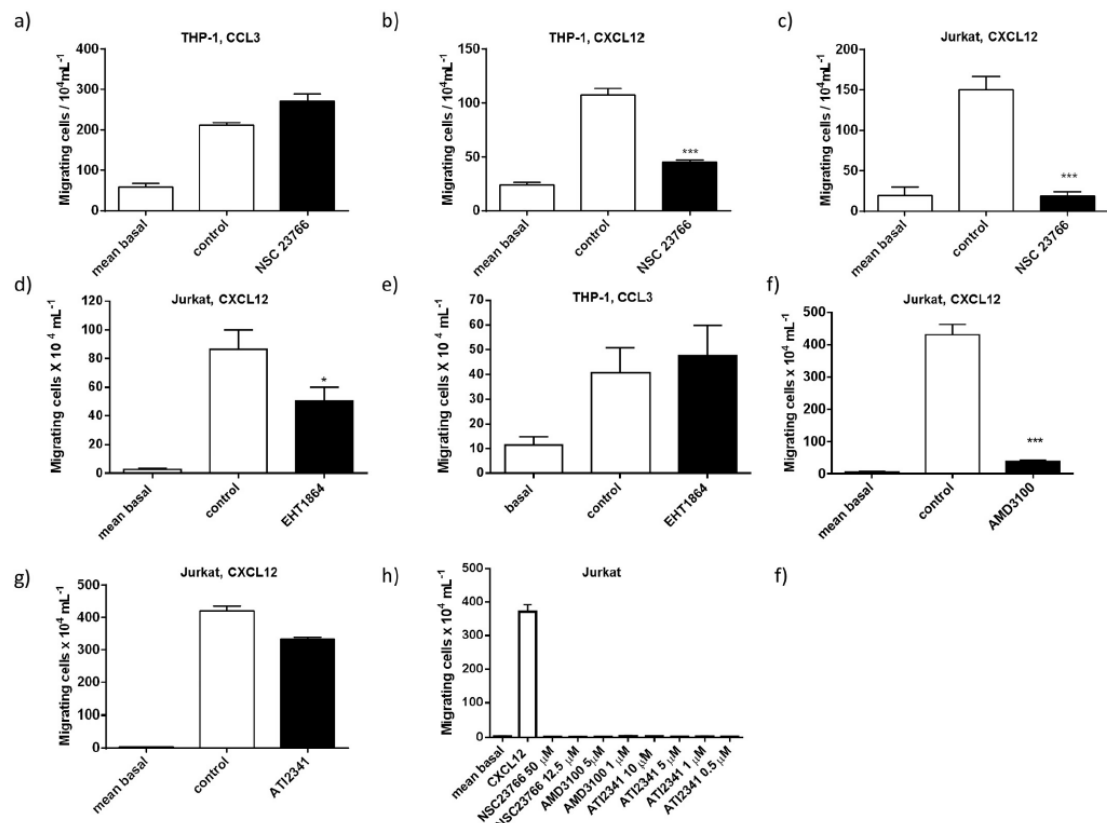
<http://dx.doi.org/10.1016/j.cellsig.2017.10.006>

Received 30 May 2017; Received in revised form 11 October 2017; Accepted 13 October 2017

Available online 16 October 2017

0898-6568/ Crown Copyright © 2017 Published by Elsevier Inc. All rights reserved.





**Fig. 1.** NSC23766 blocks CXCL12-induced chemotaxis but not CCL3. A) Shows migratory response of THP-1 cells towards 1 nM CCL3 in untreated control cells or 100 μM NSC23766 pre-treated cells. B) Cell chemotaxis towards 1 nM CXCL12 in untreated control cells or 100 μM NSC23766 pre-treated THP-1 cells. C) Cell chemotaxis towards 1 nM CXCL12 in untreated control cells or 100 μM NSC23766 pre-treated Jurkat cells. D) Cell chemotaxis towards 1 nM CXCL12 in untreated control cells or 100 nM EHT1864 pre-treated Jurkat cells. E) Cell chemotaxis towards 1 nM CCL3 in untreated control cells or 100 nM EHT1864 pre-treated THP-1 cells. F) Cell chemotaxis towards 1 nM CXCL12 in untreated control cells or 1 μM AMD3100 pre-treated Jurkat cells. G) Cell chemotaxis towards 1 nM CXCL12 in untreated control cells or 5 μM ATI2341 pre-treated Jurkat cells. H) Cell chemotaxis towards 1 nM CXCL12 or towards NSC23766, AMD3100 or ATI2341 as chemoattractants. Data shown are the mean  $\pm$  SEM of at least 3 independent experiments. (\* =  $p \leq 0.05$ , \*\*\* =  $p \leq 0.001$ , One-way ANOVA with a Tukey's multiple comparisons test as post-test).

cells [23,24]. In leukocytes, chemokine receptors control activation of a small G protein, Rac1, which induces growth of actin filaments. Recent studies have shown that Rac1 is associated with CXCL12-induced chemotaxis in breast cancer cells [24], as well as modulating cell invasion and tumour metastasis in human oesophageal cancer [25]. Direct association with Rac1 also seems to affect the conformation of CXCR4 [26] and therefore might affect chemokine binding to the receptor and activation of downstream signalling partners. In this study we examined the role of Rac1 in cell chemotaxis induced by two different chemokines, CCL3 and CXCL12 respectively, in different cellular backgrounds. These results highlight the importance of characterising cell signalling networks by single receptor, and not by families, as well as considering cellular background when analysing results.

## 2. Materials and methods

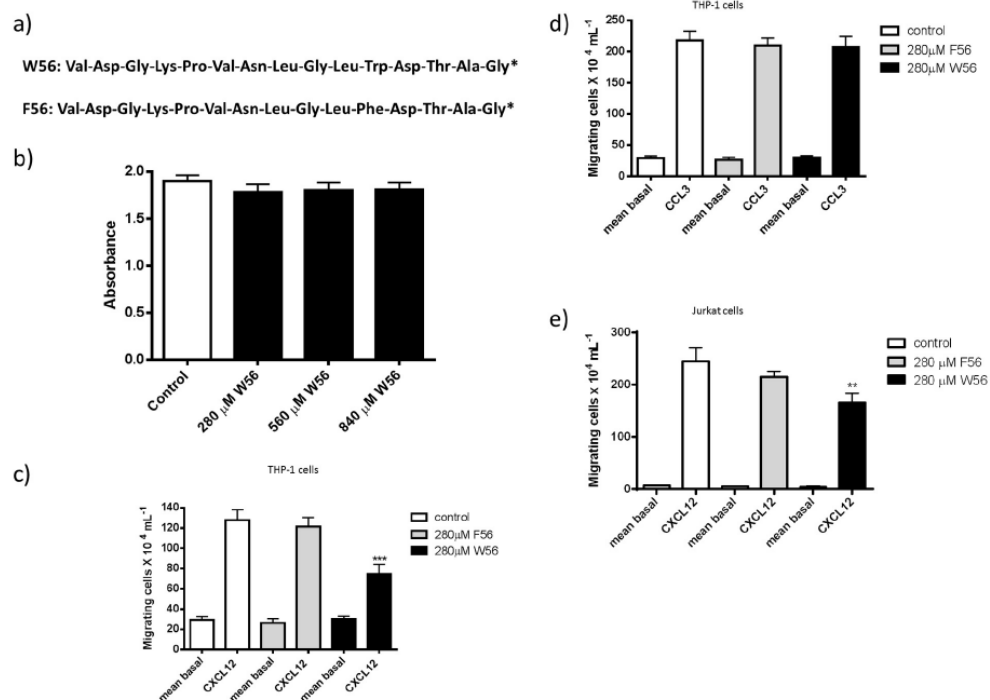
### 2.1. Cells and materials

The leukemic cell line Jurkat and the monocytic cell line THP-1 were purchased from the ATCC (Teddington, UK) and both cell lines were grown as described [5]. The breast cancer cell line MCF-7 was

obtained from the ATCC and grown in DMEM containing 10% FCS and 2 mM L-glutamine. The chemokine CXCL12 was obtained from Peprotech (London, UK); CCL3 has been described previously [16,27]. NSC23766, AMD3100, and H89 were purchased from Abcam (Cambridge, UK). ATI2341 was from Tocris Biosciences (Bristol, UK), EHT1864 was purchased from Cambridge Biosciences (Cambridge, UK). The anti-CXCR4 (12G5) antibody was from R & D Systems (Abingdon, UK) and the corresponding FITC labelled anti-mouse secondary antibody was from Sigma (Poole, UK). Rac1 Pull-down Activation Assay Kit was obtained from Cytoskeleton Inc. (Denver, USA), the CatchPoint cAMP Fluorescent Assay Kit was from Molecular Devices (Wokingham, UK). All other chemicals were from Fisher Scientific (Loughborough, UK).

### 2.2. Peptide synthesis

Two 15mer peptides, active (VDGKPVNLGLWDTAG) (W56) and inactive (VDGKPVNLGLFDTAG) (F56) were synthesized on a Multisynth Syro I automated peptide synthesiser using standard Nα-Fmoc-based solid-phase peptide synthesis. The synthesis was carried out on a NOVA PEG Rink amide polystyrene resin (substitution:



**Fig. 2.** Rac1 activation is essential for CXCL12-induced chemotaxis but not for CCL3.

A) Shows amino-acid sequence of active W56 peptide and inactive control F56 peptide, \* denotes C-terminal amide, B) MTS assays in THP-1 cells showing no toxicity against different peptide concentrations. C) Shows migratory response of THP-1 cells towards 1 nM CXCL12 in untreated control cells, inactive F56 or active W56 pre-treated cells. D) Cell chemotaxis towards 1 nM CCL3 in untreated control cells, inactive F56 or active W56 pre-treated THP-1 cells. E) Shows migratory response of Jurkat cells towards 1 nM CXCL12 in untreated control cells, inactive F56 or active W56 pre-treated cells. Data shown are the mean  $\pm$  SEM of at least 3 independent experiments. (\*\* =  $p \leq 0.01$ , \*\*\* =  $p \leq 0.001$ , One-way ANOVA with a Tukey's multiple comparisons test as post-test).

0.49 mmol/g) using methodology similar to that described by Malkinson [28], except that Fmoc de-protection was carried out with 40% piperidine ( $1 \times 10$  min) and 20% piperidine ( $2 \times 5$  min). The peptide was cleaved from the resin by shaking the resin beads in 5 mL TFA/H<sub>2</sub>O/TIPS (95:2.5:2.5% v/v) for 3 h. The solution was filtered and the resin beads washed with neat TFA and combined with the above solution. This was then evaporated under vacuum. The crude peptide was precipitated with cold diethyl ether and then filtered. The peptides were purified using reverse phase chromatography on a Biotage Isolera Four (SNAP Cartridge KP-C18-HS 12 g). Mobile phase A: 5% methanol in H<sub>2</sub>O + 0.05% TFA. Mobile phase B: 5% H<sub>2</sub>O in methanol + 0.05% TFA. Gradient 0  $\rightarrow$  100%B over 60 min. The fractions containing the peptide were evaporated under vacuum and then the peptide was freeze-dried from purified water. Purity was confirmed at 90% using analytical HPLC (ZORBAX Eclipse XBD-C18) (Mobile phase A: H<sub>2</sub>O + 0.05% TFA. Mobile phase B: methanol + 0.05% TFA. Gradient 5  $\rightarrow$  95%B over 20 min) and the peptide mass was confirmed by MALDI mass spectrometry active W56 (M + Na, 1562) and (M + K, 1578), control F56 (M + Na, 1523) and (M + K, 1539).

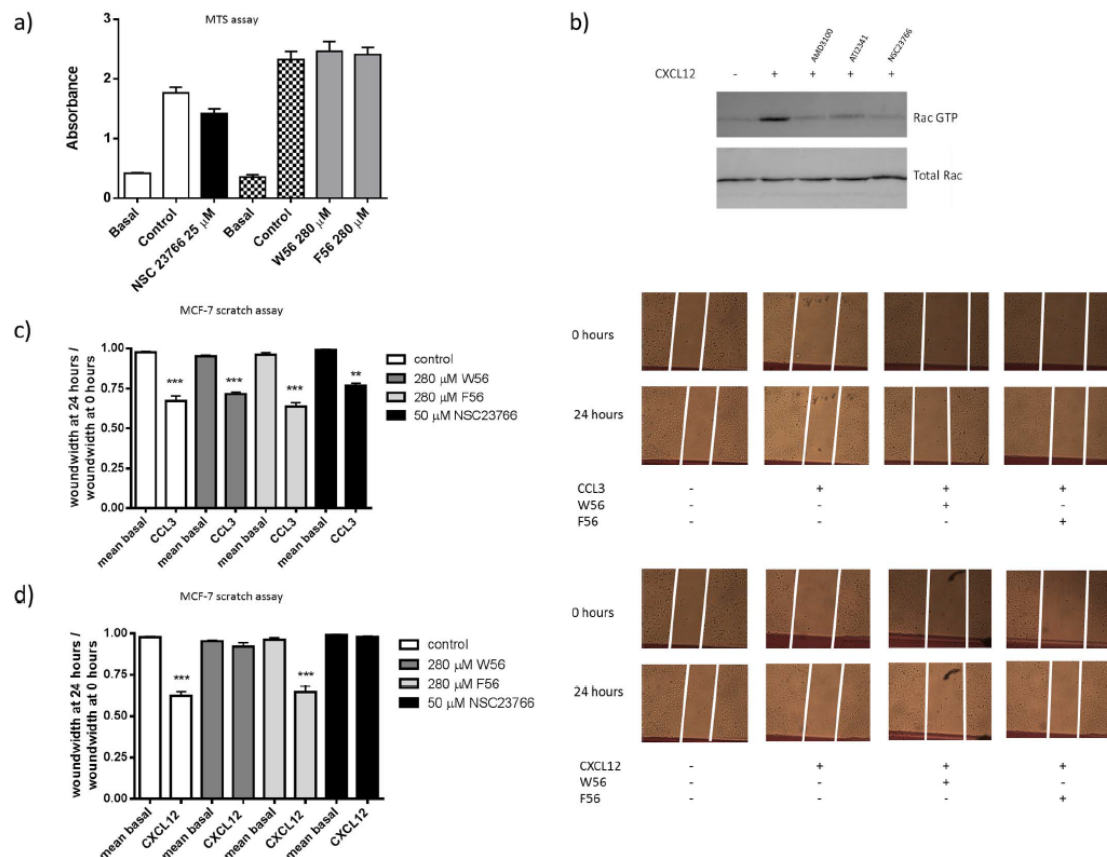
### 2.3. Chemotaxis assays

Cells were harvested and then re-suspended at a concentration of  $25 \times 10^4$  cells  $\text{mL}^{-1}$  in serum-free RPMI 1640 containing 0.1% BSA. Cells were loaded in a total volume of 20  $\mu$ L into the upper compartment of a microchemotaxis chamber (Receptor Technologies, Adderbury, UK) as described previously [5]. For inhibitor treatment,

cells were incubated for 30 min with the relevant inhibitors or vehicle control before loading onto the membrane. Chemoattractants at a concentration of 1 nM were loaded in a final volume of 31  $\mu$ L at indicated concentrations in the lower compartment. The two compartments were separated by a polyvinylpyrrolidone-free polycarbonate filter with 5  $\mu$ m pores. The chemotaxis chamber was incubated at 37  $^{\circ}\text{C}$ , 100% humidity, and 5% CO<sub>2</sub> for 4 h. The filter was then removed, and the number of cells migrating into each bottom compartment was counted using a haemocytometer. In all experiments, each data point was performed in duplicate.

### 2.4. Analysis of intracellular calcium ion concentration

MCF-7 cells were harvested and treated as described previously [29]. Cells were loaded with Fura-2 as described previously [30,31]. Inhibitors were present during the 30 min incubation period. Following incubation with inhibitors, cells were washed with calcium flux buffer and were re-suspended at  $2 \times 10^6$  cells/mL in calcium flux buffer. Chemokine-induced intracellular calcium mobilisation was determined as described by Gryniewicz [32] using a BMG Labtech Fluostar OPTIMA fluorometer. Chemokine was added after 15 s of incubation in the fluorometer. Calcium mobilisation was monitored for a further 60 s following chemokine challenge. Jurkat cells were harvested, then re-suspended in buffer as described [29]. Fluorescence was measured at 37  $^{\circ}\text{C}$  every 3.5 s. Stimulation with CXCL12 was after 30 s. Calcium mobilisation and AUC was determined in a Flexstation III ROM V3.0.22 (Molecular Devices Ltd., Wokingham, UK) using SoftMax Pro and Excel,



**Fig. 3.** Rac1 activation is essential for CXCL12-induced migration of MCF-7 cells. A) Shows MTS assay with 25  $\mu$ M NSC23766 and 280  $\mu$ M W56 or F56 over 48 h, B) Rac1 activation assay in the presence/absence of CXCL12 and AMD3100, AT12341, NSC23766, upper panel shows active Rac1, lower panel shows total Rac1 in lysate. C) Wound healing assay on MCF-7 cells after treatment with NSC23766, inactive F56 or active W56. Cell migration was induced with 10 nM CCL3 and measured after 24 h. Left side shows quantified migration, right shows representative pictures from scratch D) Wound healing assay on MCF-7 cells after treatment with NSC23766, inactive F56 or active W56. Cell migration was induced with 10 nM CXCL12 and measured after 24 h. Left side shows quantified migration, right shows representative pictures from scratch. Quantification of migration of cells into the wound: A number of 1 denotes no migration occurred whereas a number < 1 denotes cell migration. \*\* denotes a significant difference towards the corresponding control (\*\*\*) =  $p \leq 0.001$ , One-way ANOVA with a Tukey's multiple comparisons test as post-test). Data shown are the mean  $\pm$  SEM of 3 independent experiments, western blot analysis shows initial data from experiments.

and displayed using GraphPad Prism.

## 2.5. Wound healing assays

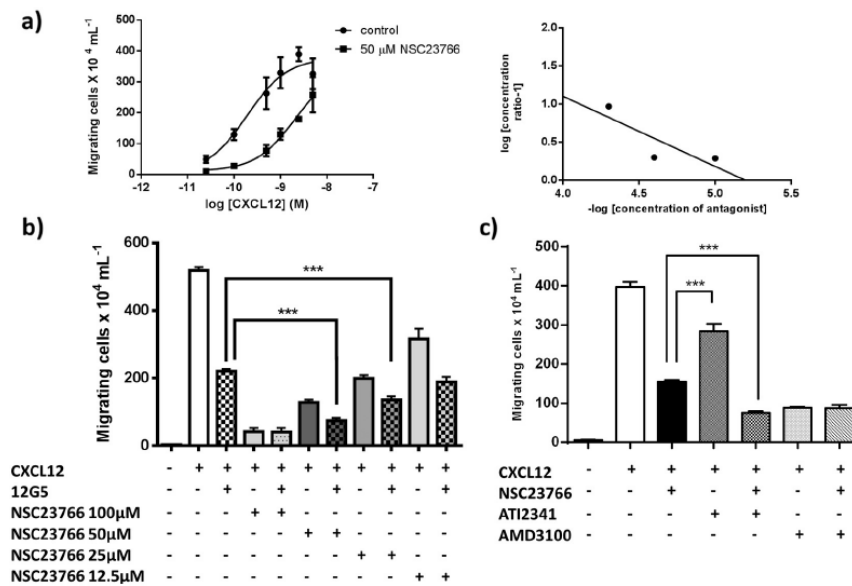
MCF-7 cells were seeded onto 24 well plates overnight. After 24 h, the cells were washed once in DMEM without supplements and incubated in DMEM without supplements. A scratch was introduced to the monolayer with 200  $\mu$ L pipette tips (time point 0). Inhibitors were added to the cells and incubated for 30 min at 37  $^{\circ}$ C, 100% humidity, and 5% CO<sub>2</sub>. Chemokines or vehicle controls were added to the cells and pictures were taken at time point zero and after 24 h using an inverted Leica microscope. Images were analysed and the width of the wound was measured for control and with inhibitor treatment (with and without chemokine) at 0 h and 24 h. The ratio of the width of the wound after 24 h divided by the width of the wound at 0 h was then used to compare the effectiveness of treatments in preventing migration, where a number of 1 denotes no migration and a number smaller than 1 denotes migration of cells.

## 2.6. Cell viability studies

MTS assays were performed using a CellTiter 96<sup>®</sup> Aqueous Non-Radioactive Cell Proliferation Assay (Promega, Southampton, UK) and has been described previously [33].

## 2.7. Internalisation assay and flow cytometry analysis

Jurkat T-cells were harvested, re-suspended at  $5 \times 10^5$  cells/mL in 0.1% BSA/RPMI with inhibitors or control (H<sub>2</sub>O) at either 37  $^{\circ}$ C or 4  $^{\circ}$ C for 30 min, then treated with CXCL12 (15 nM) at either 37  $^{\circ}$ C or 4  $^{\circ}$ C for 15 min, washed with ice-cold 0.5% BSA/PBS, suspended in anti hCXCR4 clone 12G5 antibody from R & D Systems (1:2000) for 1 h at 4  $^{\circ}$ C, washed 3 times with ice-cold 0.5% BSA/PBS, then incubated for 1 h at 4  $^{\circ}$ C with fluorescein isothiocyanate (FITC)-conjugated anti-mouse IgG antibody (1:500). Stained cells were washed, gated to exclude dead cells using FSC versus SSC and quantified using a FACS Calibur, and data analysed using CellQuest software version 3.1 (Becton Dickinson, San Jose, CA).



**Fig. 4.** NSC23766 changes potency of CXCL12 in chemotaxis assays and has an additive effect on the neutralising 12G5 antibody and ATI2341, but not on AMD3100. A) Figure on left shows a concentration response curve towards CXCL12 in untreated control cells or 50  $\mu\text{M}$  NSC23766 pre-treated Jurkat cells, right shows a Schild plot analysis in the presence of different concentrations of NSC23766. B) Shows chemotaxis towards 1 nM CXCL12 in Jurkat cells where cells have been either left untreated, pre-treated with 12G5 (1:2000) or different concentration of NSC23766 or both of them. C) Shows chemotaxis towards 1 nM CXCL12 in Jurkat cells where cells have either been treated with 50  $\mu\text{M}$  NSC23766, 5  $\mu\text{M}$  ATI2341, 0.5  $\mu\text{M}$  AMD3100 or a combination of NSC23766/ATI2341 or NSC23766/AMD3100. Data shown are the mean  $\pm$  SEM of 3 independent experiments. (\*\*\*) =  $p \leq 0.001$ , One-way ANOVA with a Tukey's multiple comparisons test as post-test).

## 2.8. cAMP assay

cAMP assays were performed as recommended by manufacturers (Molecular Devices). Briefly, cells were harvested, re-suspended in 0.75 mM IBMX in Krebs-Ringer bicarbonate buffer (KRGB) pH 7.4 at  $2 \times 10^6$  cells/mL, treated with inhibitor or control ( $\text{H}_2\text{O}$ ) for 15 min (37  $^\circ\text{C}$ , 5%,  $\text{CO}_2$ ), aliquots of 40  $\mu\text{L}$  were treated with 20  $\mu\text{M}$  forskolin for 15 min (37  $^\circ\text{C}$ , 5%,  $\text{CO}_2$ ) before timed chemokine or  $\text{H}_2\text{O}$  control addition prior to lysis using CatchPoint buffers and protocols for cAMP analysis. Results were read at excitation 530 nm, emission 585 nm, cut off 570, using Flexstation III ROM v3.0.22.

## 2.9. Rac1 activation assays

Cells were serum starved for 24 h, treated at 37  $^\circ\text{C}$  with inhibitors for 30 min then 10 nM CXCL12 for 15 min, lysed (50 mM Tris pH 7.5, 10 mM  $\text{MgCl}_2$ , 0.5 M NaCl, 2% Igepal) and 800  $\mu\text{g}$  protein/sample used in Rac1 Activation Assay, with 10  $\mu\text{g}$  protein/sample for total rac, following Rac1 Activation Assay Biochem Kit protocol (Cytoskeleton Inc.). The samples were separated on a 10% SDS-PAGE and electrophoretically transferred to a nitro-cellulose membrane. The membranes were blocked with 5% non-fat powdered milk in PBS (30 min, RT). For Western blotting, these membranes were incubated at 4  $^\circ\text{C}$  overnight with 1:500 anti-Rac1 antibody, ARC03, in TBST, no blocker, then rinsed 50 mL TBST (1 min) and then incubated with 1:10,000 goat anti-mouse HRP conjugate in TBST (1 h, RT) membrane washed with TBST (5  $\times$  10 min). The blots were developed using Pierce<sup>TM</sup> ECL western blotting substrate (ThermoFisher Scientific).

## 2.10. Analysis of data

Data were analysed using GraphPad Prism V6 (GraphPad Software). Statistical analyses were performed using a One-way ANOVA with post-

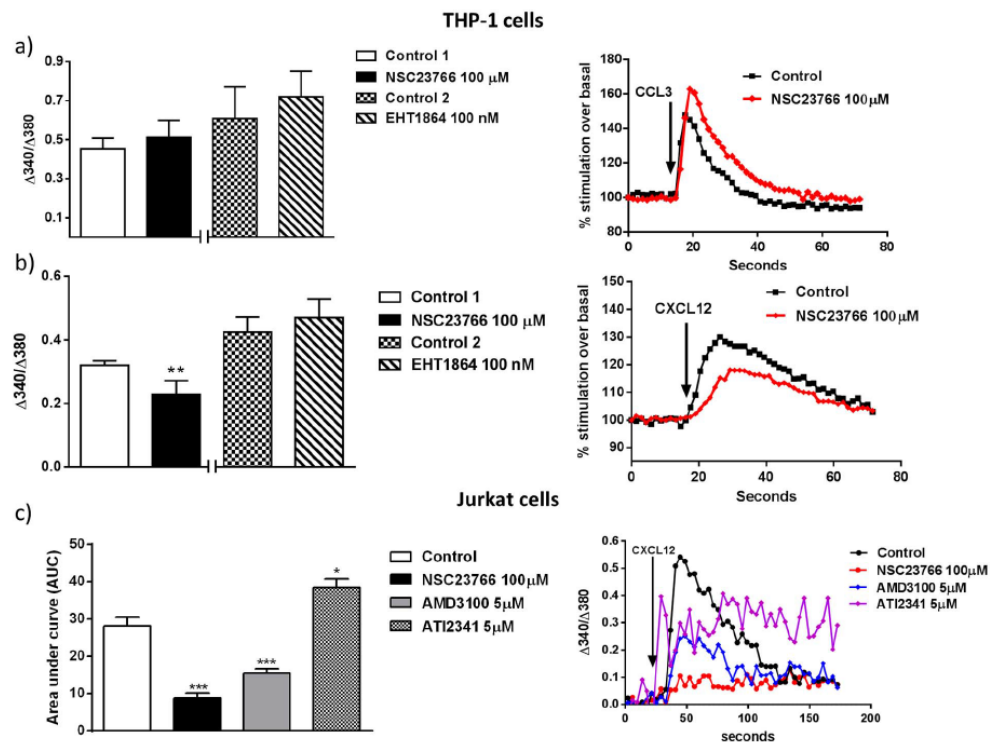
hoc Bonferroni or Tukey's multiple comparisons tests. Data represent the mean  $\pm$  SEM of at least three independent experiments.

## 3. Results

### 3.1. CXCL12-induced chemotaxis in Jurkat and THP-1 cells is blocked by Rac1 GEF inhibitor NSC23766

We set out to examine the role of Rac1 in chemokine-induced cell chemotaxis for different receptors and cell types. Whereas there was no inhibitory effect on CCL3-induced chemotaxis after pre-treatment of THP-1 cells with NSC23766, a specific Rac1-GEF interaction inhibitor [34] (Fig. 1a), there was, however, a significant reduction of chemotaxis towards CXCL12 (Fig. 1b). We confirmed the inhibitory effect of NSC23766 on CXCL12 chemotaxis in Jurkat cells (Fig. 1c), where virtually no cells migrated after NSC23766 treatment, whereas in THP-1 cells about 40% of migration was observed. Cell viability assays (MTS assays) showed that over the timeframe and concentrations used, NSC23766 exhibits only a minor toxic effect on cell growth (data not shown). The Rac1 inhibitor EHT1864 gave similar results, blocking significantly CXCL12 induced chemotaxis (Fig. 1d), but not CCL3 induced chemotaxis. (Fig. 1e). We also used the CXCR4 specific orthosteric antagonist AMD3100, to block chemotaxis in our assay (Fig. 1f). AMD3100 is a bicyclam antagonist of CXCR4 thought to bind three acidic residues Asp<sup>171</sup>, Asp<sup>262</sup> and Glu<sup>288</sup> in the main binding pocket of CXCR4 [35]. In contrast ATI2341 is an allosteric agonist derived from a CXCR4 intracellular loop 1 protein sixteen residue sequence. ATI2341 has many rotatable bonds facilitating flexible docking and a long palmitate tail facilitating cell penetration. ATI2341 had a small non-significant negative effect on CXCL12 induced chemotaxis in Jurkat cells (Fig. 1g). When used on their own, neither NSC23766, nor AMD3100 or ATI2341 induced any chemotactic responses in Jurkat cells (Fig. 1h).





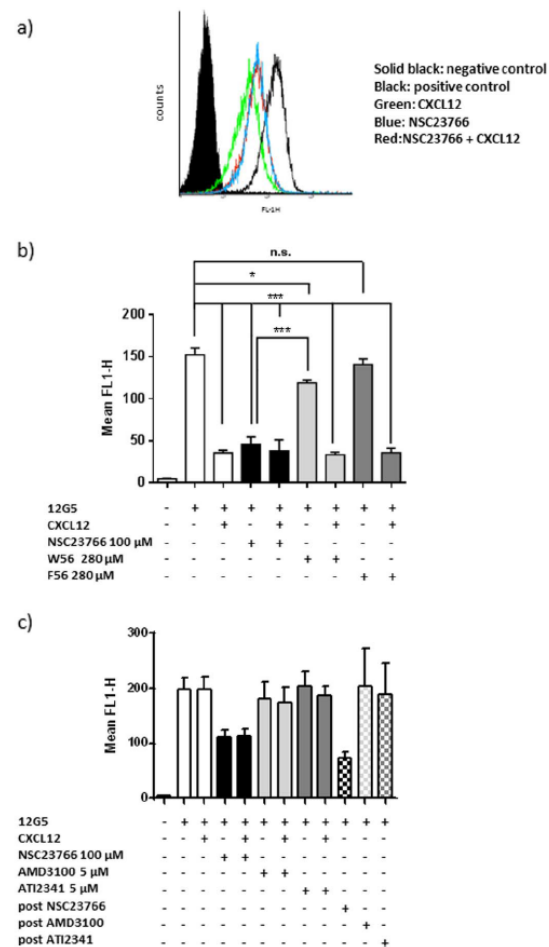
**Fig. 5.** NSC23766 does not affect the release of intracellular calcium in response to CCL3 activation in THP-1 cells. A) Figure on left, stimulation of untreated, NSC23766 or EHT 1864 treated THP-1 cells with CCL3 100 nM leads to release of intracellular calcium, on the right representative trace showing stimulation of untreated or NSC23766 treated cells with CCL3 100 nM. B) Left figure, stimulation of untreated, NSC23766 or EHT 1864 treated THP-1 cells with CXCL12 10 nM leads to release of intracellular calcium, on the right representative trace showing stimulation of untreated or NSC23766 treated cells with CXCL12 10 nM. C) Left figure, stimulation of untreated or NSC23766, AMD3100 and ATI2341 treated Jurkat cells with CXCL12 10 nM leads to release of intracellular calcium, on the right representative trace showing stimulation of untreated or inhibitor treated cells. A, B: Data in single traces were normalised to stimulation over basal. (\*\* =  $p \leq 0.01$ , paired Student's *t*-test,  $n = 3$ ), C: Area under the curve was calculated using SoftMax Pro and Excel (\*\*\* =  $p \leq 0.001$ , \* =  $p \leq 0.05$ , One-way ANOVA with a Tukey's multiple comparisons test as post-test,  $n = 6$ ).

### 3.2. A Rac1 inhibitory peptide also blocks CXCL12 induced chemotaxis, but not CCL3 in THP-1 and Jurkat cells

Small molecule inhibitors can have off-target effects and indeed it has been described that NSC23766 has additional effects on muscarinic acetylcholine receptors, where it acts a competitive antagonist [36]. We therefore synthesized a previously described peptide (W56) [37] which targets a sequence in the  $\beta 3$  region of switch 2 in Rac1 and blocks its functionality (Fig. 2a). As an internal control we used an inactive control peptide (F56), which has a key amino acid, tryptophan, substituted by phenylalanine to inactivate the peptide. Even at very high concentrations, this W56 peptide did not show any toxicity in THP-1 cells (Fig. 2b). We repeated the chemotaxis assays in THP-1 and Jurkat cells in the presence or absence of the Rac1-binding peptide (W56) and we confirmed the peptide's inhibitory effect on CXCL12-induced chemotaxis, whereas there was no effect on CCL3-induced chemotaxis (Fig. 2c, d). Similarly in Jurkat cells, the Rac1-binding peptide (W56) blocked CXCL12-induced chemotaxis in THP-1 cells (Fig. 2e). The inactive F56 peptide did not block CXCL12 or CCL3 chemotaxis (Fig. 2). Increasing the concentration of W56 to 560  $\mu$ M does not change the differences observed between the two chemokines tested (data not shown).

### 3.3. Rac1 inhibition blocks CXCL12-induced migration of adherent MCF-7 cells

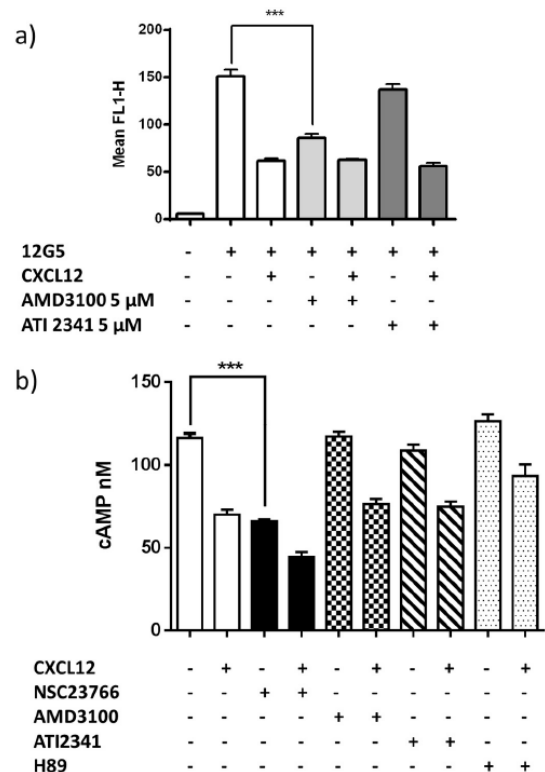
We previously observed differences in the signalling machinery utilised during cell migration with regards to adherent cells compared to suspension cells [5]. To analyse whether the use of Rac1 differs in suspension versus adherent cells, we used a cellular model of wound healing assays in the adherent breast cancer line MCF-7. Since wound healing assays expose the cells towards the drugs for a longer timeframe than a chemotaxis assay does, we repeated the MTS cell viability assay for NSC23766 on MCF-7 cells (Fig. 3a), selecting the 25  $\mu$ M dosage to treat the cells, and we used the peptide concentration of 280  $\mu$ M for W56 and F56. Rac1 activation assays showed that CXCL12 leads to activation of Rac1 in MCF-7 cells, which can be blocked by the Rac1 GEF inhibitor NSC23766 as well as by the CXCR4 antagonist AMD3100 and the allosteric agonist ATI2341 (Fig. 3b). The results of the wound healing assays mirror the results in suspension cells. Neither the active W56 peptide nor NSC23766 blocked CCL3-induced migration (Fig. 3c), whereas the active W56 peptide as well as NSC23766 blocked migration in response to CXCL12 (Fig. 3d). These results clearly show that in CCL3-induced migration compared with CXCL12-induced migration Rac1 activation is not necessary.



**Fig. 6.** NSC23766 acts as an agonist and leads to internalisation of CXCR4. A) Flow cytometry analysis of CXCR4 expression on Jurkat cells in either control cells or pre-treated cells: solid black is the negative control, black line is the positive 12G5 control, green line are control cells treated with CXCL12, blue line are cells treated with NSC23766 100  $\mu$ M, red line are cells treated with NSC23766 and CXCL12. B) Cells were pre-incubated with inhibitors for 30 min at 37 °C and internalisation of CXCR4 was induced with CXCL12 15 nM. Cells were then stained for CXCR4 expression and analysed using flow cytometry. Data is presented as mean plus S.E.M. of the mean fluorescence measured of 4 independent experiments C) Cells were kept at 4 °C for all incubation steps. Cells were either pre-incubated with inhibitors before induction of internalisation and the antibody stain or the cells were stained with 12G5 first and then incubated with inhibitors (post NSC23766, post AMD3100, post ATI2341 4 °C, 30 min). Data is presented as mean plus S.E.M. of the mean fluorescence measured of at least 6 independent experiments.

### 3.4. NSC23766 acts as a competitive antagonist in CXCL12-induced chemotaxis in Jurkat cells

To understand the action of NSC23766 in more detail, we performed a concentration response curve for CXCL12-induced chemotaxis in Jurkat cells in the presence or absence of 50  $\mu$ M NSC23766. We used a slightly lower concentration of NSC23766 as compared to our initial experiments, in order not to prevent migration completely (Fig. 4a left). The sigmoidal dose response curves clearly show a reduction in potency in the presence of NSC23766 ( $EC_{50}$  of CXCL12 in the absence of NSC23766: 0.19 nM, in the presence of NSC23766 the  $EC_{50}$  for CXCL12



**Fig. 7.** ATI2341 does not induce internalisation of CXCR4, NSC23766 acts as an agonist on CXCR4 in cAMP assays. A) Data shows levels of CXCR4 expression in Jurkat cells in control, AMD3100 or ATI2341 pre-treated cells in response to CXCL12 activation. Data shown are the mean  $\pm$  SEM of 3 independent experiments. (\*\*\*) =  $p \leq 0.001$ , One-way ANOVA with a Tukey's multiple comparisons test as post-test. B) Data show levels of cAMP in Jurkat cells after treatment with 100 nM CXCL12 for 10 min. Cells were pre-treated with 20 mM forskolin to induce cAMP production and either NSC23766, AMD3100, ATI2341, H89 or left untreated for 30 min before they were incubated with 100 nM CXCL12 for 10 min and the amount of cAMP present was measured using a CatchPoint cAMP Fluorescent Assay Kit. Data shown are the mean  $\pm$  SEM of 4 independent experiments. (\*\*\*) =  $p \leq 0.001$ , One-way ANOVA with a Tukey's multiple comparison tests as post-test.

is 2 nM), but there is no effect on the efficacy of CXCL12. De facto NSC23766 behaves like a competitive antagonist for CXCR4 in this assay and the inhibitory response is surmountable. We did further experiments in the presence of different concentrations of NSC23766 and plotted the data as Schild plot which allowed the calculation of the  $pA_2$  for NSC23766, which is 5.2 (Fig. 4a, right) and used a Gaddum/Schild  $EC_{50}$  shift to calculate the affinity as well, which is determined at 4  $\mu$ M. The CXCR4-specific antibody 12G5 is capable of blocking chemotaxis [38]. At 50 and 25  $\mu$ M concentration of NSC23766 there is an additive effect of NSC23766 treatment on inhibition of CXCL12-induced chemotaxis in the presence of the 12G5 antibody, whereas at the lower concentration of NSC23766, no significant additive effect on 12G5 occurs (Fig. 4b). At 100  $\mu$ M concentration of NSC23766 the addition of 12G5 has no effect on further reducing chemotaxis. A similar effect can be seen with the allosteric agonist ATI2341, but not with AMD3100 (Fig. 4c). This data leads us to speculate that the action of NSC23766 in this system is not solely blocking the Rac1-GEF interaction, but is also acting on the CXCR4 receptor directly.

### 3.5. NSC23766 blocks CXCL12-induced calcium release in THP-1 and Jurkat cells

NSC23766 does not block CCL3-induced release of calcium in THP-1 (Fig. 5a), and has therefore no general effect on cell signalling. In contrast, we observed a significant reduction in calcium release after CXCL12 activation in THP-1 cells which have been pre-treated with NSC23766. Again, these results point to NSC23766 having additional effects on CXCR4 rather than solely blocking Rac1-GEF (Fig. 5b). The Rac1 inhibitor EHT 1864 does not inhibit the release of calcium in these cells for both CXCL12 as well as CCL3. Intracellular calcium responses to CXCL12 in Jurkat cells pre-treated with AMD3100, NSC23766 or ATI2341 illustrate that ATI2341 clearly increases total calcium release, whereas AMD3100 and NSC23766 dramatically reduce calcium release in this cell line (Fig. 5c). This alludes to the fact that ATI2341 acts as a CXCR4 agonist with respect to calcium release, whereas both AMD3100 and NSC23766 dramatically reduced the AUC compared to control and act as antagonists (see Fig. 5c).

The addition of CXCL12 for 15 min before staining with the CXCR4 specific antibody leads to rapid internalisation of the receptor from the surface of Jurkat cells, which is measurable by a loss of fluorescence (Fig. 6a, b). Cells that were pre-incubated with NSC23766 exhibited a similar profile after 12G5 staining as cells where the receptor has been internalised (Fig. 6b), whether they have been subjected to CXCL12 treatment or not. This apparent loss of receptors could occur if Rac1 inhibition triggers receptor internalisation even if the receptor is inactive, or it could occur due to the NSC23766 competitively binding to the monoclonal antibody binding sites. It could also be due to a conformational change in the receptor which leads to a loss on antibody binding, as has been proposed by Zoughlami et al. [26]. We therefore repeated the CXCR4 internalisation experiments with the active (W56) and inactive control (F56) peptides. We did not observe any significant effects on receptor expression or internalisation (Fig. 6b). This makes it highly unlikely that general Rac1 inhibition triggers internalisation or leads to a conformational change which leads to a loss of antibody binding. We hypothesized that if NSC23766 was competing with the 12G5 antibody to bind to the receptor, then the same experiment performed at 4 °C to prevent active internalisation of CXCR4, would show the same results as experiments performed at 37 °C, where the receptor can undergo internalisation (modelling of NSC interaction with CXCR4 is supplied in the Supporting information section). This is in fact what our data shows (Fig. 6c), suggesting that NSC23766 is not acting via receptor internalisation. Furthermore, treatment with NSC23766 following primary and secondary antibody treatment produced a greater loss of receptor 12G5 staining than pre-treatment with NSC23766 before receptor staining (Fig. 6c). This suggests that although NSC23766 rapidly binds CXCR4, its affinity weakens over the timescale of the receptor staining (about 2 h) (Fig. 6c).

To verify these results we also treated Jurkat cells with AMD3100 and ATI2341 (Fig. 7a). The results show that ATI2341 (5 µM) does not induce internalisation on its own, and it does not block CXCL12-induced internalisation. AMD3100 binds to the same site on CXCR4 as the 12G5 antibody and is known to prevent antibody binding, and therefore exhibited a similar result as NSC23766 at 37 °C (Figs. 6b and 7a). However we found that the effects of 100 µM NSC23766 are considerably more pronounced than those of 5 µM AMD3100 at 4 °C (Fig. 6c).

CXCR4 receptors couple to Gαi/o heterotrimeric G proteins, so therefore we treated Jurkat cells with forskolin to induce cAMP production after pre-treating the cells with either NSC23766, AMD3100, ATI2341 or H89 (a potent, cell-permeable protein kinase A (PKA) inhibitor). 10 min activation of CXCR4 receptors with CXCL12 leads to a loss of quantifiable cAMP in the cells, which is not blocked by AMD3100, ATI2341 or H89. NSC23766 induces a reduction in cAMP levels in the absence of CXCR4 receptor activation, which is then increased by the addition of CXCL12 (Fig. 7b), suggesting that NSC23766

may also act as a CXCR4 agonist, which can induce reduction in cAMP production, but is not capable of inducing cell chemotaxis. Alternatively, NSC23766 acts as an agonist at a receptor distinct from CXCR4 and their effects are cumulative.

## 4. Discussion

Chemokine receptor-induced cell chemotaxis is a crucial step in metastasis of cancer as well as the inflammatory response [12]. The chemokine receptor CXCR4 has been of interest for a number of years, as it has been shown to be up-regulated in several cancers and its activation can lead to cancer cell metastasis [7–9,25,39–41]. Although different studies investigated how CXCL12-induced activation of CXCR4 leads to chemotaxis of cells, there are still many unanswered questions. We have shown recently that the type of cells where the receptor is expressed has an effect on which downstream signalling partners will be utilised to transduce the signal from receptor towards cell migration [5]. Also there are distinct differences in which pathways are used, depending on which receptor becomes activated [5,29]. We therefore set out to investigate how Rac1 signalling is involved with chemotaxis towards CXCL12 or CCL3 in different cell types. One of the findings in our study is that there are indeed differences in whether Rac1 activation is essential for cell chemotaxis or not. CCL3-induced chemotaxis occurs in the absence of Rac1 activation, in both suspension and adherent cell types, whereas CXCL12 chemotaxis is completely prevented when Rac1 is blocked by a specific Rac1 binding peptide or by the Rac1 inhibitor EHT 1864. This in contrast to previous studies in chronic lymphocytic leukaemia (CLL) cells, where chemotaxis towards CXCL12 relied on RhoA activation and not Rac1, which again highlights the important impact different cell types have on receptor-induced signalling [23].

Our results with the Rac1-GEF inhibitor NSC23766 are more complicated. Using NSC23766 we confirmed that CCL3-induced chemotaxis in THP-1 cells as well as MCF-7 cells occurs independently of Rac1 activation. On first sight, the data also confirms that CXCL12-induced chemotaxis is completely reliant on Rac1 activation, however, there are more dimensions to these results. Recently it has been shown that NSC23766 indeed acts as antagonist on various receptors [36,42]. NSC23766 can directly regulate NMDA receptors as indicated by their strong effects on both exogenous and synaptically evoked NMDA, indicating that NSC23766 could be a novel NMDA receptor antagonist [42]. Similarly, NSC23766 inhibits the M2 muscarinic acetylcholine receptor (M2 mAChR) and induces a concentration-dependent rightward shift of the carbachol concentration response curves at all mAChRs [36]. There have also been studies showing that Rac1 can lead to a direct conformational change in CXCR4 and that Rac1 inhibition affects this as well [26]. With this in mind, we investigated the role of NSC23766 in CXCL12-induced chemotaxis further. Concentration response curves in the presence or absence of NSC23766 clearly showed a shift in potency for CXCL12 in the presence of NSC23766, with no effect on the overall efficacy of the chemokine, which points to NSC23766 being a competitive antagonist on CXCR4 and not to NSC23766 solely blocking Rac1 activation, which was also confirmed with a Gaddum/Schild EC<sub>50</sub> shift analysis. 12G5, a CXCR4 antibody which has been shown to be dependent on receptor conformation for binding [43], can block chemotaxis of cells. In our hands there is a clear additive effect of NSC23766 and 12G5; together they block chemotaxis to greater extent than either on their own. The allosteric agonist ATI2341, which has been shown to induce chemotaxis via CXCR4 in polymorphonuclear neutrophils (PMNs) but not in lymphocytes [44], does not induce chemotaxis in Jurkat cells, but has a slight inhibitory effect on CXCL12-induced chemotaxis, acting like a weak partial agonist. This effect is synergistic with the effects seen with NSC23766, whereas AMD3100 and NSC23766 do not exhibit any synergistic effect. ATI2341 has been shown to have a very weak effect on CXCR4 internalisation [45], which we can confirm. It does not affect CXCL12-induced internalisation, nor



is there any effect visible in cAMP assays, even though ATI2341 has been shown to engage G $\alpha$ i heterotrimeric G proteins [45]; however we recognise an increase in overall calcium release in the cells in the presence of ATI2341, even if the peak release is not higher.

Unlike previous publications who linked expression levels of CXCR4 directly to the functionality of Rac1 [26], we observed further effects of NSC23766 in these experiments. Our data points to NSC23766 directly binding to CXCR4, as has been shown for other receptors [36,42] and inducing diverse signalling (see Supporting information). We have previously shown that the chemokine receptor signalling can differ depending on cell types used [5], and therefore it is not too surprising that data recorded in transfected HEK293 [26] cells do not match with cAMP assays in Jurkat cells, where a reduction in cAMP levels after NSC23766 treatment can be observed, which is further decreased by the addition of CXCL12 (Fig. 7b). These results do not necessarily disagree with the hypothesis that Rac1 blockade leads to a conformational change in CXCR4, however it would be an active conformation of the receptor and not an inactive conformation. NSC23766 can lead to the downregulation of receptors from the cell surface as has been shown for glycoprotein on platelets [46]. Our data with the W56 peptide in Jurkat cells show internalisation of CXCR4, and not a conformational change, since only in the presence of CXCL12 is there a loss of receptor expression, whereas a conformational change would show this loss in the absence of agonist as well. We also cannot confirm the Rac1 inhibition is essential for CXCR4-induced internalisation, since even in the presence of W56, the receptor internalises after activation with CXCL12.

The concept of biased agonism has become more popular within the chemokine field, since increasingly numerous examples from the field of GPCRs point to the fact that structurally different ligands acting on the same receptor can activate different signalling pathways within the cell [47–49]. An agonist may preferentially stabilize a receptor conformation over another, leading to the recruitment of a particular group of intracellular signalling molecules to the receptor and the preferential activation of one downstream signalling pathway over another [50]. Overall our data points to NSC23766 directly binding to CXCR4 and inducing specific signalling events which differ from CXCL12, and therefore confirms the concept of ligand biased signalling on the CXCR4 receptor.

#### Authorship contribution

Contribution: S.C.M designed and performed the experiments, analysed, and interpreted the data, and wrote the manuscript; L.H. and L.S. performed some experiments; A.B. did the molecular modelling; A.M. supervised the study, designed the experiments, analysed and interpreted the data, and wrote the manuscript.

#### Conflict-of-interest disclosure

The authors declare no competing financial interests.

#### Acknowledgments

We acknowledge the support for SCM from the Novartis studentship fund.

#### Appendix A. Supplementary data

Supplementary data to this article can be found online at <https://doi.org/10.1016/j.cellsig.2017.10.006>.

#### References

- [1] M. Thelen, *Nat. Immunol.* 2 (2001) 129–134.
- [2] B. Homey, A. Muller, A. Zlotnik, *Nat. Rev. Immunol.* 2 (2002) 175–184.
- [3] A. Zlotnik, Ernst Schering Res. Found. Workshop (2004) 53–58.
- [4] P. Dillenburger-Pilla, V. Patel, C.M. Mikelis, C.R. Zarate-Blades, C.L. Doci, P. Amorphimoltham, Z. Wang, D. Martin, K. Leelahavanichkul, R.T. Dorsam, A. Masedunskas, R. Weigert, A.A. Molinolo, J.S. Gutkind, *FASEB J.* 29 (2015) 1056–1068.
- [5] S.C. Mills, P.H. Goh, J. Kudatsih, S. Ncube, R. Gurung, W. Maxwell, A. Mueller, *Cell Signal.* 28 (2016) 316–324.
- [6] G.G. Vaday, D.M. Peehl, P.A. Kadam, D.M. Lawrence, *Prostate* 66 (2006) 124–134.
- [7] A. Zlotnik, *Int. J. Cancer* 119 (2006) 2026–2029.
- [8] A. Zlotnik, *Semin. Cancer Biol.* 14 (2004) 181–185.
- [9] F. Balkwill, *Semin. Cancer Biol.* 14 (2004) 171–179.
- [10] Y. Li, J. Wu, P. Zhang, *Tumour Biol.* 37 (2016) 4501–4507.
- [11] C. Delgado-Martin, C. Escribano, J.L. Pablos, L. Riol-Blanco, J.L. Rodriguez-Fernandez, *J. Biol. Chem.* 286 (2011) 37222–37236.
- [12] F. Bachelier, A. Ben-Baruch, A.M. Burkhardt, C. Combadiere, J.M. Farber, G.J. Graham, R. Horuk, A.H. Sparre-Ulrich, M. Locati, A.D. Luster, A. Mantovani, K. Matsushima, P.M. Murphy, R. Nibbs, H. Nomiya, C.A. Power, A.E. Proudfoot, M.M. Rosenkilde, A. Rot, S. Sozzani, M. Thelen, O. Yoshie, A. Zlotnik, *Pharmacol. Rev.* 66 (2014) 1–79.
- [13] C. Blanpain, I. Migeotte, B. Lee, J. Vakili, B.J. Doranz, C. Govaerts, G. Vassart, R.W. Doms, M. Parmentier, *Blood* 94 (1999) 1899–1905.
- [14] A. Mueller, E. Kelly, P.G. Strange, *Blood* 99 (2002) 785–791.
- [15] G. Germea, E. Hirsch, *Mol. Immunol.* 55 (2013) 83–86.
- [16] J.S. Kerr, R.O. Jacques, C. Moyano Cardaba, T. Tse, D. Sexton, A. Mueller, *Cell. Signal.* 25 (2013) 729–735.
- [17] A.J. Ridley, *Curr. Opin. Cell Biol.* 36 (2015) 103–112.
- [18] T.D. Pollard, G.G. Borisy, *Cell* 112 (2003) 453–465.
- [19] A.J. Ridley, *Methods Mol. Biol.* 827 (2012) 3–12.
- [20] A. Mueller, P.G. Strange, *Eur. J. Biochem.* 271 (2004) 243–252.
- [21] C.M. Ryan, J.A. Brown, E. Bourke, A.M. Prendergast, C. Kavanagh, Z. Liu, P. Owens, G. Shaw, W. Kolch, T. O'Brien, P.P. Barry, *Stem Cell Res Ther* 6 (2015) 136.
- [22] A.K. Cross, V. Richardson, S.A. Ali, I. Palmer, D.D. Taub, R.C. Rees, *Cytokine* 9 (1997) 521–528.
- [23] S.W. Hofbauer, P.W. Krenn, S. Ganghammer, D. Asslauer, U. Pichler, K. Oberacher, R. Henschler, M. Wallner, H. Kerschbaum, R. Greil, T.N. Hartmann, *Blood* 123 (2014) 2181–2188.
- [24] H. Li, L. Yang, H. Fu, J. Yan, Y. Wang, H. Guo, X. Hao, X. Xu, T. Jin, N. Zhang, *Nat. Commun.* 4 (2013) 1706.
- [25] J. Guo, X. Yu, J. Gu, Z. Lin, G. Zhao, F. Xu, C. Lu, D. Ge, *Tumour Biol.* 37 (2016) 6371–6378.
- [26] Y. Zoughlami, C. Voermans, K. Brussen, K.A. van Dort, N.A. Kootstra, D. Maussang, M.J. Smit, P.L. Hordijk, P.B. van Hennik, *Blood* 119 (2012) 2024–2032.
- [27] C. Moyano Cardaba, R.O. Jacques, J.E. Barrett, K.M. Hassell, A. Kavanagh, F.C. Remington, T. Tse, A. Mueller, *Biochem. Biophys. Res. Commun.* 418 (2012) 17–21.
- [28] J.P. Malkinson, M. Zloh, M. Kadom, R. Errington, P.J. Smith, M. Searcey, *Org. Lett.* 5 (2003) 5051–5054.
- [29] R.O. Jacques, S.C. Mills, P. Cazzonatto Zerwes, F.O. Fagade, J.E. Green, S. Downham, D.W. Sexton, A. Mueller, *Cell Biochem. Funct.* 33 (2015) 407–414.
- [30] C.M. Cardaba, A. Mueller, *Biochem. Pharmacol.* 78 (2009) 974–982.
- [31] C.M. Cardaba, J.S. Kerr, A. Mueller, *Cell. Signal.* 20 (2008) 1687–1694.
- [32] G. Gryniewicz, M. Poenie, R.Y. Tsien, *J. Biol. Chem.* 260 (1985) 3440–3450.
- [33] S. Khabbazi, R.O. Jacques, C. Moyano Cardaba, A. Mueller, *Cell Biochem. Funct.* 31 (2013) 312–318.
- [34] Y. Gao, J.B. Dickerson, F. Guo, J. Zheng, Y. Zheng, *Proc. Natl. Acad. Sci. U. S. A.* 101 (2004) 7618–7623.
- [35] M.M. Rosenkilde, L.O. Gerlach, J.S. Jakobsen, R.T. Skerfving, G.J. Bridger, T.W. Schwartz, *J. Biol. Chem.* 279 (2004) 3033–3041.
- [36] M. Levay, K.A. Krobert, K. Wittig, N. Voigt, M. Bermudez, G. Wolber, D. Dobrev, F.O. Levy, T. Wieland, *J. Pharmacol. Exp. Ther.* 347 (2013) 69–79.
- [37] Y. Gao, J. Xing, M. Streuli, T.L. Leto, Y. Zheng, *J. Biol. Chem.* 276 (2001) 47530–47541.
- [38] H. Yang, C. Lan, Y. Xiao, Y.H. Chen, *Immunol. Lett.* 88 (2003) 27–30.
- [39] B.A. Teicher, S.P. Fricker, *Clin. Cancer Res.* 16 (2010) 2927–2931.
- [40] S. Liekens, D. Schols, S. Hatse, *Curr. Pharm. Des.* 16 (2010) 3903–3920.
- [41] Y. Sun, X. Mao, C. Fan, C. Liu, A. Guo, S. Guan, Q. Jin, B. Li, F. Yao, F. Jin, *Tumour Biol.* 35 (2014) 7765–7773.
- [42] H. Hou, A.E. Chavez, C.C. Wang, H. Yang, H. Gu, B.A. Siddoway, B.J. Hall, P.E. Castillo, H. Xia, *J. Neurosci.* 34 (2014) 14006–14012.
- [43] F. Baribaud, T.G. Edwards, M. Sharron, A. Brelot, N. Heveker, K. Price, F. Mortari, M. Alizon, M. Tsang, R.W. Doms, *J. Virol.* 75 (2001) 8957–8967.
- [44] B. Tchernychev, Y. Ren, P. Sachdev, J.M. Janz, L. Haggis, A. O'Shea, E. McBride, R. Looby, Q. Deng, T. McMurry, M.A. Kazmi, T.P. Sakmar, S. Hunt III, K.E. Carlson, *Proc. Natl. Acad. Sci. U. S. A.* 107 (2010) 22255–22259.
- [45] J. Quoyer, J.M. Janz, J. Luo, Y. Ren, S. Armando, V. Lukashova, J.L. Benovic, K.E. Carlson, S.W. Hunt III, M. Bouvier, *Proc. Natl. Acad. Sci. U. S. A.* 110 (2013) E5088–E5097.
- [46] S. Duttling, J. Heidenreich, D. Cherpokova, E. Amin, S.C. Zhang, M.R. Ahmadian, C. Brakebusch, B. Nieswandt, *J. Thromb. Haemost.* 13 (2015) 827–838.
- [47] A. Steen, O. Larsen, S. Thiele, M.M. Rosenkilde, *Front. Immunol.* 5 (2014) 277.
- [48] A.J. Zweemer, J. Toraskar, L.H. Heitman, A.P. IJ, *Trends Immunol.* 35 (2014) 243–252.
- [49] C.A. Anderson, R. Solari, J.E. Pease, *J. Leukoc. Biol.* 99 (2016) 901–909.
- [50] T. Kenakin, *Br. J. Pharmacol.* 172 (2015) 4238–4253.